1-1-2004

Inflight investigation of the effects of rotor state measurement and feedback on variable stability helicopters

Marc David Alexander
Ryerson University

INFLIGHT INVESTIGATION OF THE EFFECTS OF ROTOR STATE MEASUREMENT AND FEEDBACK ON VARIABLE STABILITY HELICOPTERS

By

Marc David Alexander
Bachelors Degree - Aerospace Engineering,
Ryerson University,
Toronto, Ontario, Canada, 2000

A Thesis presented to the Ryerson University School of Graduate Studies
in partial fulfillment of the requirements for the degree of
Masters of Applied Science
in the Program of
Mechanical Engineering

Toronto, Ontario, Canada, 2004

Your file Votre référence
ISBN: 0-612-94219-8
Our file Notre référence
ISBN: 0-612-94219-8

Borrower's Page

Ryerson University requires the signatures of all persons using or photocopying this thesis. Please sign below, and give address and date.

Address/Signature/Date

ABSTRACT

Title:	Inflight Investigation of the Effects of Rotor State Measurement and Feedback on Variable Stability Helicopters
Name:	Marc David Alexander
Program:	Masters of Applied Science, Mechanical Engineering
Institution:	Ryerson University, Toronto
Year:	2004

This thesis describes a flight test evaluation of flight control laws applying rotor state measurements and feedback on the National Research Council Bell 412 Advanced Systems Research Aircraft (ASRA) and Bell 205A Airborne Simulator (AS).

Parameter estimation of a higher-order mathematical model of the ASRA rotor dynamics was achieved by Maximum Likelihood Estimation (MLE) employing coupled rotor-body equations parameterized by explicit rotor and fuselage state measurements.

Root Locus (RLM), Classical Multivariable (CMC), Eigenstructure Assignment (EAC), and Model Following control algorithms were implemented in Matlab/Simulink simulation for analysis of coupled rotor-body dynamics.

Rotorcraft performance specifications were based on compliance with ADS-33E-PRF and Cooper Harper military handling qualities.

Evaluated in desk-top and in-flight simulation, rotor state feedback of longitudinal and lateral disc tilt dynamics by modern multivariable control **significantly improves** inter-axis decoupling, disturbance rejection characteristics, rotor response dynamics, command tracking accuracy, and rigid-body bandwidth performance.

Acknowledgements

The author wishes to extend many Thanks to the National Research Council Flight Research Laboratory staff for supporting the many endeavors required throughout my research. The NRC_FRL was a wonderful environment within which to engage personal studies and experiences of my passion for experimental flight test aeronautics. Further Thanks are extended to the Ryerson University community for their many years of sustained support, development, and confidence of my skills as an Aerospace Engineer and Researcher.

I am indebted to you all.

With Gratitude:

Ryerson University
Dr. Kamran Behdinan, Research Supervisor

National Research Council – Flight Research Laboratory
Flight Mechanics and Avionics
Aircraft Maintenance
Electronics and Flight Instrumentation
Airworthiness Engineering
Design and Fabrication Services
Flight Operations and Safety
Computer Programming Support
Administration and Support Staff
Security and Cleaning Staff

Esteemed Mention:

Bill Gubbels, Research Advisor
Kris Ellis
Tim Leslie
Rob Erdos
Stephan Carignan
Ed Pinnell
Ken Hui
Jeremy Dillon

...and all NRC-FRL staff of whom I have come to know throughout this endeavor.

Dedication

Thoughts of gratitude, love, passion, and humility that words cannot express…

Table of Contents

Chapter 1 An Overview of the Rotor State Domain

Chapter 2 Parameter Estimation of Bell 412 ASRA Rotor Yoke Flap Dynamics

Chapter 3 High Bandwidth Rotorcraft Flight Control Law Design

Chapter 4 Model Following Flight Evaluation of Rotor State Feedback

Chapter 5: Conclusions and Recommendations

Appendices

References

List of Tables

List of Figures

Chapter 1

Chapter 2

Chapter 2

Appendices

Nomenclature

a_n, b_m	Transfer Function Coefficients
a_1	Longitudinal Disc Tilt, Displacement
a_0, a_{0f}, a_{0L}	Coning, Average Coning, and Average Lag Angles
a_{1f}, a_{1L}	Longitudinal Tilt and Skewing of Tip-Path-Plane
a_{2f}, a_{2L}	Rotor Weaving, Rotor Skew-Weave
b_1	Lateral Disc Tilt, Displacement
b_{1f}, b_{1L}	Lateral Tilting, Lateral Skewing
dr	Rotor Blade Element, Radial Length
e	Hinge Offset; Error vector
$\bar{e}$	Normalized Hinge Offset
f(t)	Atmospheric and Other Disturbances
g	Gravitational Acceleration
h	Fuselage Length Measure
m	Blade Element Mass
$p(\xi/z_{fd})$	Likelihood ratio for MMLE Analysis
p, q, r	Angular velocity components, helicopter about fuselage x-, y-, and z-axes
q	Displacement Vector, Constant Coefficient System
$\dot{p}, \dot{q}, \dot{r}$	Angular rate components, helicopter about fuselage x-, y-, and z-axes
r	Pilot command (or reference input) vector
$r_1, r_3, \dot{h}(3)$	Decoupling Parameters for Handling Qualities Specification
t	Time
u, v, w	Translational velocity components, helicopter along fuselage x-, y-, and z-axes
u	Control input vector of state space system model
$\dot{u}, \dot{v}, \dot{w}$	Translational rate components, helicopter along fuselage x-, y-, and z-axes
x, y, z	Mutually orthogonal fuselage axes; x-forward, y-starboard, z-downward
x, x	State vector of state space system model; Trim condition
$\dot{x}$	Perturbation Velocity
x_e	Equilibrium Value of the State Vector
y	Output vector of state space system model
z_{fd}	Flight Test Data for MMLE Analyses
A	State Matrix of state space model
A_1, B_1	Lateral and Longitudinal Harmonics of Blade Feathering, Cyclic Pitch
A_x, A_y, A_z	Vehicle Rigid-Body Accelerations
B	Control distribution matrix of state space model
C	Output matrix(state space model); Cosine component(direction cosine matrix)
C_ζ	Rotating-Frame Lead-Lag Damper Strength
D	Output matrix of state space model
D_δ	Specified Axis Control Input
F_z	Rotor Aerodynamic Force, z-axis direction
G	Gravitational Acceleration
$G_{\theta\delta g}$, $G_{\phi\delta g}$, $G_{\psi\delta g}$	Pitch, Roll, and Yaw Axial Gust Components, METS Model
G(s)	Design Plant Transfer Function
I_b, I_β	Blade Second Mass Moment Inertia
I_{xx}, I_{yy}, I_{zz}	Moment of Inertia of helicopter about x-, y-, and z-axes
$J(\xi)$	Optimization Cost Function for MMLE analysis
K	Full state feedback control gain matrix
K_H	Hub Moment Constant
K_ζ	Hub Stiffness, Lead-Lag Degree-of-Freedom
K_β	Hub Stiffness, Flap Degree-of-Freedom
L	Turbulence Integral State Length, METS Model

Lp, Mq, Nr, etc.	Moment Stability and Control Derivatives
L, M, N	External aerodynamic moments about x-, y-, and z-axes
$\overline{M}_\beta$	Aerodynamic Force due to Rotor Blade Flapping
M_a	Vehicle Mass
N_b	Number of Blades on Main Rotor
R, R	Rotor Radius; Rolling Moment
S	Sine Component, Direction Matrix
S_β	Stiffness Number, $(\lambda_\beta^2 - 1)/(\gamma/8)$
U_0	Mean Wind Speed, METS Model
X, Y, Z	External aerodynamic forces acting along the x-, y-, and z-axes
Xp, Yq, Xr, etc.	Force Stability and Control Derivatives
Z	Rotor disc height above ground
Z_{MLE}	Parameter data array for MMLE analysis
$\delta_{LAT}, \delta_{LON}, \delta_{COL}, \delta_{PED}$	Lateral, Longitudinal, Collective, Tail-Rotor Control Inputs
δ_x	Perturbation Value of the State Vector
δ_3	Rotor Pitch-Flap Coupling (also delta-3)
δF_ζ	Rotor Blade Element Lagging Force
δF_β	Rotor Blade Element Flapping Force
$\beta_0, \beta_{1c}, \beta_{1s}, \beta_2$	Collective, Longitudinal, Lateral, and Differential flapping angles
β	Cyclic Flap Degree-of-Freedom
β_p	Rotor Pre-cone Angle
ξ	Stability and Control Derivative Values for MMLE analysis
μ	Advance ratio
θ_0	Main-Rotor collective pitch angle
θ_{0T}, θ_{tr}	Tail-Rotor Collective pitch angle
θ_{1s}, θ_{1c}	Longitudinal and Lateral Cyclic pitch angles, respectively
θ_{dyn}	Rotor dynamic Twist of rotor blades
η_{Ga1}, η_{Gb1}	Rotor Turbulence Components (Longitudinal, Lateral Disc Tilt)-MFCA Model
τ	Time Delay
$\tau_{a1s}, \tau_{b1s}, \tau_b, \tau_f$	Time constants for longitudinal, lateral (disc tilt), fuselage, and rotor
τ_P	Phase Delay used in ADS-33 Specifications ($\frac{\Delta_{2\omega_{180}}}{57.3 \cdot (2\omega_{180})}$)
$\overline{v}_0$	Profile Induced Velocity
ω_d	Damped Frequency ($\omega_n\sqrt{1-\zeta^2}$)
ω_n	Natural Frequency
ω_o	Dimensionless Rotating Frequency
ω_{BW}	Bandwidth Frequency, Attitude Response
$\omega_{Bwphase}$	Bandwidth Evaluated by Phase Definition of Handling Qualities Specification
ω_{Bwgain}	Bandwidth Evaluated by Gain Definition of Handling Qualities Specification
ω_{180}	Neutral Stability Frequency at which Phase Bode Plot = -180°
ω_{RL}	Regressing Lag Mode Frequency
ω_β	Rotor Flap Natural Frequency
ω_ζ	Rotor Lead-Lag Natural Frequency
θ, ϕ, ψ	Euler angles about in pitch-, roll-, and yaw-axes
α	Vehicle Pitch Angle
α_w	Wind Standard Parameter, METS Model, $\left(2 \cdot \frac{U_0}{L}\right)$
Ω	Rotor Rotational Speed

λ	Dynamic Inflow, Mean Ratio Relative to Plane of No-Feathering
λ	Desired Pole Locations, EAC Control Law
σ	Rotor Solidity; Vertical Turbulence Intensity, METS Model
ν_β	Dimensionless rotating frame flapping frequency
ν_ζ	Dimensionless rotating frame lead-lag frequency
γ	Rotor Lock Number
γ^*	Reduced Rotor Lock Number
ψ	Rotor Azimuth Angle; Vehicle Heading Angle
ζ	Lead-Lag Degree-of-Freedom; System Damping Ratio
$\zeta_0, \zeta_{1c}, \zeta_{1s}, \zeta_2$	Collective, Longitudinal, Lateral, and Differential Lead-Lag Angles
ζ_{RF}	Rotating Frame Flap Damping Ratio
ζ_{LAG}	Rotating Frame Lag Damping Ratio

Notation

C.F.	Centrifugal Force
G.W.	Vehicle Gross Weight

Abbreviations

ABC	Advanced Blade Concept
AAH	Advanced Attack Helicopter
ADOCS	Advanced Digital/Optical Control System
AMCS	Advanced Mechanical Control System
ASRA	Advanced Systems Research Aircraft (NRC-FRL Bell 412)
CMC	Classical Multivariable Control
CR-B	Cramer-Rao Bounds
DOF	Degree-Of-Freedom
EA	Eigenstructure Assignment Control
FBW	Fly-By-Wire
FCC	Flight Control Computer
FCDE	Flight Control Development Environment
FSMS	Fuselage State Measurement System
HES	Hall Effect Sensor
HHC	Higher Harmonic Control
HLH	Heavy Lift Helicopter
HMMS	Hybrid Mathematical Model Structure
HQR	Cooper Harper Handling Qualities Rating
IBC	Individual Blade Control
IFR	Instrument Flight Rules
LQR	Linear Quadratic Regulator
LQG	Linear Quadratic Gaussian
MCT	Multiblade Coordinate Transformation
METS	Mixer Equivalent Turbulence Simulation
MFCA	Model Following Control Architecture
MIMO	Multiple-Input Multiple-Output
MMLE	Maximum Likelihood Estimation
MTE	Mission Task Element
OFE	Operational Flight Envelope
PID	Proportional-Integral-Derivative
PIO	Pilot Induced Oscillation
RASCAL	Rotorcraft Aircrew Systems Concepts Airborne Laboratory
RF	Radio Frequency
RLM	Root Locus Method

RSCM	Rotor State Computer Module
RSF	Rotor State Feedback
RSMS	Rotor State Measurement System
SAS	Stability Augmentation System
SFE	Safe Flight Envelope
SHP	Shaft Horse Power
SISO	Single-Input Single-Output
SLC	Sequential Loop Closure
TA	Transmitter Assembly
TPP	Tip Path Plane
UCE	Useable Cue Environment
VFR	Visual Flight Rules
VMC	Visual Meteorological Conditions

Institutions

DERA	Defense Evaluation and Research Agency
NRC-FRL	National Research Council – Flight Research Laboratory

Subscripts

C	Cosine Component
S	Sine Component
F	Fuselage
H	Horizontal Stabilizer
M	Main Rotor
T	Tail Rotor
V	Vertical Stabilizer

Chapter 1.0

An Overview of the Rotor State Domain

1.1 Introduction: Rotor State Measurement and Feedback Control

Helicopters typically exhibit flight dynamics that are characterized by a number of handling qualities deficiencies that require extensive vehicle design technologies, use of stability and control augmentation technologies, and refined pilot techniques.[1] The current trend in rotor systems design is towards powerful hingeless and bearingless main rotor hubs in vehicles with tailorable high bandwidth[i] digital flight control systems. The current specifications for flying qualities dictate high maneuverability and agility in the face of demanding mission tasks, degraded cue environments, normal and failed operational states, and with full and divided pilot attention.[13,14,15] Both the vehicle development and flight research cycles have in common the requirement to reduce flight test development time and cost in optimizing this complex vehicle. Feasible methods for attaining improved flight performance are required beyond that of vehicle redesign.

In the continuing trend to improve helicopter performance then, state measurement and feedback control are applied in flight control systems to extend the bandwidth capability of the helicopter. The most advanced form of feedback is the concept of integrated active control.[29] This context is illustrated in Figure 1.1 that presents a generic active control system. In an integrated active controlled vehicle, the flight state is attained by closing the loop around a myriad of sub-technologies that provide additional

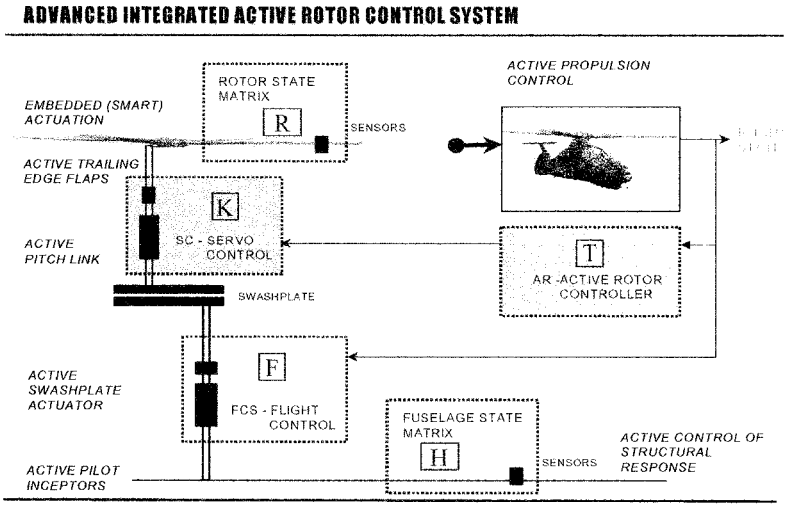

Figure 1.1 A Generic Active Control Technology Integration

systems level design flexibility. Particularly, active rotor control provides the ability to sense rotor behavior and act through additional or new control inputs to eliminate or reduce detrimental characteristics associated with the rotor blade and its operating environment. Performance enhancements are significant across the vehicle operational frequency spectrum. Fundamental to active rotor control is the concept of rotor and fuselage state measurement and feedback. Elevated operational bandwidths can

[i] Rotorcraft control bandwidth relates to characteristics of accurate command following, reduced sensitivity, agility, and stability. In the frequency domain bandwidth defines the frequency range over which control is effective, defining qualitatively that frequency at which the output will track an input sinusoid. In the time domain, high bandwidth corresponds to faster response rise times, tighter command tracking and higher control power as well as higher noise and parameter variation sensitivities.

be attained by sequentially closing the active rotor feedback and baseline vehicle control system loops with measured rotor and fuselage state behavior. This elevated local and global systems bandwidth can provide performance enhancements in areas such as control effectiveness (i.e.; robustness, signal noise rejection), handling qualities (i.e.; tracking, pointing, attitude stabilization), ride qualities (i.e.; gust/disturbance rejection, vibration and noise reduction), and flight envelope expansion (i.e.; aeromechanical stability enhancement, stall suppression).[29]

Active rotor control is currently not a feasible technology for widespread industry application due to systems complexity, reliability, and cost. However, rotor state measurement and feedback applied through upgraded sensor suites, actuators, and current digital flight control systems represent realistic concepts for near term optimization of rotorcraft performance. In the former case, access to rotor dynamics in the helicopter operational flight envelope allows for the monitoring of system integrity and stability. Further, these higher order states, in addition to those of the fuselage, may be incorporated in mathematical models through identification to provide improved vehicle models and more optimal flight control laws. In the latter case, the feedback of measured, high quality rotor state signals will provide the additional dynamic content necessary to improve helicopter gust rejection, tracking, stability, and ride and handling qualities through classical and modern multivariable control laws.

This thesis explores the design, implementation, and flight test evaluation of rotor state measurement feedback control systems on high bandwidth fly-by-wire inflight simulators. This first chapter will provide an introductory tour of the many interrelated disciplines and requirements for this investigation. This multidisciplinary nature and facets of the rotor state domain form an outline for discussions as illustrated in Figure 1.2. These interrelationships are familiar to research engineers in the areas of flight

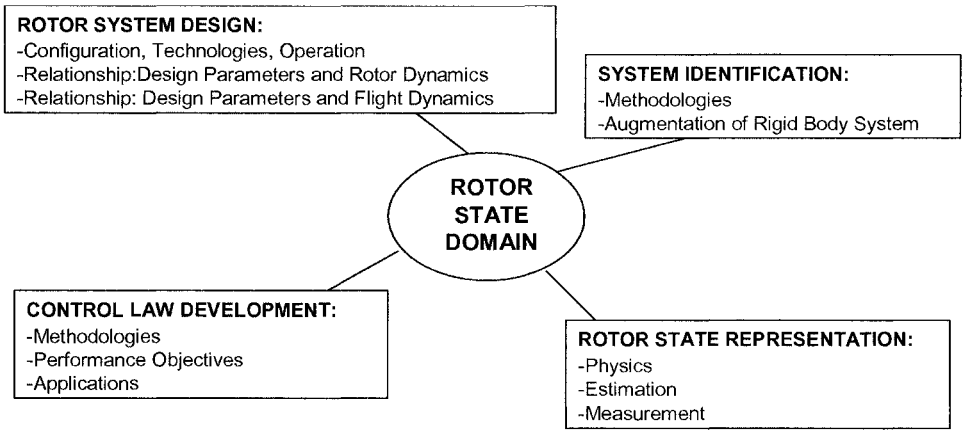

Figure 1.2 The Rotor State Domain

dynamics, helicopter design, control law design, and system identification. Further, the author will develop the motivations for this research initiative into higher order rotor dynamics and control, propose the research scope, and present the research organization. The subjects of this study are the Bell 412 Advanced Systems Research Aircraft (ASRA) and the Bell 205A Airborne Simulator (AS) of the National Research Council of Canada, Flight Research Laboratory.[110]

1.2 Rotor System Design: Characterizing Rotor and Flight Dynamics

Opening the tour is the rotor system design, its configuration, and its influence over helicopter performance. The unaugmented helicopter exhibits non-linear, unstable, and coupled dynamics that are functions of the vehicle's configuration (e.g.; main rotor type, propulsion system, flight control system) and flight state (e.g.; weight, airspeed, altitude). Flight control systems are designed to improve performance across a broad frequency spectrum as depicted in Figure 1.3, which for the helicopter extends out to some 50 Hz. Helicopter handling qualities are generally in the frequency range of 0.05 to 2 Hz (3.14 to 12.56 rad./sec.) and define required responses when control inputs are applied and when controls are free. Ride qualities generally involve gust sensitivity, vibration, and related noise characteristics of the helicopter. Critical to the flight control design process are coupled rotor/body/engine dynamics at 1 to 5 Hz (6.28 to 31.4 rad./sec.) and mid frequency rotor modes at 1.6 to 3.2 Hz (10 to 20 rad./sec.) depending on the type of rotor system. The flight control requirements of variable stability and modern rigid rotor helicopters are met by control law designs with a frequency range of 0.15 to 5 Hz (1 to 30 rad/sec). Measurement systems must operate with a high signal-to-noise ratio over the frequency range of concern. Further, system identification of mathematical models of the vehicle requires that mathematical models have response fidelity and robustness to parameter variation across the frequency spectrum of concern.

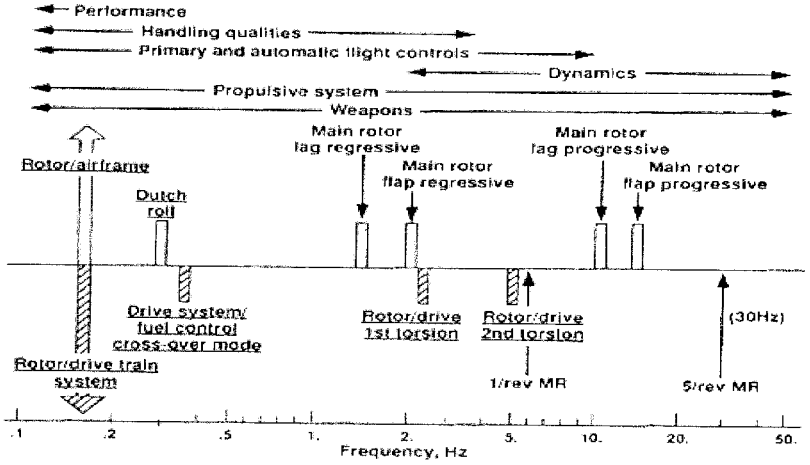

Figure 1.3 Typical Frequency Bandwidths of Helicopters[5]

The modes most of concern for researching rotor state measurement and feedback in context of the Bell 412 ASRA soft-inplane hingeless rotor include:

- **Vehicle Modes**: Longitudinal-lateral-directional stability.
- **Rotor Modes**: Disc tilt or flap regressive modes and lead-lag mode stability.
- **Control Modes**: Air/Ground resonance and aeroservoelastic coupling in the form of undesirable pilot to control systems interactions.

The development of a flight control system is complex because design requirements and performance specifications are most often mutually contradictory while stability requirements form threshold boundary conditions. The flying qualities, flight dynamics, and overall performance of a helicopter are functions of the rotor system design. For this reason designers must select main-rotor parameters to ensure the best possible vehicle performance throughout the operational flight envelope (OFE).

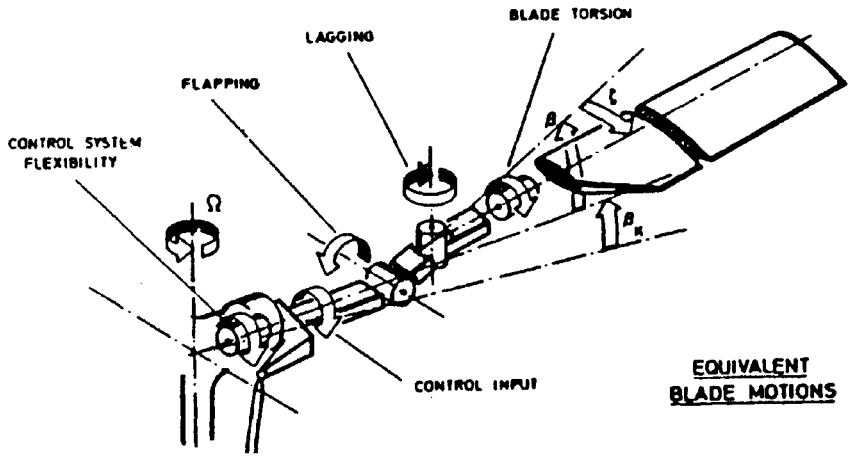

Figure 1.4 Rotor Degrees of Freedom[18]

Helicopter main-rotor systems are usually classified according to mechanical arrangement of the hub design to accommodate the blade flap and lead-lag motion; general rotor degrees-of-freedom are depicted in Figure 1.4. Fundamentally, there are 4 hub arrangements:

- Semi-Rigid Teetering
- Fully Articulated
- Hingeless
- Bearingless

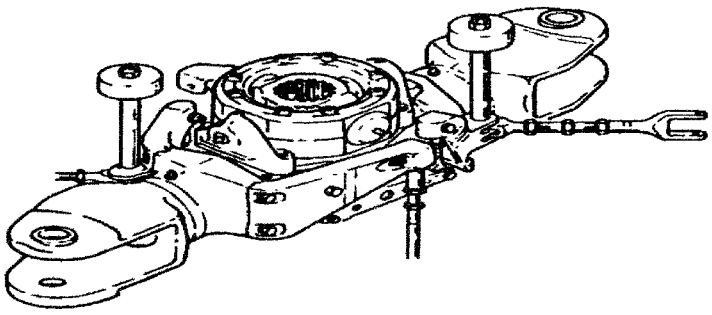

Figure 1.5 Semi-Rigid/Teetering Rotor Hub: Bell 47[8]

The semi-rigid or teetering hub was developed in the 1940's and is depicted in Figure 1.5 in typical 2-bladed configuration with the blades rigidly attached to the shaft by a pin. The major portion of the rotor-head is below the pin (under-slung) to improve stability. The rotor hub has both flapping and feathering axes. The fully articulated hub was developed in the 1920's and is depicted in Figure 1.6 and has provisions for independent rigid flapping of the rotor blades by using a hinge mechanism for each blade.

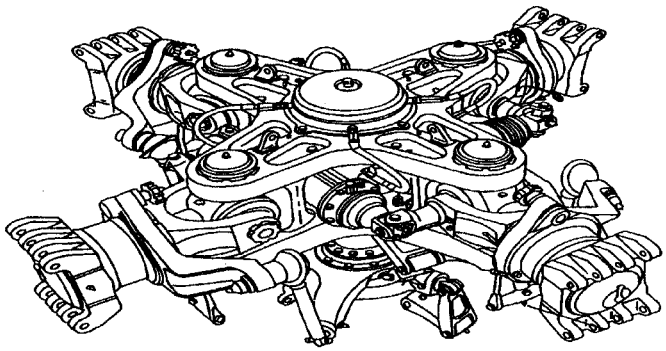

Figure1.6 Fully Articulated Rotor Hub: Sikorsky S-58[8]

Lead-lag motion is accomplished independently using both hinge and damper mechanisms to control the motion. The rotor hub also provides a feathering axis for pitch change.

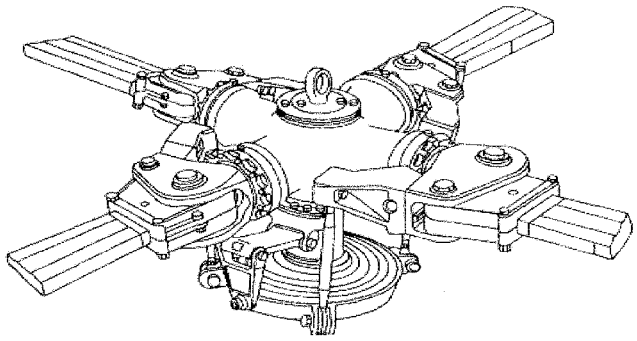

Figure 1.7 Soft Inplane Hingeless Rotor Hub - Messerschmitt-Bölkow-Blohm Bo105[8]

Since the 1960's, there has been considerable interest in hingeless rotors because of greater reliability through mechanical simplification as well as reduced drag, weight, and maintenance costs. Other advantages include better handling qualities and maneuverability through increased control power. In the so-called hingeless rotor hub as shown in Figure 1.7, the flap and lead-lag hinges are removed while bearing mechanisms impose the feathering axis. The rotor blade becomes a long, thin-member, cantilever beam in which deformations for those axes occur structurally. The bearingless rotor hub lacks all 3 hinges and bearings as shown in Figure 1.8.

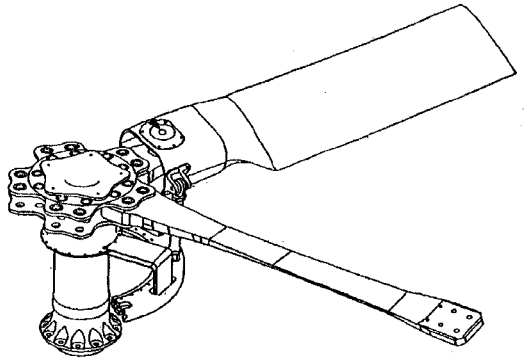

Figure 1.8 Soft Inplane Bearingless Rotor Hub; Boeing-Sikorsky RAH-66[24]

Tail rotors also require aeroelastic design considerations. They perform in similar manner to the main rotor, with blades being able to change pitch and flap either independently or collectively. Some designs include 2-bladed to 4-bladed teetering, hingeless and bearingless flex-beam designs, fenestron and FANTAIL concepts, and NOTAR concept.[16]

The NRC-FRL utilizes a teetering rotor hub based Bell 206 for flight training and vehicle modeling. The facility also employs both the Bell 205 with a teetering rotor hub and the Bell 412 with a soft-inplane hingeless main rotor hub for advanced inflight simulation. These vehicles utilize a two-bladed teetering tail rotor design for anti-torque control.

1.3 Main Rotor Dynamics: Characterizing Rotor Systems Operation

Having defined various main rotor systems, the discussions that follow highlight important facets of their dynamics. The rotor system designer selects rotor design parameters to obtain specific flight and rotor dynamic characteristics. Thus, in the design of the rotor hub and blades, fundamental design parameters define operational boundary conditions of the helicopter. Figure 1.9 illustrates the influences of various rotor system design parameters on helicopter dynamics.

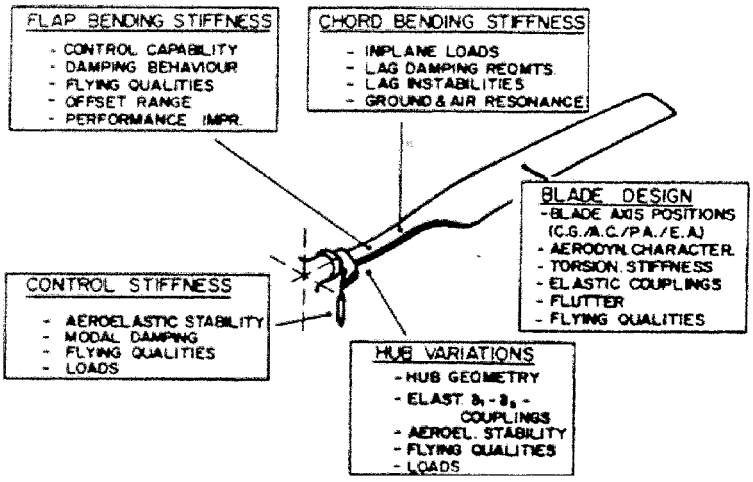

Figure 1.9 Influences of Rotor System Design[22,23]

Aeroelastic stability[17] is concerned with the relationship between force and response, defining the interaction between the fluid medium (e.g.; aerodynamics) and flexible structure (e.g.; rotor blades). In helicopter rotor dynamics, aeroelastic phenomena may be categorized as isolated rotor instabilities to 3 degrees of freedom, rotorcraft dynamic coupled body/rotor response of multiple degrees of freedom, and the aeromechanical behavior in vehicle flight dynamics. Isolated rotor dynamics and rotorcraft dynamic response determine aeromechanical stability.[3-6] Important parameters in designing these rotor systems to obtain particular flight dynamics objectives include: number of blades, rotor system kinematics, blade flap and lead-lag frequencies, hub and control system flexibilities, aeroelastic couplings, and blade balance. Aeroservoelasticity[20,21] merges the disciplines of structural dynamics, aerodynamics, and control dynamics in order to attain required levels of flying qualities. Critical to this research in high bandwidth flight control is the fact that the design of the main rotor (kinematics, design parameters, and configuration) influences the design of rotor state measurement technologies. Complex hubs limit sensor placement options. Complex kinematics not properly measured may create uncertainties and errors in rotor state data that is to be applied in vehicle monitoring, system identification, and state feedback flight control.[58]

1.3.1 Number of Blades

The number of blades may indirectly affect helicopter handling qualities as well as inter-blade coupling instabilities. For a given blade area and rotor radius, as the number of blades is increased, the resulting blade design acquires a slender, higher aspect ratio configuration. This creates a hub design featuring

elevated flap bending flexibility that impacts the hub moment production capability and thus vehicle controllability.[1,10,16] Based on multiblade dynamics, rotor systems with 3 or 4 blades exhibit different characteristic multiblade instabilities. Specifically, with regard to rotor state feedback investigation, Hohenemser and Yin[57] demonstrated that a lower stability margin exists for 3 bladed as compared to 4 bladed rotor systems with identical blade configurations.

1.3.2 Inplane and Out of Plane Rotor Dynamics

Many important effects relate to the inplane (Lead-Lag) and out-of-plane (Flap) motion of the rotor system. Blade flap dynamics are critical to vehicle flight dynamics and control due to their important role in hub moment generation. Blade lead-lag dynamics drive coupled rotor-body instabilities. The frequencies are characteristic of the helicopter type and capability as illustrated in Figure 1.10. These rotor dynamics are typically associated with a high frequency bandwidth greater than 2 Hz (12.56 rad./sec.) in hingeless rotor helicopters.[1,10,19,23] It is noted here that unlike the rotor system designer, the flight controls designer may or may not have access to this rotor state information. (i.e.; low order mathematical models and rotor state estimation applied in feedback)

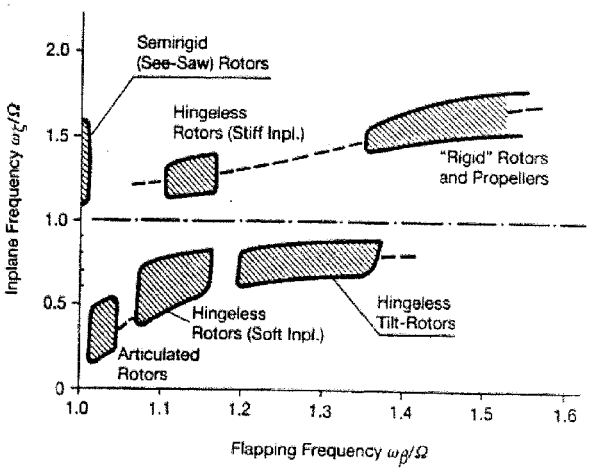

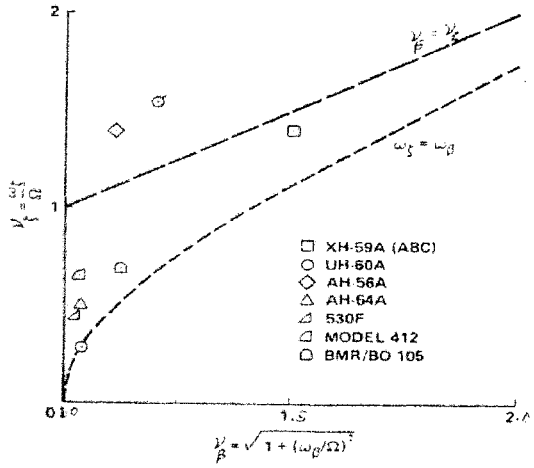

PARAMETER	ESTIMATE	HELICOPTER								
		RAH66	LYNX	BO105	BELL412	BELL427	AH64	PUMA	UH60	BELL205
Roll Convergence Mode	$-L_P = \frac{16K_H}{\gamma^* I_X \Omega}$	9.8	10.6	8.5	2.1	3.65	1.8	1.7	2.6	1.032
Regressing Flap Mode	$\frac{1}{\tau_F} = \frac{\gamma^* \Omega}{16}$	10.2	10.3	14.9	10.45		9.2	9.2	10.6	9.32
Coupled Roll-Flap Damping Ratio	$\zeta_{RF} = \sqrt{\frac{-1}{4L_P\tau_F}}$	51%	49%	66%	111%		113%	117%	101%	150%
Regressing Lag Mode	$\omega_{RL} = (1-\nu_\zeta)\Omega$	10.5	12.83	14.7	12.34		16.2		19.9	
Rotating Frame Lag Damping Ratio	$\zeta_{LAG} = \frac{C_\zeta}{2I_b\nu_\zeta\Omega}$	5%		3%			10%		43%	

Figure 1.10 Comparison of Helicopter Rotor-Body Coupling Parameters[1,7,25,90]

This means that designed vehicle stability and augmented vehicle stability margins may not be congruent providing the possibility for flight critical instabilities to occur through invalid performance prediction. Neglected or unmodelled dynamics are as critical to effective and safe rotor state feedback control as are those dynamics directly involved in the loop closure.

Why and how are lead-lag dynamics influential in rotor state measurement and feedback? Firstly, the lead-lag dynamics are the primary drivers of aeromechanical stability. These dynamics reflect the amount the center of gravity of the rotor blades, and hence the rotor disc center of gravity, is offset from hub center. The excitation of the lead-lag dynamics (i.e.; regressive lead-lag mode) is due to the vehicle rolling moment that imposes coriolis forces. These forces accompany blade flapping when lateral cyclic inputs are applied. The lead-lag frequency typically varies from 0.4 to 0.8 times rotor RPM for soft-inplane hingeless rotors such as the Bell 412 and the Bo105.[1,90,108,109] In terms of rotor state measurement then, knowledge of the lead-lag dynamics defines the resonant state (and its boundary conditions) of the coupled rotor-fuselage system. In terms of rotor state feedback the variation of lead-lag gains has important effects in feedback control. In a 1990 study of rotor state feedback control for the UH-60, Takahashi pointed out that in rotor state feedback investigations, on-axis position and rate lead-lag gains in the roll axis remove damping losses in the lead-lag modes with modest effects on flapping modes. Off-axis lead-lag gain variation had little effect in closed loop.[50,51] Further, the lead-lag gains were critical in attaining the 1/s behavior of the feedback above crossover frequency.

Why and how are flap-dynamics influential in rotor state measurement and feedback? Typically, articulated flap frequencies vary between 1.03 and 1.05 times rotor RPM; this parameter varies from 1.08 to 1.15 in hingeless rotor vehicles. The higher the flap amplitude and frequency, the higher the bending stresses at the root of the rotor blade. These higher flap frequencies in the hingeless rotor helicopter increase the hub moment capacity affecting both handling and ride qualities. The flap dynamics of the helicopter are critical to the force and moment generation of the vehicle. Blade flap response is dominated by centrifugal stiffness. As blade flap stiffness is increased the difference in fuselage attitude between hover and forward flight speeds also increases, as well as does the occurrence of pitch attitude instabilities. High rotor damping occurs at high rotor speed or given lighter rotor blades. This high damping provides the helicopter with faster disc (tip-path-plane) response to control inputs or fuselage motion.[1,5,16] In terms of rotor state measurement then, knowledge of the flap dynamics is critical in interpreting and controlling helicopter flying qualities. In particular, Tischler has illustrated that rotor state measurements for system identification and application in high bandwidth flight control law design for hingeless rotor helicopters, should show high coherence in the range of 10 to 15 rad./sec.[102,103] This is important for capturing on and off-axis dynamic response, based on the correlation between regressive flap dynamics and vehicle attitude rate response as functions of cyclic inputs. In the previously mentioned rotor state feedback application by Takahashi, it was illustrated that rotor flap gains dominate on- and off-axis pitch and roll crossover behavior. In the roll axis, flap gains offset damping losses of the flap modes.

As with the lead-lag gains, flap gains were critical in attaining the 1/s behavior of the feedback above crossover frequency.

1.3.3 Coupled Fuselage and Rotor System Dynamics

It was mentioned that the coupling of inplane and out-of-plane motions result in the handling and aeromechanical characteristics of the helicopter. The location of the flap and lead-lag eigenvalues[ii] is of importance to both the rotor and flight control systems designers[1,18,42,43,102] due to their typical stability margins. Calculated flap and lag mode eigenvalues for teetering (Bell205), articulated (Puma, UH60), hingeless (Bell412, Bo105, Lynx, AH64), and bearingless (RAH66) rotor helicopters are depicted in Figure 1.11.

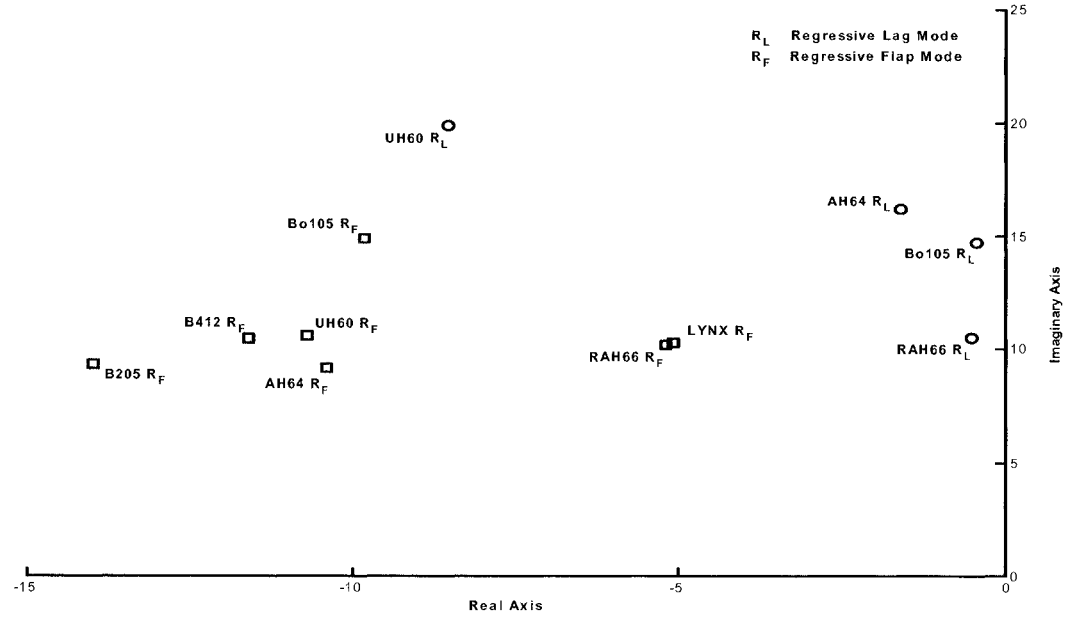

Figure 1.11 Comparison of Helicopter Flap and Lag Mode Eigenvalues[1,6,90,108,]

The lead-lag mode is typically less damped than the flap mode and thus more susceptible to destabilization. In conjunction with the damping provided by the airframe, and rotor parameters such as hub flexibility, shifting of the rotor center-of-gravity creates rotor and body interactions known as ground or air resonance[3,5,50]. As helicopters are modified, for example for variable stability, the concern that instabilities may occur is large. Helicopters of this type are used to explore the bandwidth of the vehicle's coupled flight control, actuation, and rotor systems. In terms of aeromechanics, (i.e.; coupled rotor/body dynamics), the damping required for a hingeless soft-in-plane rotor is considerably smaller than for an articulated rotor to eliminate the resonant state. The air resonance occurs when there is interaction between the regressing flap and lag modes. In Figures 1.10 and 1.11, note the susceptibility of the

[ii] In the rotorcraft rotor dynamics, multiblade coordinates allow approximation of rotor behavior operating in the rotor-rotating and fuselage-motion time frames. In the rotor-rotating frame, roots of the cyclic flap and lead-lag equations identify mode shapes by eigenvalues such as the regressing and advancing flap and lead-lag modes, respectively. Mode stability is defined by placement of the eigenvalues in the s-plane.

regressive lag modes to destabilization for the soft inplane bearingless RAH-66 and the hingeless Bo105 due to mode locations in the s-plane and low lag damping. The Bell 412 ASRA has lead-lag damping technology[108,109] to alleviate some concern over lead-lag resonant states; the Bo105 relies only on rotor structural damping.[1,16] Note the variance in lag damping provided on the articulated UH60 rotor as compared to the RAH66, Bo105, and AH64 in Figures 1.10 and 1.11. The frequency at which the resonant state occurs is lower for articulated rotors than in hingeless rotors. Research has shown that resonance in undamped hingeless rotors can occur with a doubling time of approximately 4 seconds, while that for articulated rotors occurs in a time frame 10 times smaller.[26,27] Ground resonance is more of concern for the Bell 412 ASRA and as such the current research program will not engage rotor state feedback with skids on the ground.

One of the most recent advanced coupled rotor-body interactions in high bandwidth application was studied for the digitally controlled RAH-66 Comanche. Here 2 techniques are investigated for interaction between the vehicle roll rate and the regressive lag mode. The first, currently in application on the soft in-plane bearingless main rotor RAH-66, is the application of notch filters at the regressive lag mode frequency allowing higher roll rate feedback gain tolerance in the low frequency range. The second was the flight test application of a roll rate feedback with phase lead design intended to improve the lateral axis handling qualities by reducing pilot perceived roll oscillation. This roll oscillation was a result of an air resonant state in the RAH-66 occurring at 1.7 Hz.[24,25]

Proceeding further through the introductory tour, it is emphasized that coupled rotor-body behaviors of the helicopter define the utility of rotor states and their feedback as a performance enhancement tool as well as define a propensity for events of closed loop mode destabilization.

1.3.4 Rotor System Flexibility, Blade Balance, and Moment Capability

The hub stiffness moment ($K_\beta \cdot \beta$) is proportional to the product of spring stiffness and flap angle. Hingeless rotor helicopters can generate hub moments 4 times greater than that of articulated rotor helicopters. This hub moment capability results in high control sensitivity, damping, and responsiveness at the expense of gust sensitivity. Control system flexibility is a key parameter in rotor system stability (i.e.; aeromechanics instability such as air resonance) and blade elastic coupling (i.e.; aeroelastic interaction such as pitch-flap coupling). It is critical in assessing torsional rotor dynamics in hingeless rotors that have pronounced coupling of flapwise and inplane bending. The chordwise balance of the blade can directly affect control power production, attitude damping and stability (e.g.; angle of attack stability), elastic couple stability (e.g.; blade flutter, and torsional divergence), gust sensitivity, and ride qualities (e.g.; vibration, tracking). The blade balance directly couples with control system flexibility to impact similar areas of helicopter dynamics as discussed above.[1,7,16]

For rotor state feedback research on the variable stability Bell 412 ASRA, it is the unmodeled nonlinear behavior of the rotor system, defined by such parameters as control and hub flexibility and lead-lag damper dynamics that present, physics that are difficult to predict.

1.3.5 Aeroelasticity and Aeromechanics

As shown in Table 1.1, the rotor dynamics of a helicopter are based on coupled flap, lag, and torsion dynamics of the rotor blades. The spatial orientation of the pitch axis and the stiffness of the flap, lead-lag, and torsion axes drive rotor aeroelastic stability. Designers may orient this axis to take advantage of stabilizing or destabilizing coupling effects by manipulation of the geometric hub design parameters. (i.e.; precone, droop, sweep, root offset, and torque offset).[16,22,27]

Aeroelasticity: Isolated Rotor Stability		
1DOF	2DOF	3DOF
Stall Dynamics Torsion Dynamics	Pitch-Flap Couple Flap-Lag Couple Pitch-Lag Couple	Flap-Lag-Torsion Couple
Aeromechanics: Rotorcraft Dynamic Response		
Rotor/Airframe/Engine Coupling	Airframe Response	Rotor Response
Ground Resonance Air Resonance Torque Oscillation	Fuselage Vibration Loads	Tracking Vibration Air-loads

Table 1.1 Important Rotor-Control-Airframe Responses[16-20]

The benefits and pitfalls of rotor states as applied in helicopter flight dynamics research are emerging through these discussions. However, how does the researcher proceed to apply these states in differential equations for identification of the rotor system and in feedback control for performance tailoring and enhancement? The answer is mathematical modeling of helicopter physics as discussed next in the tour of the rotor state domain.

1.4 Helicopter Modeling: State Descriptions of Helicopter Dynamics

The helicopter operational environment can by defined by complex interactions occurring in an aeroservoelastic interrelationship. These interactions are determined by structural dynamics, the augmentation bandwidth of the flight control system, and unsteady aerodynamic airloading. The entire domain is driven by mission-based pilot demands and results in vehicle flight dynamics. Modeling this environment is critical to research which aims to provide techniques for effecting optimal and robust closed loop control of multidisciplinary vehicle dynamics. For this research, modern classical and multivariable high bandwidth control development requires models for desktop simulation and for implementation in the Bell 412 ASRA flight control system. For these applications, high fidelity linearized representation of the coupled non-linear rigid-body and main-rotor dynamics is necessary for the analyses of handling qualities, ride qualities, and first order prediction of aeromechanical and aeroservoelastic stability.

1.4.1 Linearization

In essence, linearization makes the assumption that helicopter motion can be considered as a perturbation about a trim or equilibrium condition. The theory of the stability of motion for linear dynamic systems is most often expressed using linear algebra and the concepts of eigenvalues and eigenvectors. Analysis tools for complex nonlinear helicopter flight dynamics are limited and tend to be based on the assumption that non-linearities are weak. In the realm of helicopter flight nonlinear phenomena include vortex ring state, main rotor wake to tail rotor interactions, rotor stall, and rotor wake to empennage interactions. Also, in order to analyze the flight dynamics of the aircraft from first principals, Newtonian mechanics are used to develop nonlinear differential equations of state. These enable the determination of aircraft response, trajectory and attitude with time through numerical integration. [1,3,4,6]

A fundamental assumption of linearization is that the external forces X, Y, and Z and moments L, M, and N can be represented as analytic functions of the disturbed motion variables and their derivatives. Using a Taylor series expansion consisting of the force and moment functions, and their derivatives, the behavior of the helicopter can be assessed. Using small perturbation theory, during disturbed motion, the helicopter behavior can be described as a perturbation from trim whereby,

$$x = x_e + \delta x \qquad 1.1$$

The linearized equations of motion for the perturbed motion about trim for the 6DOF system may be written as:

$$\dot{x} - Ax = Bx(t) + f(t) \qquad 1.2$$

where;

f(t), represents atmospheric and other disturbances

(A, B), represent the system and control matrices, respectively

The coefficients of A and B represent the slope of the forces and moments at the trim state for definition of stability and control derivatives. The differentiation techniques of Finite Difference and System Identification are often used to determine the derivatives. These models can be derived to predict the vehicle dynamics (i.e.; by analytical solution of differential equations of motion) or to portray these dynamics (i.e.; by identification of comprehensive simulation response or flight test data). Herein, both methods are utilized to synthesize rotor state feedback control laws.

In order to model the Bell 412 ASRA for this application, a variety of states will be utilized based on required structure and state availability. In the following discussion, an overview of conventional and higher order dynamics, and their influences in the control of vehicle coupled rotor/body dynamics will be presented.

1.4.2 Rigid Body Dynamics

In the fixed reference frame the helicopter fuselage is modeled as a rigid body unless high frequency flexural modes are to be analyzed. The rigid body measurement system of the Bell 412 ASRA has the capability of capture states describing actuation, aircraft position and orientation, air data, propulsion, and fly-by-wire health states. The conventional 6DOF state vector of the helicopter used in flight dynamics studies uses a subset of these states.

Two axes systems will be used to begin the derivation of this state vector. The body axis system, shown in Figure 1.12, enables an overall accounting of those forces and moments from the mechanics of flight. The orthogonal axis system, shown in Figure 1.13, relates these forces and moments in vectorial form. The development starts with a basic body axes analysis of the helicopter in trim to introduce the helicopter flight mechanics. In this axes system we will ignore the coning and flapping of the rotor. (This limits the equations of motion to 6 – Equations 1.3 to 1.8; the complete set of 9 – Equations 1.12 to 1.20 will be incorporated into the orthogonal axes analysis that follows.) The forces and moments acting on the helicopter can be developed from a free-body diagram of the Body Axes:

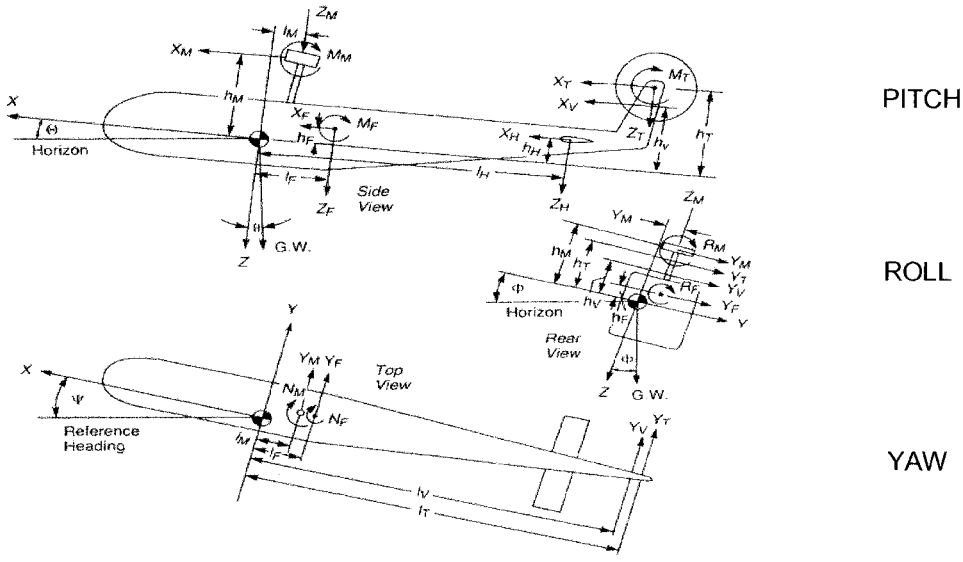

Figure 1.12 Body Axis Reference[7]

Longitudinal Force: $X_M + X_T + X_H + X_V + X_F = G.W.\sin\theta$ 1.3

Lateral Force: $Y_M + Y_T + Y_V + Y_F = -G.W.\sin\phi$ 1.4

Vertical Force: $Z_M + Z_T + Z_H + Z_V + Z_F = -G.W.\cos\theta$ 1.5

Rolling Moment: $R_M + Y_M h_M + Z_M y_M + Y_T h_T + Y_V h_V + Y_F h_F + R_F = 0$ 1.6

Pitching Moment:

$M_M - X_M h_M + Z_M l_M + M_T - X_T h_T + Z_T l_T - X_H h_H + Z_H l_H - X_V h_V + M_F + Z_F l_F + X_F h_F = 0$ 1.7

Yawing Moment: $N_M - Y_M l_M - Y_T l_T + Y_V l_V + N_F - Y_F l_F = 0$ 1.8

Consider the helicopter equations of motion described in nonlinear form:

$$\dot{x} = F(x, u, t) \quad 1.9$$

In six rigid body degrees of freedom, (accounting for coning, longitudinal and lateral flapping by equivalent time delay) the motion states and controls are given below.

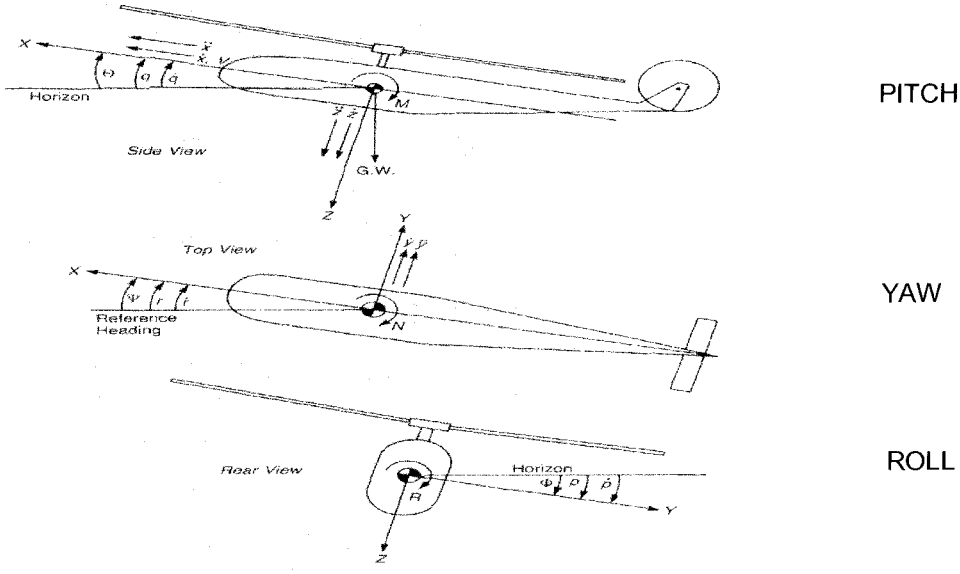

Figure 1.13 Orthogonal Axis Reference[7]

The state vector for a conventional helicopter, x, comprises 3 translational velocity components u, v, w, the 3 rotational velocity components p, q, r, and the Euler angles θ, ϕ, ψ given by:

$$x = \{u, w, q, \theta, v, p, \phi, r, \Psi\} \quad 1.10$$

The state vector may be augmented by time derivatives of the components shown.

The control vector for a conventional helicopter has four components - main rotor collective, longitudinal cyclic, lateral cyclic, and tail rotor collective given by:

$$\mathbf{u} = \{\theta_0, \theta_{1S}, \theta_{1C}, \theta_{0T}\} \quad 1.11$$

This control vector may be augmented with other dynamics such as engine parameters.

Now, applying Newtonian mechanics relating applied forces and moments to the resulting accelerations in translation and rotation assembles the 9 equations of motion[1,7].

$$\dot{u} = -(wq - vr) + \frac{X}{M_a} - g\sin\theta \qquad 1.12$$

$$\dot{v} = -(ur - wp) + \frac{Y}{M_a} + g\cos\theta\sin\phi \qquad 1.13$$

$$\dot{w} = -(vp - uq) + \frac{Z}{M_a} + g\cos\theta\sin\phi \qquad 1.14$$

$$I_{xx}\dot{p} = (I_{yy} - I_{zz})qr + I_{xz}(\dot{r} + pq) + L \qquad 1.15$$

$$I_{yy}\dot{q} = (I_{zz} - I_{xx})rp + I_{xz}(r^2 - p^2) + M \qquad 1.16$$

$$I_{zz}\dot{r} = (I_{xx} - I_{yy})pq + I_{xz}(\dot{p} - qr) + N \qquad 1.17$$

$$\dot{\phi} = p + q\sin\phi\tan\theta + r\cos\phi\tan\theta \qquad 1.18$$

$$\dot{\theta} = q\cos\phi - r\sin\phi \qquad 1.19$$

$$\dot{\psi} = q\sin\phi\sec\phi + r\cos\phi\sec\theta \qquad 1.20$$

1.4.3 Rotor Dynamics

There are 36 stability derivatives and 24 control derivatives for the conventional 6DOF rigid body system. The conventional framework above must be modified by additional rotor dynamics equations, and either state measurements or estimates for higher order modeling of helicopter response. In the hybrid 8DOF system for this research, rotor states augment the system to some 64 stability and 32 control derivatives. (Refer to Chapter 2 for derivation of the 8DOF hybrid system based on measured rotor yoke flap dynamics).

Rotor states determine the forces and moments transmitted to the fuselage from the rotor. These force-moment couples, characteristic to each type of rotor system, effect control over and interact with the rigid body states. In controlling rigid body states (i.e.; directly by pilot-demand or indirectly by structural coupling), knowledge and feedback of rigid body and rotor state dynamics provides for closed loop mode alteration. In reference to Figure 1.14, the flap and lead-lag dynamics of the rotor system in the non-rotating frame can be expressed in Fourier series form by harmonic analysis of rotating systems[3,5,82,83]. For approximation of a 4-bladed rotor, the first four terms are:

$$\beta^{(n)}(\psi_n) = a_{of} + a_{1f}\cos\psi_n + b_{1f}\sin\psi_n + a_{2f} \ldots \qquad 1.21$$

$$\zeta^{(n)}(\psi_n) = a_{oL} + a_{1L}\cos\psi_n + b_{1L}\sin\psi_n + a_{2L} \ldots \qquad 1.22$$

Other important rotor dynamics include rotor speed, blade azimuth, and blade torsion dynamics.

By applying a Multiblade Coordinate Transformation[1,44-46], a description of the rotor system in the rotating frame provides disc (tip-path-plane) dynamics as shown in Figure 1.14.

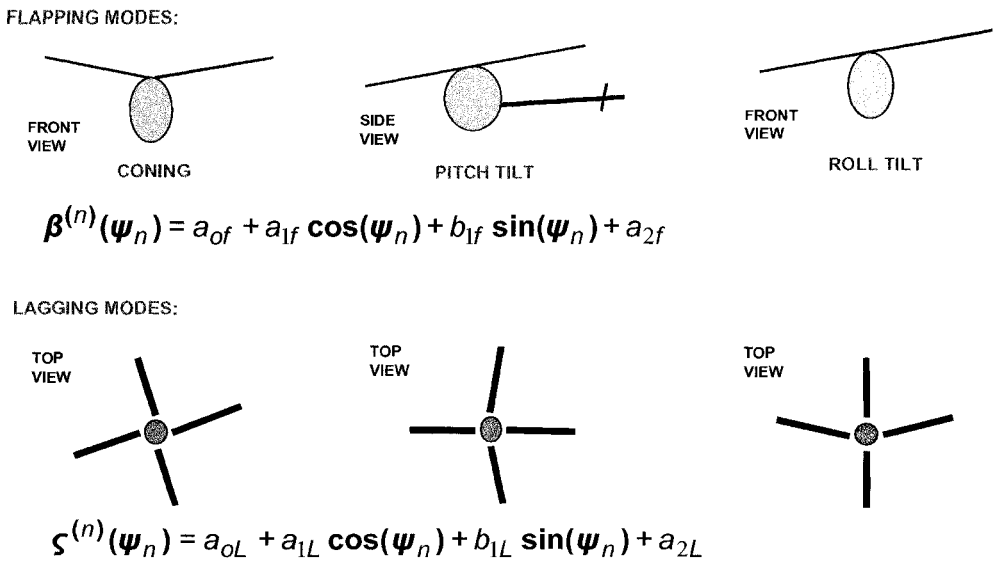

Figure 1.14 Rotor Multiblade States

The Fourier coefficients are defined as follows;

$$a_{of} = \frac{1}{Nb}\sum_{n=1}^{Nb}\beta^{(n)} \qquad 1.23 \qquad a_{oL} = \frac{1}{Nb}\sum_{n=1}^{Nb}\zeta^{(n)} \qquad 1.24$$

$$a_{1f} = \frac{2}{Nb}\sum_{n=1}^{Nb}\beta^{(n)}\cos\psi_n \qquad 1.25 \qquad a_{1L} = \frac{2}{Nb}\sum_{n=1}^{Nb}\zeta^{(n)}\cos\psi_n \qquad 1.26$$

$$b_{1f} = \frac{2}{Nb}\sum_{n=1}^{Nb}\beta^{(n)}\sin\psi_n \qquad 1.27 \qquad b_{1L} = \frac{2}{Nb}\sum_{n=1}^{Nb}\zeta^{(n)}\sin\psi_n \qquad 1.28$$

$$a_{2f} = \frac{2}{Nb}\sum_{n=1}^{Nb}\beta^{(n)}(-1)^n \qquad 1.29 \qquad a_{1f} = \frac{2}{Nb}\sum_{n=1}^{Nb}\zeta^{(n)}(-1)^n \qquad 1.30$$

Here, individual blade motions define the dynamics of the rotor disc. Thus the Fourier coefficients describing rotor disc flap dynamics are: average coning angle - (a_{of}), longitudinal tilt - (a_{1f}), and lateral tilt - (b_{1f}) dynamics. The Fourier coefficients describing rotor disc lead-lag dynamics are: average lag angle - (a_{0L}), longitudinal skewing - (a_{1L}), and lateral skewing - (b_{1L}). Other dynamics include rotor weaving - (a_{2f}), and skew/weaving - (a_{2L}). The rotating and non-rotating rotor state vectors are given by: [3,82-83]

$$x_{RRF} = [\Omega\ \psi_{(k)}\ \beta_{(k)}\ \zeta_{(k)}\ \theta_{dyn}] \qquad 1.31$$

$$x_{RNRF} = [a_{of}\ a_{1f}\ b_{1f}\ a_{1L}\ b_{1L}\ a_{2f}\ b_{2f}\ a_{2L}] \qquad 1.32$$

Again, time derivatives may be appended to the rotor state vector. The rotating frame measurement system of the Bell 412 ASRA is capable of capturing rotor yoke flap, cone, lead-lag, azimuth, and speed states. The yoke flap, cone, and lead-lag, states approximate rotor blade dynamics.

1.4.4 Higher Order Dynamics

The frequency bandwidth (or operational frequency range) of a helicopter extends from handling qualities to aeroservoelastic stability to structural dynamics as was shown in Figure 1.3. In order to perform analyses across this spectrum, various other high frequency parameters are required in the model state description. Several important helicopter interactions involving these high frequency parameters (also known as higher order dynamics) include aerodynamics, propulsion system dynamics, control systems dynamics, and rotor flexural dynamics.

Air mass dynamics are important contributors to helicopter performance stability, control, and response. Locally, blade pitch variation modifies unsteady blade surface pressures, vortex character (core size, strength, trajectory, blade vortex interaction, vortex-blade miss distance) and velocity fields. Globally, these parameters determine blade unsteady airloading and form the wake character (structure, distortion dynamics, intensity, trajectory).[9-11] The helicopter operational environment is characterized by an abundance of interactional aerodynamic effects. A principal source of interaction is the main rotor wake as it descends over the fuselage, empennage, and through the tail rotor disc. Dynamic inflow and wake have been shown to effect performance prediction (e.g.; handling qualities and aeromechanical stability), simulation (e.g.; piloted and comprehensive analytical) models, and the design of flight control laws for high bandwidth applications. A study by Chen and Hindson[12] investigated the impact of dynamic inflow on the design of a high bandwidth flight control system for the NASA CH-47B variable stability helicopter. Their results indicated that dynamic inflow affected linearized mathematical model predictions of helicopter vertical acceleration response to abrupt collective inputs. The addition of inflow dynamics created an inflow mode, destabilized the rotor-coning mode, added time delay to the main rotor's response in vertical rate of climb, and created phase lead in vertical acceleration to collective dynamics (causing transient thrust overshoot). The type of inflow model also played a part in analytical and flight data correlation. Aponso et al.[107] confirmed these results in the identification of higher order dynamics applied to analyses of CH-53E data. Curtiss[42-43] showed that increased coupling between flap regressing and body roll and pitch modes occurred when dynamic inflow was added to an analysis of hingeless rotor stability and control. The analysis involved linearized modeling of a single rotor helicopter (i.e.; articulated and hingeless rotors with 11 percent equivalent hinge offset) in hovering flight. It was also determined that this inflow caused a significant change in transient roll response to cyclic demand. These effects are significant since flap and inflow dynamics occur in similar time scales. In the area of control law development Takahashi et al.[50] and Mullen et al.[77] determined that airmass dynamics were critical to developing control laws for the UH-60 RASCAL and Bristol University hingeless rotor rig, respectively. In the former, study both dynamic inflow and wake are applied to the

linearized model of the RASCAL. Particularly in the case of dynamic wake it was found that its inclusion led to improved off-axis response correlations. For the Bristol University study involving multivariable control laws it was found that with only a quasi-steady model of inflow, the predicted performances of the multivariable control laws did not correlate with experiment. In related research in theoretical and experimental investigations on the Bo105 by Padfield[1], it was shown that body-flap models with quasi-static inflow impacted the size and damping of on-axis response as well as the sign and magnitude of coupled responses.

Propulsion and rotor system interactions influence the helicopter across a broad performance spectrum that includes handling qualities, coupled rotor/airframe/engine/drive-train dynamics, and ride qualities. With reference to Figure 1.3, a critical frequency range of excitation occurs in the region of 0 to 5 Hz where engine-load sharing and engine-torque oscillations couple with rotor torsion, flap and lead-lag modes. Important research in the area of rotor and engine state dynamics by Chen[52] suggested that performance prediction of vehicle heave rate and acceleration response were inaccurate without rotor speed dynamics. Further, pitch and roll control sensitivity and control response bandwidth decrease with droops in rotor speed. And lastly, that in the presence of collective flapping and flapping rate feedbacks most effective in attaining higher closed loop bandwidth and gust rejection, gain thresholds exist for excitation of the rotor lead-lag and rotor speed modes. It follows then that in experimentation in the high bandwidth, fly-by-wire (FBW) augmented, flight control environment of the Bell 412 ASRA that rotor state feedback, compensatory control inputs, and the coupled dynamics described present a daunting aeroservoelastic (ASE) interaction problem in the light of meeting handling qualities requirements such as ADS-33E-PRF.[13]

The control system kinematics and dynamics as well as rotor blade dynamics impart other important higher order dynamic content to the helicopter physics. Blade flap and lead-lag flexibilities contributed to errors in predicted vertical acceleration to collective response and roll rate to lateral cyclic response, respectively. These findings were based on an analytical study of the CH-53E fully articulated helicopter. Turnour and Celi[116] pointed out that rotor blade flexibility had modest effects on an analytical modeling of frequency content of the articulated UH-60 over a frequency range of 0.4 to 55 rad./sec. It was pointed out however that the effects were important to consider if high-gain flight control applications are intended. Kufeld[28] showed that control system stiffness modeling effected response correlation for predicting rotor system landing and dynamic stall events. It is important to note that these 2 studies involved high damped articulated rotor helicopters. As was mentioned in Section 1.3.4, researchers such as Hohehemser[16] and Huber[22] both indicate that control system flexibility modifies the rotor blade dynamics phenomena such as pitch-lag coupling to a significant extent in hingeless rotor helicopters. This concept of control system kinematics and dynamics is particularly important to Bell 412 ASRA operations and research requiring performance prediction since the actuation systems have been modified for supporting its FBW variable stability capability.

1.4.5 The Effects of Higher Order Dynamics on Specification Development

The relationship between rotor states and mathematical model fidelity as well as the capability of variable stability research helicopters influences the definition of modern rotorcraft specifications. Handling, ride, aeromechanical, and aeroservoelastic specifications for rotorcraft are vehicle dependent, and driven by the vehicle configuration, mission requirements, and the environment. (Note: the rotor/control system type is significant) These specifications cannot be universally applied. Table 1.2 illustrates the development of handling qualities metrics that were in many cases functions of new helicopter programs.

SPECIFICATION	YEAR	APPLICATION	COMMENTS
MIL-H-8501	1952	Helicopters	Specifically a criteria for helicopters that was inadequate for army missions, lacking treatment of envelopes and failures; limited to VMC
MIL-H-8501A	1961	Helicopters	Revision of above
AGARD 408	1962	V/STOL	
MIL-F-83300	1970	V/STOL and USAF Helicopters	Broad coverage with systematic structure and based on V/STOL data; criteria inadequate for army missions and limited to VMC
UTTAS, AAH PIDS	1971/3	UH-60; AH-64	Based on 8501A with maneuvering criteria added
AGARD 577	1973	V/STOL	
8501B (PROPOSED)	1973	Helicopters	Many new unsubstantiated requirements
DEF-STAN 00-970	1984	EH-101	Military specifications used in UK
ADS-33C	1989	LHX (RAH-66)	Basis for new MIL-SPEC; NRC-FRL applies teetering rotor based Bell 205 in criteria development
EURO-ACT	1990/3	Future European military Helicopters	Review of existing requirements with comparison to ADS-33 criteria; guidelines for optimum handling qualities of military helicopters
Tailored ADS	1992/3	Tiger; NH-90	Based on ADS-33C
ADS-33D	1994		Based on ADS-33C
ADS-33E	2000		Revision of ADS-33D

Table 1.2 Evolution of Military Rotorcraft Handling Qualities Specifications (Past 5 Decades) [2]

This presents an interesting point of view regarding specification development in analytical and experimental contexts. Firstly, analyses that were done to develop these specifications based on low order mathematical models would poorly predict helicopter performance. Secondly, experimentally developed specifications based on lower capability (i.e.; bandwidth, low axis coupling, etc.) helicopters would hinder the development of modern helicopters (i.e.; high bandwidth, high axis coupling, etc.) by creating performance capability mismatches in key design criteria.

With the development of such agile and aggressive vehicles prone to instability by powerful structural dynamic rotor systems, one must ask why are there no "rotor dynamic" specifications? ADS-33C[14] may have addressed this issue intuitively by Small Amplitude, Mid-Term Response specifications (3.3.2.2.2) and (3.3.5.2.2) since it is stated that no response should be unstable concerning rigid body mode placement (i.e.; unstable rotor modes would be non-compliant).

However other higher order dynamic thresholds are important. For example, high frequency rotor mode placement and trajectory should be standardized based on rotor type, helicopter configuration, and mission definition.

1.4.6 Rotor State Measurement Systems Development

It has been determined through research that measured rotor states are required to improve the fidelity of rotorcraft analyses and control, as well as to give access to states that theoretical estimation and observation do not predict well. For this reason, rotor state measurement technology plays a key role in

FLIGHT TEST PROJECTS		
VEHICLE	**PROGRAM**	**RSMS TECHNOLOLOGY**
Cobra AH-1G	NASA/AIRLOADS	Wireless RF
S-61	NASA/AIRLOADS	Slip-Ring Interface
H-34	NASA/AIRLOADS	Slip-Ring Interface
H-53	NASA/AIRLOADS	Slip-Ring Interface
CH-47	NASA/AIRLOADS	Slip-Ring Interface
XH-51	NASA/AIRLOADS	Slip-Ring Interface
UH-1	NASA/AIRLOADS	Slip-Ring Interface
BlackHawk UH-60	NASA/MTR – AIRLOADS NASA/TAAT – Acoustics NASA/OLS – Acoustics NASA/RASCAL NASA/RASCAL	RDAS, Slip-Ring Interface Slip-Ring Interface Slip-Ring Interface HUMS, Wireless RF LASER, Slip-Ring Interface
Stallion CH-53A	NASA/RSF	Slip-Ring Interface
Stallion CH-53G	ZFL/IBC	Slip-Ring Interface
Bo-105	(DLR/RACT)/Flight IBC	Slip-Ring Interface
Lynx ZD 559	DRA/Flight Research	
Puma XW 241	DRA/Flight Research	
MuPal-ε MH2000A	Japan NAL/Flight Research	Slip-Ring Interface
Bensen-B8 Autogyro	US Navy/Continuum Dynamics	Wireless IR

WIND-TUNNEL TEST PROJECTS		
SUBJECT	**PROGRAM**	**RSMS TECHNOLOLOGY**
Model: Rotor-Rig	(DERA/Augusta Westland)/RSF	Slip-Ring Interface
Model: NH-90	NLR/D&D	MR/TR RSMS, Slip-Ring Interface
Model: BMTR-2	(UTRC/Sikorsky)/IBC	IP, Slip-Ring Interface
Full-Scale Rotor on NASA LRTA: UH-60	NASA/IBC	RMDAS, Slip-Ring Interface

Table 1.3 Overview of Selected Rotor State Measurement Technologies (Past 4 Decades) [58-71]

attaining research fidelity and cost effectiveness in applications involving high bandwidth flight control and system identification. Data acquisition systems for sensing rotor dynamics have previously been developed for ground-rig, wind-tunnel, and in-flight testing.

Rotor state measurement systems capture data consisting of component loads, blade displacements (e.g.; linear, angular, azimuthal), blade displacement derivatives (e.g.; rate and acceleration), flow characteristics (e.g; temperature and pressure), vibration spectra, and acoustic data. Table 1.3 provides an overview of four decades of RSMS technologies. These systems were developed to support experimental research that included: rotor design (i.e.; airfoil and hub/control system design), rotor airloads assessment, health and usage monitoring, in-flight simulation, active rotor control (i.e.; HHC/IBC), flight control law design, rotor deicing technology, and production vehicle flight-testing. These previous technologies

helped shape the NRC-FRL RSMS design and integration requirements.[58] The results of the first parameter identification study applying this new measurement technology the Bell 412 ASRA are presented in the next chapter.

1.5 Effecting Control: Rotor Control by State Feedback

The introductory tour now focuses on rotor state feedback control with the intent of presenting important conclusions from previous research initiatives. In order to effect control over the complex dynamics of a helicopter, structural configurations are selected and flight control systems are designed. Beyond key flight dynamics defined by handling qualities, servo-loop performance requirements exist for ride qualities, aeromechanical stability, and aeroservoelastic stability. Thresholds exist for ride qualities based on vibration and noise, aeromechanical margins and envelopes for structural dynamics and resonance, and aeroservoelasticity constraints of the OFE for freedom from interactions between electronic flight controls, pilot demand, and servo actuation systems. The design of feedback control systems and strategies is a mature domain of research spanning several decades of helicopter development. Historically there were 3 eras in rotor state feedback control. In early development of helicopters the era of kinematic feedback was defined by the engineering of rotor kinematic and auxiliary systems for vehicle control and stabilization. Electronic flight control presented opportunities to produce electromechanical equivalents of mechanical feedback systems. However, with the understanding that higher order vehicle states were critical in flight control laws and math models, an era dedicated to the exploration of higher order rotor states was born. This era was dedicated to the development of system identification techniques for higher order rotor dynamics, of multiblade coordinate strategies for manipulating estimated and/or measured rotor states, the development of advanced rotor state measurement technologies, and development of control strategies for rotor state feedback control. This activity was crucial to proof-of-concept research applying rotor state feedback for next generation helicopter performance attainment. Finally, the era of electronic rotor state feedback provided for modern rotorcraft high bandwidth capabilities through the advancement of the digital flight control system, system identification techniques, measurement techniques, and multivariable control techniques particularly involving active control.

1.5.1 The Era of Kinematic Feedback: Attaining Stability Through Mechanization

Mechanical systems for altering rotor-vehicle control and stability included δ_3 (i.e.; kinematics relationship such that flap displacement alters collective blade pitch), Oehmichen (i.e.; kinematics relationship such that flap displacement alters adjacent blade pitch), and couplings (i.e.; kinematics displacements such as pitch-cone, pitch-lead, and pitch-flap). Historically, mechanical stabilization devices were designed either auxiliary to (non-flight critical) or as integral parts of (flight critical) the control loop.[16] In early helicopter development, designers strived to unravel complex and little understood dynamics. A significant contribution to the improvement of helicopter attitude and control instability occurred in the 1940's. Young[38] used a variety of models in order to design stabilizing devices such as rotor linkage systems, universal joints, and a stabilizing bar. The stabilizing bar was developed to full-scale for Bell Helicopters and provides a time lagged feedback of rotor-mast longitudinal and lateral angular rates causing stabilizing pitch and roll moments. Stuart III applied lift and control rotor flapping feedback in order to improve objectionable pilot control characteristics (such as stick loads, vibration, and

control latency) and unstable low-inertia roll oscillation. This was achieved using a rotor control linkage developed to full scale by Hiller. Miller[39] investigated the application of blade design modification and rotor flapping feedback to effect stabilizing control over helicopter control overshoot, attitude oscillation, and pitch-roll cross-couplings. Kaman developed servo tabs to effect control of his helicopters. As well, in comparison to the conventional single rotor helicopter designs of his competitors, this innovation and its counter-rotating configuration offered a greater amount of pitch damping and less inter-axis coupling. For the exception of Kaman's servo tab system, all these concepts represent augmentation that was auxiliary to the primary control system. [52,60]

An important body of research specific to hingeless rotor helicopters can be found in the 1970's relating to the design of rotor kinematic systems for feedback control. By this time rotorcraft research programs such as AAH (Advanced Attack Helicopters), and HLH (Heavy Lift Helicopters) defined the vehicle as a high performance, high advance ratio, agile, precision controllable, and low pilot workload vehicle capable in both VFR and IFR operating conditions.[16] As such, the helicopter designers made changes to vehicle rotor systems and designed augmentation systems for compliance. The hingeless rotor system competed with established teetering or gimballed and articulated systems, as well, the capability to apply electronics, electromechanics, and fluidics in state feedback was being explored. Examples of advanced hingeless rotor designs of this era (until 1973) include those of the Westland Lynx, Bolkow/Vertol Bo105, Bell Model 609, Lockheed AH-56 Cheyenne (CL-840), and the Sikorsky ABC coaxial concept. All of these rotor systems featured the application of advanced structural configurations and dynamics based on kinematic couplings as well as diverse options for feedback augmentation systems based on fuselage and rotor states. [16]

In terms of feedback control for hingeless rotor systems many concepts were developed. The Lockheed Gyro-Controlled Rotor (AMCS) applied fuselage pitch attitude and cyclic rotor flapping feedback by a floating gyro-swashplate system. The potential benefits of this system included higher angle-of-attack stability, lower control over-sensitivity, lower pitch-roll coupling, lower gust sensitivity, lower stick reversal, and reduced pitch-up divergence. The floating gyro-swashplate concept proved unreliable and Lockheed developed an equivalent system applying as the lagged rotor tilting moment feedback. The gyro-swashplate, eliminated by introducing cyclic actuator lag, could be implemented in either mechanical or electromechanical form. [16,41]

Thrust or tilting moment feedback (also flap-moment, proportional rotor tilting moment derivatives) were developed to modify the rotor characteristics to more acceptable forms. Used alone or in conjunction with fuselage feedback (e.g.; body rate feedback) the flap-moment concept was based on cyclic response to rotor flap-moment feedback being dominantly proportional to the integral of the moment rather than to its magnitude. This system was researched using the AH-56 Cheyenne (CL-840) rotor system. Not limited to the hingeless rotor system flap-moment feedback provided the potential for primary aircraft control or for alleviation of excessive loads and vibration as well as reducing rotor design complexity and weight.[41]

Coning or Normal Acceleration Feedback into cyclic pitch was applied to the Westland Lynx. Normal acceleration feedback to collective increases gust insensitivity and decreases pilot workload in turbulent conditions in the 120-165 knot speed range of the Lynx.[16] The combination of coning feedback into collective pitch and proportional rotor cyclic flapping feedback into cyclic pitch is equivalent to δ_3 pitch-flap coupling. Hohenemser suggests that this would produce good flapping stability at high advance ration for torsionally stiff blades outside of their reverse flow torsional divergence limit.

1.5.2 The Era of Higher Order Rotor States: Rotor State Identification, Manipulation, and Control

At this stage, well-established methods existed to feedback rotor states in mechanical, kinematic, and servo-actuated forms. With the development of the electronic flight control system, a new era in rotor state characterization and feedback control theory was born. Research in this era can be categorized by activities in the following domains:

1. System Identification of Higher Order Dynamics (including Rotor States)
2. Development of Multiblade Coordinate Strategies for Rotor State Estimation and Measurement
3. Development Control Strategies based on the Implementation of Higher Order Dynamics (including Rotor States) in Modeling and Feedback

These activities provided the tools necessary to embark on rotor state feedback research by fully digital electronic and electro-servo-hydraulic flight control systems for the myriad of performance benefits that could be brought about by advanced control concepts such as active control technology. Specifically, system identification beyond the baseline 6DOF model extended the range of fidelity of analyses and simulations in representing coupled rotor-body helicopter physics. These models were applied in the flight control design process. The multiblade coordinate strategies allowed researchers to analytically explore and manipulate rotating and non-rotating frame components of the helicopter, which played a critical role throughout this era when estimations of higher order dynamics were being replaced by measured dynamics obtained from state measurement systems.

1.5.2.1 System Identification of Higher Order Mathematical Models

Modeling of the Bell 412 ASRA soft inplane hingeless rotor dynamics and vehicle response provides unique challenges in lieu of flight control. The variable stability system that includes actuation, digitization, and inceptor technology allows the vehicle to operate at higher authority and attain higher bandwidth capability than the base vehicle (Bell 412 HP). This required that a restricted flight envelope be established which is safe guarded by manual and automated safety systems. In 6DOF representations of the Bell 412 ASRA as was developed in Section 1.4.2, the effect of the main rotor and control system (i.e.; actuators, hydraulics) are not modeled.

The theoretical vehicular response due to this quasi-steady representation leads the actual vehicle dynamics by assuming;

- First order attitude-rate response
- Instantaneous rotor-body response due to control inputs (i.e.; instantaneous tip-path-plane tilt with immediate angular acceleration response)
- Steady state rotor response absorbed in rigid body derivatives
- No high frequency dynamic content

The helicopter rotor and control system cause modal dynamics that may only be represented by single-axis equivalent time delays. This method of approximating the rotor-control response limits the frequency range of validity and applicability of the 6DOF model. Characteristics include:

- Low-mid frequency range of validity (i.e.: Out to 10 rad/sec for soft inplane hingeless vehicles) for handling qualities and simulation of rigid body response
- Unmodeled high frequency rotor and rotor-body mode content
- Restricted flight control applications

Modern helicopters and inflight simulators require capability in a much broader frequency range or bandwidth. Typically for high bandwidth flight control this range extends to 4.78 Hz (30 rad/sec) for soft inplane hingeless rotor vehicles.[95-97,102,103] This requires modeling of the rotor-control system either by state estimates or by measured state data. In system identification research, the NRC-FRL proceeded to develop hybrid representations of the Bell 412 ASRA based on estimates of rotor tip-path-plane dynamics.[99-100] These models, though improved over baseline 6DOF cases, had limited validity in high frequency mode interaction behavior of flap and lead-lag dynamics. A model with measured rotor states was required which would initially capture the soft inplane hingeless coupled roll-attitude/rotor-flap second order response. With the realization that rotor states influenced analytical results for vehicle performance prediction as well as control law effectiveness, researchers developed extended and hybrid mathematical models. These are reviewed in the following chapter on the parameter identification of a hybrid mathematical model for the Bell 412 ASRA rotor yoke flap dynamics.

1.5.2.2 Multiblade Coordinate Strategies for Rotor State Estimation and Measurement

In order to perform rotor and fuselage dynamics analyses more efficiently and effectively complex coordinate mathematics were developed. Pioneering work by such researchers as Coleman and Feingold [5] (1950's) in the area of ground resonance instability (coupled inplane blade and horizontal rotor hub vibration) and Loewy [17] (1960's) in the area of rotary-wing and propeller aeroelasticity initiated this type of analytical framework. A decade later, complex coordinates were required for emerging design challenges for modern rotor system design and optimization of rotor-fuselage stability. A body of research in multiblade coordinates in the 1970's illustrates that accessing and exploring rotor states via estimation and/or measurement was vital to making rotor dynamics theories applicable. This activity was emerging from the development of advanced rotor systems (hingeless and bearingless), of electronic

flight control technology, of system identification techniques for flight control law design, and of rotor and fuselage state measurement technologies applied in a variety of rotorcraft production and research applications.

Curtiss explored the transient and frequency response characteristics of the tip-path-plane (TPP) and the influence of flapping feedback using a complex coordinate description of the equations of motion.[44] Applicable to articulated and hingeless rotors at low advance ratios ($\mu < 0.3$), the analysis described the TPP by a single 2nd order differential equation with multiblade coordinates (where; a 4 bladed description includes coning, longitudinal and lateral TPP tilt, and TPP warp). Hohenemser et al.[45,46] published several works from the 1970 to 1974 on the application of multiblade coordinates for the assessment of rotor/body coupling stability and response for hingeless and rigid rotor configurations. The analyses assessed stability limits, eigenvalues, and transient response to controls, gusts and feedback. The types of feedback included rotor tilting to cyclic, normal acceleration to collective, coning, lagged and proportional tilting moment types.

In the 1970' and 1980's, active control technology and one of its fundamental principles, state feedback, meant that multiblade coordinate analyses needed to be developed for real-time (on-line) applications such as experimental rotor-rig and helicopter flight test activity, as opposed to simulation studies. DuVal performed a numerical simulation to evaluate the performance of a technique for on-line estimation of rotor-states in the non-rotating frame from multiple simultaneous measurements in the rotating frame.[47] The technique employed both multiblade coordinates and an observer approach to perform the TPP estimation based on flapping and flapping rate sensors. Fuller developed a Kalman filter design for estimating rotor TPP states using combinations of blade flapping and flapping rate measurements; sensor failure detection, isolation, and accommodation are also considered.[48] The rotor dynamics transformation is done analytically by Lyapanov methodology to convert the system to a time-invariant form.

Other notable mutiblade coordinate strategies in active rotor research include projects for rotor vibration attenuation such those developed by McKillip.[49]

1.5.2.3 Control Laws for Rotor State Dynamics Investigations

The goal of modern helicopter flight control is to effect optimized multivariable control to achieve optimized multidisciplinary performance based on multiobjective requirements. In reality, an expert control designer can use classical and/or modern multivariable techniques to achieve the required performance. Through decades of flight control law design research, lessons learned that are essential to this study may be categorized as follows:

1. General guidelines for the control law design process
2. Knowledge of the effects of the presence of rotor states in mathematical modeling and the impact of rotor state feedback in attaining coupled rotor-fuselage performance
3. General guidelines for the evaluation of these control laws via flight testing

In this research, several flight control algorithms are applied in simulation to predict closed loop performance of rotor state augmented linearized mathematical models applied in rotor state feedback. The predictions allow for implementation of such laws in flight test activities on the Bell 412 ASRA. Both classical and modern multivariable methods are employed. In analytical and experimental applications in rotor state feedback it is more educational and guiding to understand which control law strategies were employed and how they were employed to effect control, rather than their theoretical development. If one considers research over the past 6 decades of rotor state feedback research (Table 1.4), it is interesting to note application of very similar control techniques throughout.

INVESTIGATION	YEAR	TYPE	CONTROL LAWS
Howitt, et. al.:[53,67] Rotor Rig Hingeless	2000	Analytical/ Experimental	H-Infinity, Eigenstructure Assignment, Proportional-Integral Derivative
CH-53 Articulated[54]	1975	Analytical/ Experimental	Programmed Control Logic
Hohenemser et. al.:[57] Model Hingeless	1972+	Analytical	Root Locus Method; Proportional-Integral Derivative
Cunningham et. al.: [56] Model CH-47B Tandem	1980	Analytical	Modal Control by Eigenvalue-Eigenvector placement
Curtiss et. al.:[42-44] Model Articulated	1988	Analytical	Root Locus Method; Linear Optimal Regulator
Hall et. al,: [40] Model S-61 Articulated	1970+	Analytical	Quadratic Synthesis (Linear Quadratic Gaussian)
Takahashi: [50,51] Model UH-60 Articulated	1994+	Analytical	H-Infinity; Linear-Quadratic Regulator
Diftler:[55] Model UH-60 Articulated	1988	Analytical	Root Locus Method; Programmed Control Logic
Chen: [52] Model UH-60 Type	1992	Analytical	Linear Quadratic Regulator
Ellis:[37] Model Kaman Helicopter	1953	Analytical/ Experimental	Root Locus Method

Table 1.4 Overview of Selected Rotor State Feedback Investigations (Past 6 Decades)

The control theories typically rely heavily on classical transfer function, mode placement, and modern multivariable representations. The control techniques include from the classical context (Root Locus Method[8] (RLM), Sequential Loop Closure[87] (SLC), Proportional-Integral-Derivative[77,78] (PID)) and from modern control (Linear Quadratic Regulation[52,84] (LQR), H-Infinity[51] (H_∞), Eigenstructure Assignment[77,79] (EA)). The control structures were primarily observer (state estimate) form with some applications of full-state feedback. RLM was typically used to assess system pole trajectories due to configuration and flight condition changes. SLC closure was a natural step to the multiple bandwidths and multiple objectives of helicopter controllers; each loop designated for a given closed loop task based on its feedback parameters. It could be used for classical, modern, or combinations of these 2 control techniques. This concept is important to rotor state feedback design since measured rotor state data provides for a more optimal full-state feedback structure. In these loop closures then PID, LQR, EA, and H_∞, have been applied in rotor state feedback studies. Of these, PID and EA are purported to provide the

control designer the clearest insight of the relationship between control parameterization and helicopter physics; LQR was shown to cloud this insight.[75] H_∞ in rotor state feedback investigations has been shown to inherently assist in control tuning simplicity, objective attainment such as axis de-coupling, and robustness to uncertain dynamics and signal noise.[51] However, this was dependent on the proper control law architecture.[53,67,77]

It is notable in the research summarized above that:

- High emphasis is placed on the structure (order, states, etc.) and fidelity (structure robustness, parameter sensitivity, etc.) of the mathematical model. Specific structures are required for rotor state feedback analyses while poor model fidelity led to low control effectiveness.
- Gain influence and dynamics are indicative of helicopter dynamic complexity over the operational envelope of concern.
- The simulated controller performance and gain structure are typically over predicted to that attainable in experiment.
- Combining classical and modern multivariable methods yields flexibility in the control task.
- Of the control law techniques reviewed without including active control research, none have been applied in experimental flight-testing of rotor state feedback control on a variable stability FBW helicopter.

Research by Tischler[84] showed directly through the application of optimization that given the proper problem formulation (specifications, tuning parameters, constraints) and an experienced control law designer, many techniques could be used to effect optimal flight control over the helicopter.

1.5.3 The Era of Electronic Rotor State Feedback: Research in Rotor State Measurement, State Feedback, and Active Control

Variable stability helicopters such as the Bell 412 ASRA provide the ability to tailor response characteristics over a broad frequency range to simulate various vehicles, flight conditions, and mission types. The capability to perform inflight simulation weighs heavily on control bandwidth. A vehicle's control bandwidth relates to characteristics of accurate command following (tracking, maneuverability, pointing), reduced sensitivity (gust rejection, configuration and flight condition robustness), agility (control authority, control power, responsiveness), and stability (flight dynamic, rotor, and coupled rotor-fuselage). These characteristics determine the stringent handling qualities for vehicles applied in inflight experimentation and in modern rotorcraft design. It follows then that research in rotorcraft flight dynamics has for decades of helicopter development focused on attaining broader bandwidth capabilities. The variable stability helicopter thus presents a multidisciplinary environment within which rotor states may be applied in research to influence:

1) **Aeromechanics Analyses**: Identification of rotor design parameters, characterization of rotor/body modes, and maintenance of stability.

2) **Specifications Development**: Handling and Ride Qualities analyses for development and optimization of requirements.

3) **Ride Qualities Improvement**: Development and optimization of vehicle metrics (vibration, noise, etc.)

4) **Handling Qualities Improvement**: Development and optimization of vehicle metrics (coupling, bandwidth, etc.)

5) **Flight Control Law Design**: Development of more efficient and effective algorithms

6) **System Identification and Modeling**: Development of high fidelity and appropriately parameterized mathematical models.

7) **Aeroservoelasticity**: Identification of parameters, characterization of coupled modes, and maintenance of stability.

1.5.3.1 Rotor State Measurement and Feedback Studies

Rotor state feedback has demonstrated potential to minimize control activity as well as attenuate rotor dynamics responses that can be catalysts in coupled rotor-body instabilities. Ingle et al.[75] demonstrated that an H-Infinity controller designed with a model incorporating higher order dynamics affected more robust (i.e.; to off-design conditions) and more optimal (i.e.; less control activity) control than an Eigenstructure Assignment design with a model employing only rigid body dynamics. This analytical investigation involved a 32 state linear, time invariant hover model of the UH-60 helicopter. The DERA/Agusta-Westland hingeless rotor rig has been the subject of many rotor state feedback investigations. Howitt et al.[53] demonstrated that flap angle feedback could reduce peak-to-peak cyclic control activity and tip-path-plane deflection by some 30 percent. This finding was important since it was the case with measured rather than that of estimated rotor flap angle that achieved these benefits.

Rotor state feedback has been applied for the reduction of rotor sensitivity to gusts, control-actuation sensitivity to sensor noise. Briczinski et al.[54] (1975) investigated in flight rotor/vehicle state feedback applied to a US Navy CH-53A. The study consisted of both analytical and flight test phases based on a variety of feedback schemes. In rotor state feedback delta-3, Oehmichen, delta-3/Oehmichen, pure pitch-cone, and proportional schemes were assessed. For fuselage state feedback, angle-of-attack, normal load factor, and pitch acceleration schemes were assessed. In combined format, thrust vector control was evaluated. Ride qualities, based on delta-3, Oehmichen, pure pitch-cone, and normal load factor feedbacks, reduced transient normal load factor response to gust disturbances by 30 to 50 percent compared to baseline response. Chen[52] (1992) performed an exploratory investigation of the effects of rotor RPM variations and rotor state feedback on a UH-60 based nonlinear hover model. The mathematical model incorporated vertical and yaw axis motion, inflow dynamics, drive train with flexible shaft, and engine-governor dynamics. Feedback control was investigated by full state linear-quadratic regulation (LQR). This investigation determined that both vehicle and some rotor responses to vertical gust disturbances are substantially attenuated by rotor state feedback. It was noted that vertical attenuation was evaluated in flap dynamics however, events of response amplification were shown in

lead-lag dynamics and rotor speed variation. Takahashi[50,51] investigated rigid-body and rotor-state feedback in a series of studies based on the design of helicopter flight control laws for blade element based comprehensive models of the UH-60A BlackHawk. Control methodologies were based on model following structures developed for the RASCAL inflight simulator that incorporates command models, dynamic decoupling, inner loop feedback, and outer loop feedback. This structure was modified to accommodate rotor state feedback loops applying classical and multivariable Ricatti solution (LQR and H-Infinity) methods. Of the many findings, Takahashi determined that a significant reduction in noise sensitivity resulted from the application of rotor flap feedback. This noise was passed to actuators near the 1/rev frequency. It was also determined that disturbances in pure longitudinal and lateral air-mass translations could be significantly attenuated in all axes. In a stability augmentation study of the UH-60A, Diftler[55] attempted to improve the roll characteristics of the vehicle by varying control-system/SAS bandwidth and applying rotor flap feedback (combined lateral flap tilt and tilt rate) to lateral control. It was determined that at low bandwidth, the flap feedback dampened the regressive flap mode and destabilized the primary servo mode. At high bandwidth, the flap feedback dampened the regressive flap mode, stabilized the primary servo mode, and destabilized the progressive flap mode. Applying δ_3 coupling (i.e.; decreasing blade pitch as blade flaps up producing collective flap feedback) and roll rate feedback destabilized the rotor regressive flap mode.

Through closed loop rotor state feedback, research has shown that higher closed loop bandwidths are attainable, controllers are more robust to model uncertainty and feedback gain variation, vehicle response can exhibit reduced inter-axis coupling, and the control law design process made more apparent. In modern research, many of these findings were demonstrated in analytical and experimental investigations on the previously mentioned DERA/August-Westland hingeless rotor rig. In an early study, Cunningham et al.[56] applied a modal EA technique to study high gain feedback control on the NASA CH-47B variable stability tandem rotor helicopter by higher order mathematical models and rotor/fuselage state feedback. State feedback of rotor coning and lateral flapping angles to longitudinal and lateral control, respectively, allowed for higher bandwidths of rigid body modes to be attained. However, the designs resulted in rigid body feedback gains being too high to accommodate sensor noise and actuator nonlinearity of the CH-47B's technology era.

Many researchers over some 6 decades of flight control research have illustrated that flight controllers designed without rotor dynamics over-predict the feedback gain limits for rotor mode stability. Further, mathematical models without this high frequency content do not represent key dynamics of concern leading to false performance predictions, poorly mapped stability margins, or ineffective control law designs. Neglected rotor dynamics could be classified as modeling errors or uncertainties in the control law design process. These errors or uncertainties typically stem from plant modeling and output measurement anomalies in the closed loop system output.

In a 1953 study, Ellis[37] showed that neglecting rotor dynamics in an analysis of an attitude feedback compensator for an articulated helicopter led to an over-prediction of the maximum feedback capabilities.

Further he concluded that without rotor dynamics, controllers produced unsatisfactory performance at low feedback gain. As well, satisfactory performance resulted at a particular feedback gain with better controller capability. In 1973, Hall and Bryson[40] demonstrated destabilization of a helicopter model's flap regressive mode by a hover hold controller design without rotor dynamics. Other results indicated the correlation between feedback gain and vehicle performance. The instability increased relative to increased controller gain for tighter tracking of the helicopter hover position.

The over prediction of lateral axis bandwidth associated with rotor flap and higher order dynamics was demonstrated in a 1986 study of the NASA CH-47B variable stability helicopter. Here, Chen and Hindson[72] demonstrated the effects of rotor, sensor, servo actuator, and digitization dynamics on an LQG roll axis controller. The coupled rotor-fuselage model neglected cross-coupling effects (yaw rate, translational velocities) and included tip-path-plane flap dynamics. The study resulted in an analytical prediction of roll oscillation that was 10 percent greater than that measured in flight. Further, it was shown that increasing roll rate gain destabilized the regressing flap mode. As well, the other higher order dynamics included in the analysis limited achievable feedback gain and overall performance.

In 1987, Miller and White[76] investigate the impact of flap, lead-lag, drive-system, and inflow dynamics on helicopter handling qualities. A comprehensive linear rotor-fuselage model is developed from nonlinear equations of motion by an exponential basis function technique; simulation results are compared to UH-60A and CH-47B flight cases. Inclusion of inflow dynamics improved correlation of predicted flap regressive/rigid body modal frequencies with flight test data. Lead-lag dynamics could be destabilized by lateral/directional feedback before the flap regressive mode in the presence of time delay and lag damper parameter variation. Also, neglecting lead-lag dynamics resulted in over-prediction of achievable directional axis bandwidth.

Tischler and Curtiss obtain similar conclusions on hingeless rotor coupled rotor-fuselage dynamics with regards, to modeling and feedback of flap and lead-lag dynamics. In the former case, the Bo105 is the subject of a system identification and control law design study for roll axis augmentation. Tischler[102,103] illustrates the requirement for accurate knowledge of rotor dynamics as control system lags determine feedback gain bandwidth. Both Tischler and Curtiss conclude that for a single rotor hingeless helicopter coupled body/rotor flapping modes limit attitude feedback gain while lead-lag modes limit attitude-rate feedback gain. An important finding by Curtiss was that the instability limit for attitude-rate gain was a function of non-linear lag damper characteristics whereby the effective lag damping decreases with increasing amplitude above a threshold.[42,43] Tischler's study demonstrated very decisively that that lower order models without lead-lag dynamics are only valid when the identification is band-limited to the particular frequency range of interest. (i.e.; for the research herein, this points to an upper-limit of the rotor flap regressive modal frequency of the Bell 412 ASRA). Mullen and Brinson[77] in 1999 found that model uncertainty could impact predicted and experimental control law performances. In their study of multivariable control laws, the DERA/Augusta-Westland experimental hingeless rotor rig is mathematically modeled for a hover condition. States included were 6 rotor states (i.e.; coning, flapping,

and their rates of change), 3 actuator states (i.e.; collective, lateral, and longitudinal cyclic), and quasi-static rotor inflow. Control design techniques included classical multivariable (CMV, based on Nyquist-array method) and classical multivariable plus H-infinity (CMVH, based on CMV and an H-infinity compensation). In this study, the interplay between model fidelity and the control law technique effected the attainment of predicted bandwidths, damping, and cross coupling. Among the findings was the fact that the performance improvements for the CMVH design over the CMV predicted in simulation were not as marked as those found during experimentation on the rotor rig.

Beyond vehicle system identification and flight control law design, incorporation of higher order dynamics in mathematical models has improved the simulated/analytical data correlation to flight data in applications such as comprehensive rotorcraft modeling codes and piloted simulations. Several important conclusions were derived from Lewis[88] in research based on a UH-60 aeroelastic blade element model investigation for a piloted rotorcraft simulation. In control law design, it was found that using a rigid blade plant led to the design of controllers with low control gains due to unmodeled blade elasticity. Pilots evaluating elastic and rigid blade simulations perceived increased control sensitivity that in effect increased with airspeed. As well, elastic blade models increased the level of excitation and broadened the frequency range of the simulated helicopter modes. Inclusion of higher harmonic inflow provided improved flight data correlation and system damping. It was also reported that the modeling technique of incorporating consistent aerodynamic and structural dynamic modal content properly predicted avoidance modes.

1.5.3.2 Rotor and Fuselage State Feedback in Active Controls Research

Particular studies have illustrated that rotor states are critical in designing and analyzing rotorcraft for aeromechanical stability. The majority of benefits for the maintaining aeromechanical stability through feedback control are derived from research in active rotor control concepts.[30,31,32] Straub et. al[36] investigated active rotor state feedback influences in the augmentation of coupled rotor-fuselage stability. In the hover regime, it was determined that sine components of lag displacement, lag rate or acceleration, or body roll rate or acceleration were most effective in improving damping. Weller et al. and Gandhi et al.[33-35] applied fuselage and rotor state feedback actively through swashplate and individual blade control to investigate alleviation of resonant states. Fuselage state feedback applied to a bearingless main rotor in hover was used to attain aeromechanical stability through damping. It was determined that 1 percent additional damping could be attained by applying body rate feedback. This result was beyond that attainable by body attitude feedback. In another study, rotor state feedback through individual blade control was more effective at stabilizing ground resonance than either aeroelastic couplings or active swashplate control based on fuselage state feedback. Further important findings on active rotor control and its application of rotor state feedback may be found in previous research by the author on the integration of active rotor control into modern helicopters.[29]

1.6 Motivation and Research Proposal

The previous discussions have highlighted the effects and interaction of rotor states in rotorcraft dynamics, performance, stability, and control. Throughout this review of rotor state dynamics it has been illustrated that rotor state feedback has been applied kinematically in rotor system design, electronically in digital flight control, and actively through concepts such as active rotor technology. Bandwidth related benefits have been reported across this spectrum of activity. Further, the presence of rotor states in mathematical models of the vehicle has improved model fidelity.

With the recent installation of an RSMS on the Bell 412 ASRA, the NRC-FRL has not as yet researched the influence of measured rotor state data in parameter identification or in high-bandwidth flight control applications. Further, in some 6 decades of non-active control based rotor state feedback research reviewed herein, there are no findings suggesting that rotor state feedback has been successfully engaged on a variable stability FBW helicopter.

With access to the technologies and resources for higher order system identification and the variable stability FBW capability of the Bell 412 ASRA, the author embarks on a study to explore the effects of rotor state measurement and feedback through flight test investigation. The areas to be addressed include the commissioning of a Rotor State Measurement System (RSMS) for normal and research operations, thorough understanding of coupled rotor-body physics, the development and analysis of a higher order mathematical model of the ASRA incorporating rotor dynamics, and the development and analysis of classical and modern flight control laws employing both rotor state measurement and feedback.

The proposed research aims to investigate:

- What are the limitations and deficiencies of the RSMS in high bandwidth operations and how might the system be improved?
- What are the characteristics of the rotor flap and lead-lag dynamics of the ASRA's soft inplane hingeless rotor system as compared to other helicopters?
- How does this rotor system interact with the ASRA fuselage and advanced variable stability FBW flight control system?
- To what level of fidelity can a higher order mathematical model of the ASRA be developed given the influences of system identification methodology, current NRC-FRL desk-top analysis simulation tools, rotor state measurement technology, and the ASRA high bandwidth rotor/flight–control capability?
- How effective, efficient, and robust are classical and modern multivariable flight control law methods based on higher order models and state feedback in attaining next generation performance benefits under military specifications? These benefits include:
    - Gust Disturbance Rejection
    - Axis-Decoupling
    - Signal Noise Insensitivity
    - Robustness to Off-Design Conditions
    - Reduction of Pilot Workload
    - Prediction of and Maintenance of Stability Margins
    - Maneuverability

- How compliant is this research with requirements for safety (FBW variable stability engagement), and for military handling qualities (ADS-33E-PRF) specifications?
- What recommendations can be developed from this research in support of NRC-FRL future high-bandwidth rotorcraft investigations?

1.7 Organization of Research

An overview and analysis of the parameter identification process and analysis of the mathematical model of the Bell 412 ASRA is presented in Chapter 2. The development of flight control laws and closed loop simulated behavior of the vehicle will be discussed in Chapter 3. In Chapter 4, the ground and flight test evaluation of control laws will be reviewed. Preparations, experiment design, test result comparisons to prediction, and performance evaluations will be discussed. And finally, Chapter 5 provides conclusions and recommendations that evolved from this investigation in high bandwidth flight control.

Chapter 2.0

Parameter Estimation of Bell 412 ASRA Rotor Yoke Flap Dynamics

2.1 Introduction: Rotor State Parameter Identification

The following study was undertaken by the NRC-FRL in order to develop high fidelity mathematical models of the Bell 412 ASRA rigid body fuselage augmented with rotor hub yoke flap dynamics. The final Hybrid Mathematical Model Structure (HMMS) was attained with the expert contributions in aircraft identification by Hui and Mikjaniec, and in model refinement by Bell 412 ASRA manager, Gubbels. The approach herein involves parameter identification[iii], which comprises 2 components:

- **System Identification**: procedures and techniques to address the mathematical model structure and equations of motion defining the coupled rotor-fuselage system

- **Parameter Estimation**: procedures and techniques to address the quantification of vehicle stability and control derivatives contained in the equations of motion

In the former case, a hybrid model structure was derived from first principles of rotorcraft coupled rotor-fuselage equations of motion, as well as based on the integration of the rotor state measurement system (RSMS) on the Bell 412 ASRA. Previous research in soft-inplane hingeless rotor parameter estimation involving both the Bo105 and the Bell 412 provided guidelines for this derivation.
In the latter case, the stability and control derivatives were obtained by an NRC-FRL time domain optimization technique based on Maximum Likelihood Estimation (MLE). Constraints in the optimization space for the MLE process included:

- Approximation of the kinematics and dynamics of the Bell 412 ASRA hub
- Measurement limitations of the RSMS
- Non-linearities and unknown dynamics in the high bandwidth flight dynamics environment

This chapter documents this parameter estimation investigation in overview the NRC-FRL requirement and previous research identifying the need for mathematical models augmented with rotor state data. The Bell 412 ASRA and its fuselage state and rotor state measurement systems (FSMS and RSMS, respectively) are described. The vehicles application in a data gathering flight test program highlights its many research capabilities. The chapter provides an in-depth discussion of the parameter identification process and analysis of the final 8DOF model structure.

[iii] In modern rotorcraft research, system identification is generally the term used for the entire parameter identification process.

2.2 Motivation and Previous Research

The recent installation of a Rotor State Measurement System (RSMS) for capturing flap and lead-lag dynamics of the Bell 412's hingeless rotor system has broadened the scope of the NRC-FRL rotorcraft program. The rotor system data can be used for safety monitoring in Fly-By-Wire (FBW) operations, identification research, and flight control system development using rotor state feedback. The motivation for installing the RSMS was to gain access to high quality rotor state data, which is a common theme in helicopter development and research over the past 6 decades.[58]

The Bell 412's soft inplane hingeless configuration combined with a high bandwidth FBW control system is indicative of the helicopter design trend towards achieving superior, mission-tailored handling qualities. This rotor system provides highly coupled and unstable bare airframe response at the cost of lower maintenance requirements, higher control power, and lower time delays. The variable stability control system is used to reduce off-axis cross-coupling, vary control bandwidth, and provide desired response modes based on the given mission task. The classical and modern multivariable helicopter flight control design techniques require accurate descriptions of the coupled rotor/body system in order to effect control. Typically, linearized mathematical models are utilized. In context rotor and flight control systems interactions, previous research has shown the effects of neglecting rotor system dynamics. This includes the inability to attain the high bandwidth flight control requirements of Level 1 handling qualities and aeromechanical/aeroservoelastic stability.

In the preceding chapter it was illustrated that in early helicopter design, knowledge of rotor dynamics and their feedback through hub design kinematics were essential in reducing the unfavorable characteristics of the helicopter. Rotor design parameter and configuration variation was critical in the 1960's and 1970's as advanced rotor systems such as hingeless and bearingless concepts emerged. Designers relied on structural characteristics and axis couplings to achieve flight aeromechanical stability and handling qualities. As the concept of electronic flight control emerged, electronic equivalents of the above concepts could be implemented through feedback control laws. Throughout these eras, the effects of rotor dynamics in the flight control systems design was explored.

Our introductory tour led to several compelling conclusions that motivate the need for higher order mathematical model application in the design of high bandwidth flight control laws:

1. Unmodeled dynamics lead to falsely predicting the maximum gains that can be achieved in the actual coupled rotor-fuselage vehicle.
2. Unmodeled dynamics could lead to control law designs that show poor overall control performance (i.e.; robustness to modeling errors and off design conditions, noise rejection, input tracking, and minimization of control energy)

These points are critical in hingeless and bearingless vehicles with high bandwidth flight control systems where bare-airframe stability thresholds are low and highly configuration dependent.[16]

2.3 Description of the Bell 412 Advanced Systems Research Aircraft

The Flight Research Laboratory of the National Research Council of Canada operates two variable stability research rotorcraft: The Bell 205A Airborne Simulator and the Bell 412HP Advanced Systems Research Aircraft. A myriad of projects have been conducted with these facilities such as pure research in handling qualities and flight controls, developmental systems testing, flight test simulation or rehearsal, and training test pilots and flight test engineers from the various test pilot schools.[110,111]

Figure 2.1 The NRC-FRL Bell 412 Advanced Systems Research Aircraft (ASRA)

The Bell 412 Advanced Systems Research Aircraft (ARSA) as shown in Figure 2.1 is an airborne research simulator derived from the Bell 412HP helicopter[108,109]. The Bell 412 is a medium, twin-engine helicopter with a gross take-off weight of 11,900 lbs, powered by a PT6T-3BE twin-pac turboshaft engine, rated at 1800 SHP. This aircraft has a 4-bladed soft-inplane hingeless rotor system featuring high control power and low response time delays. Installed in the ASRA is an experimental, single string fly-by-wire control system used for research purposes only. The single string architecture consists of:

- a single set of FBW actuators
- one flight control computer
- a single set of aircraft state sensors

These features significantly reduce the maintenance and operating costs associated with the aircraft's project systems. The single string design philosophy incorporates an inherent reliance on automated safety monitoring systems and a safety pilot to guard against system failure or exceedance of the operational flight envelope. An independent computer known as the health-monitoring unit (HMU), assists the safety pilot by monitoring critical aircraft parameters and ensuring that the aircraft response does not exceed an allowable envelope. The HMU is the core of the ASRA safety system. It performs a wide variety of relatively simple monitoring functions, but its most important role is to provide a prediction of the aircraft worst-case future state if the present command is in error. Should the HMU detect a potential problem, the FBW system is disengaged and control is automatically passed back to the safety pilot.[111]

The Bell 412 ASRA has a dedicated array of measurement technologies in order to provide real-time flight data throughout the OFE. This data can be used in real-time inflight process and safety monitoring and control system feedback, as well as in post-flight analyses such as aircraft modeling and stability assessment. This suite of technologies can be categorized in either Non-Rotating (Fuselage) or the Rotating (Rotor) frames as shown in Figure 2.2.

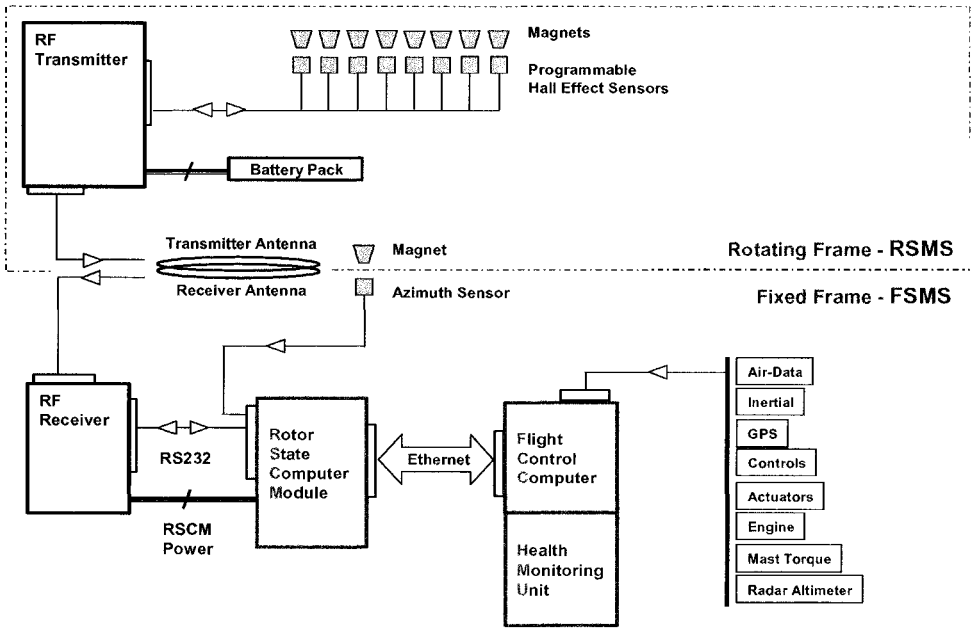

Figure 2.2 Bell 412 ASRA State Measurement Systems

2.3.1 Fuselage State Measurement System (FSMS)

The Bell 412 ASRA is an inflight simulator with bandwidth capabilities comparable to the UH-60 and performance characteristics inherent to other hingeless and rigid rotor vehicles such as the Bo105 and the Lynx, respectively.[1,90] The primary measurement suite for the vehicle consisting of an array of sensors, termed the fuselage state measurement system (FSMS), continues to be modified since the vehicle's

inception in 1993. This system provides real-time data sets of control/actuator positions, air data measurement, aircraft position (Global, Inertial, Radar Altimeter), propulsion system, and FBW health monitoring (Power, Internal Command, Command Validation, Actuator Drive, and Watch-Dog Timers).

2.3.2 Rotor State Measurement System (RSMS)

Extension of the capabilities of the Bell 412 ASRA is of primary importance to the NRC rotorcraft research program, particularly in the area of high bandwidth flight control. It was determined that the best method of achieving this was to install a Rotor State Measurement System (RSMS) for capturing state dynamics of the Bell 412's hingeless rotor system. The primary systems integration was completed in 2000.[58] The RSMS was designed to capture rotor yoke deflections and calculates longitudinal and lateral flapping and lead-lag, disc coning, blade azimuth, and rotor speed states based on wireless radio frequency technology. As shown in Figures 2.2 and 2.3 then is a fully integrated airworthy, reliable, and easily transferable technology. The installed weight of the RSMS of less than 20 lbs. consists of a sensor suite and transmitter pod in the rotating frame, and a receiver and a rotor state computer module (RSCM) in the non-rotating frame. In the rotating frame the RSMS incorporates the Transmitter Assembly (TA), 8 Hall Effect Sensors (HES) for flap and lead-lag dynamics, and a rotor RPM/Azimuth HES. In the fixed frame, the Rotor State Computer Module (RSCM) is mounted inside the vehicle while the Receiver Assembly (RA) is mounted on the upper deck, beneath the aft roof cowling.

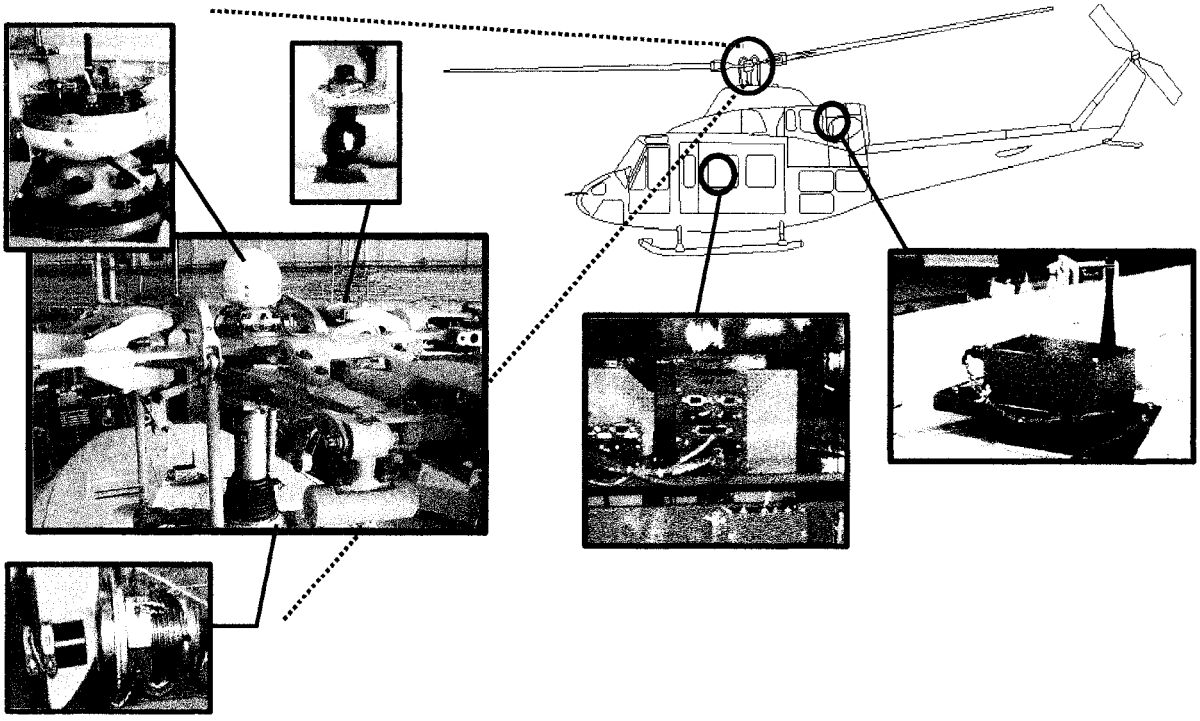

Figure 2.3 Bell 412 ASRA Rotor State Measurement Systems Integration

2.4 System Identification Methodology: Derivation of the Hybrid Model Structure

Hybrid Mathematical Model Structures (HMMS) specifically for incorporating rotor dynamics into mathematical models have been synthesized by several researchers. Typically, six degree of freedom (6DOF) rigid body models are used to describe helicopter dynamics in the low to mid frequency range (e.g. out to 10 rad/s for hingeless Bo105 and Bell 412 rotors) for pilot simulation, simulation validation, and handling qualities analyses. These formulations account for rotor dynamics by time delays and absorbing the steady state rotor flapping effects into the rigid body stability derivatives. Model fidelity must be compatible with the analytical application. In high bandwidth flight control applications such as inflight simulation, high frequency coupled rotor/body flap and lead-lag dynamics are necessary for tight command tracking, robustness to disturbances and variations in flight conditions, and precise/agile maneuver tracking. These high frequency dynamics occurring out to 30 rad/s (e.g. for hingeless Bo105 and Bell 412) are unattainable by 6DOF models. Hence, research into the development of hybrid formulations that append the rotor-fuselage flap and lead-lag dynamics to the rigid body structure are extensive. [1,95-97,99,100,102,103]

Two important contributions to HMMS development were extended equations of rotor dynamics and model structures with 8 or more degrees-of-freedom appending these rotor dynamics to the base 6DOF formulation. Talbot et al.[92] and Padfield et al.[94] developed extended equations (i.e.; 2 rotor degrees of freedom) of the rotor system. In the former case, a theoretical coupled body attitude-rate rotor-flapping model of a nonlinear, total force and moment model for single rotor helicopters was developed. In the latter case, a similar isolated model incorporating coupled rotor/inflow dynamics that was driven by rigid body attitude rates was developed. Many applications of HMMS having more than 8DOF emerged as researchers expanded their capability to model the coupled rotor-fuselage system as applied to flight control applications. Mullen[77] et al. utilized a hybrid 8DOF model of the DERA/Agusta-Westland experimental rotor rig to assess multi-variable control schemes. This structure was also used for rotor state feedback research. The rotor states were obtained both by state estimation and measurement. Kaletka et al. developed several forms of hybrid models (≥8DOF) for studying Bo105 coupled rotor/body dynamics for its model following inflight simulation capability. The rotor states were obtained both by state estimation (approximation of lead-lag dynamics) and measurement (blade flapping dynamics). Kaletka et al.[95-97] also investigated the application of the previously mentioned Talbot coupled rotor body model for their application. Hansen[98] developed hybrid model structures for the CH53A. The first model incorporated body acceleration, control rate, and coning and regressive flap dynamics. The second model incorporated tip path plane regressive flap dynamics. Hui[98,99] developed an 8DOF HMMS for the Bell 412 ASRA applying the Talbot and Chen[92,93] coupled rotor-body equations. Initially rotor state estimates were used to parameterize the model. In this study measured rotor state data obtained from the RSMS is applied in the system identification of the Bell 412 ASRA. Blackwell[101] developed a blade flapping and

inflow hybrid 8DOF model for the MK50 Sea-King helicopter. Tishler et al. developed several helicopter HMMS including a 9DOF for the Bo105[102,103], 10DOF for the SH-2G[104], and 12DOF for the S-92[105]. The S-92 model included coupled dynamics of the fuselage, flapping, coning, dynamic inflow, lead-lag, and engine degrees-of-freedom. In terms of lead-lag dynamics, Tischler applied a method by Fletcher to model the regressive lead-lag dynamics as a dipole filter on roll rate and pitch rate.

The system identification of HMMS requires the derivation of equations of motion describing the extended rotor dynamics of concern and of the chosen model structure. Linearized mathematical models may then be developed in 3 ways[106]:

i) Analytical or numerical linearization of non-linear equations of motion
ii) Application of parameter estimation techniques to time histories from non-linear mathematical simulation models
iii) Application of parameter estimation techniques to flight test data

2.5 Representation of Hingeless Rotor Dynamics of the Bell 412ASRA

From first principals, the RSMS was installed on the Bell 412 ASRA's soft inplane hingeless hub requiring compatible equations of kinematics and motion for the coupled rotor and fuselage in order to proceed with the mathematical model development. In the following section, three levels of representation illustrate characteristics of the rotor dynamics in flap and lead-lag degrees-of-freedom, however, as will be shown only Levels 2 and 3 were applied mainly due to limitations imposed by the current RSMS configuration.

2.5.1 Level 1: Accurate Representations of Rotor Physics[3,4,5,6,35]

The physical representations of the rotor flap and lag dynamics can be derived from a 6DOF ground – hover rigid blade aeromechanical stability model based on the perturbation flap and lag equations. The rotor blades are assumed to be rigid, have uniform mass density, and undergo flap and lag motion, about spring-restrained offset hinges. The blade root flap and lag stiffness, along with the hinge offsets determine the fundamental frequencies. The aerodynamic loads on the rotor blades are calculated using quasi-steady strip theory, assuming uniform inflow. The fuselage is assumed to undergo rigid body pitch and roll motion about its center of mass. The center of mass is located directly below the rotor hub by a distance, h. The fuselage physical properties required are pitch and roll inertia, stiffness, and damping.

The rotor-fuselage equations of motion are linearized about the equilibrium trim condition to obtain the perturbation equations. The perturbation flap and lag equations for the individual blades are transformed to the non-rotating coordinate system using Multiblade Coordinate Transforms (MCT). This transformation yields a collective, differential, and two cyclic equations in the non-rotating coordinate system for flap and lag motions. However, only the cyclic flap and lag equations need to be retained.

The collective and differential flap and lag equations do not couple with the fuselage motions and hence can be dropped from this aeromechanical stability analysis. The rotor fuselage model thus has 6 degrees-of-freedom encompassing cyclic flap, cyclic lag, fuselage roll, and fuselage pitch. In the non-rotating (or fuselage) frame the resulting constant coefficient system can be represented in the following form:

$$[M]\{\ddot{q}\}+[C]\{\dot{q}\}+[K]\{q\}=\{0\} \qquad 2.1$$

where; $[M]$, $[C]$, and $[K]$ are 6x6 Mass, Damping, and Stiffness matrices.

The eigenvalues of this constant coefficient system yield open-loop modal frequencies and decay rates. Complete model physics would constitute perturbation equations for blade flap and lag, body pitch and roll, aerodynamic moment, and aeromechanical stability computation.

2.5.1.1 Rotor Blade Flap Response

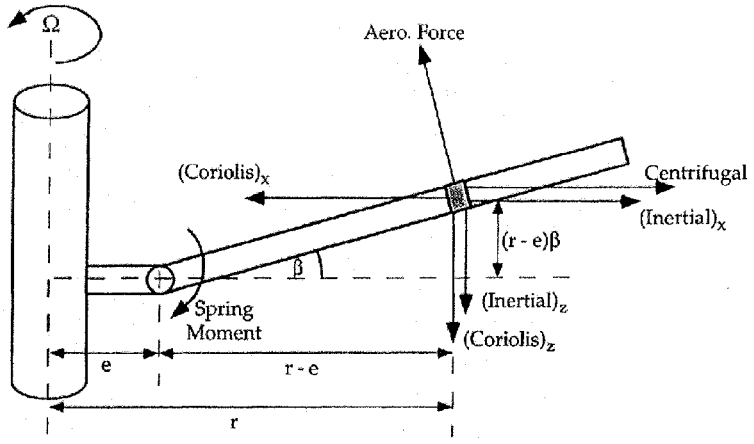

Figure 2.4 Force Resolution for Blade Flap Degree-of-Freedom[6]

Resolving along the radial and vertical directions in Figure 2.4, we can express the forces acting on a blade element that cause flapping as follows:

Force	Magnitude	Moment Arm
Centrifugal	$(mdr)\Omega^2 r$	$(r-e)\beta$
$(Coriolis)_x$	$2(mdr)\Omega(r-e)\dot{\zeta}$	$(r-e)\beta$
$(Coriolis)_z$	$2(mdr)(p\cos\psi+q\sin\psi)r\Omega$	$(r-e)$
$(Inertial)_x$	$(mdr)[h+(r-e)\beta](\dot{p}\sin\psi-\dot{q}\cos\psi)+(mdr)(r-e)\beta\ddot{\beta}$	$(r-e)\beta$
$(Inertial)_z$	$(mdr)r(\dot{p}\sin\psi-\dot{q}\cos\psi)+(mdr)(r-e)\ddot{\beta}$	$(r-e)$
Aerodynamic	$\delta F_\beta dr$	$(r-e)$
Spring	$K_\beta\beta$	

Table 2.1 Tabulation of Blade Element Forces, Flap Degree-of-Freedom

Taking moments about the flap hinge (flap-up, positive) we obtain:

$$0 = -\int_e^R (mdr)\Omega^2(r-e)\beta + \int_e^R 2(mdr)\Omega(r-e)^2\beta\dot{\zeta} - \int_e^R 2(mdr)(p\cos\psi + q\sin\psi)r(r-e)\Omega + \ldots$$
$$\ldots - \int_e^R (mdr)[h + (r-e)\beta](\dot{p}\sin\psi - \dot{q}\cos\psi)(r-e)\beta - \int_e^R (mdr)(r-e)^2\beta^2\ddot{\beta} - \int_e^R (mdr)r(r-e)(\dot{p}\sin\psi - \dot{q}\cos\psi) + \ldots \quad 2.2$$
$$\ldots - \int_e^R (mdr)(r-e)^2\ddot{\beta} + \int_e^R \delta F_\beta dr(r-e) - K_\beta\beta$$

Using definitions, $I_\beta = \int_e^R (mdr)(r-e)^2$ for the blade second moment of inertia, and $S_\beta = \int_e^R (mdr)(r-e)$ for the blade first moment of inertia, the perturbation equation can be written as:

$$I_\beta(1+\beta^2)\ddot{\beta} + I_\beta\Omega^2(1 + e\frac{S_\beta}{I_\beta} + \frac{K_\beta}{I_\beta\Omega^2})\beta - 2I_\beta\Omega\beta\dot{\zeta} + I_\beta(1 + h\beta\frac{S_\beta}{I_\beta} + e\frac{S_\beta}{I_\beta} + \beta^2)(\dot{p}\sin\psi - \dot{q}\cos\psi) + \ldots \quad 2.3$$
$$\ldots + 2I_\beta(1 + e\frac{S_\beta}{I_\beta})\Omega(p\cos\psi - q\sin\psi) = \int_e^R (r-e)\delta F_\beta dr$$

After linearization of this equation about a trim condition (e.g.; by Taylor's theorem for analytic functions[1]) and transformation to the non-rotating frame using a Multiblade Coordinate Transform[1] (MCT), the cyclic flap equations are presented in coupled form as:

$$\begin{bmatrix}\beta_{1c}'' \\ \beta_{1s}''\end{bmatrix} + 2\begin{bmatrix}\beta_{1s}' \\ -\beta_{1c}'\end{bmatrix} + (\nu_\beta{}^2 - 1)\begin{bmatrix}\beta_{1c} \\ \beta_{1s}\end{bmatrix} - 2\beta_0\begin{bmatrix}\zeta_{1c}' + \zeta_{1s} \\ \zeta_{1s}' - \zeta_{1c}\end{bmatrix} + (1 + \beta_0\bar{h}S_{\beta'} + \bar{e}S_{\beta'})\begin{bmatrix}-q'' \\ p''\end{bmatrix} + 2(1 + \bar{e}S_{\beta'})\begin{bmatrix}p' \\ q'\end{bmatrix} - \begin{bmatrix}\gamma\delta M_{\beta c}^{AERO} \\ \gamma\delta M_{\beta s}^{AERO}\end{bmatrix} = 0 \quad 2.4$$

where:

$$(\,)' = \Omega(\,);\quad (\,)'' = \Omega^2(\,) \quad 2.5$$

$$\bar{c} = \frac{e}{R-e},\ \bar{h} = \frac{h}{R-e};\qquad \text{Normalized Hinge Offset and Helicopter Center-of-Mass} \quad 2.6$$

$$S_{\beta'} = \frac{(R-e)S_\beta}{I_\beta};\qquad \text{Normalized Blade Stiffness} \quad 2.7$$

$$\nu_\beta{}^2 = 1 + \bar{e}S_{\beta'} + \frac{K_\beta}{I_\beta\Omega^2} + \frac{\gamma}{8}\tan\delta_3;\qquad \text{Non-Dimensional Rotating Frame Flapping Frequency} \quad 2.8$$

$$\gamma\delta M_\beta^{AERO} = \frac{1}{I_\beta\Omega^2}\int_e^R (r-e)\delta F_\beta dr;\qquad \text{Perturbation Aerodynamic Flap Moments} \quad 2.9$$

$$\gamma\delta M_{\beta c}^{AERO} = \frac{2}{N_b}\sum_{i=1}^{N_b}\gamma\delta M_{\beta i}^{AERO}\cos\psi_i\ ,\ \gamma\delta M_{\beta s}^{AERO} = \frac{2}{N_b}\sum_{i=1}^{N_b}\gamma\delta M_{\beta i}^{AERO}\sin\psi_i \quad 2.10$$

Blade flap or out-of-plane response occurs normal to the plane of rotor rotation. Beyond handling qualities, rotor flap response is associated with vibration characteristics, aeroelastic stability, and rotor performance. The fundamental rotating flap frequency is an important indicator of rotor performance,

flight stability, and dynamics. The flapping frequency for the Bell 412 ASRA may be estimated by a relationship incorporating the flap frequency ratio, hub stiffness, and the hinge offset such that;

$$\nu_\beta = \sqrt{1 + \frac{3}{2}\cdot\frac{e}{R} + \frac{K_\beta}{I_\beta \cdot \Omega^2}} \qquad 2.11$$

The flapping or first out-of-plane frequencies for the Bell 412ASRA and Bo105 are approximately (1.031/rev., 1.117/rev.), respectively. The flapping Equation 2.4 shows important characteristics of the helicopter rotor system. Firstly the perturbation aerodynamic flap moment requires knowledge of components of the velocity flow-field. Low order approximations are available for axis-symmetric (i.e.; hover/ground) conditions however these are not valid at high advance ratios. A notable component of the aerodynamic flap moment is its dependence on pitch-flap coupling and pitch-lag coupling stiffness parameters of the rotor system. Secondly, the Delta-3 (δ_3) term in the non-dimensional flap frequency equation for a hingeless rotor helicopter defines pitch-flap coupling for soft inplane hub configurations where the feather axis participates in flapping motion. This represents a form of kinematic rotor state feedback.

2.5.1.2 Rotor Blade Lead-Lag Response[3,4,5,6,35]

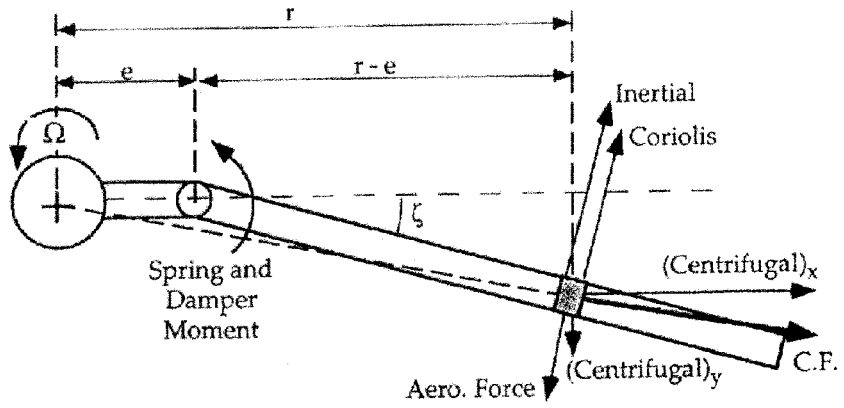

Figure 2.5 Force Resolution for Blade Lead-Lag Degree-of-Freedom[6]

Resolving along the radial and horizontal directions as shown in Figure 2.5, we can express the forces acting on a blade element that cause lead-lag as follows:

Force	Magnitude	Moment Arm
$(\text{Centrifugal})_x$	$(mdr)\Omega^2 r$	$(r-e)\zeta$
$(\text{Centrifugal})_y$	$(mdr)\Omega^2(r-e)\zeta$	$(r-e)$
Coriolis	$2(mdr)\Omega(r-e)\dot{\beta}\beta$	$(r-e)$
Inertial	$(mdr)[h+(r-e)\beta](\dot{p}\cos\psi-\dot{q}\sin\psi)+(mdr)(r-e)\ddot{\zeta}$	$(r-e)$
Aerodynamic	$\delta F_\zeta dr$	$(r-e)$
Spring	$K_\zeta\zeta$	
Lag Damper	$C_\zeta\zeta$	

Table 2.2 Tabulation of Blade Element Forces, Lead-Lag Degree-of-Freedom

Taking moments about the lead-lag hinge (lag back, positive) we obtain:

$$\begin{aligned}0=&-\int_e^R(mdr)\Omega^2 r(r-e)\zeta+\int_e^R(mdr)\Omega^2(r-e)^2\zeta-\int_e^R 2(mdr)\Omega(r-e)^2\beta\dot{\beta}+\ldots\\&\ldots-\int_e^R(mdr)[h+(r-e)\beta](\dot{p}\cos\psi-\dot{q}\sin\psi)(r-e)-\int_e^R(mdr)(r-e)^2\ddot{\zeta}+\ldots\\&\ldots-\int_e^R(mdr)(r-e)^2\ddot{\zeta}+\int_e^R\delta F_\zeta dr(r-e)-K_\zeta\zeta-C_\zeta\dot{\zeta}\end{aligned}\qquad 2.12$$

Using definitions for the blade second moment of inertia, I_β, and for the blade first moment of inertia, S_β, the perturbation equation can be written as:

$$I_\beta\ddot{\zeta}+C_\zeta\dot{\zeta}+I_\beta\Omega^2\left(e\frac{S_\beta}{I_\beta}+\frac{K_\zeta}{I_\beta\Omega^2}\right)\zeta+2I_\beta\Omega\beta\dot{\beta}+I_\beta\left(h\frac{S_\beta}{I_\beta}+\beta\right)(\dot{p}\cos\psi-\dot{q}\sin\psi)=\int_e^R(r-e)\delta F_\zeta dr \qquad 2.13$$

After linearization of this equation about a trim condition and transformation to the non-rotating frame using a Multiblade Coordinate Transform (MCT), the cyclic lag equations are presented in coupled form as:

$$\begin{bmatrix}\zeta_{1c}''\\ \zeta_{1s}''\end{bmatrix}+2\begin{bmatrix}\zeta_{1s}''\\ -\zeta_{1c}''\end{bmatrix}+(\nu_\zeta^2-1)\begin{bmatrix}\zeta_{1c}\\ \zeta_{1s}\end{bmatrix}-gl\begin{bmatrix}\zeta_{1c}'+\zeta_{1s}\\ \zeta_{1s}'-\zeta_{1c}\end{bmatrix}+2\beta_0\begin{bmatrix}\beta_{1c}'+\beta_{1s}\\ \beta_{1s}'-\beta_{1c}\end{bmatrix}+(\bar{h}S_{\beta'}+\beta_0)\begin{bmatrix}p''\\ q''\end{bmatrix}-\begin{bmatrix}\gamma\delta M_{\zeta c}^{AERO}\\ \gamma\delta M_{\zeta s}^{AERO}\end{bmatrix}=0 \qquad 2.14$$

Additional definitions:

$$(\,)'=\Omega(\,);\quad(\,)''=\Omega^2(\,) \qquad 2.15$$

$$gl=\frac{C_\zeta}{I_\beta\Omega}; \qquad \text{Lag Damping Geometry} \qquad 2.16$$

$$\nu_\zeta^2=\bar{e}S_{\beta'}+\frac{K_\zeta}{I_\beta\Omega^2}; \qquad \text{Non-Dimensional Rotating Frame Lagging Frequency} \qquad 2.17$$

$$\gamma\delta M_\zeta^{AERO}=\frac{1}{I_\beta\Omega^2}\int_e^R(r-e)\delta F_\zeta dr; \qquad \text{Perturbation Aerodynamic Lag Moments} \qquad 2.18$$

$$\gamma\delta M_{\zeta c}^{AERO}=\frac{2}{N_b}\sum_{i=1}^{N_b}\gamma\delta M_{\zeta i}^{AERO}\cos\psi_i\ ,\quad \gamma\delta M_{\zeta s}^{AERO}=\frac{2}{N_b}\sum_{i=1}^{N_b}\gamma\delta M_{\zeta i}^{AERO}\sin\psi_i \qquad 2.19$$

This aeromechanical analysis highlights several important characteristics of the helicopter coupled rotor/fuselage response. The lead-lag dynamics of hingeless rotor helicopter is affected by the lead-lag flexural kinematics; parameters include damping, C_ζ and stiffness, K_ζ. In the Bell 412ASRA, the lead-lag mode will be significantly damped due to the use of elastomeric dampers while in case of the Bo105 for instance no dampers are used (i.e.; blade/hub flexibilities define this damping). Referring to Figure 1.10 note then that the Bo105 has only 3% lag damping. The lead-lag or first in-plane frequencies of the Bell 412 ASRA and the Bo105 are (0.65/rev., 0.73/rev.), respectively. Without accurate knowledge of the damper characteristics the lag damping of the Bell 412 ASRA cannot be computed over its operational flight envelop (OFE). Data from Chopra[6] (Figures 1.10 and 2.6) suggest that the regressing lag mode natural frequency of the Bell 412 ASRA lies at 12.34 rad./sec. The value of 14.7 rad./sec. for the Bo105 in Figure 1.10 is off that in Figure 2.6 by some 19%. The flap regressive mode frequency of 10.45 rad/sec. for the Bell 412 ASRA (Figure 1.10) matches well with Chopra's data with only some 1.44% deviation.

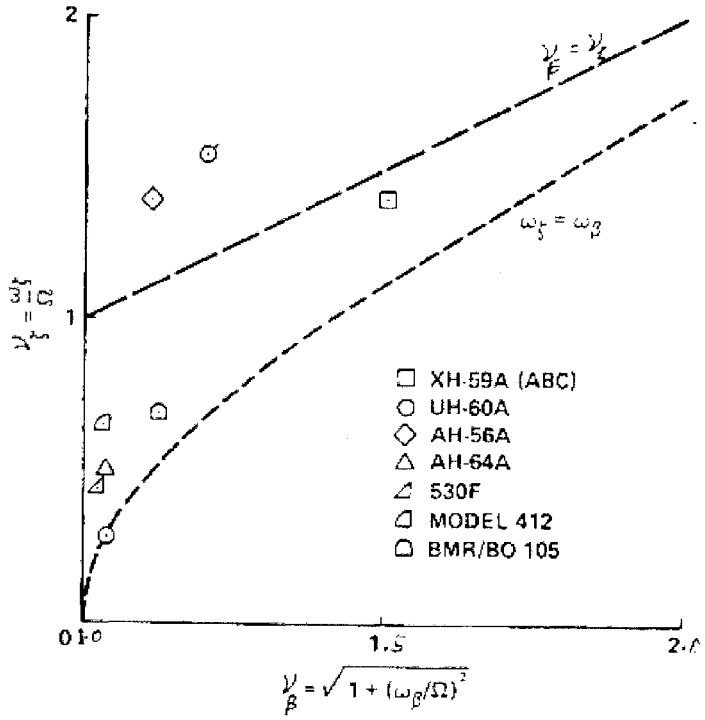

Figure 2.6 Rotor Dimensionless Frequencies for Several Helicopters[6]

Further, in the present study there is a lack of detailed information on lead-lag dynamics and their structural/damper design, blade root flap and lag stiffness, aerodynamic loading and inflow, and defined vehicle attitude pitch and roll inertia, stiffness, and damping. This data is proprietary to Bell Helicopter Textron and approximations of it mean that results would be unreliable for prediction of a safe-flight envelope for the Bell 412 ASRA under feedback control. It is then evident that a reduced order linearization of the coupled rotor-fuselage system is required.

2.5.2 Level 2: Approximate Coupled Rotor Flap Response

A hybrid model structure was selected and evaluated for this application. The frequency range of validity required would include a linearization model capable of representing classical attitude response modes (short period, Dutch roll, phugoid, spiral) and coupled body/rotor regressive flap dynamics. Control and actuator data was available for modeling. Lead-lag dynamics and inflow would have to be approximated or inferred since the Bell 412 measurement systems could not provide this data. The hybrid model was also required to have fidelity in rotor state measurement and flight control applications of soft-inplane hingeless rotor dynamics. This also implied a range of fidelity for flight control where research by Tischler[102] suggests soft inplane hingeless rotor models (such as that of the Bell 412 ASRA) should be accurate out to 20 rad/s with dynamic modes valid by 0.3 to 3 times crossover frequency. Hence, the HMMS would be developed by explicitly incorporating the differential equations for coupled rotor-body dynamics. Research by Chen and Talbot et al. allowed for the development of a linearized representation of the related rotor flap to body attitude-rate dynamics[92,93]. Specifically a coupled equation for rotor flap and body pitch and roll rate dynamics that has been widely used in the desired contexts mentioned. This equation is given by;

$$\begin{bmatrix}\ddot{a}_1\\ \ddot{b}_1\end{bmatrix}+\Omega\begin{bmatrix}\frac{\gamma}{8} & 2\\ -2 & \frac{\gamma}{8}\end{bmatrix}\begin{bmatrix}\dot{a}_1\\ \dot{b}_1\end{bmatrix}+\Omega^2\begin{bmatrix}0 & \frac{\gamma}{8}\\ -\frac{\gamma}{8} & 0\end{bmatrix}\begin{bmatrix}a_1\\ b_1\end{bmatrix}-\Omega^2\begin{bmatrix}\frac{\gamma}{8}A_1-2\frac{p}{\Omega}-\frac{\gamma}{8}\frac{q}{\Omega}\\ \frac{\gamma}{8}B_1-2\frac{q}{\Omega}-\frac{\gamma}{8}\frac{p}{\Omega}\end{bmatrix}=0 \qquad 2.20$$

Research by Kaletka and Hui confirmed the applicability of this representation for flapping dynamics of the soft-inplane hingeless Bo-105 and Bell 412 helicopters, respectively. Lead-lag dynamics, higher order aerodynamics such as inflow, and engine dynamics are neglected. However, Tischler, Kaletka, and Hui attempted to model lead-lag dynamics by dipole representation with limited fidelity overall.[95-97,100,102,103] The fundamental modeling of rotor flap dynamics was critical to the installation of the RSMS as well as in the application of rotor state data compatibly in this particular hybrid model. The modeling of rigid blade offset hinge flap dynamics is derived next.

2.5.3 Level 3: Rigid Blade Offset Hinge Model[3,4,5]

To assist in the prediction of flap dynamics a simple rigid flapping model was useful. This was especially so in the installation of the RSMS and estimation of rotor parameters such as spring stiffness and flap frequencies. The blade is assumed rigid and hinged at a distance, e, from the rotation axis. It is also assumed that there is a flap bending spring at the hinge. This configuration represents the dynamics of an articulated blade with hinge offset as well as an approximation of hingeless rotor dynamics. In the case of the hingeless rotor, the model captures those dynamics associated with the fundamental flap mode shape and frequency.

Referring to Figure 2.4, resolving along the radial and vertical directions, we can express the forces acting on a blade element that cause flapping as follows:

Force	Magnitude	Moment Arm
Inertial	$(mdr)(r-e)\ddot{\beta}$	$(r-e)$
Centrifugal	$2(mdr)\Omega(r-e)\dot{\zeta}$	$(r-e)\beta$
Aerodynamic	$F_z dr$	$(r-e)$
Spring	$K_\beta(\beta-\beta_P)$	

Table 2.3 Tabulation of Blade Element Forces, Flap Degree-of-Freedom - Rigid Blade Offset Hinge

Here note that β_P, the precone angle is introduced by the hinge-spring in the absence of external forces. Taking moments about the flap hinge (flap-up, positive) we obtain:

$$0=\int_e^R m(r-e)^2 dr\ddot{\beta}+\int_e^R m\Omega^2(r-e)dr\beta-\int_e^R F_z(r-e)dr+K_\beta(\beta-\beta_P) \qquad 2.21$$

The flap equation may be written as;

$$I_\beta\left\{\ddot{\beta}+\Omega^2\left(1+\frac{e\int_e^R m(r-e)dr}{I_\beta}\right)\beta+\frac{K_\beta}{I_\beta}(\beta-\beta_P)\right\}=\int_e^R F_z(r-e)dr \qquad 2.22$$

Written in non-dimensional terms (dividing by $I_b\Omega^2$);

$$I_{\beta'}(\beta''+\nu^2\beta)=\frac{K_\beta}{I_b}\frac{1}{\Omega^2}\beta_P+\gamma\overline{M}_\beta \qquad 2.23$$

where, ν_β is the non-dimensional flap frequency given by: $\nu_\beta=1+\dfrac{e\int_e^R m(r-e)dr}{I_\beta}+\dfrac{K_\beta}{I_\beta\Omega^2}$ 2.24

The second term is simplified by the uniform blade simplification, $\dfrac{e\int_e^R m(r-e)dr}{I_\beta}\cong\dfrac{3c}{2(R-e)}$ 2.25

The third term, non-rotating natural frequency, is made dimensionless using rotational frequency, such that; $\dfrac{K_\beta}{I_\beta}=\omega_o^{\,2}$ 2.26

The flap equation is re-written (assume $I_{\beta'}=\dfrac{I_\beta}{I_b}$ is unity) to give;

$$\beta''+\nu_\beta^{\,2}\beta=\frac{\omega_o^{\,2}}{\Omega^2}\beta_P+\gamma\overline{M}_\beta \qquad 2.27$$

2.6 Model Structure Selection and Kinematic Compatibility of the Integrated RSMS

The methodology for developing hybrid mathematical model for the hingeless rotor helicopter is discussed next. These HMMS augment the 6DOF rigid body structure with rotor states and other higher order dynamics. For this research the model structure selected is shown in Figure 2.7 below.

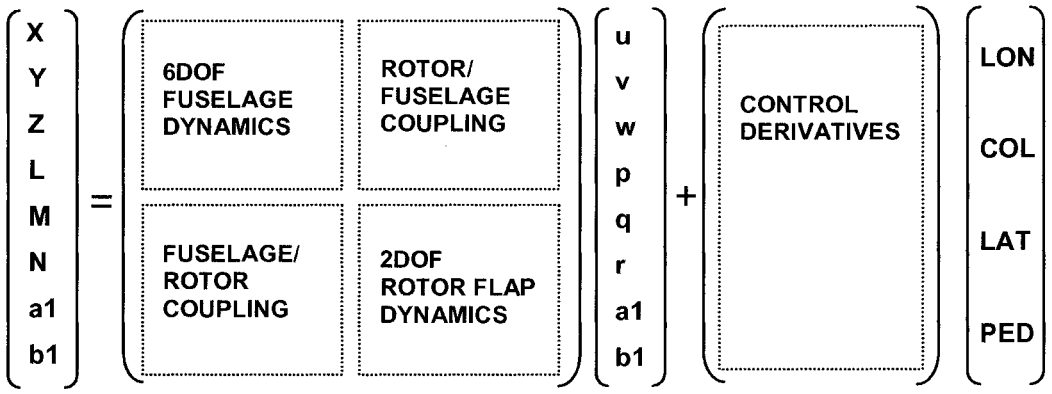

Figure 2.7 Model Structure – Augmented Rotor Yoke Flap Dynamics

In order to apply the Level 2 model differential equation to the parameter identification algorithm, several processing steps were performed. These were required to apply the rotor state measurements compatibly with the differential system.

2.6.1 Elimination of Terms

For computation, a first order representation is developed by neglecting the flapping accelerations terms of the coupled rotor-body equation (Equation 2.20) that do not significantly impact model fidelity in the frequency range of handling qualities. The first order representation is then given by:

$$\begin{bmatrix}\dot{a}_1\\ \dot{b}_1\end{bmatrix}+\frac{\Omega}{\frac{\gamma^2}{64}+4}\begin{bmatrix}\frac{\gamma}{4} & \frac{\gamma^2}{64}\\ -\frac{\gamma^2}{64} & \frac{\gamma}{4}\end{bmatrix}\begin{bmatrix}a_1\\ b_1\end{bmatrix}-\frac{\Omega}{\frac{\gamma^2}{64}+4}\begin{bmatrix}\frac{\gamma^2}{64}A_1-\frac{\gamma}{4}B_1\\ \frac{\gamma}{4}A_1+\frac{\gamma^2}{64}B_1\end{bmatrix}+\begin{bmatrix}q\\ p\end{bmatrix}=0 \qquad 2.28$$

This assumption was validated by previous research applied in context of hingeless rotor state measurement application of the Bell 412 ASRA helicopter. Hui[99,100] demonstrated that flapping accelerations do not have significant effects in flight dynamics modeling out to 20 rad/s. Similar finding were illustrated by Kaletka et al. and Von Grunhagen et al. in Bo105 applications[74]. Referring back to Equation 2.4 for Level 1 modeling of the coupled rotor-body system, note that that the pitch-roll term coupling is critical and cannot be dropped, as might be the case for Equations 2.20 and 2.28.

2.6.2 Data Fitting

In order to parameterize this differential equation, point profiles and simulations were performed to identify coefficients to fit flight test data. The point profiles served as a means of rapid verification of the relationship between rotor longitudinal disc tilt, control input, and vehicle attitude-rate. The differential equations are separated into their longitudinal and lateral components as follows:

$$\dot{a}_1 + K_{a_1} a_1 - K_{A_1} A_1 + q = 0$$
$$\dot{b}_1 + K_{b_1} b_1 - K_{B_1} B_1 + p = 0 \qquad 2.29$$

Theoretical flap dynamics analyses by Bramwell et al.[4] predict by rigid hinge offset modeling the coning, longitudinal, and lateral disc tilt as given by;

$$a_0 = \frac{\gamma}{8}\left[\theta_0(1+\mu^2) + \frac{4}{3}\lambda\right] \qquad 2.30$$

$$a_1 = \frac{2\mu(4\theta_0/3 + \lambda)}{1-\mu^2/2} \qquad 2.31$$

$$b_1 = \frac{4(\mu a_0 + 1.1\nu^{0.5}\lambda_i)/3}{1+\mu^2/2} \qquad 2.32$$

Based on some developmental RSMS flight test data as shown in Figure 2.8, point calculations for u=60knots at μ=0.129 show that:

- The coupled body-flap differential equation for longitudinal disc tilt under-predicted the Bell 412 ASRA attitude-pitch rate by some 15% (prior assumptions and neglecting trim condition).
- The theoretical longitudinal disc tilt was over-predicted by some 40% (neglecting inflow, and trim condition).

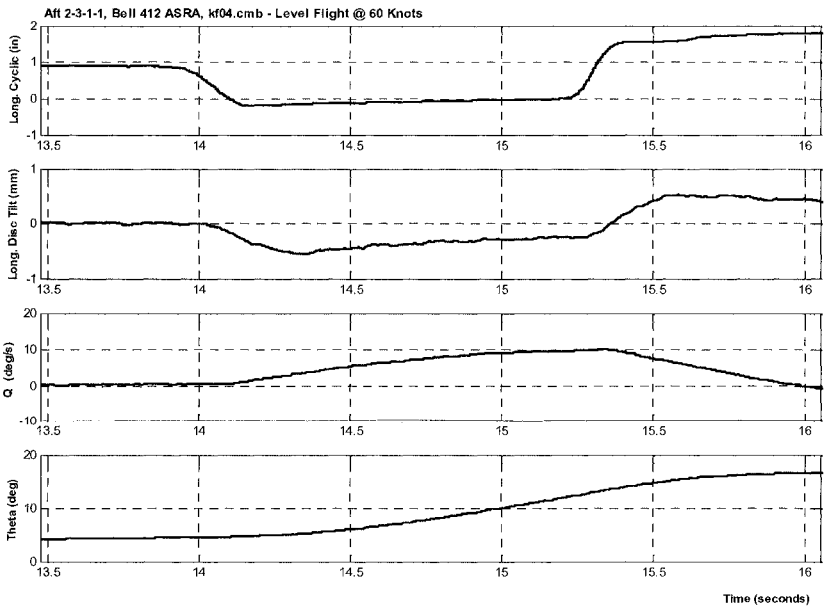

Figure 2.8 Bell 412 ASRA FSMS/RSMS Flight Test Data – Aft 2-3-1-1, 60 Knots, Level Flight

2.6.3 Frequency Range of Validity

The flapping displacement of the yoke measured by the RSMS was assumed linearly related to the rotor blade flap angle based on a rigid blade offset hinge model. Presented as the Level 3 rigid-blade offset hinge model of rotor flap dynamics (Section 2.5.3), this representation of the correlation between rotor yoke flap and rotor blade flap motion is a standard approximation of articulated and hingeless rotor dynamics. The frequency range of validity of this assumption extends to the first flap mode, which is the measurement capability of the RSMS.

2.6.4 Predicted Model Accuracy

An accounting of neglected dynamics, assumptions, and procedures was tabulated as shown in Table 2.4 to overview the contributors to HMMS fidelity with helicopter physics. A ranking of 1 to 5 was imposed where 5 represented the domain most penalizing to this acquired fidelity. This was a crucial step in the overall research project in order to put into perspective the limitations/fidelity of the mathematical model, the impacts on the flight control design process, and the boundary conditions for safe flight testing. Based on the combined assumptions of the RSMS capability and the tabulation:

The Bell 412 ASRA Hybrid Mathematical Model Structure (HMMS) will have inaccuracies that must be accounted for as model uncertainty in the flight control law design process. Various accumulating effects include neglected dynamics, linear assumptions in rigid offset hinge modeling, single point sensing band-limiting rotor mode fidelity, and the lack of higher order dynamics (lead-lag, engine, airmass) which make the rotor state analysis aeroservoelastically compatible. It is thus purported that the model will show poor robustness to off-design flight conditions showing sensitivity to such factors as parameter variation and model structure.

Due to the lack of lead-lag monitoring the author suggests:

An incremental gain approach will be required for safe ground and flight-testing. On this point it is critical to point out that the rotor state feedback system not be engaged with skids on the ground to eliminate the posibility of ground resonance, that actuator monitoring thresholds be tightened within the 200% FBW disengage limits to mitigate against oscillatory behaviors that could be damaging to the vehicle in flight trials, and that restrictions placed on pilot input excitation to levels below 3 Hz as gains are incrementally advanced through their design ranges.[110,111]

Assumptions (A) Neglected Dynamics (ND) Procedure (P)	Impact	Rank
(A) RSMS Measurement Capability: captures pure on-axis rotor hub yoke response (ND/A) RSMS Measurement Limitations: 1st order (1st flap bending mode) rotor response, rotor yoke dynamics correlate to rotor blade dynamics	The RSMS captures gross motion and low frequency behavior of the rotor system. Single-point sensing restricts modal sensing to first-order fundamental flap dynamics. Rotor hub dynamics are out of phase with blade dynamics.[1,58,95,97,103]	5
(ND) Airmass Dynamics – Inflow, Wake	Airmass dynamics are critical in obtaining aeroelastic compatibility in analyses. Lack of these dynamics reduces fidelities such as coupled rotor/body off-axis response and rotor vertical acceleration responses.[9,12,88]	3
(ND) Engine Dynamics	Engine dynamics couple with the airframe to modify aeromechanical, control, and flight dynamics. In a rotor state feedback investigation, then penalties for not modeling propulsion system effects rate as moderately penalizing. This issue might depend on flight test investigations evaluating oscillatory engine-torque and/or collective input response that could couple with lead-lag dynamics to create resonance.[52]	+/-3
(ND) Rotor Dynamics - Lead-Lag, Torsion	Higher order rotor dynamics, especially lead-lag dynamics are critical to aeromechanical stability and resonance. Without these dynamics the stability margins for resonance based on vehicle configuration, damping, and feedback control may only be estimated.[58,93,95,97,103]	5
(A/ND) Coupled Rotor/Body Equation: derived for hovering flight but appropriate for forward flight, acceleration terms may be dropped	Chen's coupled rotor/body equation has been validated by Kaletka, Hui, and Tischler in identification of hingeless rotor helicopters (>8DOF) from hover out to some 120knots. The original report in 1980, suggests the flapping equation is limited to advance ratios of 0.3.[58,93,95,97,103] For the Bell 412ASRA: R=23ft, RPM=33.93 rad./sec. $\mu = 0.3 = \frac{v_{LIMIT}}{(33.93)(23)}$; v_{LIMIT} = 234.12 ft/sec. (138.71 knots). Further, the rotor flap dynamics at high flight speeds are damped; the flap activity is much higher for the Bell 412 at hover/low-speed. The authors above have also validated neglecting the acceleration terms without excess penalty.	3
(A) Single Point Model: Parameter Estimation of a single 60 knot design point for flight control law development is sufficient representation	The helicopter's dynamics vary as a function of vehicle configuration, aerodynamic properties, and flight dynamics (maneuvers, speed, etc.). A multivariable control law can deal with a certain percentage of uncertainty; here uncertainties are high (rotor state physics, digitization/implementation, off-design flight conditions...)[73]	3
(A) Acceleration Data Filtering: will not influence model structure or fidelity	Acceleration filtering should not be a problem. Digital 4 Hz cutoff Butterworth filter (no added time delay) selected; no removal of helicopter high working bandwidth frequencies (rotor blade harmonics). Filtering techniques with zero phase shift critical. Identification process sensitive to phase errors.[90]	3
(P) Parameter Estimation: Time Domain (a priori data, low frequency weighting, etc.) vs. Frequency Domain (no a priori data, low frequency/steady-state fidelity)	**Time Domain** parameter estimation weights helicopter dynamics on low frequency response, thus transfer function models show poor coherence. "A priori" physics are problematic here since the RSMS installations are uncorrelated and identification process (rotor states) is new to the NRC-FRL. (i.e.; non-linearities and sensor/structure compatibility etc. are unknowns). In the **Frequency Domain**, parameter identification is accurate from mid to high frequencies that are more important to complex coupled/controlled/piloted rotor-body physics.[89,91]	+/-3
Comment: Experience/ System Identification/ Flight Control Law Design	Hui is a time domain specialist while Tischler is a frequency domain specialist. Both are renowned for their mathematical modeling of rotorcraft. Both have myriads of identifications of rotorcraft. Decisions along this research project influence: model accuracy, control law effectiveness, feedback stability margins, and flight safety.	5

Table 2.4 Tabulation of Assumptions, Neglected Dynamics, and Procedures Influencing Convergence and Fidelity of the Final HMMS Parameterization

2.7 Parameter Estimation Methodology: Quantification of Stability and Control Derivatives

The parameter estimation problem herein begins by assuming that the rotorcraft dynamics of concern can be modeled by a set of dynamic equations containing unknown parameters. Through a flight test based on a calibrated sensor suite and control input profile, the vehicle is excited in the frequency range of concern. The values of the unknown parameters are then inferred from the requirement that the model prediction should match actual response. Measurement errors, low fidelity representation of dynamics and non-linearities, and state or process noise, complicate the identification process.

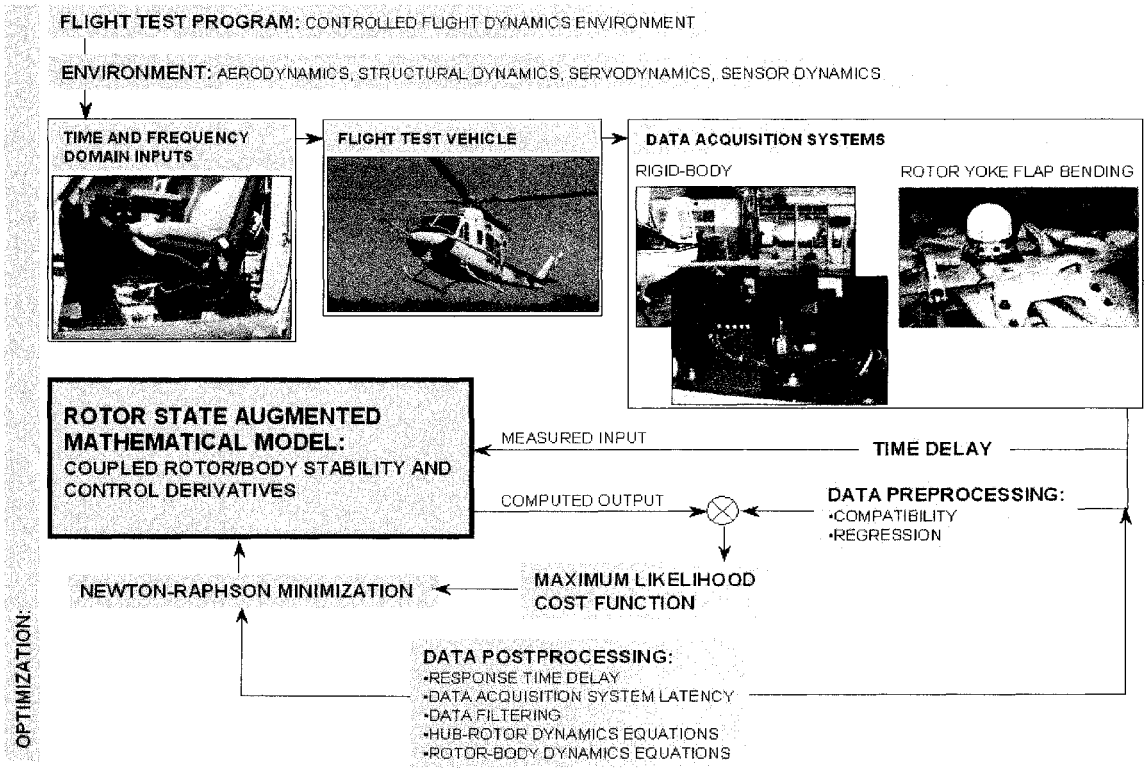

Figure 2.9 Parameter Estimation Procedure for Coupled Rotor/Body Dynamics

The particular algorithm for identification of the HMMS in this study is the NRC-FRL modified version of NASA's Maximum Likelihood Estimation (MMLE3)[89] code for time domain parameter estimation. The MMLE3 procedure has been applied to many NRC-FRL projects in both fixed and rotary wing applications. The particular framework for this project is illustrated in Figure 2.9.

In overview, the MMLE3 routine is used in the calculation of helicopter stability and control derivatives, ξ, based on flight test data, z_{fd}, by maximizing the probable values of ξ given z_{fd}, or of the likelihood ratio, $p(\xi / z_{fd})$. The MMLE3 objective is cast in state and observer form with an optimization driven by a cost function, $J(\xi)$. This cost function is based on the vehicle response and state non-linearity, which in

this case, involves both the well-understood rigid body dynamics, and previously unidentified rotor state measurements from a largely uncommissoned rotor state measurement system. To obtain convergence, this optimization involves the Newton-Raphson method requiring starting estimates close enough to the minimal error solution values. Also known as *a priori* derivatives, these estimates were chosen to be a set of validated derivatives and conditions from previous Bell 412 ASRA identifications. The iterative procedure for MMLE3 was done off-line in order that the model structure, data, rotor state equation coefficients, and resulting response is validated as shown in Figure 2.10.

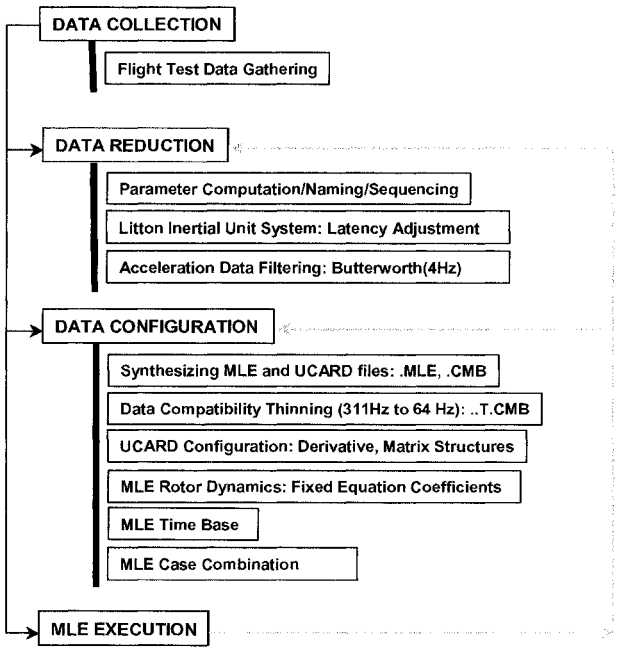

Figure 2.10 MMLE-Based Validation Procedure

Convergence accuracy, correlation, and validity of the HMMS may be evaluated by metrics such as Cramer-Rao Bounds (C-RB). These bounds estimate the minimum achievable standard deviation in the converged parameters and reflect high parameter insensitivity and/or parameter correlation. The parameters with the largest C-RB have the poorest relative confidence. A commonly used threshold in system identification research is to set $C\text{-}RB_i < 20\%$.[103]

The MMLE procedure was computationally intensive requiring some 4 software environments. The parameter estimation computations were performed in Visual Fortran. Matlab/Simulink provided an environment for model response and control analyses. The NRC-FRL standard flight-test data analysis code, Playback, was used for primary desktop data interpretation while Ghostview allowed the response trajectories to be printed out in standard format for comparative study.

Major tasks in the MMLE process are described in the discussion that follows.

2.7.1 Data Collection: Data Gathering Flight Test

The primary flight test for data gathering occurred on March 27, 2003 on the Bell 412 ASRA (C-FPGV); sortie (A033343). The main objectives of the flight were:

1. To develop an accurate, forward flight mathematical model
2. To validate the model with respect to previous flight test results as well as against the current NRC-FRL rotor state estimated models
3. To validate the RSMS installation and recent architecture optimizations

Performed in smooth air conditions, the target speed and altitude was 60 knots and 2500 feet respectively. The Bell 412 ASRA was configured for dual engine operation, SAS off, and heater off; the takeoff weight was 10045.7 lbs. The test maneuvers consisted of ground calibrations and ground points for capturing steady state flight control computer (FCC), FSMS and RSMS, and piloted/manual cyclic control reference outputs. Time domain tests by piloted/manual 2-3-1-1 pulses and step inputs were executed for on-axis excitation. Frequency domain tests by piloted/manual frequency sweeps were executed for on-axis excitation over 0.1 to 3 Hz (0.63 to 18.84 rad./sec.). The project manager of the Bell 412 ASRA, Gubbels, acted as flight engineer for monitoring and critiquing of the flight test while the author acted as support engineer for recording and call out of test points. The pilot for this particular flight was NRC-FRL research pilot Erdos. The flight data downloaded from the aircraft included some 80 parameters with digital samplings of 64 Hz for rigid body and 311 Hz for rotor states data sets.

As step inputs do not contain the frequency content necessary to identify coupled rotor/body response of the hingeless rotor and high bandwidth actuator system, frequency sweeps were applied for the identification flight-testing. Not only is the correct frequency content required but also the purity of on-axis excitation. Pilots have the tendency to couple the desired on-axis frequency sweep and off-axis stabilization control inputs. This correlation can decrease the identification accuracy. Frequency sweep data from this flight test in the time and frequency domain are depicted in Figures 2.11 to 2.16.

The spectral analyses shown in Figures 2.13 to 2.16 are in bode form using a Hanning window type for a data sample rate of 311 samples/sec. The frequency range of concern is 1 to 30 rad./sec. using 200 windows of 8192-point window length and data smoothing set at 100 points per decade.

In Figures 2.11 and 2.12 there is some partial off-axis correlation along with the presence of digital signal noise. In the longitudinal sweep, the dominant longitudinal input occurs at 10% cyclic, 5% lateral, and 3% pedal throws. The lateral sweep shows 9% dominant lateral cyclic, and both 4% for longitudinal cyclic and pedal throws. The collective control appears digitally noisy since this control was not displaced; this noise is of very low magnitude. The vehicle responses appear symmetric longitudinally and laterally.

In Figures 2.13 to 2.16 the frequency content of the flight test appears on target for both the safety of the aircraft and the required spectral content for identification. The data shows several characteristic features

of the soft inplane hingeless rotor system and it's physics during flight. The coherence extends out to the 20 rad./sec. range; the rotor flap regressive modes are expected to be in the 10-15 rad./sec. band. The dips in coherences depicted are present due to several factors. Firstly, very high trim excursions occurred in the frequency sweep testing of the powerful hingeless rotor system. Secondly, as mentioned, was the presence of related control axis correlations. And thirdly, was the presence of nonlinearities such as output noise that during high frequency control decreases coherence at high frequency bounds. Other dips in the coherences indicate the various modes of the vehicle: spiral, pitch and roll subsidence, Dutch roll, and phugoid. There is high correlation between coupled attitude-roll rate and rotor-lateral disc tilt. This is indicative of a high effective roll-damping derivative, Lp, and high response derivative couplings in pitch (|Mp/Mq|, |Mp/Lp|) and roll (|Lq/Lp|, |Lq/Mq|). Only the rotor flap regressive mode is present as lead-lag measurements were not available for this particular flight. The lead-lag dynamics should be well damped as the Bell 412 ASRA has lead-lag dampers.[102,103]

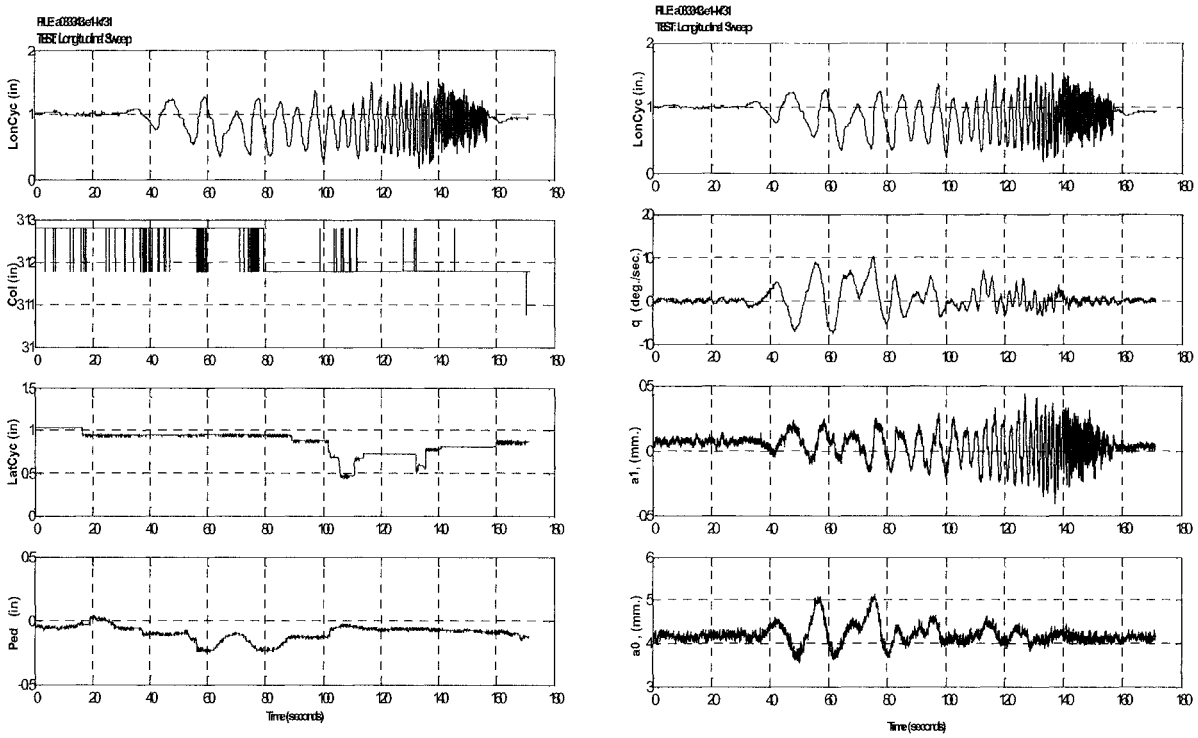

Figure 2.11 Time Histories of Longitudinal Cyclic Sweep: Off-Axis Control, Primary-Response

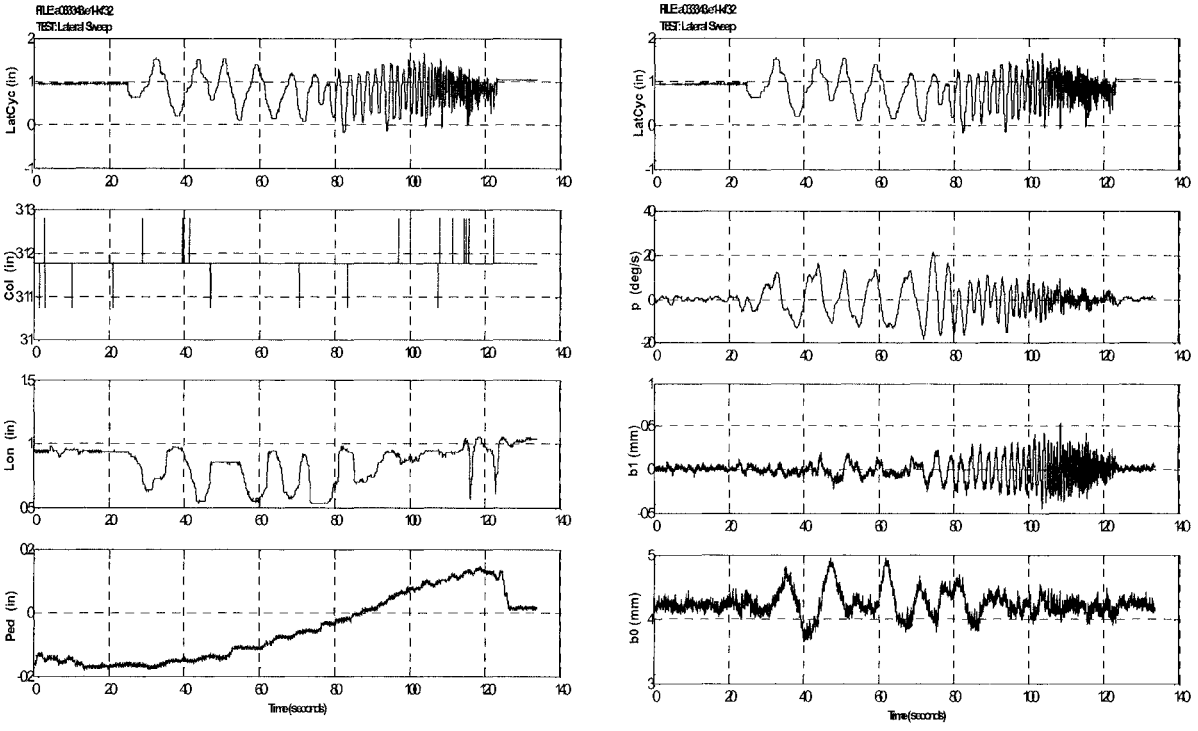

Figure 2.12 Time Histories of Lateral Cyclic Sweep: Off-Axis Control, Primary-Axis Response

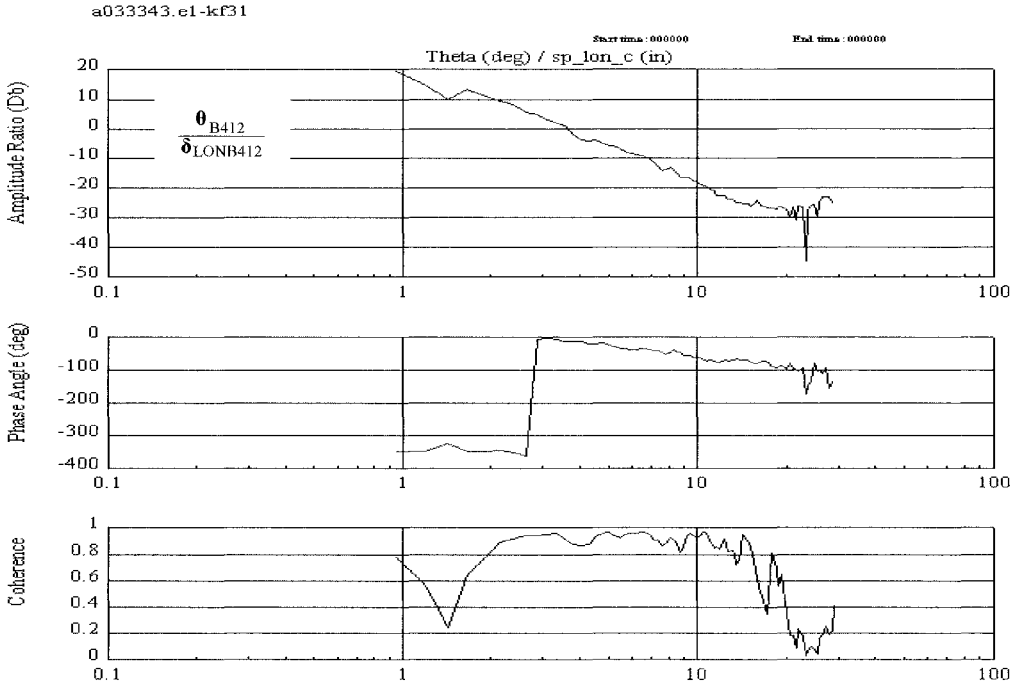

Figure 2.13 Frequency Response Identification – Longitudinal Axis Rigid Body Response

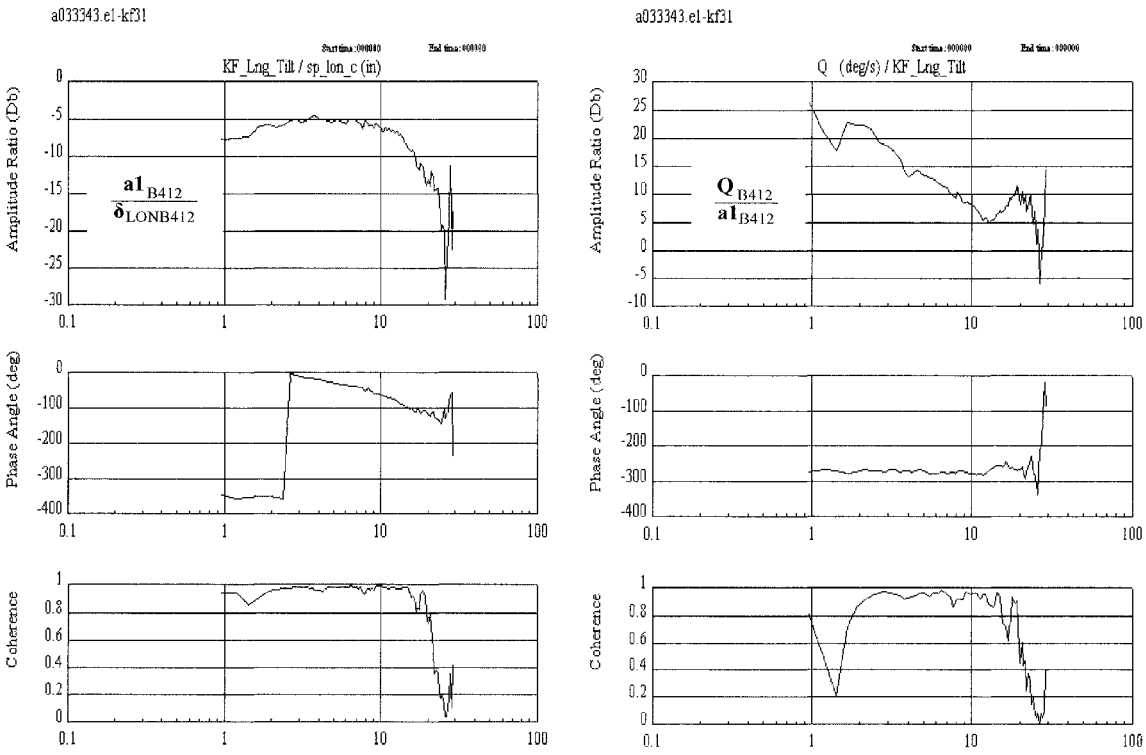

Figure 2.14 Frequency Response Identification – Longitudinal Axis Rotor Disc Tilt Response

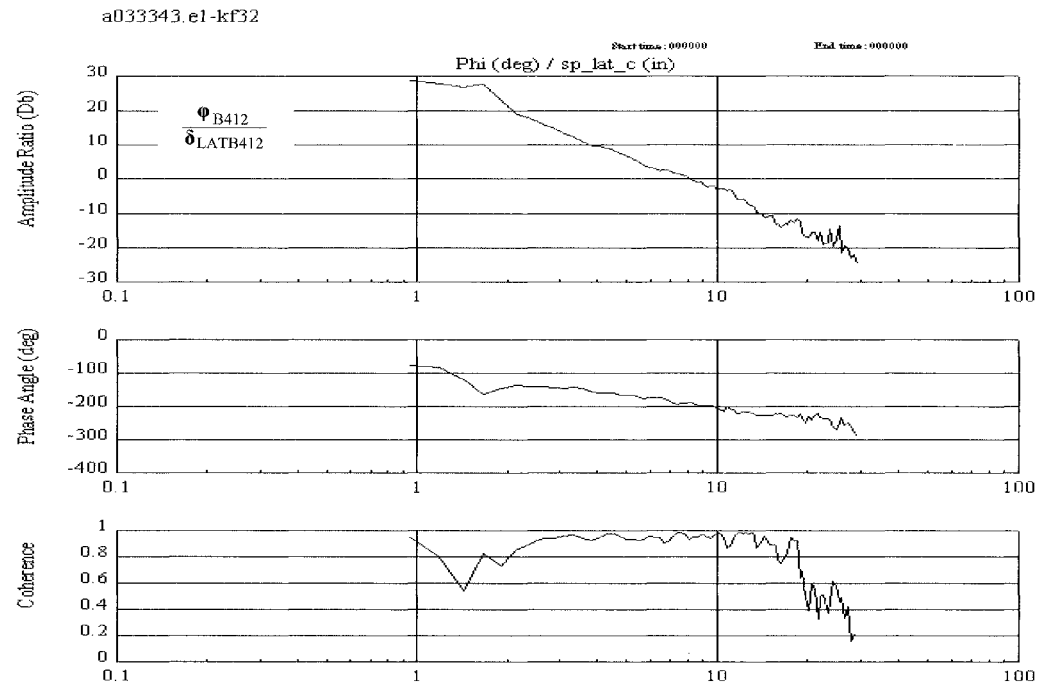

Figure 2.15 Frequency Response Identification – Lateral Axis Rigid Body Response

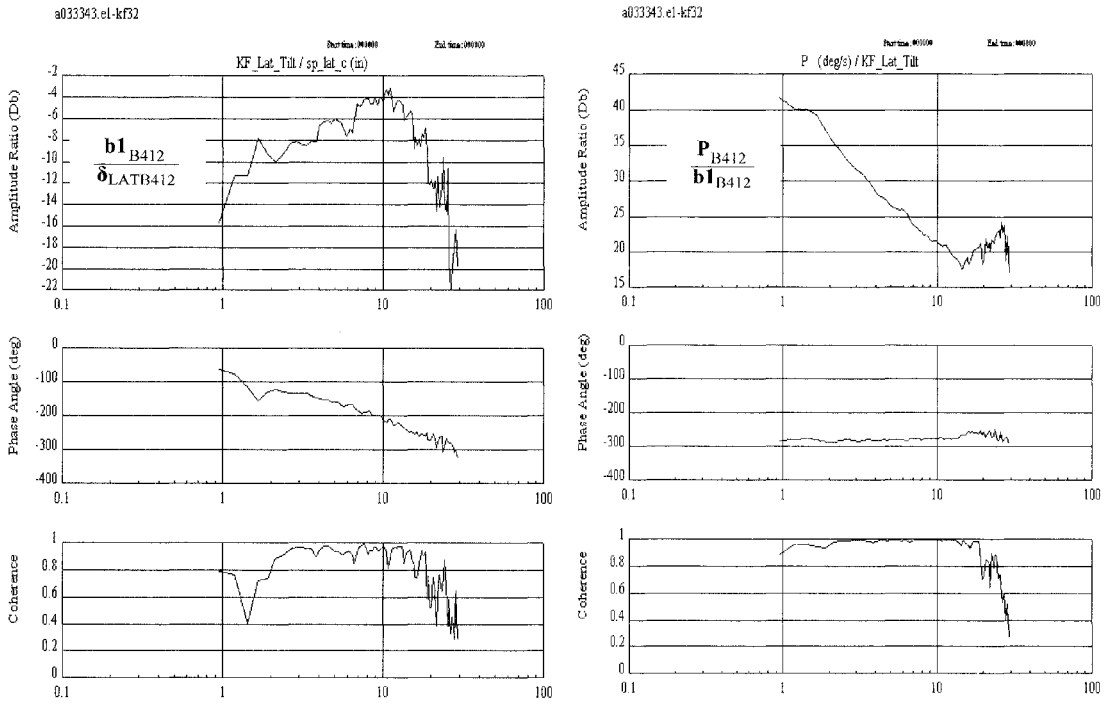

Figure 2.16 Frequency Response Identification – Lateral Axis Rotor Disc Tilt Response

2.7.2 Data Reduction

The data reduction process involved 3 important tasks. The data from the aircraft was re-organized into a standard 20-parameter structured array. The array includes:

$$Z_{MLE} = [\alpha\ \beta\ u\ v\ w\ \phi\ \theta\ q\ p\ r\ A_x\ A_y\ A_z\ \theta_{1c}\ \theta_{1s}\ \theta_{tr}\ \theta_o\ a_o\ a_1\ b_1] \quad 2.33$$

At this stage the data contained information sampled at incompatible rates. Several terms of this array required calculation based on the flight configuration of the vehicle. Data time scale adjustments were required. These stemmed from the various incompatible digitized data streams emerging from the many measurement systems and data filtering due to low signal to noise ratio of the acceleration measurements. This data normalizing is described below.

2.7.3 Transport Delay and Sampling Rate Adjustment

Time delays are used in the system identification process to account for instrumentation system and flight dynamics effects in a simplified manner. For data acquisition systems installations, acquired flight test data is adjusted in post-processing by accounting for the system operational latencies and sampling rates. The Bell 412 ASRA is instrumented with a Litton 92 Inertial Reference Unit (LTN-92) for rigid body accelerations, rates, attitudes, ground speed, and position information. Rotor state data was appropriately adjusted to account for these latencies depicted in Table 2.5. [110,111]

Parameter	Update/Output Rate (Hz)	Transport Delay (ms)
Pitch Angle	64	60
Roll Angle	64	50
Body Pitch Rate	64	50
Body Roll Rate	64	50
Body Yaw Rate	64	50
Body Longitudinal Acceleration	64	60
Body Lateral Acceleration	64	60
Body Normal Acceleration	64	60

Table 2.5 LTN-92 Systems Operation

Instrumentation sampling rates provided another systems dependent time frame issue to be addressed. The rigid body and rotor state data acquisition systems operate at different sampling rates; 64 Hz (typical) and 311 Hz (nominal), respectively. This required thinning of the rotor state data for analytical compatibility.

For vehicle math model development, time delays are used to appropriately model the relationship between control input, rotor response and vehicle rigid body response in absence of comprehensive

vehicle measurements. For this investigation a series of time delays were iterated upon to obtain proper response compatibility for the Bell 412 ASRA as shown in Figures 2.17 and Table 2.6.

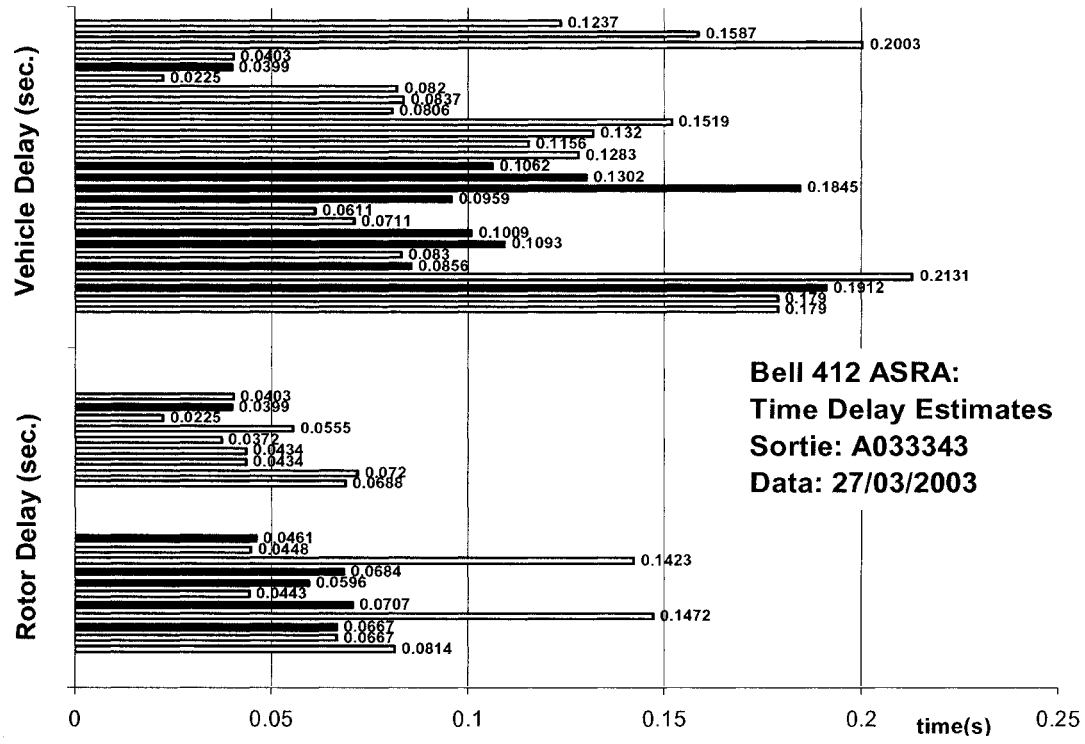

Figure 2.17 Compiled Estimates of Rotor and Vehicle Response Delays

Determination of the time delays was evaluated using a Matlab/Simulink graphical user interface. This method produced a significantly scattered result, however an initial guess for the MMLE routine was determined by comparing previous Bell 412 ASRA data sets, averaging, and elimination of outlying data points.

Response Delay	Longitudinal (ms)	Collective (ms)	Lateral (ms)	Pedal (ms)	Rotor Flap (ms)
Historical Data	50	50	25	35	40
Iteration 1	80	85	40	60	
Iteration 2	70	70	40	50	
Final	**55**	**55**	**30**	**40**	**40**

Table 2.6 Bell 412 ASRA HMMS Response Time Delays

2.7.4 Acceleration Data Filtering

During the system identification process, data analysis showed the presence of high frequency noise in the acceleration components of the flight test data sets. This characteristic was ascertained to be due to rotor hub track/balance or instrumentation arrangement deviations that were different from previous NRC-FRL system identification flights. It was decided that data filtering would be applied to eliminate the unwanted excitation from the acceleration data. The selected filter was a 4 Hz Butterworth format implemented without added time delay. One could increase the filter order and reduce filter cutoff however care needs to be taken not to intercept the useful aircraft bandwidth frequencies.

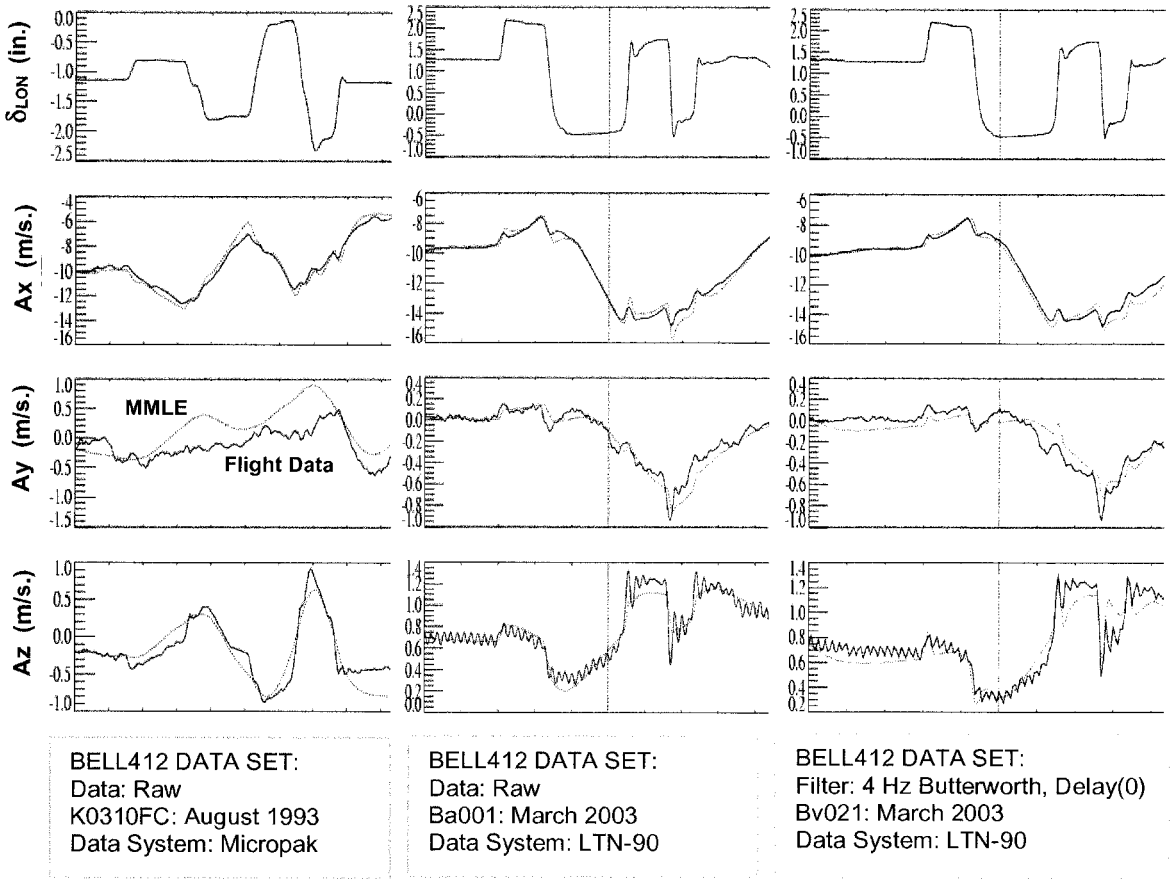

Figure 2.18 Comparison of Bell 412 ASRA Historical, Present, and Filtered Flight Test Data Sets

2.7.5 Development of Rotor Hub Yoke to Blade Dynamics Relationships

A relationship between RSMS flap sensor output and blade deflection was determined through static blade pull tests. Static (RPM = 0) blade-yoke flap bending mode shape functions were determined for high, mid, and low collective settings as illustrated in Figure 2.19.

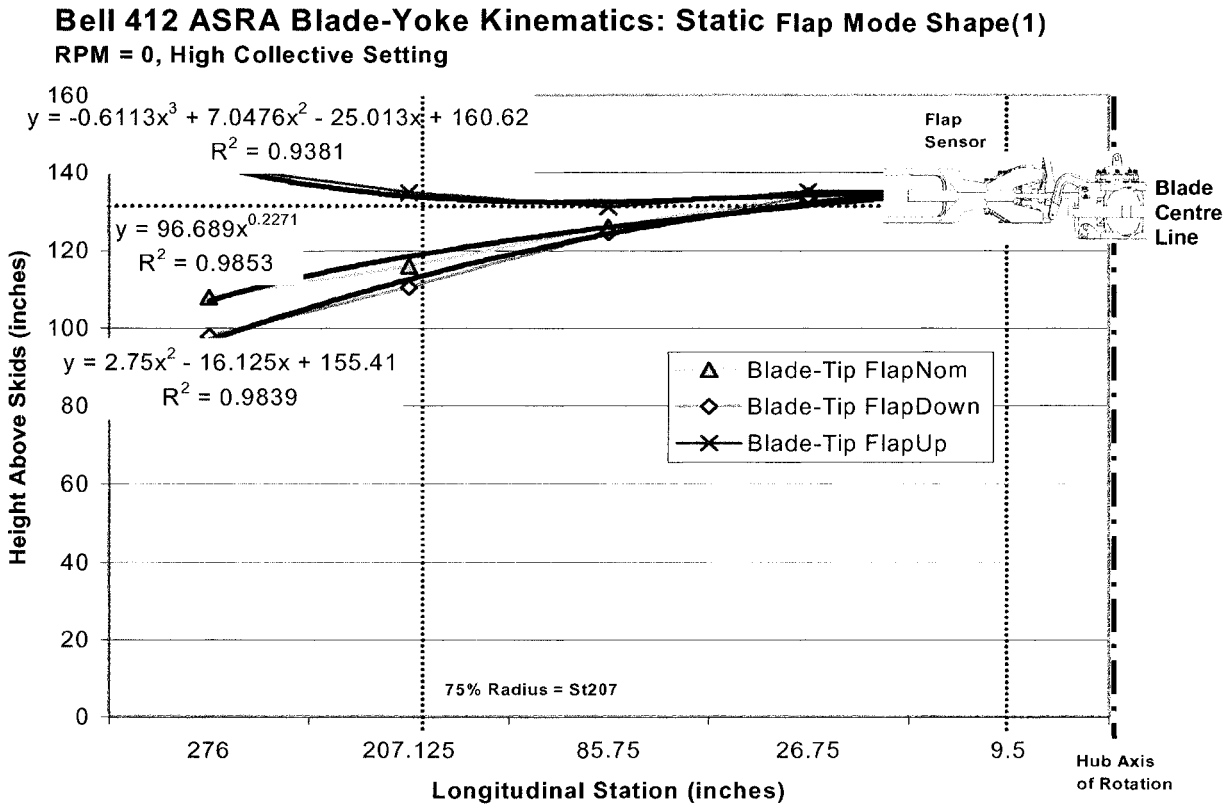

Figure 2.19 Blade-Yoke Static Flap Bending Mode Shapes

Though useful for calibration of the RSMS, the relationships would not allow for proper parameterization of the coupled rotor/body flap dynamics equations. This was due to the static condition that does not replicate blade or hub dynamics influenced by the aerodynamic, structural dynamic, or servodynamic environment of the rotor system in operation. Similar findings by Kaletka et. al[95-97] illustrated that a ground or in-flight experiment would be required to accurately obtain the hub to blade calibration data.

2.7.6 Angular Scaling of Measured Rotor State Data

Regression plots, based on the evaluated blade mode shape functions, as depicted in Figure 2.20 were used to assess the basis for scaling the rotor state flap data displacement measurement (mm. units) to an angular measurement. This analysis applied the rigid blade offset hinge rotor model developed in Section 2.5.3. The analysis confirmed that the stability and control derivatives would be scaled by a linear

approximation of the bending slope of the rotor blade. As such the coefficients of longitudinal and lateral rotor flap terms (a_1 and b_1, respectively) in the coupled rotor/body equation would not change and thus would not assist in the MMLE convergence. Results suggested there was thus no advantage of using the scaled values.

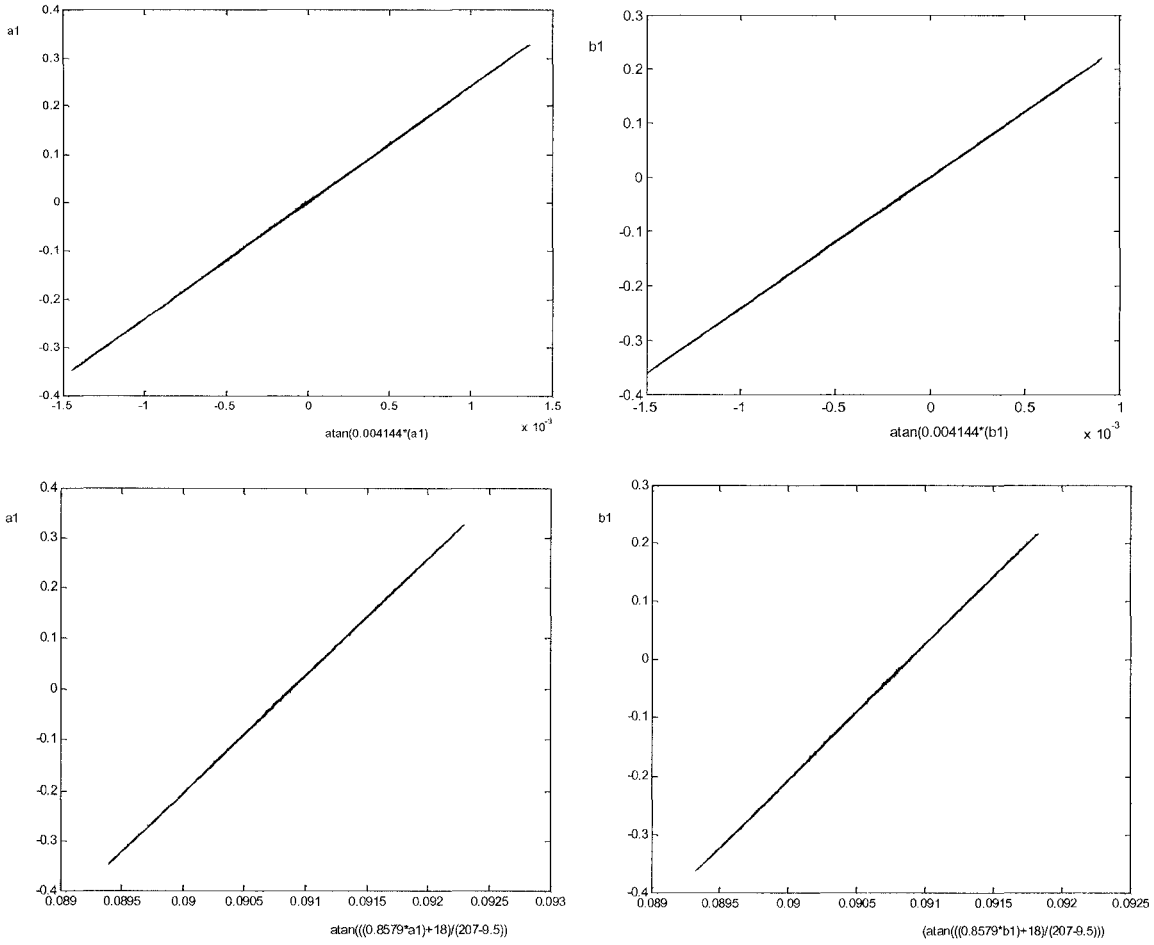

Figure 2.20 Regression Trends for Rotor State Data Scaling

For parameterization of the MMLE routine, the rotor hub yoke flap sensor outputs for longitudinal and lateral disc tilt were implemented directly in the rotor-body dynamics equations by assessing coefficients through simulation. This assumption is based on the rigid blade flap bending model and overall allows for a first order, first flap bending mode fidelity of the extracted mathematical model. This fidelity is low since it is known that the flap regressive response of the soft-inplane hingeless rotor shows a damped second order response that is highly coupled with body attitude-roll dynamics. This physical characteristic is depicted later in Section 2.8.8.

In any event, this limits the validity of the high frequency prediction of the final MLE based 8DOF HMMS model in the range of 2Hz (12.6 rad./sec.).

2.7.7 Development of Rotor Hub to Rigid Body Dynamics Relationships

In order to properly integrate the coupled rotor-body Equation 2.28 in the MMLE routine, a Matlab/Simulink simulation was developed as shown in Figure 2.21 to correlate trend results with flight test data based on manual iteration of the rotor state coefficients.

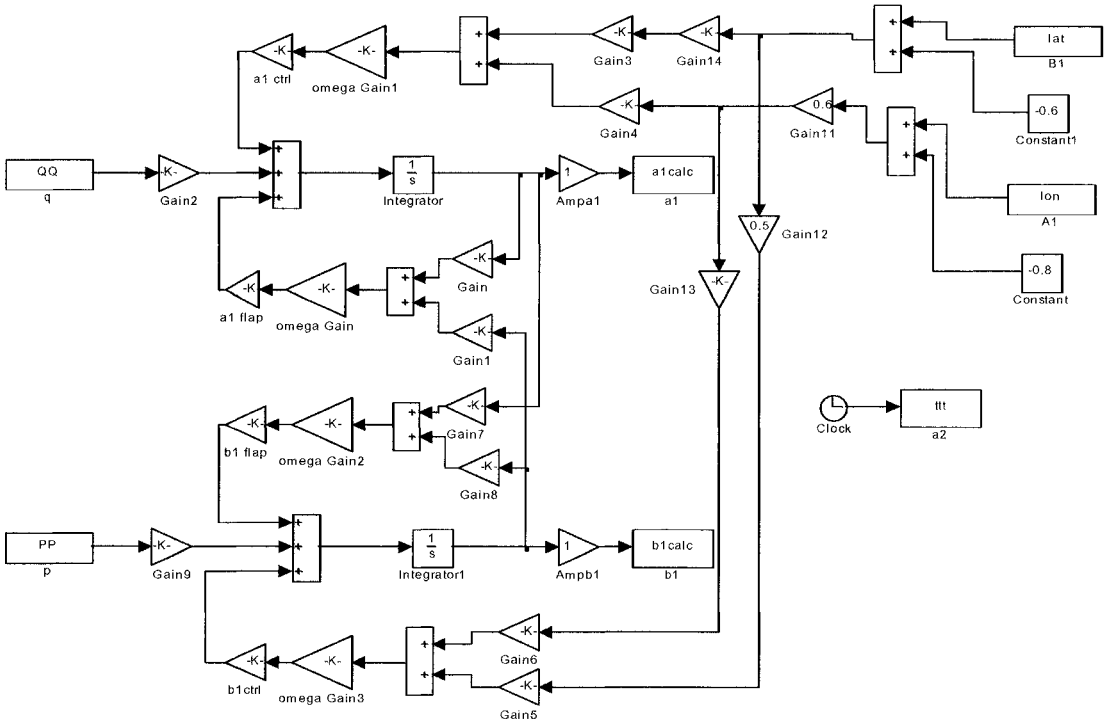

Figure 2.21 Simulink Representation of the Coupled Rotor/Body System

Through iteration to account for unmodeled and unmeasured dynamics such as aerodynamics and structural non-linearities, coefficients of this equation were obtained. Figure 2.22 depicts the computed lateral and longitudinal disc tilt responses to longitudinal and lateral 2-3-1-1 flight test step input data.

The parameterization applied in the MMLE execution was then based on the following equations:

$$\dot{a}_1 - 0.18164(B_1 - 0.8) - 6.29928(A_1 - 0.8) + 10.4988a_1 + 3.6328b_1 - 0.2269q = 0 \qquad 2.34$$

$$\dot{b}_1 - 0.21797(A_1 - 0.8) + 5.2494(B_1 - 0.8) - 3.6328a_1 + 10.4988b_1 - 0.224328p = 0 \qquad 2.35$$

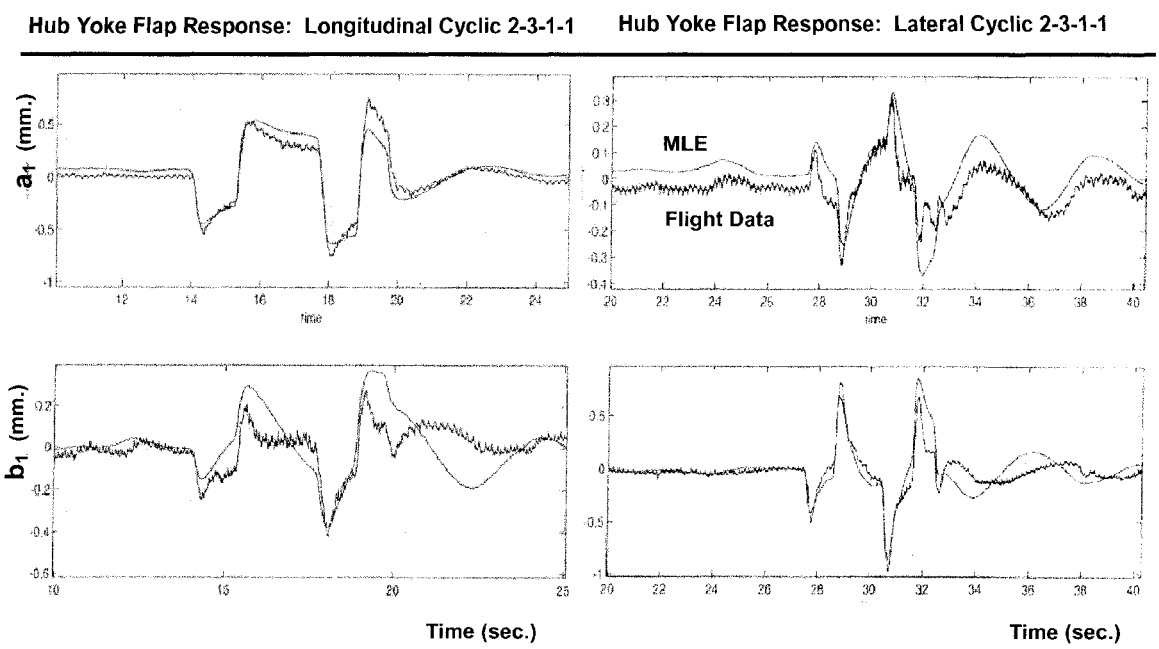

Figure 2.22 Correlation-Computed Rotor Hub Yoke Flap Response with Bell412 ASRA Flight Test Data

In each case, on-axis response shows better correlation than the off-axis response. For this research in rotor state feedback since longitudinal flap dynamics would typically be more weighted than the lateral case, for flight control purposes the correlation was deemed acceptable overall.

2.8 Discussion and Results

An iterative application of the MLE procedure was used to obtain time domain response trajectories of the Bell 412 ASRA. The parameter estimation was applied with and without rotor flap (longitudinal disc tilt) measurement for comparison of a 6DOF and 8DOF math model structure.

2.8.1 Baseline 6DOF Correlation

In Figure 2.23, the MLE convergence is good for on-axis response of the 6DOF model structure. The off-axis correlations are not always favorable however. Particularly, the off-axis pitch and yaw rates, and vertical and lateral translational velocities show poor matching.

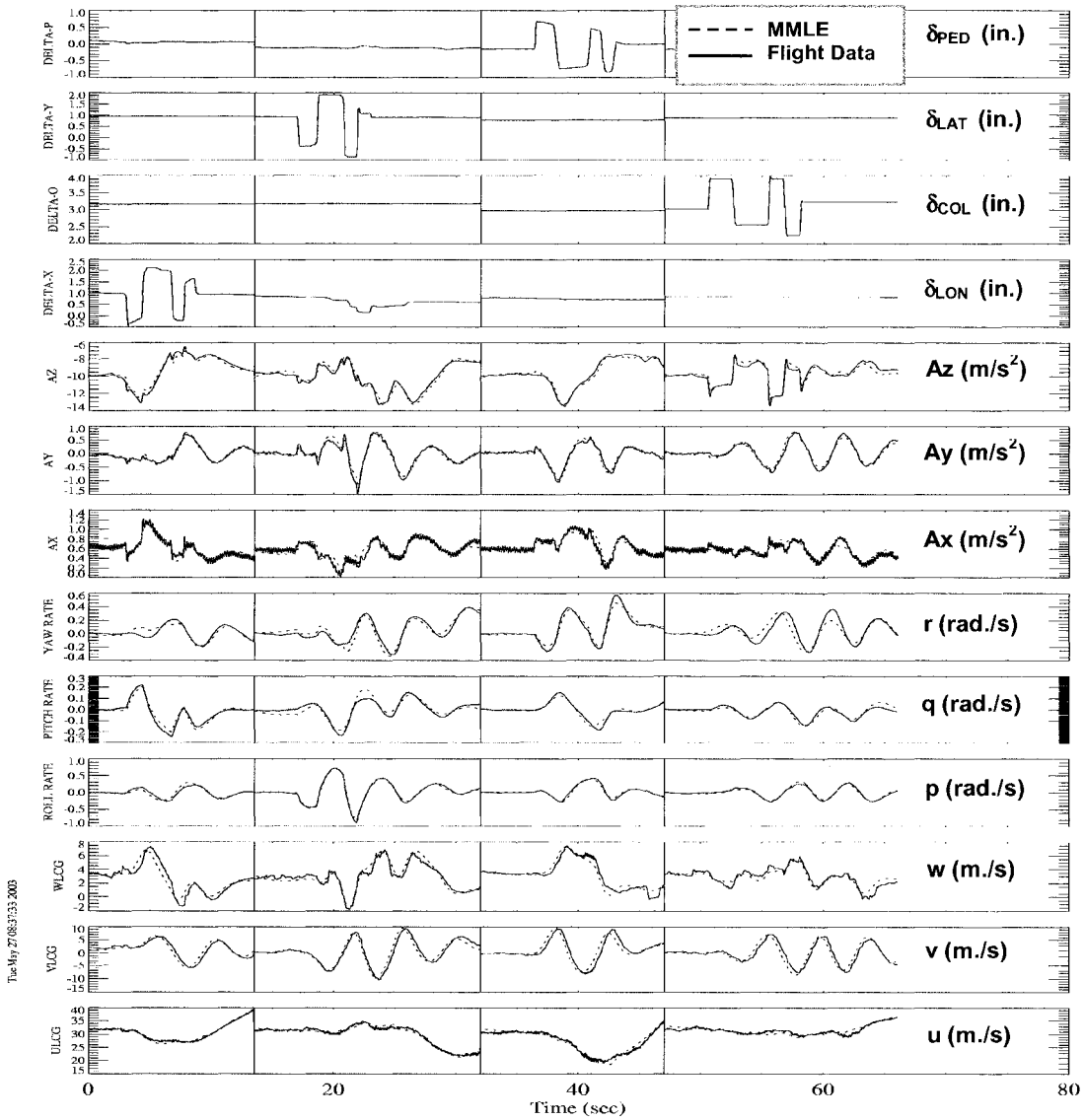

Figure 2.23 Bell 412 ASRA 6DOF Model Response - CASE: B4a004

2.8.2 8DOF Correlation Without Main Rotor RPM: Free Coefficients

Next the 8DOF model was synthesized with all flapping derivatives set to iterate. A sensitivity analysis was performed through a variety of MMLE configurations setting fuselage, control, and rotor state flap parameters in the differential equations to be fixed or to iterate.

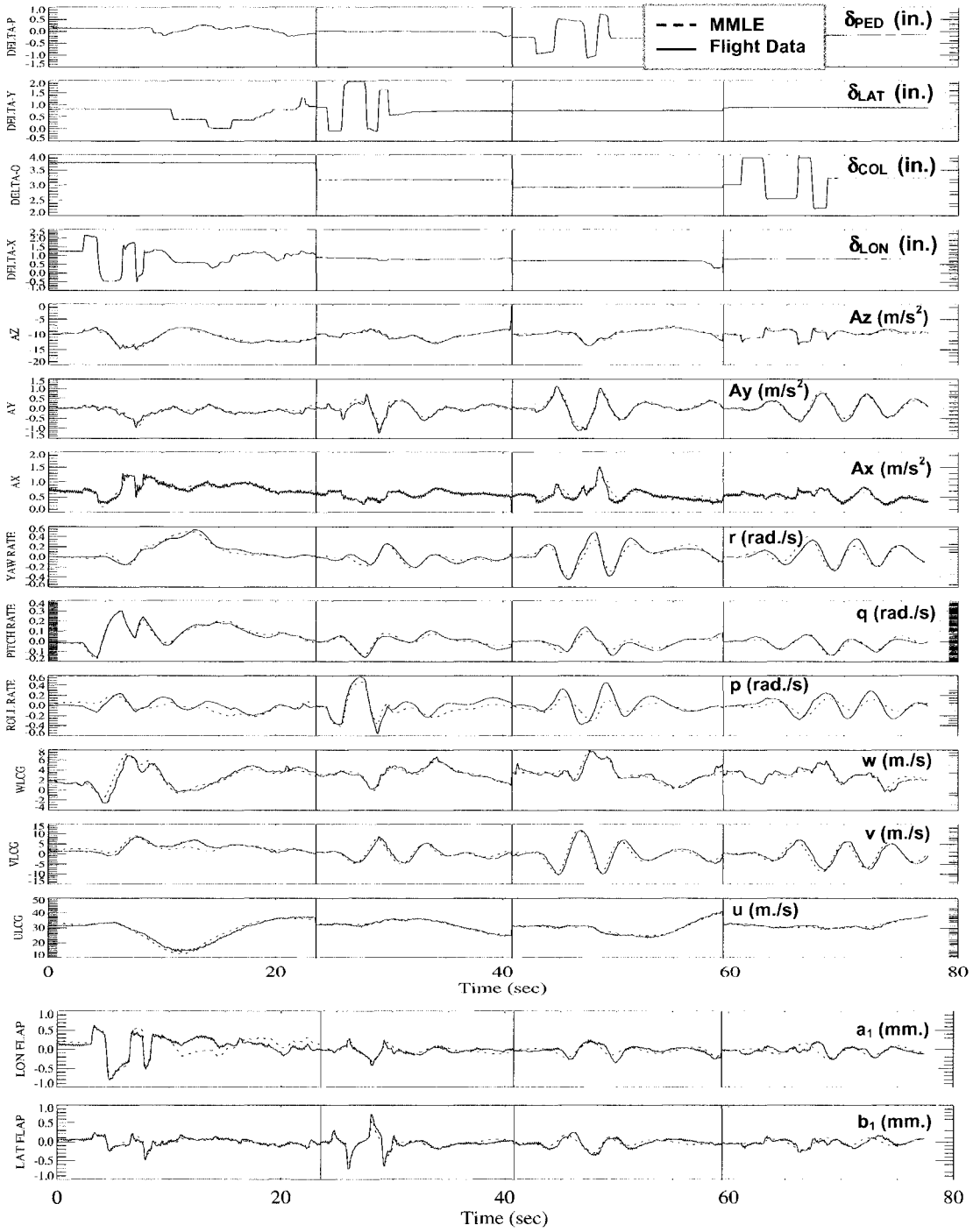

Figure 2.24 Bell 412 ASRA 8DOF Without Main Rotor RPM Model Response - CASE: F001withpqfree

The first case included parameters for attitude-rates (roll and pitch) together and independently. Overall there were no significant deviations in effects to fuselage response or rotor flap response through the sensitivity analysis. The trend overall was that on-axis longitudinal flap response correlation was poor while the on-axis lateral flap correlation showed better matching. This trend is demonstrated in Figure 2.24 for both attitude-rates (roll and pitch) free to iterate. Compared to the baseline 6DOF correlation (Figure 2.23) the fuselage response has degraded particularly in both on-axis and off-axis roll rate response.

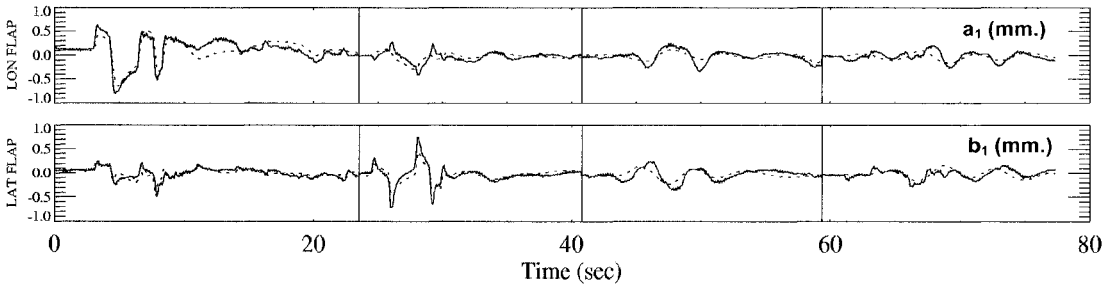

Figure 2.25 Bell 412 ASRA 8DOF Model Response - CASE: F001a_andbdot_and_controls_free

The second case involved iterating rotor flap states (longitudinal and lateral) and controls together. As shown in Figure 2.25, for lateral flap, longitudinal flap rate, and controls iterating, the rotor longitudinal flap response improves however overall rotor flap responses are poorly correlated. As shown in Figure 2.26, for longitudinal flap, lateral flap rate, and controls iterating, the rotor flap responses are poorly correlated with lateral flap response worsening. The fuselage responses retain good matching.

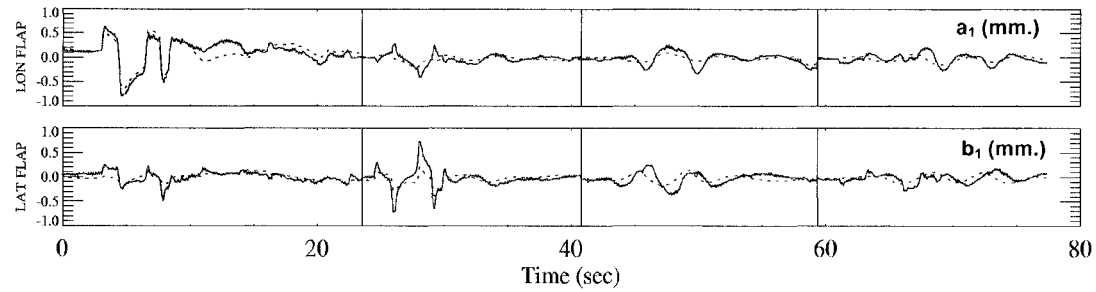

Figure 2.26 Bell 412 ASRA 8DOF Model Response - CASE: F001with_b_and_a_dot_equations_free

The third case involved iterating rotor flap rate states and controls together. For longitudinal flap rate, and controls iterating, and for lateral flap rate, and controls iterating, the rotor flap responses are poorly correlated with longitudinal flap response showing poorest correlation (Figure 2.27). The fuselage responses again retain good matching. With the same case analyzed again with controls fixed, Figure 2.28 depicts the results were similar.

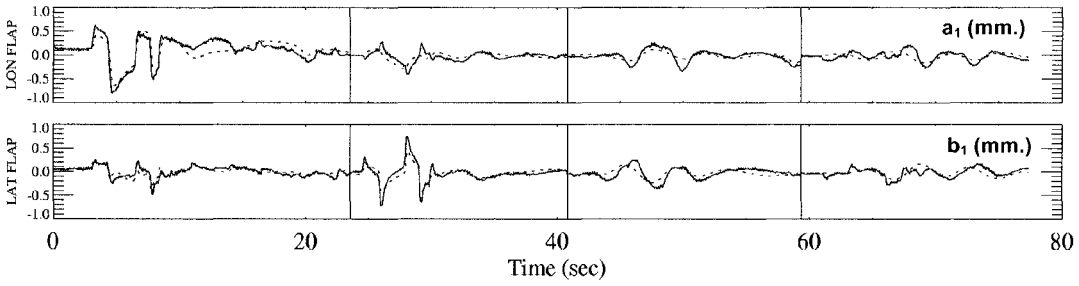

Figure 2.27 Bell 412 ASRA 8DOF Model Response - CASE: F001adotcontrolsfree

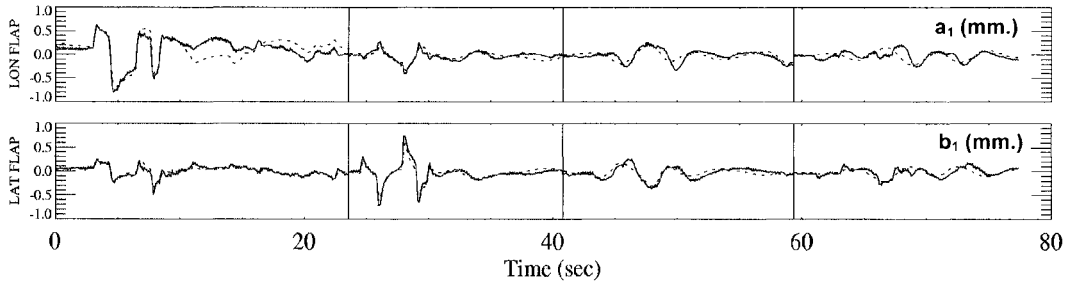

Figure 2.28 Bell 412 ASRA 8DOF Model Response - CASE: F001bdotcontrolsfree

2.8.3 8DOF Correlation Without Main Rotor RPM: Forced Coefficients

In this analysis, the coefficients computed in Equations 2.34 and 2.35 were set in the MLE routine forcing the regression to accept the rotor flap state time histories they represented. It was difficult to make the MLE model run to converge. The longitudinal and lateral time histories showed worsened correlation and the fuselage state match was degraded as compared to the 6dof baseline.

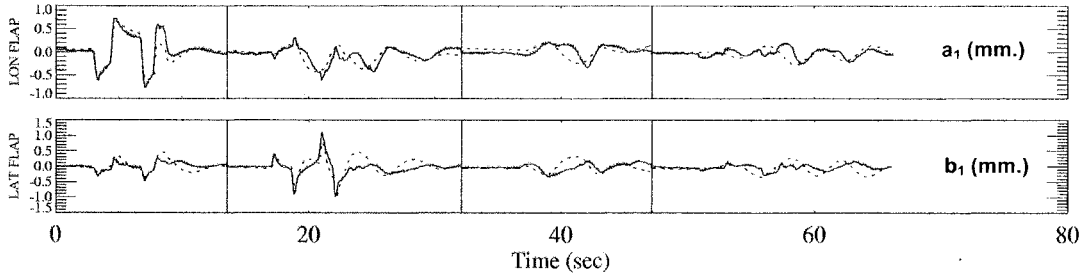

Figure 2.29 Bell 412 ASRA 8DOF Model Response - CASE: F024xtermsfree

2.8.4 6DOF and 8DOF Correlations With Main Rotor RPM

The final sensitivity analysis prior to final validation involved including main rotor RPM (MRRPM) as a control state. The MMLE routine parameterized in this way had more confidence in the fuselage measurements and the rotor dynamics did not converge as depicted in Figure 2.30.

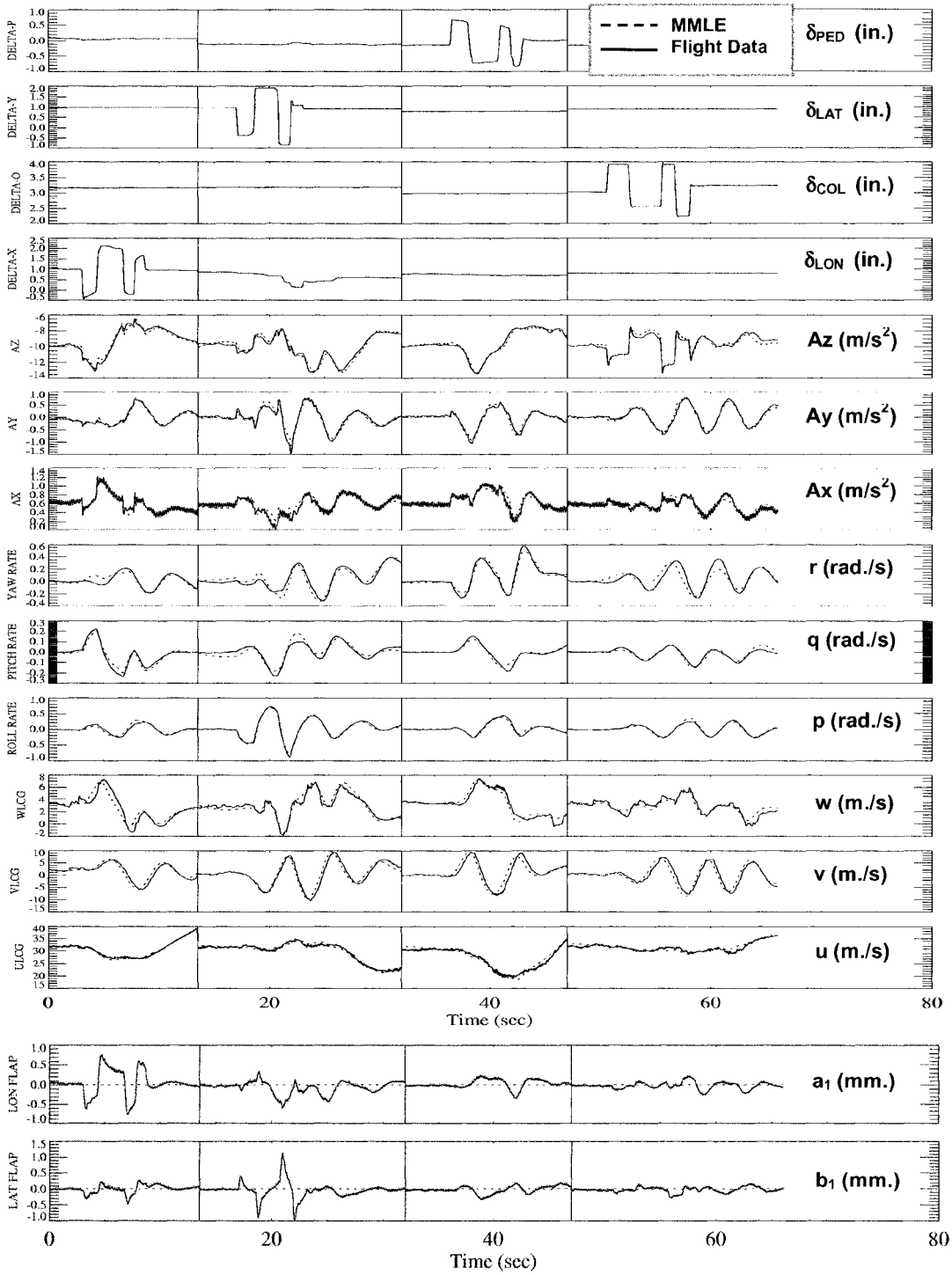

Figure 2.30 Bell 412 ASRA 8DOF With Main Rotor RPM Model Response - CASE: B4f044

2.8.5 Final Validation and Model Selection

The final model was selected as shown in Figure 2.31 to proceed with the flight control law design process. In comparison to a previous study by Hui[100] in the development of a hybrid math model of the Bell 412 ASRA using estimated rotor flap dynamics the response correlations are not improved. Much uncertainty has been incorporated in this model that must be accounted for in the selected methodology for modern multivariable flight control. This scenario is typical of complex helicopter flight dynamics.

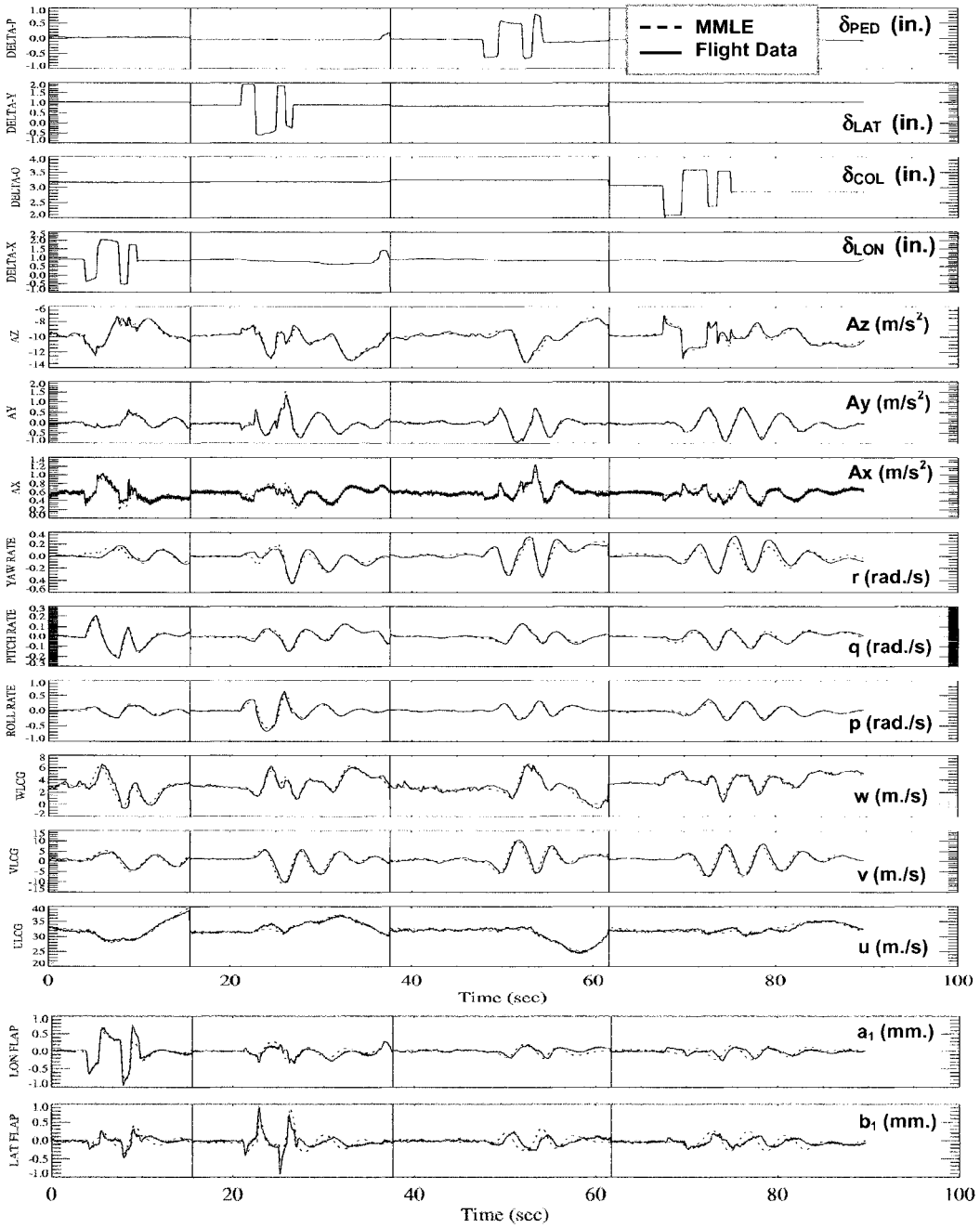

Figure 2.31 Bell 412 ASRA Final Validation Model – CASE: B4v023

2.8.6 Time and Frequency Response Analyses of the Selected Hybrid Mathematical Model Structure (HMMS)

The mathematical model is now analyzed to expose features of the Bell 412 ASRA and its hingeless rotor system. Time domain and frequency domain responses of the coupled bare-airframe are depicted in Figures 2.32 to 2.40 spanning 5 second and 100 rad./sec. ranges, respectively.

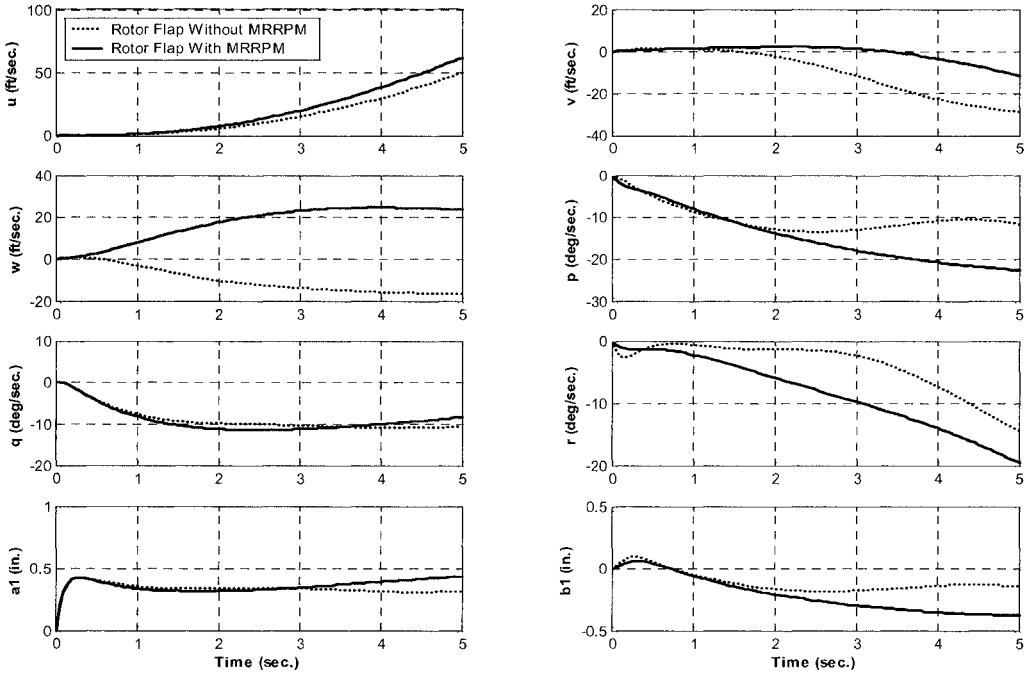

Figure 2.32 Coupled Open Loop Time History Response to One Inch Longitudinal Cyclic Step

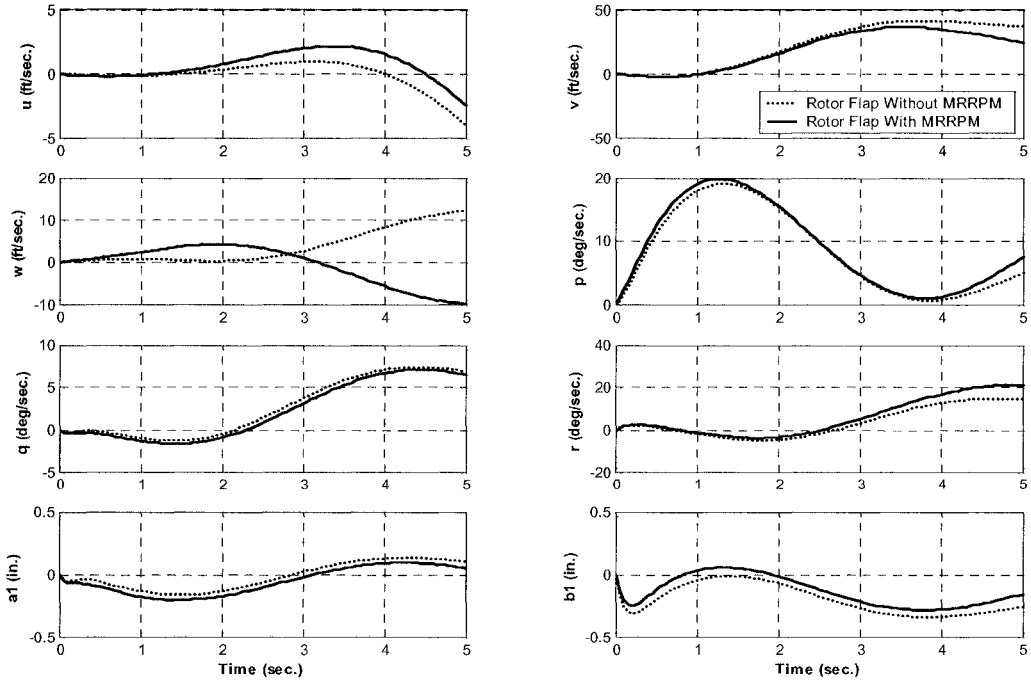

Figure 2.33 Coupled Open Loop Time History Response to One Inch Lateral Cyclic Step

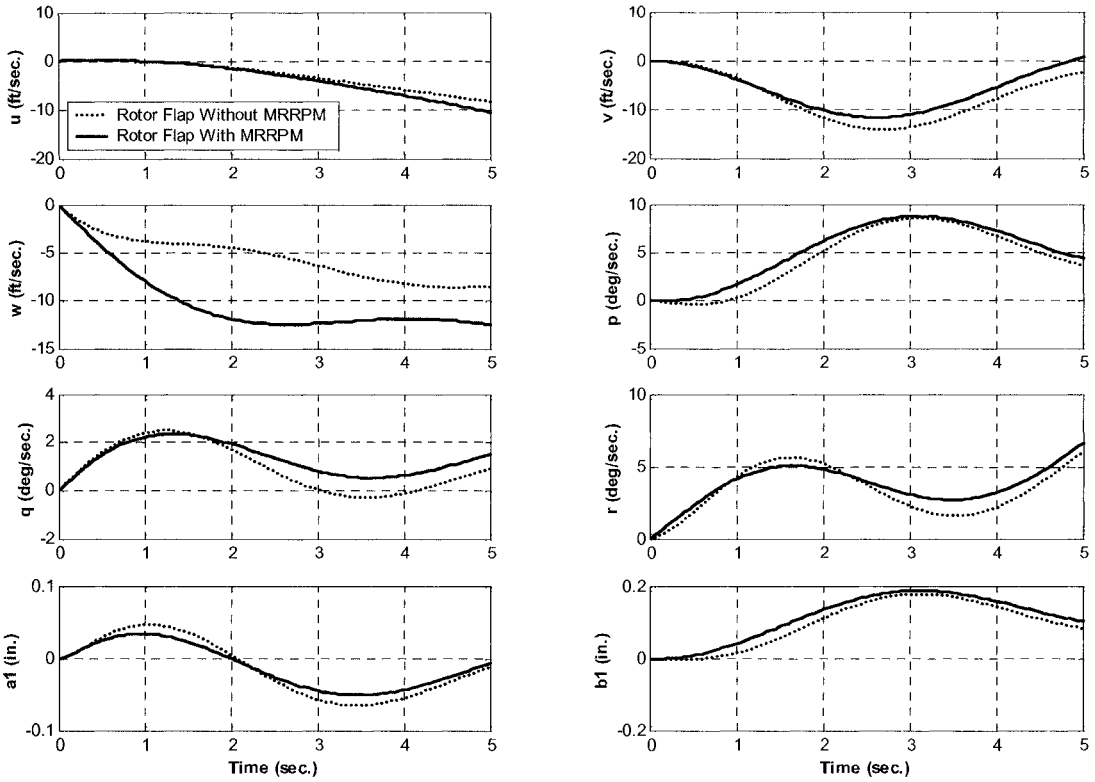

Figure 2.34 Coupled Open Loop Time History Response to One Inch Collective Step

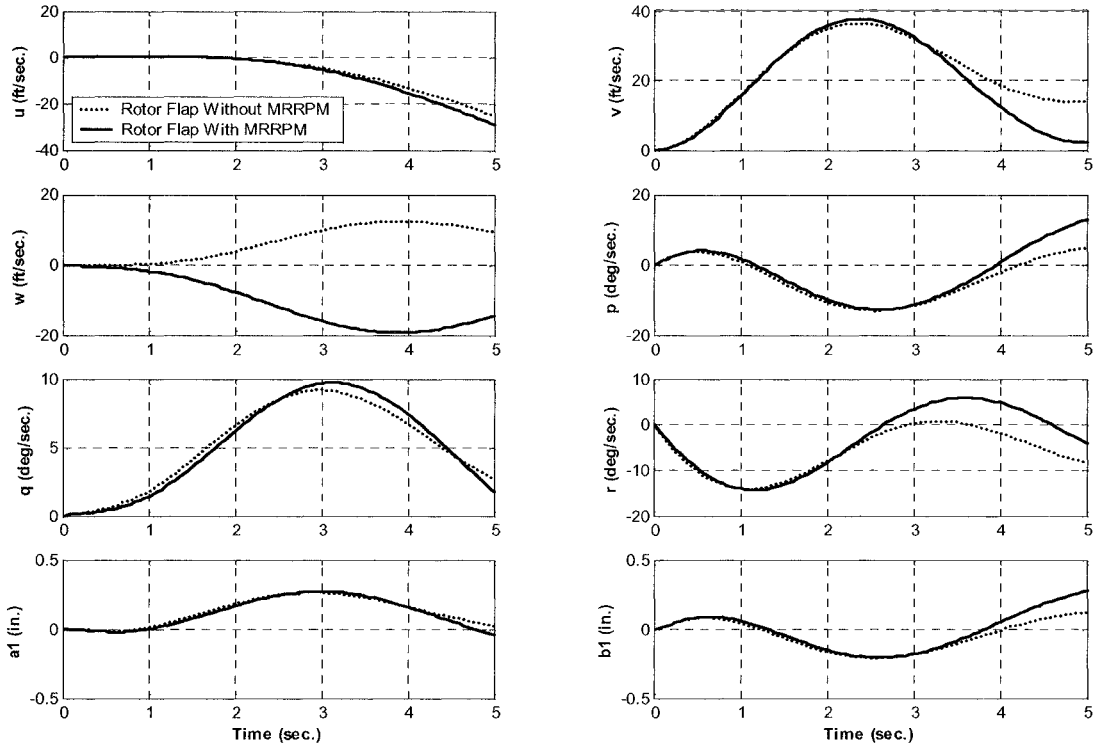

Figure 2.35 Coupled Open Loop Time History Response to One Inch Tail Rotor Collective Step

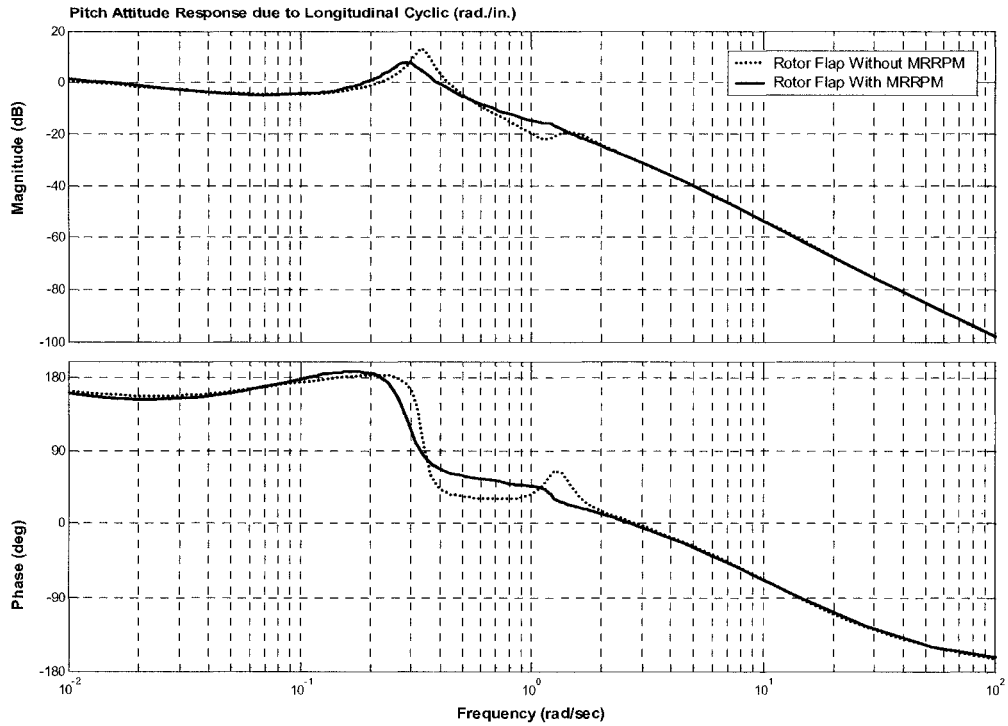

Figure 2.36 Coupled Open Loop Rigid Body Frequency Response in Pitch

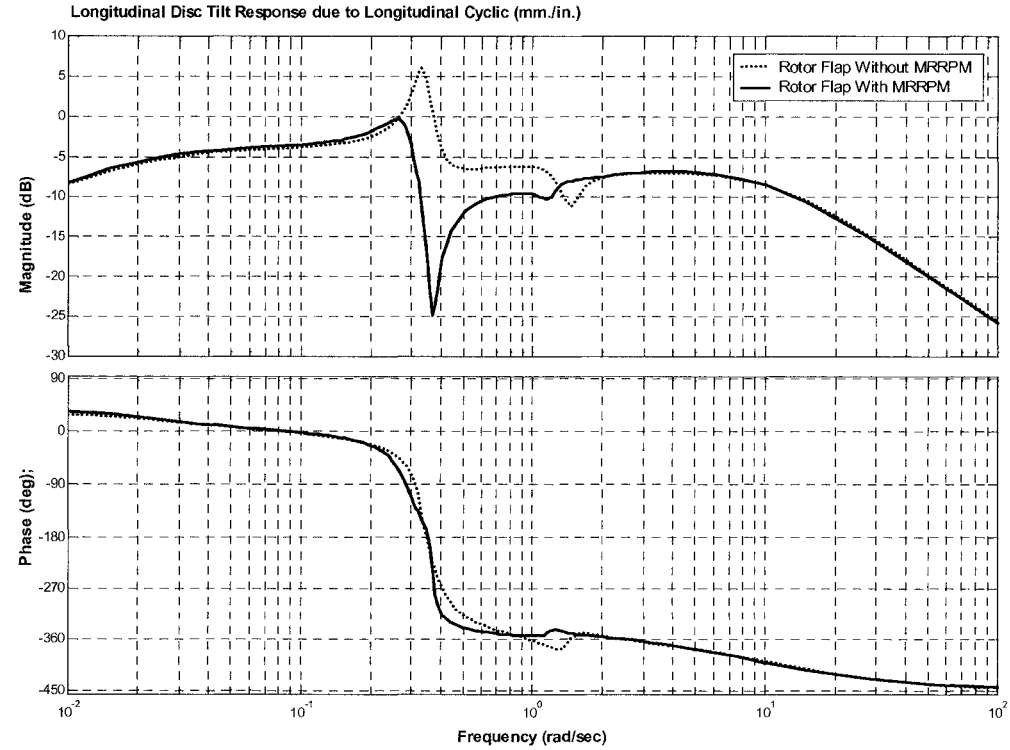

Figure 2.37 Coupled Open Loop Rotor Flap Frequency Response in Pitch

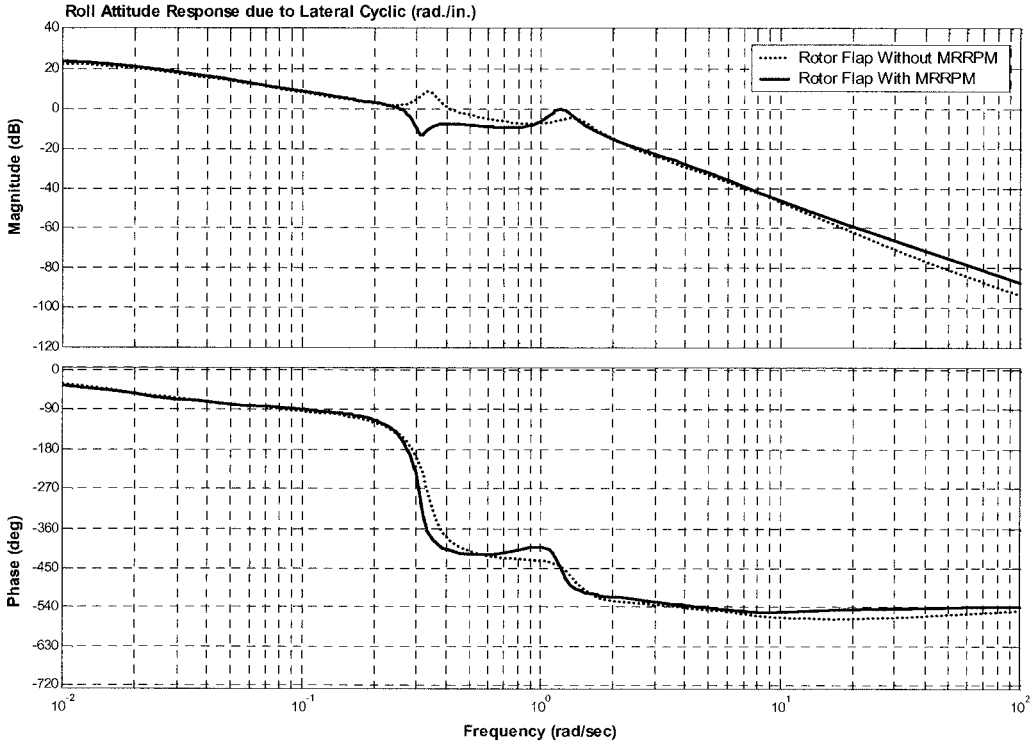

Figure 2.38 Coupled Open Loop Rigid Body Frequency Response in Roll

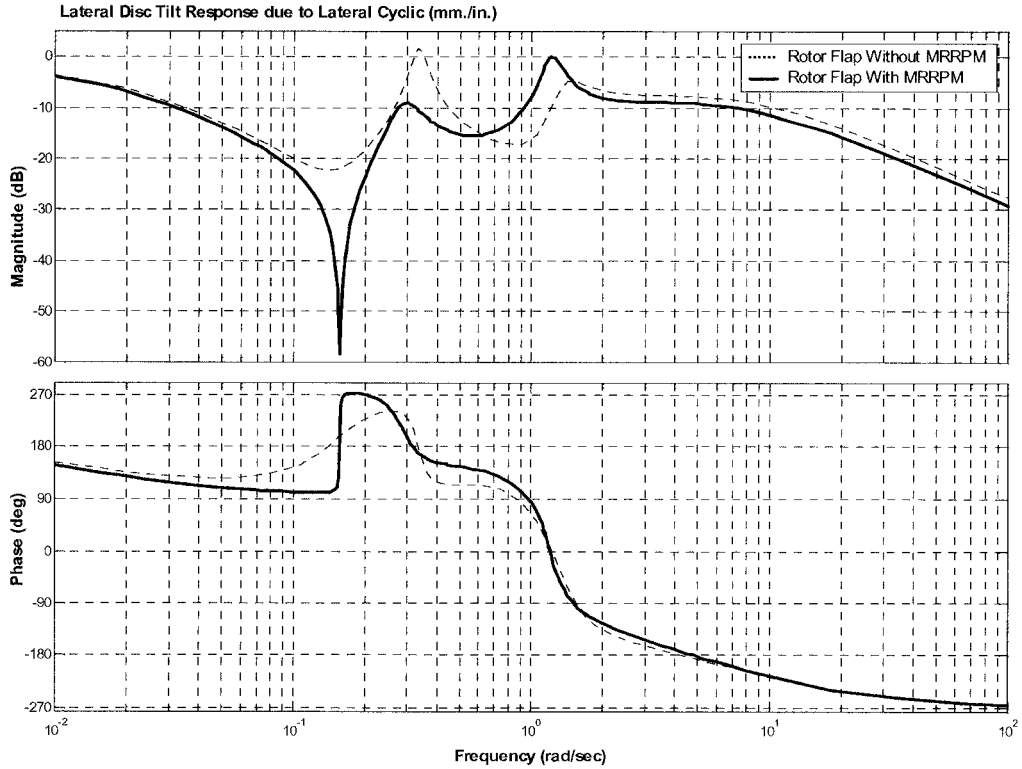

Figure 2.39 Coupled Open Loop Rotor Flap Frequency Response in Roll

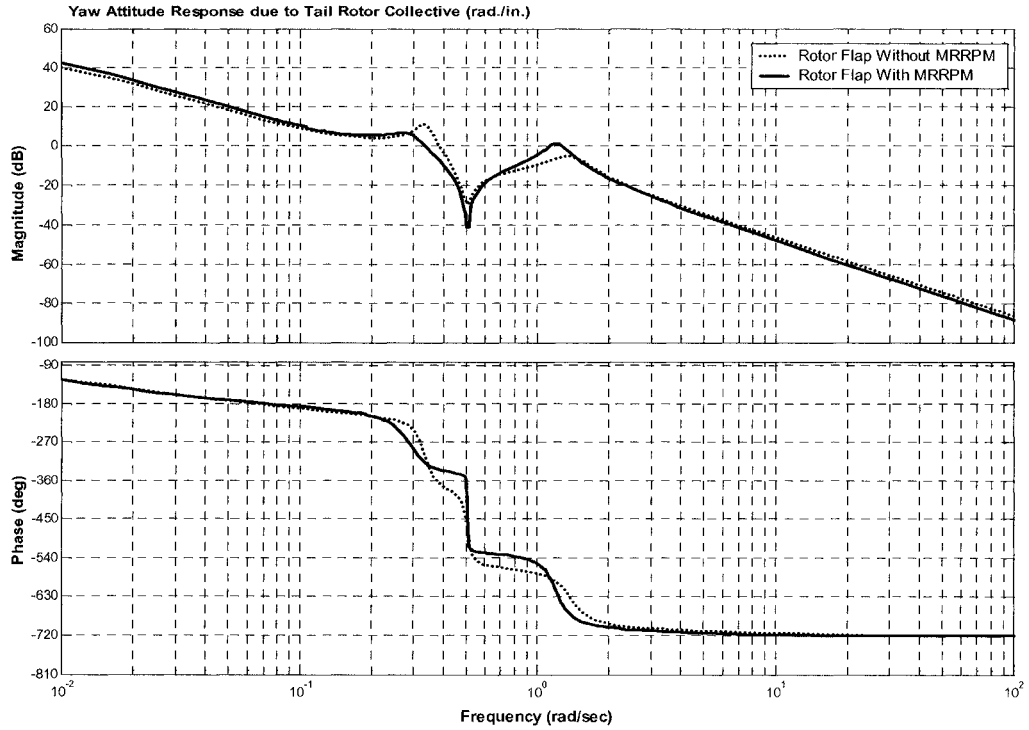

Figure 2.40 Coupled Open Loop Rigid Body Frequency Response in Yaw

The pitch rate to longitudinal cyclic and corresponding longitudinal disc tilt follow the control input in opposite sign as shown in Figure 2.32 with supporting dynamics showing the pilot pushing cyclic forward. This correlates with flight test data in Figure 2.8 for an aft cyclic step. The roll rate response to lateral cyclic responds positively then reverses as shown in Figure 2.33; the supporting responses indicates a right cyclic input. The off-axis couplings in yaw, pitch, and heave, are all significant in this axis. Comparatively, the heave velocity responses diverge for the With- and Without-MRRPM cases indicating a sign convention anomaly. This anomaly is present in all control axes as shown in Figures 2.32 to 2.35. Comparing the longitudinal response (Figure 2.32) and lateral response (Figure 2.33), the axis coupling is more significant in the former response. The longitudinal and lateral disc tilt responses tend to mimic their attitude-rate responses.

In Figure 2.34, there is significant coupling between heave, pitch, and roll axes for a collective step. The coupling in yaw to pitch axis is notably high for the tail-rotor collective step in Figure 2.35 with rotor responses being similar in magnitude to the other axes. Both of these couplings contribute to poor handling qualities ratings by virtue of high pilot workload of the vehicle. This is a well defined example of the impact vehicle characteristics have on the pilot's ability to perform mission tasks through divided attention control of the aircraft.

In Figures 2.36 to 2.40, the longitudinal, lateral and directional characteristics are presented in the frequency domain. The bare-airframe pitch attitude response shows a roll off at some 0.3 rad./sec. and out-of-phase response. The longitudinal axis will be further scrutinized in Section 2.8.7. The bare-airframe roll attitude response to lateral cyclic in Figure 2.38 shows the vehicle is stable with a positive gain margin and phase margins of +4dB and +40 degrees, respectively. The roll off occurs at 1.5 rad./sec. after some coupling peaks. The first peak in magnitude is characteristic of the Dutch roll mode at approximately 0.3 rad./sec. The HMMS, for both with and without main rotor RPM cases, do not correlate in response for this mode placement, however. The rotor longitudinal and lateral disc tilt dynamics show frequency content out to 10 rad./sec. before drop off in magnitude occurs. This confirms the Bell 412 ASRA bandwidth features of the rotor system and corroborates the frequency dynamics previously mentioned in Section 1.3 of Chapter 1, and Section 2.5 of the present chapter.

It must always be kept in mind that time history representations of response tend to poorly represent helicopter pilot control input dynamics or coupled rotor/vehicle dynamics.[91] Typical time history parameters such as rise-time, time-to-double amplitude, settling time, and time delays weight the control and rotor/vehicle physics on low frequency response phenomena. These dynamics are occurring at high frequencies and, as is being emphasized by this research in higher order rotor states, must be retained with fidelity in analyses of helicopter dynamics. With regard to the rigid body dynamics then, frequency responses (Figures 2.36, 2.38, and 2.40) show significant coupled rotor-body dynamics in the ranges of 0.1-2.5 rad./sec. This coupling is more distinctly shown in the longitudinal and lateral rotor disc tilt responses (Figures 2.37 and 2.39) whereby rotor regressive (lateral and longitudinal flap) and rigid body (pitch/roll, yaw/heave, etc.) modes are interacting, impacting the handling qualities frequency spectrum. In the next section, the response of the Bell 412ASRA is further assessed through frequency domain analysis.

2.8.7 Compliance with ADS-33E-PRF Military Handling Qualities Specifications

The presented coupled responses cloud the designers understanding of the helicopter control task. An uncoupled axis profile typically consists of a reduced order state space form and the respective attitude and/or rate and disc tilt transfer functions. The following discussions focus on the standard Without Main-Rotor RPM (MRRPM) case for analysis. In order to assess the compliance of the vehicle to specifications for rotorcraft handling qualities, **ADS-33E-PRF** and **ADS-33C** specifications are assessed for a **Target Acquisition and Tracking (TA+T)** subset[13,14]. These specifications define response types, mission tasks elements, useable cue environments, system functionality, and pilot workload of the vehicle in its operational flight envelope (OFE). The rigid body and rotor longitudinal disc tilt dynamics covering, low and high frequency contributions, are illustrated in Figures 2.41, 2.42, and 2.43. (Refer to Appendix A for general guidelines on specification compliance.)

Coupled Response:
States: $x = [u\ v\ w\ p\ q\ r\ \theta\ \phi\ \psi\ a_1\ b_1]$

Regressive Flap Mode:
(-9.3737, 3.6692) rad./sec.

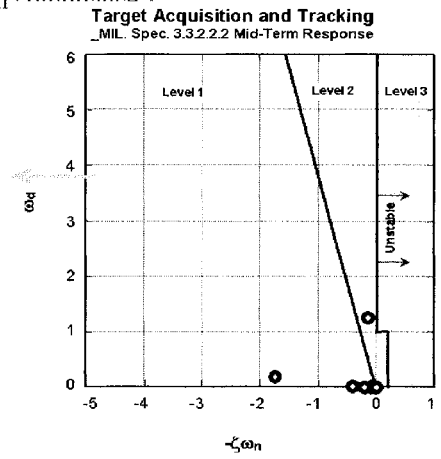

Figure 2.41 Bare-Airframe Coupled Longitudinal Poles for ADS-33C

Uncoupled Longitudinal Response:
States: $x = [u\ w\ q\ \theta\ a_1]$

Rotor Flap Regressive Mode:
(-9.5713, 0) rad./sec.

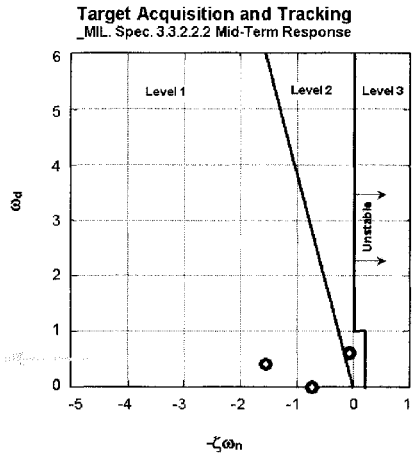

Figure 2.42 Bare-Airframe Uncoupled Longitudinal Poles for ADS-33C

Uncoupled Lateral Response:
States: $x = [v\ w\ p\ r\ \phi\ b_1]$

Rotor Flap Regressive Mode:
(-9.066, 0) rad./sec.

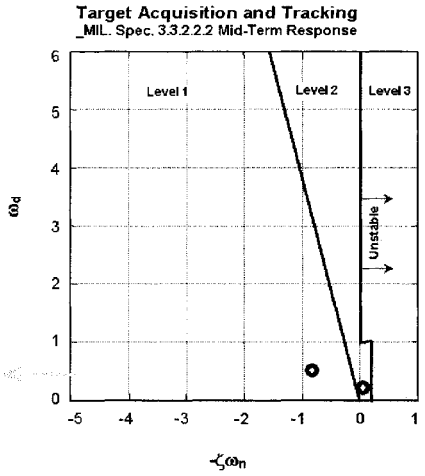

Figure 2.43 Bare-Airframe Uncoupled Lateral Poles for ADS-33C

With contributions for the rotor and its time delay, and the pitch angle response, the Bell 412 ASRA depicts Level 3 bare-airframe uncoupled longitudinal and lateral responses of Level 3 in Figures 2.44 and 2.45. Directionally, for an uncoupled yaw axis response, a marginal Level 2 rating was assessed as shown in Figure 2.46.

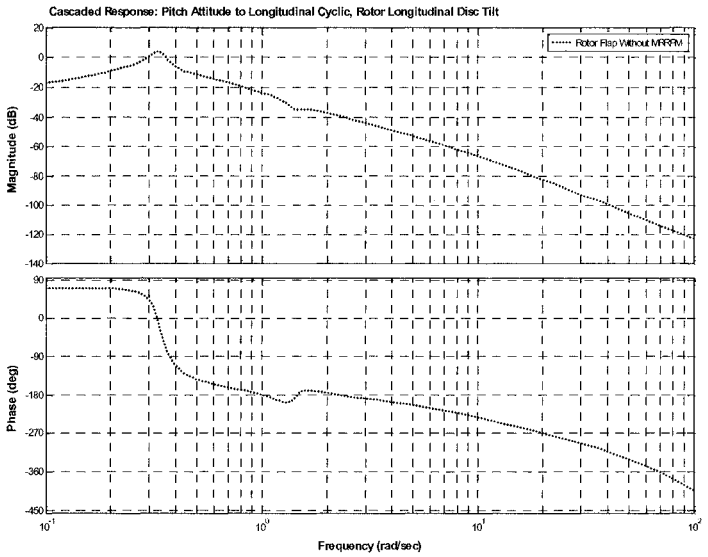

Uncoupled Longitudinal Response:
States: $x = [u\ w\ q\ \theta\ a_1]$

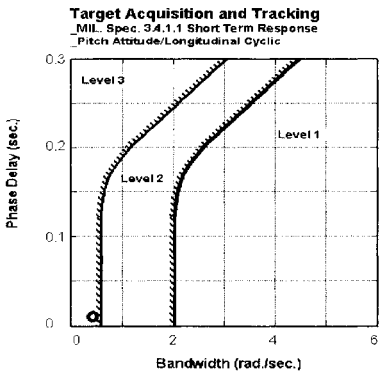

Figure 2.44 Bare-Airframe Rating for Longitudinally Uncoupled, Target Acquisition and Tracking - ADS-33E-PRF

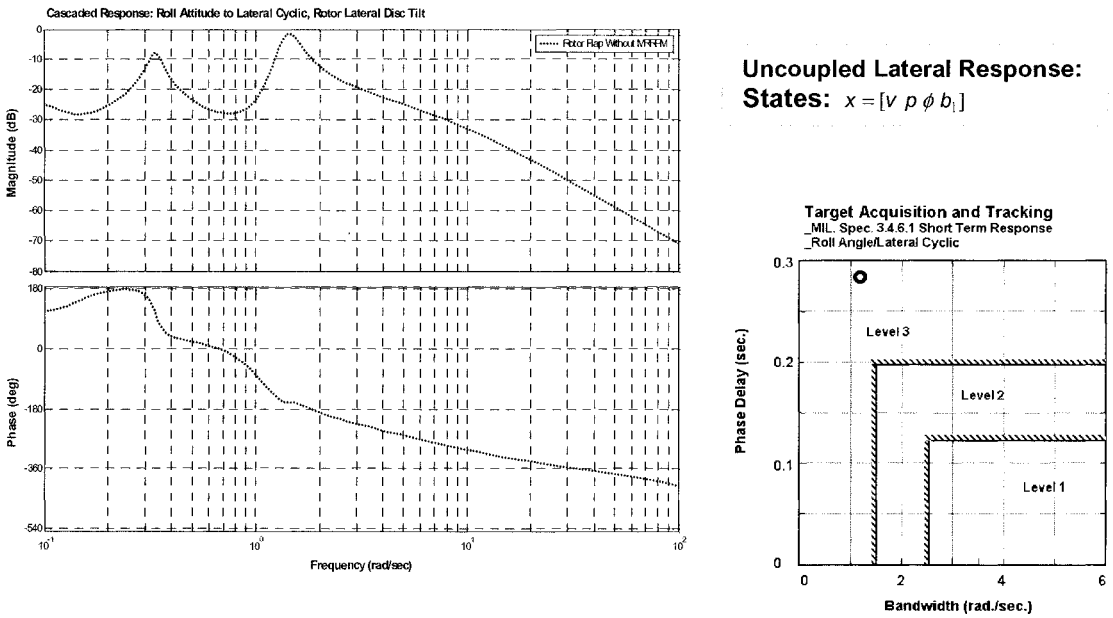

Figure 2.45 Bare-Airframe Rating for Laterally Uncoupled, Target Acquisition and Tracking - ADS-33E-PRF

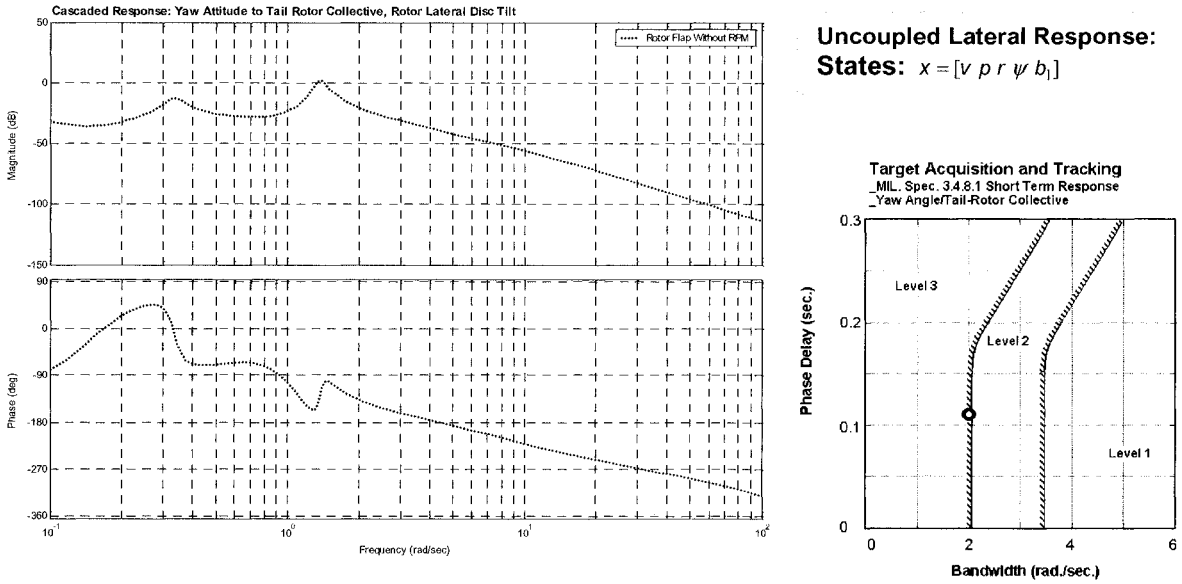

Figure 2.46 Bare-Airframe Rating for Directionally Uncoupled, Target Acquisition and Tracking - ADS-33E-PRF

The directional coupling of the helicopter may be assessed in all axes. An important coupling for aggressive maneuvering occurs between directional pointing (yaw axis) and collective control (heave input). The Bell 412 ASRA depicts a Level 3 bare-airframe rating for this specification as shown in Figure 2.47.

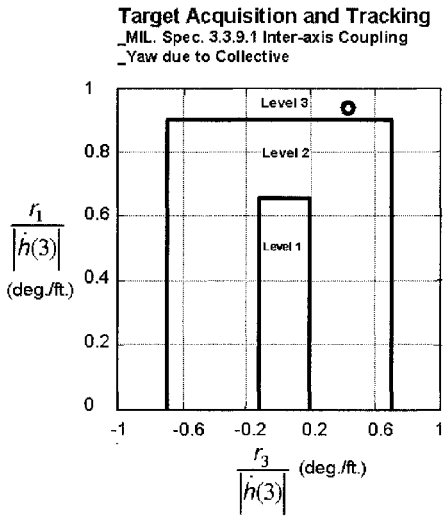

Figure 2.47 Bare-Airframe Rating for Yaw-Collective Coupling, Target Acquisition and Tracking - ADS-33E-PRF

Other critical couplings for aggressive maneuvering include pitch attitude to longitudinal cyclic and roll attitude due to lateral cyclic. As shown in Figure 2.48, the Bell 412 ASRA bare-airframe response rates Level 2 in this specification.

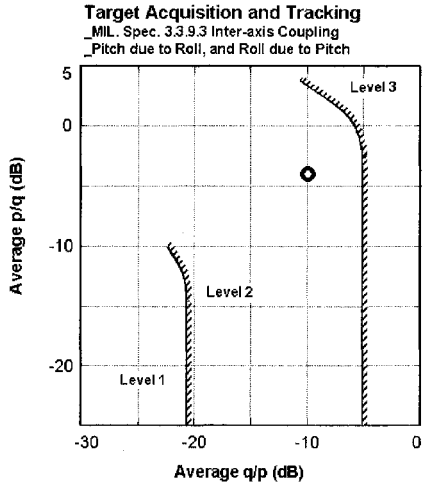

Figure 2.48 Bare-Airframe Pitch-Roll and Roll-Pitch Coupling, Target Acquisition and Tracking - ADS-33E-PRF

2.8.8 HMMS Spectral Content: Coupled Rotor-Body Dynamics Modal Placement

Data from the vehicle RSMS was used to assess the power spectral density of raw rotor yoke flap dynamics as shown in Figure 2.49. This harmonic analysis depicts the nominal main rotor frequency content including the 1 per rev (5.4 Hz), 2 per rev (10.8 Hz), and 4 per rev (21.6 Hz) frequencies.

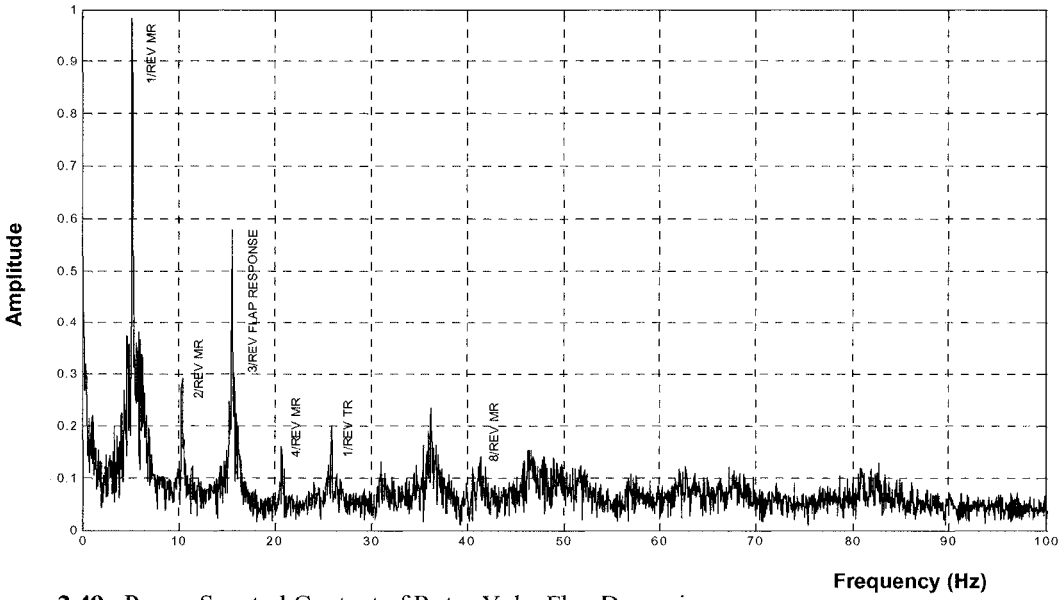

Figure 2.49 Power Spectral Content of Rotor Yoke Flap Dynamics

The 3 per rev harmonic at 16.2 Hz shows the high flap-wise bending mode amplitude response of the main rotor blade. There are aerodynamic forces that excite the rotor at the 3 per rev frequency in forward flight, and it is common to see high 3 per rev amplitudes due to flap-wise bending. This excitation of the flap-wise rotor response is characteristic of hingeless rotors with large effective hinge offset. This offset allows for the development of high hub moments and thus creates an agile helicopter with high control sensitivity and damping. These effects though favorable come at the expense of high gust sensitivity. The expectation then is that this rotor flap response dominates a spectral bandwidth of the coupled rotor-body system in:

- On-axis pitch rate response
- On-axis roll rate and attitude response
- On axis longitudinal and lateral rotor flap response

These dynamics should correlate with the mathematical model representation of the complex hingeless rotor helicopter physics. The modal content of the HMMS for the case without main rotor RPM for longitudinal and lateral dynamics are depicted in Figures 2.50 to 2.53. For modes with large magnitude separation, it is the bode magnitude of the axis transfer function which dictates the dominant modal response. The on-axis longitudinal and lateral flap regressive modes correctly depict second order behaviors and dominate their respective responses as shown in Figures 2.50 and 2.51. The regressive flap modes are associated with the rolling motion of the helicopter however these associations are not

confirmed by the on-axis roll rate response in Figure 2.53 where the rotor modes should dominate. In the longitudinal axis, the pitch rate to longitudinal axis transfer function is dominated by the rotor flap regressive mode, but only after roll-off of the coupled pitch-roll mode, in a range of 4.5 out to 30 rad./sec. The pitch and roll subsidence modes have a first-order behavior as expected since they are real modes.

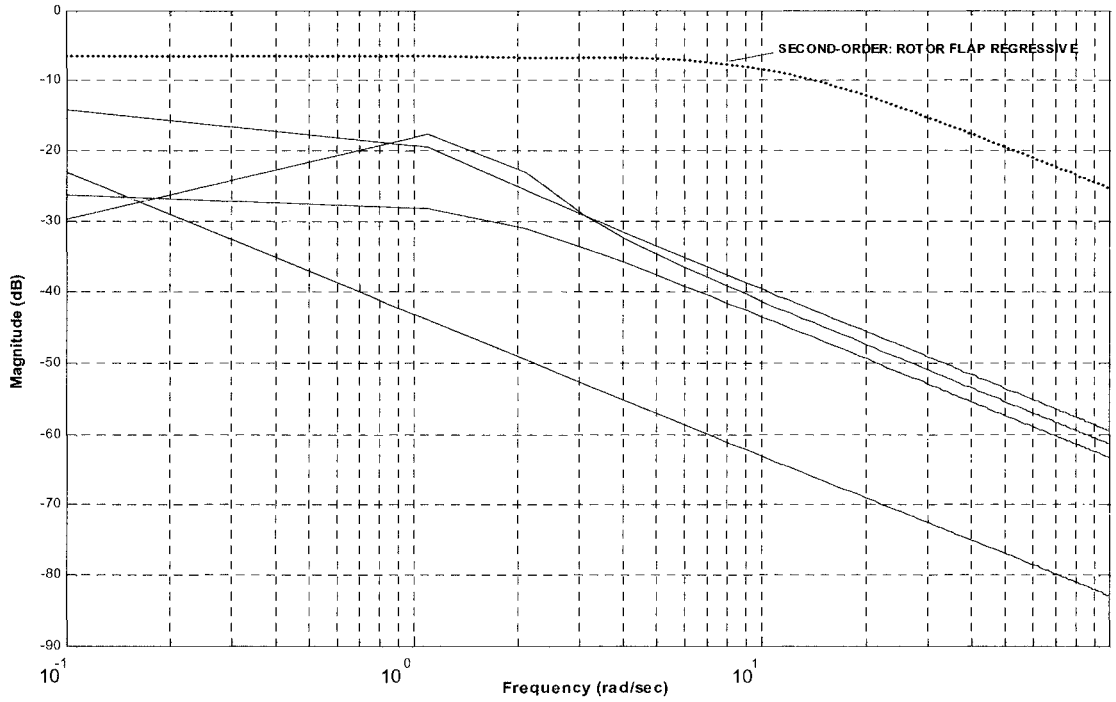

Figure 2.50 Modal Content, On-Axis Longitudinal Disc Tilt Response – Without Main Rotor RPM

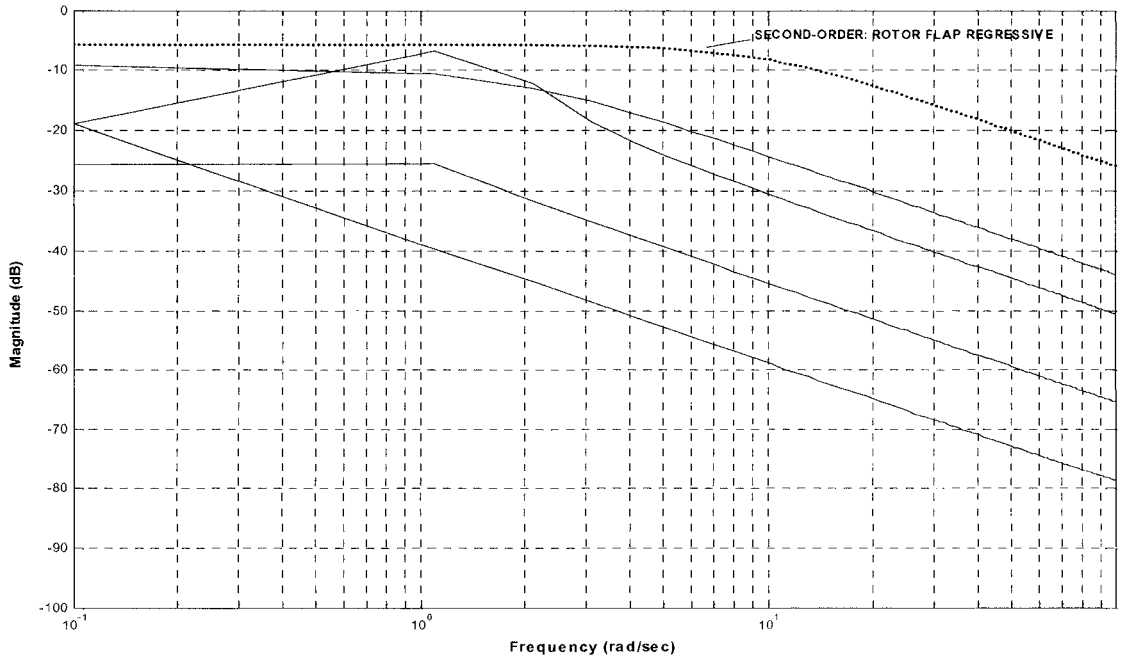

Figure 2.51 Modal Content, On-Axis Lateral Disc Tilt Response – Without Main Rotor RPM

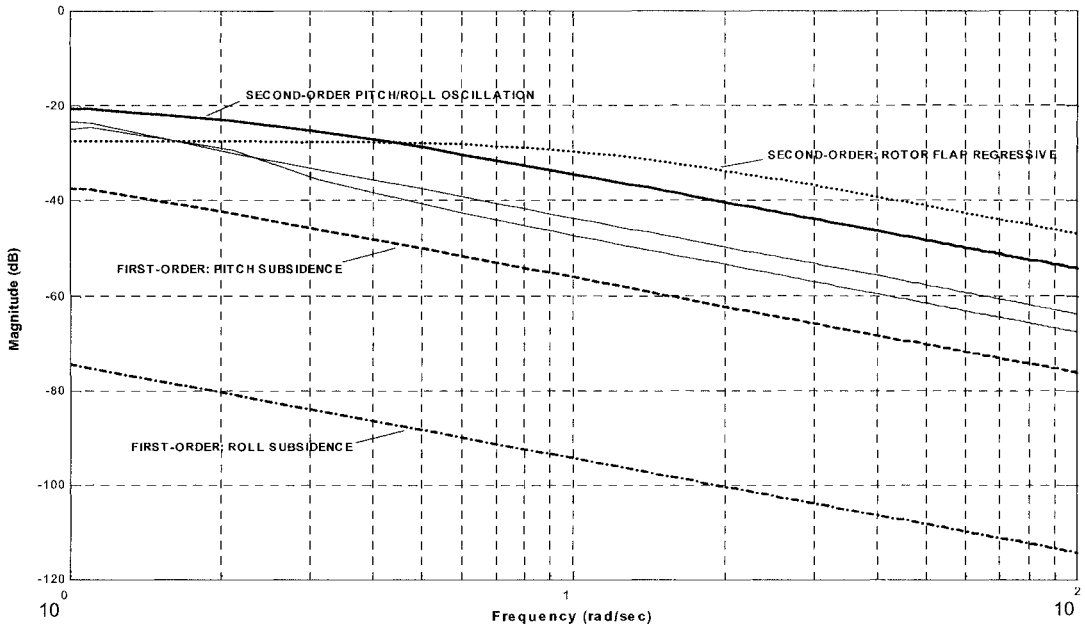

Figure 2.52 Modal Content, Pitch Rate to Longitudinal Cyclic Response – Without Main Rotor RPM

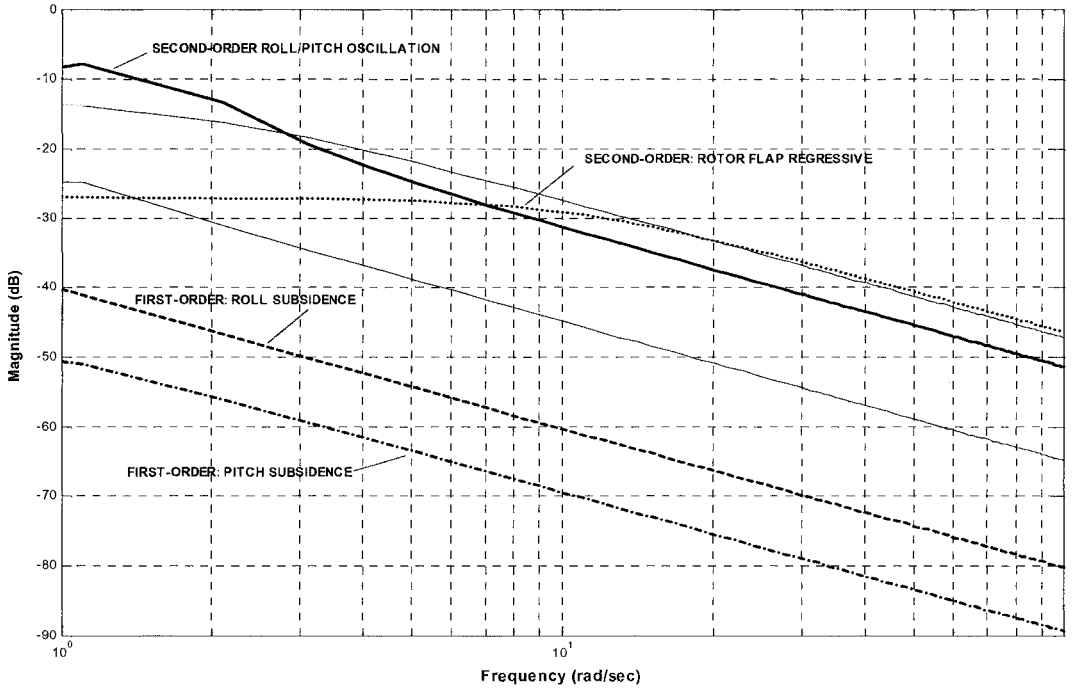

Figure 2.53 Modal Content, Roll Rate to Lateral Cyclic Response – Without Main Rotor RPM

This analysis might then seem to display some anomaly in physics however if it is considered that the hingeless rotor system generates some 4 times the hub moment of an articulated helicopter which dictates the level of cross-couplings of the vehicle, then the responses above define well the hingeless rotor coupled rotor/body dynamics.

As a final analysis of the modes it is worthwhile to compare the Bell 412 ASRA mode placement to other helicopters and thus perform a general "sanity check" of this HMMS.

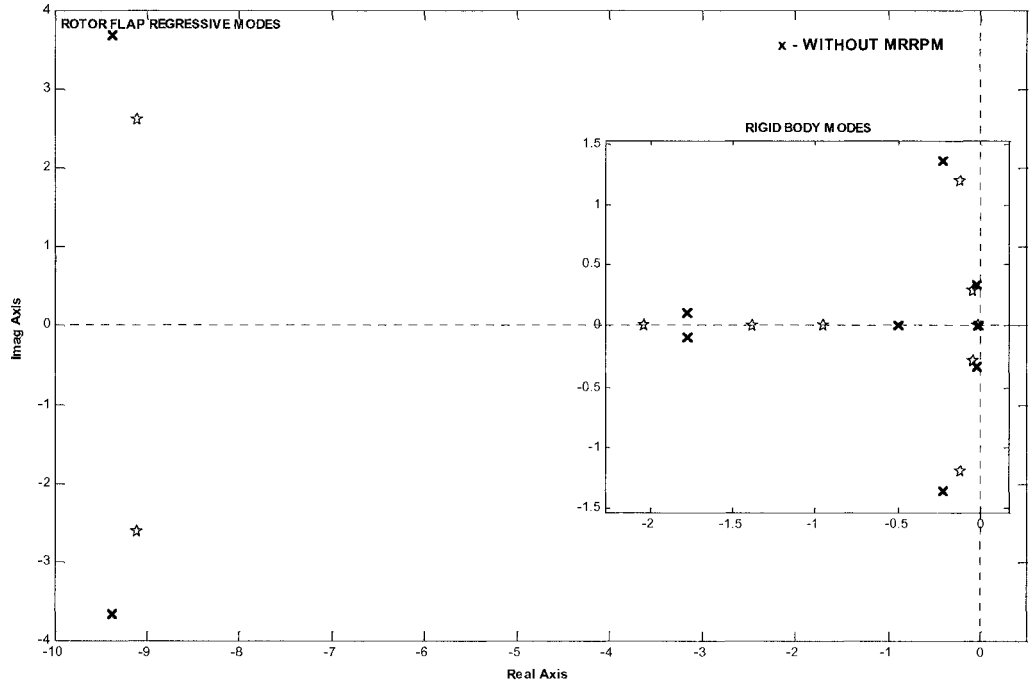

Figure 2.54 Modal Placement of Bell 412ASRA HMMS - Without and With Main Rotor RPM

MODE	HELICOPTER			
	BELL412ASRA ROTOR: HINGELESS SOFT INPLANE MODEL: 8DOF, WITHOUT MRRPM TRIM: 60KTS	BELL412ASRA ROTOR: HINGELESS SOFT INPLANE MODEL: 8DOF, WITH MRRPM TRIM: 60KTS	BO105 ROTOR: HINGELESS SOFT INPLANE MODEL: 9DOF TRIM: 80KTS	
			KALETKA	TISCHLER
Pitch Phugoid	[+0.0712, 0.335]	[+0.0987, 1.2]	[-0.22, 0.34]	[-0.394, 0.302]
Dutch Roll	[+0.161, 1.38]	[+0.156, 0.288]	[+0.14, 2.53]	[+0.219, 2.609]
Spiral	(0.0167)	(0.0151)	(0.03)	(0.0507)
Pitch-1	(0.495)	(0.946)	(0.43)	(0.448)
Pitch-2		(2.03)		(5.843)
Pitch/Roll Oscillation	[0.998, 1.78]			
Roll/Flap			[0.77, 13.5]	[0.788. 12.57]
Regressing Flap Mode	[0.931, 10.1]	[0.961, 9.47]	[0.91, 7.38]	
Longitudinal Flap				(15.93)
Lead/Lag Approx.			[0.015, 14.7]	[0.0557, 15.59]

Notation:

$[\zeta, \omega_0]$ implies $s^2 + 2\zeta\omega_0 s + \omega_0^2$, where ζ = damping, ω_0 = undamped natural frequency (rad./sec.)

$(1/T)$ implies $(s + 1/T)$, (rad./sec.)

Table 2.7 Comparison of Soft-Inplane Hingeless Modal Dynamics; Bell412 ASRA, Bo105[1,90,103,108,109]

Figure 2.54 depicts the mode placement of the rigid-body and rotor longitudinal disc tilt dynamics for the HMMS. The prominent features of the placement are the rotor modes that correlate well between the 2 models. There is however discrepancy of the rigid body modes such that the case without main rotor RPM seems to indicate the development of coupling of body pitch and/or roll behavior at 1.75 rad./sec. In any event, the HMMS analyses are complex and modes interact to such a high degree for the hingeless rotor helicopter that the mode labels for the Bell 412 ASRA depicted in Table 2.7 must be taken as approximations.

2.8.9 Model Fidelity: Derivative Representation of Helicopter Physics

Analysis of hybrid mathematical models is complex if the model structure has inherent derivative correlation. For many of the hybrid mathematical models reviewed, the derivative structure typically included:

- Absent quasi-steady rotor moment derivatives (Lp, Lq, Mp, Mq)
- Absent quasi-steady rotor force derivatives (Xp, Xq, Yq)
- Absent quasi-steady rotor cyclic control derivatives (L1c, L1s, M1c, M1s, X1c, X1s, Y1c, Y1s)

These quasi-steady terms are a result of 6DOF assumptions for low accuracy simple time delay rotor modeling that are inadequate for high bandwidth flight control and handling qualities applications.

The hybrid model structures aim to:

- Capture by explicit rotor equations, the rotor control response and angular rate response effects
- Improve model sensitivity to parameter variation etc. (robustness) by minimization of parameter correlation
- Represent with fidelity the helicopter physics by the derivatives

The derivatives of the Bell 412 ASRA HMMS indicate important characteristics for application of high bandwidth flight control by rotor state feedback. The final HMMS parameterization is shown in Appendix B. There are 12 derivatives with Cramer-Rao Bounds that break the 20% threshold for high parameter insensitivity, parameter correlation, and confidence; these derivatives are Xu, Xp, Xq, Yq, Zu, Zq, La1, Zped, Lcol, Mped, Ncol, and b1lon. Some point calculations will illuminate features of this helicopter.

The roll flapping spring derivative, L_{b1s}, sets the frequency of the hingeless rotor second-order coupled roll/flapping second order mode and the upper limit bandwidth of the 6DOF model such that $\zeta_{RF} = \sqrt{L_{b1s}}$. In the case of the Bell 412 model, this derivative by conversion indicates that the limit is some 9.91 rad./sec. and corresponds to modal placements as indicated in Figure 2.54. The Bell 412 ASRA time constants indicate rotor to rigid body time frame response due to pilot control. For a variety of applications it is appropriate to estimate longitudinal and lateral flapping time constants as equal, $\tau_f \equiv \tau_{b_{1s}} \equiv \tau_{a_{1s}}$, however this does not seem to be the case for this analysis. An approximation shown by

Kaletka[96,97] suggests the rotor flap time constant to be $\tau_b = \left|\frac{L_p}{L_{b1}}\right|$ which indicates a value of 0.0805s. During model development, the longitudinal flap time constant was established to be $\tau_{a1s} = 0.04s$, again suggesting that these constants are not equal. Tomashoski and Tischler[104] apply another estimate by Heffley that suggests $\frac{1}{\tau_f} = \frac{\gamma^* \Omega}{16}\left(1 - \frac{8e}{3R}\right)$, (where; $\gamma^* = \frac{\gamma}{1 + \frac{a\sigma}{16\bar{\upsilon}_0}}$) which provides a high value of 0.1622s.

The roll-flap damping ratio may be estimated by the roll damping and the rotor flap time constant by $\zeta_{RF} = \sqrt{\frac{-1}{4L_P\tau_F}}$. This value corresponds to 134.9% compared to 111% in Figure 1.10. Overall, in magnitude, this indicates the highly damped rotor flap dynamics of the Bell 412 ASRA.

The roll and pitch flapping spring ratio determine the helicopter's ratio of pitch and roll moment of inertia is 1.2345 given by $\left|\frac{L_{b1s}}{M_{b1c}}\right|$. The pitch response couplings, $\left|\frac{M_p}{M_q}\right|$ and $\left|\frac{M_p}{L_p}\right|$, and roll response couplings, $\left|\frac{L_q}{M_q}\right|$ and $\left|\frac{L_q}{L_p}\right|$, which are typically large for helicopters, have null values for the Bell 412 ASRA as defined by the hybrid model given that the Lq, Mp, and Mq derivatives are absent. Their effects are explicitly defined by the incorporated rotor flap dynamics equations and measurements.

The pitch spring constant to roll spring constant defines the ratio of the helicopter's pitch to roll inertia, which is typically on the order of 3.0. Inertias for the Bell 412 ASRA are (I_{xx}=15027800 lbin^2, I_{yy}=67080400 lbin^2) at W=7428.4lb giving a ratio of 4.464. Further then, the pitch spring constant Ma1s should be 1/3 of the roll spring Lb1s; for the Bell 4 ASRA however, this ratio is 0.81.

The parameters that should compare well with the Bo105 hingeless soft inplane rotor helicopter are the flapping spring constants, off-axis response, and the control couplings. The lateral flapping spring constant Kb1s, is 0.001844 by $\left|\frac{L_{\delta LAT}}{L_{b1s}}\right|$, which compares to a value of 0.001045 for the Bo105[90,103]. The off-axis control responses in roll, $\left|\frac{L_{\delta LON}}{L_{\delta LAT}}\right|$, and pitch, $\left|\frac{M_{\delta LON}}{M_{\delta LAT}}\right|$, are both significant (1.1562, 0.8086), indicating highly coupled, high workload, bare-airframe flying characteristics. The pitch control to collective and longitudinal stick control couple, $\left|\frac{M_{\delta COL}}{M_{\delta LON}}\right|$, is of moderate magnitude, (0.4926), indicating considerable collective to longitudinal cyclic coupling.

2.9 Conclusions

A Hybrid Mathematical Model Structure (HMMS) was developed for the Bell 412 ASRA based on measured rotor yoke flap dynamic data from the RSMS. The data indicates:

- Rotor response degrades the nominal 6DOF rigid body response correlation indicating a poor convergence by MMLE. This result can be attributed to the many neglected dynamics, assumptions, and procedures required to extract the model based on the limited resources of this contract.
- The RSMS primary limitation is attributed to single-point and off-blade sensing. Single-point sensing does not capture high order physics such as modes beyond first order and multi-axis mode coupling, or allow for sensor/data cross-correlation. The off-blade sensing does not capture the physics of the rotor system. For example, research has shown that the rotor blade dynamics are out of phase with hub dynamics.
- The HMMS primary limitation is the neglecting of higher order dynamics that have been shown to impact the system identification of HMMS models. These include airmass dynamics and coupled rotor/fuselage/engine dynamics.
- The HMMS structure is thought to suffer from the application of a priori knowledge of soft inplane hingeless dynamics, which were only estimated prior to this contract. Further, the structure requires some further development to match parameter identification and flight control design requirements.
- The lack of lead-lag dynamics is of significant concern to the flight control law development process however, the knowledge that in previous flight tests the lead-lag mode could not be excited as well as the comparison of mode placements with other helicopters indicates this mode has significant damping in uncontrolled form. The effects of temperature, control system dynamics, and feedback dynamics on this mode require further assessment.
- The typically poor off-axis correlation that the HMMS depicts is a remnant of neglected dynamics (rotor dynamics), RSMS data fidelity (purity of rotor dynamics measurements), and model structure (absent and correlated derivatives).
- Through the author's analyses the HMMS is band-limited in high frequency prediction in the range of 2Hz (12.6 rad./sec.) just beyond the rotor flap regressive mode.
- The fidelity of the HMMS is deemed average. The Bell 412 ASRA vehicle manager and system senior aerospace engineer of the NRC-FRL authorized clearance of the 8DOF mathematical model for flight control law development for inflight rotor state feedback investigations.

Chapter 3.0

High Bandwidth Rotorcraft Flight Control Law Design

3.1 Introduction: Flight Control Law Design

In this chapter the author designs model following control laws, which access explicitly the rotor states of the hybrid mathematical model structure (HMMS) for high bandwidth feedback control. Model following control laws provide modularity in the sense that a variety of command models may be configured to alter the closed loop response type. Further, control law design is a challenging optimization procedure whereby trim variables, specifications (handling qualities, aeromechanical stability bounds, etc.), feedback gains, design cross-over frequency, bandwidth, uncertainty and non-linearity of response, and coupled vehicle dynamics are just a few parameters in the design space. It is thus required that control law designs be easily tuned for ground simulation and in-flight engagement.

The control laws described in this chapter are designed to assess the proper gain structures that will be required for implementation in flight on the Bell 412 ASRA.

In this thesis, Classical techniques are used to interpret SISO input-to-output behaviors for rotor system stability, handling/ride qualities metrics, component modeling (actuators, filters, etc.), and response representations. These techniques are based on transfer-function representations that characterize particular helicopter dynamic response with minimal dimensionality. Modern multivariable methods are used to effect control of the helicopter in an effort to attain multiple objectives in the presence of highly non-linear and uncertain dynamics. Although transfer functions are still the most effective form of single axis representation, modern control relies on MIMO state-space representations to capture axis cross-coupled dynamics.

There are 4 guiding principles critical to the control law design process in a Classical framework that include the feedback loop dynamics (open and closed loop), transfer function model structure, frequency domain analyses (Root Locus, Bode, Spectral responses), and time domain analyses (time histories, transient response, etc.). Throughout the following discussion and development, these points serve as guiding principals in the design process.

In a Modern control context model uncertainty that may be associated with mathematical model errors, unknown rotor response dynamics, signal sensor noise, and other non-linearities complicate the control law design process. The fundamental objectives for a multi-axis, multivariable control law include:

- **Flight Envelope Robustness** of the flight control law to changes in the design point condition. This is critical to helicopter flight dynamics that are a function of such variables as vehicle configuration as altered by mission requirements, fuel usage, and atmospheric conditions.
- **Disturbance Rejection** capability associated with perturbation dynamics that are injected into the helicopter control system, rotor system, and digital flight control paths.
- **Command Tracking** of manually generated or digitally developed flight control inputs, of desired flight trajectory, and of desired vehicle dynamics including rigid-body and rotor state forms associated with helicopter performance.

- **Rotor-Control Activity Attenuation** for providing the helicopter with the most efficient usage of its rotor, control, and actuator authorities directed at attaining specified flight characteristics.

In what follows, an investigation into the effects of rotor states and their feedback in closed loop control of helicopter flight dynamic and aeromechanics will be undertaken. In Chapter 1, several control law design techniques were reviewed. Herein, the trajectories and placements of modes in the s-plane that characterize modal dynamics of the helicopter's coupled rotor/body system are of primary concern and interest. As such the author will focus on modal dynamics analysis from a theoretical and experimental perspective by Classical Root Locus Analysis theory, Classical Multivariable control of full-state dynamics, and Eigenstructure Assignment control in full-state feedback form.

3.2 Classical and Modern Multivariable Control of High Bandwidth Helicopters

An introductory tour of the high-bandwidth rotorcraft flight control domain specific to the variable stability helicopter is in order. Discussions will address transfer functions, time and frequency domain dynamics in terms of handling qualities requirements, and the control law design requirements for this study.

3.2.1 Transfer Function Modeling

In order to design control laws for the helicopter, a variety of models are required to represent its physics. The most important model that researchers use for single input and single output analyses is the transfer function that may be derived as follows. A typical time invariant linearization of the rotorcraft may be given by;

$$\dot{x}(t) = [A] \cdot x(t) + [B] \cdot u(t) \qquad 3.1$$

$$y(t) = [C] \cdot x(t) + [B] \cdot u(t) \qquad 3.2$$

where;

x(t) = state vector, u(t) = control vector, y(t)= output,

A = state matrix, B = control distribution matrix, D = control feed-forward matrix

The system may be represented in the frequency domain in transfer function coefficient form G(s), such that;

$$G(s) = \frac{(b_o s^m + b_1 s^{m-1} + \ldots + b_m) e^{-\tau s}}{s^n + a_1 s^{n-1} + \ldots + a_n} \qquad 3.3$$

This form defines the model structure that comprises;

- Input and output variables
- Frequency range of validity based on application
- Numerator and denominator polynomial orders (m, n)
- Component modeling, (e.g.; equivalent time delay), in transfer function form

The state space linearization that was used to derive G(s) in the case of rotor dynamics analyses is not the conventional 6DOF representation of helicopter flight dynamics, but a rotor-state augmented 8DOF system defined by the Bell 412 parameter estimated HMMS.

Input and output variables in this case extend to represent SISO fuselage to control and rotor TPP to control response. This in itself is significant in allowing higher fidelity modeling of the time frame relationship between pilot control, gust input, fuselage response, and rotor response.

Both state space and transfer function models represent derivations of the actual response (parametric models) that were derived from flight test (time, frequency sweep) data gathering from the Bell 412 (non-parametric) models. The frequency range of validity for this research extends out to 20 rad/sec. for high bandwidth variable stability application. Depending on the type of application then, the transfer function structures will be parameterized on low order and high order forms encompassing;

- Classical attitude response modes
- Regressing rotor flap modes (lead-lag modes – not modeled herein)
- Airmass Dynamics (inflow – not modeled herein)
- Actuator dynamics (equivalent time delay or by transfer function component modeling)

In in-flight simulation, high bandwidth servo-electro hydraulic actuators drive the augmented fly-by-wire control system. Modeling these actuators (i.e.; rate and deflection limits) is critical in assessing feedback gain thresholds. These thresholds are also functions of other higher order dynamics such as;

- Sensor noise
- In-plane rotor dynamics
- Inflow dynamics
- Phase margin requirements and high frequency model uncertainty (rotor and structural flexure modes)
- Propulsion system dynamics
- Digital implementation (phase delay, time delay, etc.)

Thus for this research components such as the Bell 412 ASRA actuators are modeled based on detailed design and operational data as component transfer functions.

3.2.2 Dynamics in the Time Domain: Transient Response of the Rotor, Servo, and Fuselage

In the time domain, system stability is derived from analyzing the excited system transient time history. Interpretation of the time history for modal information is dependent upon the correct type of input excitation being applied. Rotor modal data can give researchers invaluable trend data regarding aeromechanical events. Vehicle stability data can allow for the evaluation of characteristic handling qualities response types.

The most important concepts for this research are the following 2 issues: time domain representation of helicopter physics and, monitoring of unstable transient response. Helicopter physics are governed by broad frequency spectrums as was illustrated in Chapters 1 and 2. Handling qualities reside in the lower frequency band while rotor dynamics and aeromechanics in the upper band. It is important that in the application of control inputs, the representation of helicopter physics by mathematical models, and in the observation of coupled rotor/body response, that the researcher realizes that time domain response does not always appropriately represent helicopter dynamics. The time domain response tends to misrepresent pilot control activity, weighting low frequency behavior. This same weighting is true in time domain system identification.

The dynamics in time and frequency domains are required to be bound by specifications for helicopter flight characteristics. The discussion that follows highlights the ADS-33E-PRF and ADS-33C specifications[13,14] applied in this research effort.

3.2.3 Military Rotorcraft Handling Qualities Specifications

The National Research Council Flight Research Laboratory has international expertise in the application of the ADS-33 rotorcraft handling qualities standard[110]. The following discussion will initiate the reader in the area of this helicopter handling qualities specification. The primary objective of applying these specifications is to standardize the results of this research such that they are industry/military relevant, establish a design space for flight control law development, and establish metrics of compliance for the desk-top simulation and ground/flight test portions of this project.

Handling qualities requirements have emerged as a direct result of vehicle design. As was depicted in Table 1.2, ADS-33 military specifications define the capability of the latest generation of light-armed reconnaissance helicopter (LHX program). The helicopter performs a wide variety of tasks over broad operational and safe flight envelopes (OFE and SFE, respectively), consequently ADS-33 categorizes helicopter missions into components or Mission Task Elements (MTE). Response types for these MTE are defined in terms of the flight envelope, the flight condition, and the pilot's workload.

Some key elements of ADS-33 include mission, maneuvers, flight envelope/condition, pilot workload, operable states (failed or functional), and useable cues.

3.2.3.1 Mission Definition

For this research a 60-knot forward flight Target Acquisition and Tracking (TA+T) task is specified for flight control law design and the flight test engagement. In ADS-33, the ground speed range is defined from hover (less than 5kts), low speed (15 to 45kts) and forward flight (greater than 45 knots). It is useful to define a mission for studying ADS-33 compliance. For a forward flight phase military TA+T mission, tasks could be broken down based on altitude. A high altitude TA+T of multiple targets might include climbing and descending through a reference altitude, long-term slalom maneuvers to adjust target

alignment relative to heading, and the final target engagement which could be defined by a radar observation or a weapons engagement. A low altitude TA+T of multiple targets might include aggressive Nap-Of-Earth (NOE) flight terrain following and vehicle masking, aggressive slalom and sharp turns for TA+T, high variation in forward flight speed, and the final target engagements by attitude capture tasks.

3.2.3.2 Maneuvers and Mission Task Elements (MTE's)

As a variable-stability helicopter, the mission of the Bell 412 ASRA is to evaluate integrated control laws and flight technologies. Its mission then is one of emulating a variety of helicopter characteristics based on technology, control response, and mission definition. The maneuvers performed are defined by MTE's that are role-relevant to the vehicle. The ADS-33 MTE's defined above are based on 5 categorizations: precision tasks, aggressive tasks, approach tasks, precision tasks in degraded visual environments, and moderately aggressive tasks in degraded visual environments.

3.2.3.3 Flight Envelope

The defined TA+T mission involved the helicopter's operational and safe flight envelopes (OFE and SFE, respectively). The OFE defines the speed, altitude, vehicle orientations, loading, etc., based on configuration. The handling qualities requirement interplay with both the OFE and SFE of the helicopter to determine its operational capability.

3.2.3.4 Flight Conditions

The ADS-33 specification defines the environmental conditions within which the mission is performed. This dictates the environmental or outside world Useable Cue Environment (UCE) given to the pilot to perform his/her task. These conditions could include Instrument Flight Rules (IFR) and Degraded Visual Environment (DVE) that are based on parameters such as the range of visibility, atmospheric conditions (i.e.; precipitation, temperature, winds, etc.), and terrain features, to name a few.

3.2.3.5 Pilot Workload

While performing the said forward flight TA+T, the pilot must contend with cockpit management tasks. His/her workload is graded based on the divided attention devoted to both flying and systems operations of the vehicle. The bare-airframe vehicle response stability relative to the level of divided attention is a critical handling qualities metric defining pilot workload to control the vehicle.

3.2.3.6 Response Types

As the Bell 412 ASRA evaluates rotor state feedback control by emulating our TA+T mission, a variety of response types may be used to allow the pilot to tailor the vehicle's response to a specific mission task. Most helicopters exhibit an unaugmented or bare-airframe Rate Command (RC) response type that is non-compliant with military handling requirements. As was shown in Chapter 2, without feedback control

the helicopter is highly cross-coupled, (heave, longitudinal, lateral, and directional axes), has low bandwidth for axis stability, and has unstable low frequency rigid body dynamics. The compliant RC response provides proportional control of angular velocities about the vehicle pitch, roll, and yaw axes due to pilot control input. Pilots prefer this response for agile response under operations that feature fully attended cockpit management and good external visual cueing.

The ACAH response provides proportional control of vehicle attitude angle to pilot cyclic control. Upon removing the control input the helicopter returns to pre-input trim.

For precision hovering mission tasks, the Translational Rate Command Position Hold (TRCPH) response type is desired. This response type produces a constant translational rate upon pilot input and position hold for no control input. The TRCPH is also applicable in NOE maneuvers in degrading external visual cue conditions.[13,14,74]

3.2.4 Control Law Design Requirements

A subset of ADS-33-E-PRF and ADS-33C forward flight requirements are to be applied in this research to establish guidelines for the flight control law design process. The methodologies for compliance with these requirements are outlined in the Appendix A of this document.

3.2.4.1 Fidelity-Robustness

Overall the primary requirement is to evaluate the HMMS for overall fidelity and robustness to the flight control effort. Thus minimal changes should be required to implement the control laws on the flight test vehicle. Further, the gain structures for feedback should effect designed control action with good model following over an off-design margin. The design point is the 60-knot forward flight condition with Attitude Command Attitude Hold (ACAH) response.

3.2.4.2 Disturbance Rejection

Rotor state feedback has the potential to improve the controller's ability to reject both gust attitude-rate inducing dynamics and control-actuation signal noise perturbation. Standard gust and signal noise are injected to assess controller performance.

3.2.4.3 Attitude Bandwidth and Phase Delay

To ensure input control response over the closed loop system bandwidth with moderate input frequencies, bandwidth and phase delay are bound. The compliance is defined for pitch, roll, and yaw attitude frequency response.

3.2.4.4 Mode Placement

Of particular importance in this study is the requirement of mode location, trajectory, and interaction in the s-plane. This specification in ADS-33C was based on low frequency rigid-body dynamics. However, requirements for this project include the rotor flap and lead-lag dynamics out to 20 rad./sec.

3.2.4.5 Control Power

The TA+T task requires high maneuverability and agility, thus control power is critical in the attainment of both attitude rates and vertical axis response. Compliance with specifications under these groupings are developed based on large amplitude attitude change, vertical axis velocity, and rotor disc tilt response due to longitudinal control response

3.2.4.6 Axis De-coupling

Decoupling of the pitch, roll, yaw, and heave dynamics of the ASRA will be evaluated through compliance with several ADS-33 metrics. These include the forward flight pitch-to-roll and roll-to-pitch coupling, and the hover/low-speed yaw response due to collective specifications.

3.3 Modeling the Physics of the Bell 412 ASRA

Mathematical, transfer function, and linear and non-linear simulation models were used throughout this investigation to create a basis for predicting the helicopter performance due to rotor state feedback applied in real-time.

3.3.1 Mathematical Models

As was developed in Chapter 2, the 8DOF hybrid mathematical model structure (HMMS) is used as the baseline design plant for flight control law design. The fuselage is modeled as a rigid body. Rotor dynamics are based on the soft inplane hingeless hub yoke flap-bending dynamics. Torsional and lead-lag rotor dynamics are not modeled because the frequency bandwidth of such dynamics are beyond the range of compatibility for handling qualities. As well, these dynamics could not be measured for explicit application in this investigation. The rotor inflow airmass dynamics is not included primarily because they could not be measured for explicit application. It should be noted that both of these omissions will lead to the accruing of uncertainty in the overall design and fidelity-robustness effects.

The control vector is defined as:

$$u = [\theta_{1c}\ \theta_{1s}\ \theta_0\ \theta_{tr}] \tag{3.4}$$

The output vector **y** is defined as:

$$y = [p\ \ q\ \ w\ \ r\ \ \phi\ \ \theta\ \ u\ \ v\ \ \psi]^T \tag{3.5}$$

In order to retain non-singularity in the design plants no poles or perfect integrators may be present. As such caution must be applied with regards to the heading state, which results from integration of yaw rate. The removal of this state is studied in this research specifically for control law synthesis of Eigenstructure Assignment control. The state space representation of the system is then represented in linearized dynamics by standard state and output equations of the form illustrated by Equations 3.1 and 3.2. These equations may be visualized in standard control block diagram form as shown in Figure 3.1 that represents the design plant from a flight control design perspective.

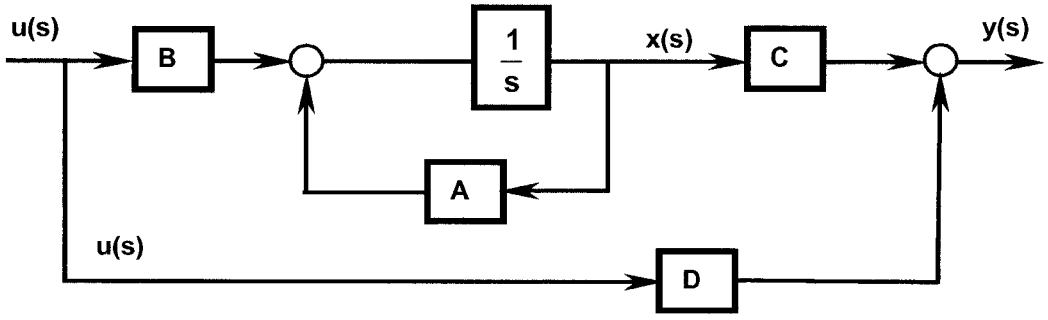

Figure 3.1 Design Plant, G(s)

The matrix [*D*], would be non-zero if there were direct couplings between the control inputs and any of the measured outputs. This can happen, for example, if a velocity vector is located downstream of a control surface. In the present application, the control feed-forward matrix [*D*] has been assumed to be zero. The design plant, defined earlier, is represented by the transfer function, *G*(*s*) as follows:

$$G(s)=[C](sI-[A])^{-1}[B]+[D] \qquad 3.6$$

G(*s*) is a complex function containing the magnitude and phase information of the output response to the sinusoidal input. The design plants are defined by the following state variables that encompass rigid body motion, and rotor hub yoke flap dynamics:

1. State description of the six degrees of freedom rigid body motion of the helicopter's fuselage. Attitude-rates and attitude-angles are primarily used for fuselage state feedback.
2. State description the flapping of the rotor hub yoke in the non-rotating frame. The hub yoke flap parameters β_0, β_{1c}, and β_{1s}, that are related to the flapping angle $\beta^{(k)}$ of the k^{th} blade. The parameters used for rotor state feedback are longitudinal and lateral disc-tilt dynamics, a_1 and b_1 respectively, describing the tip-path-plane.

Note that time derivatives (rates, accelerations) are applied where required.

The 8DOF hybrid mathematical structure (HMMS), and thus G(s), represents the Bell 412 ASRA at a 60 knot design point; the rotor speed Ω (Nominal=324RPM) is constant.

Actuator modeling of the Bell 412 ASRA is unconventional in that the variable stability FBW installation on the aircraft includes both the standard Bell 412HP actuators and the ASRA project actuators. The dynamics of the standard Bell 412HP actuators controlling the swashplate and tail rotor collective are modeled by four (4) identical second order transfer functions, $G_{acto}(s)$:

$$G_{acto}(s)=\frac{\delta_{act}(s)}{\theta_{com}(s)}=\frac{1600}{s^2+55.95s+1600} \qquad 3.7$$

The dynamics of the Bell 412 ASRA fly-by-wire (project), actuators, which are in series with those above, are modeled by four(4) identical second order transfer functions, $G_{actp}(s)$:

$$G_{actp}(s)=\frac{\delta_{act}(s)}{\theta_{com}(s)}=\frac{3600}{s^2+83.9s+3600} \qquad 3.8$$

The design plant state vector may be defined by 15 parameters:

$$x_{15}=[u\ v\ w\ p\ q\ r\ \theta\ \phi\ \psi\ a_1\ b_1\ \delta_{LON}\ \delta_{LAT}\ \delta_{COL}\ \delta_{PED}] \qquad 3.9$$

Reduced order models were created throughout the design process to represent and scrutinize various dynamics of the helicopter. From the 8DOF state matrix then, the general procedure involves state partitioning, expansion, and discarding based on the output dimension required.

3.3.2 State Space Models

The fully coupled state space system is defined by an 11 state matrix that is represented by;

$$\begin{bmatrix} \dot{u} \\ \dot{v} \\ \dot{w} \\ \dot{p} \\ \dot{q} \\ \dot{r} \\ \dot{\theta} \\ \dot{\phi} \\ \dot{\psi} \\ \dot{a}_1 \\ \dot{b}_1 \end{bmatrix} = \begin{bmatrix} X_u & X_v & X_w & X_p & X_q & X_r & -g\cdot\cos\theta_0 & 0 & 0 & X_{a_1} & X_{a_1} \\ Y_u & Y_v & Y_w & Y_p & Y_q & Y_r + u_0 & 0 & g\cdot\sin\theta_0 & 0 & Y_{a_1} & Y_{b_1} \\ Z_u & Z_v & Z_w & Z_p & Z_q + u_0 & Z_r & -g\cdot\sin\theta_0 & 0 & 0 & Z_{a_1} & Z_{b_1} \\ L_u & L_v & L_w & L_p & L_q & L_r & 0 & 0 & 0 & L_{a_1} & L_{b_1} \\ M_u & M_v & M_w & M_p & M_q & M_r & 0 & 0 & 0 & M_{a_1} & M_{b_1} \\ N_u & N_v & N_w & N_p & N_q & N_r & 0 & 0 & 0 & N_{a_1} & N_{b_1} \\ 0 & 0 & 0 & 0 & 1 & 0 & 0 & 0 & 0 & 0 & 0 \\ 0 & 0 & 0 & 1 & 0 & \tan\theta_0 & 0 & 0 & 0 & 0 & 0 \\ 0 & 0 & 0 & 0 & 0 & \sec\theta_0 & 0 & 0 & 0 & 0 & 0 \\ 0 & 0 & 0 & 0 & a_{1_q} & 0 & 0 & 0 & 0 & a_{1_{a_1}} & b_{1_{b_1}} \\ 0 & 0 & 0 & b_{1_p} & 0 & 0 & 0 & 0 & 0 & b_{1_{a_1}} & a_{1_{b_1}} \end{bmatrix} \begin{bmatrix} u \\ v \\ w \\ p \\ q \\ r \\ \theta \\ \phi \\ \psi \\ a_1 \\ b_1 \end{bmatrix}$$

$$u = \begin{bmatrix} \delta_{LON} \\ \delta_{COL} \\ \delta_{LAT} \\ \delta_{PED} \end{bmatrix} \qquad 3.10$$

For this research the standard reduced order models included uncoupled longitudinal and lateral/directional dynamics. Reduced order modeling of the longitudinal dynamics involved the uncoupled state space form:

$$\begin{bmatrix} \dot{u} \\ \dot{w} \\ \dot{q} \\ \dot{\theta} \\ \dot{a}_1 \end{bmatrix} = \begin{bmatrix} X_u & X_w & X_q & -g\cdot\cos\theta_0 & X_{a1} \\ Z_u & Z_w & Z_q + u_0 & -g\cdot\sin\theta_0 & Z_{a1} \\ M_u & N_w & M_q & 0 & N_{a1} \\ 0 & 0 & 1 & 0 & 0 \\ 0 & 0 & a_{1_q} & 0 & a_{1a1} \end{bmatrix} \begin{bmatrix} u \\ w \\ q \\ \theta \\ a_1 \end{bmatrix} \qquad 3.11$$

$$u = \begin{bmatrix} \delta_{COL} \\ \delta_{LON} \end{bmatrix}$$

Reduced order modeling of the lateral/directional dynamics involved the uncoupled state space form:

$$\begin{bmatrix} \dot{v} \\ \dot{p} \\ \dot{r} \\ \dot{\phi} \\ \dot{b}_1 \end{bmatrix} = \begin{bmatrix} Y_v & Y_p & Y_r & -g\cdot\cos\theta_0 & Y_{b1} \\ L_v & L_p & L_r & 0 & L_{b1} \\ N_v & N_p & N_r & 0 & N_{b1} \\ 0 & 1 & 1 & 0 & 0 \\ 0 & b_{1_p} & 0 & 0 & b_{1_{b1}} \end{bmatrix} \begin{bmatrix} v \\ p \\ r \\ \phi \\ b_1 \end{bmatrix} \qquad 3.12$$

$$u = \begin{bmatrix} \delta_{LAT} \\ \delta_{PED} \end{bmatrix}$$

3.3.3 Uncoupled Non-Linear Simulation Model of Fuselage and Rotor State Feedback

For developmental work, a simple single axis, uncoupled simulation model was applied to evaluate and assess feedback control characteristics as shown in Figure 3.2. These models could use either transfer function or state space dynamics to describe the vehicle's axis or component of concern.

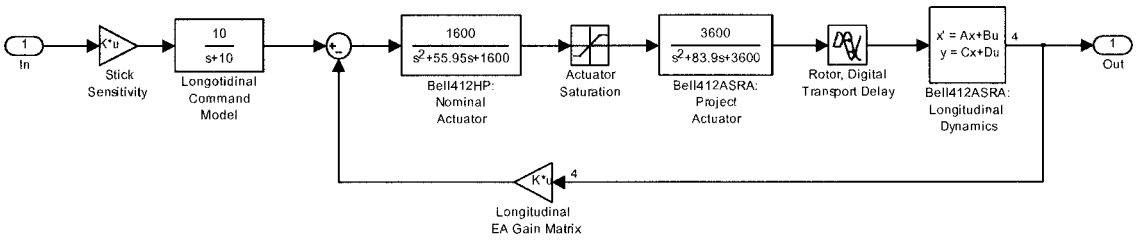

Figure 3.2 Standard, Single-Axis Control Format

For vehicle axis simulation, the single axis format consisted of a command set (command model and stick sensitivity, Bell 412 ASRA nominal and project actuation descriptions), non-linearities (rotor, digital transport delay, and actuator saturation limits), and the vehicle dynamics. The helicopter has inherently linear dynamics in terms of control response and thus these low order uncoupled simulations were highly representative of the aircraft at design point conditions.

3.3.4 Coupled Non-Linear Simulation Model of Fuselage and Rotor State Feedback

For model implementation an updated coupled nonlinear simulation was developed by Gubbels and Ellis to simulate the Bell 412 ASRA flight dynamics. This model structure was developed to correct deficiencies found in the original NRC-FRL Bell 412 ASRA validation model previously employed.
The model structure is shown in Figure 3.3 and consists of several interacting subsystems. The pilot input subsystem contains the basic longitudinal, lateral, directional, and collective input set from the pilot. The kinematics subsystem integrates the angular rates to obtain the vehicle Euler angle attitudes. This subsystem requires input from initial trim Euler angles and 8DOF state attitude-rates. The kinematic equations use the classical Euler angle representation:

$$\dot{\phi} = p + \tan\theta(q\sin\phi + r\cos\phi) \qquad 3.13$$

$$\dot{\theta} = q\cos\phi - r\sin\phi \qquad 3.14$$

$$\dot{\psi} = \frac{q\sin\phi + r\cos\phi}{\cos\theta} \qquad 3.15$$

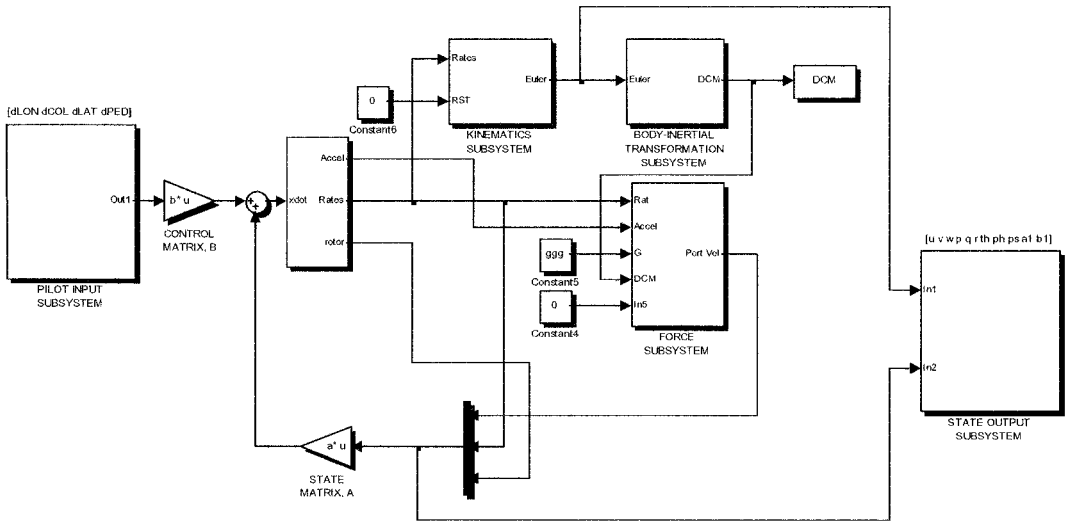

Figure 3.3 Baseline Coupled Non-Linear Simulation Environment (BNLSE)

The output is sent to the vehicle state vector and to the input of the body-inertial transformation subsystem. The latter subsystem computes the direction cosine matrix required for transformation from inertial to the body frame. The direction cosine matrix (DCM) is given by;

$$DCM = \begin{bmatrix} C_\theta C_\psi & C_\theta S_\psi & -S_\theta \\ S_\phi S_\theta C_\psi - C_\phi C_\psi & S_\phi S_\theta S_\psi + C_\theta C_\psi & S_\phi C_\theta \\ C_\phi S_\theta C_\psi + S_\phi S_\psi & C_\phi S_\theta S_\psi - S\phi C_\psi & C_\phi C_\theta \end{bmatrix} \qquad 3.16$$

This model forms the computational subsystem for the simulation employed by the author in flight control algorithm development. The primary additions to the base model is the control actuation subsystem and non-linearities which include:

- Bell 412HP Actuators
- Bell 412ASRA Project Actuators
- Actuation Limits
- Digitization and Non-Linearity Time and Phase Delay Dynamics

For fully coupled non-linear simulation the baseline model is incorporated in a flight control development environment (FCDE) that incorporates the Bell 412 ASRA control-actuation loop, trim settings, and disturbance injection blocks as shown in Figure 3.4.

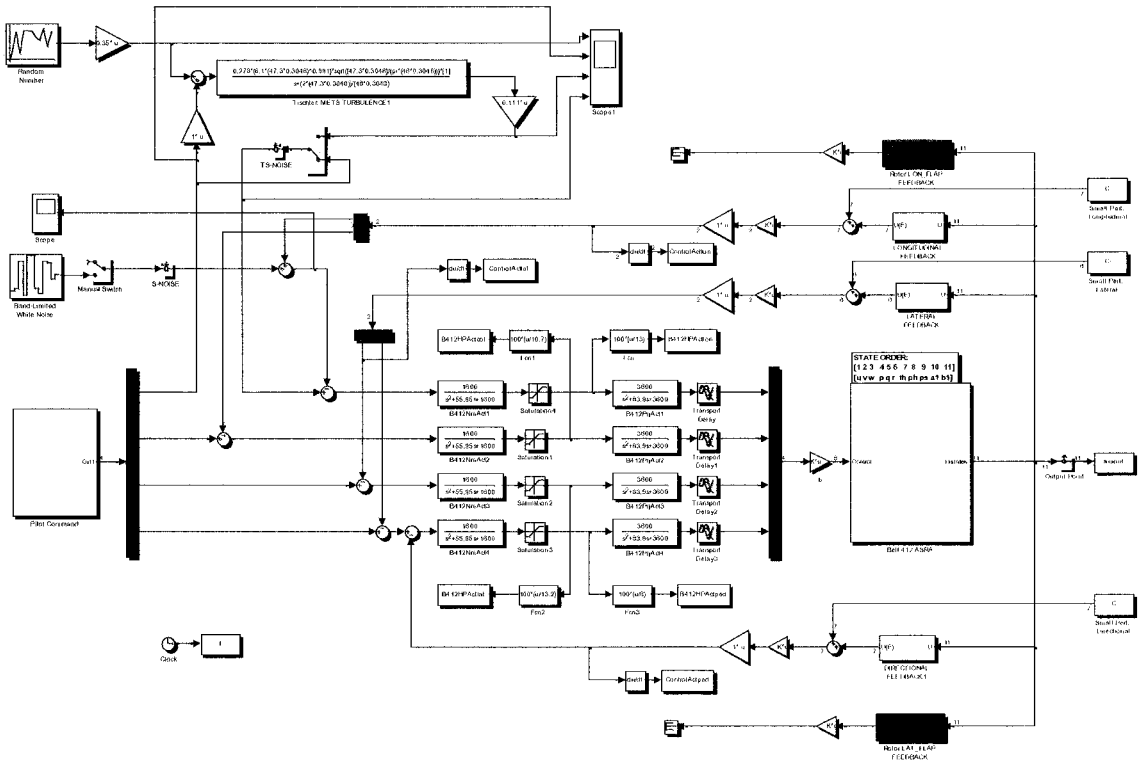

Figure 3.4 Flight Control Development Environment (FCDE)

3.3.5 Model Validation

Prior to implementation the simulation tools were validated to ensure the physics of the Bell 412ASRA were being properly represented. These physics were evaluated without the rotor state feedback and for a single 60-knot design point. Figures 3.5 to 3.8 present the model validation results depicting correlation quality between a Bell 412 ASRA flight test data set and the BNLSE based on the 8DOF Hybrid Mathematical Model Structure (HMMS). These figures show the HMMS and flight test data correlation for a longitudinal 2-3-1-1 cyclic control input. Similar trend results were demonstrated in the lateral and directional axes demonstrating a high level of confidence in these simulation tools.

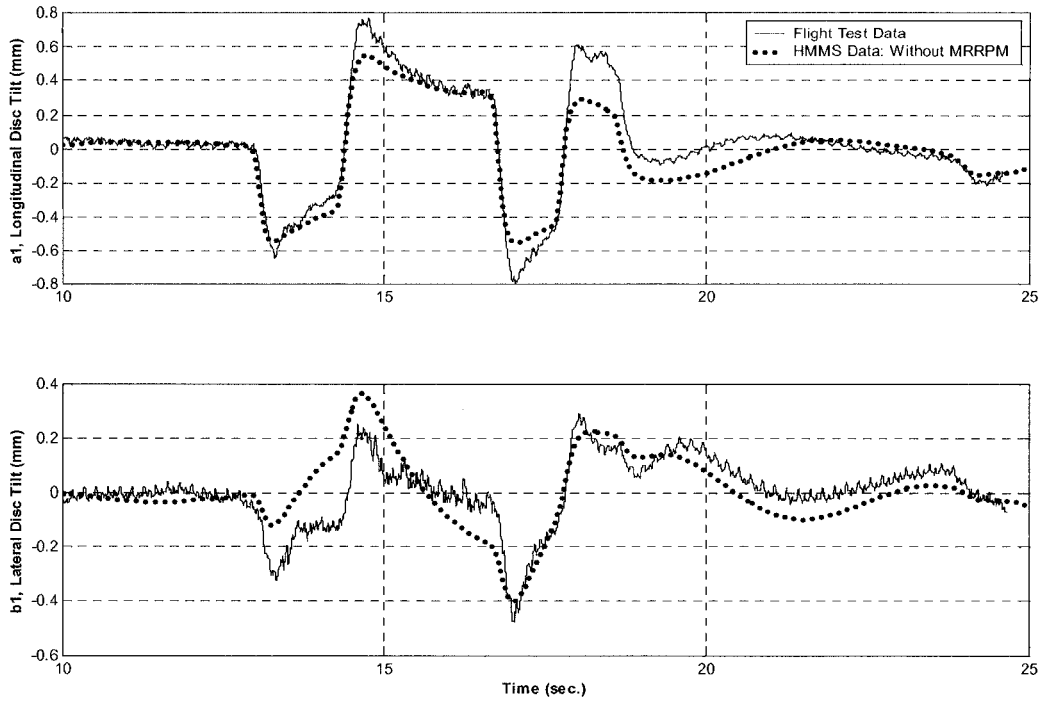

Figure 3.5 Validation Results – Rotor Disc Tilt Dynamics

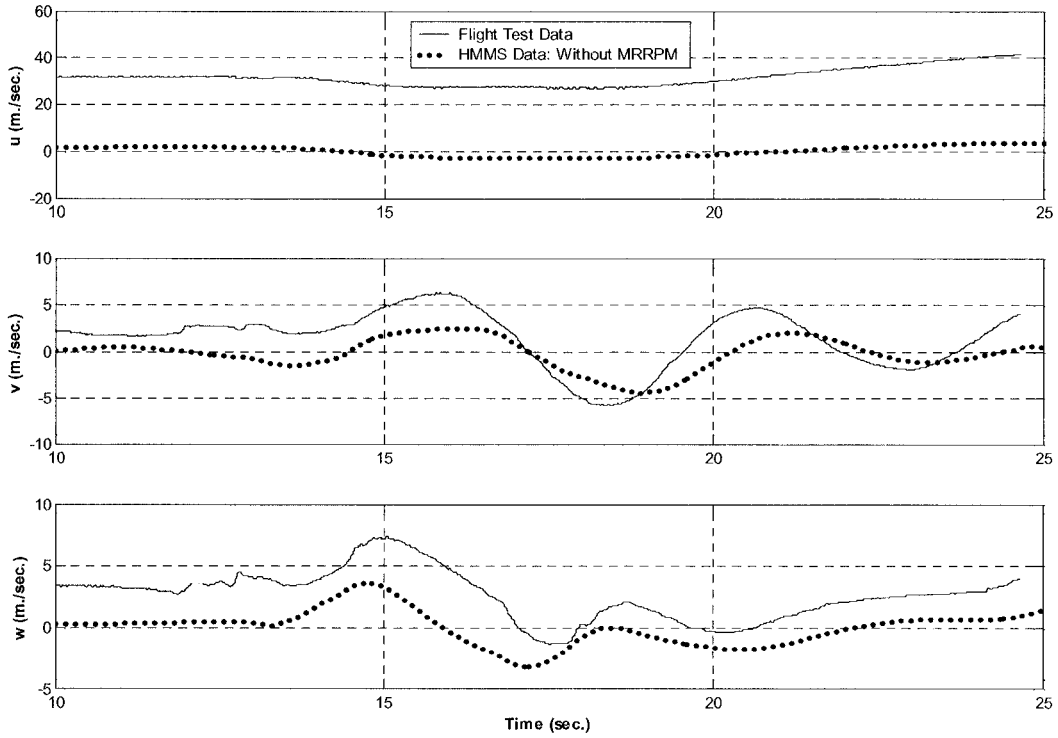

Figure 3.6 Validation Results – Translational Velocities

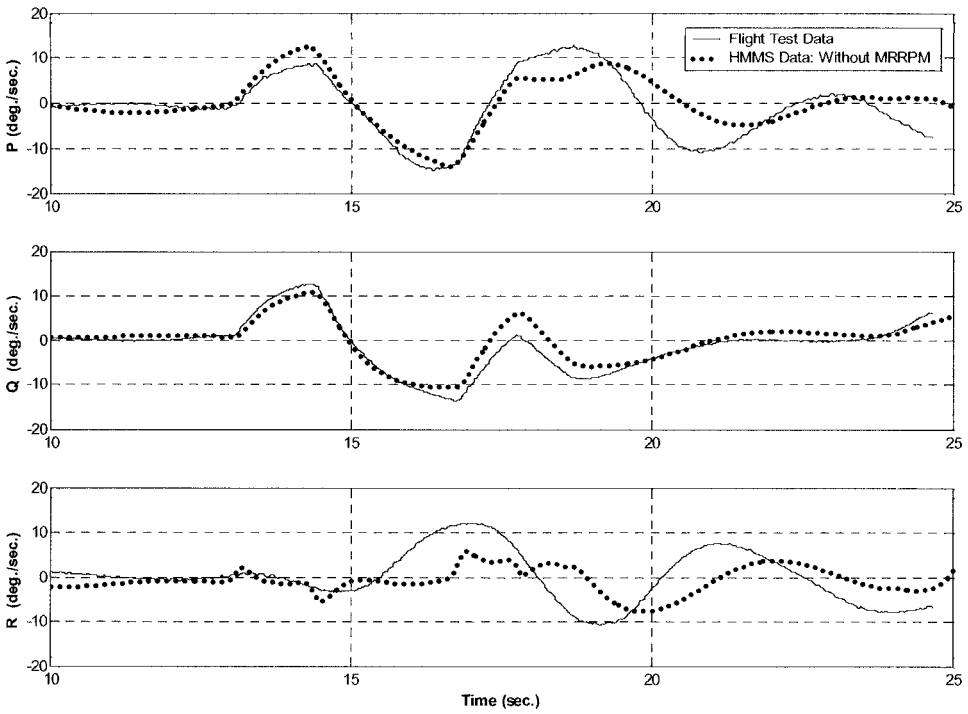

Figure 3.7 Validation Results – Attitude-Rates

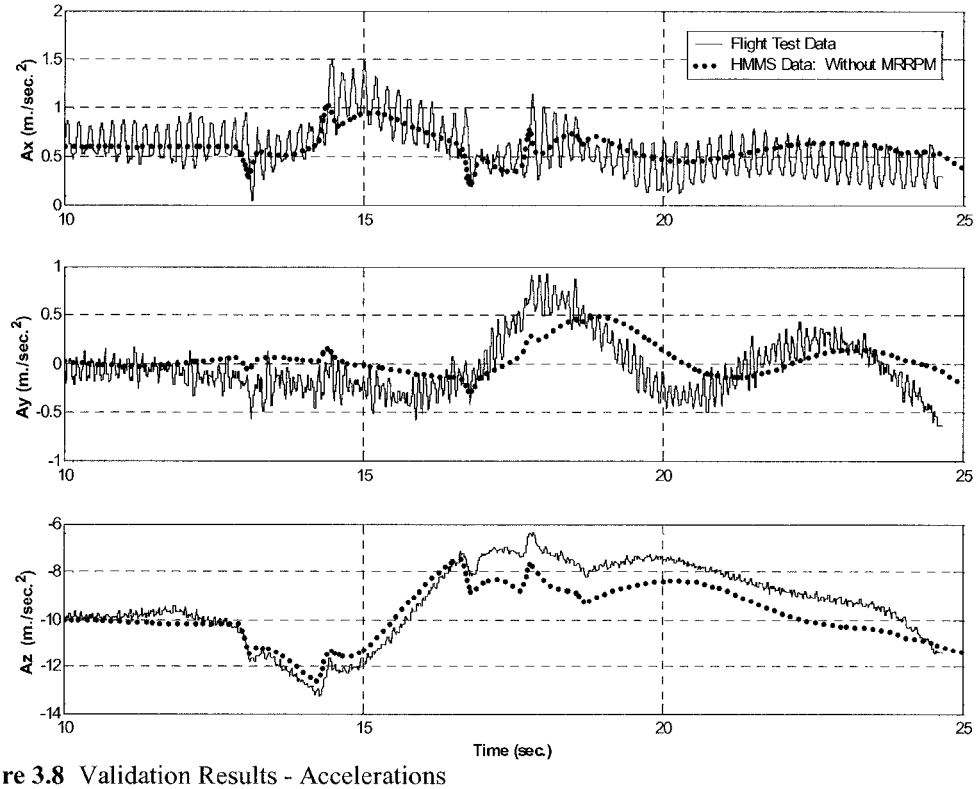

Figure 3.8 Validation Results - Accelerations

The validation results are average in terms of overall time history matching. There are several characteristics that relate to HMMS development fidelity. The rotor dynamics show better correlation in longitudinal as opposed to lateral flap dynamics, which is in agreement with the analyses in parameter identification analyses (Chapter 2). In particular it is noted that vehicle response demonstrates the HMMS is deficient in off-axis correlation with flight data. Tischler[102,103] demonstrated that higher order system identification models should have high coherence across the rotor modal frequency range (i.e.; some 10 to 15 rad./sec. for hingeless rotors). By reference to Figures 2.13 and 2.16 of Chapter 2, we note that the coherence of longitudinal and lateral rigid-body and rotor disc tilt dynamics begin to drop out in the 13 to 18 rad./sec range. The forward flight speed (Figure 3.6) shows the design flight or trim velocity correction (30 m/s or 60 knots). The other translational velocities show less off-trim correlation as depicted in Figure 3.6. The accelerations match well, although A_y and A_z depict some off-phasing at approximately 12.5 seconds; this may be yaw attitude-rate, R, depicting both off phase response and coupling with what appears to be rotor flap or vehicle acceleration dynamics. The characteristic high frequency noise in the acceleration data is thought to be due to the tracking of the rotor system.

Next the validation of the FCDE was primarily based on repetitively ensuring "sanity" of the overall vehicle trim conditions. This process was repeated throughout the flight control design process. The null-control input vehicle trim responses are shown in Figures 3.9 to 3.10.

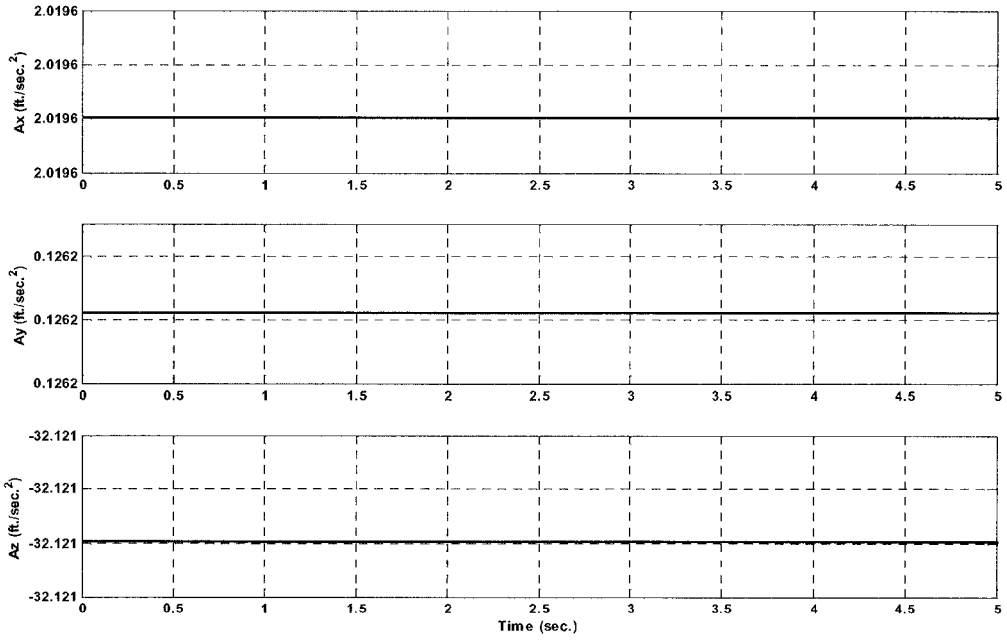

Figure 3.9 FCDE – Null Control Acceleration Response

The trim conditions depicted in Figure 3.10 of the FCDE time history response due to the initial state Euler angles given by $[\theta\ \phi\ \psi]$ = [3.5979, -0.2252, 257.5006] degrees. These angles were extracted, from the system identification flight test data gathered as mentioned in Chapter 2. The flight test point is from a longitudinal cyclic step (CASE kf06.cmb) with conditions including a pressure altitude of 2320 ft., fuel status of 8875.7 lb., and indicated airspeed of 63 knots.

The acceleration response (Figure 3.10) depicts the effects of the initial Euler angles, by developing initial longitudinal and lateral accelerations; gravitational acceleration is also nominally depicted. The time history shows null responses with exception of the Euler angles.

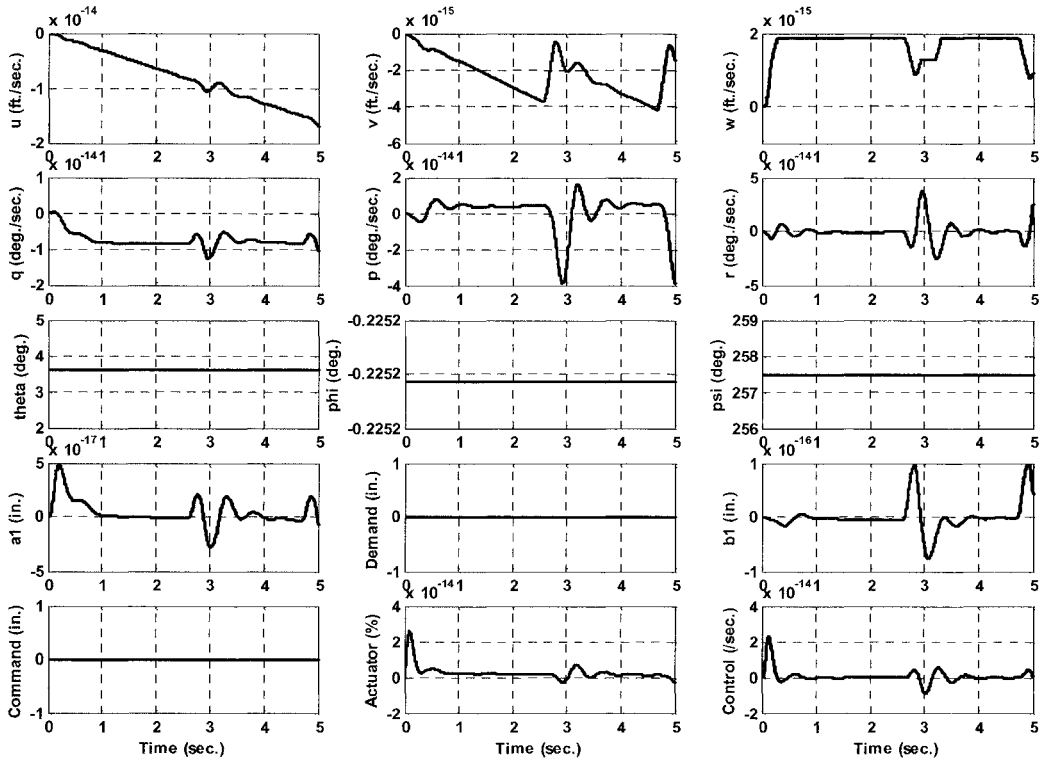

Figure 3.10 FCDE – Null Control Time History Response

With the simulation tools in place and the specifications tabulated we now proceed to explore the effects of rotor state feedback on the hingeless soft-inplane Bell 412 ASRA from first principals. The ADS-33 specifications for military rotorcraft will be referred to repeatedly in an effort to bound and optimize performance.

3.4 Theoretical Developments of High Bandwidth Feedback Gain by Classical Control Methodology

In this research, a Classical framework is applied to develop an understanding of the effects of rotor state modes and feedback in closed loop control as well as to synthesize Classical Multivariable control laws. The maximum closed loop feedback gains are limited by several parameters in the flight control law design space:

i. Sensor noise associated with the data acquired from the aircraft in real time but also having been acquired during the system identification of the aircraft

ii. Aeromechanical stability influences specifically associated with the out-of-plane (rotor flap dynamics) and more critically inplane (lead-lag dynamics) of the hingeless rotor system. For this research, an important indicator of inplane aeromechanical stability will be actuator activity (magnitude, phase).

iii. Vehicular phase margin requirements which are an accumulation of phase contributions from actuators digitization, rotor system dynamics, pilot dynamics, and unmodelled dynamics

iv. Vehicular latencies that are accrued largely through the high bandwidth variable stability flight control system's digital implementation

These limitations place restrictions on the capability to effect control over mode trajectory and placement in the s-plane in order to achieve desired response. Research into highly augmented rotorcraft flight control by Tischler[78] and Takahashi[87] establishes some requirements on this procedure. Results from system identification and flight controls research on helicopters such as the UH-60 ADOCS and Bo105 helicopters establishes trends to follow for the high bandwidth environment of in-flight simulation based on articulated and hingeless rotor dynamics.

In the area or rotor state feedback and higher order dynamics Classical control laws have been a fundamental tool in analyses. Mullen et al.[77] applied SISO as well as Classical Multivariable/Modern controllers to experiments of hingeless rotor state feedback on the DERA-Augusta Westland Rotor Rig. Much earlier in a flight test initiative, Briczinski et al.[54] reported on a 1975 study featuring combined rigid-body and rotor-state feedback control of a Sikorsky CH-53A helicopter. Investigations aimed to determine specifically how rotor tip-path-plane and rigid-body state feedbacks altered rotor and fuselage response and to evaluate the practical limitations of in-flight digital signal feedback in FBW context.

In what follows the author embarks on an exploration of the effect of hingeless rotor dynamics in closed loop feedback control by attitude command controllers.

3.4.1 Design of Classical Attitude Command Attitude Hold (ACAH) Controllers

For this flight test investigation, the ACAH response type was chosen for characterizing a baseline piloted control response. ACAH requires the feedback of attitude and attitude-rate signals. The response type will typically be driven by a command model in the control law which is a second order transfer function defined by:

$$\frac{\theta_{com}}{\delta(s)}(s) = \frac{M_\delta \omega^2}{s^2 + 2\zeta\omega s + \omega^2} \qquad 3.17$$

$$\frac{\phi_{com}}{\delta(s)}(s) = \frac{L_\delta \omega^2}{s^2 + 2\zeta\omega s + \omega^2} \qquad 3.18$$

The stabilization cross-over frequencies (ω_c) and ACAH characteristic bandwidths (ω_{BW}) are based on of 3-6 rad./sec. and 2-4 rad./sec. respectively. For high bandwidth flight control, a high cross over frequency suppresses low frequency dynamics by zero cancellation and lead-compensation by attitude and attitude-rate feedback. However the high bandwidth is restricted due to rotor mode stability and digitization requirements of the control systems.

In the area of rotor mode instability of the Bell 412ASRA two points are made with regard to out-of-plane and inplane dynamics. Firstly, setting high rigid body feedback gains to attain the crossover frequencies necessary for high bandwidths is limited by the destabilization of the rotor flap regressive mode. This point will be highlighted in the next section by Root Locus analyses.

Secondly the unknown nature of the lead-lag dynamics is critical to aeromechanical stability. Unfortunately for this program, the lead-lag dynamics were not identified and can only be estimated prior to flight test trials. Setting high rigid body gains can lead to the coupling of the rigid body and lead-lag rotor dynamics. [42,43]

To mitigate against aeromechanical events, we begin with rotor response predictions using other helicopters to establish proper trends. The Bell 412 ASRA soft inplane hingeless rotor system incorporates lead-lag dampers. Data for this discussion is referenced from Figure 1.10, Figure 2.54, and Table 2.7. The HMMS has predicted the regressive flap mode lies at approximately 9.5 rad./sec. We assume that the Bell 412 inplane dynamics are damped far more than say either the AH64 or Bo105 hingeless rotor helicopters. For a regressive-lag damping of 75% giving a lag mode frequency of 12.34 rad./sec., this places the flap and lag mode eigenvalues as shown in Figure 3.11; the estimated Bell 412 lag mode is highlighted. This illustrates the effect of the damping designed into the inplane (lead-lag) rotor dynamics of the utility-based Bell 412. Now, let's select a high design cross-over frequency of 6 rad./sec (0.25/rev.). The Bo105 without lag dampers has a non-rotating frame regressive lag frequency greater than 0.4; this parameter in the Bell 412 ASRA is postulated to be less than 0.4. This suggests that the design cross over frequency and inplane dynamics have good separation and helps mitigate against

coupled rotor body phenomena. Precautions will be made during the flight test program such that the flight control laws will not be engaged on the ground and to use incremental gains and control input magnitudes/phasing.

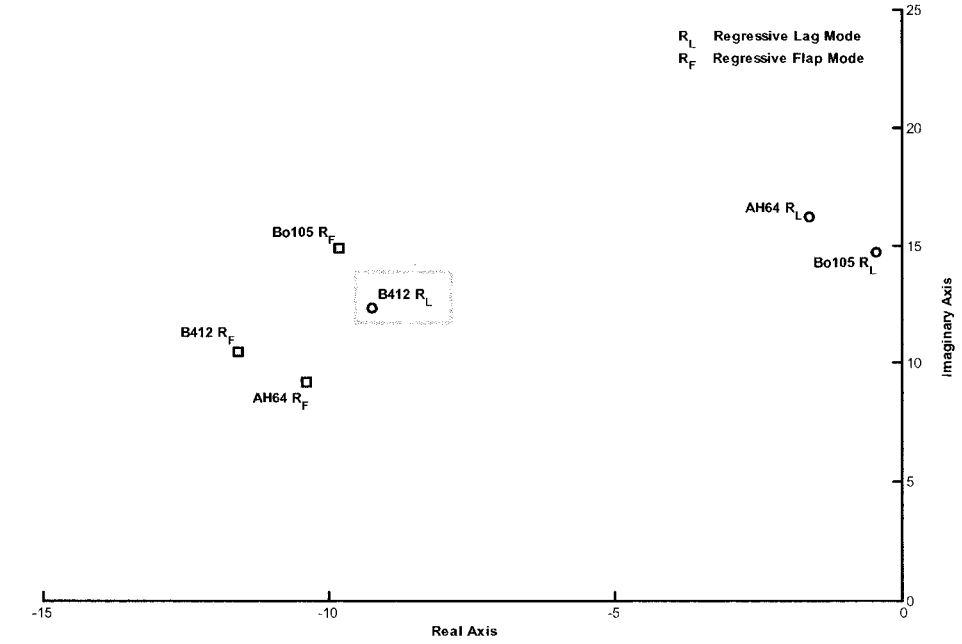

Figure 3.11 Prediction of the Bell 412 ASRA Rotor Mode Locations

The next point to bring forward is that of actuation activity and phase delay limits for achieving aeromechanical stability and handling qualities requirements. Plotting the combined rotor to actuator phase contribution allows us to assess the time and frequency frame dynamics of the augmented vehicle.

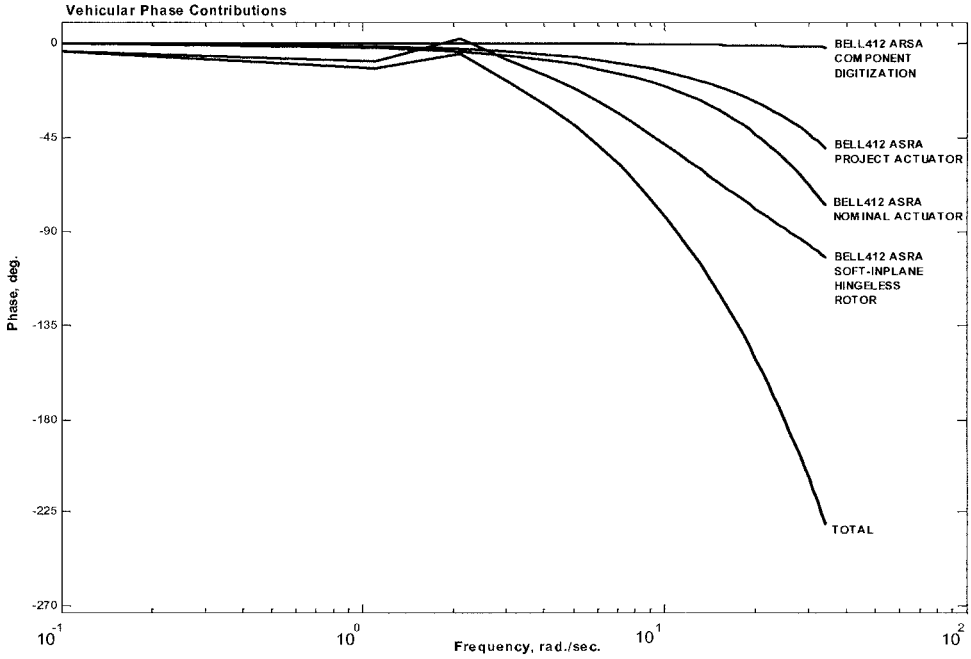

Figure 3.12 Bell 412 ASRA Vehicular Phase Contributions

Depicted in Figure 3.12 is an estimate of the Bell 412 ASRA high frequency phase contributions. At a design cross over frequency of some 6 rad./sec., the hingeless rotor system and rigid body dynamics contribute some 50ms of latency to the overall flight dynamics. The component digitization depicted is for a single digital element such as a filter or the LTN-90 Inertial unit. The combined phase lags for the complete ASRA digital architecture create substantial phase delay. In order to design a flight control law a relationship must be developed between the rotor dynamics equations, and 4 key parameters – open loop and design cross over frequencies, phase margin, the effective vehicular time delay, and gain values. ADS-33 requirements for handling qualities suggest a phase delay limit of 100 msec. be imposed on the integrated control system. For the Bell 412 ASRA at a design cross-over frequency of 6 rad/sec., the phase margin is 47.5 deg. This sets an elevated time delay of some 138 ms with digitization (non-linear) dynamics incorporated.

Another avenue is to predict the phase delay based on the ACAH bandwidth requirements. The predicted achievable bandwidth is defined as the lowest frequency at which the augmented vehicle exhibits 45deg of phase margin or 6dB of gain margin as defined in Figure 3.13. Setting the design cross over frequency equivalent to the required ACAH bandwidth of 4 rad./sec. then the phase lag is 31.25 deg. suggesting a phase delay of 136 ms is associated with this design. This is still elevated, and handling qualities will suffer. To reduce the time delay to the 100 ms requirement, we would require 76deg. of phase lead. Tischler suggests that the maximum amount of phase lead that can be provided by classical attitude and attitude rate feedbacks is some 75 degrees.[78]

Hence, without further filtering techniques which add more delay and non-linearity, the rigid body feedback cannot achieve the design goals. In what follows it will be shown that rotor state feedback can be used to attain the desired design requirements.

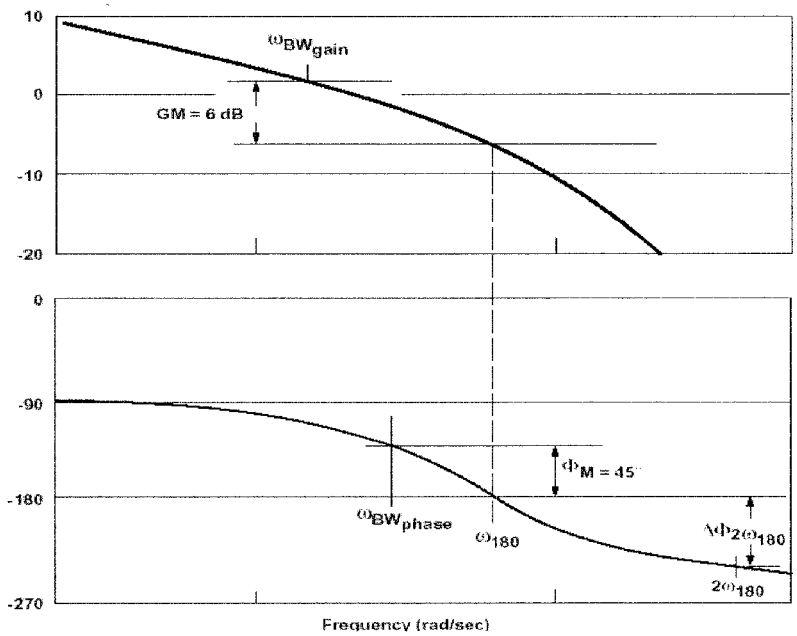

Figure 3.13 Definition of ADS-33E-PRF Bandwidth and Phase Delay Criteria[13]

3.4.2 Exploring the Effects of Rotor State Feedback

It has been suggested by previous research that rotor state feedback can provide additional lead to access higher levels of bandwidth. The next theoretical development aims to determine if this is indeed the case, and to establish the gain structures for ACAH control. To develop an estimate of the gains for effecting control, we must again relate the crossover frequency, phase margin, and effective time delay. Two cases are explored consisting of state feedbacks with and without rotor disc tilt dynamics.

3.4.2.1 Case I: Without Rotor State Feedback

First let us consider the case without rotor state feedback. Using pure gains on attitude and attitude-rate signals we obtain the closed loop compensators, H(s), for the pitch and roll axes:

$$H(s)_{RBC\theta} = K_q(s) + K_\theta \qquad 3.19$$

$$H(s)_{RBC\phi} = K_p(s) + K_\phi \qquad 3.20$$

In each case, a ratio of attitude-rate to attitude gain will achieve the desired control response. Thus, the compensators are simplified as follows:

$$H(s)_{RBC\theta} = \alpha_{2\theta}(s) + \alpha_{1\theta} \quad \text{where; } \alpha_{1\theta} = K_\theta,\ \alpha_{2\theta} = \frac{K_q}{K_\theta} \qquad 3.21$$

$$H(s)_{RBC\phi} = \alpha_{2\phi}(s) + \alpha_{1\phi} \quad \text{where; } \alpha_{1\phi} = K_\phi,\ \alpha_{2\phi} = \frac{K_p}{K_\phi} \qquad 3.22$$

In order to adhere to the handling qualities requirements of Figure 3.13, the feedback gains are to be selected by the following conditions: [78]

- **Condition 1.0:** Phase Margin, Φ_M, is 45 deg.
- **Condition 2.0:** Gain Margin, **GM**, is greater than 6 dB
- **Condition 3.0:** Cross-Over Frequency occurs at maximum phase such that, $\frac{\partial\Phi(\omega)}{\partial\omega} = 0$
- **Condition 4.0:** Phase and Cross-Over Frequency are linearly related such that $\Phi(\omega) = -57.3 \cdot \tau_o \cdot \omega$ deg., where τ_o represents the system time delay, and ω, the design cross-over frequency.

Relating these conditions yields the phase response related to phase delay, cross-over frequency, and feedback gain. This relationship is developed in Equation 3.23 that is the geometrical interpretation of the said parameters as illustrated in Figure 3.13, and is given by:

$$\Phi(\omega) = -180 - 57.3 \cdot \tau_o \cdot \omega + \tan^{-1}(\alpha_2)\omega \qquad 3.23$$

Solving Equation 3.23 based on Conditions 1.0 and 2.0. yields:

$$\frac{\partial \Phi(\omega)}{\partial \omega} = -57.3\tau_e + \frac{57.3(\alpha_2)}{1+(\alpha_2)^2(\omega^2)} \qquad 3.24$$

Solving Equation 3.24 for the maximum condition yields a cross-over frequency fit for estimating the effects of rigid body feedback in the presence of effective time delay.

$$\omega_c = \sqrt{\frac{1}{\tau_e \cdot \alpha_2} - \frac{1}{\alpha_2^2}} \qquad 3.25$$

This relationship is plotted as shown in Figure 3.14.

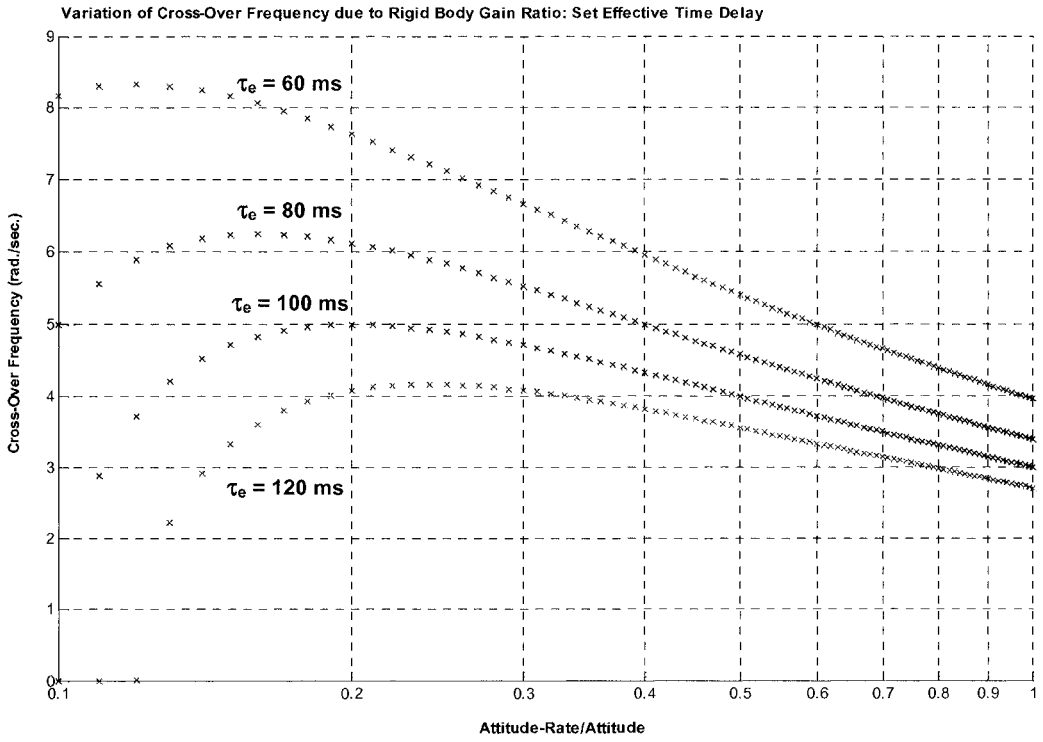

Figure 3.14 Cross –Over Frequency Variation due to Rigid-Body Gain Ratio

3.4.2.2 Case II: With Rotor State Feedback

For the case with rotor state feedback, pure gains on attitude, attitude-rate, and rotor state signals yields the closed loop compensators, H(s), for the pitch and roll axes:

$$H(s)_{RSC\theta} = K_q(s) + K_\theta + K_{a1} \quad 3.26$$

$$H(s)_{RSC\phi} = K_p(s) + K_\phi + K_{b1} \quad 3.27$$

In each case, a ratio of attitude-rate to attitude gain and rotor state gain will achieve the desired control response. Thus, the compensators are simplified as follows:

$$H(s)_{RSC\theta} = (\alpha_{2\theta}(s)+1)\alpha_{1\theta} \quad \text{where; } \alpha_{1\theta} = K_\theta + K_{a1},\ \alpha_{2\theta} = \frac{K_q}{K_\theta + K_{a1}} \quad 3.28$$

$$H(s)_{RSC\phi} = (\alpha_{2\phi}(s)+1)\alpha_{1\phi} \quad \text{where; } \alpha_{1\phi} = K_\phi + K_{b1},\ \alpha_{2\phi} = \frac{K_p}{K_\phi + K_{b1}} \quad 3.29$$

Proceeding through a similar analysis to obtain the cross-over frequency fit as shown in Figure 3.15 establishes some important findings on rigid-body and rotor state feedback.

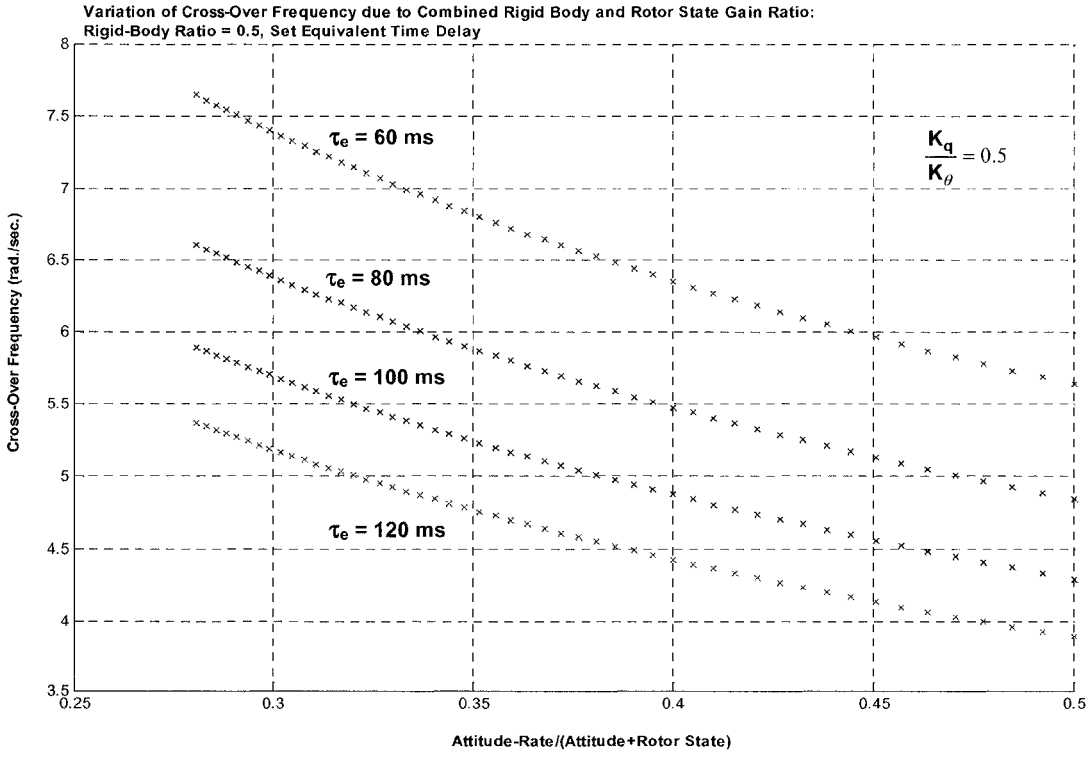

Figure 3.15 Cross –Over Frequency Variation due to Combined Rigid-Body/Rotor-State Gain Ratio

What is the basic effect of rotor state feedback in the presence of rigid body feedback and latency? At the set attitude-rate to attitude ratio and equivalent time delay of 0.5 and 100 ms, respectively, a cross-over frequency of 4.3 rad./sec. was achieved with combined rotor-state and rigid body feedback. A value of 3.2 rad./sec. was the limit achievable for solely rigid-body feedback.

The author summarizes some important trends based on these findings:

- At specific gain ratios, either solely based on rigid body dynamics or incorporating rotor state dynamics, there are specific cross-over frequencies and bandwidths that may be attained given the phase delay accrued in digitization and implementation of the flight control system.
- For rigid body feedback, increasing attitude-rate gain for a constant attitude gain decreases the ability to attain cross-over frequency and system bandwidth within bounds of stability. Conversely, decreasing attitude-rate gain for a constant attitude gain increases the ability to attain the frequency-bandwidth requirement until a threshold gain ratio.
- For rigid body feedback, increasing the attitude gain for a constant attitude-rate gain increases the ability to attain cross-over frequency and system bandwidth within bounds of stability until a threshold gain ratio. Conversely, decreasing attitude gain for a constant attitude-rate gain decreases the ability to attain frequency-bandwidth requirements.
- Increasing levels of phase delay decrease the ability to attain cross-over frequency and system bandwidth within bounds of stability.
- For a constant rigid body attitude-rate to attitude gain ratio, increasing rotor state feedback gain increases the ability to attain cross-over frequency and bandwidth within bounds of stability, and until an attitude gain ratio threshold.
- Though alterations of gain may allow for attainment of bandwidth-frequency requirements, system stability is not assured by observing these trends. This is especially the case for higher order rotor state investigations where body and rotor mode placement, trajectory, and interaction are highly non-linear phenomenon. For example, a helicopter might not be able to access the bandwidth benefits of rotor state feedback based on the elevated bandwidth causing coupled rotor-body resonant conditions or more simply, rotor system band-limiting not allowing higher performance in the controlled design space.

With these trends established we raise other questions. What happens to helicopter stability in the presence of rotor states? What happens to the helicopter stability in the presence of rotor states and rotor feedback? How do these higher-order dynamics interact to describe the non-linear helicopter flight dynamics?

In the following section, the author assesses rigid-body and rotor mode dynamics due to rigid-body feedback by classical modal analysis techniques.

3.5 Linear Control Law Development

In the study of hingeless rotor dynamics, the location of modes such as disc tilt (flap dynamics) and lead-lag dynamics in advancing and regressing forms in the s-plane indicate coupled rotor-body stability. More importantly is the trajectory of these modes as parameters in the rotorcraft design and flight performance envelopes are modified. The Root locus Method (RLM) has been applied in the assessment of rotor state dynamics and feedback effects, in helicopter system identification, and flight control law design. The method is applied herein to assess gain structure and math model robustness to parameter changes as well as to analyze the mode interactions and trajectories in closed-loop.

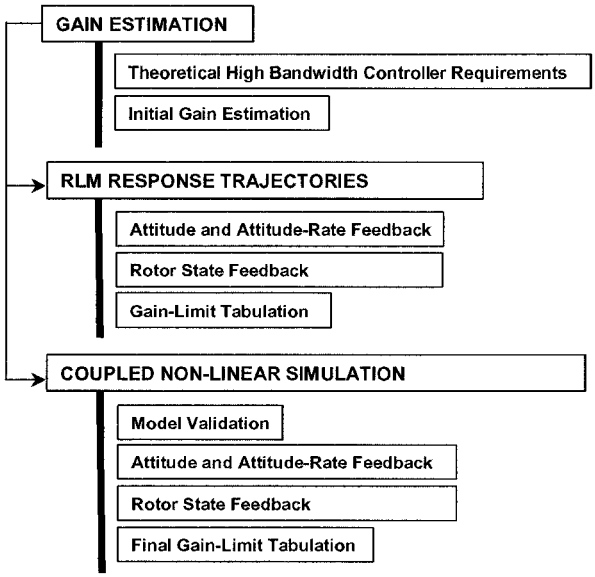

Figure 3.16 RLM Methodology

3.5.1 The Root Locus Method (RLM): Basic Theory

The RLM methodology (Figure 3.16) applied herein was coded in Matlab in order to plot pole, time history, and frequency response trajectories of the closed loop characteristic transfer function relationships for rigid body and rotor state feedback gain variation. The RLM method relies on design gain parameter variation of a feedback controller as shown in Figure 3.17, and the root trajectories of the return difference ratio. The closed loop transfer function for this system is derived such as;

$$Y(s) = G_{tf}(s)[U(s) - Z(s)] \text{ where; } Z(s) = H(s)Y(s),\ G_{tf} = \text{Transfer Function of } G(s) \qquad 3.30$$

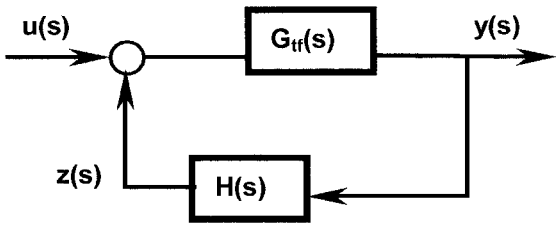

Figure 3.17 Closed Loop Feedback Controller

Substituting Z(s) into Equation 3.30, we obtain the following closed loop transfer function;

$$\frac{Y(s)}{U(s)} = \frac{G_{tf}(s)}{1+G_{tf}(s)H(s)} \qquad 3.31$$

The characteristic equation or return difference function is given by $1+G_{tf}(s)H(s)=0$ and $G_{tf}(s)H(s)$ is the return ratio. The RLM determines stability by investigating whether this return difference of the feedback loop becomes zero for any value of s in the positive s-plane. If the characteristic equation is zero for a pole in the positive s-plane, then the closed-loop system must be unstable.

The trajectory of the locus of the each of the roots of the return difference function gives flight control designers an indication of the system stability margin[81]. Further, indications of modal interactions such as those between the rigid-body and rotor dynamics are critical to the assessment of the helicopter's operation. Typically, the RLM method assesses pole trajectories alone however, for helicopter analyses, time and frequency domain trajectories due to controller variation are critical in highlighting these modal interactions. (It is noted that feedback and feedforward systems may be analyzed in this way by modifying the closed loop transfer function.)

Both full-order and reduced order uncoupled representations in transfer function form of the Bell 412 ASRA longitudinal, lateral, and directional dynamics are assessed. These create approximations of vehicle response outside of the nonlinear fully coupled Simulink simulation environment. The results from the RLM analysis will provide a performance prediction of the actual vehicle response for gain structuring. In general, initial guesses on gains from the NRC-FRL researchers and vehicle managers were used prior to initiating gain estimations from both the theoretical analysis in high bandwidth flight control and from the RLM analyses.

3.5.2 RLM Trajectory Analysis: Longitudinal Axis Control of Full- and Reduced-Order Dynamics

Full-order uncoupled, reduced order-uncoupled, and rotor state to control transfer functions are used to represent the vehicle dynamics. Each denominator factor represents open loop rigid body and rotor longitudinal disc tilt dynamics. The eigenvalues and eigenvectors describe specific vehicular modal dynamics.

The full-order uncoupled longitudinal axis transfer function for this analysis is a 10th order representation given by;

$$\frac{\theta}{\delta_{LON}} = \frac{0.1263s(s-19.17)(s+10.83)(s+1.7736)(s+0.8196)(s+0.2978)(s+0.0406)(s^2+0.3684s+1.4588)}{s(s+0.4945)(s+0.0167)(s^2+3.5467s+3.1549)(s^2+0.0477s+0.126)(s^2+0.4443s+1.8994)(s^2+18.7449s+101.324)} \quad 3.32$$

Uncoupling the Bell 412 ASRA model structure is important to both confirm/isolate findings as well as assist in the determination of appropriate model structures for the control law design process. The goal will be to represent the vehicle rigid body and rotor dynamics with the minimum dimensionality that offers both fidelity and robust/safe closed loop performance.

The reduced-order uncoupled longitudinal axis transfer function for this analysis is 5th order representation given by;

$$\frac{\theta}{\delta_{LON}} = \frac{0.1263s(s-0.000398)(s+0.8647)(s-17.9577)}{s(s+9.5713)(s^2-0.0444s+0.05494)(s^2+1.8104s+1.0209)} \quad 3.33$$

In what follows the effects of rigid body gain variations on helicopter rigid-body and rotor state dynamics are explored by assessing the trajectories of poles (by pole-zero mapping), time domain response (by time history mapping, and frequency response (bode frequency response mapping).

3.5.2.1 Effects of Pitch Rate Feedback on Full-Order Flight Dynamics

The feedback of pitch rate for positive gain variation shows trend destabilization of the rotor flap regressive modes as shown in Figure 3.18. In the frequency range of 1-10/rad./sec., this compensation correlates to increased phase lead and increased magnitude of the gain cross over frequency in longitudinal attitude response (Figure 3.19). The phase bandwidth varies from 2 to 6 rad./s with phase delay variation between 0.096 and 0.044 sec. The pitch rate feedback stabilizes rigid body dynamics in general for positive gain variation, there is some destabilization of the real component of the pitch/roll oscillation mode. If gain variation is negative then the pitch rate feedback gain limitation is the Phugoid mode. (Note lead lag dynamics are not modeled and rotor flap dynamics are further damped.)

In terms of the influence of pitch rate feedback on longitudinal disc tilt dynamics, Figure 3.20 shows the correlation between rotor and on-axis pitch dynamics of the Bell 412 ASRA. At the rotor rotating frequency of 5.4 Hz (33.9 rad./sec.), the rotor longitudinal disc tilt is some 30deg. out of phase with the attitude response due to pilot cyclic pitch. The crossover frequency of this rotor dynamic occurs at more than twice the bandwidth of the attitude response. The off-axis rotor lateral disc tilt response to pitch rate feedback (Figure 3.21) shows the rotor response some 45deg. off phase with longitudinal tilt and mode coupling the 1-3 rad/sec. range. The resulting time domain responses are depicted in Figure 3.22. The response characterizes the helicopter's initial rate response due to longitudinal unit step. Flight velocity diverges as is to be expected while heave velocity stabilizes. Again the correlation between pitch dynamics (rate and attitude) and rotor lap dynamics (longitudinal disc tilt) is to be noted. The off-axis responses in roll and yaw indicate the complexity and tonality of the response that is highly coupled.

3.5.2.2 Effects of Pitch Rate Feedback on Reduced-Order Flight Dynamics

Pitch rate feedback variation as applied to the reduced-order longitudinal transfer function model shows, in Figures 3.23 and 3.24, the direct coupling of longitudinal rotor flap regressive and roll modes in the region of 4.5 rad./sec. The stabilization and destabilization of Phugoid dynamics concurs with the full-order case based on positive or negative gain variation, respectively. The frequency domain longitudinal attitude and longitudinal disc tilt response trends correlate well with the full-order case as depicted in Figures 3.19 and 3.20 and Figures 3.25 and 3.26. As is expected, less low frequency (0.1 to 10 rad./sec.) modal coupling is depicted in the reduced-order analysis. The lack of coupling is well demonstrated in the time domain trends (Figure 3.27) where a well-established rate command response is attained with high correlation between attitude pitch rate and longitudinal disc tilt.

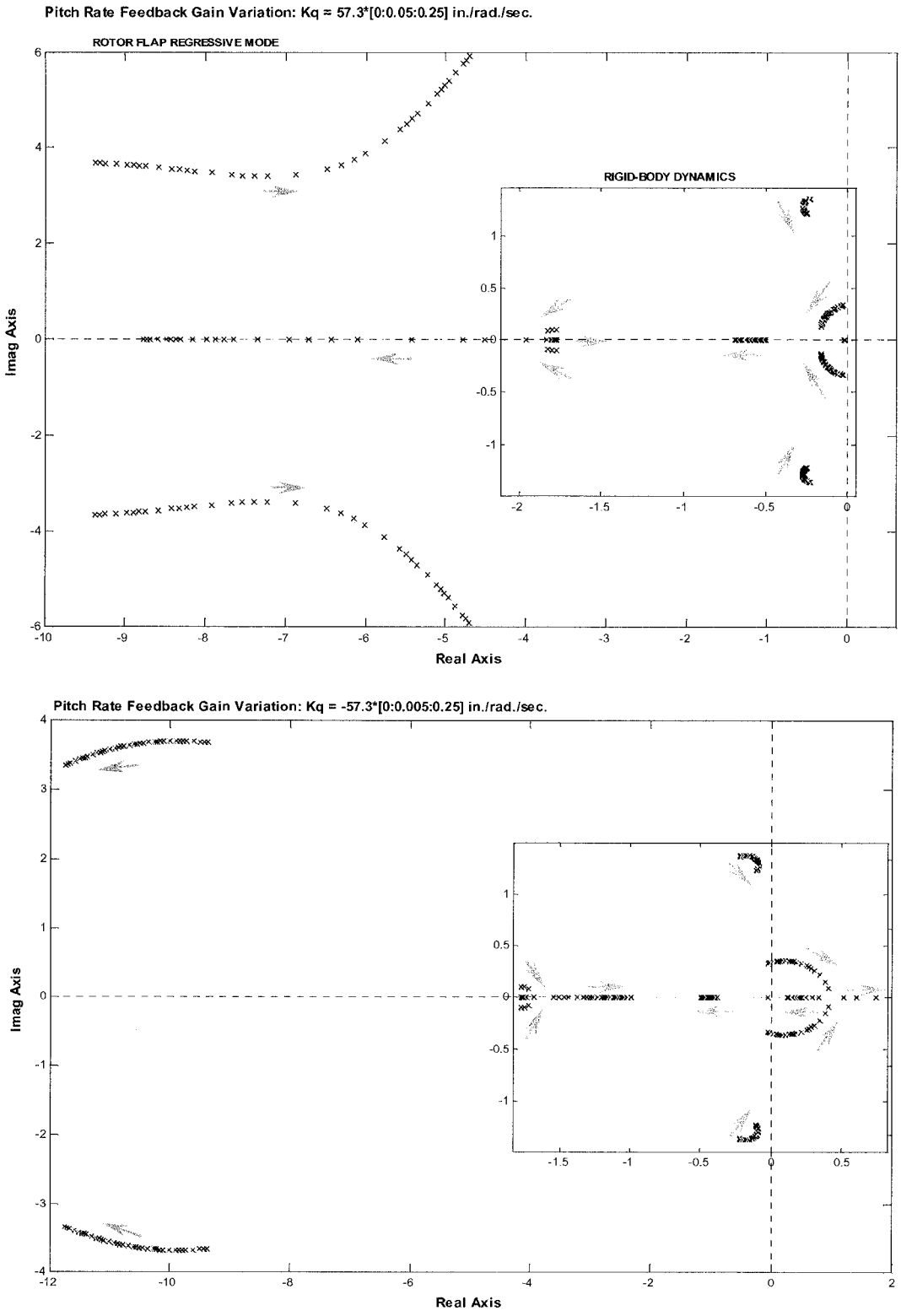

Figure 3.18 Pitch Rate Feedback Mode Trajectories
-Effects on Full-Order Closed Loop Longitudinal Axis Dynamics
-(Top) Positive Gain Variation, (Bottom) Negative Gain Variation

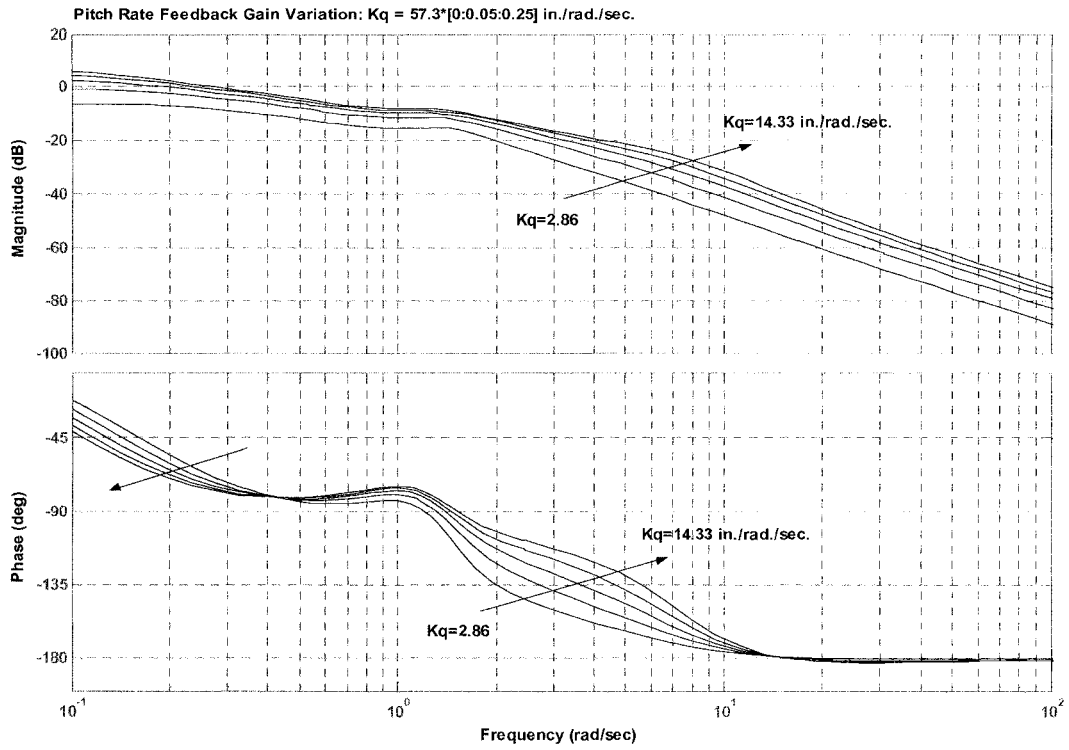

Figure 3.19 Pitch Rate Feedback Frequency Response Trajectory for Full-Order Dynamics -Pitch Attitude to Longitudinal Cyclic Dynamics, Positive Gain Variation

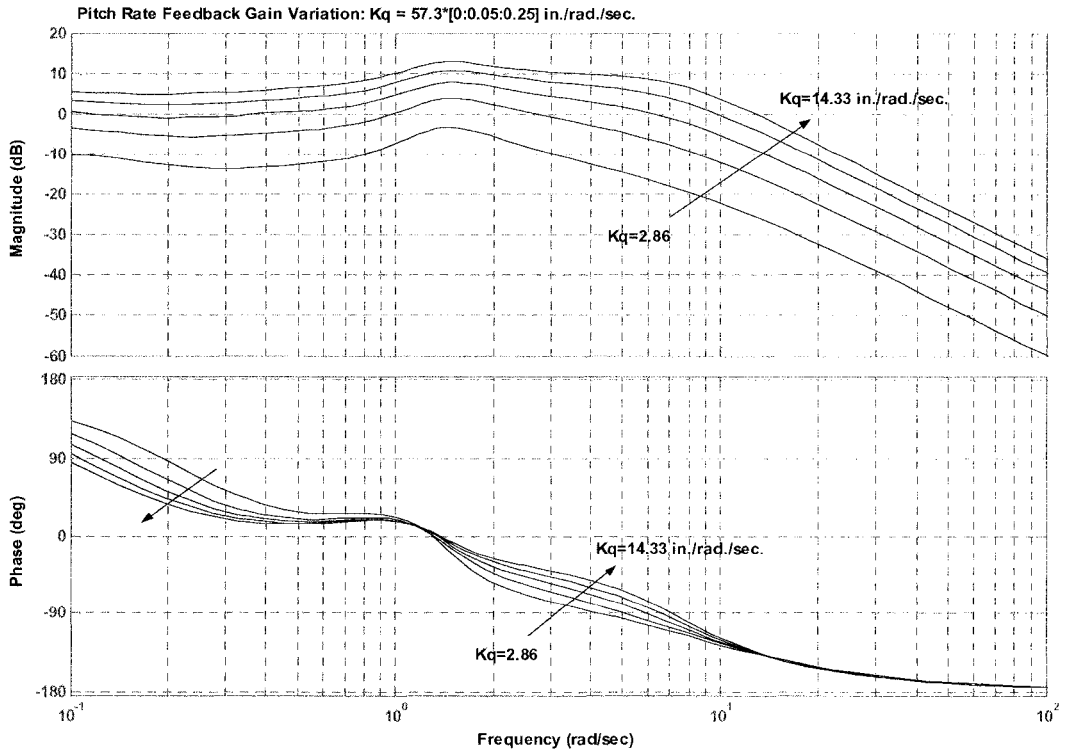

Figure 3.20 Pitch Rate Feedback Frequency Response Trajectory for Full-Order Dynamics -Longitudinal Disc Tilt to Longitudinal Cyclic Dynamics, -Positive Gain Variation

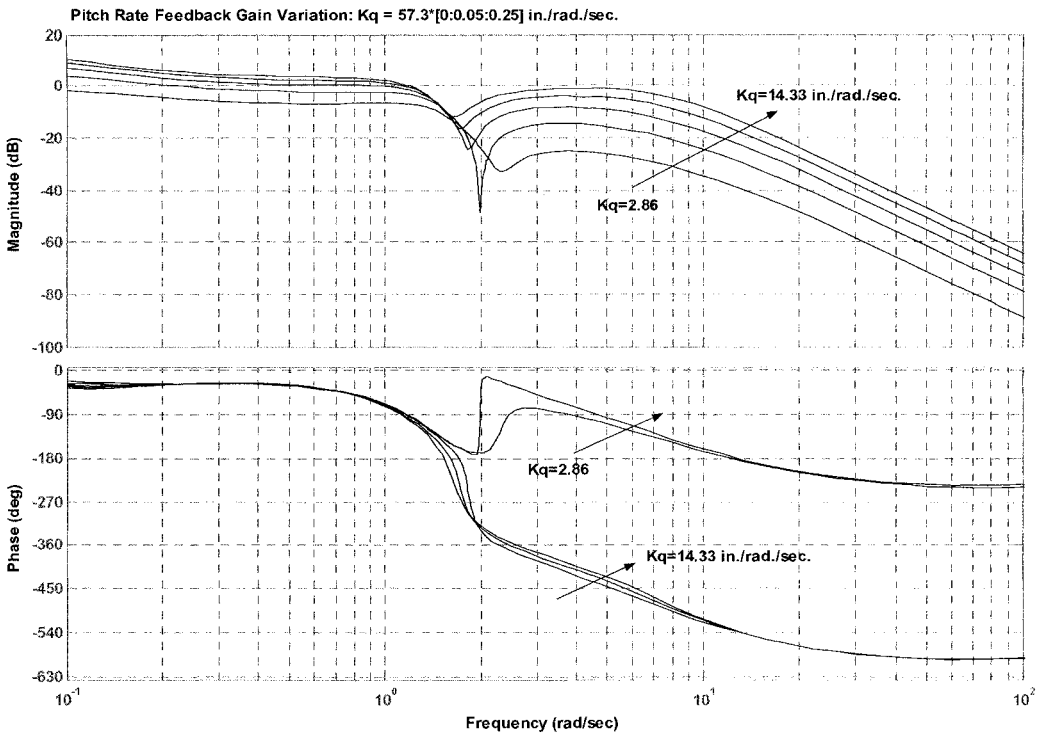

Figure 3.21 Pitch Rate Feedback Frequency Response Trajectory for Full-Order Dynamics
-Lateral Disc Tilt to Longitudinal Cyclic Dynamics
-Positive Gain Variation

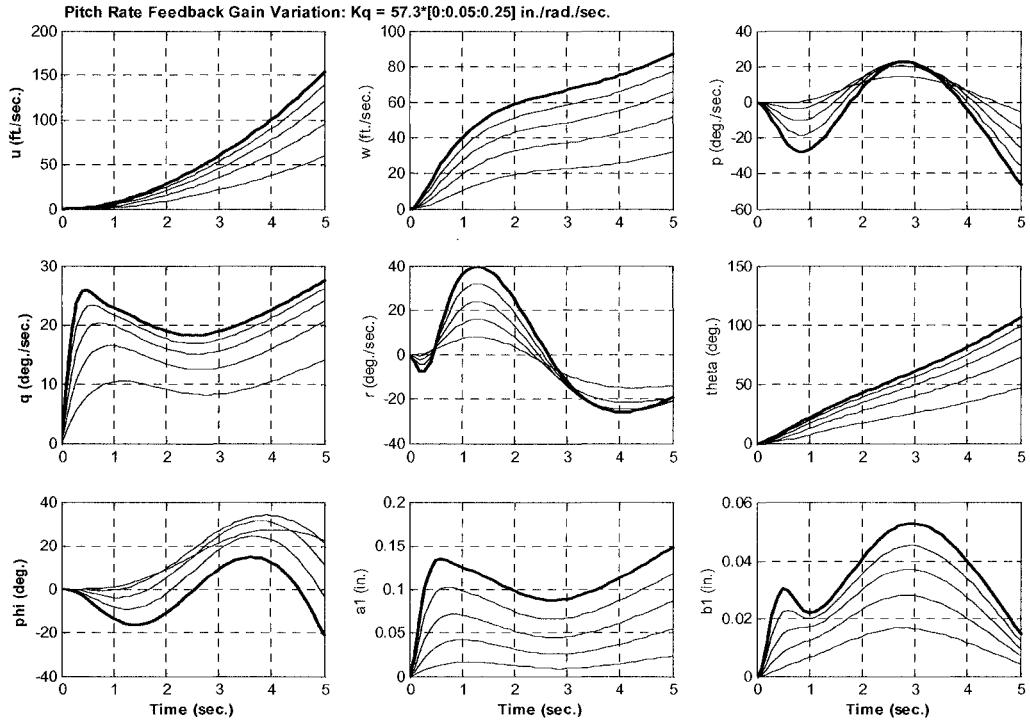

Figure 3.22 Pitch Rate Feedback Longitudinal Unit Step Response Trajectory for Full-Order Dynamics
-Positive Gain Variation

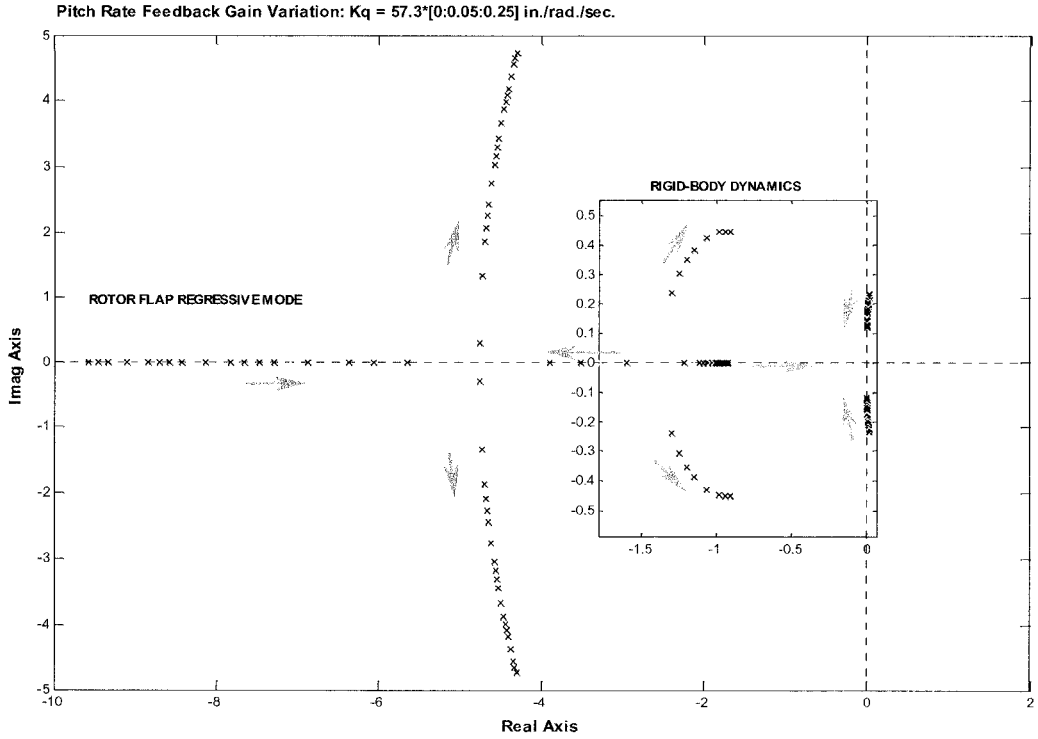

Figure 3.23 Pitch Rate Feedback Mode Trajectories
-Effects on Reduced-Order Closed Loop Longitudinal Axis Dynamics
-Positive Gain Variation

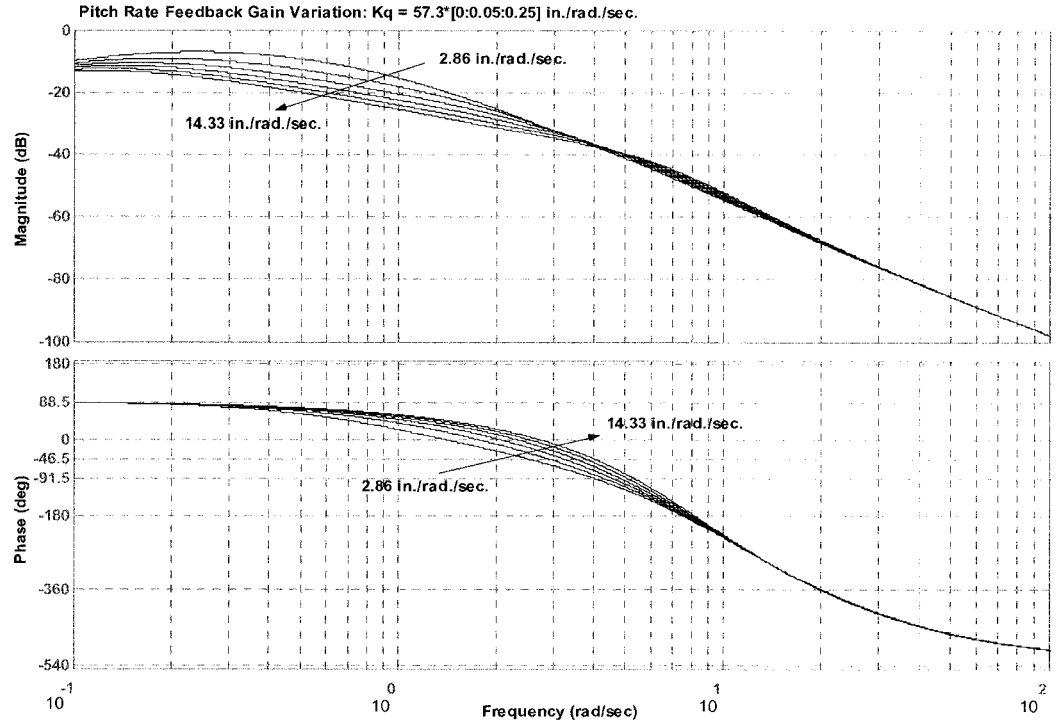

Figure 3.24 Pitch Rate Feedback Frequency Response Trajectory for Reduced-Order Dynamics
- Pitch Attitude to Longitudinal Cyclic Dynamics
- Positive Gain Variation

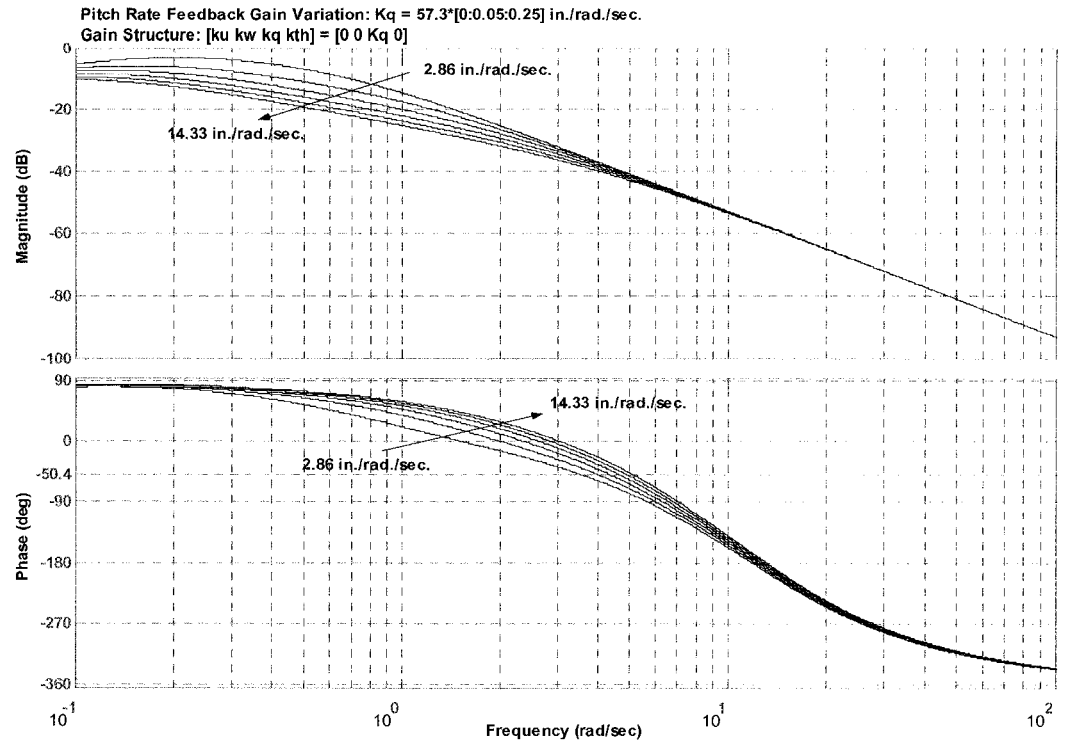

Figure 3.25 Pitch Rate Feedback Frequency Response Trajectory for Reduced-Order Dynamics
-Pitch Attitude to Longitudinal Cyclic Dynamics,
-Negative Gain Variation, Without Rotor State in Model Structure

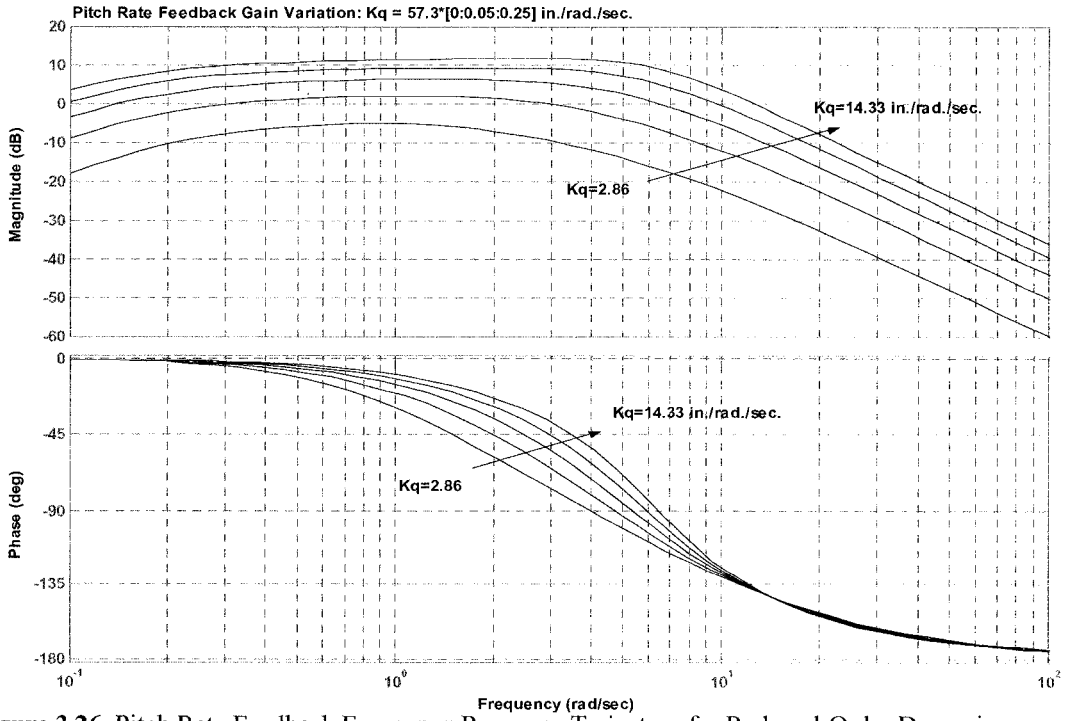

Figure 3.26 Pitch Rate Feedback Frequency Response Trajectory for Reduced-Order Dynamics
-Longitudinal Disc Tilt to Longitudinal Cyclic Dynamics
-Positive Gain Variation

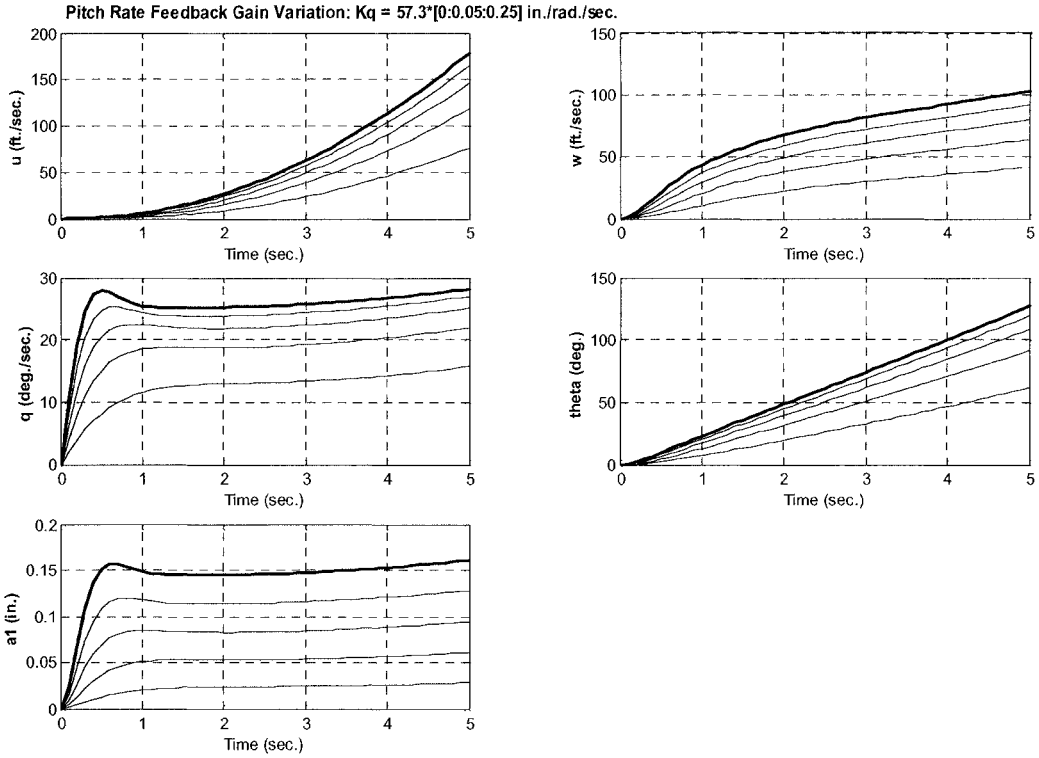

Figure 3.27 Pitch Rate Feedback Longitudinal Unit Step Response Trajectory for Reduced-Order Dynamics

3.5.2.3 Effects of Pitch Attitude Feedback on Full-Order Flight Dynamics

The effects of pitch attitude gain variation are illustrated using a base gain structure with a pitch rate gain of 0.48 in./rad./sec. The feedback of pitch attitude for positive gain variation shows further damping of the rotor flap regressive modes while all rigid body dynamics tend towards destabilization. The gain limits as depicted in Figure 3.28, without lead-lag dynamics modeled, involves the Dutch roll mode at a gain of 0.6 in./rad. In pitch attitude response, this compensation correlates to increased phase lead out to 7 rad./sec. and increased magnitude of gain cross over frequency only in the 0.1 – 0.7 rad/sec. range as shown in Figure 3.29. The effect on pitch attitude to longitudinal cyclic response remains steady exceeding Level 1 with a phase bandwidth of 8.5 rad./sec, and phase delay of 0.023 sec.

With pitch attitude gain variation, the longitudinal disc tilt response (Figure 3.30) is less correlated to the vehicle pitch rate response even though a rate feedback gain exists. As in pitch rate gain variation, off-axis mode coupling is depicted between 1-2 rad/sec. in the lateral disc tilt to longitudinal cyclic responses as shown in Figures 3.21 and 3.31. The pitch attitude gain variation has modest effects on lead and magnitude over the 0.1-2 rad./sec. range for both on- and off-axis rotor response.

The time domain response (Figure 3.32) shows the control structure seeking a pitch attitude command response. The combined pitch rate and attitude gains result in slightly more longitudinal and lateral disc tilt activity than for pure pitch rate feedback. The heave velocity tends to stabilization more exactly for this feedback structure.

3.5.2.4 Effects of Pitch Attitude Feedback on Reduced-Order Flight Dynamics

The pitch Phugoid mode limits the positive gain feedback of pitch attitude at 0.475 in./rad., stabilizing all other body and rotor modes captured by the reduced order model structure (Figure 3.33). The stabilization of the pitch axis rigid body modes was clouded by the vehicle interactions in the full-order analysis. The frequency domain longitudinal attitude and disc tilt responses correlate well with the full-order analysis with less vehicle dynamics illustrated in the 0.1-10 rad/sec. range as shown by Figures 3.29 and Figures 3.34 to 3.36. The pitch attitude response depicts slightly lower phase bandwidth and delay parameters.

In the time domain, the reduced-order response illustrates in Figure 3.37 the capture of the attitude command as well as the response correlations between rotor disc tilt and vehicle on-axis response more distinctly.

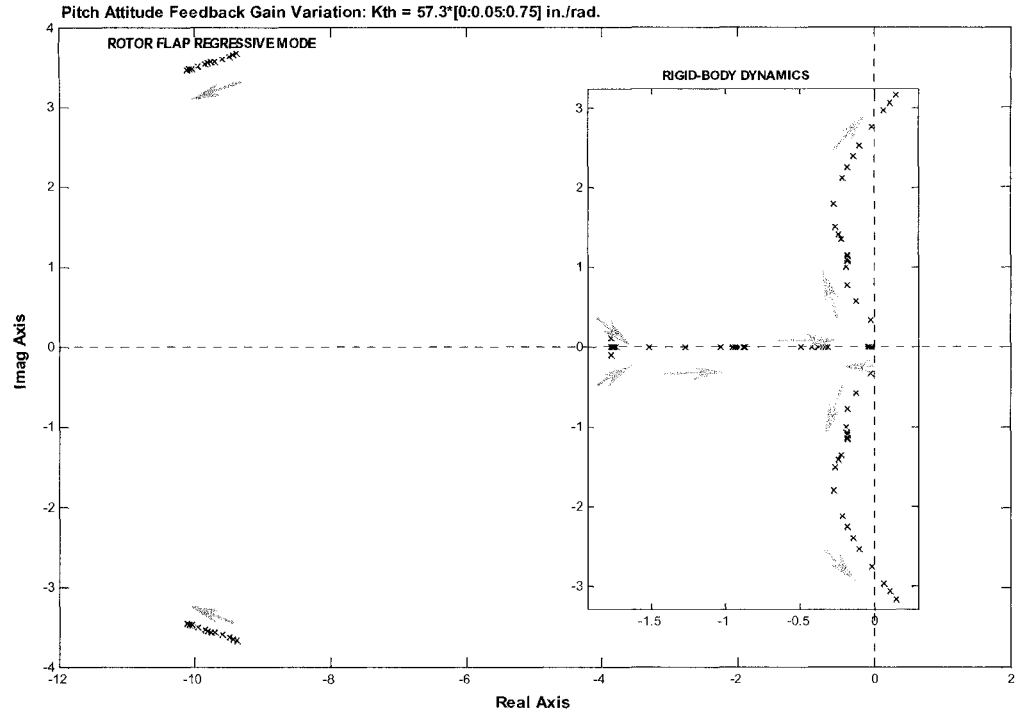

Figure 3.28 Pitch Attitude Feedback Mode Trajectories
-Effects on Full-Order Closed Loop Longitudinal Axis Dynamics

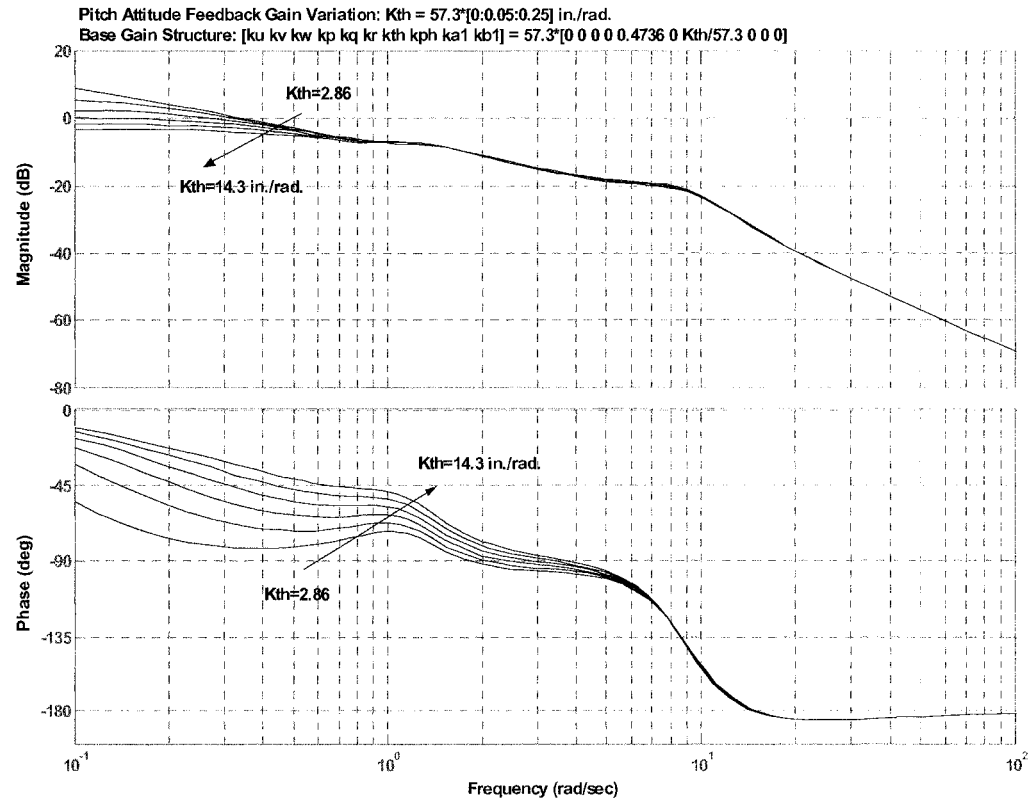

Figure 3.29 Pitch Attitude Feedback Frequency Response Trajectory for Full-Order Dynamics
-Pitch Attitude to Longitudinal Cyclic Dynamics

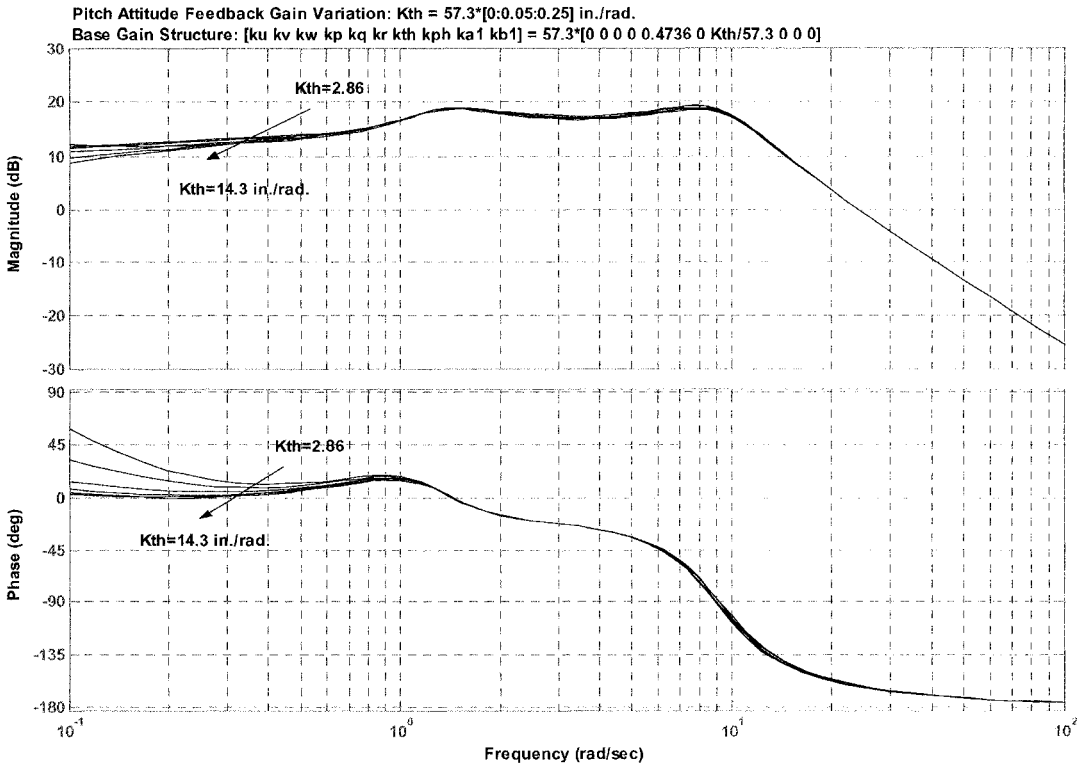

Figure 3.30 Pitch Attitude Feedback Frequency Response Trajectory for Full-Order Dynamics -Longitudinal Disc Tilt to Longitudinal Cyclic Dynamics

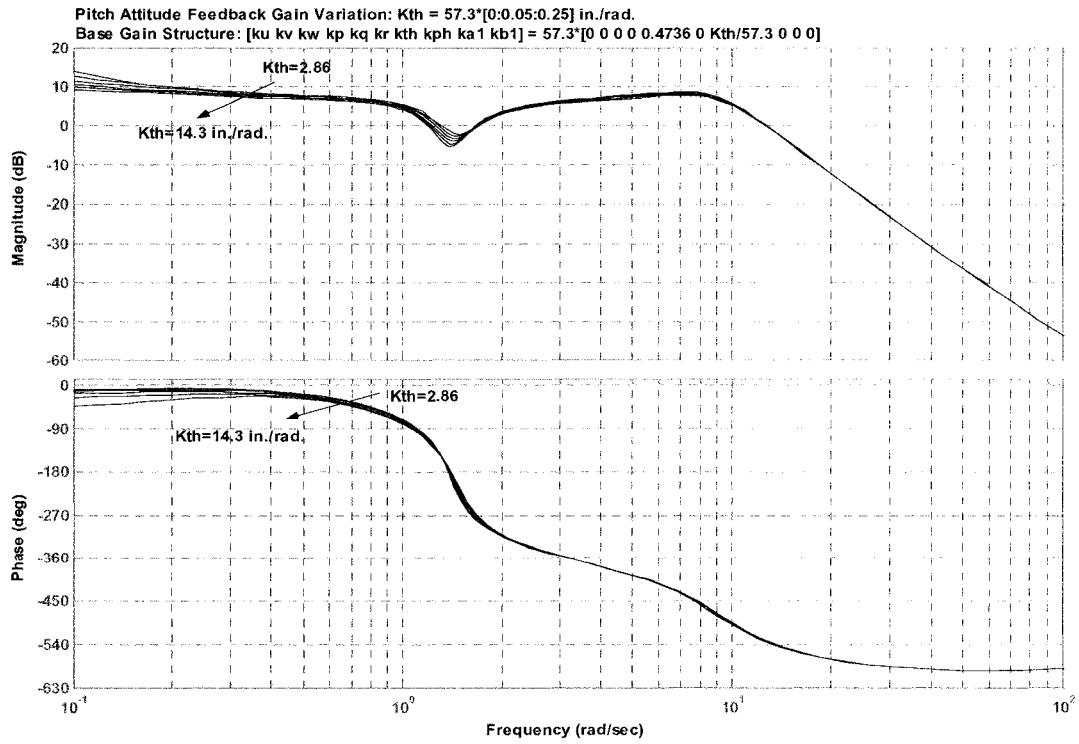

Figure 3.31 Pitch Attitude Feedback Frequency Response Trajectory for Full-Order Dynamics -Lateral Disc Tilt to Longitudinal Cyclic Dynamics

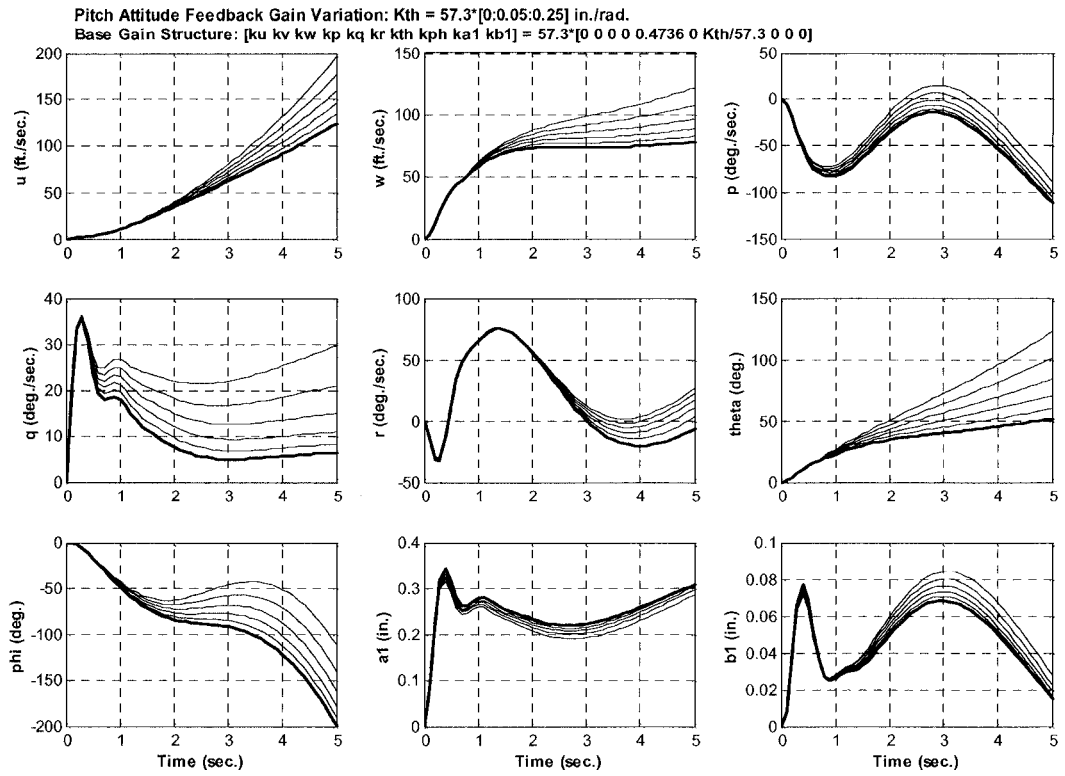

Figure 3.32 Pitch Attitude Feedback Longitudinal Unit Step Response Trajectory for Full-Order Dynamics

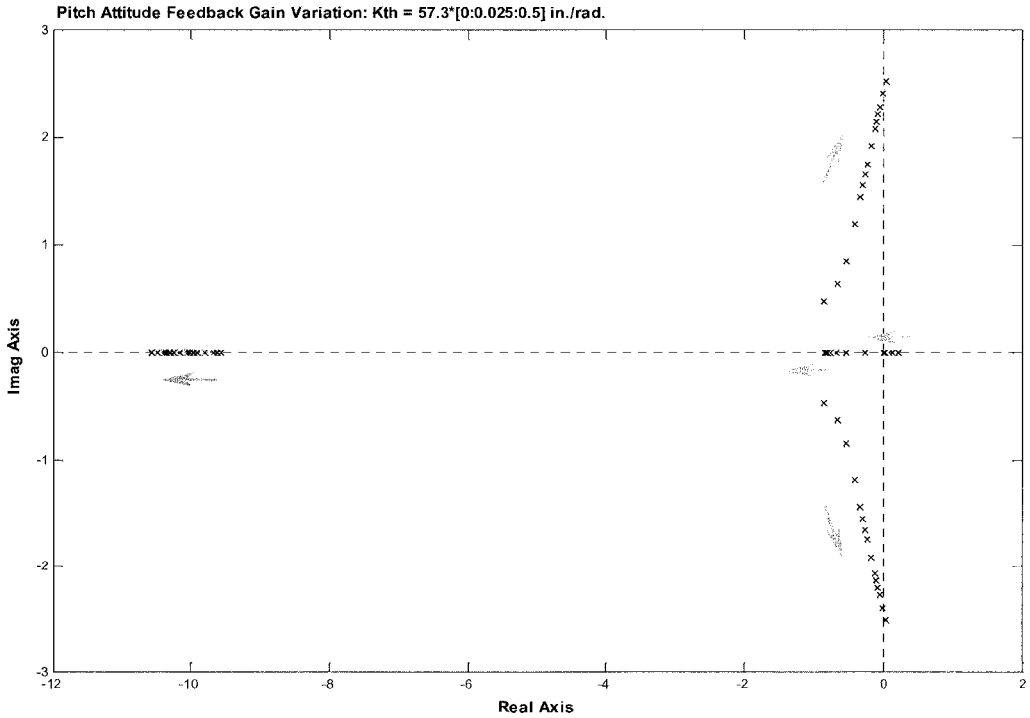

Figure 3.33 Pitch Attitude Feedback Mode Trajectory
-Effects on Reduced-Order Closed Loop Longitudinal Axis Dynamics

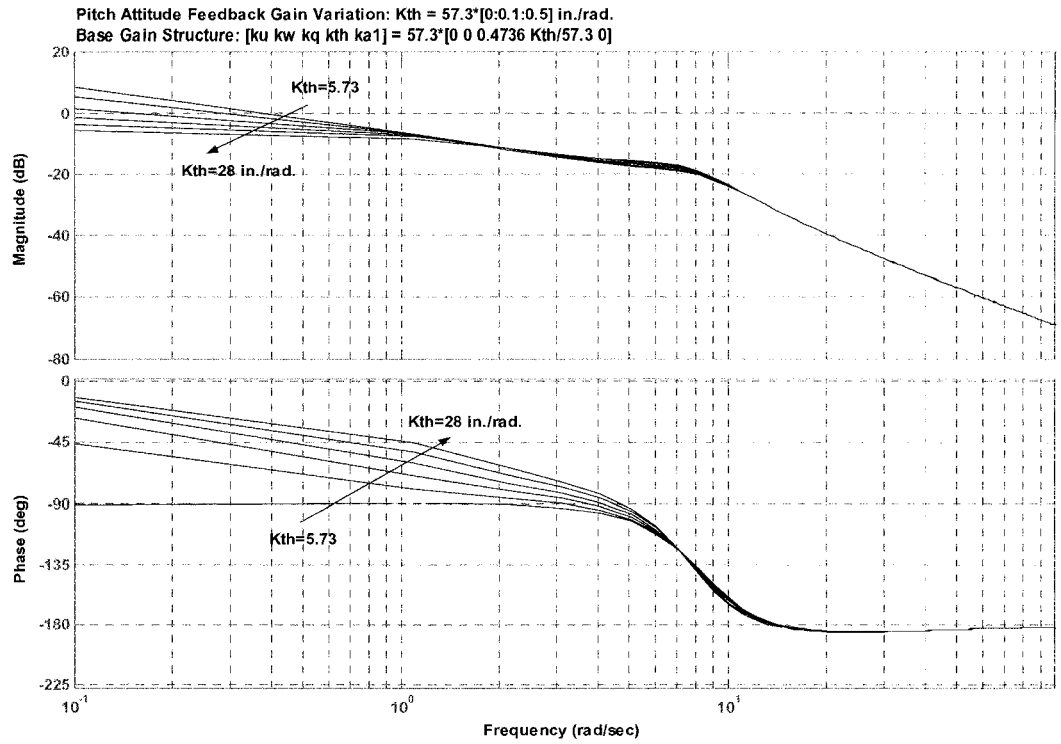

Figure 3.34 Pitch Attitude Feedback Frequency Response Trajectory, Reduced-Order Dynamics -Pitch Attitude to Longitudinal Cyclic Dynamics

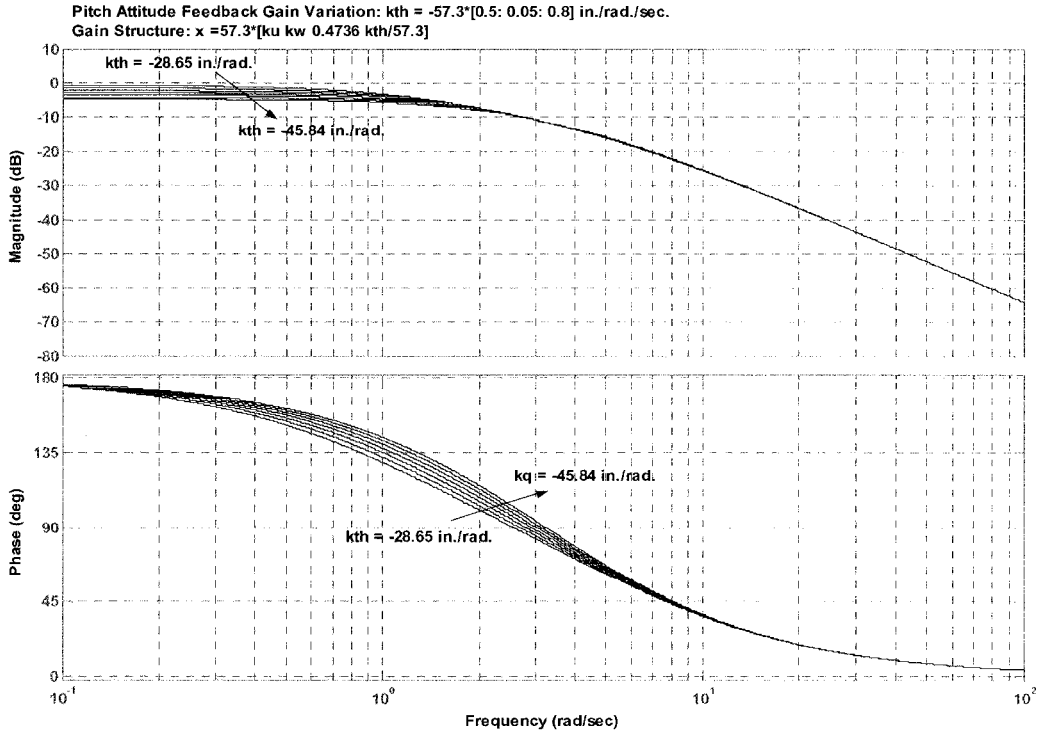

Figure 3.35 Pitch Attitude Feedback Frequency Response Trajectory, Reduced-Order Dynamics -Pitch Attitude to Longitudinal Cyclic Dynamics -Without Rotor State in Model Structure

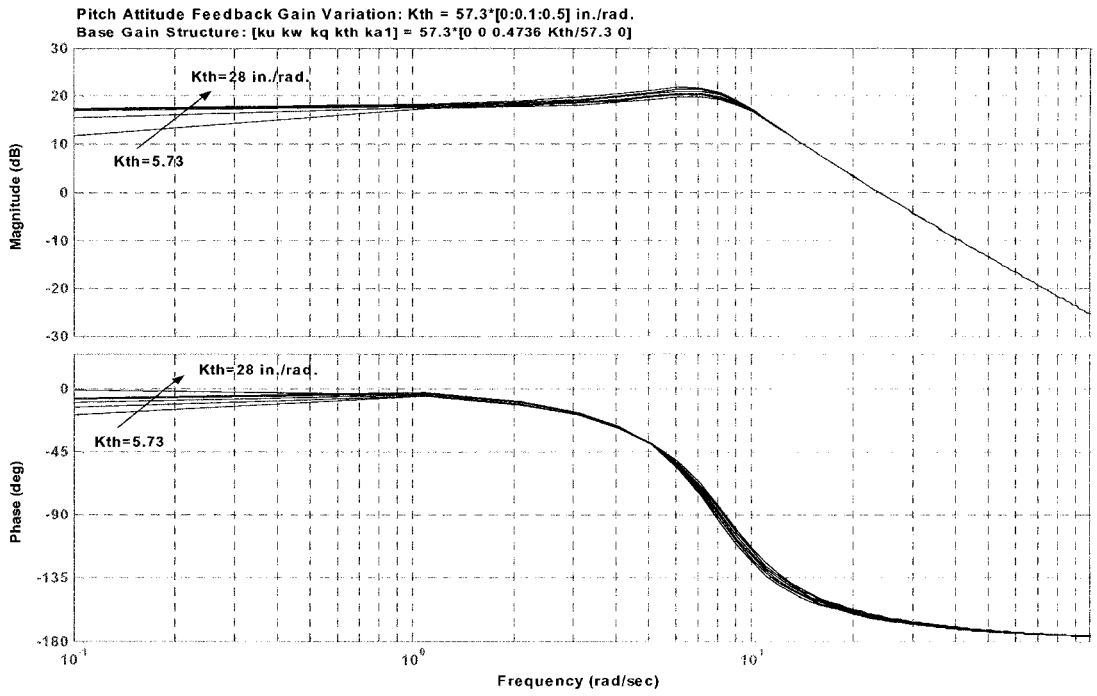

Figure 3.36 Pitch Attitude Feedback Frequency Response Trajectory, Reduced-Order Dynamics -Longitudinal Disc Tilt to Longitudinal Cyclic Dynamics

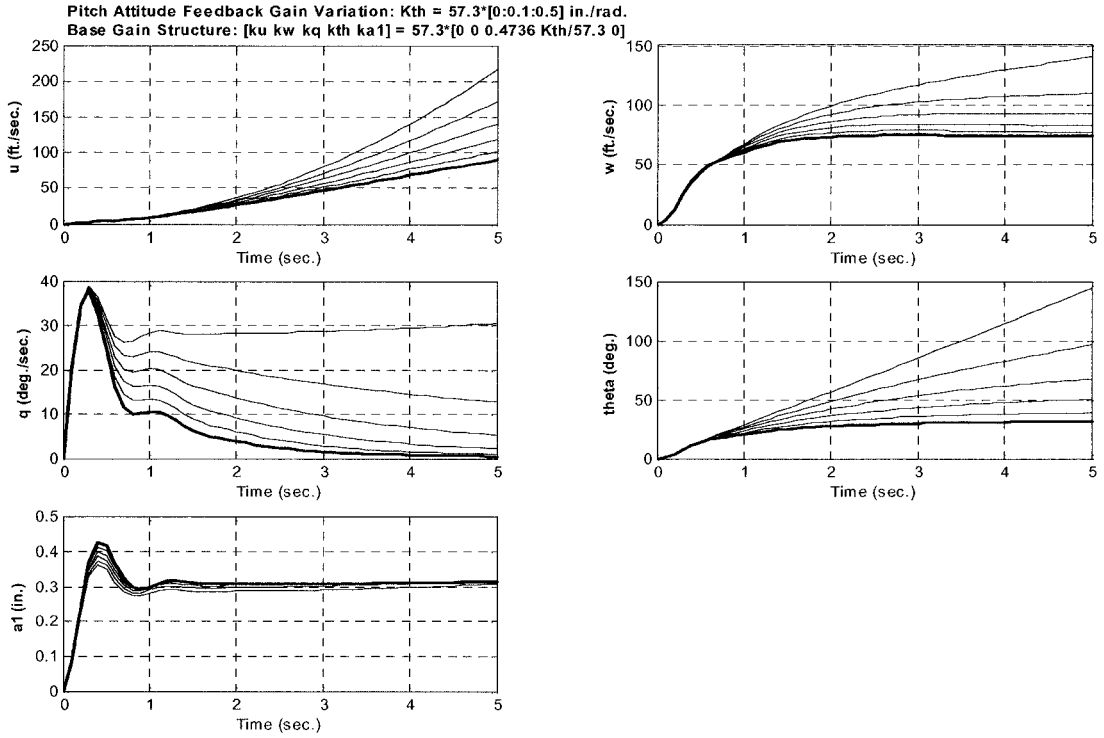

Figure 3.37 Pitch Attitude Feedback Longitudinal Unit Step Response Trajectory for Reduced-Order Dynamics

3.5.2.5 Specification Compliance: Overall Effects of Pitch Rate and Attitude Feedback

The effects of pitch attitude and attitude rate feedback on specification compliance are shown in Figures 3.38 and 3.39. The effect of rate feedback on pitch attitude to longitudinal cyclic specification ADS-33 results in a transition from marginal Level 2 to Level 1 rating.

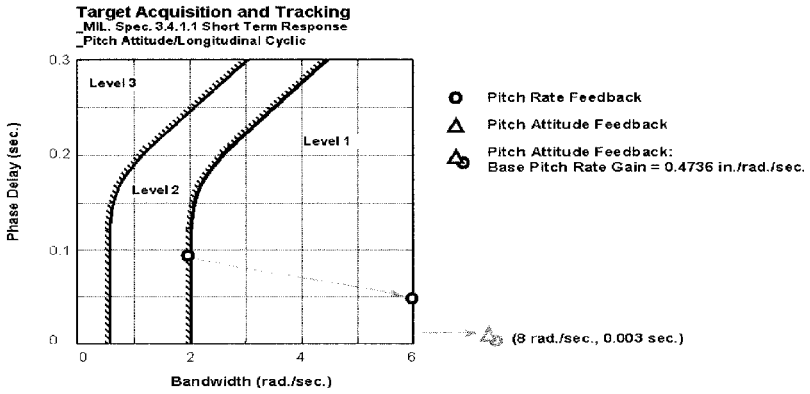

Figure 3.38 ADS-33E-PRF Rating Trajectory – Comparison of the Effects of Pitch Attitude and Pitch Rate Feedback

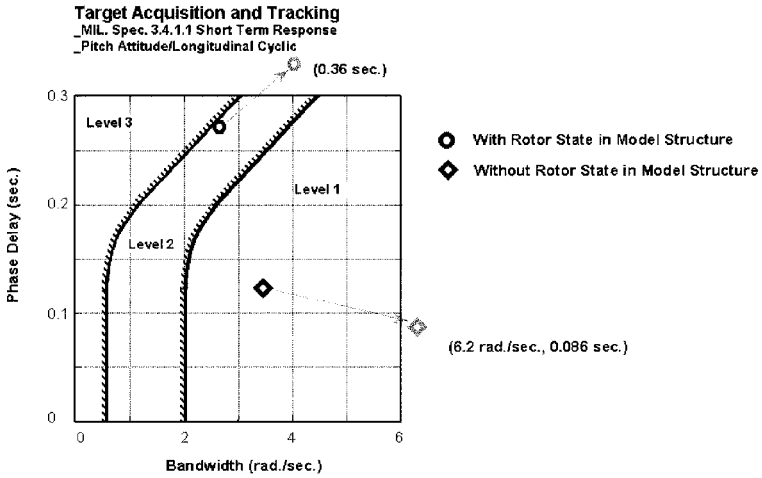

Figure 3.39 ADS-33E-PRF Rating Trajectory – Pitch Rate Feedback With and Without Rotor State Dynamics (6DOF base model for comparison)

Overall it was determined that in the presence of rotor longitudinal disc tilt dynamics, pitch rate feedback had more of an effect on mode displacement and interaction than did combined pitch attitude-rate feedback as shown in Figure 3.38. In particular, this rate feedback caused rotor-body coupling not displayed by the combined feedback case. Applied to a rate type response, pitch attitude feedback affects mainly low frequency dynamics (0.1-10 rad./sec.). In reference to Figure 3.39, the effects for the same attitude-rate feedback with and without presence of rotor states in the model structure (i.e. the 8DOF HMMS characterization compared to its baseline 6DOF development model) are demonstrated. It is shown that rotor states place limits on the attainable bandwidth by SISO feedback; note that the particular gains and delay push the compliance points beyond thresholds in both cases.

3.5.3 RLM Trajectory Analysis Lateral Axis Control: Full- and Reduced-Order Dynamics

The full-order uncoupled lateral axis transfer function for this analysis is a 10^{th} order representation:

$$\frac{\phi}{\delta_{LAT}} = \frac{0.1562s(s+31.2674)(s+12.0064)(s+1.754)(s+0.4864)(s-0.0188)(s^2-0.1455s+0.103)}{s(s+0.4945)(s+0.0167)(s^2+3.5467s+3.1549)(s^2+0.0478s+0.1124)(s^2+0.4443s+1.8994)(s^2+18.7479s+101.3304)} \quad 3.34$$

The reduced-order uncoupled lateral axis transfer function for this analysis is a 5^{th} order representation:

$$\frac{\phi}{\delta_{LAT}} = \frac{0.1562s(s+35.879)(s-0.0171)(s^2+1.6784+0.7689)}{s(s+9.0659)(s^2+0.0522s+0.34)(s^2+2.8415s+2.1506)} \quad 3.35$$

Establishing both the coupled and the minimum dimensional or reduced order response for lateral dynamics was more difficult. Lateral dynamics involve a highly coupled, lower inertia axis than that of the longitudinal case.

3.5.3.1 Effects of Roll Rate Feedback on Full-Order Flight Dynamics

In Figure 3.40, roll rate feedback by a negative gain variation shows trend destabilization of the rotor flap regressive mode with gain limits established by the Phugoid and spiral modes in absence of rotor lead-lag dynamics. A positive gain variation defines the Dutch roll mode as one of the limiting rigid body modes at 0.45 in./rad./sec. The full-order model roll attitude and rotor disc tilt to lateral cyclic responses (Figures 3.41 to 3.43) show considerable off-axis dynamics. Effects are particularly noticeable for phase information. The destabilization of the Phugoid and spiral dynamics is seen as the principal cause of these dynamics occurring in the low frequency bandwidth range. The time responses as shown in Figure 3.44 are more indicative of this axis coupling showing high responses in lateral translation, pitch rate, and yaw rate. The roll rate feedback establishes a rate command response with the roll rate response mirroring the lateral disc tilt response.

3.5.3.2 Effects of Roll Rate Feedback on Reduced-Order Flight Dynamics

The reduced-order dynamics in roll are most complex. A negative roll rate gain variation shows mode interaction of the rotor and vehicle, (i.e.; flap regressive and roll dynamics, respectively), in Figure 3.45. Initial destabilization of the rotor regressive mode changes to improved damping by alteration of the real mode into a complex form when the modes interact at 5.5 rad./sec. The presence of the lateral disc tilt dynamics in the reduced-order model affected both phase and magnitude correlation compared to the full-order analysis. Without lateral disc tilt dynamics the roll attitude to lateral cyclic response had characteristic gain and phase trajectories as shown in Figure 3.47. The addition of the lateral disc tilt in the gain structuring (Figure 3.46) caused the limiting of attainable phase bandwidth. Figures 3.42 and 3.48 illustrate trend correlation of roll rate feedback and lateral disc tilt dynamics in both full- and reduced-order analyses. The time history (Figure 3.49) shows a high initial roll rate response that decays as if a significant yaw attitude command response is established by the unit roll step input.

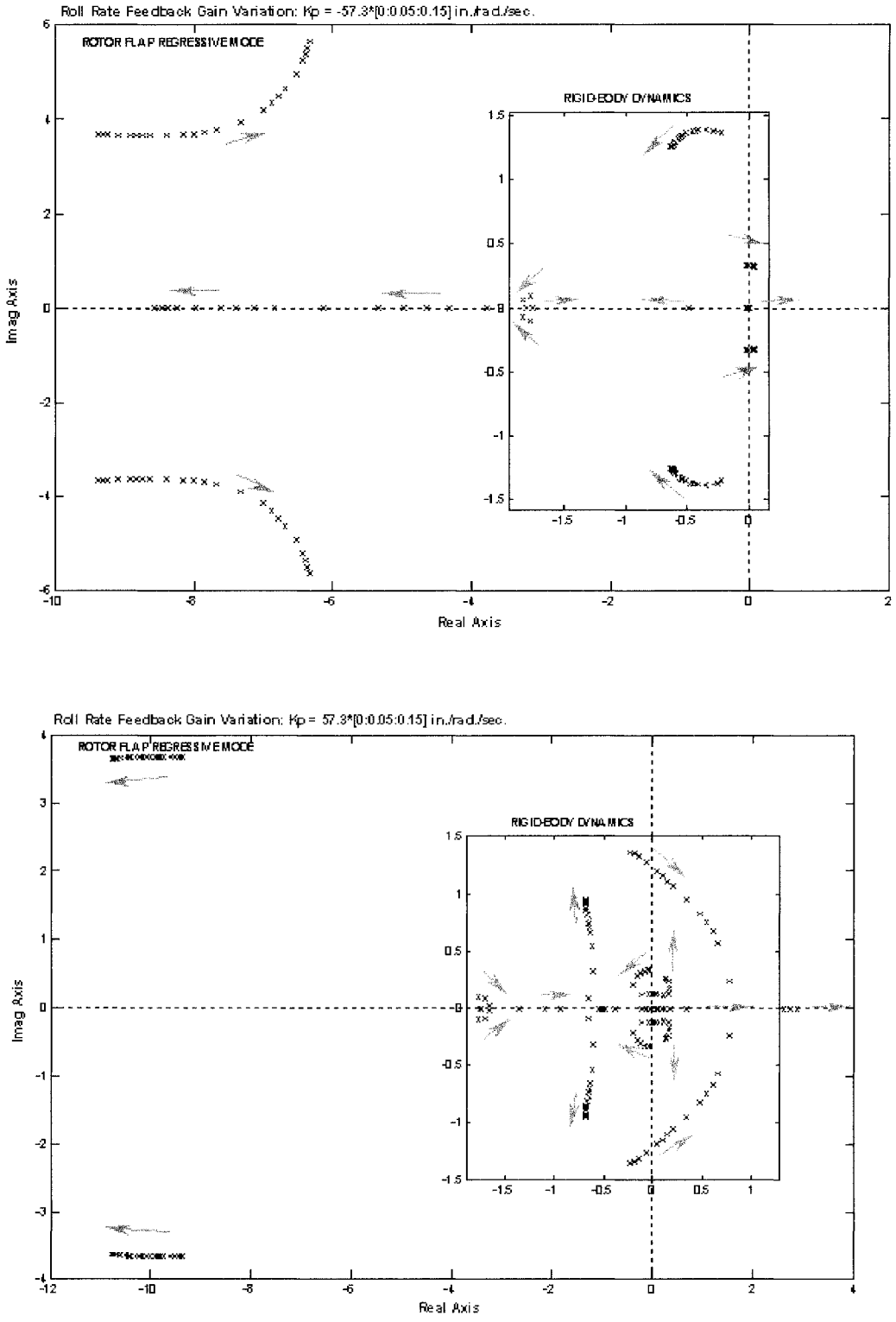

Figure 3.40 Roll Rate Feedback Mode Trajectories
-Effects on Full-Order Closed Loop Lateral Axis Dynamics
-(Top) Negative Gain Variation, (Bottom) Positive Gain Variation

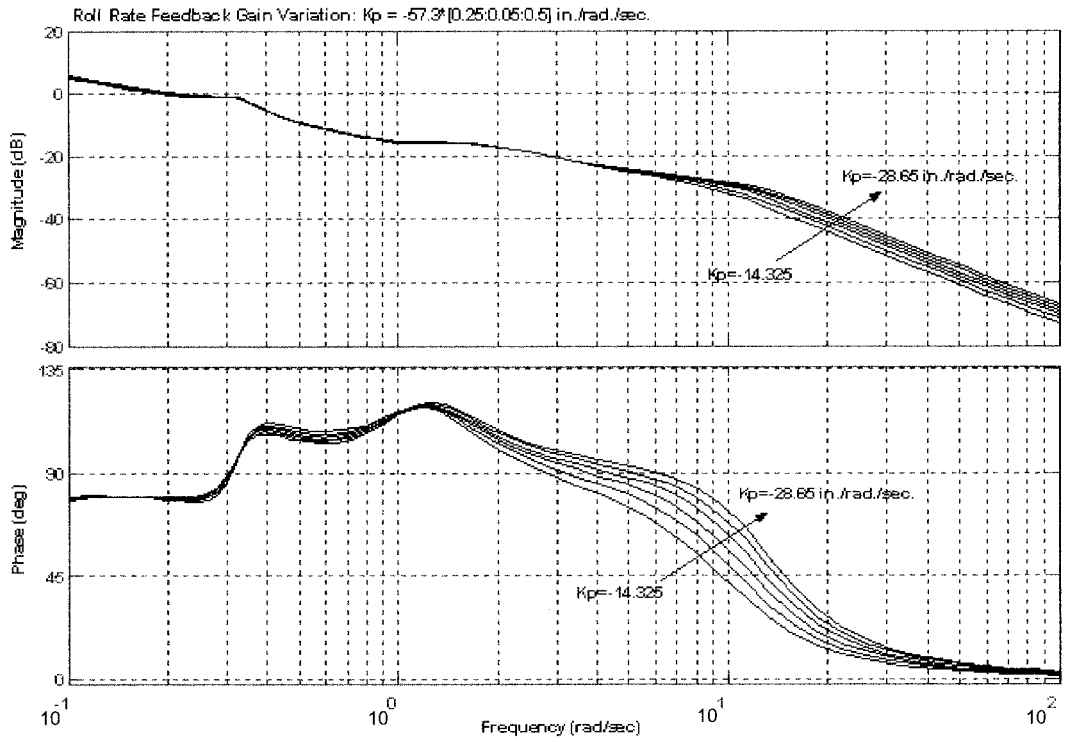

Figure 3.41 Roll Rate Feedback Frequency Response Trajectory for Full-Order Dynamics -Roll Attitude to Lateral Cyclic Dynamics

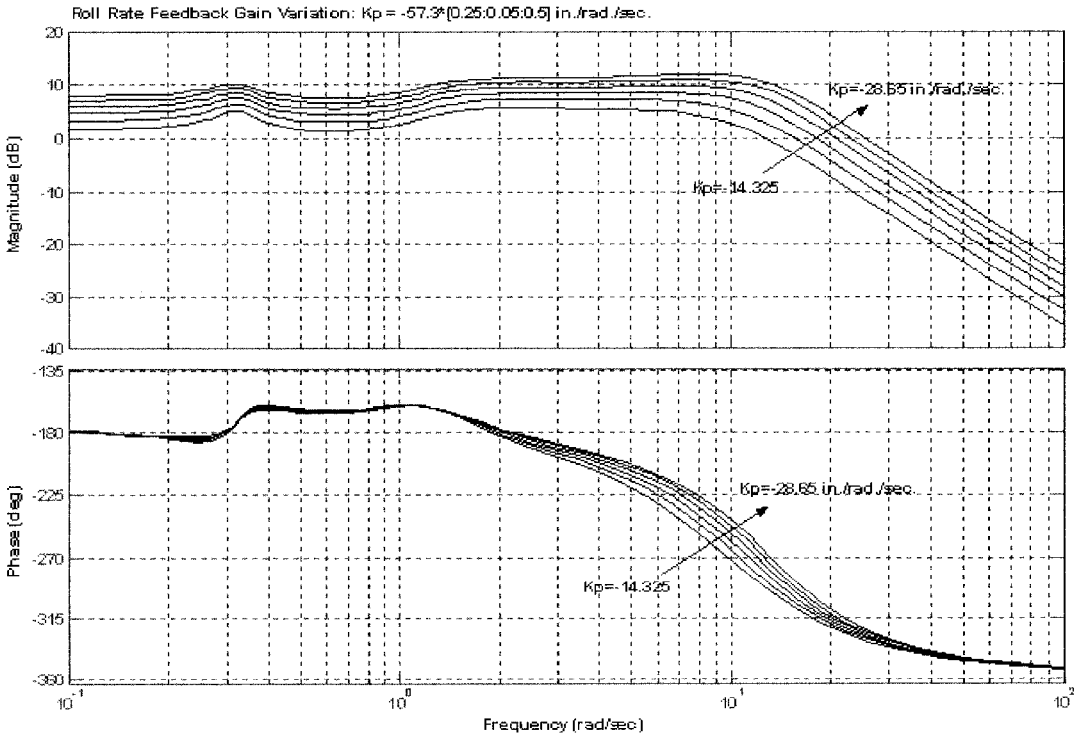

Figure 3.42 Roll Rate Feedback Frequency Response Trajectory for Full-Order Dynamics -Lateral Disc Tilt to Lateral Cyclic Dynamics

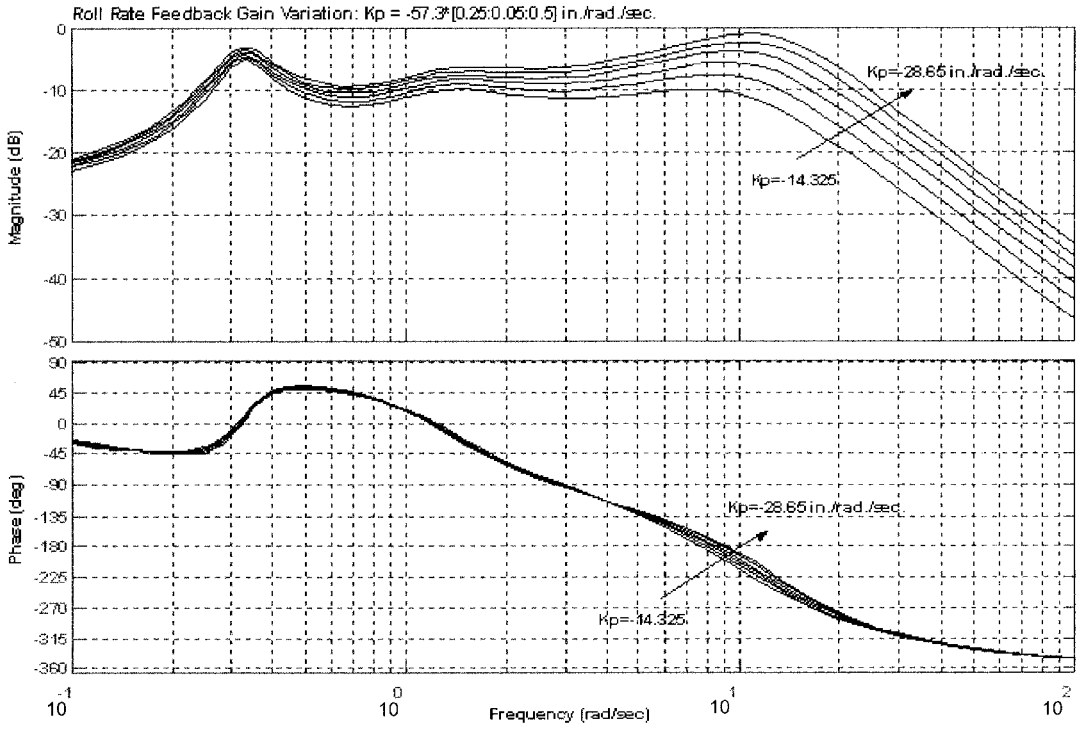

Figure 3.43 Roll Rate Feedback Frequency Response Trajectory for Full-Order Dynamics -Longitudinal Disc Tilt to Lateral Cyclic Dynamics

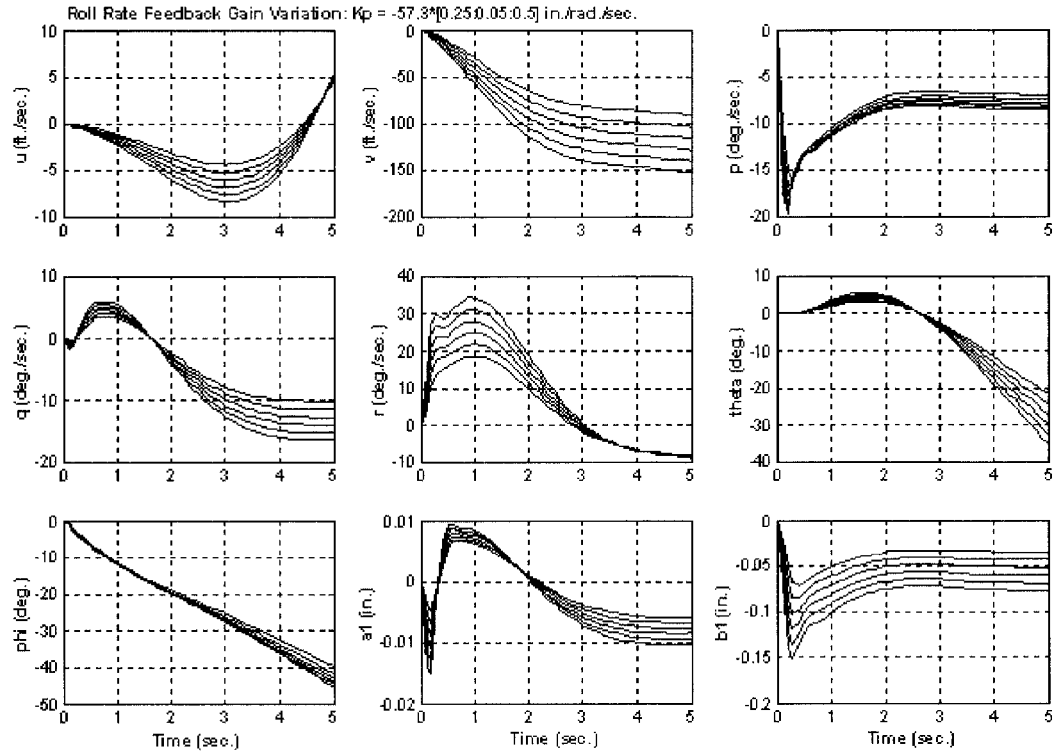

Figure 3.44 Roll Rate Feedback Lateral Unit Step Response Trajectory for Full-Order Dynamics

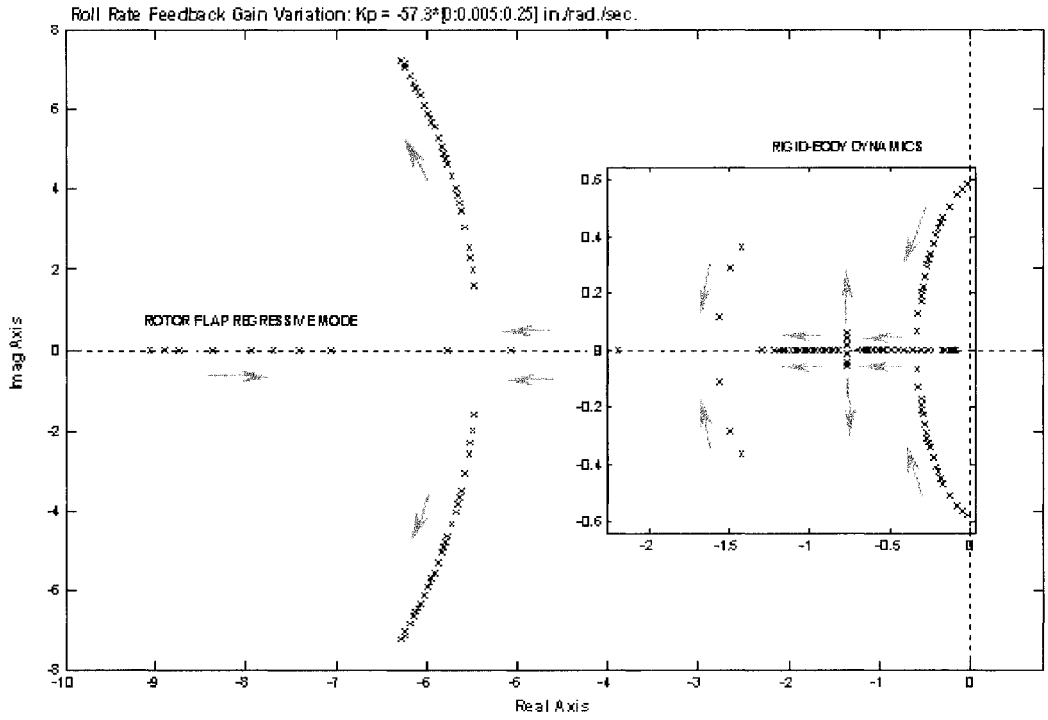

Figure 3.45 Roll Rate Feedback Mode Trajectories
-Effects on Reduced-Order Closed Loop Lateral Axis Dynamics

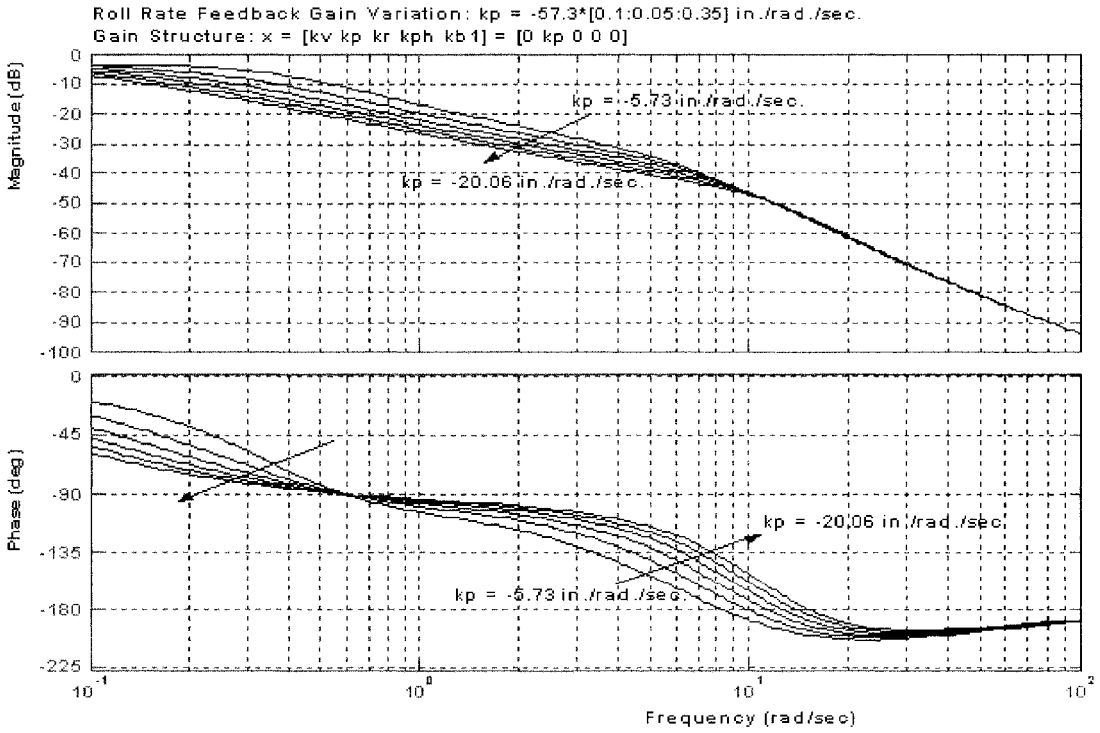

Figure 3.46 Roll Rate Feedback Frequency Response Trajectory for Reduced-Order Dynamics
-Roll Attitude to Lateral Cyclic Dynamics

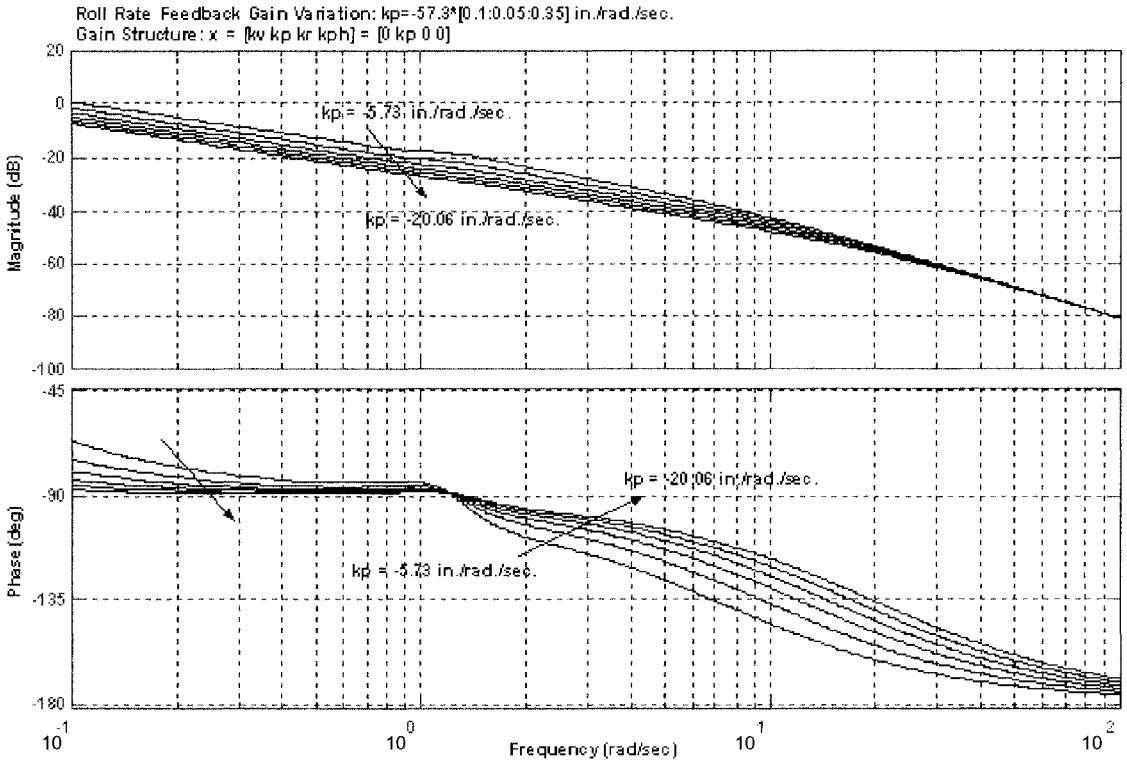

Figure 3.47 Roll Rate Feedback Frequency Response Trajectory for Reduced-Order Dynamics
-Roll Attitude to Lateral Cyclic Dynamics
-Without Rotor State in Model Structure

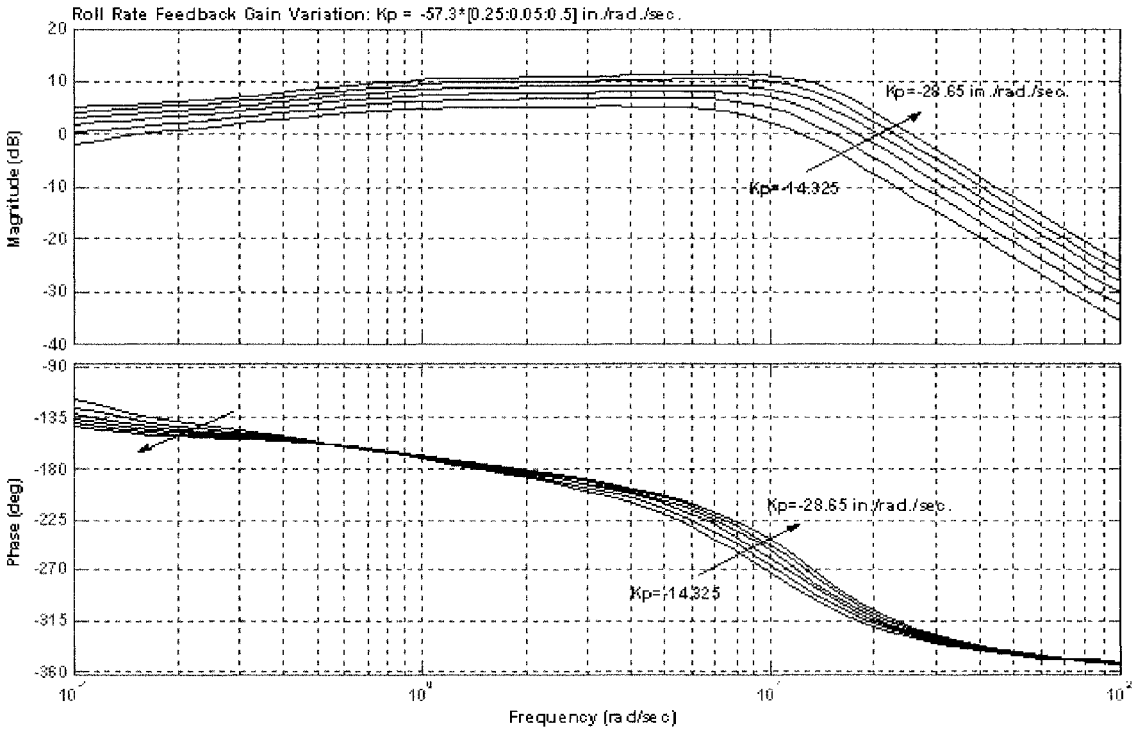

Figure 3.48 Roll Rate Feedback Frequency Response Trajectory for Reduced-Order Dynamics
-Lateral Disc Tilt to Lateral Cyclic Dynamics

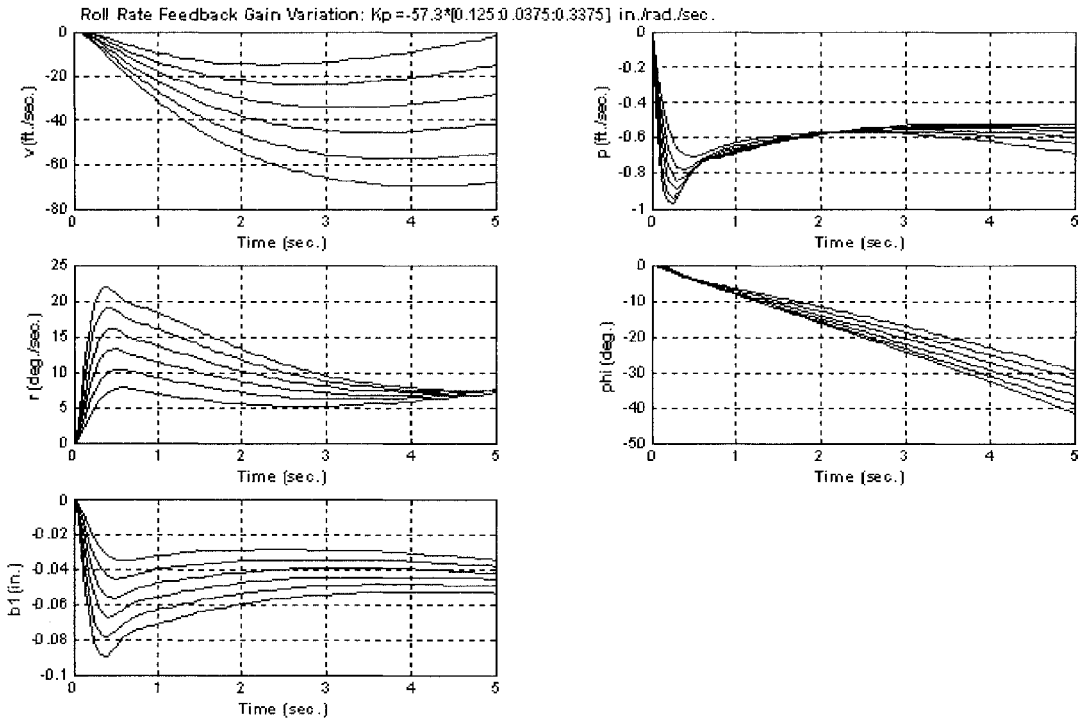

Figure 3.49 Roll Rate Feedback Lateral Unit Step Response Trajectory for Reduced-Order Dynamics

3.5.3.3 Effects of Roll Attitude Feedback on Full-Order Flight Dynamics

The effects of roll attitude variation are illustrated with a base gain structure incorporating a roll rate gain of –0.8595 in./rad./sec. As shown in Figure 3.50, the feedback of roll attitude effects the 0.1 to 3.0 rad/sec. frequency range, with a basic phase bandwidth range of 5.0 to 5.7 rad/sec. The phase delay is approximately 0.0022 sec. The effects on phase remain in the 0.1 to 5.0 rad/sec. range. The frequency spectrum shows significant coupling of low and high frequency dynamics. The resulting time domain response indicates a difficult design case, particularly in coupling between the roll and yaw dynamics as depicted by Figure 3.51

3.5.3.4 Effects of Roll Attitude Feedback on Reduced-Order Flight Dynamics

In a reduced-order format, the effects of roll attitude variation are also illustrated with a base gain structure incorporating a roll rate gain of –0.8595 in./rad./sec. As shown in Figure 3.52, the feedback of roll attitude effects the 0.1 to 1.5 rad/sec. magnitude range, with phase lead in the range of 2.6 to 2.9 rad/sec. The phase delay is approximately 0.004 sec. The effect on phase lead occurs over the 0.1 to 4.0 rad/sec. range. In Figure 3.53, without the rotor disc tilt dynamics, there is excitation of rigid-body dynamics with a narrowing of effected phase bandwidth to 1.8 rad./sec to 2.7 rad./sec.
In the time domain (Figure 3.54), the reduced-order response shows capture of an attitude command type response in roll and response correlation between the rotor disc tilt and vehicle on-axis response.

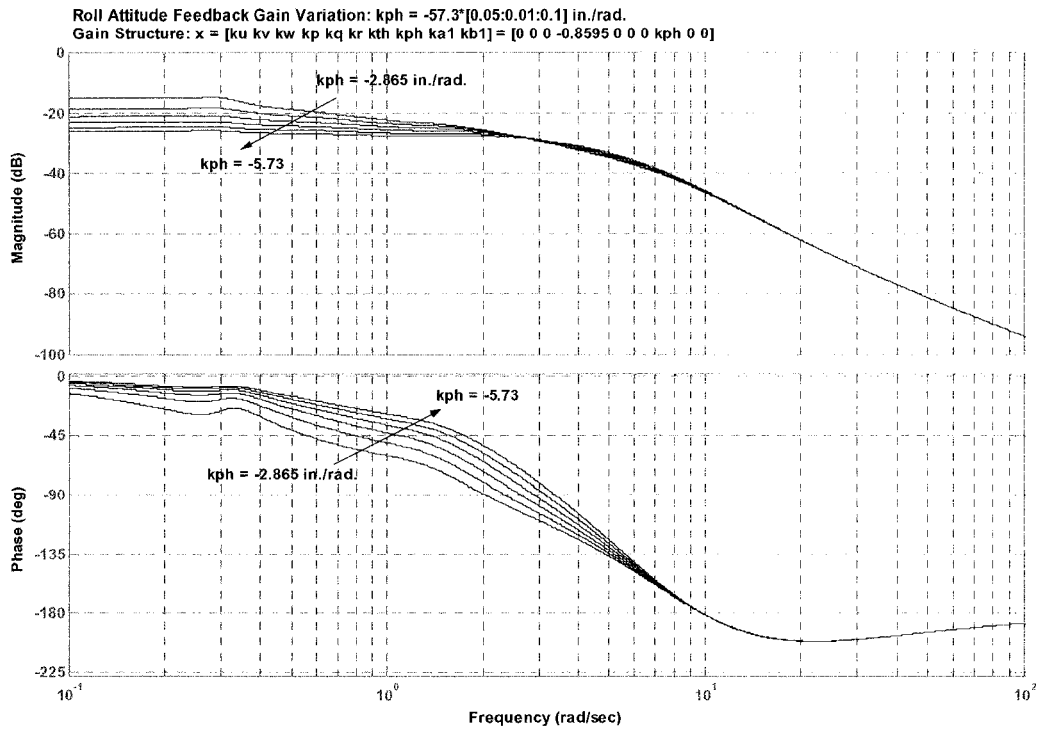

Figure 3.50 Roll Attitude Feedback Frequency Response Trajectory for Full-Order Dynamics -Roll Attitude to Lateral Cyclic Dynamics

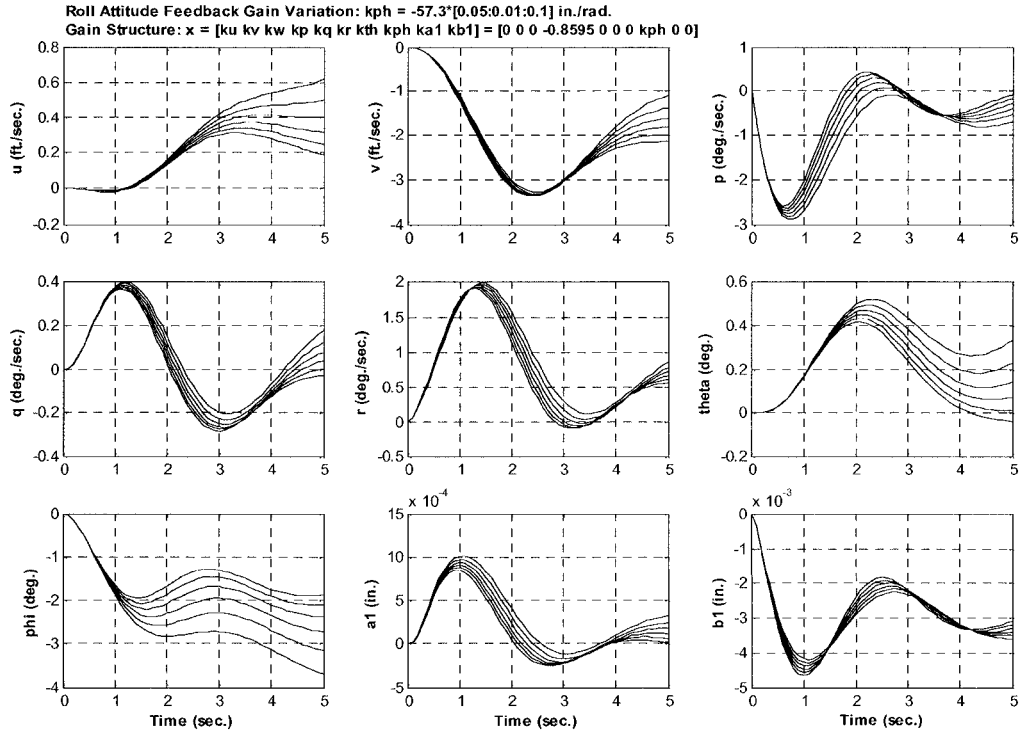

Figure 3.51 Roll Attitude Feedback Lateral Unit Step Response Trajectory for Full-Order Dynamics

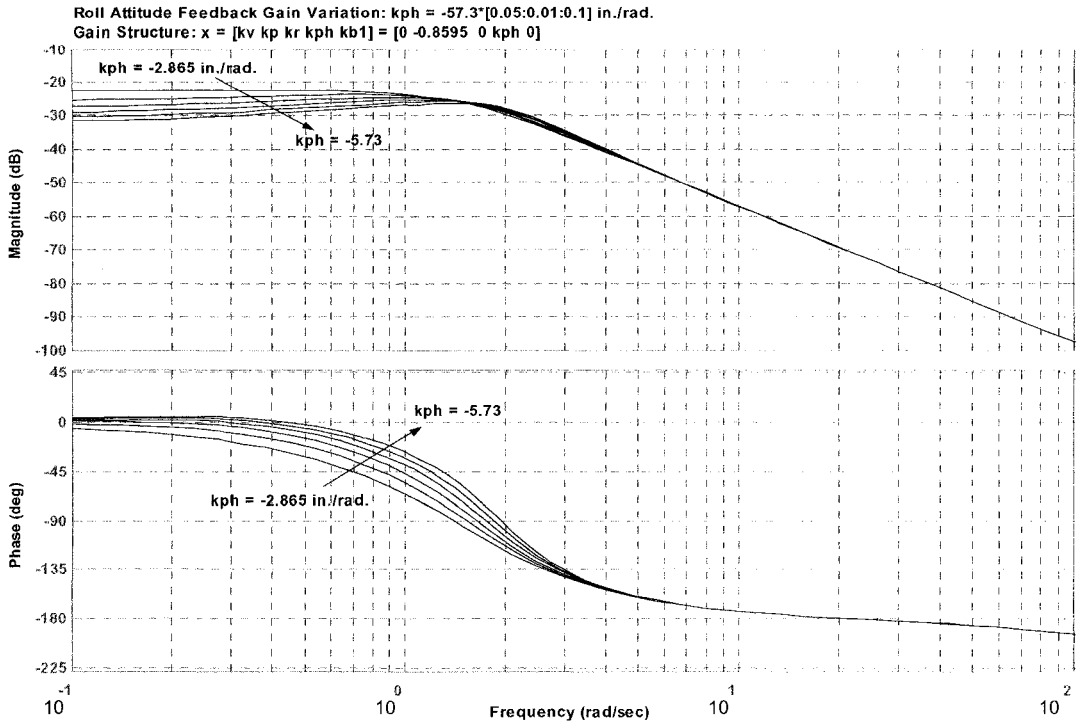

Figure 3.52 Roll Attitude Feedback Frequency Response Trajectory for Reduced-Order Dynamics -Roll Attitude to Lateral Cyclic Dynamics

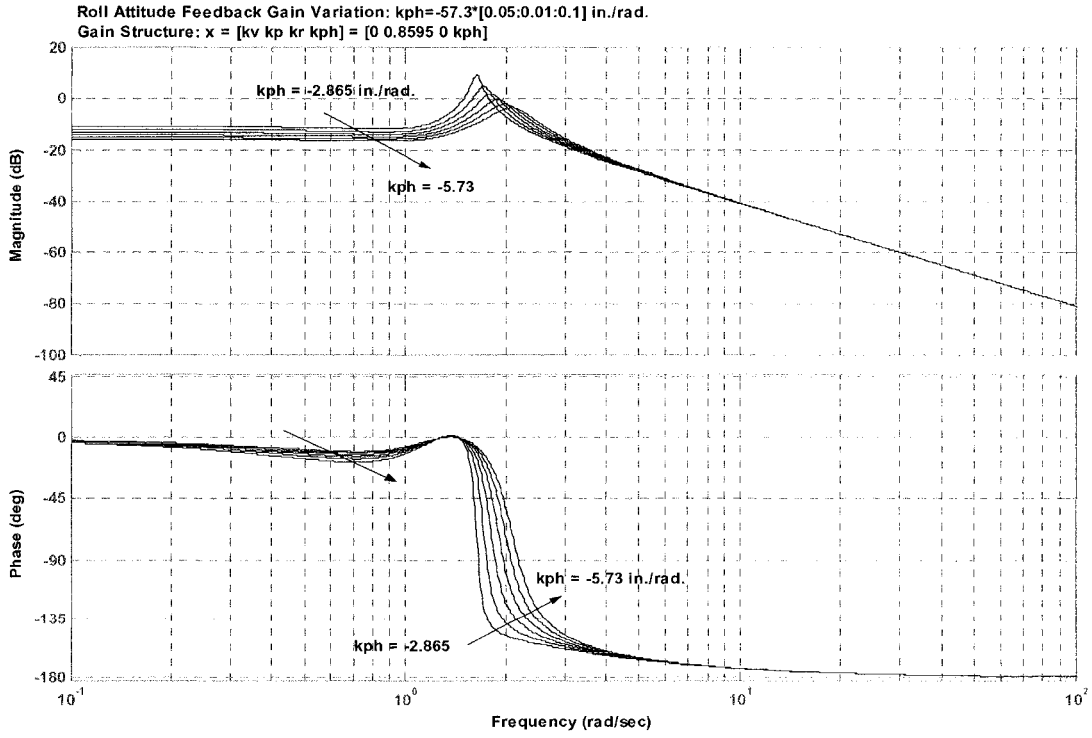

Figure 3.53 Roll Attitude Feedback Frequency Response Trajectory for Reduced-Order Dynamics -Roll Attitude to Lateral Cyclic Dynamics -Without Rotor State in Model Structure

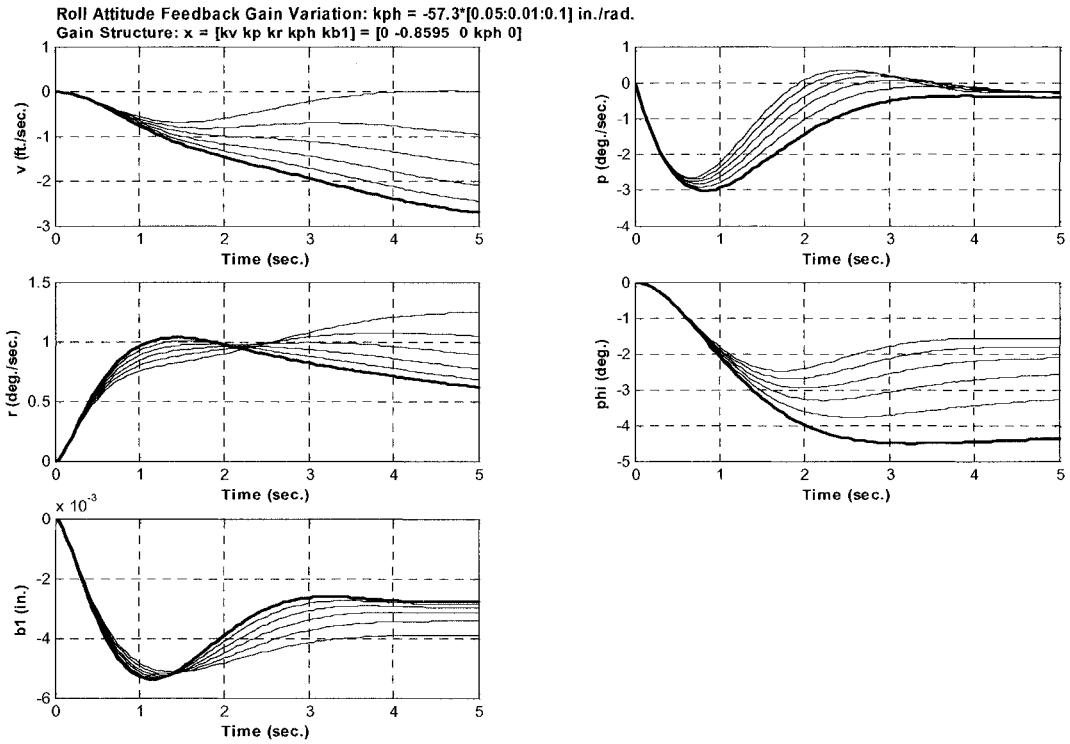

Figure 3.54 Roll Attitude Feedback Lateral Unit Step Response Trajectory for Reduced Order Dynamics

3.5.3.5 Specification Compliance: Overall Effects of Roll Attitude and Rate Feedback

The specification compliances due to roll rate and attitude and rotor state dynamics and feedback are depicted in Figures 3.55 and 3.56. The roll rate and attitude feedbacks cause transition of the bandwidth compliance from Level 2 to Level 1 as shown in Figure 3.55. As with the pitch axis feedback dynamics, the rate feedback is more influential in the transition.

The presence of rotor lateral disc tilt dynamics causes limiting of the attainable frequency bandwidth as shown in Figure 3.56. Aggressive gain choices lead to the over running of the compliance bounds.

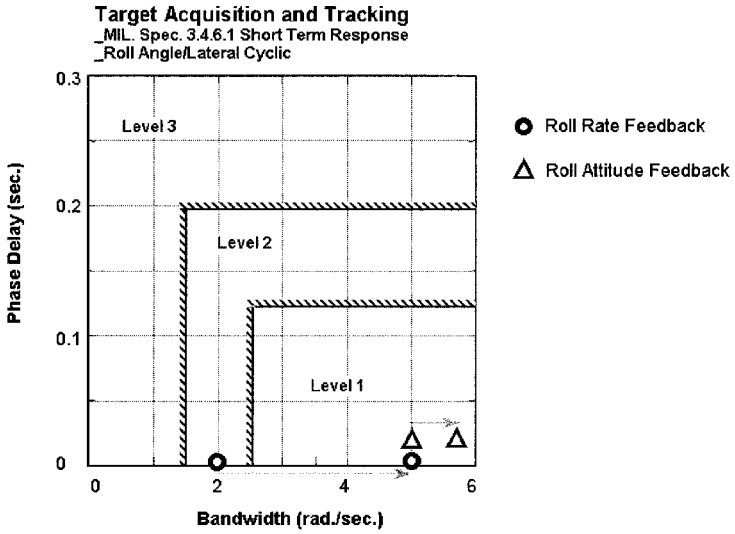

Figure 3.55 ADS-33E-PRF Rating Trajectory – Comparison of the Effects of Roll Attitude and Roll Rate Feedback

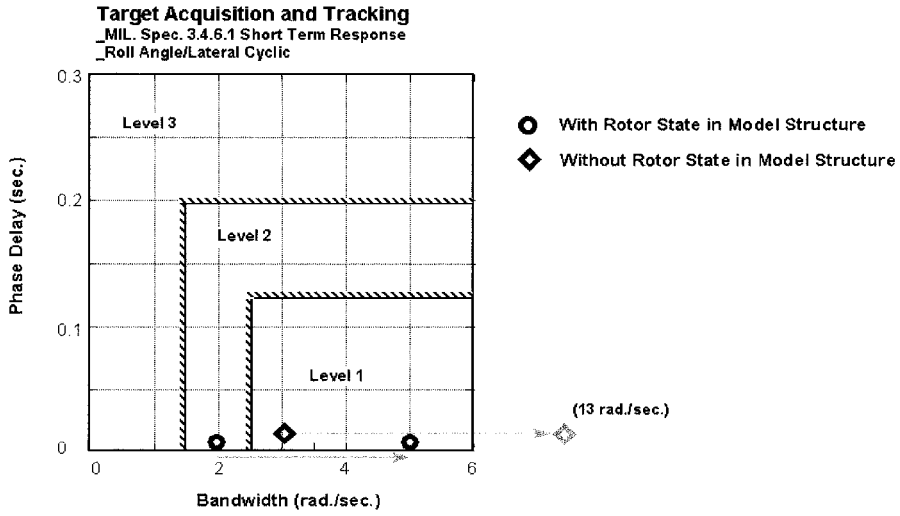

Figure 3.56 ADS-33E-PRF Rating Trajectory – Roll rate Feedback With and Without Rotor State Dynamics (6dof base model for comparison)

3.5.4 Summary of the RLM Analysis

In summary, the RLM method produced an understanding of the coupled rotor-body behavior of the hingeless rotor helicopter in context of rotor disc tilt dynamics. Findings are summarized below with attained effective control performance tabulated in Table 3.1.

In reference to Table 3.1, the results are favorable for gain prediction needed for the control law design process. The RLM method as applied herein did not formally address the implication of phase and latency inducing control/actuation dynamics. The compliance results also indicate some overly aggressive gain selections such that several case bandwidths in both pitch and roll would be unattainable by the Bell 412 ASRA. In conjunction, both of these concerns would further push the gain choices into unacceptable margins.

AXIS BANDWIDTHS (RAD./SEC.)	GAIN PARAMETERIZATIONS			
	Kp=- [5.73 – 20] (in./rad./sec.)	Kϕ = - [2.87 – 5.73] (in./rad.)	Kq = - [2.86 – 14.33] (in./rad./sec.)	Kθ = [2.86 – 14.33] (in./rad.)
$BW\theta_{NRS}$			3.5 – 6.2	8.0
$BW\theta_{RS}$			2.2 – 4.2	
$BW\phi_{NRS}$	3.0 – 13.0	5.0 – 5.7		
$BW\phi_{RS}$	2.0 – 5.0			

Notation:
NRS = **Without** Rotor State in Model Structure
RS = **With** Rotor State in Model Structure

Table 3.1 Summary of Root Locus Method (RLM) Effective Controls

The author believes that the overall modal trends produced by RLM are valid and raise important design directions and stability concerns necessary for the next step in flight control design. This crucial step is the development of the Classical Multivariable and Modern Eigenstructure Assignment control laws. In what follows these control laws aim to directly assess the effects of rotor states and their feedback on helicopter flight control. In Sections 3.5.4.1 and 3.5.4.2 important axis specific results are highlighted.

3.5.4.1 RLM Longitudinal Control Summary

The RLM result summary for longitudinal control is as follows:

- Pitch rate feedback has the effect of high mode propagation causing coupled rotor-body interaction not exhibited by pitch attitude-rate feedback
- Pitch rate feedback caused higher bandwidth alteration (phase lead development) than the pitch attitude-rate feedback
- Combined pitch attitude and rate feedback affected primarily low frequency rigid-body dynamics. The bandwidth modifications exceeded Level 1 boundaries at some gain parameterizations.
- Both pitch attitude and rate feedback influenced rotor flap mode off-axis dynamics
- A comparison of modal dynamics due to gain variation with and without rotor flap states in model structure indicates that the rotor states placed limits on the attainable bandwidth by the RLM SISO feedback

3.5.4.2 RLM Lateral Control Summary

The RLM result summary for lateral control is as follows:

- Roll rate has more effect on mode trajectory than roll attitude
- Unlike pitch attitude, roll attitude caused significant low and high frequency effects as well as phase modification based on model order
- Roll attitude had only modest effects on bandwidth. The bandwidth modifications exceeded Level 1 boundaries at some gain parameterizations.
- Modal dynamics, due to gain variation with and without rotor flap states in model structure, limit attainable bandwidth by the presence of rotor states by RLM SISO feedback
- Lateral/Directional dynamics are more complex than longitudinal and present a significant controller design challenge

3.6 Multivariable Control Law Development

The previous development has illustrated the theoretical effects of rotor state dynamics in closed loop control. The following analysis aims to develop and prepare controllers for the flight test portion of this research project. The overall goal to provide a performance prediction for the Bell 412 ASRA manager and flight crews for implementing the controllers safely.

3.6.1 Classical Multivariable Control (CMC) Without Rotor State Feedback

The Attitude Command Attitude Hold (ACAH) response type develops a vehicle attitude proportional to the cyclic control deflection force. This type of controller allows the pilot to manage the flying of the aircraft without attitude stabilization. Using the vehicle rate and attitude gyro sensors, this controller is useful in IFR flight conditions where useable environmental cues are low. The ACAH response is achieved by gain selection as well as command model applications that create the desired trajectories to be followed. The closed loop vehicle responses are given by:

$$\frac{\theta}{\delta(s)}(s)=\frac{M_\delta\omega^2}{s^2+k_q(2\zeta\omega)M_\delta s+M_\delta k_\theta\omega^2} \tag{3.36}$$

$$\frac{\phi}{\delta(s)}(s)=\frac{L_\delta\omega^2}{s^2+k_p(2\zeta\omega)L_\delta s+L_\delta k_\phi\omega^2} \tag{3.37}$$

$$\frac{\psi}{\delta(s)}(s)=\frac{N_\delta\omega^2}{s^2+k_\psi(2\zeta\omega)N_\delta s+N_\delta k_\psi\omega^2} \tag{3.38}$$

The system frequency is selected based on the desired vehicle output response. Here, by ADS-33E-PRF criterion the desired pitch, roll, and yaw bandwidths are 2-4 rad./sec, 2.5-6 rad./sec., and 3.5-6 rad./sec. respectively. The rigid-body gains were selected and adjusted to achieve the desired responses based on;

$$k_{Attitude}=\frac{\omega^2}{D_\delta} \tag{3.39}$$

$$k_{Attitude-Rate}=\frac{2\zeta\omega}{D_\delta} \tag{3.40}$$

These theoretical gains and command model parameters are suggested based on the NRC-FRL Flight Test Pilot/Engineering course for ACAH design in single input single output (SISO) control.

Table 3.2 depicts the multi-axis system. This synthesis however did not produce favorable closed loop multi-axis response and required significant empirical adjustment to attain desired control effect. The classical controller (CMC) was then re-designed and optimized manually within the non-linear model (FCDE); the final controller is tabulated in Table 3.3.

$CMC\text{-}ACAH_{THEORY}$	GAIN STRUCTURES		ACAH COMMAND MODELS
AXIS RESPONSE TYPE	ATTITUDE	ATTITUDE-RATE	
LONGITUDINAL ACAH	50.6730	126.6825	$\frac{0.0982}{s^2+1.9909s+12.4433}$
LATERAL ACAH	40.973	102.4328	$\frac{-0.2347}{s^2-0.0220s-24.042}$
DIRECTIONAL ACAH	-14.0443	-35.1108	$\frac{-7.212}{s^2-40.959s-255.999}$

ku, kv, kw = in./m./sec.;
kp, kq, kr = in./rad./sec.; $k\theta, k\phi, k\psi$ = in./rad.
ka1, kb1= in./mm.

Table 3.2 Theoretical Classical Attitude Command Attitude Hold (ACAH) Structure

A first-order command model was applied assuming the vehicle behaved in bare-airframe form as a first order system. It is suggested that the command model bandwidth be 2 to 3 times that of the axis crossover frequency. Figures 3.57 to 3.71 depict simulated responses of the coupled helicopter due to 5-inch step inputs. Due the longitudinal step input, the rigid body accelerations trim out well as shown in

CMC-ACAH AXIS RESPONSE TYPE	GAIN STRUCTURE ku, kv, kw = in./m./sec.; kp, kq, kr = in./rad./sec.; $k\theta, k\phi, k\psi$ = in./rad. ka1, kb1= in./mm.
LONGITUDINAL ACAH	Cyclic Gain: [ku kw kq $k\theta$] = [0.000 0.000 15.2 30.1]
LATERAL ACAH	Cyclic Gain: [kv kp kr $k\phi$] = [0.000 -7.68 0.000 -24.34]
DIRECTIONAL RC	Tail-Rotor Collective Gain: [kr] = [8.78]

Table 3.3 Classical Multivariable Control (CMC) Attitude Command Attitude Hold (ACAH) Structure

Figure 3.57, with gravitational acceleration depicted as reference. The vehicle coupling is already evident in lateral and longitudinal accelerated body dynamics. The vehicular responses shown in Figure 3.58 consist primarily of the pitch rate and attitude ACAH structure due to the commanded step. Forward velocity rises as the ASRA's nose pitches forward due to disc tilt. Note the rotor dynamics (a_1) lead the rate (q) response. Coupled response is evident in roll, yaw, and heave dynamics. The axis control coupling is best illustrated in off-axis driven actuation-control as in Figures 3.59 and 3.60 where the on-axis requirement is higher in the primary axis by 4% and 9% in lateral and directional actuation. The control rate indicates a low energy usage post input. The initial control rates tend to oscillate as the controller seeks the vehicle rate and responds to MIMO activity.

Due to the lateral step, one notices the significant coupling of the roll rate and the rotor longitudinal flap dynamics (pitch rate dynamics) of Figure 3.63 though overall the couplings are of similar magnitudes in

all axes as shown in Figure 3.64. The yaw dynamics as in the longitudinal case are driven to develop a rate excursion type excursion. The control usage depicted in Figure 3.65 emphasizes the cross-coupled nature of the helicopter.

The tail-rotor collective step (Figure 3.68) attains the desired rate command in yaw as well as attaining good attitude capture in the pitch and roll axes. The yaw dynamics develop the least amount of rotor activity though only a 1.5 inch. commanded step is applied as shown in Figures 3.69 and 3.70.

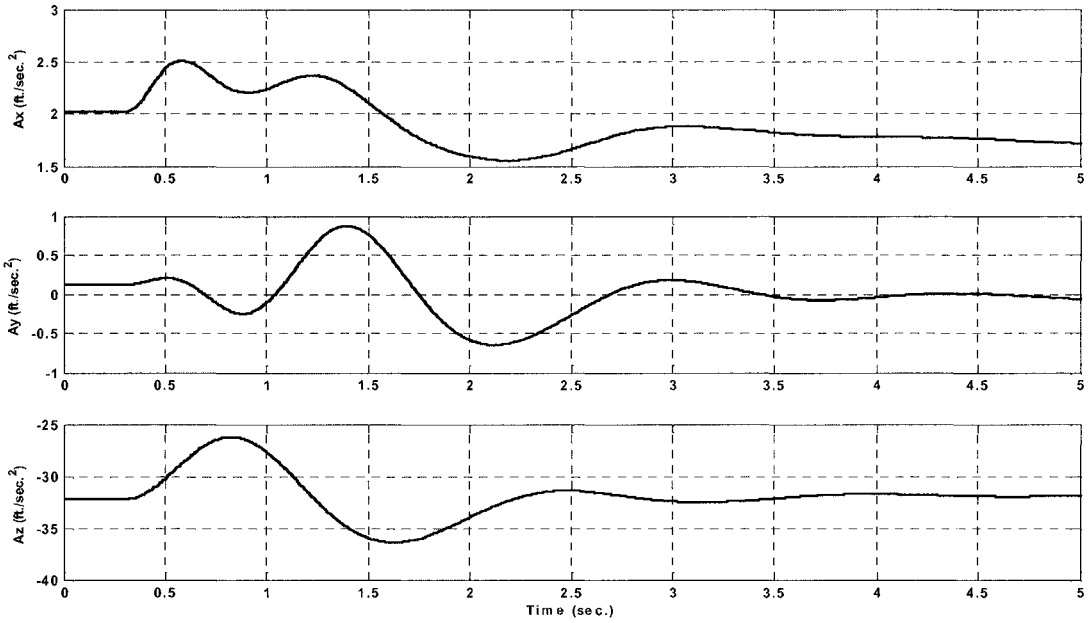

Figure 3.57 CMC Controller Acceleration Response due to Longitudinal Step

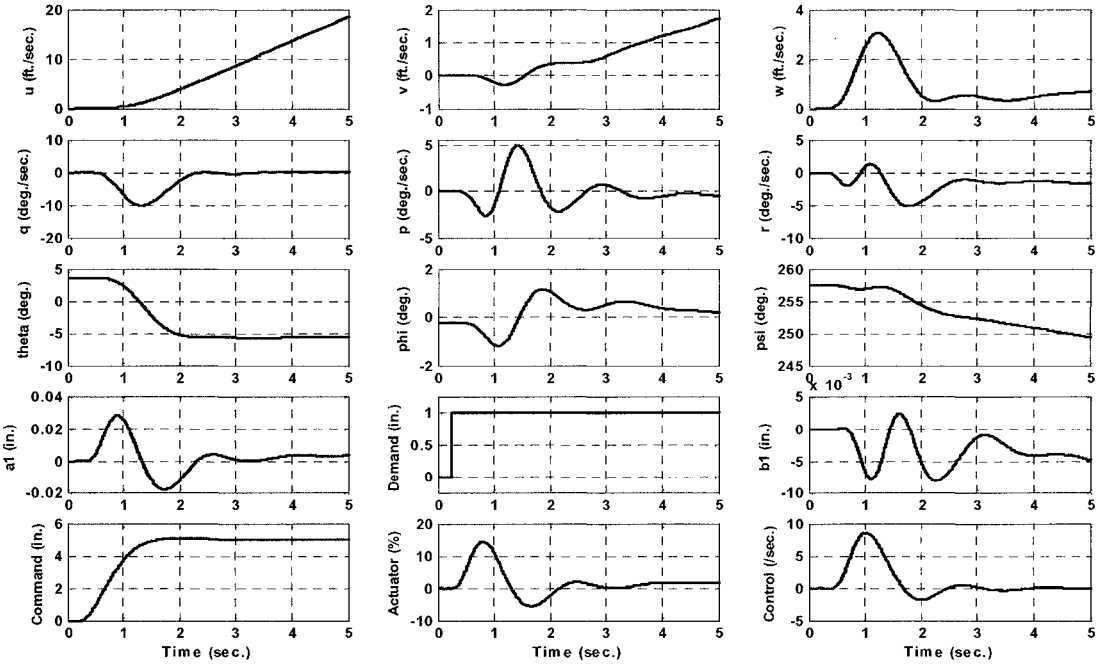

Figure 3.58 CMC Controller Time History Response due to Longitudinal Step

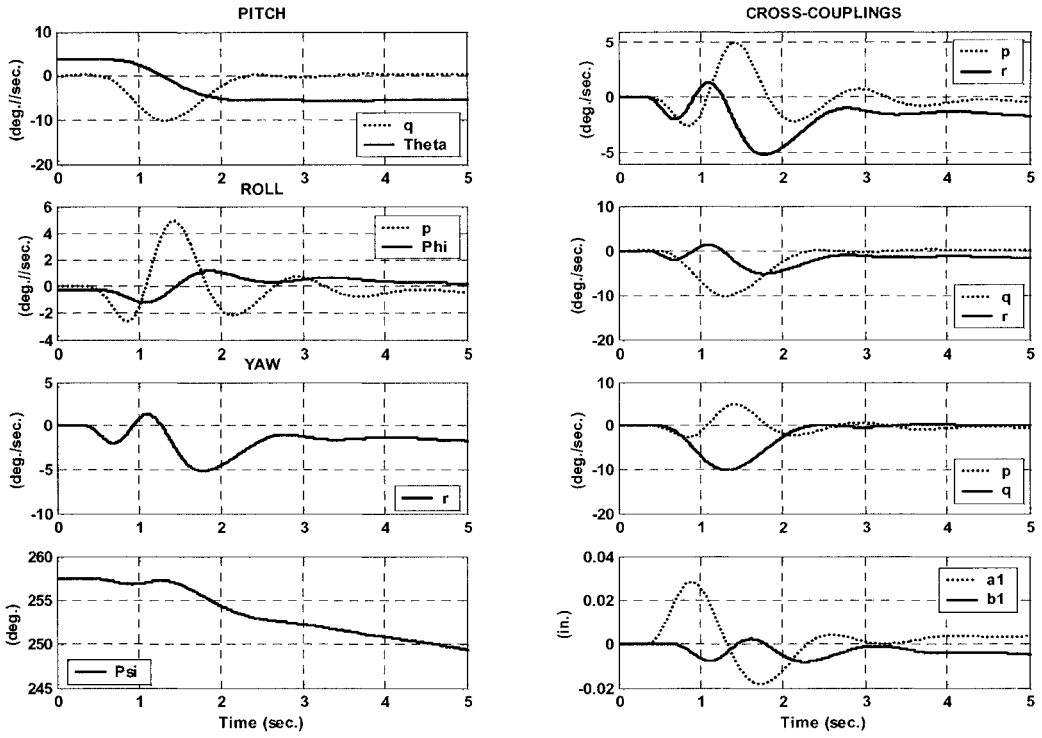

Figure 3.59 CMC Controller Cross Coupling Responses due to Longitudinal Step

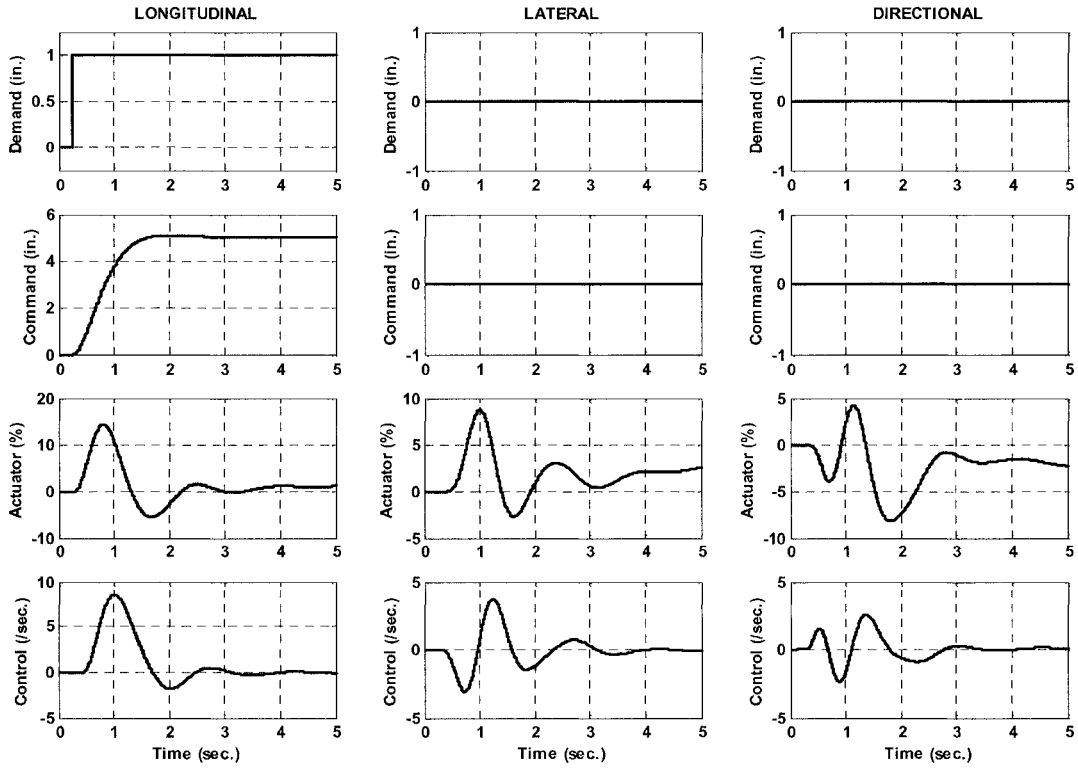

Figure 3.60 CMC Controller, Control Usage due to Longitudinal Step

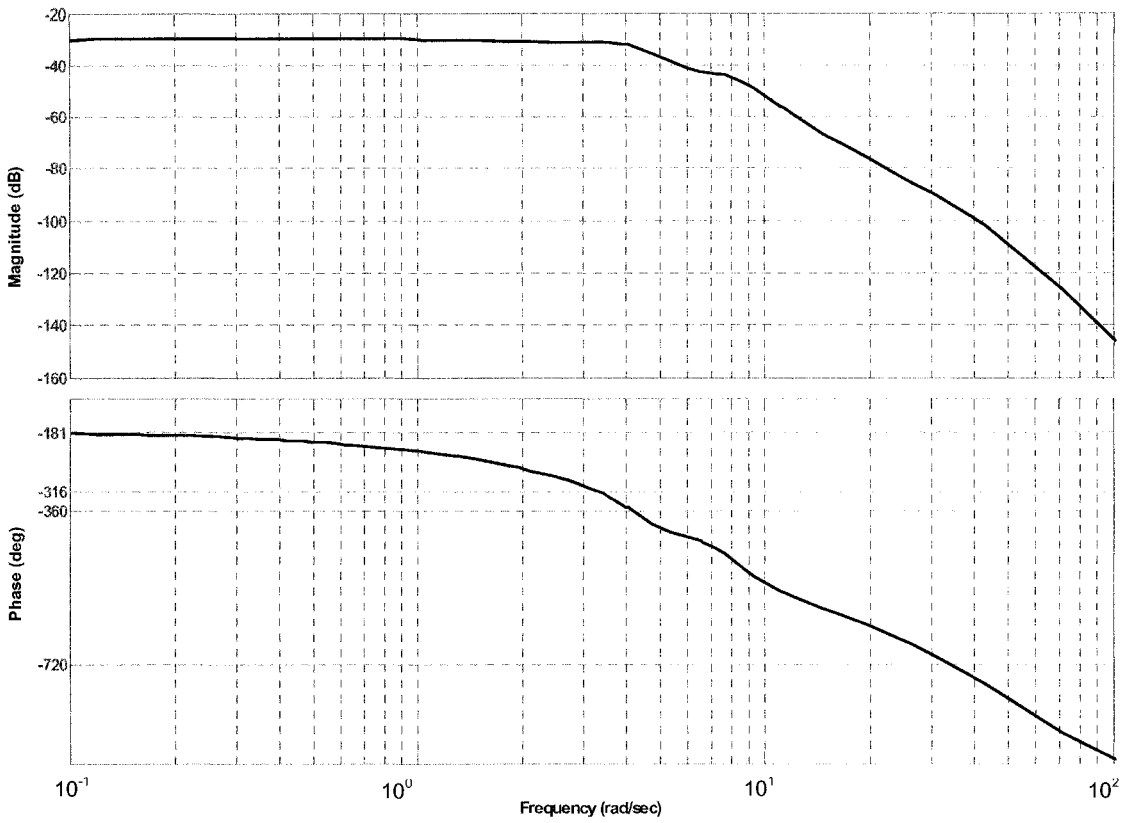

Figure 3.61 CMC Controller: Longitudinal Frequency Response

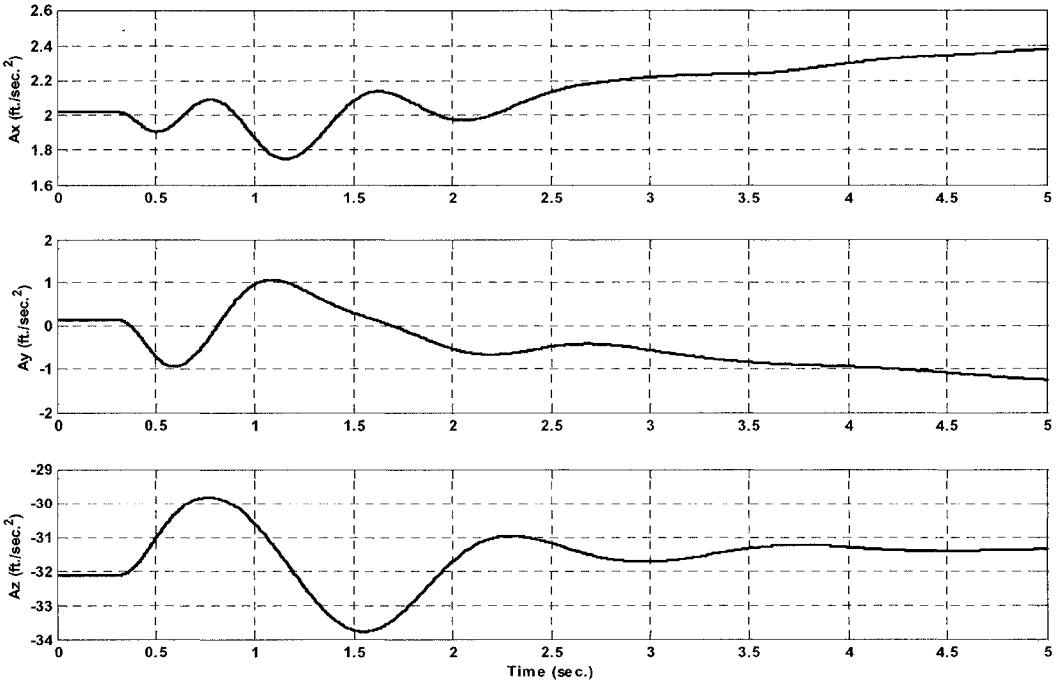

Figure 3.62 CMC Controller Acceleration Response due to Lateral Step

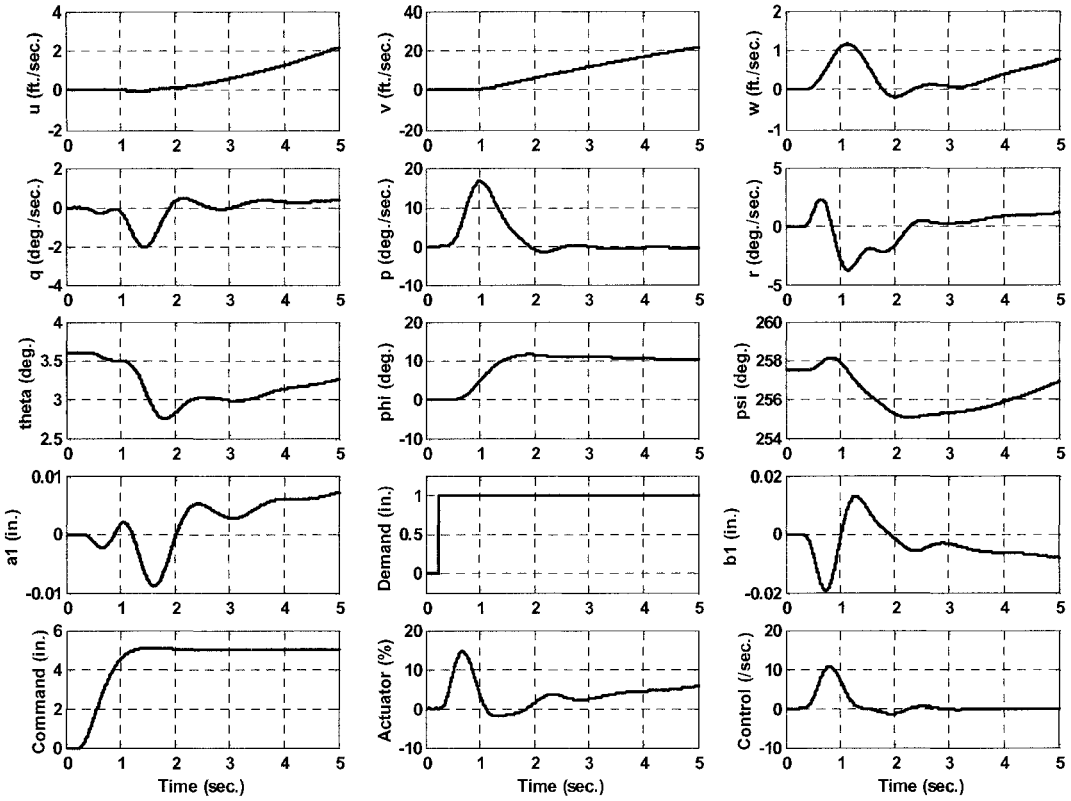

Figure 3.63 CMC Controller Time History Response due to Lateral Step

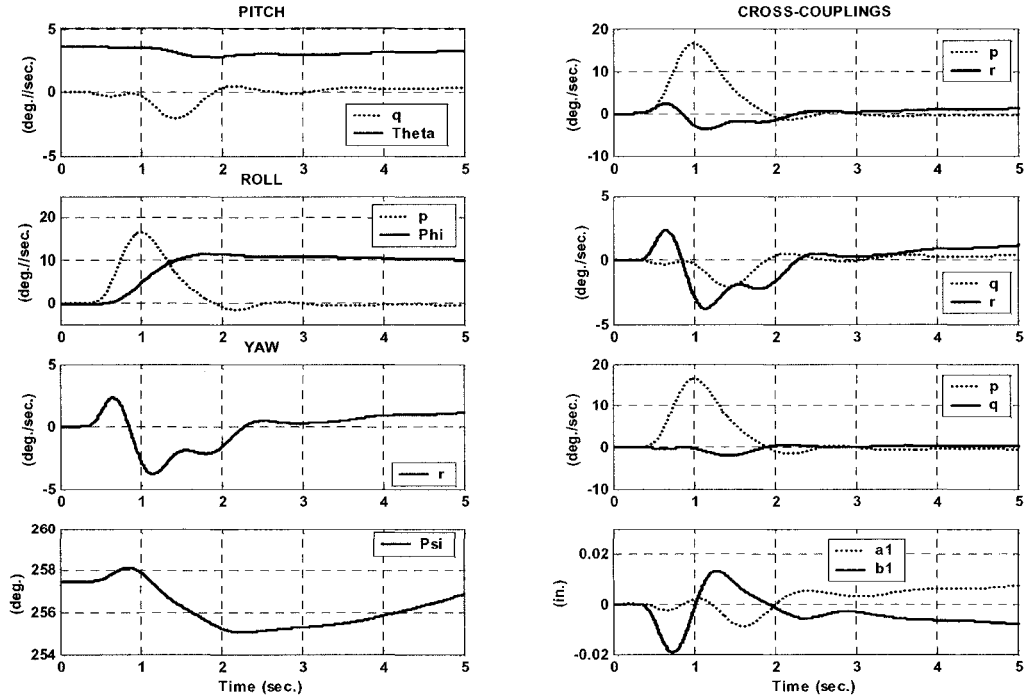

Figure 3.64 CMC Controller Cross Coupling Responses due to Lateral Step

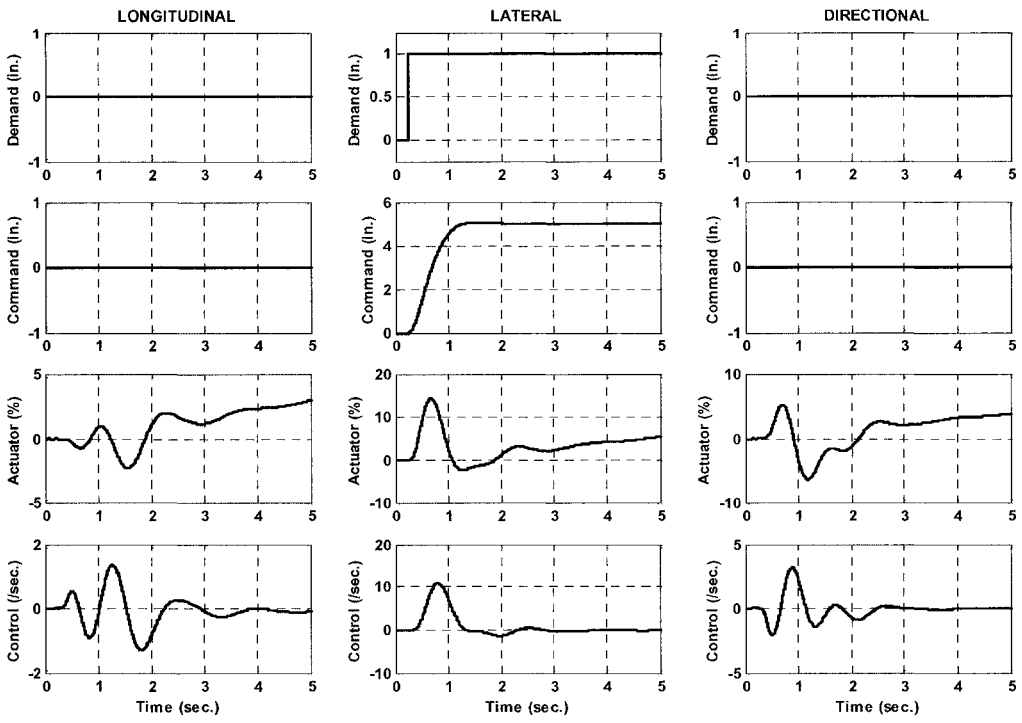

Figure 3.65 CMC Controller, Control Usage due to Lateral Step

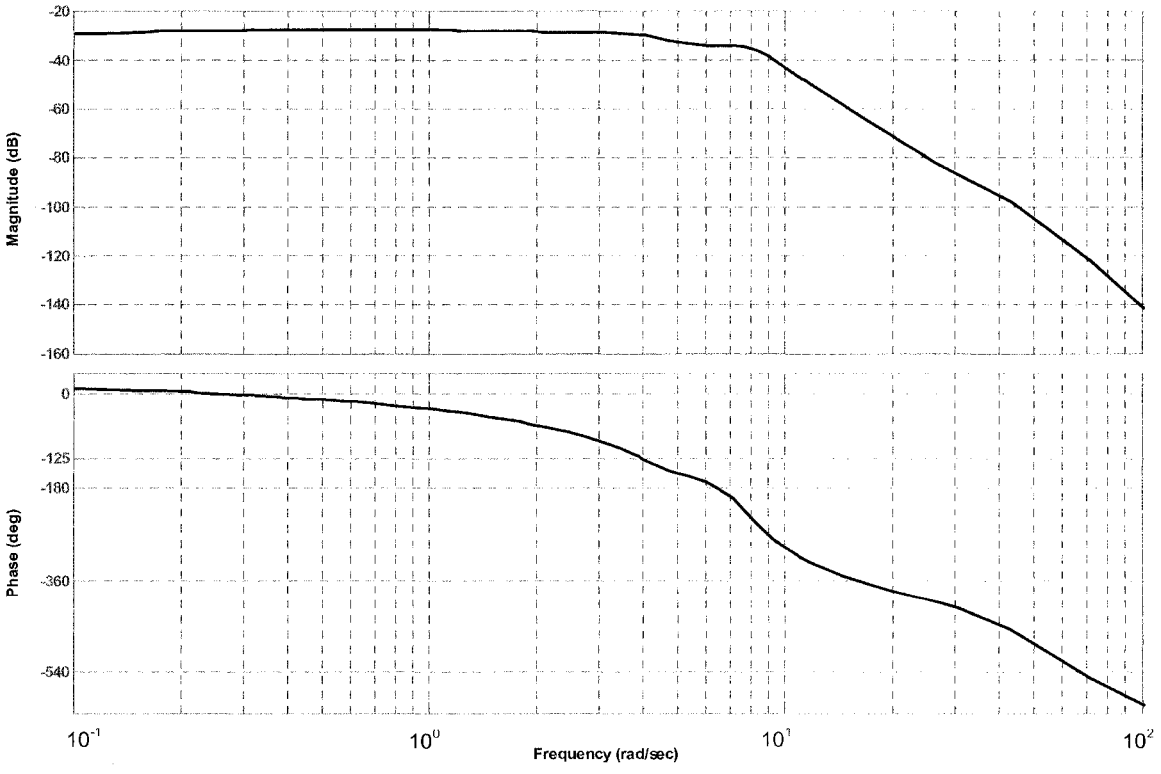

Figure 3.66 CMC Controller Lateral Frequency Response

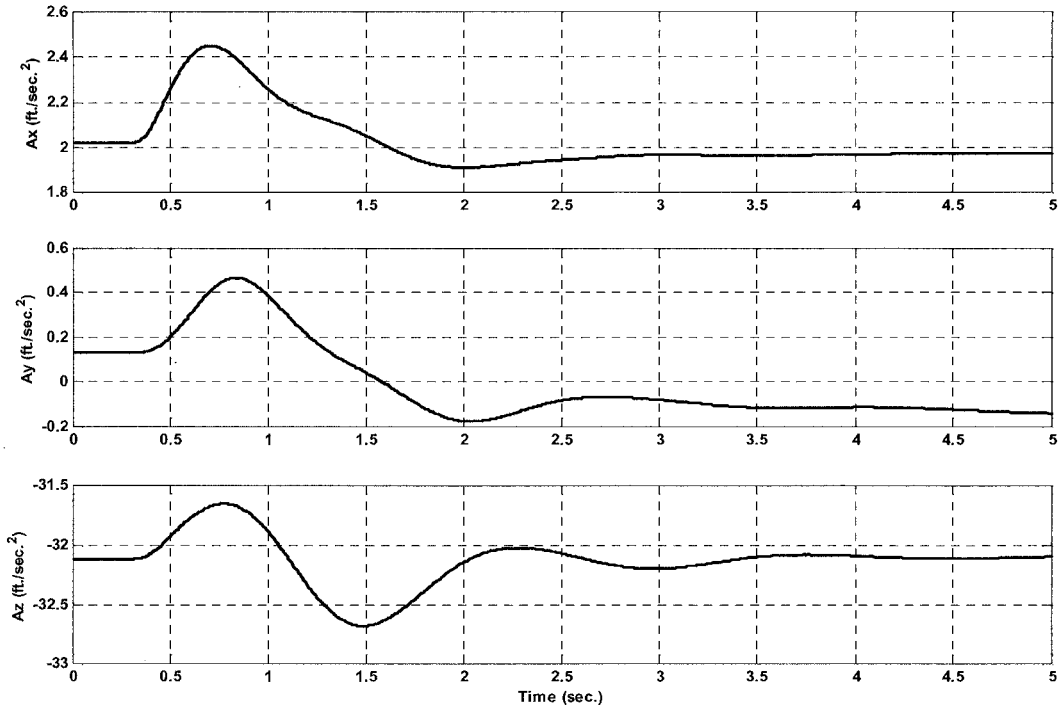

Figure 3.67 CMC Controller Acceleration Response due to Tail Rotor Collective Step

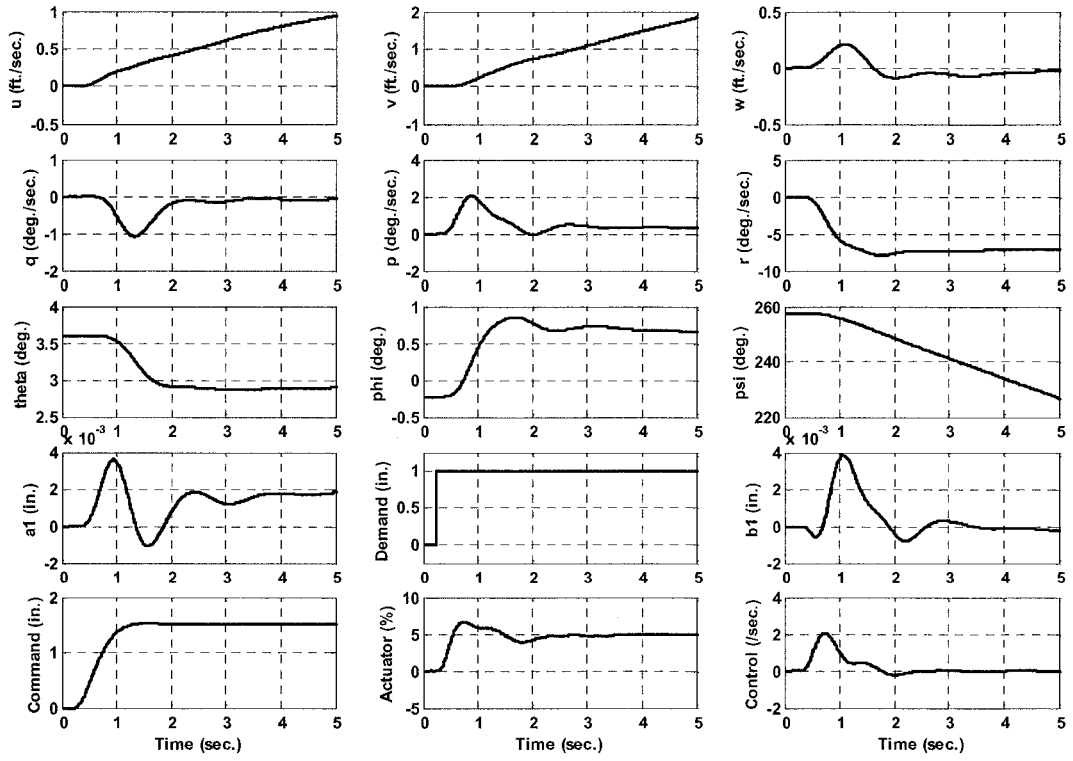

Figure 3.68 CMC Controller Time History Response due to Tail Rotor Collective Step

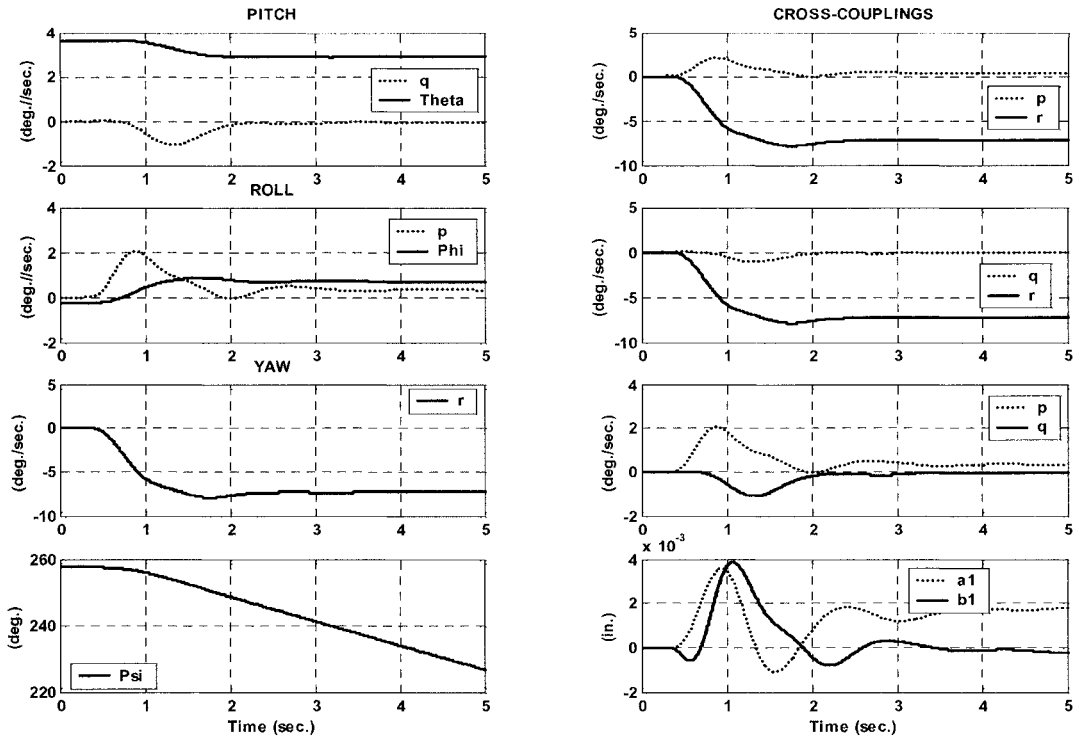

Figure 3.69 CMC Controller Cross Coupling Responses due to Tail Rotor Collective Step

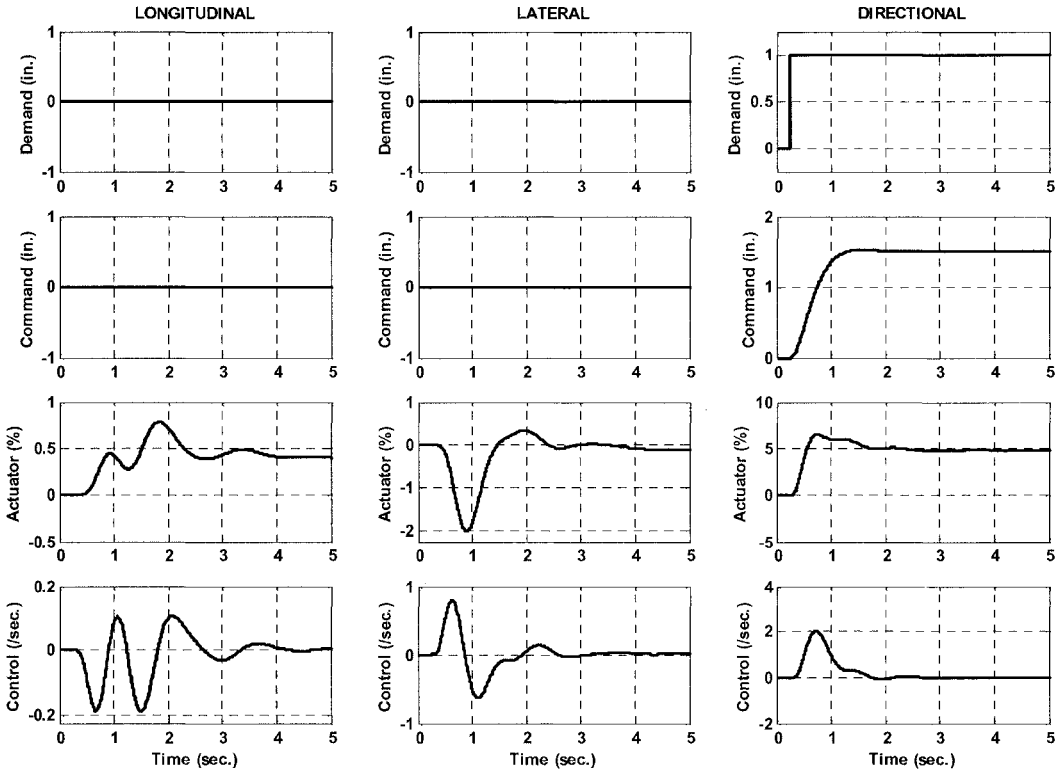

Figure 3.70 CMC Controller, Control Usage due to Tail Rotor Collective Step

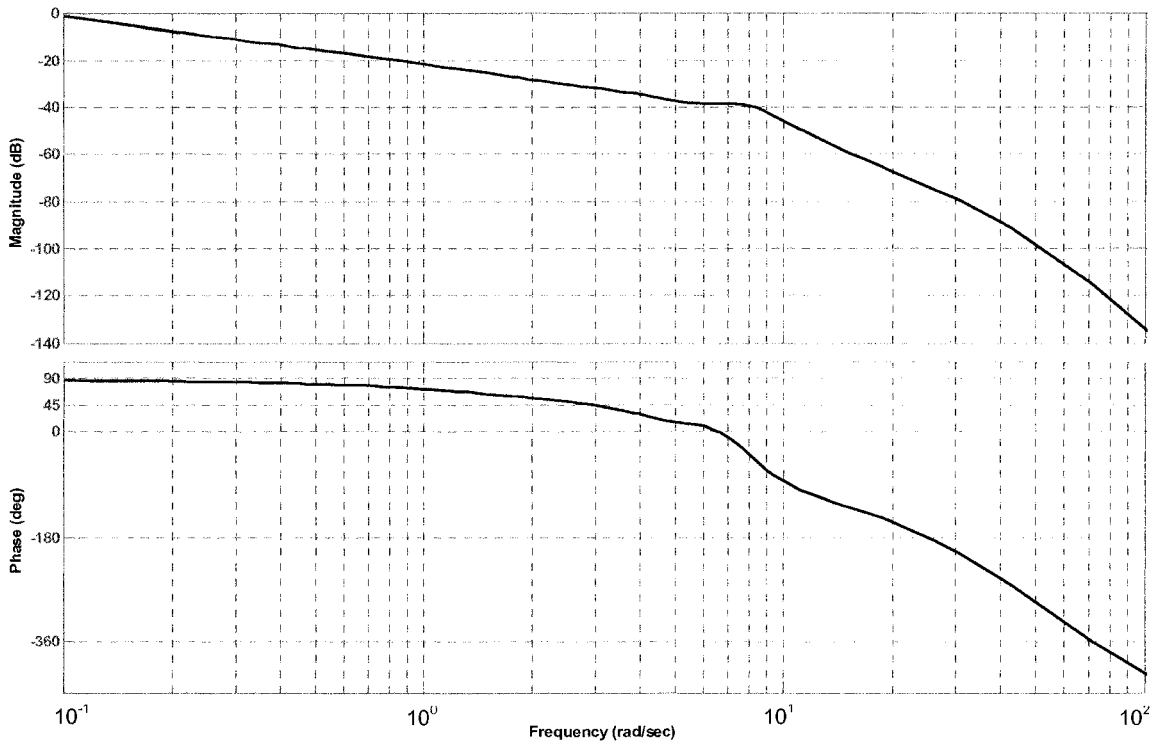

Figure 3.71 CMC Controller, Directional Frequency Response

The longitudinal frequency response as shown in Figure 3.61 is unwrapped, in correct phase and magnitude, and thus the phase bandwidth may be assessed at 135 degrees from phase response commencement. In the longitudinal axis a bandwidth and phase delay of 3.2 rad./sec. and 0.255 seconds, respectively, was assessed at this particular gain structure.

The lateral frequency response is unwrapped, and in correct phase and magnitude. As shown in Figure 3.66 the phase bandwidth frequency response for the lateral axis is assessed at 135 degrees from phase response commencement to be 4.0 rad./sec. at a phase delay of some 0.197 seconds.

At 60 knots, the helicopter is highly stable and damped directionally. Thus, control strategies for rate command are typically used. However, such control does not afford turn coordination control non-linearity that results in the increasing pilot workload throughout the turn. The rate commanded vehicle will tend to over-control the force and moment requirements causing excessive yaw dynamics. Thus rate damped type control is another control strategy to over-come this non-linear control response. Here, rate command was used for yaw control. The directional frequency response is depicted in Figure 3.71. The rate response is 90 degrees out of phase with the attitude response and thus phase bandwidth must be assessed at 45 degrees from 90 degree commencement or 135 degrees from 180 degrees commencement; this, depending on directional control to response sign convention. The directional phase bandwidth is thus assessed to be 3.1 rad./sec. with a phase delay of 0.146 seconds.

3.6.2 Specification Compliance: Attained Axis Bandwidth Without Rotor State Feedback

The ADS-33-PRF compliances resulting from these frequency responses are depicted in Figures 3.72. The pitch axis depicts Level 1 compliance while those of the roll and yaw axes are Level 2. The trajectories of axis bandwidths from the bare-aircraft dynamics of the Bell 412 ASRA as assessed in Chapter 2 is significant for all axes indicating the ability of the CMC closed loop control in mode stabilization.

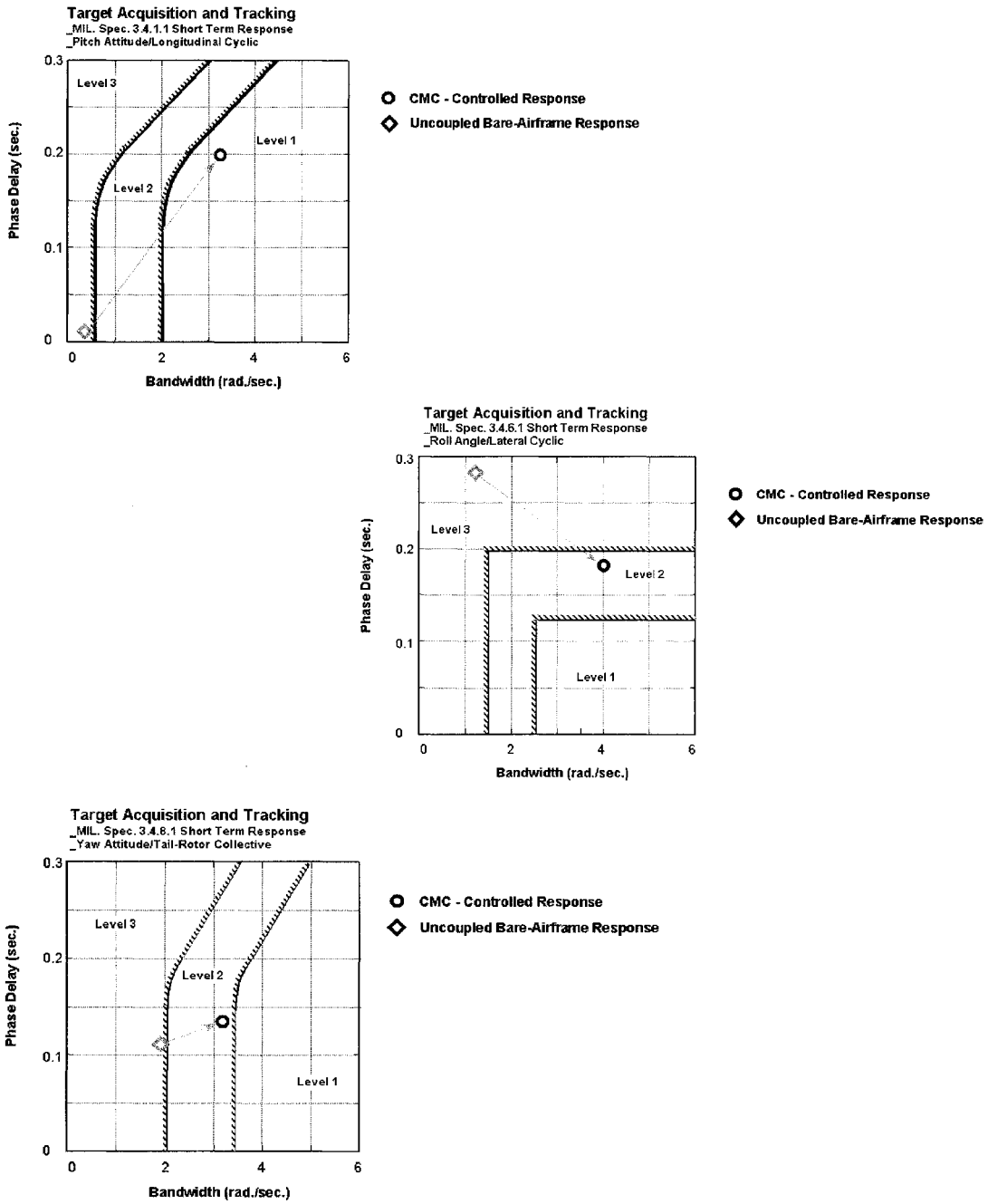

Figure 3.72 CMC Controller Response Compliance – ADS-33E-PRF

3.6.3 Effects of Rotor State Feedback by Classical Multivariable Control (CMC)

The effects of rotor state feedback are now investigated on the baseline classical controller. The author illustrates some of the benefits and capabilities provided by classical multivariable control affected in the presence of longitudinal and lateral disc tilt feedback. In the proceeding section the author evaluates the EAC controller for a variety of task elements critical to attaining modern helicopter flight dynamic and aeromechanics responses. The assessed tasks include:

- Rigid-Body Frequency Bandwidth Extension
- Aeromechanical Stability Gain Thresholds Evaluation
- Disturbance Attenuation Assessment
- Command Tracking Assessment

3.6.3.1 Bandwidth Frequency Modification

For this particular simulation, a gain structure of -1.25 in./mm. and 1.15 in./mm. of longitudinal and lateral disc tilt feedback is evaluated.

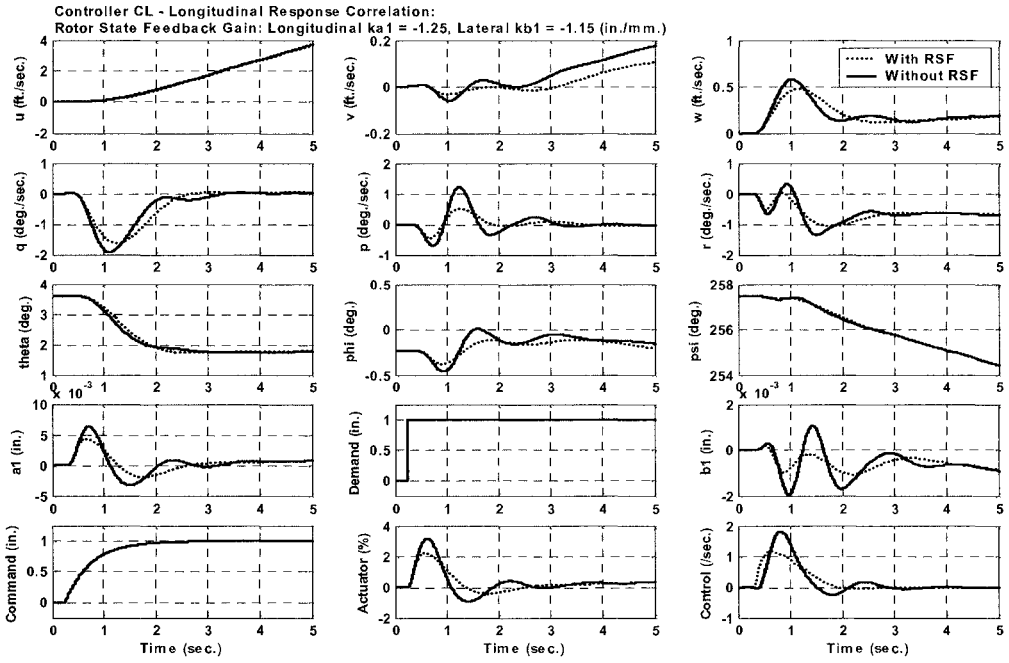

Figure 3.73 CMC Controller, Time History Response, Longitudinal Unit Step, With and Without Rotor State Feedback

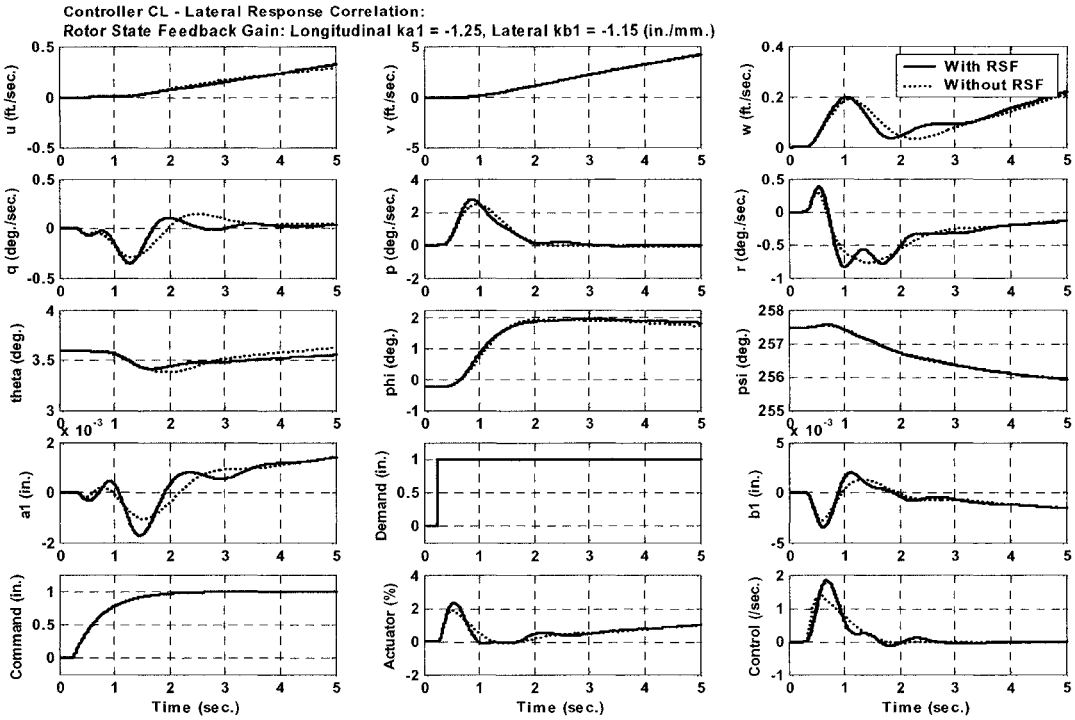

Figure 3.74 CMC Controller, Time History Response, Lateral Unit Step, With and Without Rotor State Feedback

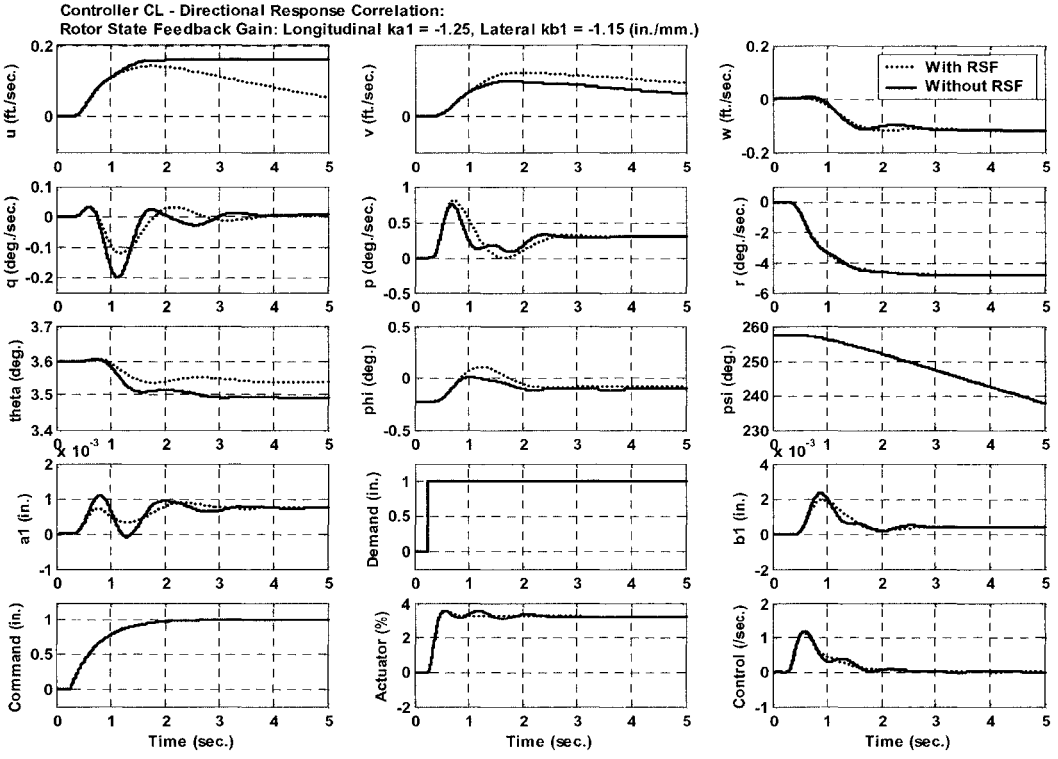

Figure 3.75 CMC Controller, Time History Response, Directional Unit Step, With and Without Rotor State Feedback

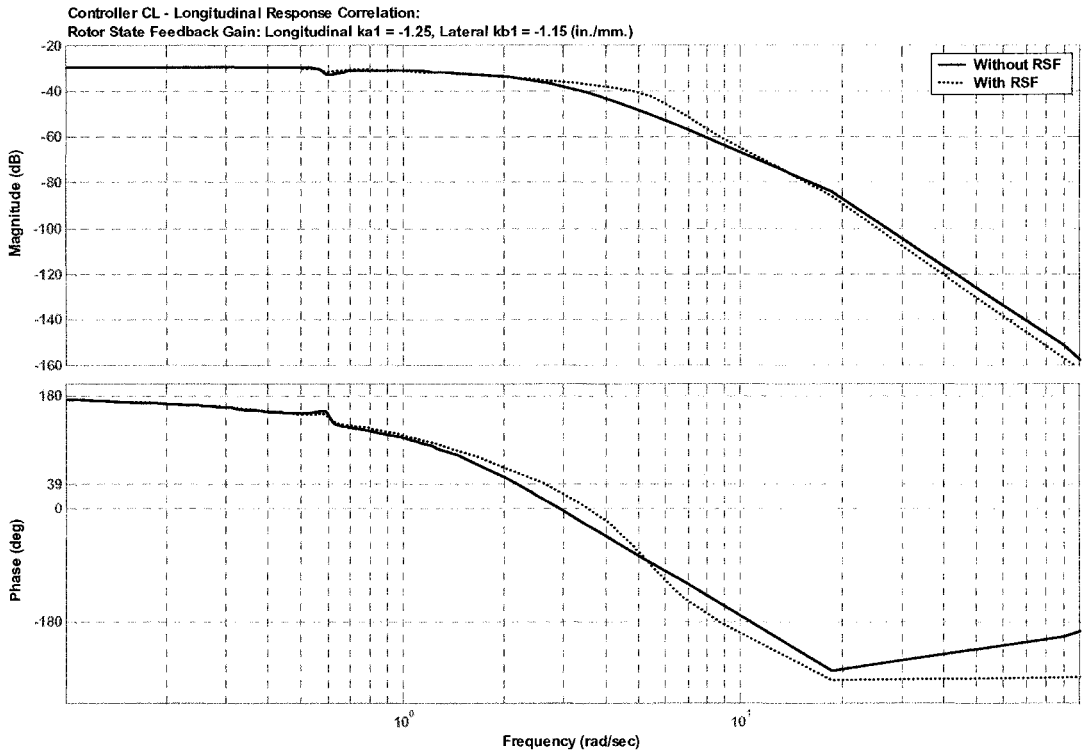

Figure 3.76 CMC Controller, Longitudinal Axis Frequency Response, With and Without Rotor State Feedback

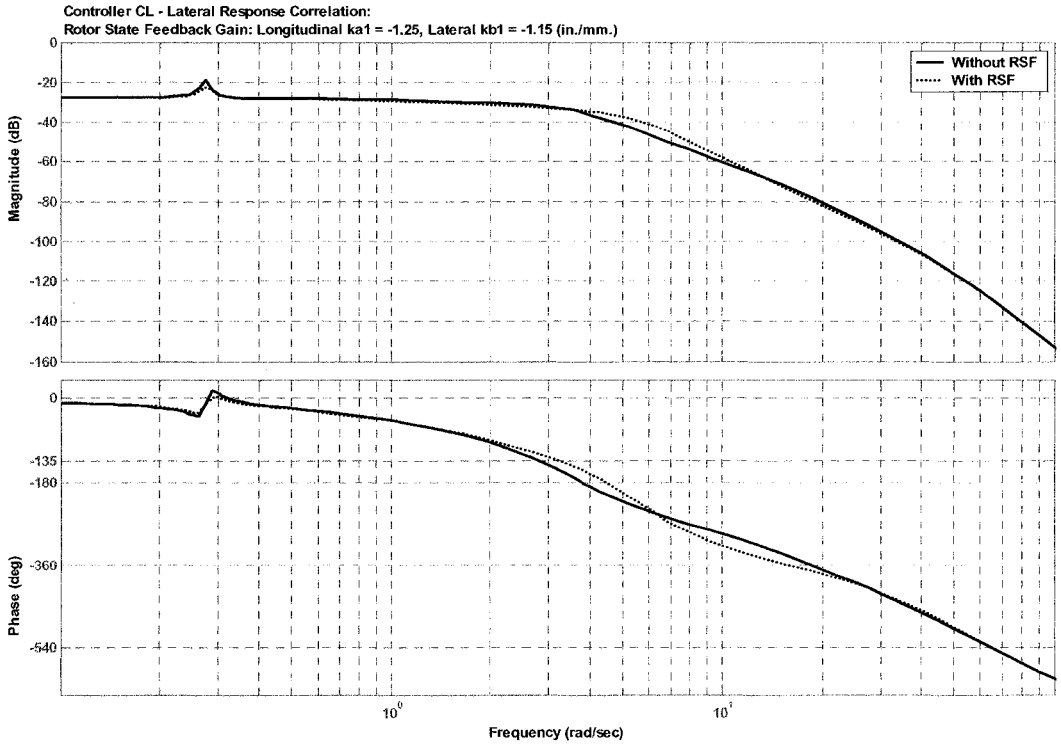

Figure 3.77 CMC Controller, Lateral Axis Frequency Response, With and Without Rotor State Feedback

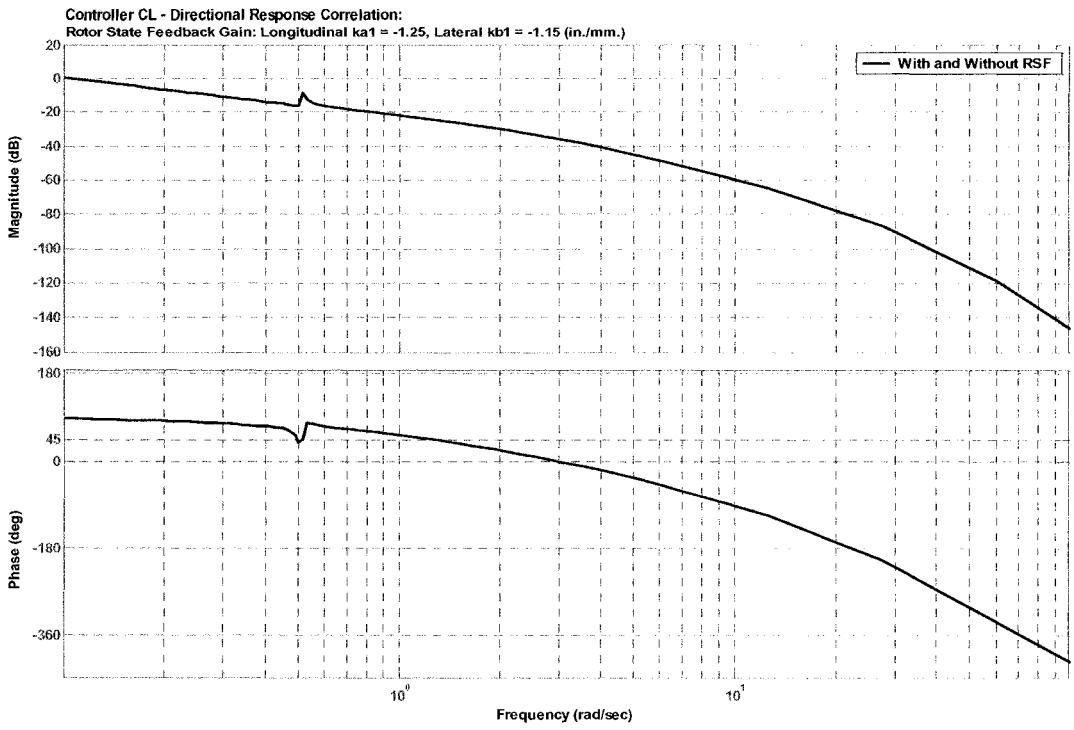

Figure 3.78 CMC Controller, Directional Axis Frequency Response, With and Without Rotor State Feedback

As shown in Figures 3.73 to 3.75, a time domain simulation in the non-linear FCDE applying a unit step input command in all axes was executed for a 5 second span. In the rigid body dynamics, the most prevalent features of rotor state feedback in the longitudinal step response are the reduction of pitch-rate, off-axis roll –rate, and off-axis yaw activities. In the yaw step response, the rigid body reduction of related pitch-rate and forward velocity excursion is notes. The roll axis response exhibits the least dynamics reduction. These effects are due to the rotor state feedback producing phase lead (bandwidth modification) in the axes of concern. In the rotor/control dynamics, reductions in the longitudinal and lateral disc tilt requirements and the control-actuator usages are prevalent in pitch and roll axes, with modest off-axis yaw response.

As was illustrated in the RLM analysis, elevated levels of bandwidth could be attained in the presence of rotor states. Here rotor state feedback in simulation shows the pitch bandwidth was improved by 23%, roll by 21%, and yaw remained constant as depicted in Figures 3.76, 3.77, and 3.78. The particular gain structure however did not produce optimal control from the classical controller. The effects of rotor state feedback was to drive the vehicle response to a poor Level 3 ADS-33 compliance. As shown in Figure 3.79, this was primarily due to the heightened phase delay acquired by the classical controller.

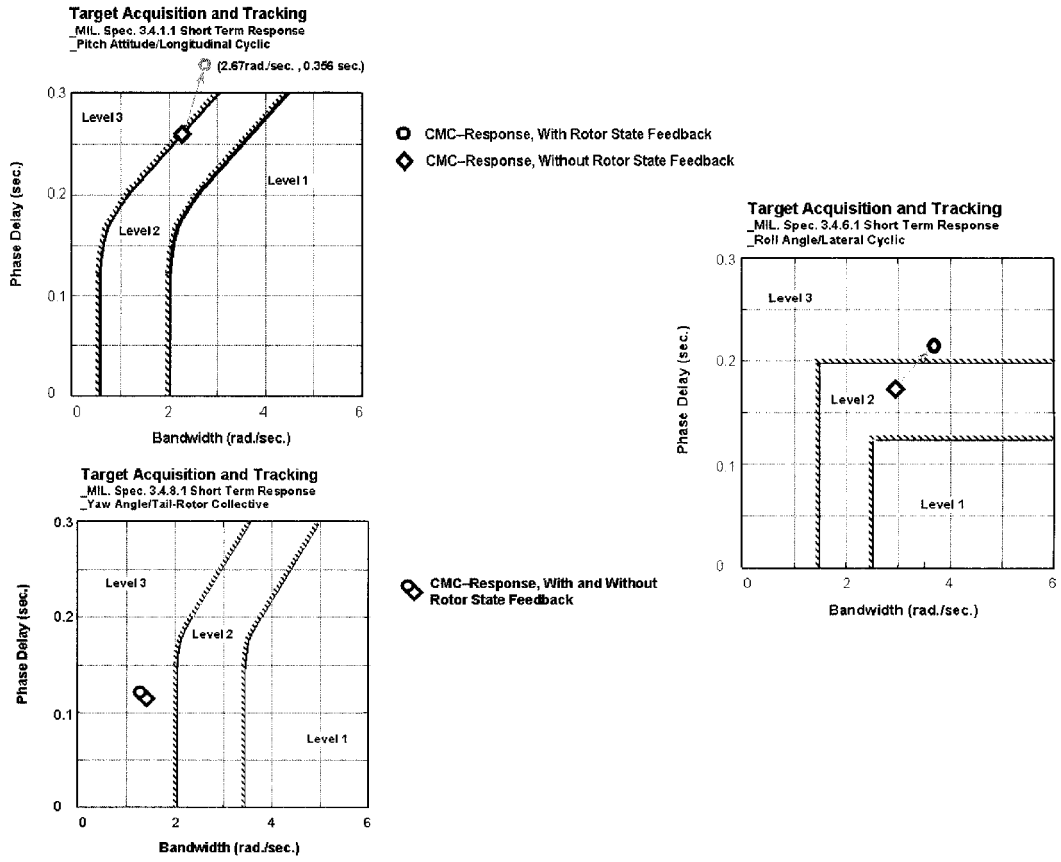

Figure 3.79 CMC Controller Compliance - ADS-33E-PRF, With and Without Rotor State Feedback

3.6.3.2 Aeromechanical Stability

An exploration of coupled rotor-body instability was performed by varying the gains through a positive and negative range. Due to the fact that the bandwidths and base gains for these rotor state controllers can be driven excessive as was demonstrated by the RLM analysis, the aeromechanically stable gain thresholds for flight testing were set at the lowest range of each gain variation at the lowest bandwidth of the 3 vehicle axes. The instability characteristics at select rotor state gain were important to observe since they predict the character of coupled rotor-body resonant states due to both on- and off-axis rigid-body and rotor state feedbacks. Results are summarized below in Table 3.4.

CONTROL INPUT: LONGITUDINAL STEP ROTOR STATE FEEDBACK GAIN	GAIN VARIATION (IN./MM.)	COMMENTS
Longitudinal On-Axis, a1	-6.0 < 0 < 1.0	
Longitudinal Off-Axis, b1	-2.0 < 0 < 1.0	
Lateral Cross-Axis, a1	-3.0 < 0 < 2.0	
Lateral Cross-Axis, b1	-5.0 < 0 < 1.5	**Divergent Oscillations, ka1 = +1.5**
Directional Cross-Axis, a1	-5.0 < 0 < 5.0	
Directional Cross-Axis, b1	-3.0 < 0 < 2.0	

CONTROL INPUT: LATERAL STEP ROTOR STATE FEEDBACK GAIN	GAIN VARIATION (IN./MM.)	COMMENTS
Lateral On-Axis, a1	-4.0 < 0 < +2.0	
Lateral Off-Axis, b1	-3.0 < 0 < +0.5	
Longitudinal Cross-Axis, a1	-4.0 < 0 < +1.5	**Divergent Oscillations, ka1 = +1.5**
Longitudinal Cross-Axis, b1	-1.0 < 0 < +1.0	
Directional Cross-Axis, a1	-10.0 < 0 < +3.0	
Directional Cross-Axis, b1	-2.0 < 0 < +2.0	**Divergent Oscillations, ka1 = -3.5**

CONTROL INPUT: DIRECTIONAL STEP ROTOR STATE FEEDBACK GAIN	GAIN VARIATION (IN./MM.)	COMMENTS
Directional On-Axis, a1	-5.0 < 0 < +2.0	
Directional Off-Axis, b1	-2.0 < 0 < +2.0	
Longitudinal Cross-Axis, a1	-4.0 < 0 < +1.0	
Longitudinal Cross-Axis, b1	-1.0 < 0 < +2.0	**Divergent Oscillations, ka1 = +2.0**
Lateral Cross-Axis, a1	-2.0 < 0 < +2.0	
Lateral Cross-Axis, b1	-4.0 < 0 < +1.75	**Divergent Oscillation, kb1 = +1.75**

Table 3.4 Classical Multivariable Control (CMC) Aeromechanical Gain Thresholds

Again with the soft-inplane hingeless rotor there existed the possibility of driving unknown dynamics, such as lead-lag modes, unstable causing ground or air resonant states.

3.6.3.3 Attenuation of Vehicular Disturbance Response

Signal noise in the form of a turbulence model developed by Tischler et.al[113] was introduced to assess the effects of rotor state feedback on noise rejection. Turbulence models may be generated by modeling of the theoretical equations identifying empirical data, or by turbulence emulation from flight-testing. The NRC-FRL and NASA have derived turbulence models for the Bell 205 and the UH-60. In the case of the NRC Bell 205 angular rates and vertical accelerations were identified by, first order inverse model of the aircraft and then applied to the vehicle actuators to emulate the effects of the atmospheric disturbance in hover.[112]

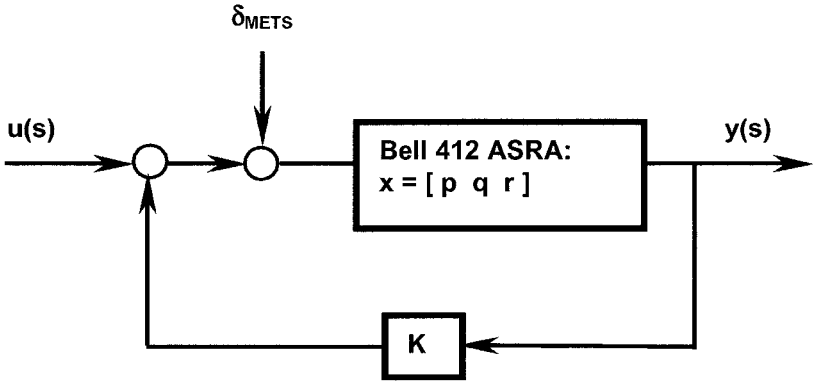

Figure 3.80 Control Disturbance Injection

Here the parameters of the Mixer Equivalent Turbulence Simulation mode (METS) were applied to the Bell 412 ASRA actuation control block of the non-linear simulation model to emulate turbulence activity as shown in Figure 3.80.

$$G_{\theta\delta_g} = 0.278\sigma^{0.991}\sqrt{\frac{U_0}{\pi L}}\left(\frac{1}{s+\alpha_w}\right), \text{ Longitudinal} \qquad 3.41$$

$$G_{\phi\delta_g} = 0.501\sigma^{0.748}\sqrt{\frac{U_0}{\pi L}}\left(\frac{1}{s+\alpha_w}\right), \text{ Lateral} \qquad 3.42$$

$$G_{\psi\delta_g} = 0.068\sigma^{0.549}\sqrt{\frac{3U_0}{\pi L}}\left(\frac{s+10.2\alpha_w}{(s+0.53\alpha_w)(s+1.48\alpha_w)}\right), \text{ Directional} \qquad 3.43$$

where; $\alpha_w = \frac{2U_0}{L}$

An initial test of the CMC controller for disturbance rejection involved a calibrated 0.5 sec. pulse of longitudinal, lateral, heave, and directional input. As shown in Figures 3.81 to 3.84, both cases with and without rotor state feedback are correlated. The parameterizations of the rotor state feedback gains were – 2.5 and 2.5 in./mm in longitudinal and lateral disc tilt for pitch and roll axis responses. The directional gains were 0.75 in./mm of lateral disc tilt feedback to lateral and directional vehicle axes.

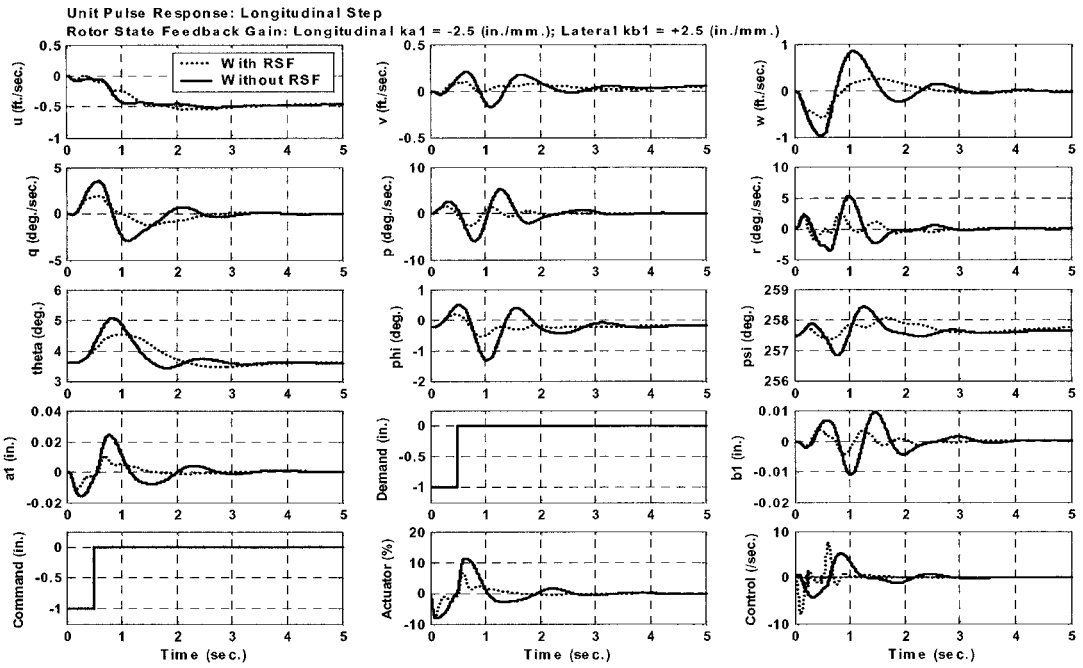

Figure 3.81 CMC Controller Longitudinal Unit Pulse Disturbance Rejection due to Rotor State Feedback

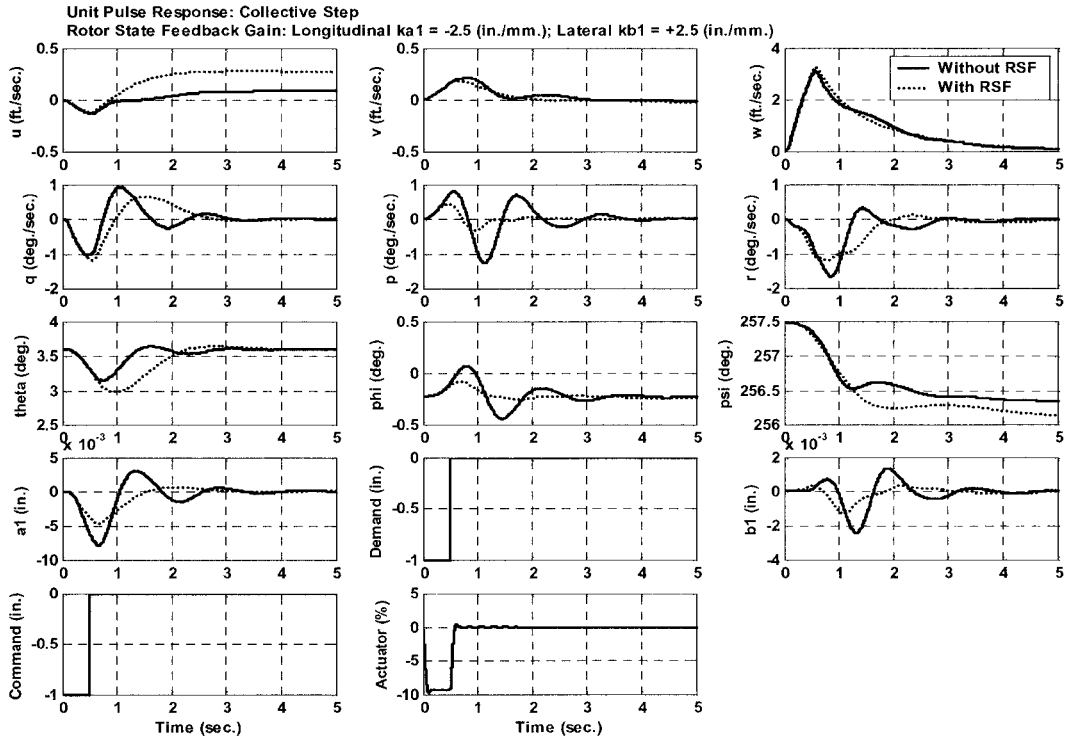

Figure 3.82 CMC Controller Collective Unit Pulse Disturbance Rejection due to Rotor State Feedback

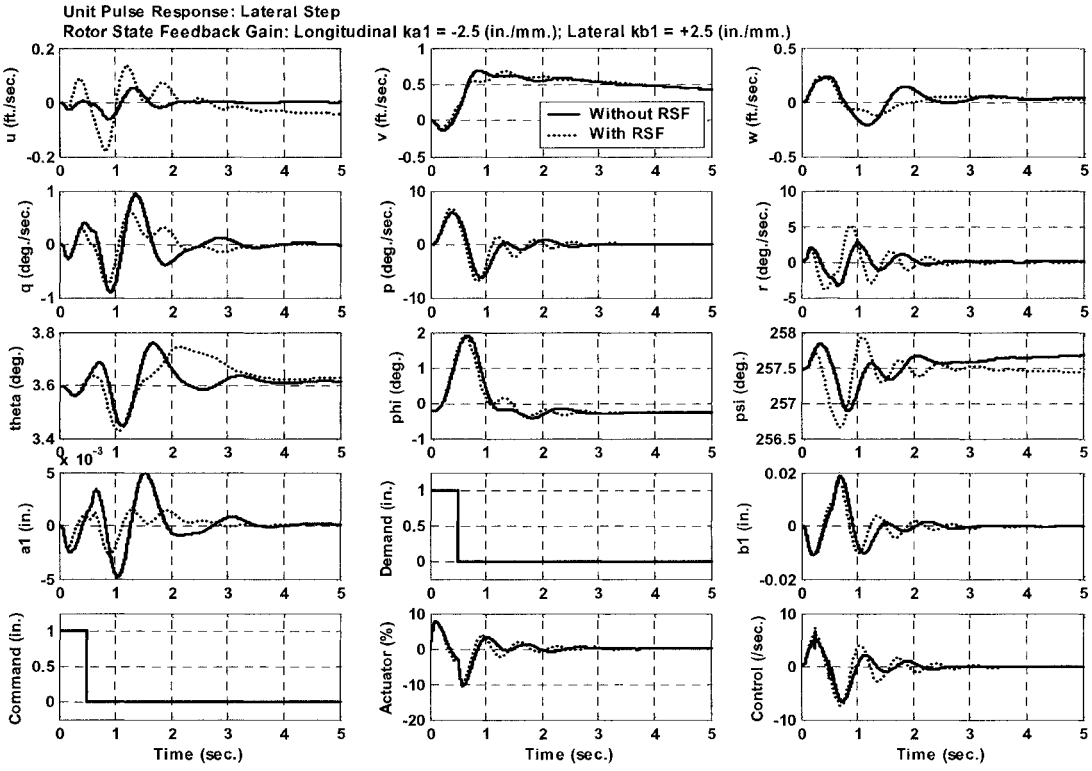

Figure 3.83 CMC Controller Lateral Unit Pulse Disturbance Rejection due to Rotor State Feedback

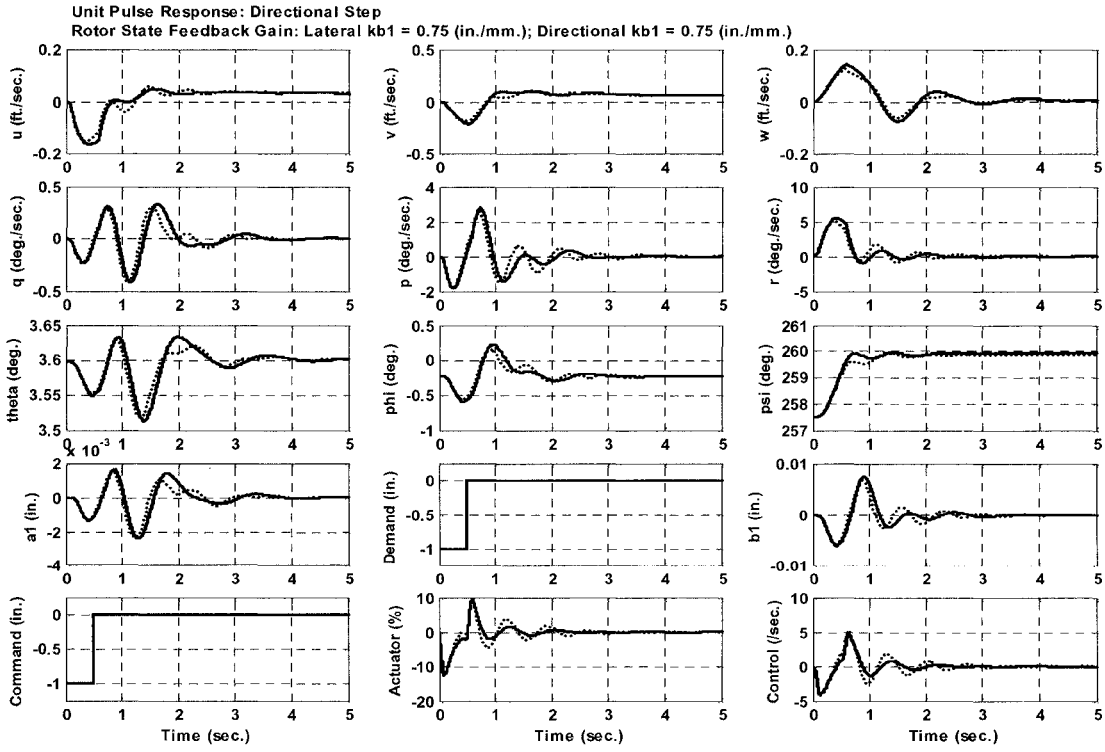

Figure 3.84 CMC Controller Directional Unit Pulse Disturbance Rejection due to Rotor State Feedback

As shown in Figures 3.81 to 3.84, significant levels of attenuation of pulse-induced energy could be achieved. In the longitudinal case, 50% on-axis pitch rate and disc tilt and 60% off-axis roll- and yaw rate, and 50% lateral disc tilt attenuations could be observed.

In the heave response (Figure 3.82), 50% reductions in both longitudinal and lateral disc tilt activity could be assessed. However there was some response magnification of yaw and pitch attitude.

The lateral dynamics (Figure 3.83) depicted a 60% reduction in off-axis longitudinal rotor disc tilt action while 30% magnification of the yaw attitude and rate dynamics.

The directional dynamics (Figure 3.84) remained largely unchanged.

The coupling of rigid-body and rotor dynamics has been illustrated to be a dominant feature of the feedback control. The classical controller has demonstrated that rotor and actuator activity attenuation is possible with rotor state feedback in both on- and off-axis cases as illustrated above. In order to evaluate atmospheric disturbance rejection, a turbulence rejection task was evaluated. Here, the Tischler[113] METS model was introduced to the ASRA control actuation block emulating a dither disturbance in the heave axis. The rotor state gain structure was changed such that –0.75 in./mm. of longitudinal and lateral disc tilt were in the feedback path. In Figures 3.85 and 3.86, response attenuations across all attitude rates and actuation axes, as well as rotor activities are depicted. This widespread attenuation again is due to the bandwidth alteration of the controlled coupled-rotor body system.

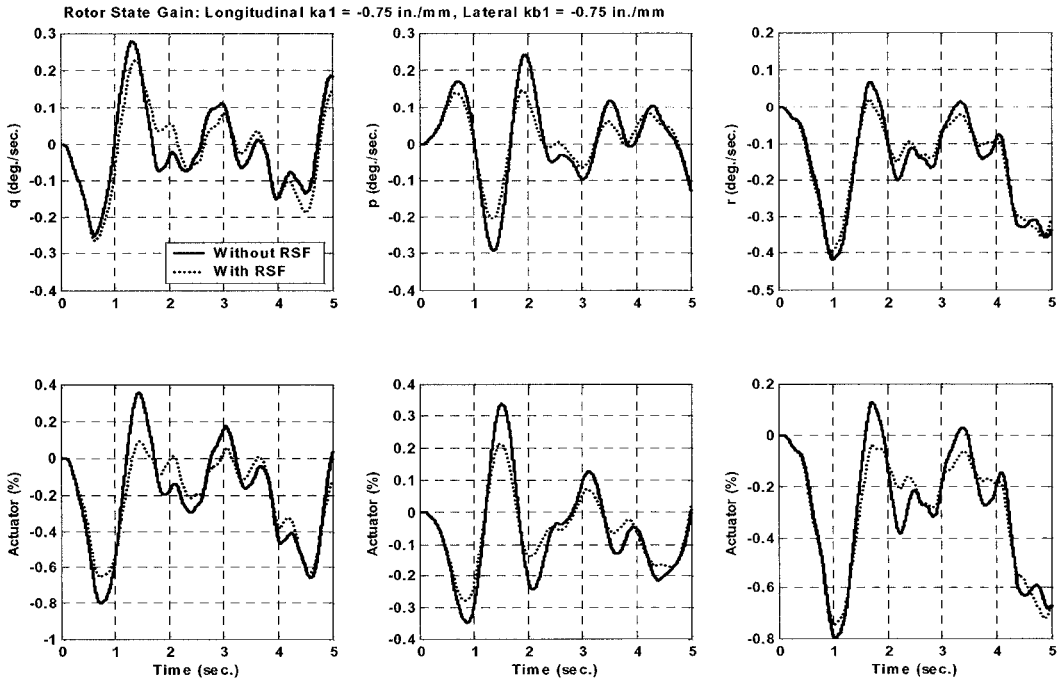

Figure 3.85 CMC Controller Heave-Axis Injected Signal Noise Rejection due to Rotor State Feedback for Rigid Body and Actuator Dynamics

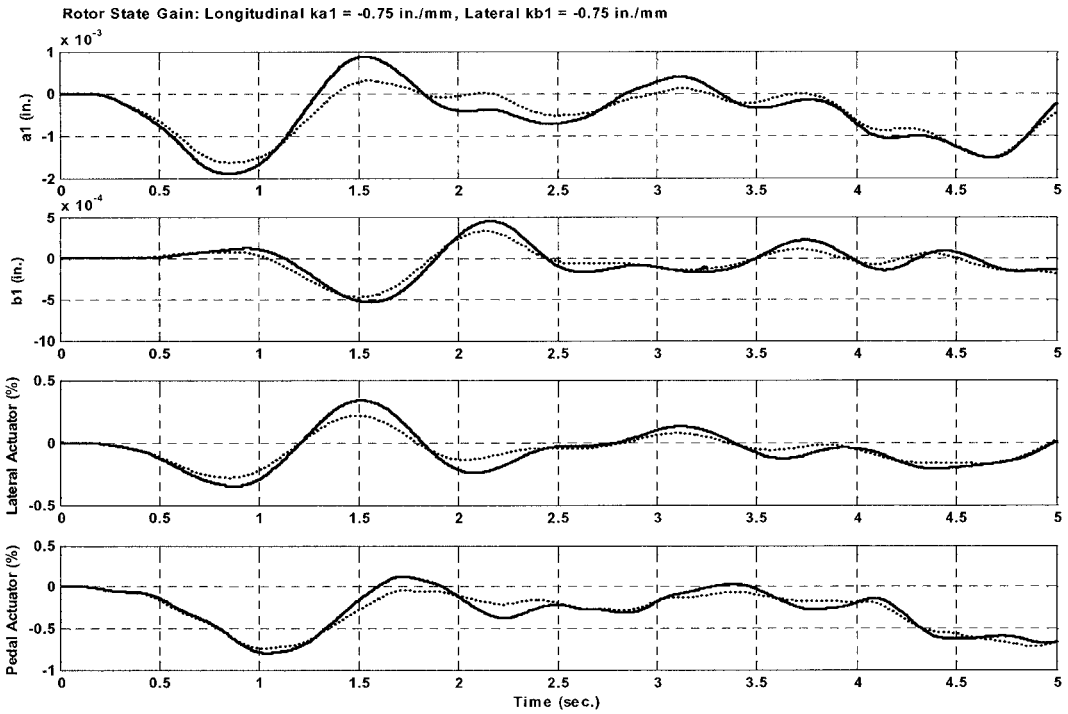

Figure 3.86 CMC Controller Heave-Axis Injected Signal Noise Rejection due to Rotor State Feedback for Actuator and Rotor Dynamics

3.6.3.4 Command Tracking Accuracy

High bandwidth variable stability research requires control systems capable of tightly tracking pilot or flight control computer generated commands. Rotor state feedback promotes this command tracking by adjusting system bandwidth command model response. Command tracking is demanding for a controller requiring optimal use of actuators, effecting of the vehicle trajectory by attitude and attitude-rate feedback dynamics, and reducing pilot workload through axis coupling interactions.

A roll ACAH tracking objective was set using a first-order command model and longitudinal and lateral disc tilt feedbacks of 1.0 in,/mm and –1.75 in./mm, respectively. Figure 3.87 illustrates how the CMC controller reacts with and without a first-order command model in tracking the roll ACAH response, without rotor state feedback. The effect is to reduce the peak excursions of rigid-body, control/actuator, and rotor responses. The CMC controller in the presence of rotor state feedback did little to command-tracking performance of the roll ACAH design objective as shown in Figure 3.88. However, off-axis activity in pitch and roll rates/attitudes slightly increased. Interestingly the longitudinal and lateral disc tilt response activities are slightly decreased indicating an overall vehicle state trimming effect confirmed by the near steady-state forward velocity.

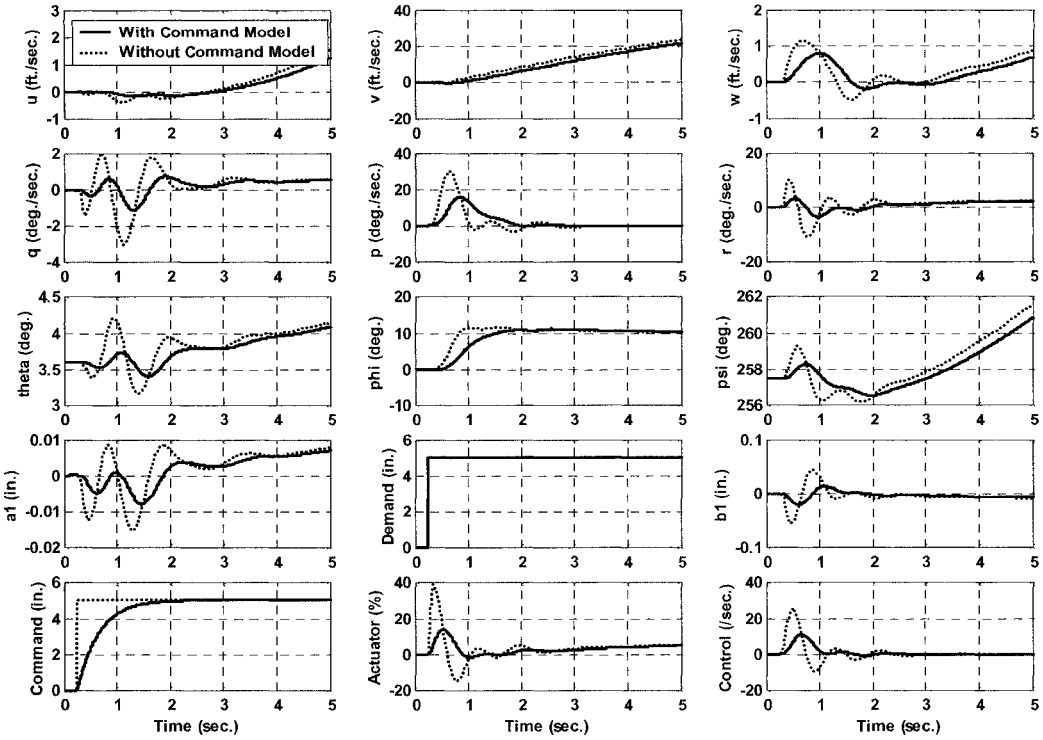

Figure 3.87 CMC Controller Response Tracking – With and Without Command Model

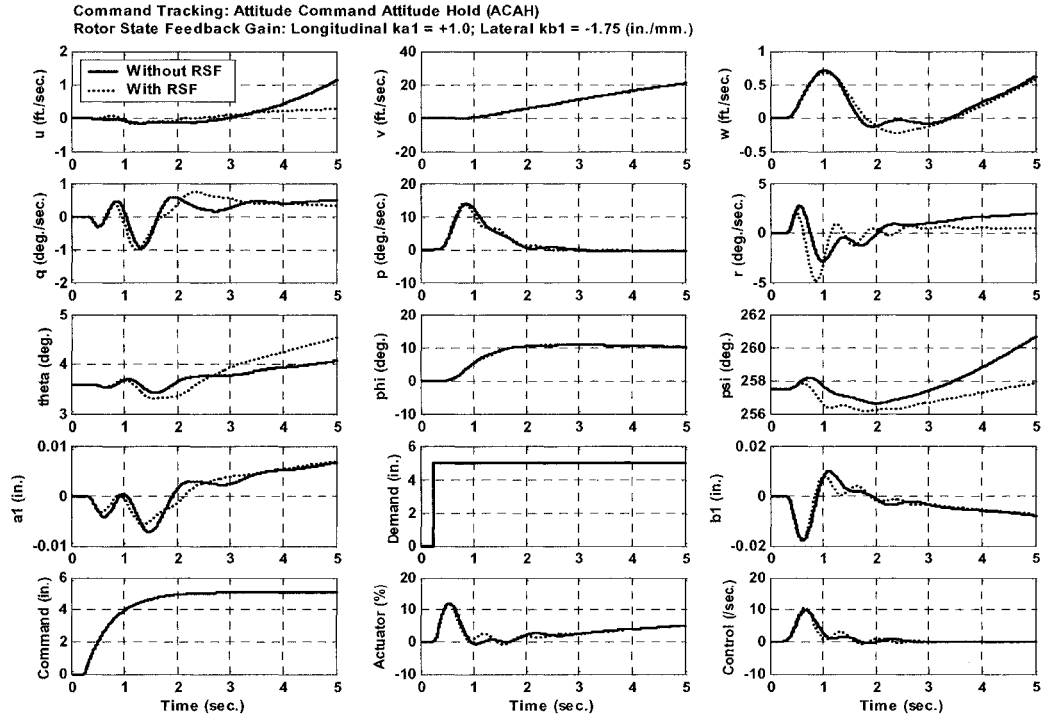

Figure 3.88 CMC Controller Command Tracking – Roll Attitude Hold by Rotor State Feedback

3.6.4 Summary: Classical Multivariable Control (CMC) Performance

The CMC control design methodology did not produce optimal multivariable designs though the benefits of rotor state feedback were very clear. The ADS-33 compliances as tabulated in Table 3.5, show that the handling qualities ratings transitioned to Level 3 in the presence of rotor state feedback.

Rotor state feedback did significantly improve disturbance rejection, reduce rotor/control activity, and alter coupled rotor/body modes. This latter point produced both beneficial and detrimental effects. The degraded control performance by the mode alteration caused undesirable on- and off-axis couplings (such as those shown in the aeromechanical stability assessment) and accruing of penalizing phase delay (as is illustrated by the low handling qualities ratings).

Overall the CMC controller was inefficient primarily due to the lack of modal control.

CONTROLLER	EFFECTIVE BANDWIDTH (BW) PERFORMANCE					
	BW_θ (rad./sec.)	RATING	BW_ϕ (rad./sec.)	RATING	BW_ψ (rad./sec.)	RATING
CMC_{NRSF}	3.2	L1	4.0	L2	3.1	L2
CMC_{RSF}	2.67	L3	3.6	L3	1.3	L3

Notation:
NRSF = **Without** Rotor State Feedback
RSF = **With** Rotor State Feedback
L1, L2, L3 = Level 1, Level 2, Level 3, with respect to ADS-33EPRF Compliance

Table 3.5 Summary of Classical Multivariable Control (CMC) Effective Controls

In what follows, the author effects more directed, flexible, and insightful control over the vehicular modal dynamics through the structuring of eigenvalues and eigenvectors. These modal dynamics are particularly difficult to control in the presence of rotor state feedback applied in the non-linear helicopter environment.

3.6.5 Modern Multivariable Eigenstructure Assignment Control (EAC)

Eigenstructure assignment (EAC) was applied to the design of Attitude and Rate Command control of the Bell 412 ASRA. EAC strategies involve the placement of eigenvalues and eigenvectors for the design of linear time-invariant multivariable control systems. The eigenvalues are the principal factors that govern the system stability and rates of decay (or rise) of various components of the system dynamic response. The right and left eigenvectors, on the other hand, are dual factors that together determine the relative shape of the system dynamic response. Performance requirements, such as off design point parameter variation insensitivity and robustness can also be improved through appropriate choice of the closed-loop system eigenstructure.

Handling qualities specifications are frequency domain based whereas EAC techniques are time domain based. In order to satisfy the handling qualities specifications the EAC closed-loop eigenstructure is parameterized to yield the specified frequency-response and modal decoupling characteristics. It is this eigenstructure that defines the desired eigenvalues and eigenvectors.

3.6.5.1 Eigenstructure Assignment Control (EAC) Methodology

Eigenstructure Assignment allows the designer to directly incorporate vehicle flight dynamics requirements based on eigenvalues and eigenvectors in the controller development. This control design approach has been used in many fixed-wing and rotary wing applications. Research thrusts by EAC control has included the attainment of handling qualities, aeroelastic stability, investigation of higher order dynamics and rotor state feedback, and control robustness.

Hughes[79], Ingle[75], and Howitt[76,80] investigated the impact of rotor dynamics on helicopter high bandwidth control using EAC algorithms. Hughes et. al developed an ACAH controller for handling qualities attainment and decoupled tracking. The EAC technique provides inherent visibility of the relationship between control and system dynamics. Augmentation of the rigid body system was made by appending 6 rotor states for second order rotor flap modeling of the Lynx rigid rotor helicopter at 80 knots.

Hughes results show deterioration in bandwidth/phase delay requirements for pitch, roll, and yaw channels. Levels of coupling and stability were robust to the additional high frequency dynamics. Two EAC controllers were developed featuring components including full state feedback, pre-compensation, output feedback, and proportional plus integral control. It was found that the controllers suffered a lack of robustness to unmodeled dynamics. Ingle's results enforced the fact that EAC algorithms are well tailored to efficient control synthesis tailored to design criteria. The study illustrated robust control of the UH-60 articulated rotor helicopter rigid body model to augmentation with higher order dynamics including rotor flap, lag, and torsion, inflow and rotor/body aerodynamics, and actuator dynamics. The EAC algorithm used incorporated a full state feedback structure based on estimated states by Kalman filter based Loop

Transfer Recovery. The algorithm was not optimal in control usage and was not robust to off-design point helicopter flight or configuration conditions.

Hybrid EAC and H-Infinity control was applied by Samblacant et al.[79] for stabilization and controller simplification. The EAC inner loop was tasked with axis decoupling, while the H-Infinity outer loop provided improved performance attainment for attitude and rate command response types in the presence of parameter variation. The most significant result was the ability of the hybrid algorithm to reduce the typically high H-Infinity compensator order thus providing efficient control.

Howitt et al.[67,80] applied an EAC technique to the investigation of rotor state flapping feedback.

For the present research, 3 eigenstructure assignment algorithms were attempted in an assessment of the most effective method for control synthesis. It should be noted that the advantage of rotor state measurement is that it eliminates the need for state estimation since rotor states are available for feedback where rank C > rank A. With this configuration the most basic and computationally efficient EAC algorithm can be coded in full state feedback form. The methodology for EAC design then involved 2 fundamental steps:

- **Step 1**: Design of a full state feedback gain matrix K with direct application of handling qualities requirements for vehicle response type attainment
- **Step 2**: Design optimization for coupled response

Several typical design strategies were neglected for this study that included pre-filtering and model scaling. Typically, a pre-filtering gain matrix is also synthesized to decouple the vehicle response. This is not favorable in the control law design process as robustness of the final controller may be jeopardized. Furthermore, depending upon the requirement for decoupling, an associated elevated decoupling control activity requirement may promote actuator saturation. Both of these penalties are significant since they can dramatically impact the onset of aeromechanical events. As such, decoupling was not applied in the control laws synthesized herein relying solely on the inherent MIMO design and rotor state feedback capabilities for such control.

Another important feature of the design developed was that scaling of the HMMS was not applied in order to fully investigate the fidelity of the mathematical structure, and robustness to the inflight test design and implementation cycle on the rotor state feedback control laws under investigation. The HMMS was thus unscaled in both vehicle state dynamics, and control distribution for altering of perceived control power. The following sections outline the EAC methods investigated, which include Direct, Recursive, and Robust formulations[79].

3.6.5.2 Method I: Direct Eigenstructure Assignment[79]

A direct EAC (non-iterative) procedure developed by Juang et al. was used for state feedback controller design. The algorithm has a 3-step process:

- **Step 1**: Selection of the desired eigenvalue and eigenvector matrices from performance specifications.
- **Step 2**: Computation of the desired eigenvector matrix associated with the desired eigenvalues
- **Step 3**: Computation of control gains by projection of the desired eigenvector into the allowable subspace.

The criterion for the gain computation is to choose the eigenvector from the allowable eigenvector subspace which minimizes the least squares problem defined by $\min_{R_i} \| R_i - R_{di} \|_2$ for i = 1,2,...,n, where the vectors, R, represent the desired and achievable closed loop eigenvectors of the allowable subspace. The algorithm allows for the direct projection of the set of real mutually orthogonal vectors into the allowable eigenvector subspaces. Computed are the state-feedback controller, K, the achieved eigenvalue vector, a, and the eigenvector matrix, Ra, for the system (A,B) given the desired eigenvalues, d, based on a unitary eigenvector matrix, Ud.

3.6.5.3 Method II: Recursive State Feedback Eigenstructure Assignment[79]

An indirect or iterative method of EAC was also applied such that the overall measure of conditioning of the eigen-problem could be assessed. Given the right and left eigenvector matrices, R_a and L_a respectively, the sensitivity of the closed-loop system is defined by;

$$J_s = \| R_a \|_2 \| L_a \|_2 \qquad 3.44$$

Recursive EAC chooses the closed-loop eigenvectors for the allowable subspaces based on the desired closed loop eigenvector matrix so that the sensitivity of the system is minimized.

The state-feedback EAC method by (Kautsky, et al., – Method 0) was applied to choose vectors Ra_j (j=1,2,...,n) from the allowable eigenvector space such as to minimize the following conditioning measure:

$$J = \| R_a^{-1} \|_2^2 \qquad 3.45$$

Computed are the constant real state-feedback gain matrix, K, and the achieved eigenstructure (a, Ra).

3.6.5.4 Method III: Robust Eigenstructure Assignment by Genetic and Gradient Based Optimization[79]

Based on robust performance indices defined in the frequency domain (such as ADS-33 handling qualities), it was desired to locate the eigenvalue set in a well-defined subspace to meet requirements of a practical control system (i.e.; stability, minimal response coupling, and robustness to unmeasured dynamics, etc.). This results in eigenvalue constraints.

The algorithm applied combines sensitivity and complementary sensitivity functions of the closed loop system in the frequency domain as a robust performance index defined by;

$$J_c(K) = \sup_{\omega \in F} \overline{\sigma} \left\{ \begin{bmatrix} W_1 S \\ W_2 KS \end{bmatrix} \right\} \qquad 3.46$$

where;

$$G = -(j\omega I - A)^{-1} B$$
$$S = (I + GK)^{-1}$$
$$KS = K(I + GK)^{-1}$$

W_1 and W_2 are weighting matrices, F is the frequency range of interest, $\overline{\sigma}\{.\}$ denotes the largest singular value of the matrix of concern, S is the sensitivity function, and KS is the complementary sensitivity function. The minimization of the function J_c applies over the whole set of stabilizing controllers, K, such that;

$$\min_K J_C(K) \qquad 3.47$$

Overall, the aim of the optimization can be interpreted as an improvement in performance directed at disturbance rejection and robust stability insensitivity to modeling errors.

3.6.5.5 Eigenstructure Assignment Control (EAC) Specifications

The benefit of the EAC method is that the pole placement specifications from ADS-33 may easily integrated into the eigenstructure although there is no guarantee of performance matching. The desired eigenstructure for this research was derived from ADS-33 specifications for the Target Acquisition and Tracking mission (i.e.; a Rate Response Type requirement) was one originally developed by Ingle[75]. This served as an initial condition for the designs herein.

For x=[p w q r ϕ θ u v ψ], the desired eigenstructure is given by;

$$Ad = \begin{bmatrix} -\lambda_p & 0 & 0 & 0 & 0 & 0 & 0 & 0 & 0 \\ 0 & -\lambda_q & 0 & 0 & 0 & 0 & 0 & 0 & 0 \\ 0 & 0 & -\lambda_w & 0 & 0 & 0 & 0 & 0 & 0 \\ 0 & 0 & 0 & -\lambda_r & 0 & 0 & 0 & 0 & 0 \\ 1 & 0 & 0 & 0 & 0 & 0 & 0 & 0 & 0 \\ 0 & 1 & 0 & 0 & 0 & 0 & 0 & 0 & 0 \\ 0 & 1 & 0 & 0 & 0 & \lambda_q & -\lambda_u & 0 & 0 \\ 1 & 0 & 0 & 0 & \lambda_p & 0 & 0 & -\lambda_v & 0 \\ 0 & 0 & 0 & 1 & 0 & 0 & 0 & 0 & 0 \end{bmatrix} \qquad 3.48$$

$$Bd = \begin{bmatrix} \lambda_p & 0 & 0 & 0 \\ 0 & -\lambda_q & 0 & 0 \\ 0 & 0 & -\lambda_w & 0 \\ 0 & 0 & 0 & -\lambda_r \\ 0 & 0 & 0 & 0 \\ 0 & 0 & 0 & 0 \\ 0 & 0 & 0 & 0 \\ 0 & 0 & 0 & 0 \\ 0 & 0 & 0 & 0 \end{bmatrix}$$

These desired poles λ_i^d were then chosen in an attempt to satisfy the handling qualities specifications. In a first order system, the pole locations are equivalent to the specification bandwidth. The pole locations are selected from Level 1 boundaries of ADS-33E-PRF specifications 3.4.1.1, 3.4.6.1, and 3.4.8.1 for a Target Acquisition and Tracking Task (TA+T). These criteria are a first estimate of the desired pole locations for pitch, roll, and yaw axes.

The eigenvalues of Ad define the desired pole locations. From Level 1 boundaries:

- Roll Bounds: $\lambda_p \geq 4.0$ rad./sec (Spec. 3.3.2.1)
- Pitch Bounds: $\lambda_q \geq 4.0$ rad./sec (Spec. 3.3.2.1)
- Yaw Bounds: $\lambda_r \geq 5.0$ rad./sec (Spec. 3.3.5.1)
- Heave Bounds: $\lambda_w \geq 3.5$ rad./sec (Spec. 3.3.10.1)

The values of λ_u and λ_v remain fixed at their open loop values from the system **A** matrix. Ingle[75] suggests this will assist in the retaining of the physical relationship between forward and sideward velocity, and roll and pitch in the closed loop system. Optimization of the response from this design process was obtained by manual migration of these pole locations to improve command tracking, robustness, and account for higher order dynamic effects.

3.6.5.6 Initial Gain Synthesis by Direct Eigenstructure Assignment

The Direct EAC Algorithm was selected for gain synthesis and evaluation of reduced-order response non-linear simulation. For longitudinal dynamics representation of the Bell 412 ASRA a reduced order state vector x is extracted from the design plant, such that x = [u, w, q, θ, a1].

The command implemented was given by the rapid first-order transfer function;

$$\theta_{COM} = \frac{8}{s+8} \qquad 3.49$$

Table 3.6 shows the synthesized state-feedback control gains, K, achieved eigenvalues, a, and the eigenvector matrix for the systems (A, B), Ra, of for a 60 knot design point, for longitudinal axis control.

To assess the overall performance of this controller synthesis algorithm, the controller is tested in both reduced-order uncoupled linear and coupled non-linear simulation environments with responses depicted in Figures 3.89 and 3.90, respectively.

EAC-RC (Eigenstructure Assignment-Rate Command Controller)
Reduced-Order Design Axis: Longitudinal

GAIN STRUCTURE	[ku kw kq kθ ka1] = [0.0381	0.3389	19.0737	0.1849	-1.3286]
ACHIEVED EIGENVALUES	[λu λw λq λθ λa1] = [-0.0011	0.0000	-3.5000	-2.0000	-10.0000]
EIGENVECTOR MATRIX	0.5125	0.0000	0.0013	-0.0008	-0.0210
	0.0122	0.0000	-0.0324	-0.1298	0.0446
	-0.0000	-0.0000	0.0024	0.0044	-0.0142
	0.0001	0.0000	-0.0007	-0.0022	0.0014
	0.0071	0.0000	0.0150	0.0172	-0.2050

Units:
ku, kv, kw = in./m./sec.;
kp, kq, kr = in./rad./sec.; kθ, kϕ, kψ = in./rad.
ka1, kb1= in./mm.

Table 3.6 Eigenstructure Assignment Control (EAC) Synthesis, Reduced-Order Longitudinal Axis Rate Command (RC)

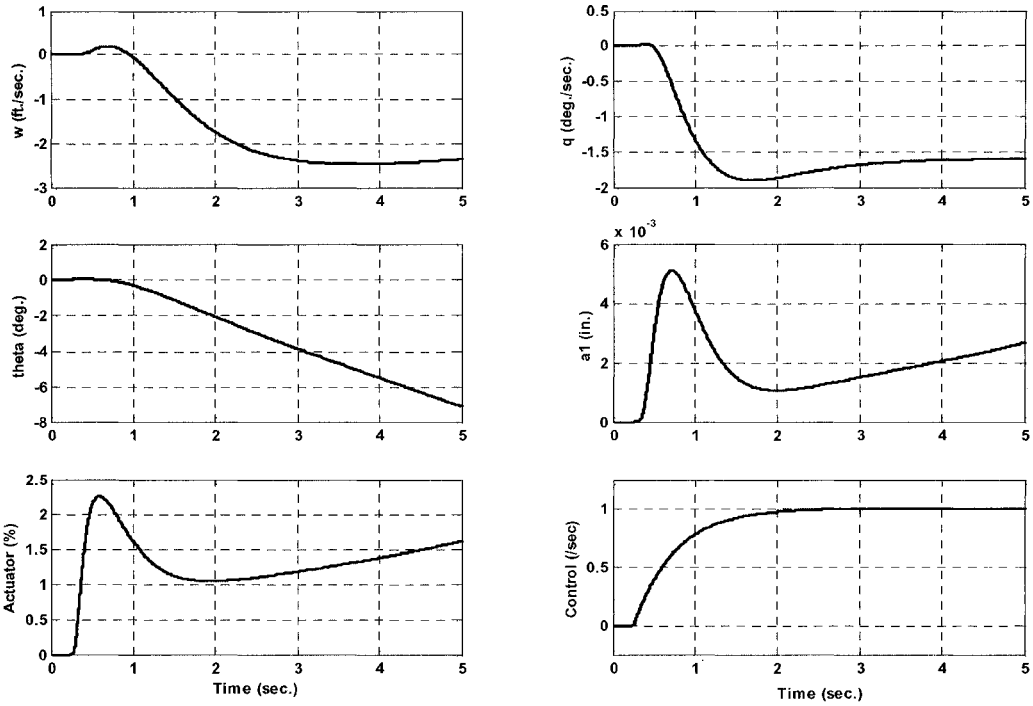

Figure 3.89 EAC Reduced-Order Uncoupled Longitudinal Unit Step Response by Rate Command Control

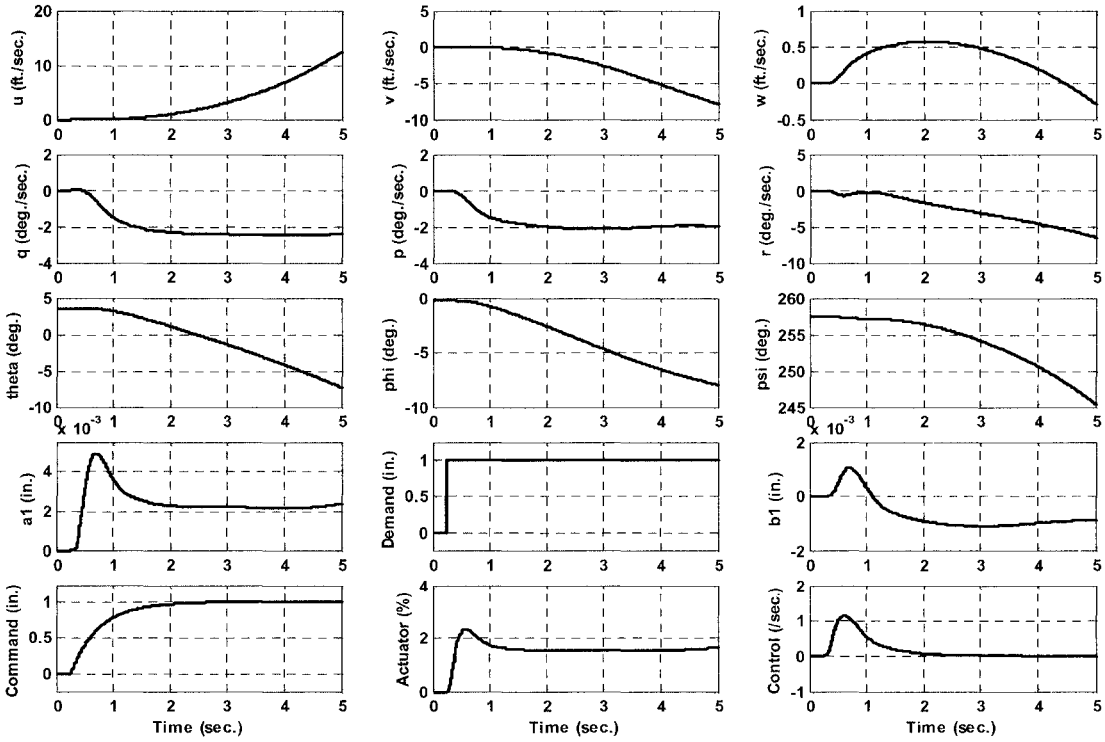

Figure 3.90 EAC Reduced-Order Coupled, Longitudinal Unit Step Response by Rate Command Control

The next step in the design process was to synthesize a multi-axis controller for non-linear simulation in the Bell 412 ASRA FCDE. This controller would serve as a baseline for examination of the effects of rotor state feedback. Table 3.7 depicts the gain structure developed by the Direct Eigenstructure Assignment procedure.

EAC-ACAH	**AXIS GAIN STRUCTURE**
AXIS RESPONSE TYPE	
LONGITUDINAL ACAH	Cyclic Gain: [ku kw kq kθ ka1] = [0.085 0.000 22.486 35.104]
LATERAL ACAH	Cyclic Gain: [kv kp kr kϕ] = [0.005 -5.756 -0.754 -15.34] Tail-Rotor Collective Gain: [kv kp kr kϕ] = [0.000 0.535 0.353 0.000]
DIRECTIONAL ACAH	Tail-Rotor Collective Gain: [kv kp kr kϕ kψ] = [0.534 0.935 20.78 0.000 30.75]

Units:
ku, kv, kw = in./m./sec.;
kp, kq, kr = in./rad./sec.; kθ , kϕ, kψ = in./rad.
ka1, kb1= in./mm.

Table 3.7 Eigenstructure Assignment Control (EAC) Synthesis, Multi-Axis Attitude Command Attitude Hold (ACAH)

The gain structures are then implemented in the non-linear simulation environment (FCDE) using a variety of command models, stick sensitivities, and non-linearities in order to evaluate controller performance and the effects of rotor state feedback.

3.6.6 Eigenstructure Assignment Control (EAC) Without Rotor State Feedback

In the absence of rotor state feedback, the EAC controller depicts a multi-axis pitch, roll, and yaw ACAH command response as shown in Figures 3.92 through 3.106 as simulated in the non-linear FCDE. The following discussion summarizes the trends observed.

In all axes, the vehicle acceleration responses depicted in Figures 3.92, 3.97, and 3.102, for 5 inch longitudinal and lateral cyclic and 1.5 inch tail-rotor collective steps, illustrate 2 points. Firstly, the EAC controller has good disturbance rejection and secondly, the helicopter has a highly damped nature at the 60 knot design point. The trends show the least excursion in longitudinal axis acceleration of 0.6 ft./sec.^{2} due to tail-rotor collective step, while the highest excursion is in vertical acceleration of some 13 ft./sec.^{2}. This illustrates the Bell 412 ASRA's damped yaw response at 60 knots and high pitch inertia that is 4.5 times that of roll inertia.

Due to the 5-inch. commanded longitudinal step response, the Bell 412 ASRA depicts significant pitch-roll couplings as shown in Figures 3.93 to 3.95. However, the controller performs well in both off-axis rate damping (roll and yaw). Actuator usage remains below 20% with oscillatory response decaying within 3 seconds as depicted in Figures 3.95. The rotor responses are stable and well damped, reacting with 0.0042 in./deg./sec. and 0.0015 in./deg./sec. of on-axis and off-axis rotor yoke flap deflection to maximum-attitude rate response.

The 5 inch. commanded lateral step response as shown in Figures 3.98 and 3.99, shows less overall coupling to pitch and yaw axes. Yaw attitude response is shown to be divergent due to the development of a 2 deg./sec. yaw attitude-rate response. Heave response also has a divergent tendency. Keeping in mind that the non-linear simulation response is valid within the first 3 seconds for small perturbation activity, the responses at high commanded inputs are acceptable. The actuator usage remains in the 20% margin with a strong yaw actuator requirement as shown in Figure 3.100. The rotor hub yoke responses are 0.0012 in./deg./sec. and 0.0102 in./deg./sec. for on- and off-axis activity.

The yaw axis responses in Figures 3.103, 3.104, and 3.105 depict elevated coupling to roll axis response for a 1.5 inch commanded tail-rotor collective step. The low pitch attitude and attitude-rate responses developed are noted. More of interest are the rotor hub yoke responses of longitudinal disc tilt to pitch rate of 0.0081 in./deg./sec. and lateral disc tilt to roll rate of 0.00188 in./deg./sec. Comparatively to the other axes considering the lower step magnitude, it is noted that the rotor system responded with the same orders of magnitude. Figure 3.105 illustrates that the actuator usage is moderate given the same considerations.

In terms of ADS-33E-PRF specifications for bandwidth and phase delay, frequency responses of Figures 3.96, 3.101, and 3.106 translate into the compliances shown in Figure 3.91. The EAC controller in the presence of rotor hub yoke dynamics has successfully tuned the bare-airframe response to Level 1 thresholds.

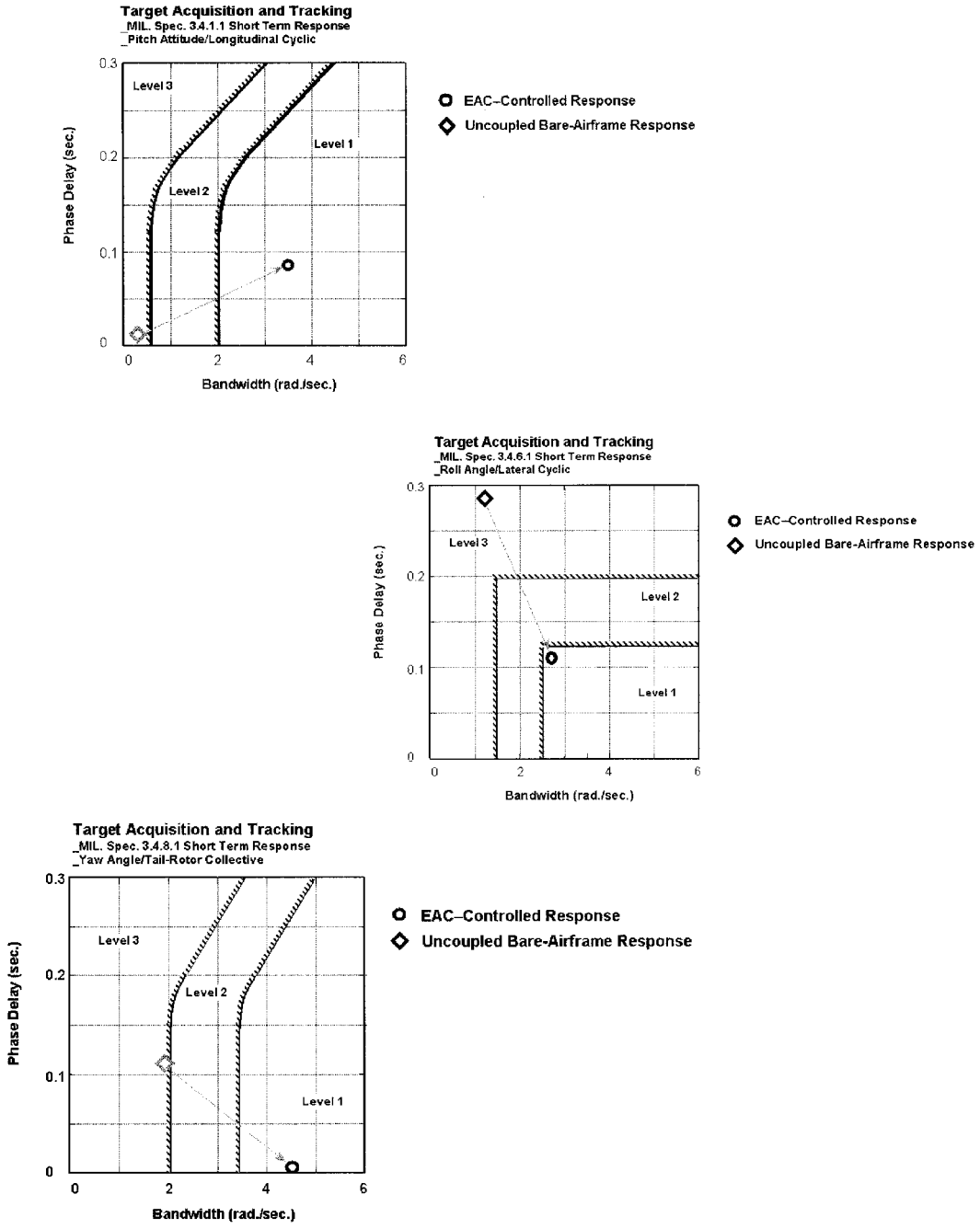

Figure 3.91 EAC Controller Response Compliance – ADS-33E-PRF

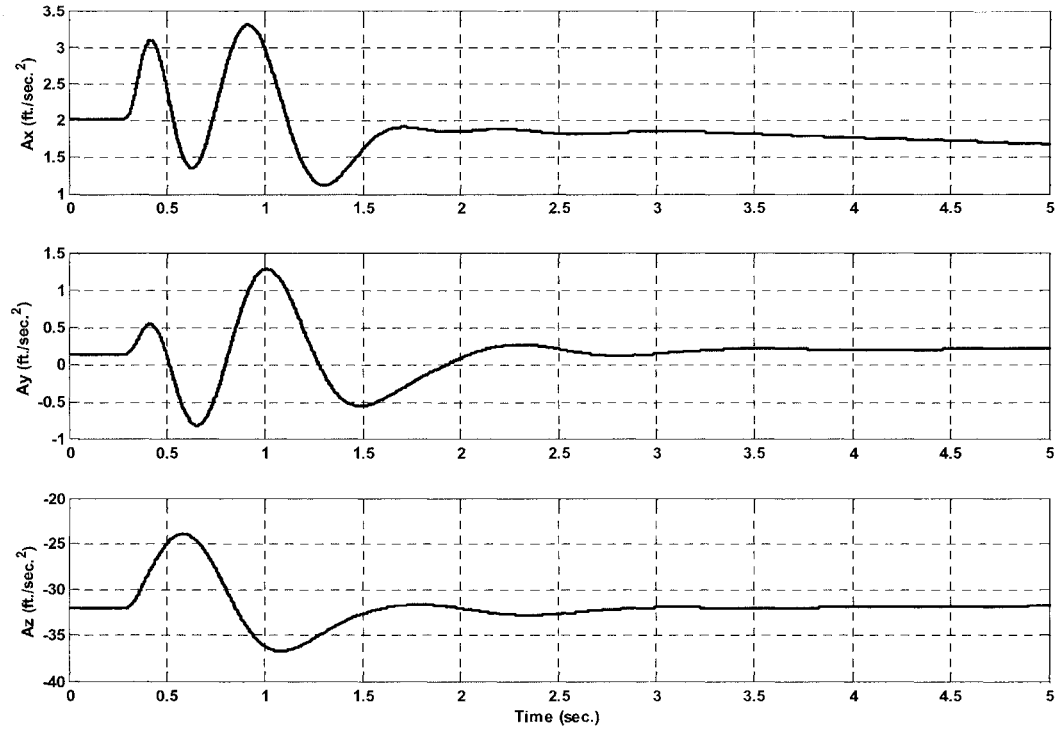

Figure 3.92 EAC Controller Acceleration Response due to Longitudinal Step

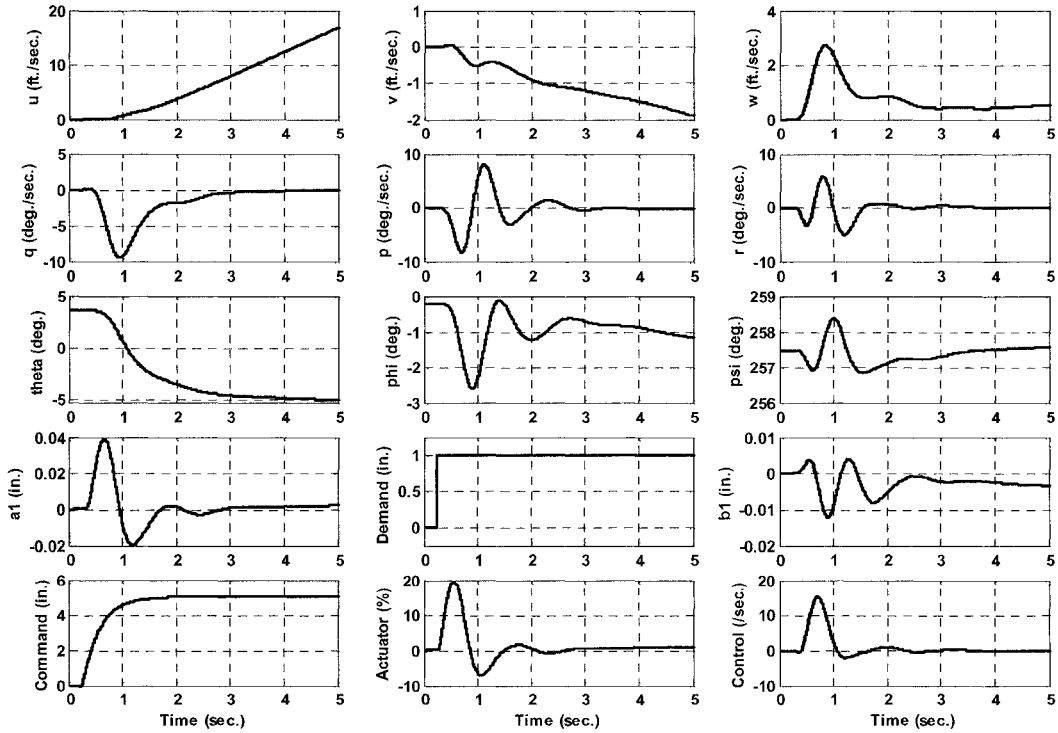

Figure 3.93 EAC Controller Time History Response due to Longitudinal Step

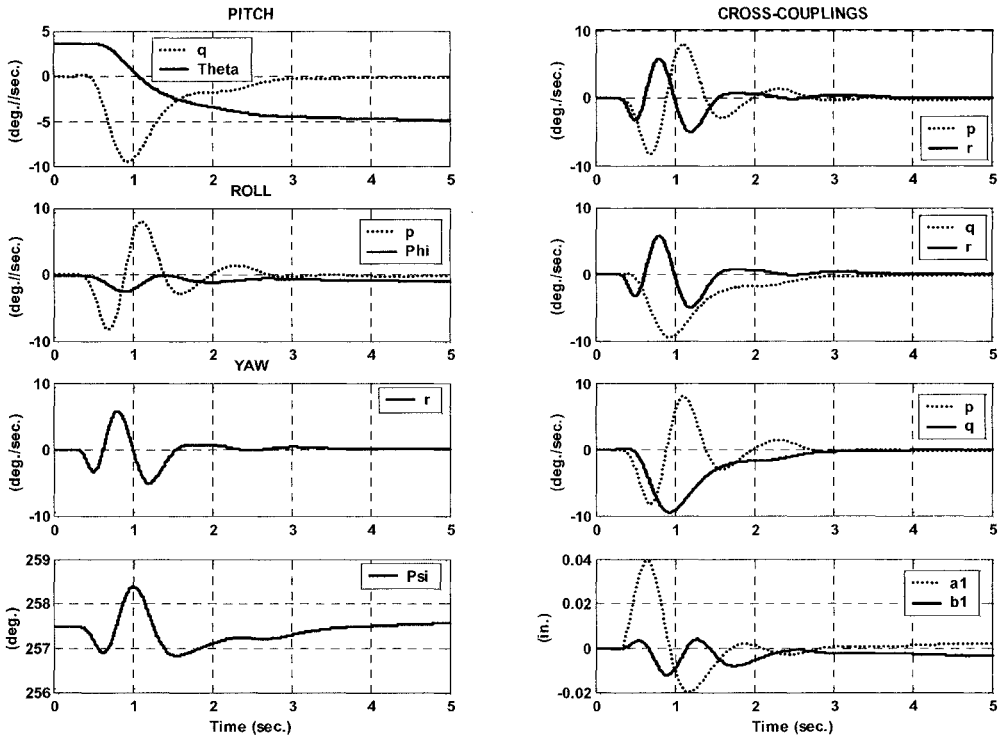

Figure 3.94 EAC Controller Cross Coupling Response due to Longitudinal Step

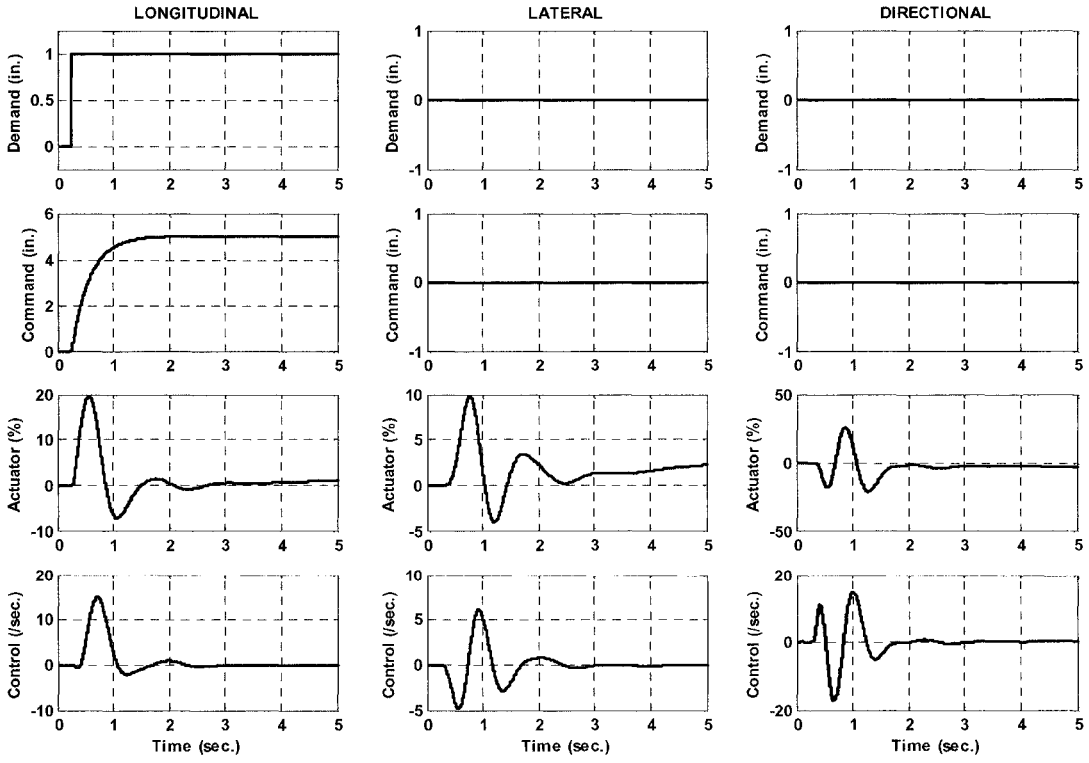

Figure 3.95 EAC Controller, Control Usage due to Longitudinal Step

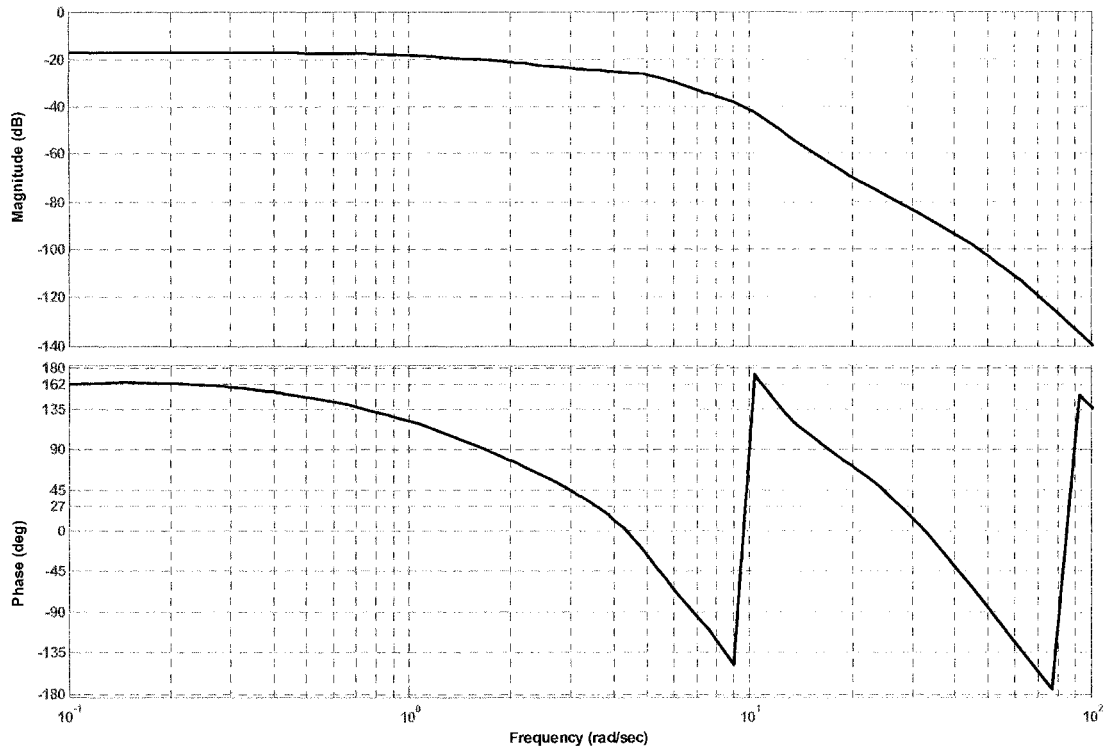

Figure 3.96 EAC Controller Longitudinal Frequency Response

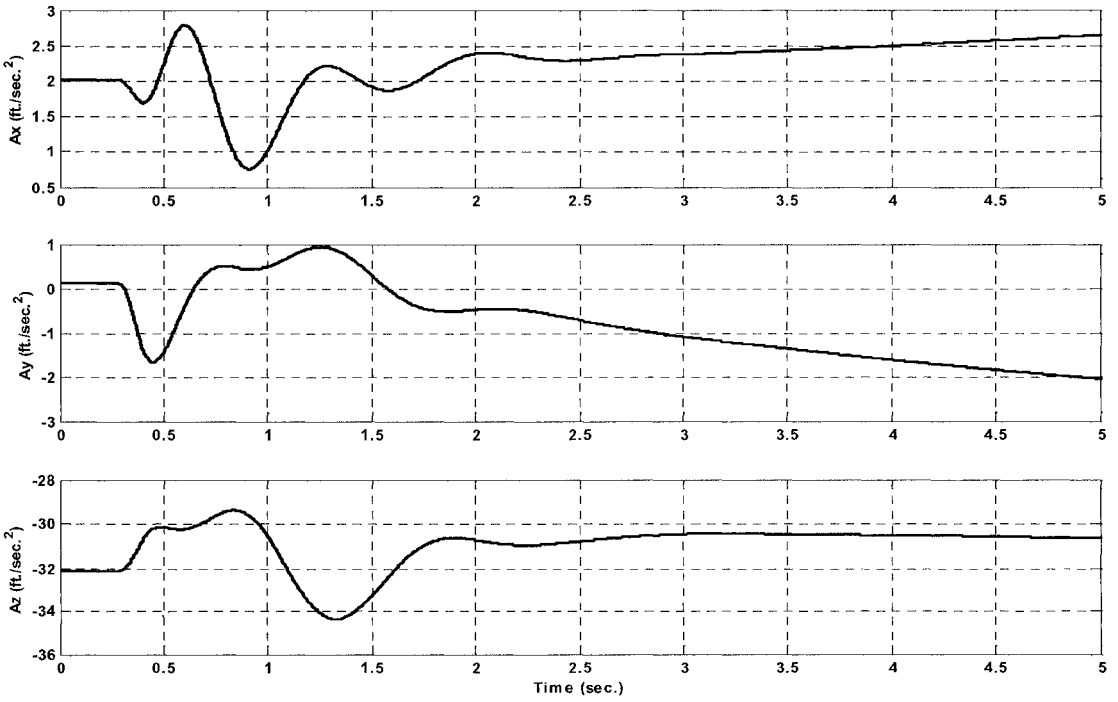

Figure 3.97 EAC Controller Acceleration Response due to Lateral Step

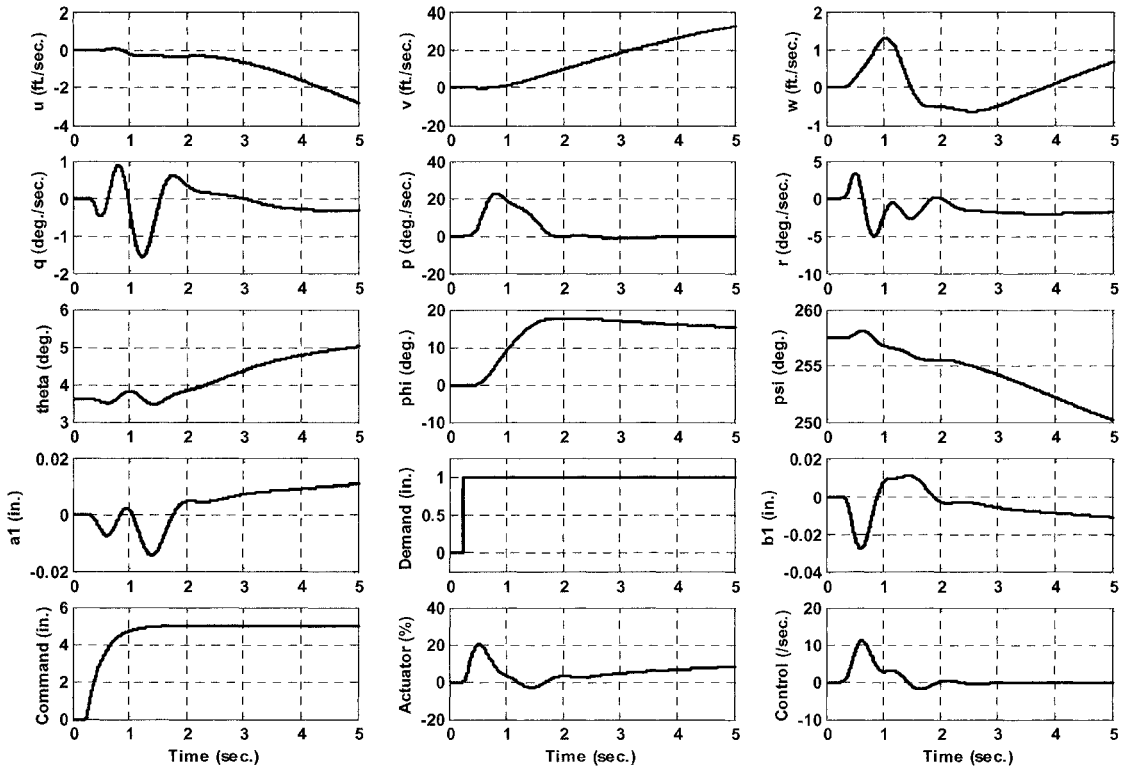

Figure 3.98 EAC Controller Time History Response due to Lateral Step

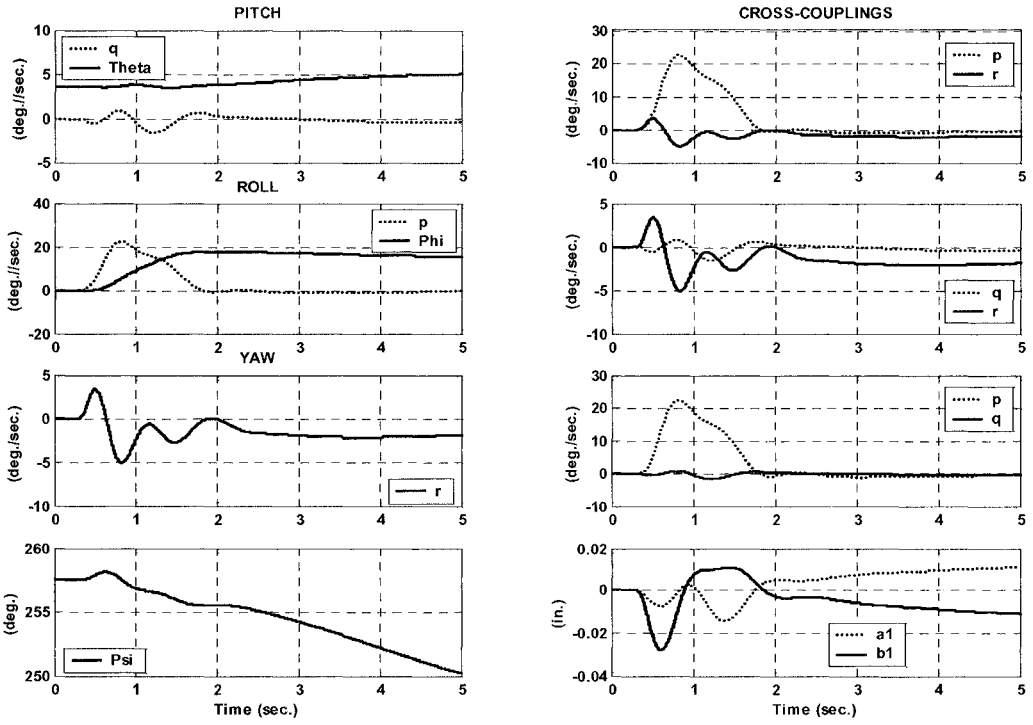

Figure 3.99 Controller EAC Cross Coupling Response due to Lateral Step

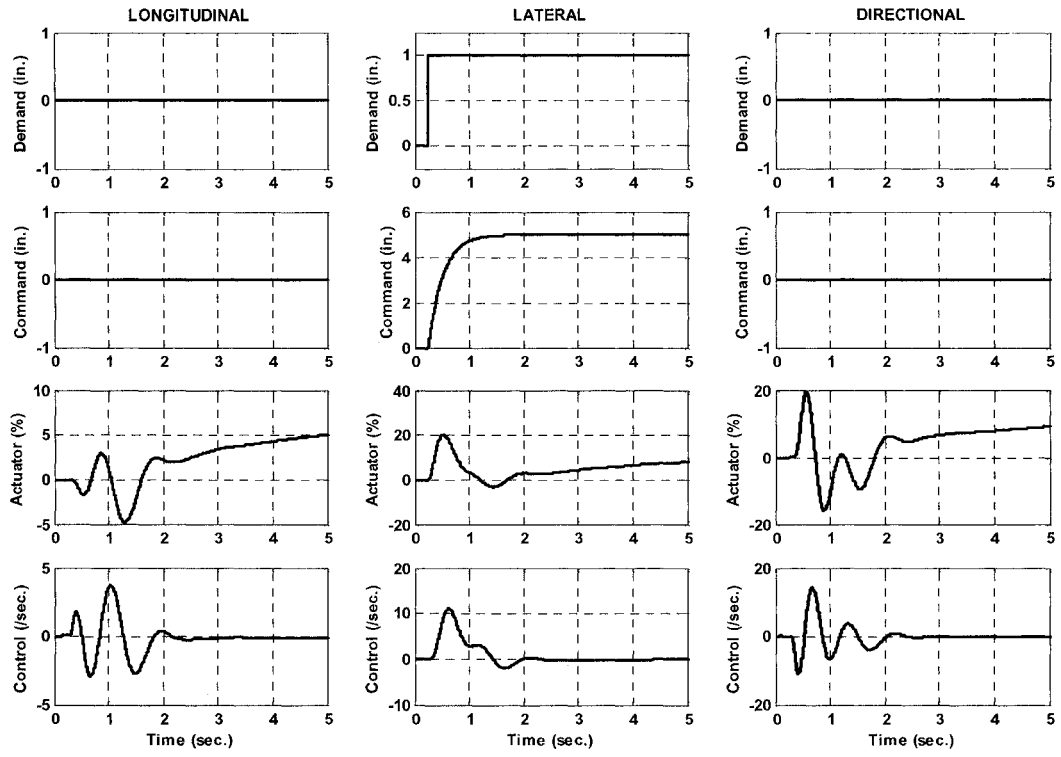

Figure 3.100 EAC Control Usage due to Lateral Step

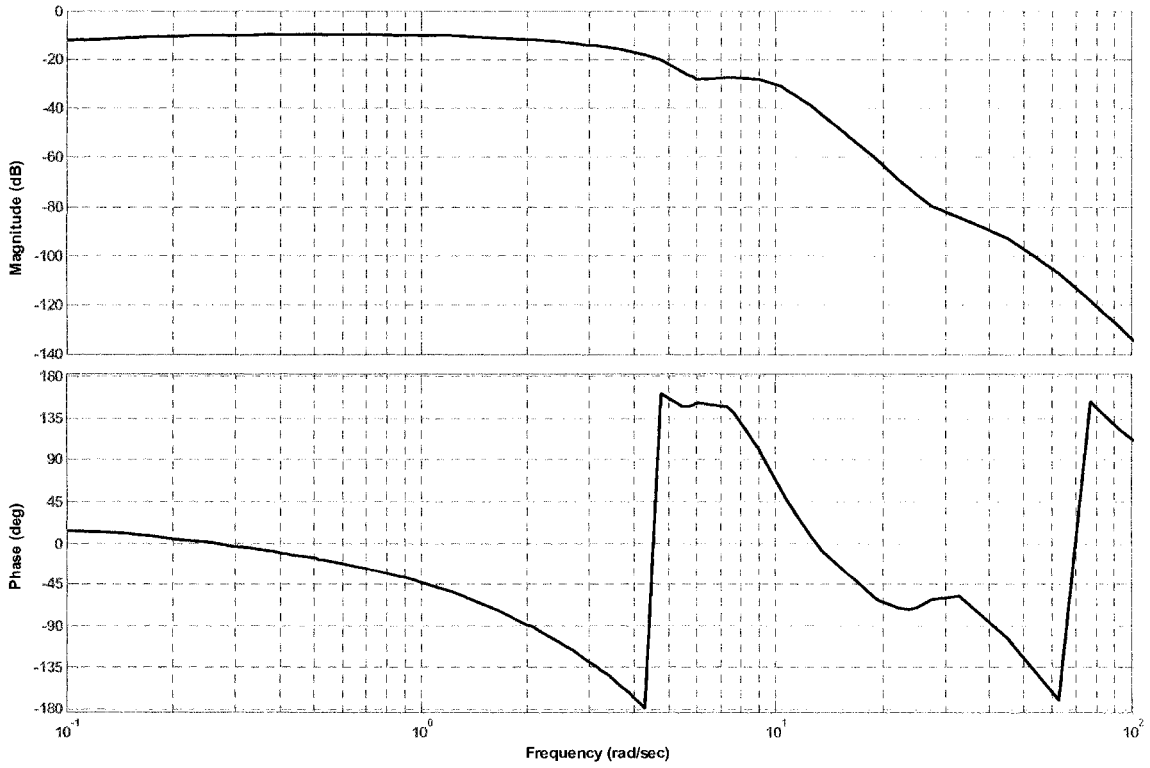

Figure 3.101 EAC Controller Lateral Frequency Response

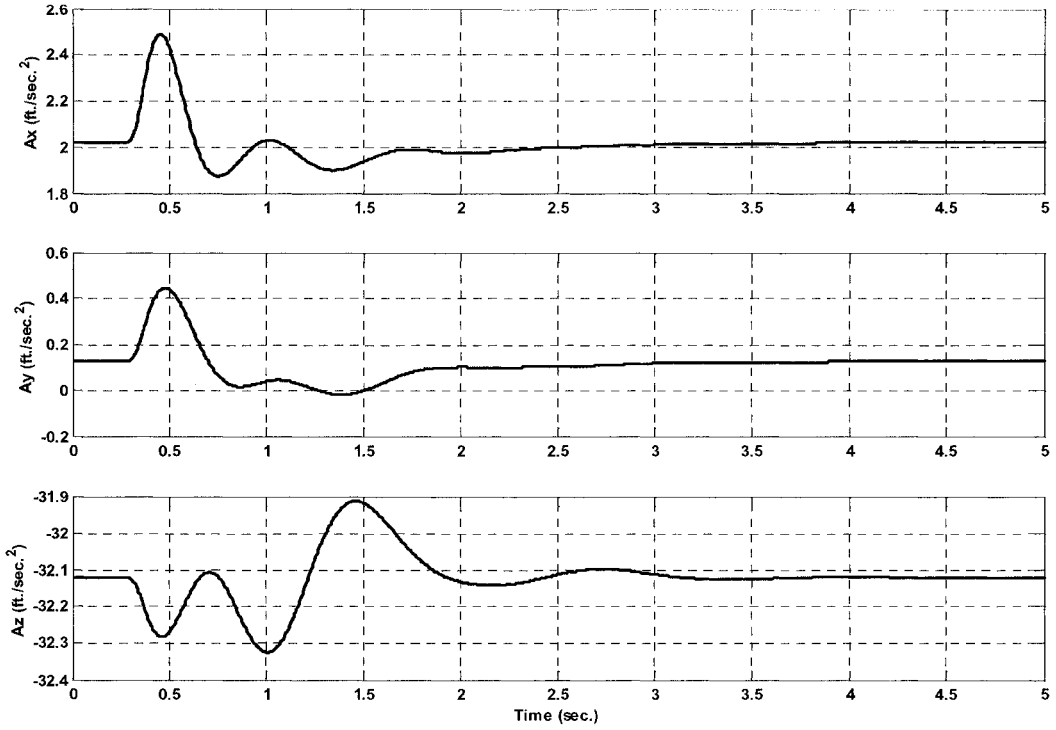

Figure 3.102 EAC Controller Acceleration Response due to Tail Rotor Collective Step

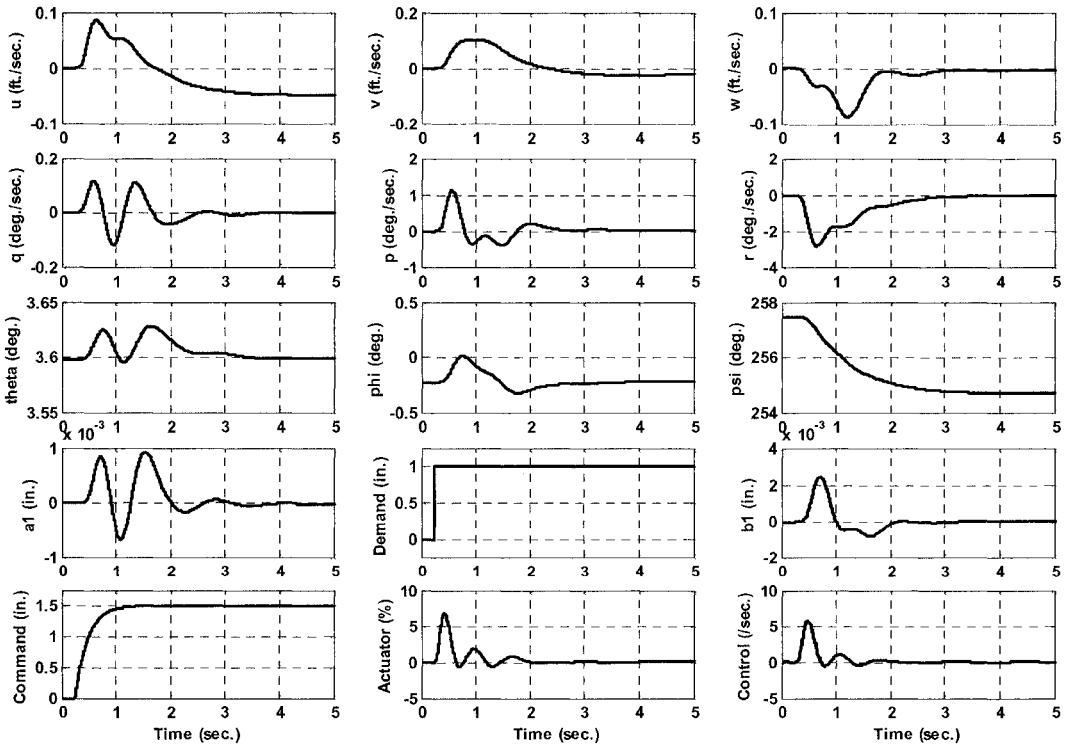

Figure 3.103 EAC Controller Time History Response due to Tail Rotor Collective Step

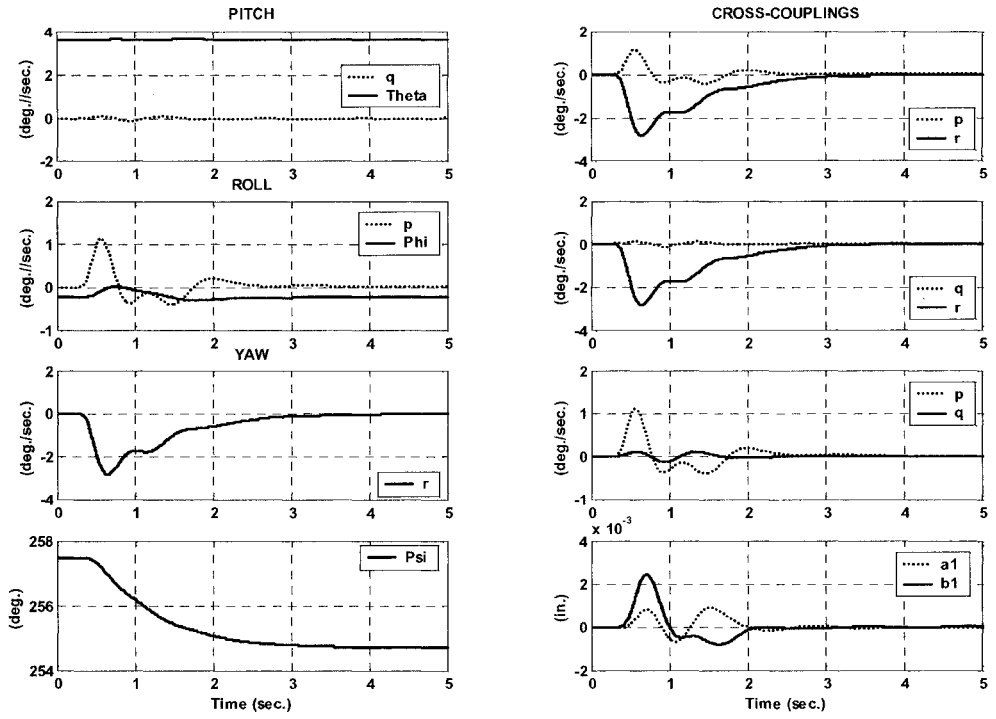

Figure 3.104 EAC Controller, Cross Coupling Response due to Tail Rotor Collective Step

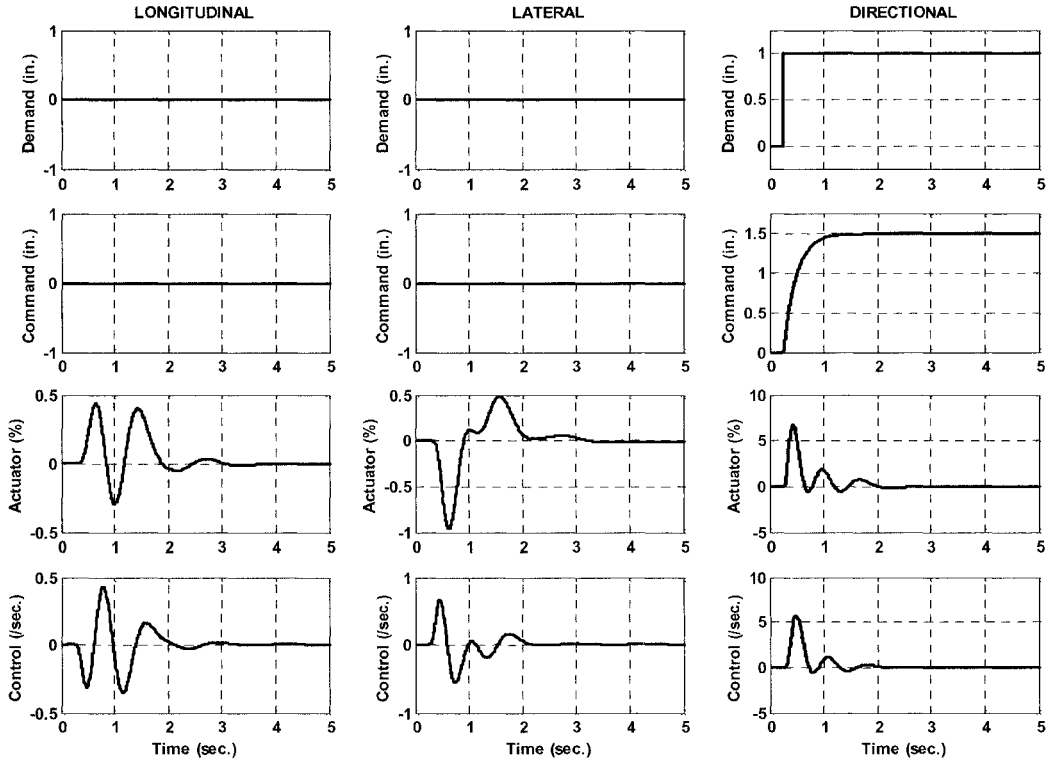

Figure 3.105 EAC Controller, Control Usage due to Tail Rotor Collective Step

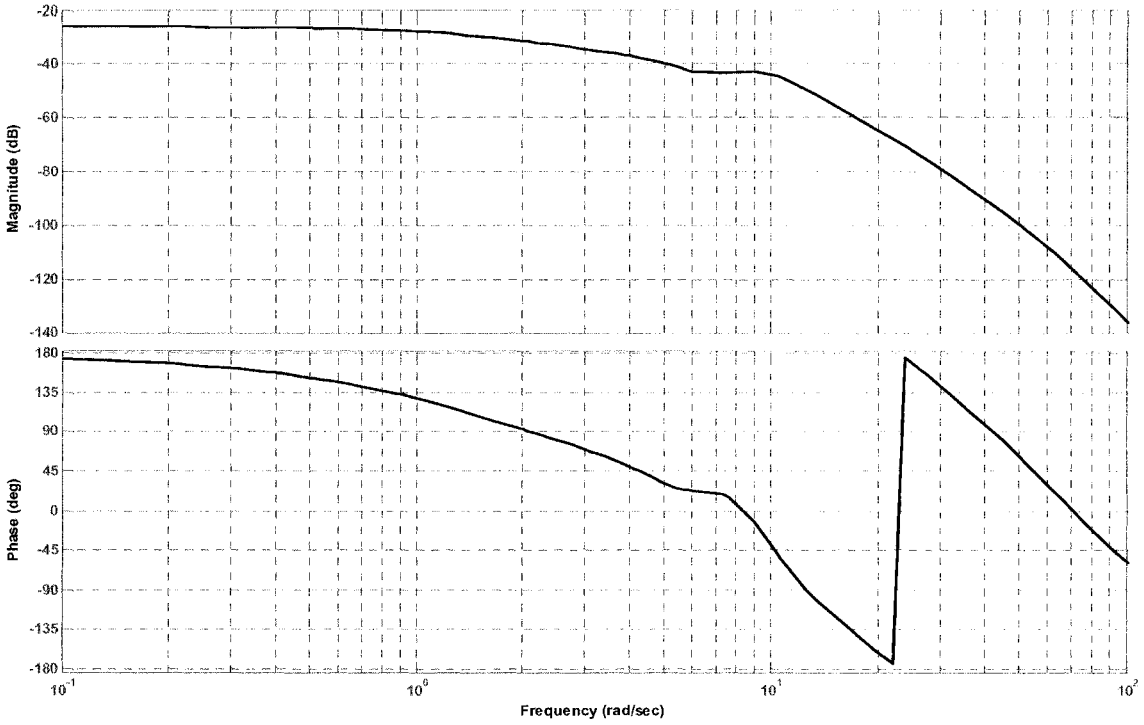

Figure 3.106 EAC Controller Directional Frequency Response

3.6.7 Effects of Rotor State Feedback by Eigenstructure Assignment Control (EAC)

The benefits of rotor state feedback have been highlighted throughout our discussions in high bandwidth flight control, system identification, and higher order dynamics research. In the proceeding section the author evaluates the EAC controller for a variety of task elements critical to attaining modern helicopter flight dynamic and aeromechanics response. The tasks include:

- Rigid-Body Frequency Bandwidth Extension
- Aeromechanical Stability Gain Threshold Evaluation
- Disturbance Attenuation Assessment
- Command Tracking Assessment
- Axis Decoupling Assessment

3.6.7.1 Bandwidth Frequency Modification

To investigate the effects of an EAC controller with rotor state feedback on rigid-body bandwidth performance, a simple design was synthesized. The EAC controller applying only single-axis rotor state feedback showed both beneficial and degrading effects on vehicle rigid-body bandwidth performance as parameterized in Figures 3.107 to 3.109. For this non-linear simulation, the pitch bandwidth was improved by 42.5 %, the roll by 54.4 %, and the yaw remained constant as summarized in Figure 3.110. The gain structure simulated did produce an optimal controller for a rotor state feedback application. The effects of rotor state feedback increased bandwidth and thus drove the rigid-body dynamics into Level 1 ADS-33 compliance for pitch and roll; the yaw axis remained at Level 3. The author's aggressive choices for cross-over frequency and control parameterization was the cause of the heightened phase delays acquired by the eigenstructure assignment controllers without rotor state feedback.

Next, EAC controllers are further scrutinized and optimized by an investigation of aeromechanical stability bounds.

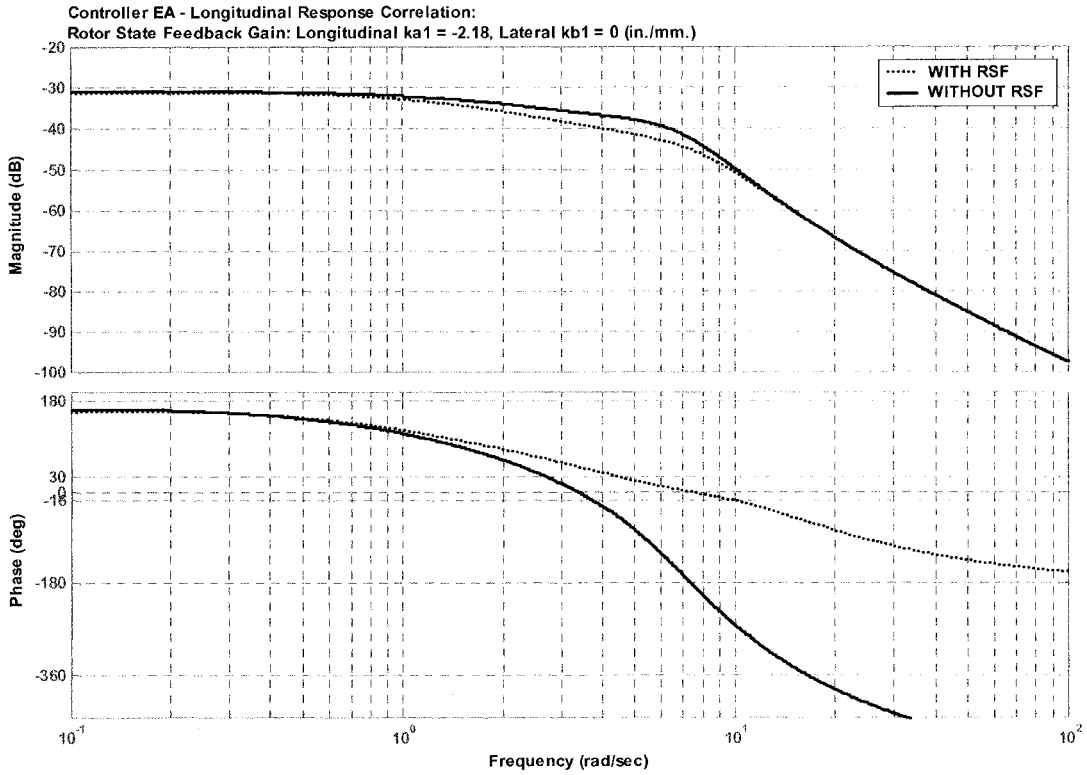

Figure 3.107 EAC Controller, Longitudinal Axis Frequency Response, With and Without Rotor State Feedback

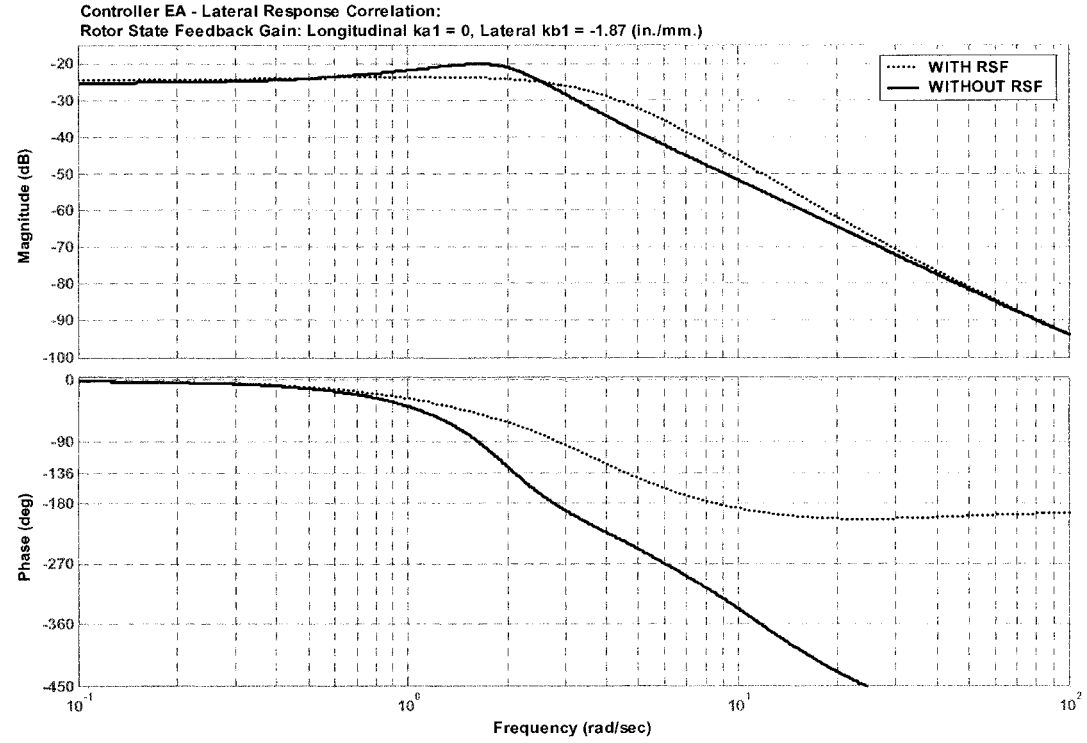

Figure 3.108 EAC Controller, Lateral Axis Frequency Response, With and Without Rotor State Feedback

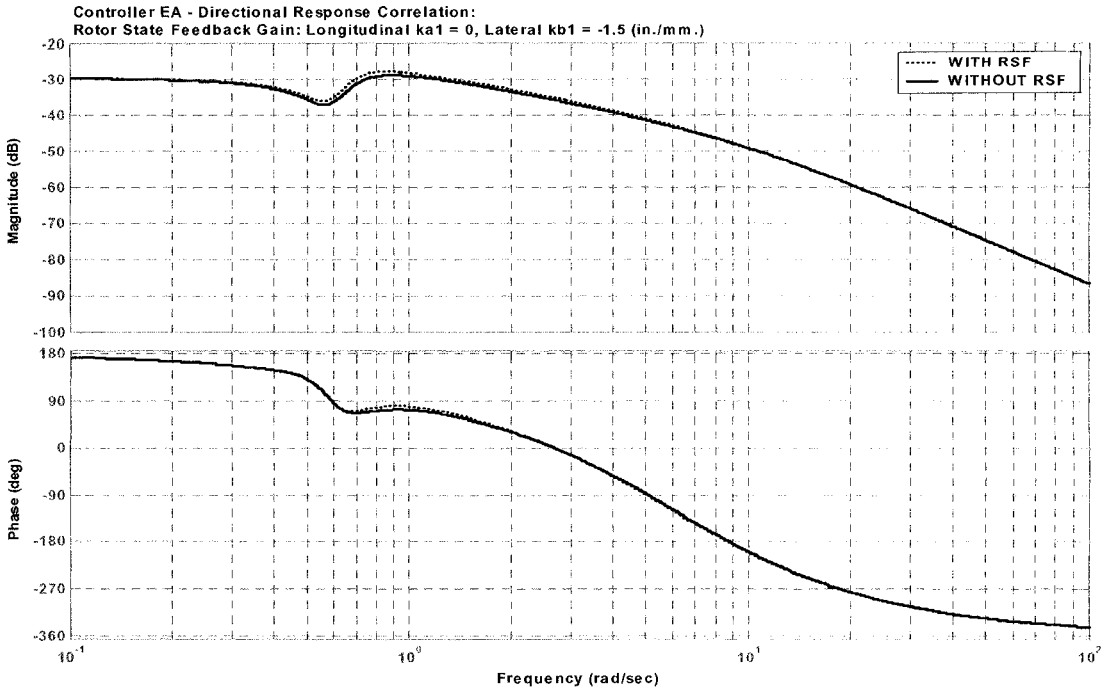

Figure 3.109 EAC Controller, Directional Axis Frequency Response, With and Without RSF

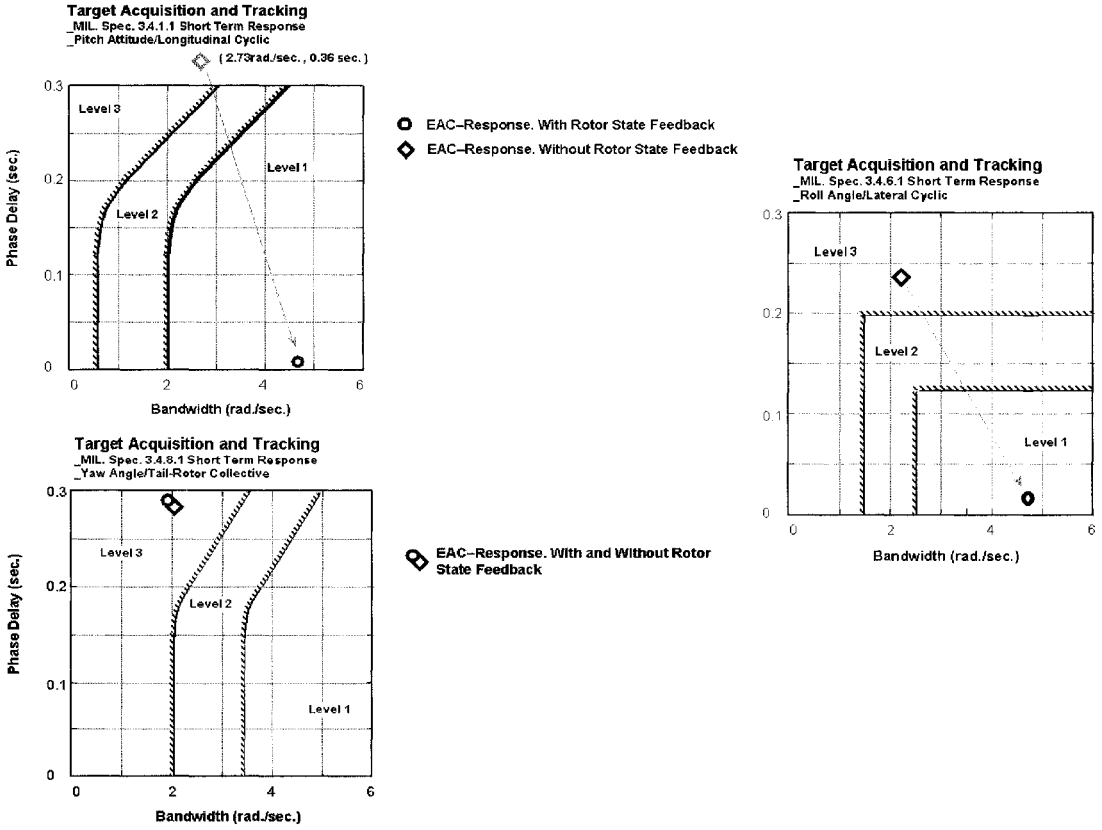

Figure 3.110 EAC Controller Response Compliance – ADS-33E-PRF,With and Without Rotor State Feedback

3.6.7.2 Aeromechanical Stability

As in the classical case, an exploration of coupled rotor-body instability was performed by varying the rotor state feedback gains, individually, through positive and negative ranges. This resulted in the stability margins depicted in Table 3.8. To note are the effects of off-axis rotor state feedback on coupled rotor-body interaction and stability.

CONTROL INPUT: LONGITUDINAL STEP ROTOR STATE FEEDBACK GAIN	GAIN VARIATION (IN./MM.)	COMMENTS
Longitudinal On-Axis, a1	-5 < 0 < +1	**Divergent Oscillations, ka1 = +1**
Longitudinal Off-Axis, b1	-3 < 0 <+1.5	
Lateral Cross-Axis, a1	-6 < 0 <+3	**High Yaw Actuator Activity, ka1 = +3**
Lateral Cross-Axis, b1	-7 < 0 <+5	
Directional Cross-Axis, a1	-5 < 0 <+3	**High Yaw Actuator Activity, ka1 = +3**
Directional Cross-Axis, b1	-7 < 0 < +7	**High Yaw Actuator Activity, kb1 = +7**

CONTROL INPUT: LATERAL STEP ROTOR STATE FEEDBACK GAIN	GAIN VARIATION (IN./MM.)	COMMENTS
Lateral On-Axis, a1	-7 < 0 < +5	**Robust to High Gain**
Lateral Off-Axis, b1	-7 < 0 < +4	
Longitudinal Cross-Axis, a1	-5 < 0 < 0.75	
Longitudinal Cross-Axis, b1	-3 < 0 < +0.75	
Directional Cross-Axis, a1	-7 < 0 < +5	**Robust to High Gain**
Directional Cross-Axis, b1	-7 < 0 < +4	

CONTROL INPUT: DIRECTIONAL STEP ROTOR STATE FEEDBACK GAIN	GAIN VARIATION (IN./MM.)	COMMENTS
Directional On-Axis, a1	-7 < 0 < +7	
Directional Off-Axis, b1	-7 < 0 < +6	
Longitudinal Cross-Axis, a1	-5 < 0 < +1	**Divergent Oscillations, ka1 = +1**
Longitudinal Cross-Axis, b1	-3 < 0 < +2	**Divergent Oscillations, kb1 = +2**
Lateral Cross-Axis, a1	-7 < 0 < +5	
Lateral Cross-Axis, b1	-7 < 0 < +5	

Table 3.8 Eigenstructure Assignment Control (EAC) Aeromechanical Gain Thresholds

3.6.7.3 Attenuation of Vehicular Disturbance Response

Disturbances are injected into the helicopter control system and rotor system throughout the operational envelope. These are the result of interactional aerodynamics associated with the coupled rotor/body system, the atmospheric environment, digitization, and signal noise.

To first test the closed loop EAC controller for disturbance rejection, a calibrated 0.5 sec. pulse of longitudinal, lateral, heave, and directional input is injected to observe the vehicle response. Both cases with and without rotor state feedback are applied.

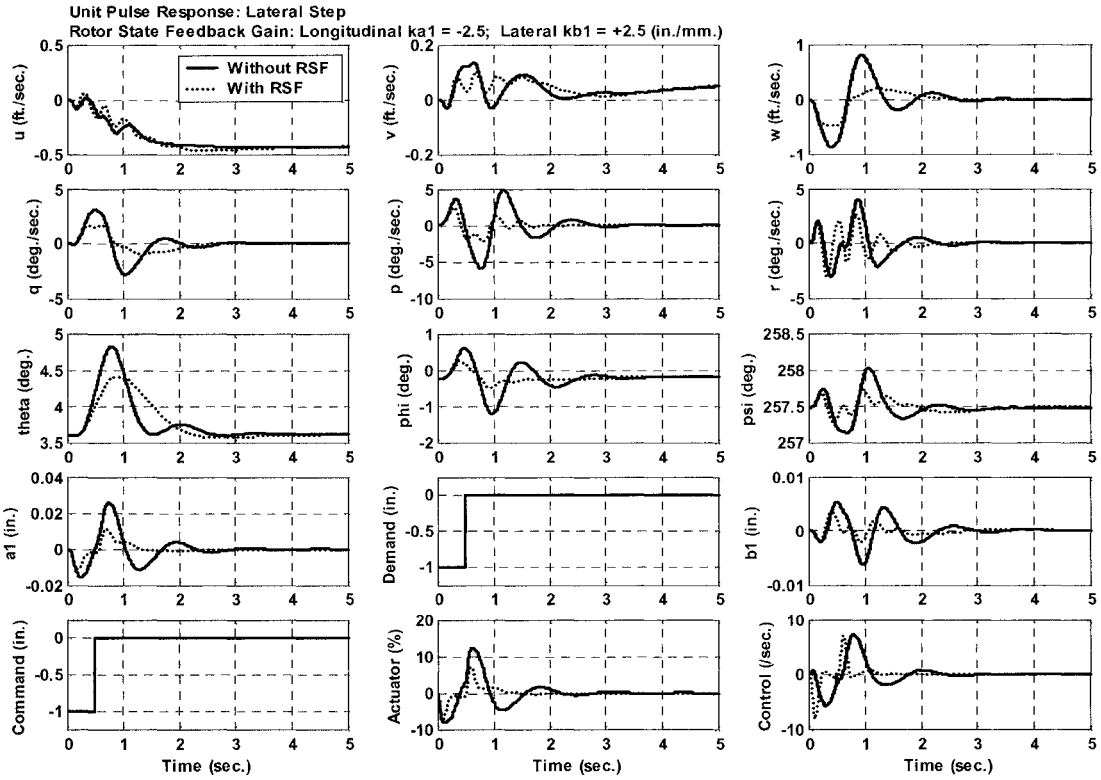

Figure 3.111 EAC Controller Longitudinal Unit Pulse Disturbance Rejection due to Rotor State Feedback

Rotor state feedback is shown in Figure 3.111 to extend the longitudinal axis bandwidth illustrated by reductions in rigid-body and control and rotor response magnitudes.

In lateral axis response, the effects are less with some amplification in forward flight trim velocity and yaw axis response magnitudes (Figure 3.112).

In the directional axis, the effects of the particular rotor state feedback are small as shown in Figure 3.113.

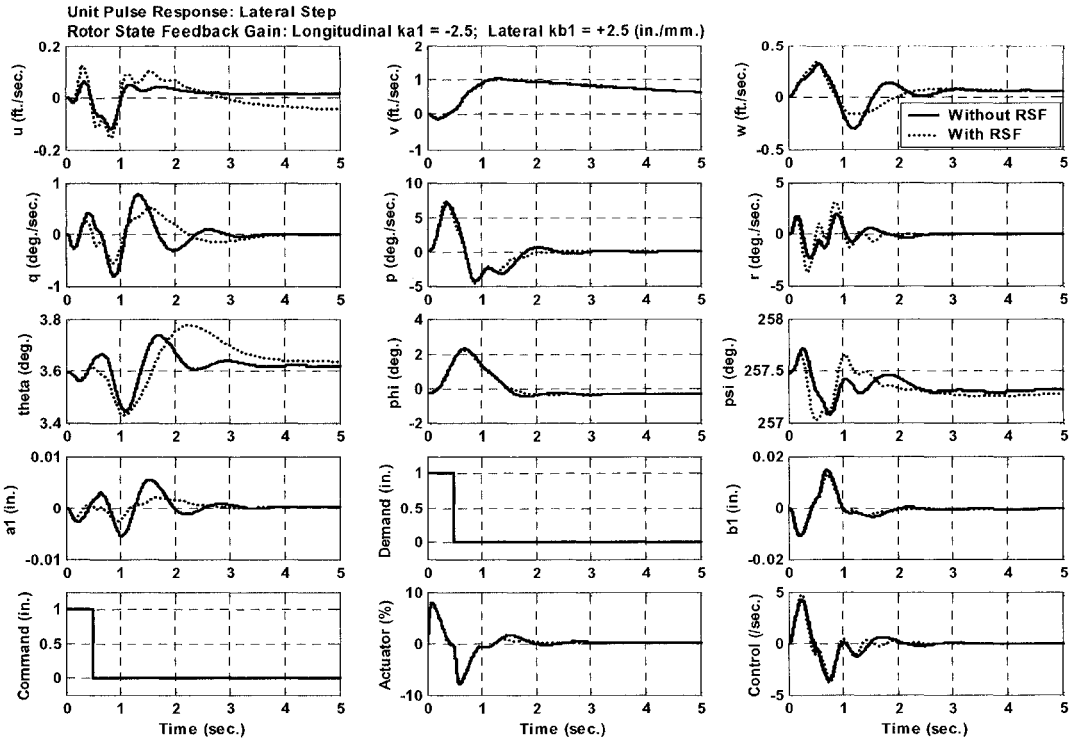

Figure 3.112 EAC Controller Lateral Unit Pulse Disturbance Rejection due to Rotor State Feedback

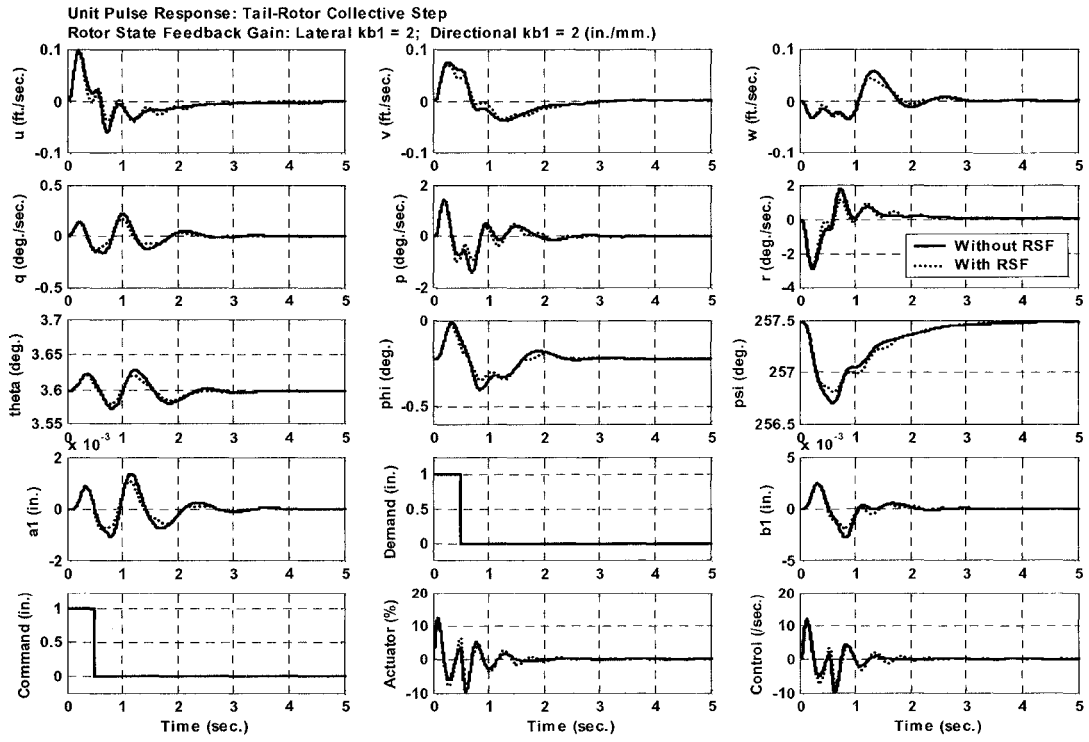

Figure 3.113 EAC Controller Tail-Rotor Collective Unit Pulse Disturbance Rejection due to Rotor State Feedback

In order to emulate other extraneous disturbances signal noise rejection is evaluated due to rotor state feedback gain variation. Signal noise in the form of a turbulence model developed by Tischler et al.[113] was introduced to assess the effects of rotor state feedback on noise rejection. The parameters of the Mixer Equivalent Turbulence Simulation mode (METS) were applied to the Bell 412 ASRA actuation control block of the non-linear simulation model to emulate turbulence activity. This particular model is injected at the control actuators (mixer or swashplate) to emulate a form of control dither disturbance. The longitudinal control axis disturbance component shown in Equation 3.41 was injected into the FCDE with pilot controls trimmed. As depicted in Figure 3.114, the presence of rotor state feedback promoted peak-to-peak attenuation of the injected disturbances in all axes in both the vehicle and actuator activity. The rotor state gains applied in this case were a longitudinal axis, longitudinal disc tilt (a_1) gain of 2 in./mm., and lateral axis, lateral disc tilt (b_1) gain of –3 in./mm. The analysis shows reductions of 47%, 49%, and 40%, in pitch, roll, and yaw rates, respectively. Reductions in actuator activity are shown to be 52%, 63%, and 22% for the same respective axes.

This attenuation extends to include rotor hub yoke activity as shown in Figure 3.115 that correlates to the reduction in rotor blade flap displacement. The reductions demonstrated are 58% and 52% in longitudinal and lateral disc tilt response, respectively.

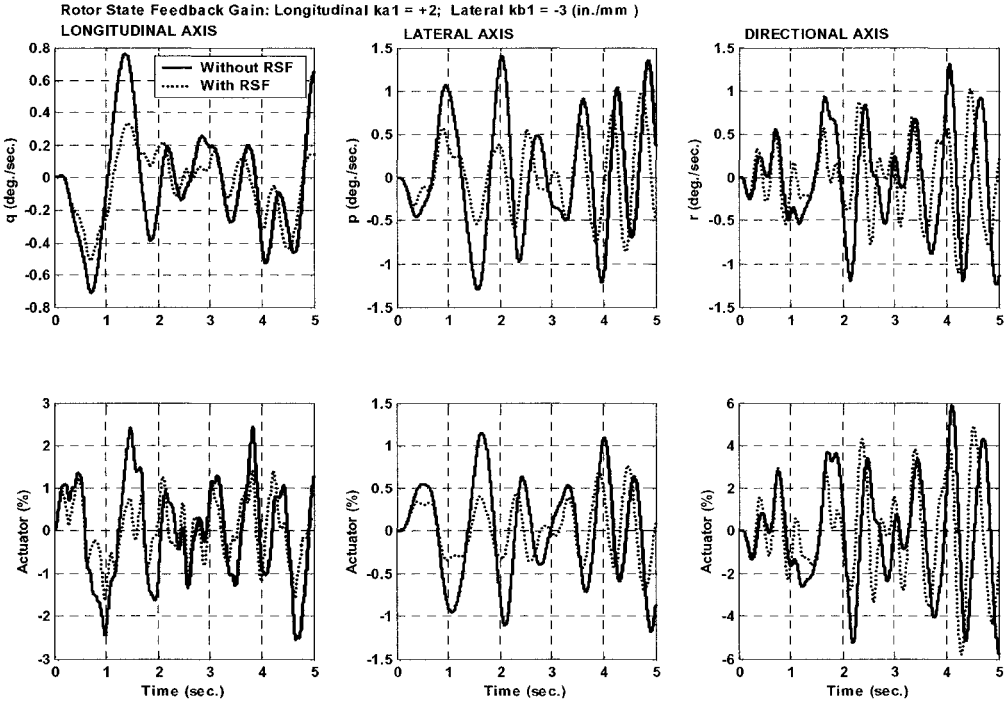

Figure 3.114 EAC Signal Noise Rejection due to Rotor State Feedback for Rigid-Body and Actuator Dynamics

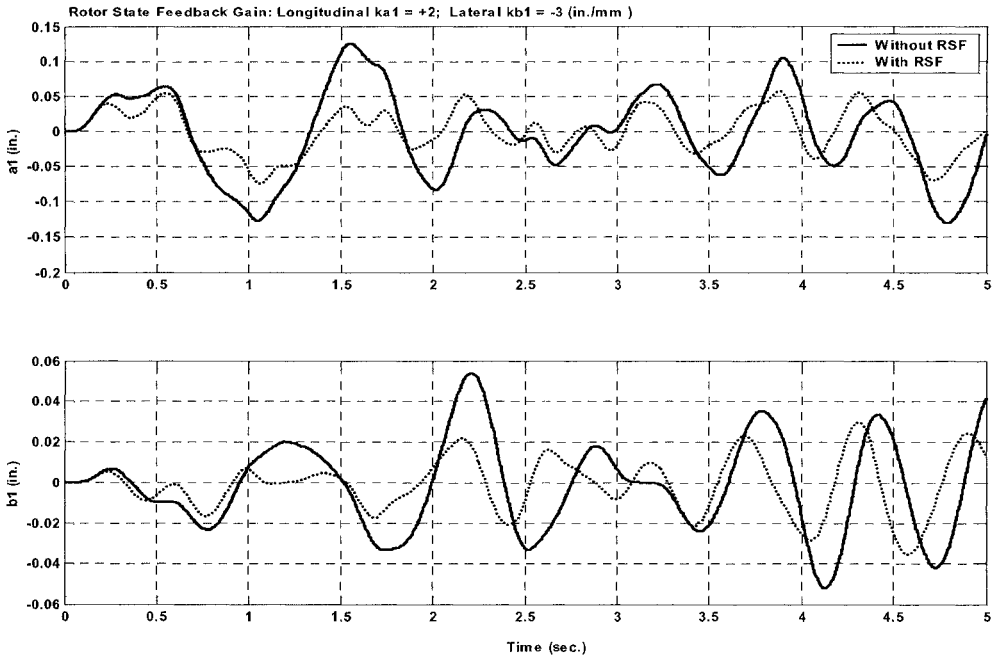

Figure 3.115 EAC Signal Noise Rejection due to Rotor State Feedback for Rotor Dynamics

3.6.7.4 Command Tracking Accuracy

In Figure 3.116, the response of the EAC controller to tracking the pitch ACAH design objective without a command model is illustrated. The command model constrains the maximum excursion of the responses overall in order to follow the command model. In Figure 3.117, the EAC controller applying a rapid first order command model as well as longitudinal and lateral disc tilt feedbacks of 2 in./mm provide a more optimal tracking of the pitch attitude hold objective. It is also noted that this improved tracking performance occurs by more optimal control usage, reduction in rotor disc displacement, and the reduction of axis coupling.

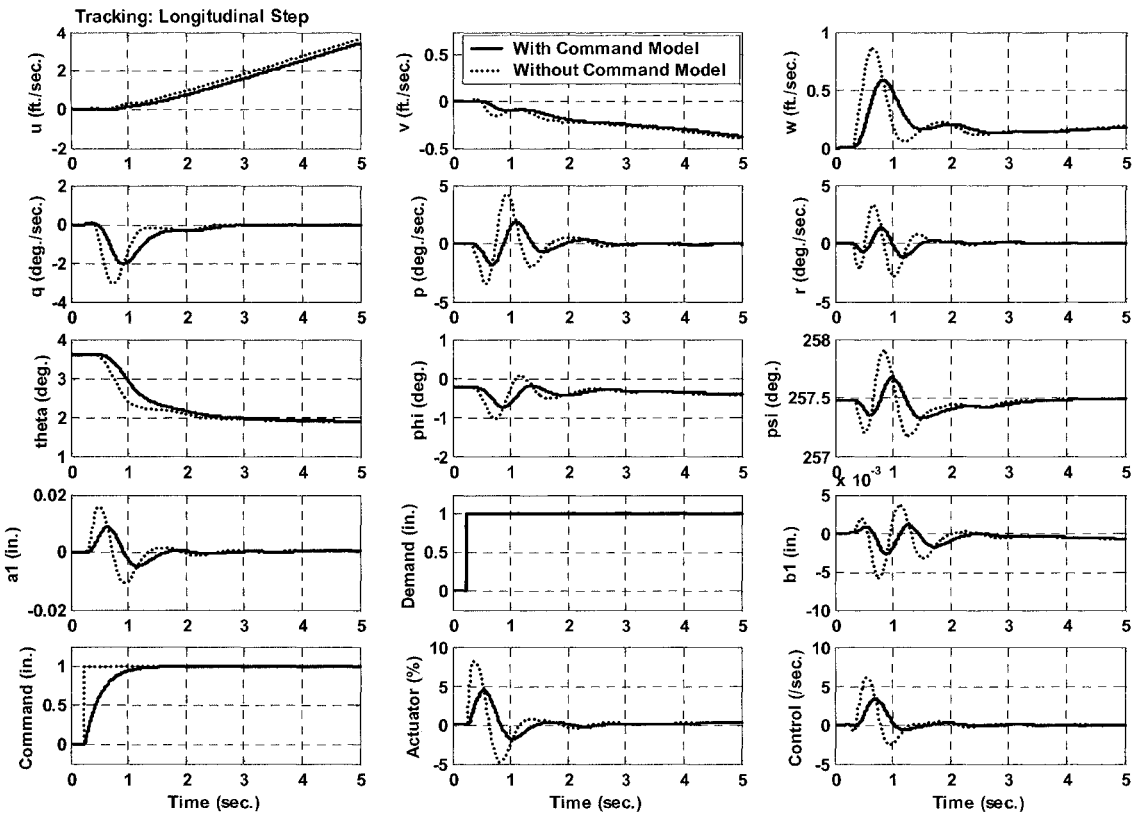

Figure 3.116 EAC Response Tracking - With and Without Command Model

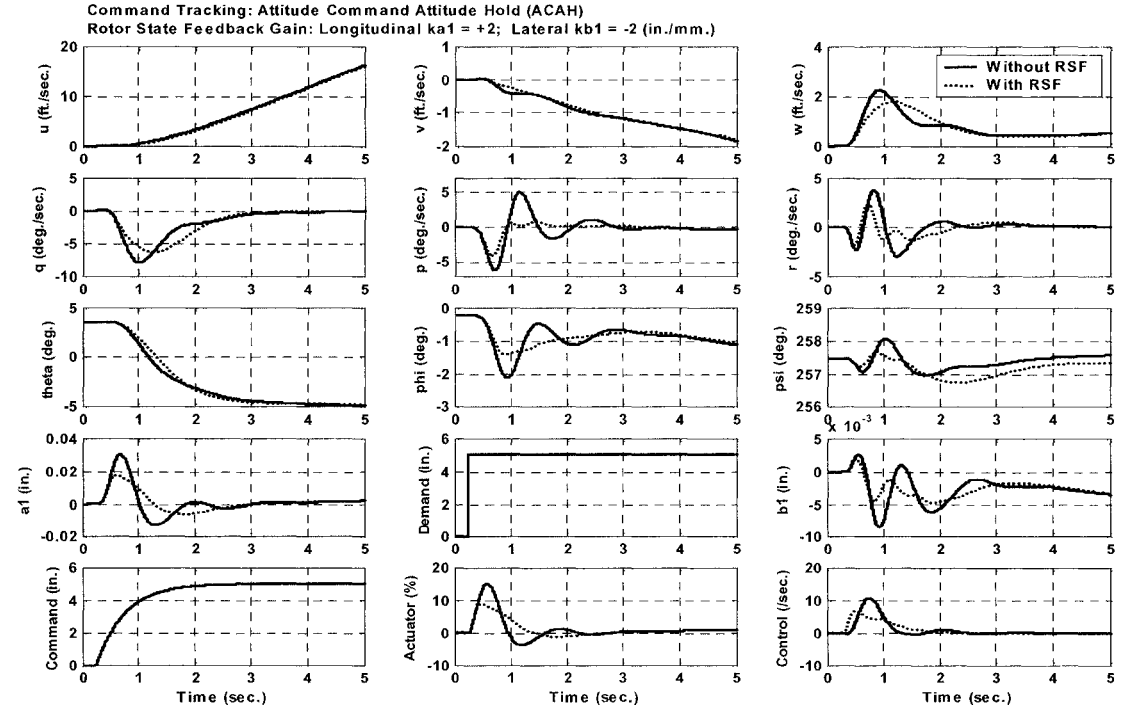

Figure 3.117 EAC Command Tracking - Pitch Attitude Hold by Rotor State Feedback

3.6.7.5 Attenuation of Rotor/Actuator Activity

The coupling of rigid-body and rotor dynamics has been illustrated to be a dominant feature of the feedback control. This coupling must be controlled since this it yields elevated on- and off-axis response, which produces excessive loading and oscillation in these axes. The result of this excess response can damage the helicopter by out-of-phase control activity, as well as vibratory and fatigue loading conditions of both the control and rotor system. Rozak[82,83] et al performed research illustrating that multivariable controllers based on high bandwidth requirements and specifications can elevate the potential for rotor hub component fatigue. In order to mitigate against this damage bandwidth compliance must be strict for both the helicopter design restrictions and specifications, decoupling control must be applied, and closed loop response to disturbances must be attenuated.

The attenuation of actuator and control rate usages, and rotor hub yoke activity was repeatedly shown in previous simulations. The reductions are important for high bandwidth simulators such as ASRA where elevated control-actuation demands tend towards saturation of the FBW and rotor/control systems.

3.6.7.6 Axis-Decoupling

The reduction of pilot workload in mission tasks is critical in attaining modern helicopter handling qualities compliance. The hingeless rotor's high hub moment capability portends to particularly high inter-axis coupling requiring a SAS for artificial improvement of vehicle characteristics.

The application of rotor state feedback is effective in decoupling both the pitch due to lateral cyclic and roll due to longitudinal cyclic interaction as shown in Figure 3.118. In this case 2 in./mm. of longitudinal on-axis disc tilt and lateral on-axis disc tilt were applied to assess decoupling.

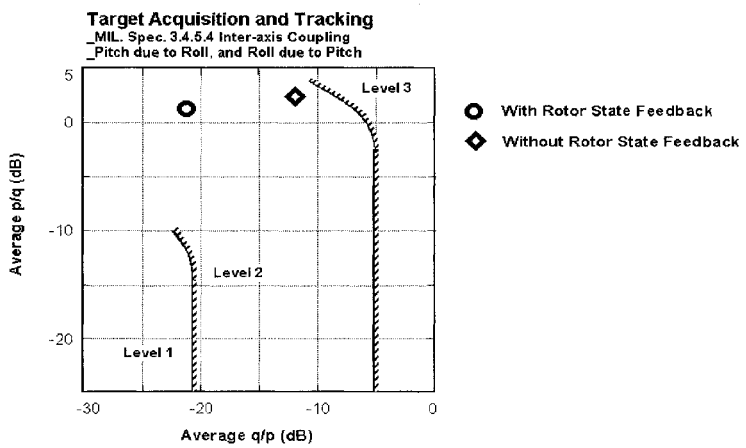

Figure 3.118 EAC Controller Compliance – ADS-33E-PRF Pitch-Roll and Roll-Pitch Coupling

Another important coupling for aggressive Target Acquisition and Tracking (TA+T) involves the yaw-collective interaction. A 5 in. collective step was applied to the ASRA non-linear simulation in the presence of the same rotor state gains as previously mentioned as shown in Figure 3.119. In Figures 3.120 and 3.121, the rotor state feedback of longitudinal disc tilt to pedal is applied.

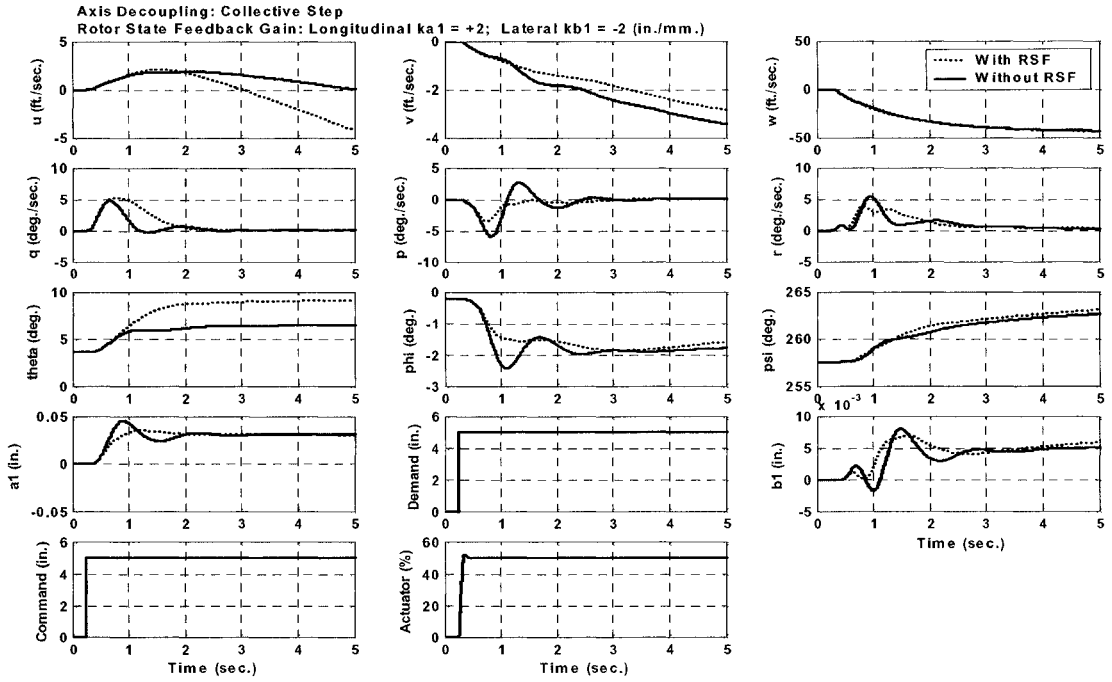

Figure 3.119 EAC Controller, Collective Step Time History Response – Longitudinal and Lateral Rotor Disc Tilt Feedback

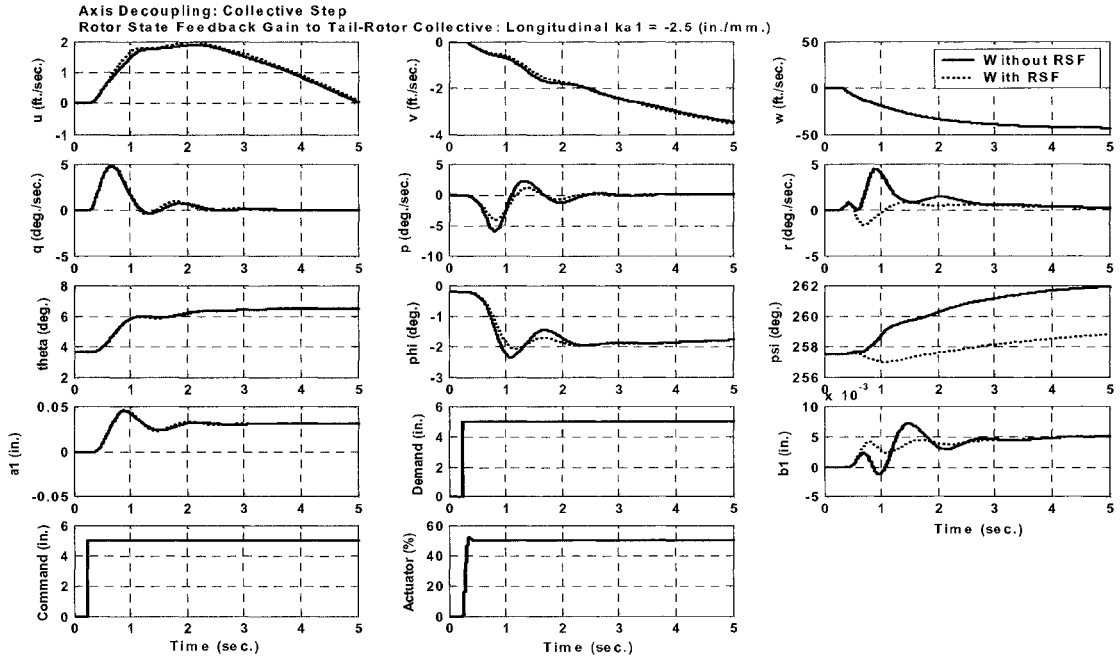

Figure 3.120 EAC Controller, Collective Step Time History Response – Longitudinal Rotor Disc Tilt Feedback to Pedal

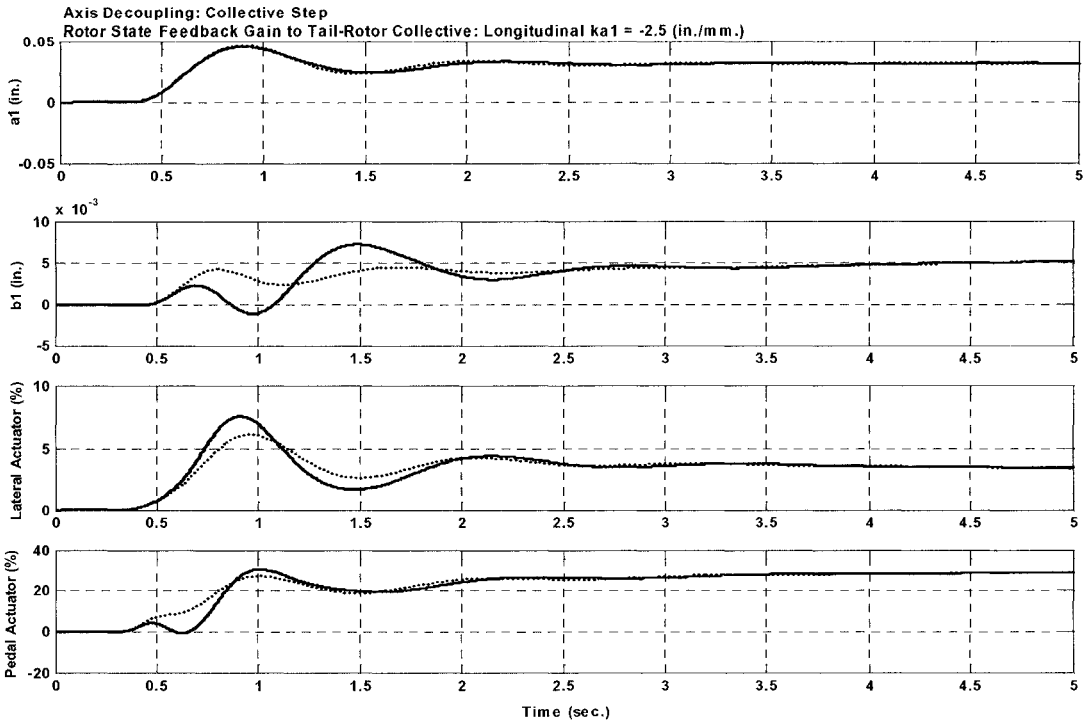

Figure 3.121 EAC Controller, Collective Step Time History Response – Longitudinal Rotor Disc Tilt Feedback to Pedal, Off-Axis Decoupling

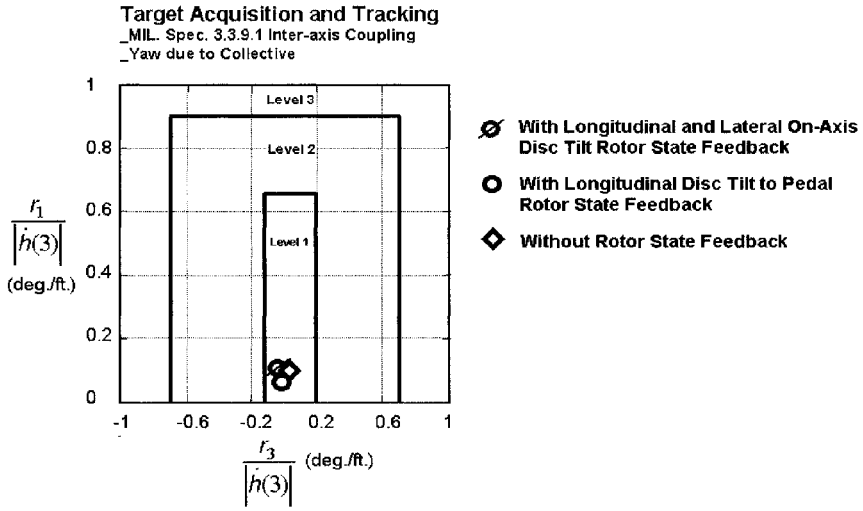

Figure 3.122 EAC Controller Compliance - ADS-33E-PRF Yaw due to Collective Coupling, Target Acquisition and Tracking

As shown in Figure 3.121, rotor state feedback reduces the maximum off-axis lateral disc tilt and associated actuator response excursions by 32% and 18%, respectively. Figure 3.122 illustrates that the overall compliance of the controlled responses remained consistently Level 1 with or without rotor state feedback.

3.6.8 Summary: Eigenstructure Assignment Control (EAC) Performance

The EAC control design methodology produced optimal modern controllers. With explicit application of ADS-33E-PRF military handling qualities specifications, the compliances remained in Level 1 bounds with the exception of the yaw axis. In the yaw axis, the unconventional application of yaw attitude and rotor state to pedal feedbacks, and the aggressive gain parameterization caused the poor compliance.

It has been clearly demonstrated that modal control is an important feature required to attain the requirements of coupled rotor-body stability and performance in the presence of rotor states and their feedback.

CONTROLLER	EFFECTIVE BANDWIDTH (BW) PERFORMANCE					
	BW_θ (rad./sec.)	RATING	BW_ϕ (rad./sec.)	RATING	BW_ψ (rad./sec.)	RATING
EAC_{NRSF}	3.4	L1	2.8	L1	4.5	L1
EAC_{RSF}	4.75	L1	4.6	L1	2.0	L3

Notation:
NRSF = **Without** Rotor State Feedback
RSF = **With** Rotor State Feedback
L1, L2, L3 = Level 1, Level 2, Level 3, with respect to ADS-33EPRF Compliance

Table 3.9 Summary of Eigenstructure Assignment Control (EAC) Effective Controls

3.7 Conclusions

The control law design process incorporated 3 control law design methodologies for synthesis of the final flight test controller group. These included Root Locus, Classical Multivariable, and Modern Eigenstructure Assignment methods. The following sections summarize the author's findings.

3.7.1 Simulation Results

Through both full- and reduced order simulations the following results are highlighted:

- The Eigenstructure Assignment Controller (EAC) provided the most optimal/efficient procedure and insightful way to design controllers that adhere to handling qualities design specifications. Modal control is the highlight of this technique.
- The Root Locus method (RLM) remains an invaluable tool in evaluating the effects of rotor states and feedback in flight control law design. The technique of trajectory analysis (typically pole-zero mapping) extended to time and frequency response mapping is innovative and further gives insight to the flight control design process.
- The Classical Multivariable control law (CMC) proved to be difficult to design without translation velocity feedbacks in the gain structure.
- In simulation, the rotor state feedback of longitudinal and lateral disc tilt dynamics by either classical or modern multivariable control laws **significantly improves** inter-axis decoupling, vehicular rigid-body and rotor response insensitivity to disturbances, optimal actuator/control usage and activity, optimal response of rotor dynamics, command tracking accuracy, and rigid-body bandwidth performance.

3.7.2 Selection of the Flight Test Controller Group

For flight test evaluation purposes a bank of controllers are assembled to evaluate the feedback characteristics due to rotor states. For the both the CMC and EAC controllers, an attitude command attitude hold (ACAH) structure was developed from baseline controllers. The rotor state feedback structures have base design gains. However, as was demonstrated by the above analysis, there are defined envelopes for the pilots to alter the gains via pilot interfaces in the ASRA cockpit in real-time, within margins of safety. Overall, this method will provide the aircraft managers and pilots with several controllers with the option of variable rotor state feedback gains. The baseline control structures presented to the flight test group (NRC-FRL Vehicle Managers: Gubbels and Ellis, NRC-FRL Test Pilots: Carignan and Leslie) are tabulated in Table 3.10.

CMC-ACAH$_{RSF}$	**GAIN STRUCTURE**
AXIS RESPONSE TYPE	
LONGITUDINAL ACAH$_{RSF}$	Cyclic Gain: [ku kw kq kθ **ka1 kb1**] = [0.000 0.000 15.2 30.1 **ka1 kb1**] Main Rotor Collective Gain: [ku kw kq kθ **ka1 kb1**] = [0.00 0.00 15.2 30.1 **ka1 kb1**]
LATERAL ACAH$_{RSF}$	Cyclic Gain: [kv kp kr kϕ **ka1 kb1**] = [0.000 -7.68 0.000 -24.34 **ka1 kb1**] Tail-Rotor Collective Gain: [kv kp kr kϕ **ka1 kb1**] = [0 0 0 0 0 **ka1 kb1**]
DIRECTIONAL RC$_{RSF}$	Tail-Rotor Collective Gain: [kr] = [8.78 **ka1 kb1**]

EAC-ACAH$_{RSF}$	**GAIN STRUCTURE**
AXIS RESPONSE TYPE	
LONGITUDINAL ACAH$_{RSF}$	Cyclic Gain: [ku kw kq kθ **ka1 kb1**] = [0.085 0.000 22.486 35.104 **ka1 kb1**]
LATERAL ACAH$_{RSF}$	Cyclic Gain: [kv kp kr kϕ **ka1 kb1**] = [0.005 -5.756 -0.754 -15.34 **ka1 kb1**] Tail-Rotor Collective Gain: [kv kp kr kϕ **ka1 kb1**] = [0.00 0.535 0.353 0.00 **ka1 kb1**]
DIRECTIONAL ACAH$_{RSF}$	Tail-Rotor Collective Gain: [kv kp kr kϕ kψ **ka1 kb1**] = [0.534 0.935 20.78 0.000 30.75 **ka1 kb1**]

Units:
ku, kv, kw = in./m./sec.;
kp, kq, kr = in./rad./sec.; kθ,kϕ,kψ = in./rad.;
ka1, kb1= in./mm.

Table 3.10 Flight Test Controller Group

Chapter 4.0

Model Following Flight Evaluation of Rotor State Feedback

4.1 Introduction: The Rotor State Feedback Flight Test Investigation

The flight test portion of this research took full advantage of the abilities of an in-flight helicopter simulation to investigate the control laws developed in Chapter 3. Due to operational issues, the Bell 412 Advanced Systems Research Aircraft (ASRA) was not available by the end of this contract to perform a rotor state feedback evaluation. As such, the managers of the Bell 412 ASRA and the Bell 205A Airborne Simulator (AS) research helicopters developed a model following concept that would allow the latter helicopter to emulate the former within bandwidth thresholds. This model following concept evaluated control laws based on in-flight model following of vehicular rigid-body dynamics that resulted from the rotor state feedback. This process allowed the controllers to be evaluated for handling qualities (i.e.; attitude tracking, axis cross-coupling) and disturbance rejection (i.e.; rigid-body disturbance attenuation) in a realistic in-flight environment. This removed some of the uncertainties associated with the results of the desk-top and ground-based simulation studies. In order to develop this task, a simulation environment was developed by Ellis and Gubbels to explore this concept. The following chapter will provide a description of the Bell 205A Airborne Simulator, a correlation analysis of the 2 vehicles (comparing rigid body dynamics, rotor dynamics, bandwidth capability), description of the model following ground and flight test plan, and a description of flight test results highlighting correlations with simulated results from Chapter 3.

4.2 Description of the Bell 205A Airborne Simulator (AS)

The Bell 205A Airborne Simulator (AS) is the NRC-FRL's third generation variable stability helicopter. The aircraft as shown in Figure 4.1, has been involved in programs such as the development of handling qualities specifications, display and night vision goggle (NVG) technologies, deck landing research, rotorcraft technology validations, and flight test aircrew training.[110]

Figure 4.1 Bell 205A Airborne Simulator (AS)

The Bell 205A AS is derived from the Bell 205A-1 helicopter. This medium class, single-engine helicopter is powered by a Lycoming T53 engine rated at 1100 SHP and has a gross take-off weight of 9500lbs. The Bell 205 features a teetering rotor hub that results in its lower bandwidth capability when compared to the hingeless rotor Bell 412 ASRA. The aircraft has an experimental full-authority fly-by-wire system and performed its first FBW engagement in 1971. The latest upgrades to the system include a VME-based flight-control-computer (FCC) and a digitally implemented, real-time programmable, hydro-mechanical force-feel system.

Other major modifications include:

- Removal of the main-rotor stabilizer bar
- Fixing of the Horizontal Stabilizer
- Installation of FBW actuation support systems including AC generator, right-seat FBW controls, instrumentation/computer suite, and the FBW electro-hydraulic actuators

The FBW architecture and protocols are the same as that of the Bell 412 ASRA whereby the aircraft features a simplex experimental control system, dual pilot operation by safety (left seat) and evaluation (right seat) pilots, automated or manual FBW disengage capability, and a fully fault tolerant control architecture. The FCC architecture has been designed to allow rapid optimization of control laws and vehicle variable stability parameters. Researcher and aircrew interfaces are vital to allow real-time as well as pre-/post- flight analyses for research purposes; two important interfaces are the researchers' own computer workstation and the aircrews' FBW control panel. Figure 4.2 presents the interface environment for the Bell 205A AS from the pilot perspective. The aircrew interfaces with the Bell 205 variable system with a dedicated suite of in-flight programmable switching and display technology. Many programmable inputs are available allowing pilots to remain focused on their mission tasks and conduct in-flight research without, in many cases, having to remove their hands from the controls.

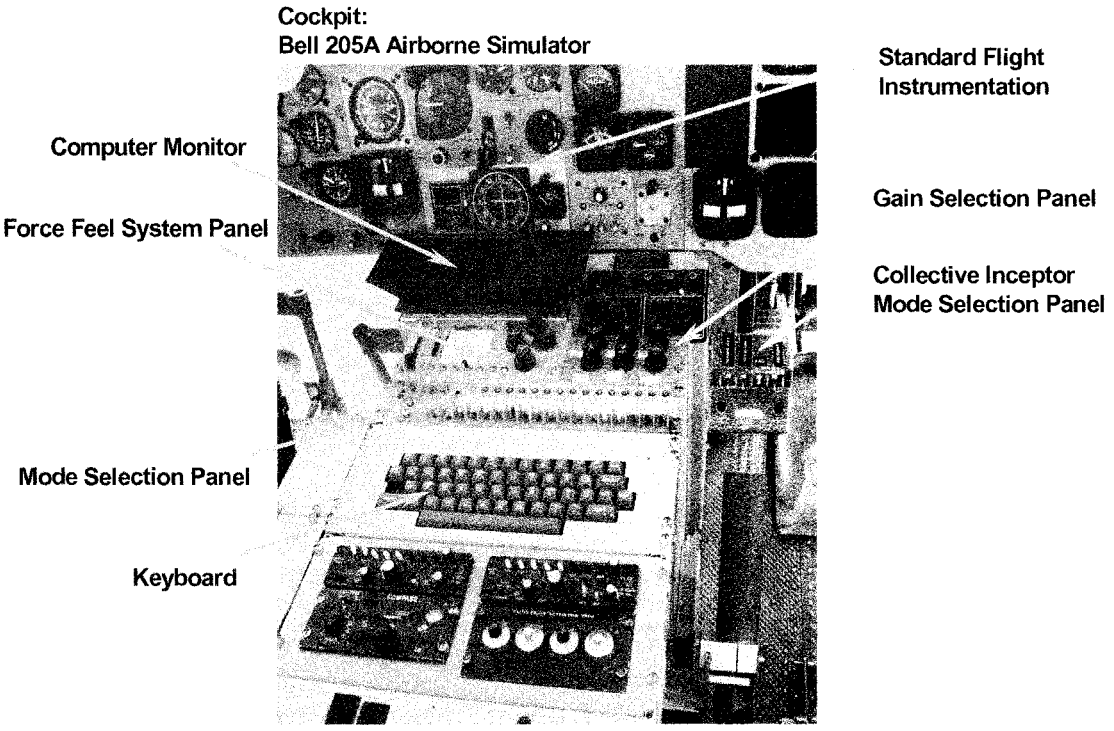

Figure 4.2 Fly-By-Wire Aircrew Interface – Bell 205A AS Cockpit

In comparison to the ASRA, the Bell 205A AS does not have a rotor state measurement capability. The Bell 205A AS flight control system has a sample rate of 64Hz causing 15msec. of latency in isolation. Other latencies including actuator/control response, mechanical control linkage free-play, teetering rotor system, and non-linearities contribute the Bell 205A AS accruing some 150msec. of time delay as compared to the 75msec. of the Bell 412 ASRA. The variable stability system features a Motorola 68040 processor running OS-9 in real-time based on a C code architecture. Other systems include the LN200 inertial navigation system, electro-hydraulic-actuators, instrumentation (air data, rigid body rates, attitudes, pilot/actuator position, etc.)[110,111], and project interfacing (pilot control switching, project panels, project display). The aircraft features a FBW force feel system to provide artificial cues (force and position) at the tail-rotor pedals and cyclic stick. A 4-axis side-arm controller has also been installed in the aircraft for alternate inceptor flight control.

4.3 Description of the Model Following Control Architecture (MFCA)

The MFCA developed by Ellis and Gubbels, consists of a physics representation of the Bell 205A AS and Bell 412 ASRA in closed loop feedback based on an attitude and attitude-rate following of the Bell 412 ASRA response. In order to evaluate rotor state feedback the MFCA implements and simulates the author's developed flight control laws in flight test by using Bell 205A AS evaluation pilot (EP) control and vehicle response inputs, and the Bell 412 ASRA rotor state feedback altered response.

The MFCA exists in SIMULINK format for desktop simulation as shown in Figure 4.3 as well as a C coded format for direct upload to the Bell 205A AS Flight Control Computer (FCC). The primary difference, then, between the MFCA and all other simulation environments in this report is that it is a real-time physics model that must conform to airworthiness standards required by the flight test aircraft. The MFCA consists of the following primary components:

- **Helicopter State Dynamics**: Bell412ASRA (8DOF HMMS), Bell 205A AS (6DOF)
- **Feedback System Dynamics**: Bell 205A AS Mixed Rate Signal, Feedback Control Law Gains
- **Feed-forward System Dynamics**: Input and Actuation Dynamics
- **Non-linearities**: Turbulence Model, Filters, Latencies, etc.

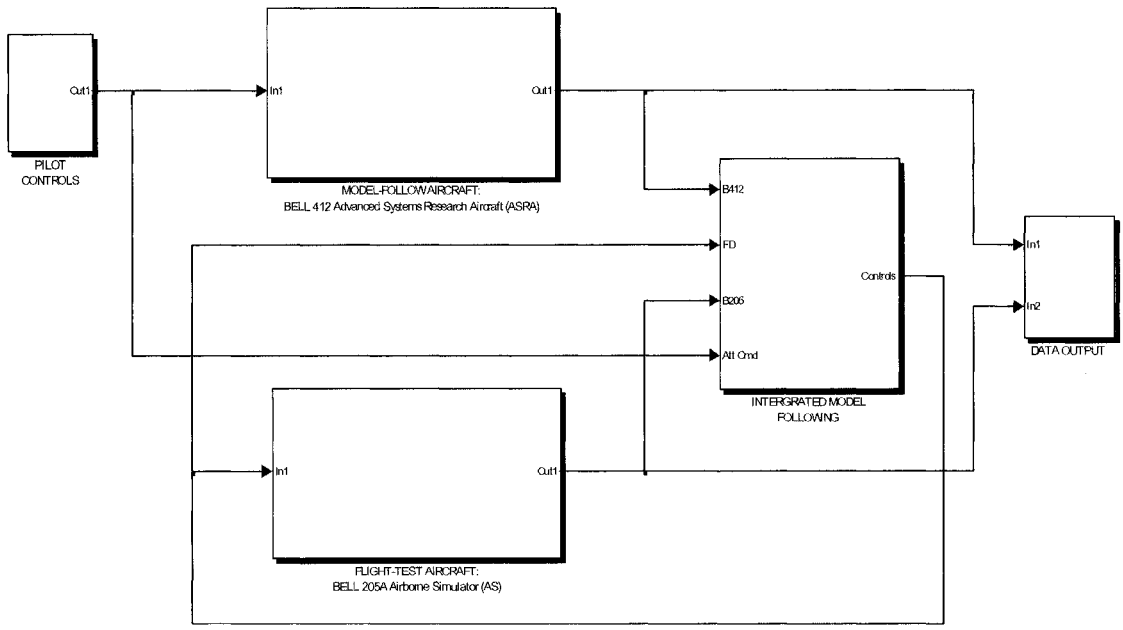

Figure 4.3 Model Following Control Architecture (MFCA)

The model following simulation was conducted onboard the Bell 205A AS applying its developed flight control architecture and rotor state feedback gain structure. The overall functionality of the system as implemented was as follows;

1. Control inputs from the evaluation pilot (EP) commanded the controllers developed in this report (either Classical Multivariable (CMC) or Eigenstructure Assignment (EAC))
2. Using the control input and feedback response from the Bell 412ASRA model (HMMS), the MFCA computed model following states. These states were subtracted from the measured Bell 205A AS states to create the commands to its actuators.
3. Bell 412ASRA HMMS states that were not to be model followed (such as the translational velocities u, v, and w) could be filtered using a high-pass filter option in the MFCA to prevent their divergence and hence conflict or divergence/disengagement of the in-flight simulation.

Others parameters such as gearing or sensitivities (pitch, roll, collective), force-feel stick characteristics, the type of filtering, and the model following gains were coded into the Bell 205A AS pilot interfaces for in-flight tuning. With this flight control configuration, the evaluation pilot had the opportunity to evaluate the controllers with rotor state feedback and without rotor state feedback, with and without active turbulence, and the raw Bell 412 ASRA in a single flight engagement.

4.3.1 Helicopter State Dynamics

The dynamics of these helicopters are similar in rigid-body context, however their bandwidth capability and the method by which hub forces and moments are applied to the aircraft fuselage differ substantially.

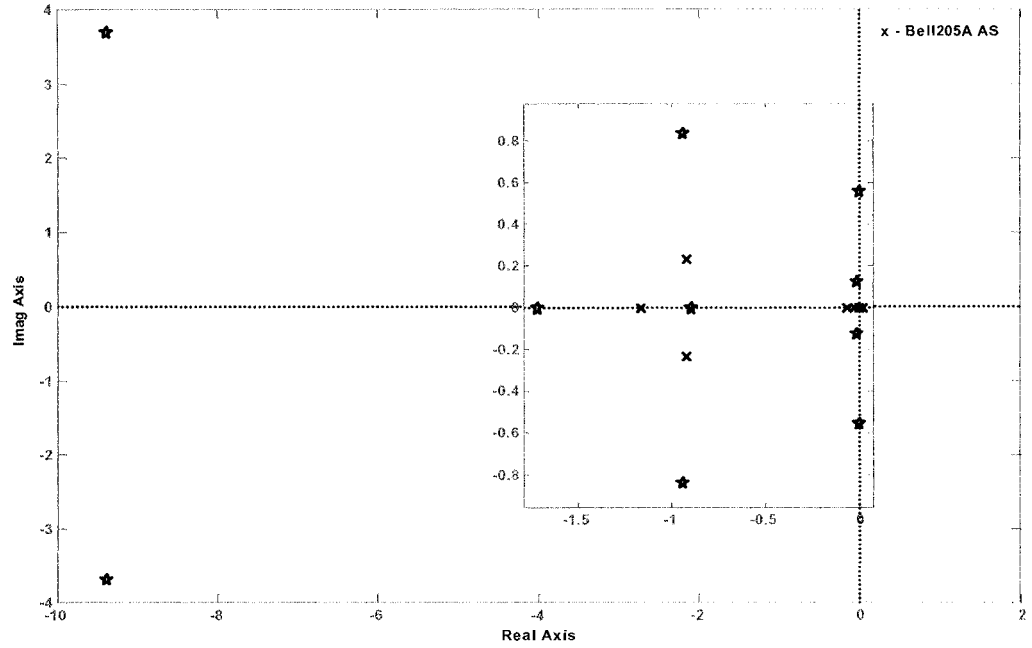

Figure 4.4 Modal Placements of Bell 205A AS and Bell 412 ASRA

	BELL412ASRA ROTOR: HINGELESS SOFT INPLANE MODEL: 8DOF, WITH MRRPM TRIM: 60KTS	BELL205A AS ROTOR: TEETERING, WITHOUT STABILIZER BAR MODEL: 6DOF TRIM: 60KTS
Pitch Phugoid	[+0.0987, 1.2]	(0.0296)
Dutch Roll	[+0.156, 0.288]	(0.0677)
Spiral	(0.0151)	(0.0186)
Pitch-1	(0.946)	
Pitch-2	(2.03)	(1.17)
Pitch/Roll Oscillation		[+0.97, 0.948]
Roll/Flap		
Regressing Flap Mode	[0.961, 9.47]	
Longitudinal Flap		
Lead/Lag Approx.		

Notation:

$[\zeta, \omega_0]$ implies $s^2 + 2\zeta\omega_0 s + \omega_0{}^2$,

where ζ = damping, ω_0 = undamped natural frequency (rad./sec.)

$(1/T)$ implies $(s + 1/T)$, (rad./sec.)

Table 4.1 Comparison of Modal Dynamics; Bell412 ASRA, Bell205A AS

Figure 4.4 and Table 4.1 compare the respective aircraft dynamics by mode placement and description. The Bell 412 ASRA features a soft-inplane hingeless rotor system that develops substantial hub-moments by blade root flexural bending. The hub tilting moment, more than the thrust moment with respect to the vehicle center-of-gravity, provides pitch-roll control and damping. The hingeless rotor features high control power and low time constants compared to articulated or teetering rotor helicopters. The Bell 205A AS features a teetering rotor hub (without the standard stabilizer bar) that does not generate hub moments. Vehicle pitch-roll control is achieved using only the moment of the rotor thrust vector with respect to the vehicle center-of-gravity. Control power is a function of g-loading and as such, the Bell 205 has a maneuverability limit defined when the g-loading is null. This corresponds to almost zero control power in this particular aircraft.

In terms of 6DOF rigid-body physics some comparisons of the two helicopters illustrate these performance differences. (Note: The 6DOF mathematical models used in this comparison are for a 60-knot forward flight linearization.) The vehicular time constants indicate rotor to rigid body time frame response due to pilot control. An estimate of rotor flap time constant given by $\frac{1}{\tau_f} = \frac{\gamma^* \Omega}{16}$ suggests that the Bell 205 and Bell 412 have 0.1073 sec. and 0.0957 sec. response frames, respectively. An estimate of the rigid body roll time constant given by $\frac{1}{\tau_p} = -\frac{1}{L_p}$ suggests that the Bell 205 and Bell 412 have 0.968 sec. and 0.487 sec. response time frames, respectively. The roll-flap damping ratio is estimated by the roll damping and the rotor flap time constant by $\zeta_{RF} = \sqrt{\frac{-1}{4 L_P \tau_F}}$. These values correspond to 150% compared to 111% for the Bell 205 and Bell 412, respectively. The heave damping derivative, Z_w, suggests blade-loading characteristics; values of -0.834 sec.$^{-1}$ for the Bell 412 and -0.998 sec.$^{-1}$ for the Bell 205 show the latter rotor system initially reacts more aggressively to gust/control perturbations than the former.

Most interestingly are the resulting off-axis control responses. (Note: In the following, the bracketed expressions define Bell 205 dynamics first and Bell 412 dynamics second.). The off-axis control responses are given in roll, $\left|\frac{L_{\delta LON}}{L_{\delta LAT}}\right|$ by (0.2489, 0.1824), and pitch, $\left|\frac{M_{\delta LON}}{M_{\delta LAT}}\right|$ by (12.778, 7.2779). These values suggest the Bell 205 is more coupled in roll and pitch than the Bell 412. The pitch control to collective and longitudinal stick control couple, $\left|\frac{M_{\delta COL}}{M_{\delta LON}}\right|$, is given by (0.1739, 0.1642), indicating that the Bell 205 has more control coupling than the Bell 412. These last findings are incorrect and their result highlights 2 important findings supported by our analyses in Chapters 2 and 3. Firstly, rigid rotors with high effective hinge offsets typically exhibit greater degrees of axis and control cross-coupling than those with lower offsets. Secondly, the cross-coupling terms in mathematical linearization are difficult to evaluate with accuracy using current system identification techniques.

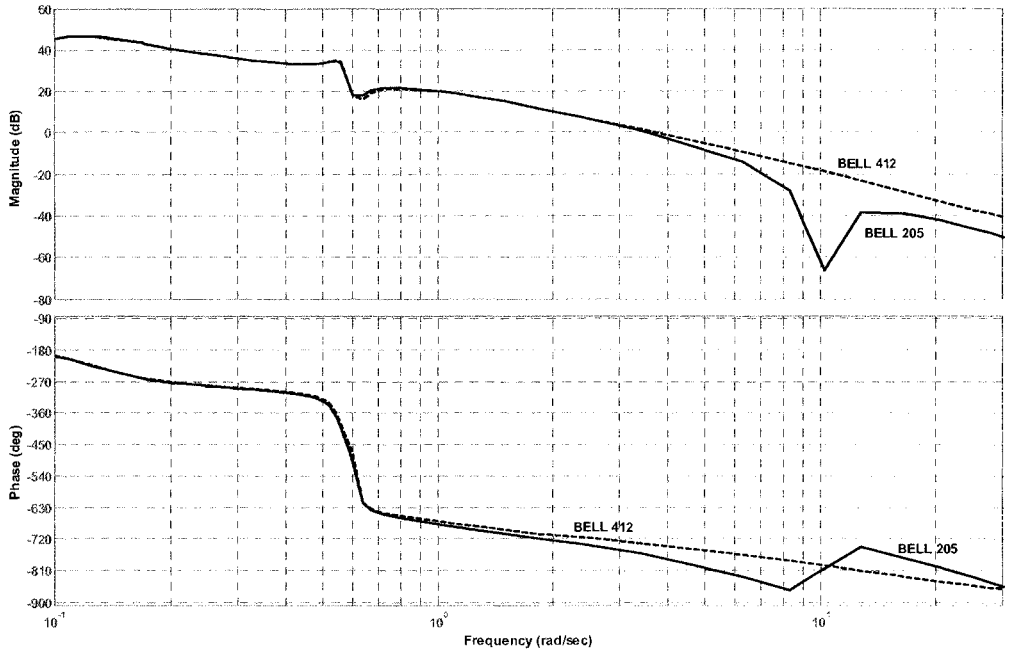

Figure 4.5 Longitudinal Frequency Response Comparison of the Bell 412 ASRA and Bell 205A AS

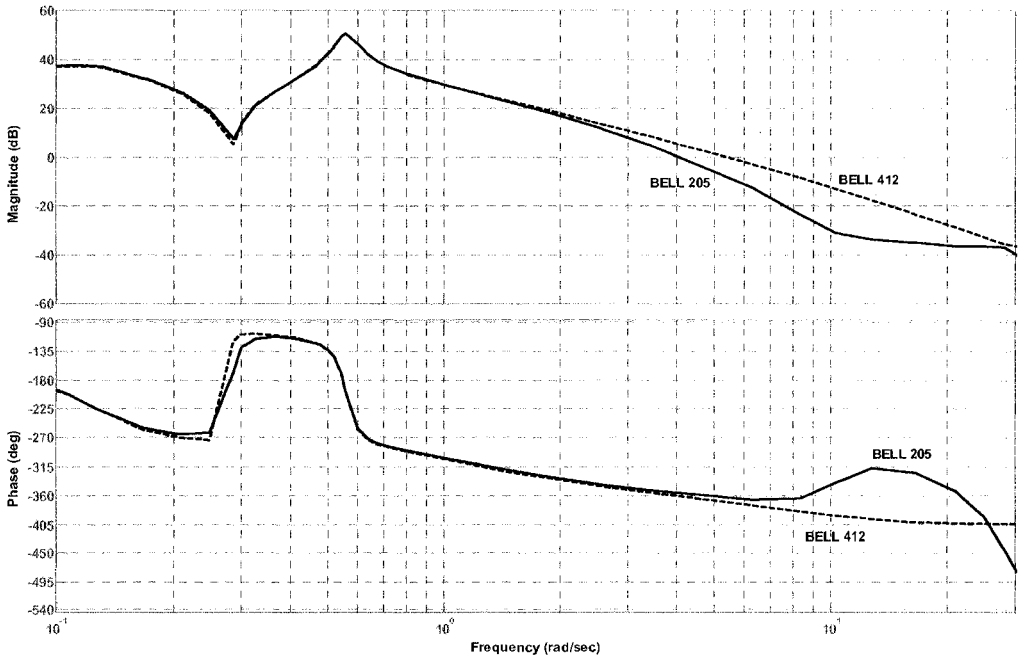

Figure 4.6 Lateral Frequency Response Comparison of the Bell 412 ASRA and Bell 205A AS

Finally in Figures 4.5 and 4.6, the Bell 205A AS and Bell 412 ASRA frequency responses are compared by the non-linear model following (MFCA) simulation. The responses highlight inherent bandwidth capabilities of these differing rotor hub arrangements though the time latency advantage of the Bell 412 ASRA is not depicted.

When combined with the MFCA implementation, these dynamics form conditions on the model following flight evaluation due to rotor state feedback that would not have existed if the test were to be done on the Bell 412 ASRA itself. As was shown in Chapter 2 where the Bell 412 ASRA HMMS model system identification showed band-limits at 12.6 rad./sec., so too is the real-time band limiting derived from the differing rotor systems in closed loop in flight simulation. This, however, does not limit the evaluation of handling qualities induced by rotor state feedback. In non-dimensional terms then the present model following in-flight investigation is based on the host aircraft (Bell 205A AS) handling qualities. Some perspectives on in-flight simulation on the Bell 205A AS versus the Bell 412 ASRA include;

- **Aeromechanical Stability:** Lead-Lag Dynamics
  In the development of rotor state feedback for the hingeless rotor system lead-lag instabilities were of concern. Though the teetering rotor hub is a hingeless hub with a hinge offset; lead-lag dynamics in the model-following flight are not limiting. The limits of concern were primarily imposed by the higher pitch and roll bandwidth of Bell 412 dynamics, and non-linearity modeling in the MFCA (i.e.; time and phase latencies). This could bring about effects such as biodynamic resonance in the FBW pilot controls under high workload tasks.

- **Bandwidth: Vehicular Rotor-Control Optimal Threshold**
  Whether ones considers the Bell 412 ASRA or Bell 205A AS flight dynamics, beyond elevated bandwidths in pitch and roll of, for example, 3.5 rads./sec. and 6.0 rad./sec. respectively – the vehicle handling qualities ratings would decline due to harsh and overly aggressive response. Thus, limiting the design point bandwidths of the rotor state feedback control laws appropriately for the given vehicle's rotor-control system will in no way limit the in-flight evaluation of rotor state feedback effects. Again, the flight test would focus on matching rigid-body attitude and attitude-rate dynamics based on the simulated effects of rotor state feedback applied to the ASRA in the MFCA.

- **Rotor State Feedback Application:** Performance Attainment
  Rotor state feedback performance benefits for this flight test investigation could not rely on host aircraft rotor state measurements or estimates. This curtailed the benefits to be demonstrated on the host Bell 205 to rigid body tracking accuracy, attitude capture accuracy, axis-decoupling

improvement, and bandwidth improvements that could provide rigid-body disturbance rejection. Direct disturbance rejection at the Bell 205A AS rotor hub could thus not be evaluated.

- **Model Following Control Physics:** Attaining Pilot Perceived Bell 412ASRA Handling Qualities

The MFCA achieves model following by relating input and response time frames, on- and off-axis response characteristics, and effects of rotor state feedback and turbulence. Set in a robust, closed loop, feedback and feed-forward structure, the MFCA uses filters to bind state divergences and delays to correlate the rigid-body response. This allows the required pilot perceptions of handling qualities to correlate for these two aircraft. The MFCA once implemented on the Bell 205 achieves model following of Bell 412ASRA pitch and roll rates and attitudes by relying on total accumulated Bell 205A AS latency to account for the entire dual aircraft system. The Bell 412 ASRA latency is not appended in the control loop. It is important to realize that the pilot's perception and ability to achieve their mission tasks will be based on both proper time based and phase based latencies of the MFCA.

4.3.2 MFCA Turbulence Model

The MFCA required a turbulence model for flight test evaluation of the achievable disturbance rejection effects that could be induced by effective rotor state feedback. This model allows the Bell 205A AS to respond to the effects turbulence injected into the onboard simulation of Bell 412ASRA rotor state controlled dynamics. Unlike the model implemented in Chapter 3, which simulated control system disturbances, the MFCA would apply a turbulence model directly into the rotor system dynamics of the Bell 412 ASRA's longitudinal and lateral rotor states, creating rigid-body pitch and roll excursions.

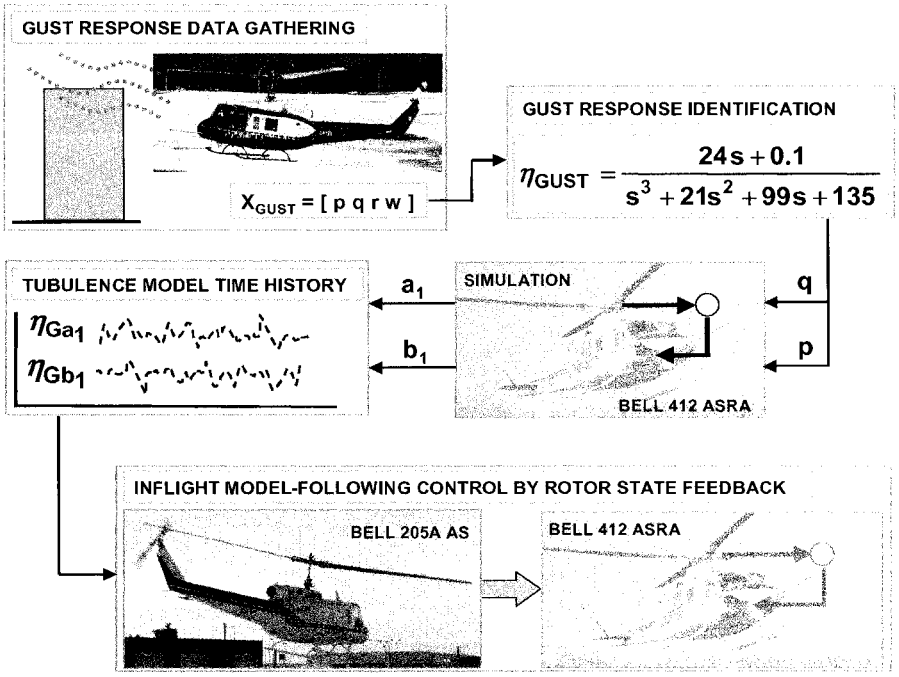

Figure 4.7 Turbulence Modeling Process

The particular process for implementing this experimental turbulence model is shown in Figure 4.7 which relies on historical data derived from the Bell 205A AS in atmospheric disturbance and bandwidth research. In a 1990 study, Baillie and Morgan[112] investigated the effects of disturbance rejection on the handling qualities of the Bell 205. The research involved a flight test investigation in which the Bell 205 was flown in turbulent conditions in order to create a physics model of the disturbances based on the vehicle's rigid-body responses. The model would be used for in-flight simulation of turbulence by injecting scaled and filtered angular and vertical motion dynamics into the Bell 205 actuators. The turbulence data from this report is depicted in Figure 4.8 as a time history turbulence response of the aircraft pitch and roll axis actuators. Using this data a power spectral density (PSD) of the time history data was developed. This frequency response data forms a standard environmental response data set that would be used for this research.

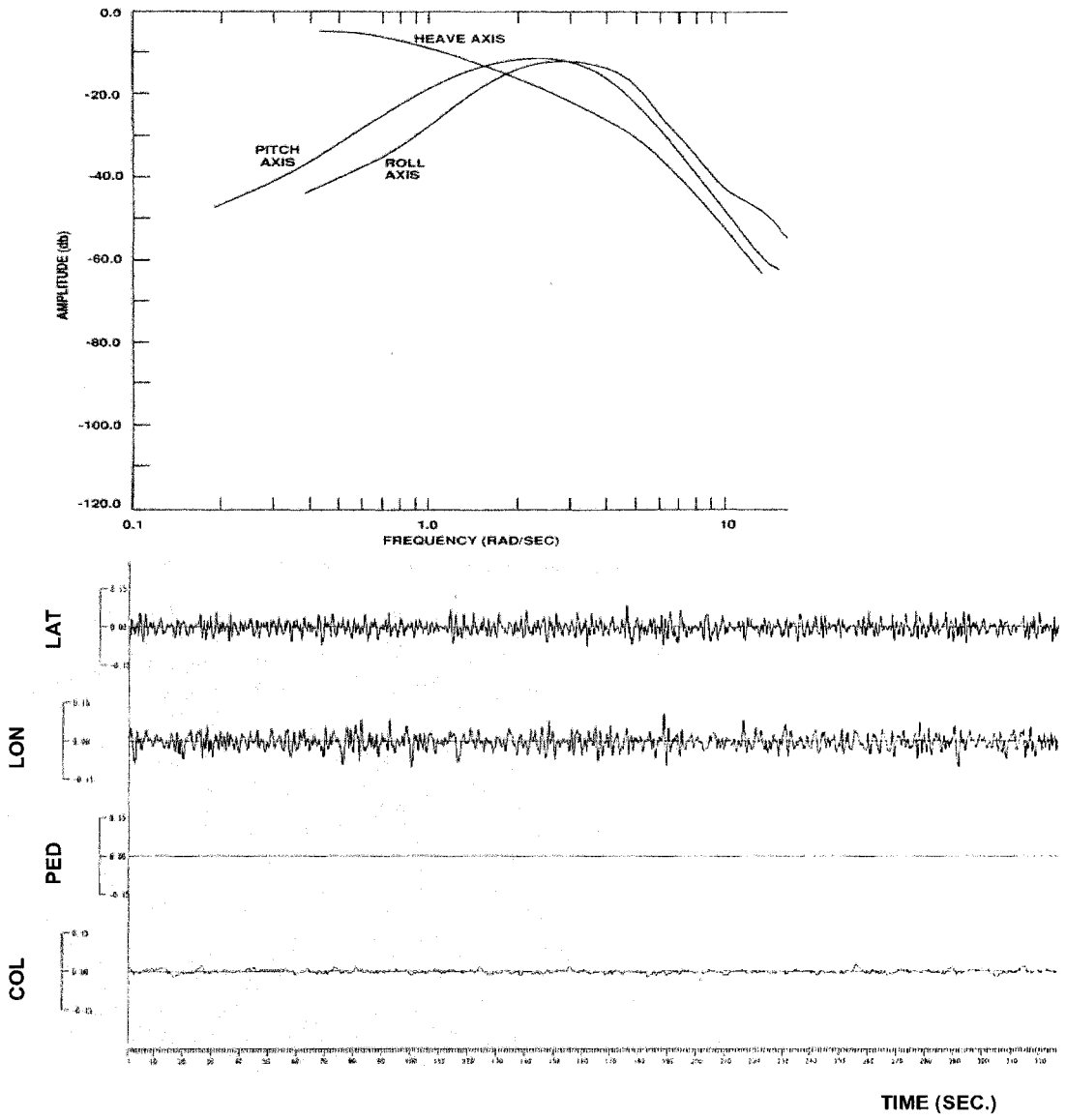

Figure 4.8 Turbulence Data, Bell 205A AS: (Bottom) Time History, (Top) Power Spectral Density[112]

The procedure for implementation of the MFCA turbulence model involved an analytical identification of the PSD data. The transfer function model of the disturbance was developed by fitting a transfer function to the PSD data for synthesis of the following 3rd order transfer function;

$$\eta_{GUST} = \frac{24s + 0.1}{s^3 + 21s^2 + 99s + 135} \qquad 4.1$$

The frequency response of this model is depicted in Figure 4.9, below.

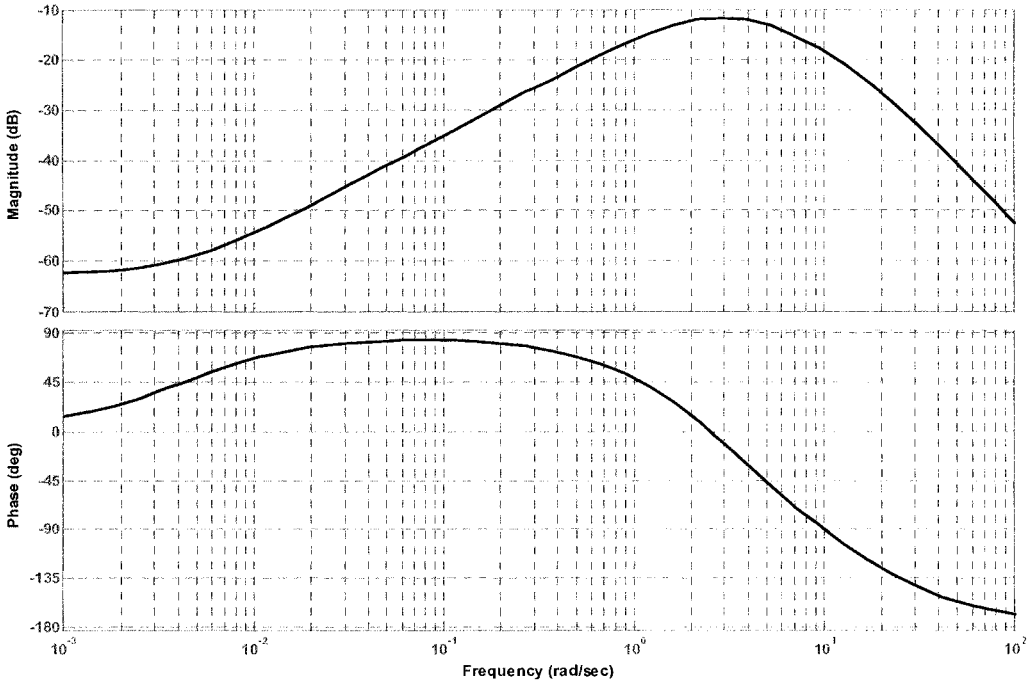

Figure 4.9 Frequency Response, Identified Turbulence Model

This model acts as a band pass filter with a peak frequency at –11.6 dB and 2.89 rad./sec. Applying this transfer function model to the Bell 412ASRA simulation resulted in the development of theoretical pitch and roll disturbance dynamics that would be used to evaluate the ability of the rotor state feedback based control laws in gust rejection, ride qualities, and handling qualities tasks.

The developmental assumptions for implementation of this turbulence model are as follows:

- **Vehicular Gust Response**

  The Bell 412 and Bell 205 platforms are of similar size (Mission Weights: W_{B412} = 10045 lbs., W_{B205} = 7557 lbs., Rotor Diameters: R_{B412} = 23ft, R_{B205} = 24ft), and thus will respond to gusts in similar frequency, amplitude, and time frames. This allows measured Bell 205 turbulence data to be applied in this study.

- **Rotor State Feedback Controller Evaluation**

  The rotor state feedback control laws apply longitudinal and lateral disc tilt feedback primarily to pitch and roll axis vehicle dynamics. Thus turbulence emulation in these axes was deemed sufficient for the to evaluation of control law performance based on the pitch and roll excursions it caused. The vertical gust dynamics were ignored.

- **Rotor-Flap and Attitude-Rate Response Correlation**
  As was shown in Chapter 2 and 3 there is correlation between the rotor longitudinal and lateral disc tilt (flap) and rigid-body pitch and roll attitude-rate dynamics. Turbulence modeling techniques by rigid-body pitch and roll dynamics emulation[1] may thus be modified to employ rotor longitudinal and lateral rotor disc tilt (flap) disturbances.

In what follows, the assumptions and conditions of the MFCA are validated prior to the ground and flight test program.

4.3.3 MFCA Physics Validation

The helicopter response physics of the MFCA are validated to ensure proper parameterization. As shown in Figure 4.10, the simulation responds with null outputs due to dead controls at trim.
In Figures 4.11 to 4.14, longitudinal and lateral pulses, respectively, are injected into the controls to evaluate a feedback control test case. In this instance, the EAC controller was implemented without rotor state feedback. The results in Figure 4.11 show that the Bell 412 ASRA dynamics lead the Bell 205A AS response. The longitudinal control power (i.e.; pitch attitude response to a unit pulse input) is some 20% higher for the Bell 205A AS; that of roll shows near identical response between both aircraft. This corroborates findings of the derivative comparisons for heave damping in Section 4.3.1.
Also in Figure 4.11, the cross coupling in pitch for the both aircraft, due to longitudinal unit pulse input, are of similar in magnitude. In Figure 4.12 the cross-coupling in roll, due to lateral unit pulse inputs, shows the Bell 205 initially reacting some 28% more in pitch rate than the Bell 412ASRA.

Most importantly is the rotor dynamics correlation. Recall that the objective of the MFCA flight engagement is to have the Bell 205 emulate the rigid body rate and attitudes of the Bell 412 ASRA due to it's simulated rotor state feedback. Thus, in Figures 4.13 and 4.14, the rigid body Bell 205A AS and Bell 412 ASRA attitude rates are well correlated. The rotor response is scaled by a factor of 100 to depict correlation to rigid-body dynamics. It can be seen that due to a longitudinal pulse the ASRA's rotor state response leads both of the helicopters' rigid-body response. A similar analysis in the roll axis shows the rotor disc reacting in a similar time frame as the rigid body dynamics.

Through this exercise, it was shown that the Bell 205A AS should exhibit sufficient fidelity to follow the modeled Bell 412 ASRA dynamics in flight.

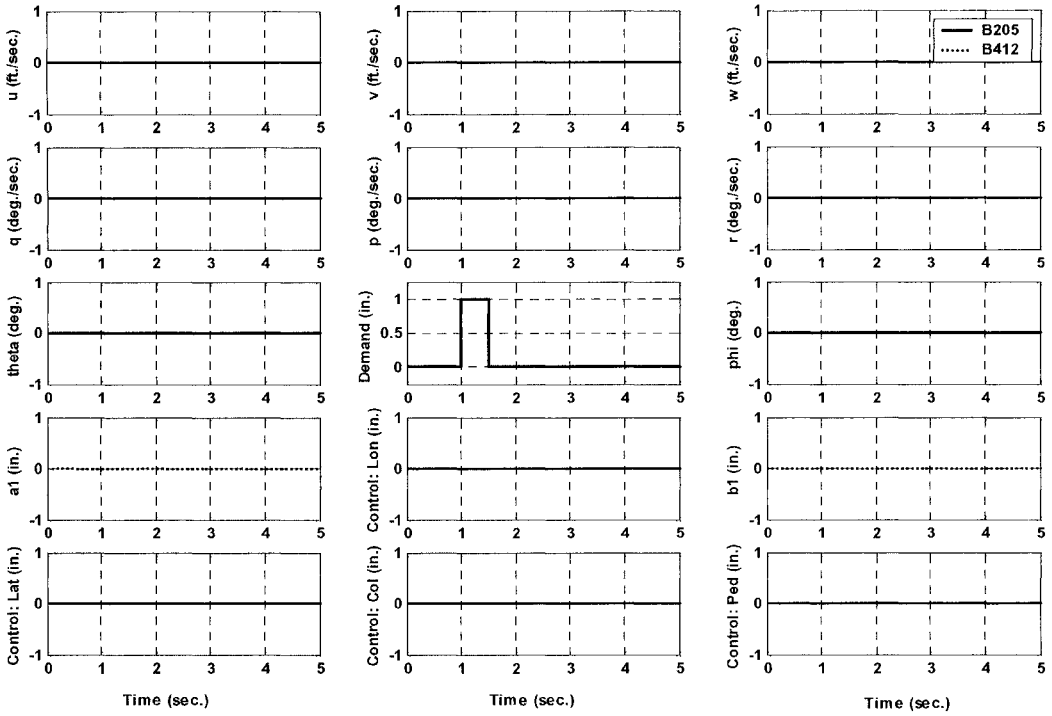

Figure 4.10 MFCA Time History Response Comparison, Bell 412 ASRA and Bell 205A AS
-Conditions: Trim, Dead Controls

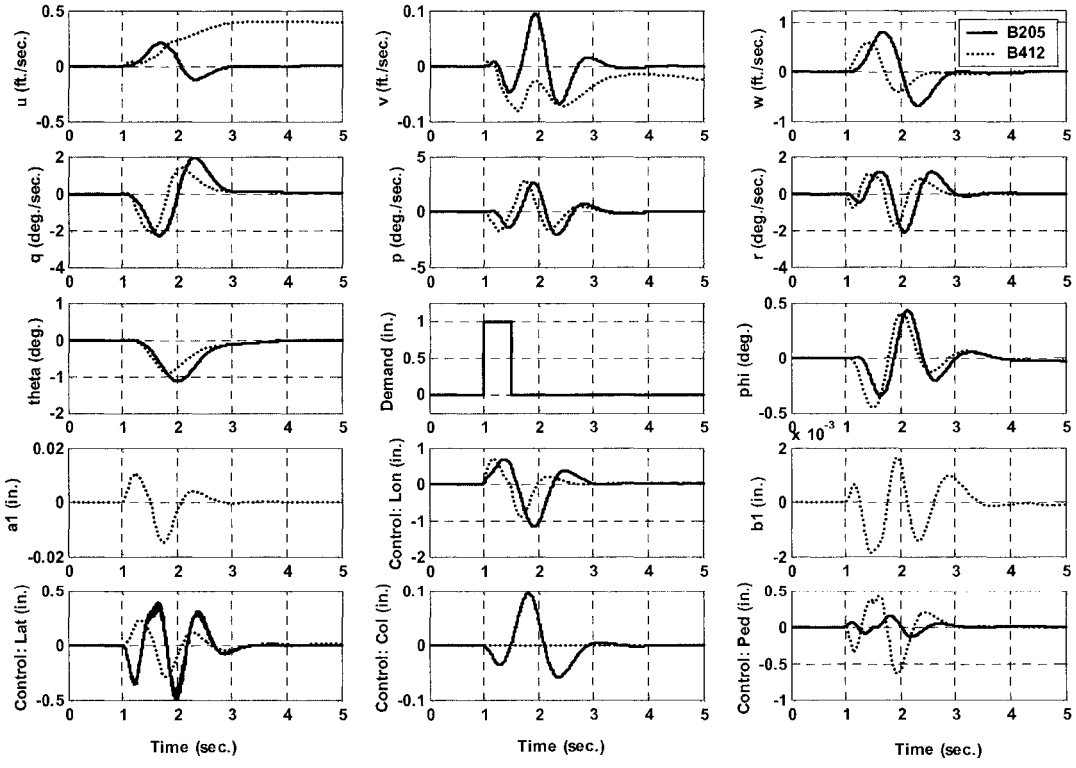

Figure 4.11 MFCA Time History Response Comparison, Bell 412 ASRA and Bell 205A AS
-Unit Pulse, Longitudinal Axis, EAC Controller Without RSF

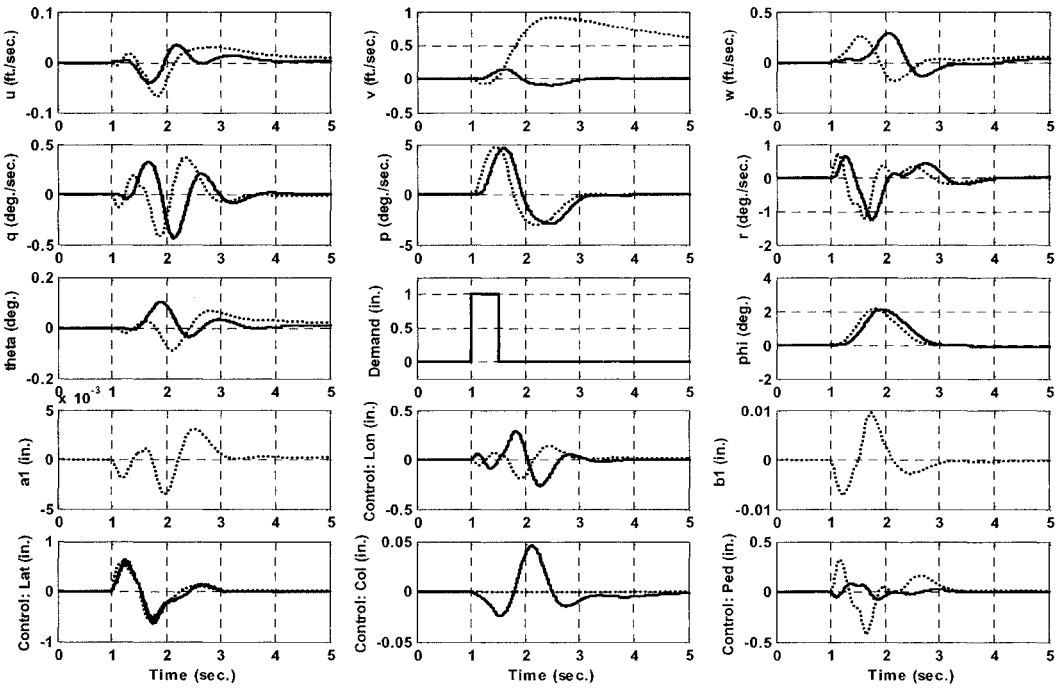

Figure 4.12 MFCA Time History Response Comparison, Bell 412 ASRA and Bell 205A AS -Unit Pulse, Lateral Axis, EAC Controller Without RSF

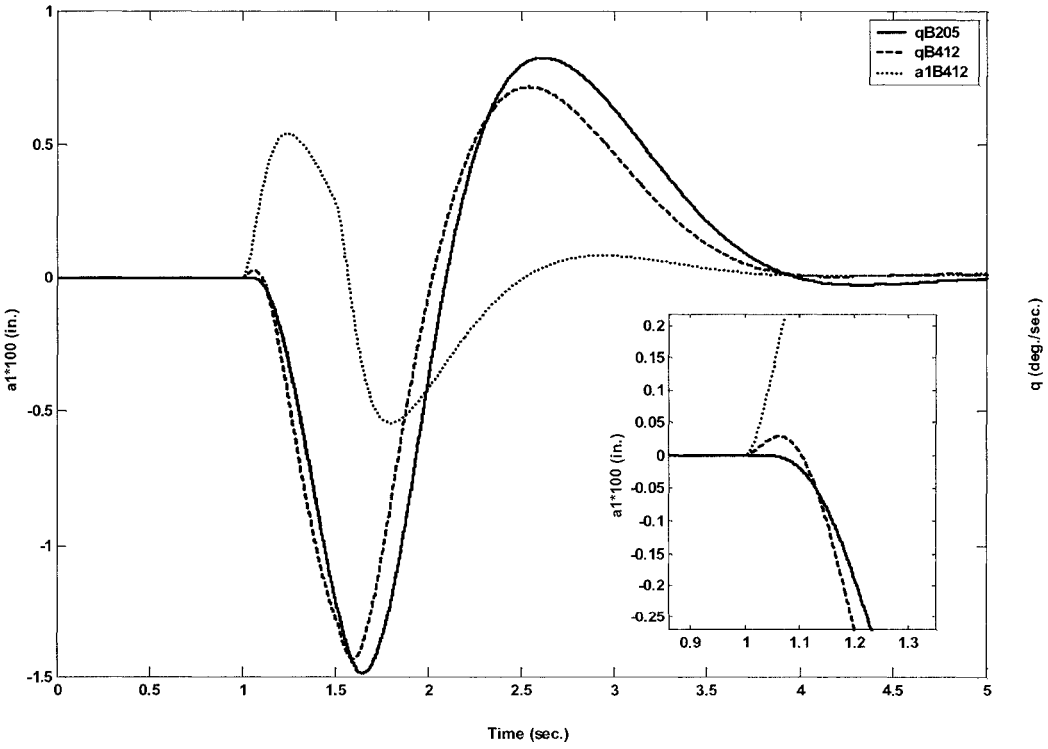

Figure 4.13 MFCA Coupled Rotor-Body Response Comparison, Bell 412 ASRA and Bell 205A AS -Conditions: Unit Pulse Longitudinal Axis, EAC Controller Without RSF

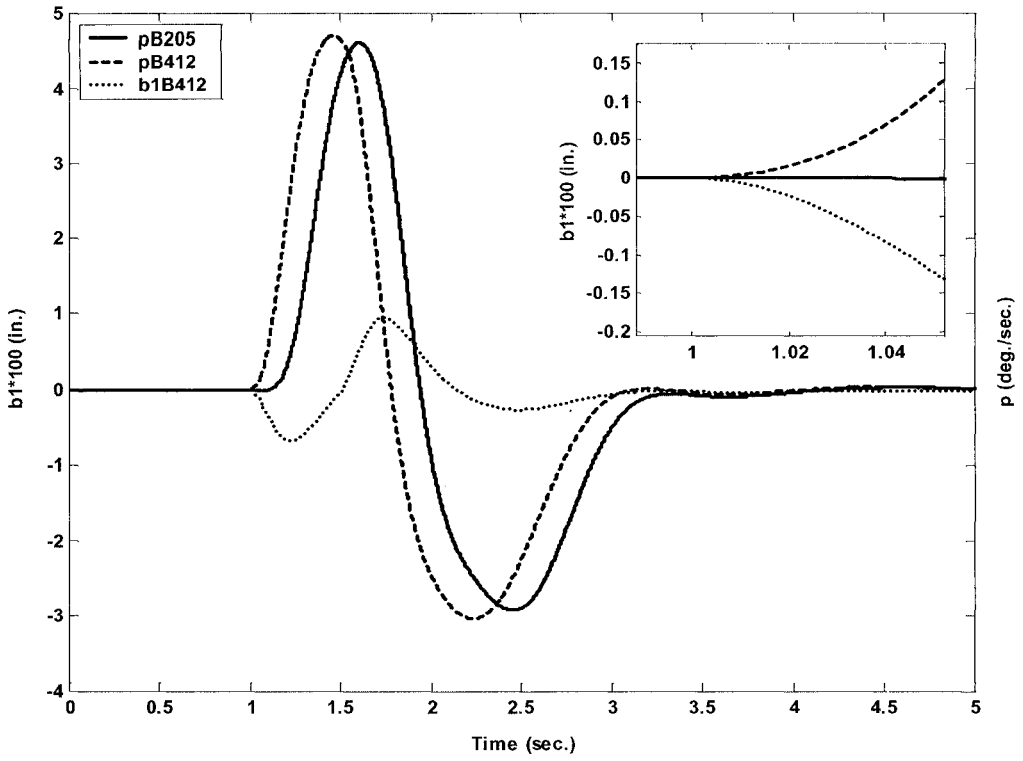

Figure 4.14 MFCA Coupled Rotor-Body Response Comparison, Bell 412 ASRA and Bell 205A AS -Conditions: Unit Pulse Lateral Axis, EAC Controller Without RSF

4.3.4 Flight Controller Selection

The controller selected for in-flight evaluation was the multivariable eigenstructure assignment controller (EAC). The structuring uses the following state vector representative of the Bell 412ASRA HMMS model;

$$\dot{x} = [u\ v\ w\ p\ q\ r\ a_1\ b_1\ \theta\ \phi\ \psi] \qquad 4.2$$

The gain structure for EAC is given by the following matrices for with and without rotor state feedback dynamics cases:

$$\mathbf{K}_{EAC} = \begin{bmatrix} 0.085 & 0.0 & 0.0 & 0.0 & 22.486 & 0.0 & 0.0 & 0.0 & 35.104 & 0.0 & 0.0 \\ 0.0 & 0.0 & 0.0 & 0.0 & 0.0 & 0.0 & 0.0 & 0.0 & 0.0 & 0.0 & 0.0 \\ 0.0 & 0.05 & 0.0 & -5.75 & 0.0 & -0.754 & 0.0 & 0.0 & 0.0 & -15.34 & 0.0 \\ 0.0 & 0.534 & 0.0 & 1.47 & 0.0 & 21.1330 & 0.0 & 0.0 & 0.0 & 0.0 & 0.0 \end{bmatrix} \qquad 4.3$$

$$\mathbf{K}_{EAC_{RSF}} = \begin{bmatrix} 0.085 & 0.0 & 0.0 & 0.0 & 22.486 & 0.0 & -2.7360 & 0.0 & 35.104 & 0.0 & 0.0 \\ 0.0 & 0.0 & 0.0 & 0.0 & 0.0 & 0.0 & 0.0 & 0.0 & 0.0 & 0.0 & 0.0 \\ 0.0 & 0.05 & 0.0 & -5.75 & 0.0 & -0.754 & 0.0 & 2.650 & 0.0 & -15.34 & 0.0 \\ 0.0 & 0.534 & 0.0 & 1.47 & 0.0 & 21.1330 & 0.0 & 0.0 & 0.0 & 0.0 & 0.0 \end{bmatrix}$$

Originally some experimentation was done with the feedback of ψ in directional dynamics and r and ψ states from lateral cyclic to pedal in order to achieve a turn coordination capability. However, since the given yaw angle was not scheduled with side-slip, the vehicle had a tendency to be unstable (oscillatory and divergent). The yaw-angle feedback was thus removed from the controller.

Table 4.2 depicts the stick sensitivities (or cyclic control gearing) that were typical of this flight test.

CASE	SENSITIVITIES			
	LATERAL		LONGITUDINAL	
	BELL 205 (DEG./IN.)	BELL412 (DEG./IN.)	BELL 205 (DEG./IN.)	BELL412 (DEG./IN.)
RSF-OFF	2.0	2.0	1.15	0.8
RSF-ON	1.83	1.95	0.83	0.72
Command Model Simulated: $\theta_{COM} = \frac{8}{s+8}$				

Table 4.2 Stick Gearing (Sensitivities) for MFCA Development

Figures 4.15 to 4.18 depict the predicted bandwidth performances of the EAC controllers as simulated in the MFCA. Compliances with ADS-33E-PRF[13] specifications are summarized in Table 4.3.

AXIS	MFCA PREDICTED BANDWIDTH (BW) PERFORMANCE							
	BELL205 BW_{NRSF} (rad./sec.)	RATING	BELL412 BW_{NRSF} (rad./sec.)	RATING	BELL205 BW_{RSF} (rad./sec.)	RATING	BELL412 BW_{RSF} (rad./sec.)	RATING
PITCH	4.0	L1	5.5	L1	3.1	L1	3.4	L1
ROLL	4.22	L1	5.05	L1	3.05	L1	3.5	L1

Notation:
NRSF = **Without** Rotor State Feedback
RSF = **With** Rotor State Feedback
L1, L2, L3 = Level 1, Level 2, Level 3, with respect to ADS-33EPRF Compliance

Table 4.3 Summary of Eigenstructure Assignment Control (EAC) Effective Controls, MFCA Prediction

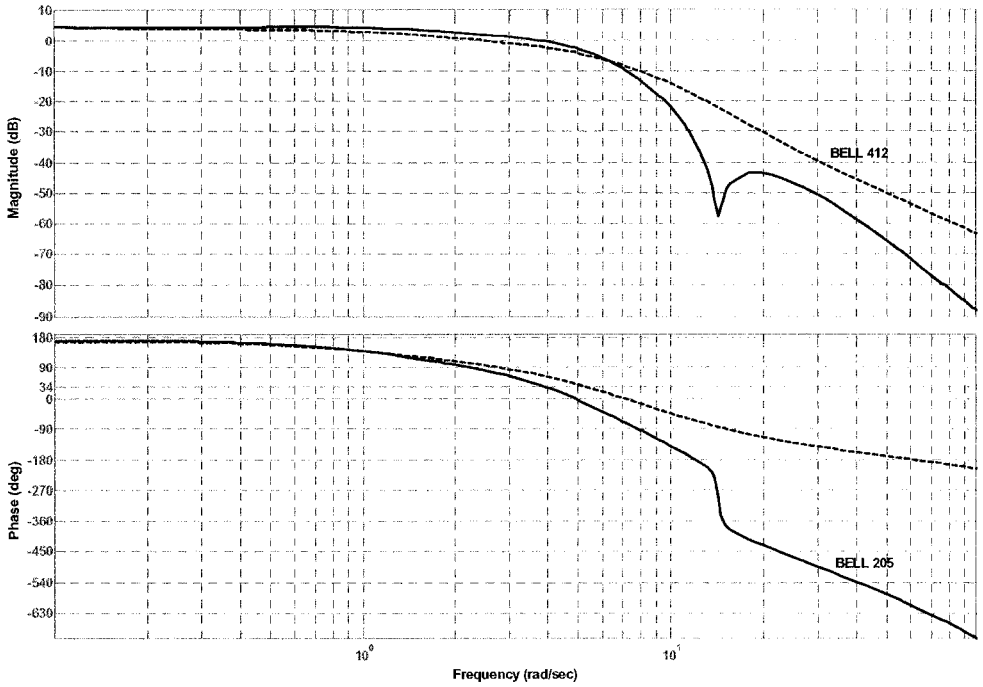

Figure 4.15 MFCA Longitudinal Frequency Response, CASE: Without RSF

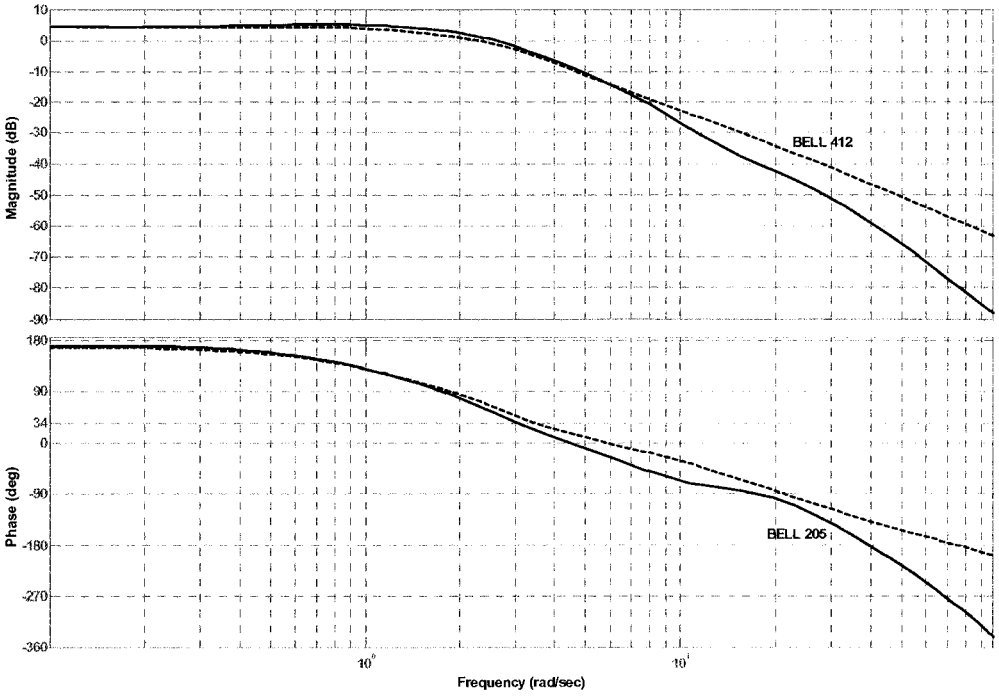

Figure 4.16 MFCA Longitudinal Frequency Response – Case: With RSF

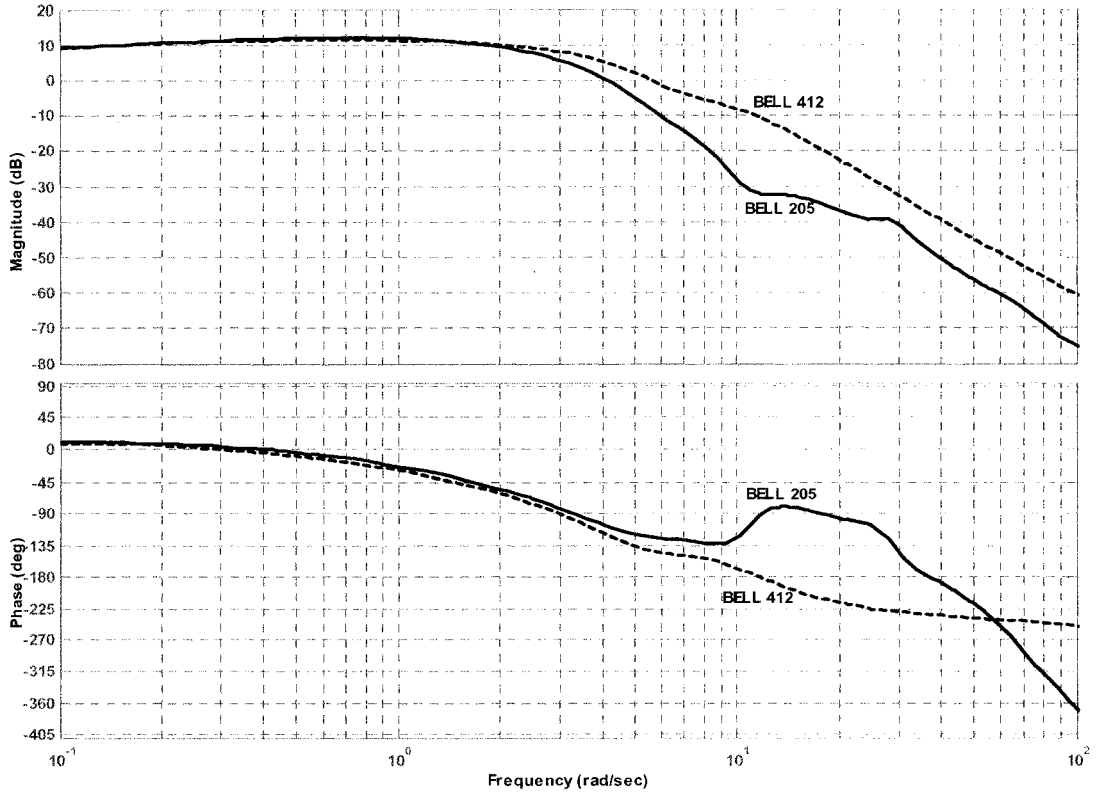

Figure 4.17 MFCA Lateral Frequency Response, CASE: Without RSF

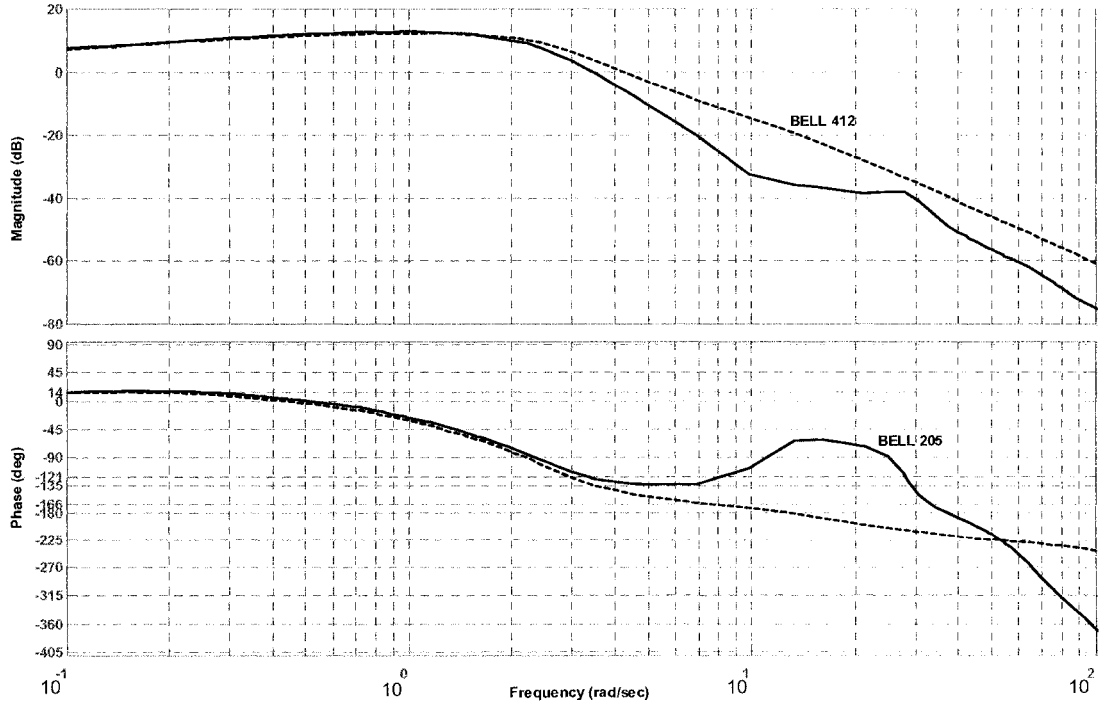

Figure 4.18 MFCA Lateral Frequency Response, CASE: With RSF

4.4 In-flight Evaluation of the Rotor State Feedback By Model Following Control

The purpose of the flight evaluation was to test the effectiveness of rotor state feedback in terms of handling qualities, performance, and disturbance rejection in a realistic flight environment.[114,115] The engagement incorporating multivariable control, variable stability helicopter performance, and handling qualities specifications would rely on important lessons learned from the many previous engagements undertaken at the NRC Flight Research Laboratory[85,86]. The data required for analyses was based on the ADS-33E-PRF Target Acquisition and Tracking (TA+T) short-term military handling requirements. The flight test was performed to gather data based on simulated rotor state feedback and simulated turbulence cases. The test matrix for the flight test evaluation included experiments for both ground and flight test implementation. The ground test portion consisted of baseline tests to ensure the control laws were correctly coded, parameterized, and implemented on the host Bell 205A AS flight control computer (FCC). The in-flight evaluation was graded by quantitative (ADS-33E-PRF) and qualitative (Cooper Harper Rating Scale) helicopter flight dynamics metrics.

4.4.1 Ground Test Planning

In order to proceed to flight test clearance and evaluation of the control laws a ground test plan was required to:

- Assess the stability boundaries for programming the pilot interfaces
- Evaluate the control law robustness to off design conditions
- Mitigate against safety of flight concerns regarding instabilities, procedures, and system faults/errors
- Brief flight test crews for standardizing the evaluations

The overall goal of the ground test was to perform a comprehensive control system performance, failure detection, and safety redundancy management test of the Bell 205A AS due to the integration of experimental flight control laws. Several components of this ground test are depicted in Table 4.4.

√	TEST POINT	GROUND TEST MATRIX
√	INPUT RESPONSE QUALIFICATION	o Evaluate model data for stability and consistency within the MFCA o Evaluate MFCA compatibility for implementation in the Bell205A AS
√	COMPATIBILITY	o Evaluate proper sign convention for feedback, control, and response computations o Ensure that the Safety Pilot controls mirror the Evaluation Pilot controls o Evaluate the Safety Pilot control action due to the research feedback system o Evaluate pilot interfaces for correct data coding and switch functionality
√	TURBULENCE QUALIFICATION	o Evaluate the characteristics of the turbulence model in application to the MFCA (i.e.: Assess response of the Bell 205A AS to the Bell412 ASRA turbulence response)

Table 4.4 Ground Test Matrix

4.4.2 Ground Test Experimental Arrangement

The experimental arrangement is depicted in Figure 4.19. The arrangement consisted of the Bell 205A AS seated on its mobile pad, a ground power unit, and the hydraulic test cart. In this configuration, the host Bell 205ASRA is powered (hydraulically and electrically) and connected via computer Ethernet connection to a computer workstation allowing preparations for flight-testing.

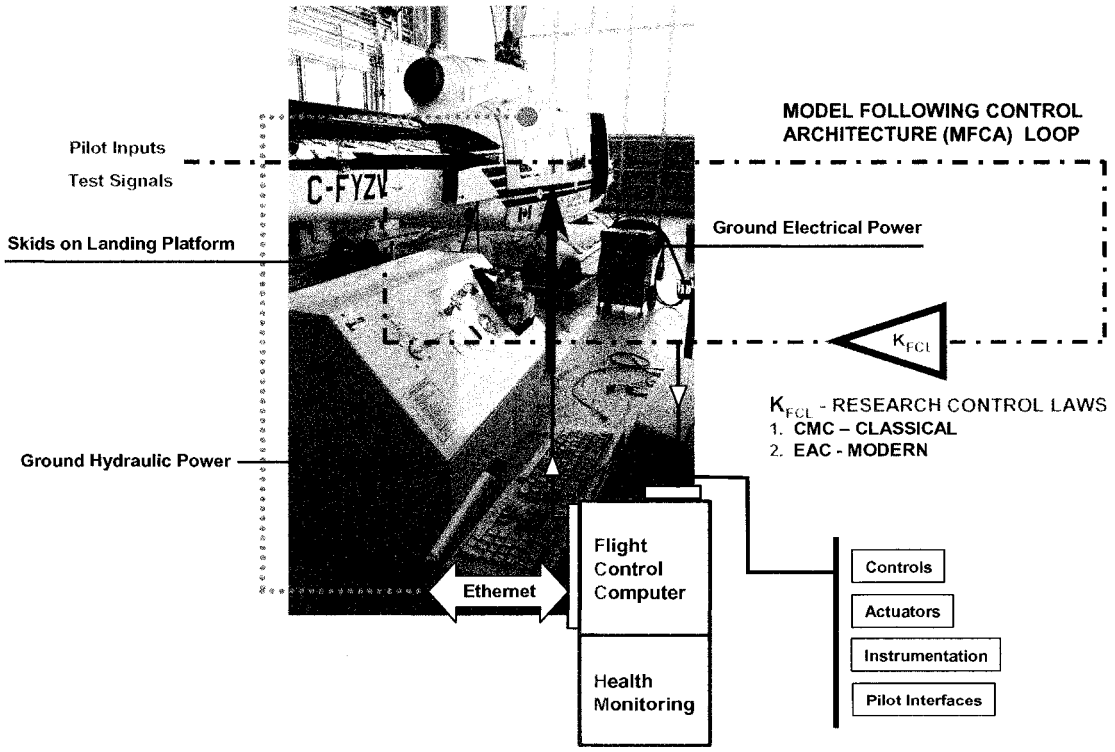

Figure 4.19 Bell 205A AS, Ground Test Configuration

Typical developmental tasks for implementing the control laws included:

- **Coding:** Fundamental helicopter flight control and dynamics equations were translated into C-code for use by the Bell 205A AS flight control computer (FCC).
- **Signal Injection:** Artificial test signals such as rates and attitudes were injected into the aircraft's inertial and flight control systems. This was done in order to evaluate the magnitude, phasing, and convention of the model following actuator/control response. In the FBW system the validation extends from the inertial system to the electro-hydraulic actuation control system and the pilot controls. Any errors found through this process were corrected in the C-code at this point.
- **Control Airworthiness:** Control law attributes were assessed to predict problems before in-flight engagements. Here such issues as computational time frame, signal noise, data recording,

and flight control system standards were a few of the parameters that were involved in "sanity" and safety checking the model following experiment.

- **Pilot Preparations:** Pilots were prepared for the flight-test engagements by briefing them on pot (i.e.; switching) functions of the experimental aircrew interface. Here several pre-evaluation flights were used to standardize the pilots' flight test technique and use of the experimental FBW interfaces.

Overall there were no major or uncommon problems with the developmental ground testing.

4.4.3 Flight Test Planning

With the successful completion of the ground testing, a detailed flight test plan was developed consisting of basic evaluation flights to shake-down the experimental implementation to the final handling qualities evaluation. ADS-33E-PRF defines response types required to achieve Level 1 or 2 handling qualities for a wide variety of mission task elements (MTE), in different useable cue environments (UCE) for normal and failed states with full and divided pilot attention. As an example, a military pilot's operational sortie may include a collection of maneuvers or MTE's to achieve the mission goals. The MTE's of primary concern for this flight test investigation included the slalom and roll attitude captures. In the context of this evaluation, these elements were performed with modifications to the ADS-33E-PRF standards.

4.4.3.1 Slalom Maneuver

The slalom MTE is depicted in Figure 4.20.

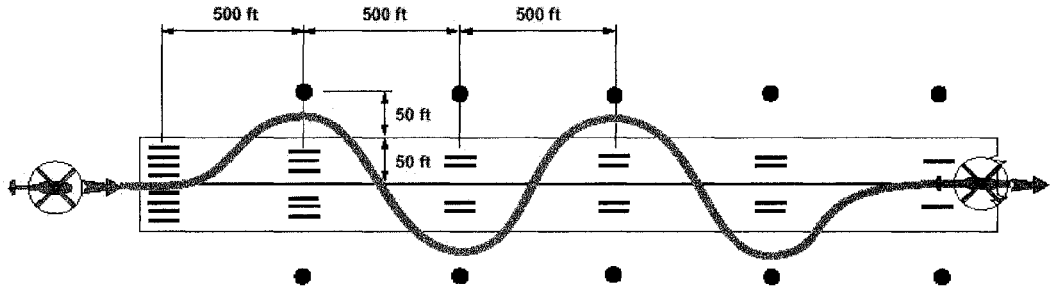

Figure 4.20 The Slalom Mission Task Element (MTE)[13]

As defined by ADS-33E-PRF, the slalom MTE is used to evaluate aggressive, Nap-of-Earth (NOE), forward flight dynamics including turn coordination and inter-axis coupling. The actual maneuver is described as follows:

"Initiate the maneuver in level un-accelerated flight lined up with the center-line of the test course. Perform a series of smooth turns at 500ft. intervals (at least twice to each side of the course). The turns shall be at least 50ft from the centerline, with a maximum lateral error of 50ft. The maneuver is to be accomplished below the reference altitude. Complete the maneuver on the centerline in coordinated flight." [13]

4.4.3.2 Roll Attitude Capture

The roll attitude capture as depicted in Figure 4.21 is a sub-task of many ADS-33 required flight test maneuvers and is an essential capability of helicopter lateral-directional dynamics. This qualitative task was devised by the pilots to assess rotor state feedback effects in isolated control (i.e.; low pilot workload) conditions.

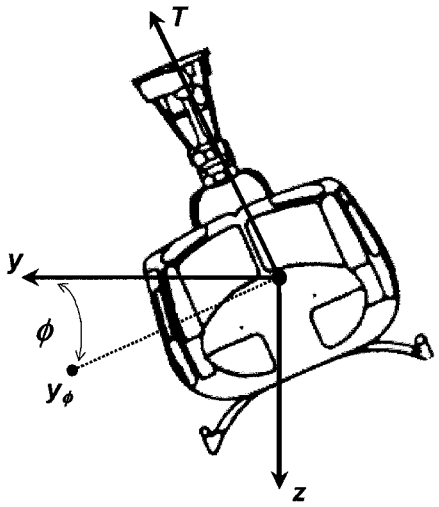

Figure 4.21 Roll Attitude Capture Task

The primary requirements included:

- Maintenance of Altitude
- Maintenance of rotor, torque, and standard operational limits
- Capture of attitude (On-axis roll-attitude by ±3°, Off-axis pitch-attitude within ±3°)

Combined with the Cooper-Harper rating scale (Figure 4.22), the ADS-33E-PRF based flight investigation provided both strict qualitative and quantitative means of evaluating the interacting pilot/ air-vehicle system. The use of simulated turbulence further addressed rigid-body disturbance rejection capabilities for the rotor state feedback active and inactive cases.

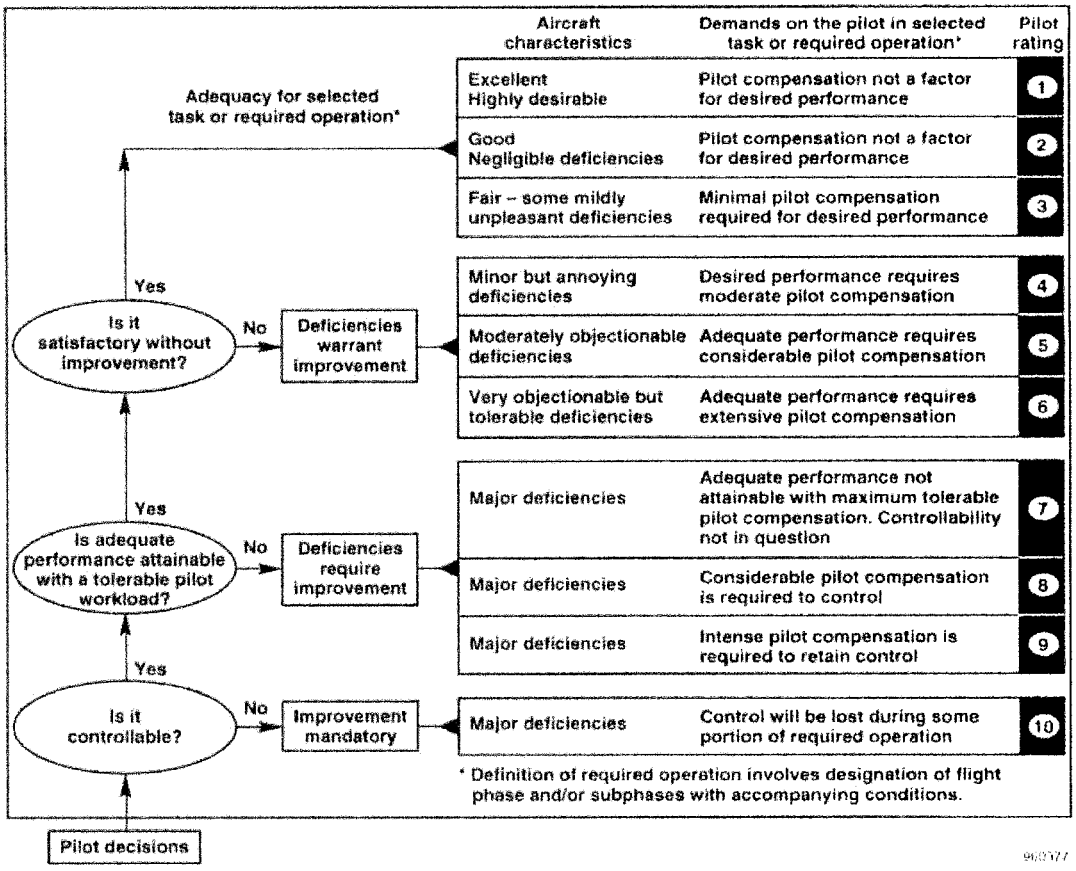

Figure 4.22 Cooper Harper Rating[1,114]

4.5 Flight Test Results

The first ground and flight engagements of the model following rotor state feedback control law occurred on December 16, 2003. Some 5 flight tests were executed consisting of developmental engagements, optimization engagements, and data gathering flights. The NRC-FRL flight test crews consisted of:

- **Flight Researcher Crew:** Ellis and Gubbels
- **Experimental Flight Test Pilots:** Carignan and Leslie

The experimental flight test pilots have over 2500 hours of flight experience. The flight researchers are managers of the Bell 205A AS and Bell 412ASRA and have extensive experience in variable stability flight controls research.

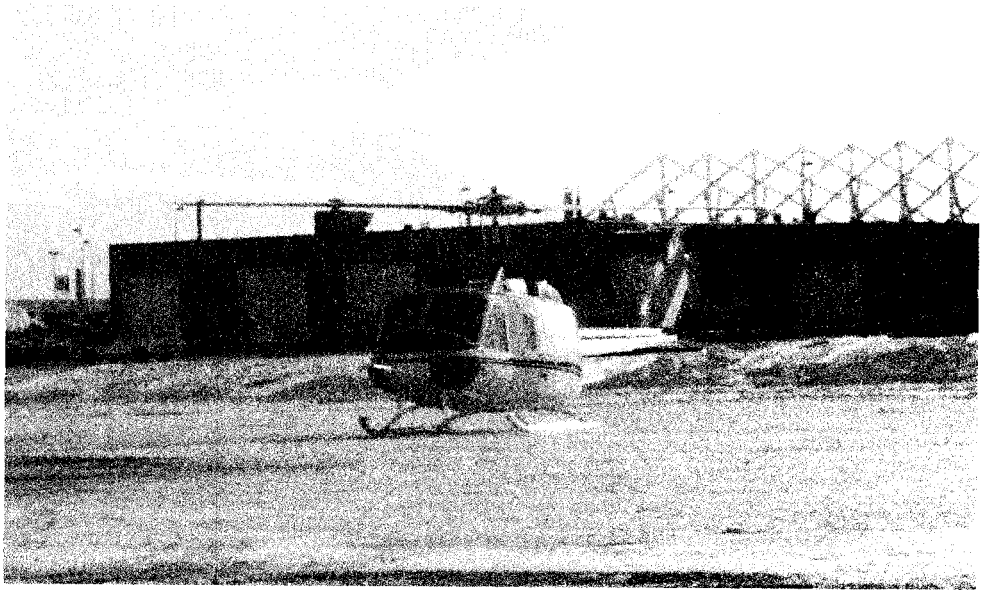

Figure 4.23 Bell 205A AS Ground Run – Handling Qualities Evaluation of Rotor State Feedback by Eigenstructure Assignment Control (EAC)

The handling qualities evaluation took place on December 19, 2003. The weather for the flight test was favorable with light winds and no turbulence, a temperature of –11°C, visibility of 15 statue miles, and an altimeter setting of 29.68 in./Hg. The helicopter is shown in Figure 4.23 and a typical weight and balance is shown in Figure 4.24.

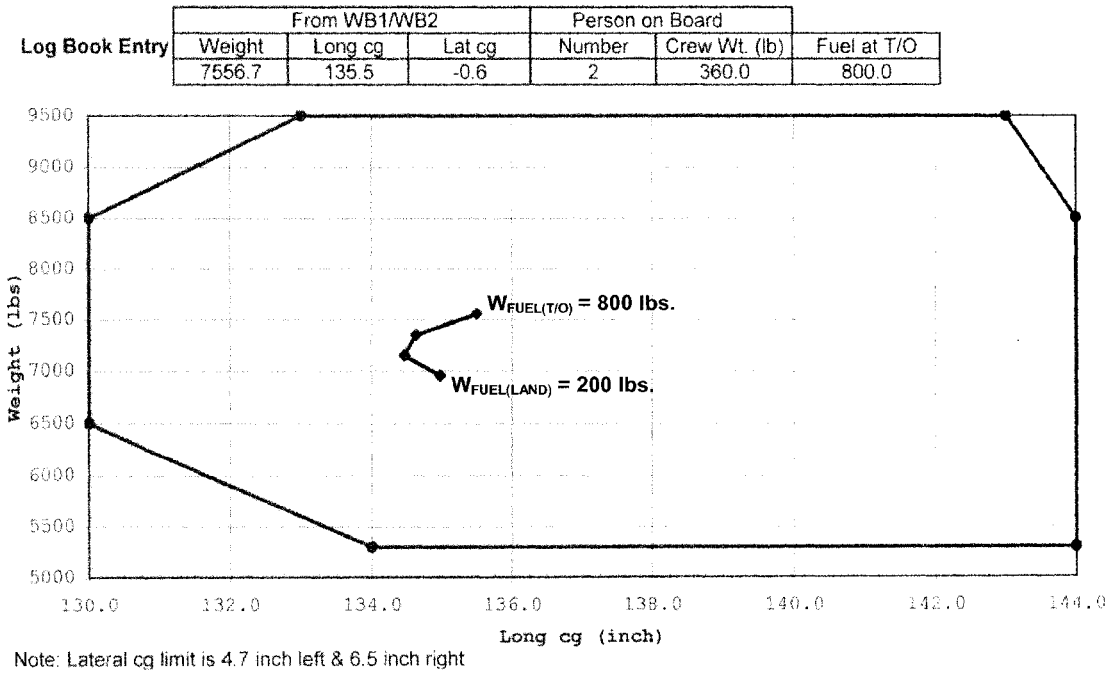

Figure 4.24 Bell 205A AS Typical Flight Test Weight and Balance Envelope

The MFCA and rotor state feedback control laws were put through rigorous trials in inclement weather (environmental turbulence, light rain/snow, gusting winds, low to high useable cue environments), off design conditions (speed and altitude off-design events by 20 knots and 4000ft, respectively), and a high workload environment (inside an international airport circuit). The conditions for the slalom test points, although not thought to be optimum by the pilots, consisted of the high workload environment of the Ottawa International Airport based on Runway 32. This required the pilots to be both aggressive on task and highly diligent in flight management.

In the following discussion several highlights of the flight test engagements are reviewed in order to evaluate the benefits of rotor state feedback. Recall that throughout our discussions, the Bell 412 ASRA results are from the MFCA in-flight simulation which is driven by actual aircraft responses from the host Bell 205A AS.

4.5.1 Initial Pilot Assessment

EVENT	MODEL	TURBULENCE CASE	SENSITIVITIES			EVAULATION PILOT COMMENTS
			LAT (DEG./IN)	LON (DEG./IN)	PED (DEG./IN)	
1	BASELINE BELL 412ASRA	OFF	0.5	0.5	1.0	o BASELINE BELL 412ASRA: More "**squirrelly**" than actual vehicle o SAS-OFF Dynamics of BELL 412 ASRA simulation evident o Sensitivities of 2.0 made the aircraft **unstable**
2	RSF-OFF	OFF	2.5	2.0	2.0	
3	RSF-ON	OFF	3.3	2.5	2.0	

Table 4.5 Baseline Sensitivity Settings

The evaluation pilot commenced assessment of the aircraft by setting the baseline gain, sensitivity, and force feel settings of the Bell 205A AS to his level of aggression and comfort as shown in Table 4.5. The control configuration of the aircraft was unknown to the evaluation pilot because the safety pilot randomly selected the test point for each engagement. The evaluation pilot commented that throughout the baseline evaluations he was changing gearing or modifying the MTE to achieve task performance. In the slalom task it was reported that until the proper sensitivities could be assessed, he was not able to maintain the 60-knot desired slalom airspeed requirement due to vehicular instability.

All who flew the EAC controllers at this stage commented that there was some unpredictability, wobbliness, or inaccuracy in their ACAH response resulting in low HQR ratings. This instability stemmed from a turn-coordination gain structure applying yaw-angle and yaw-rate feedbacks. The gain structure was non-optimal due to the fact that no side-slip scheduling had been applied. In fact this destabilization effect may have clouded the ability to thoroughly assess the controller had it not been for marked reductions in disturbance response and the lack of axis cross-coupling reported. This, in itself, is a testament to the robustness of the rotor state feedback control effect on the aircraft overall.

The aircrews commented that the turbulence model developed mainly roll disturbance dynamics that had overly sharp onset response. Actual gust disturbances exhibit dulled- or damped-onset response with distinct heave components. However, the turbulence was still deemed to provide realistic pitch and roll excursions as would result from moderate turbulence. The models had excellent airspeed capturing that remained steady on task. With regards to sensitivities the stability bound was set at 2.0 deg./in.

4.5.2 Response Correlation and Dynamics Assessment

The correlation between the host aircraft (Bell 205A AS) and that under simulation (Bell 412ASRA) was good overall. Rigid-body and rotor state dynamics are depicted in Figures 4.25 to 4.27 for representative slalom tasks. The event studied features both turbulence and rotor state feedback.

The match of the vehicle dynamics in Figure 4.25 indicates that the MFCA has a good physical representation of the helicopter physics. There are 2 important features regarding this matching. The first is the correlation between the Bell 205 aircraft and the Bell 412 simulation attitude rates. The lower bandwidth of the teetering rotor is evident in the comparison of attitude-rate peaks. Here the teetering rotor response to roll rate peaks are more than that required for the hingeless rotor Bell 412 ASRA. The second feature is that hingeless rotor flap response is similar in magnitude to the teetering hub, however the latter does not produce a hub moment. The Bell 412 with its hingeless hub can accelerate the rigid-body dynamics faster than either the articulated or teetering design. The Bell 205A AS teetering rotor inducing rigid-body response matches the ASRA's maximum roll rate though with an elevated time constant.

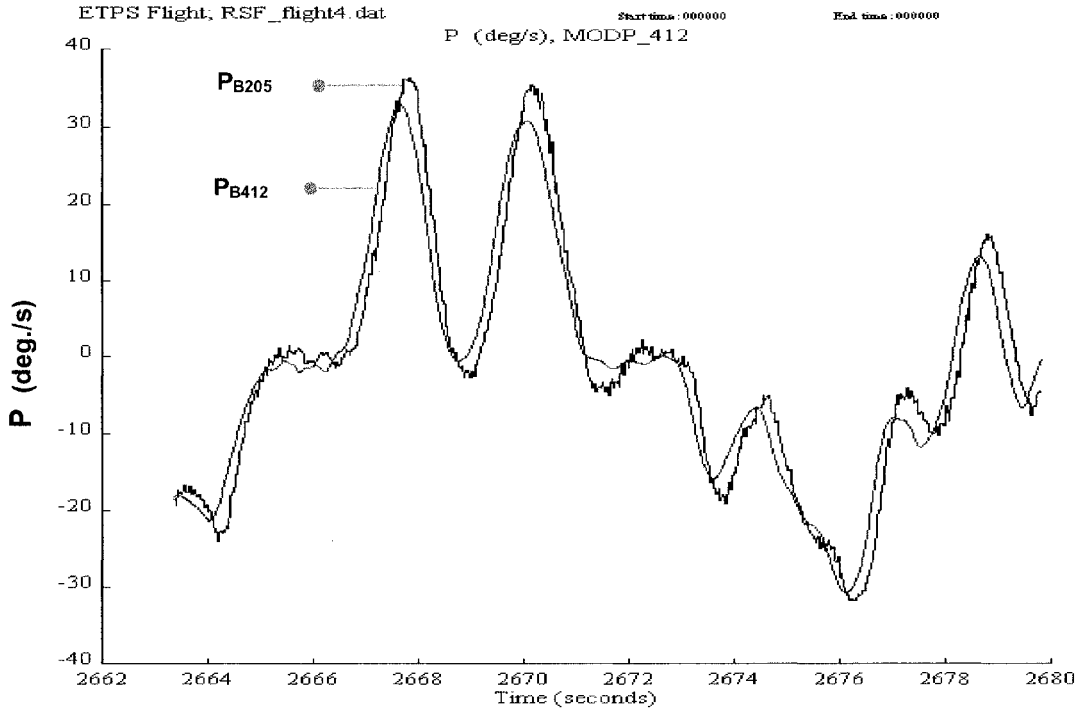

Figure 4.25 Flight Dynamics Response – Slalom Event, Roll-Rate Response Correlation – With Turbulence and Rotor State Feedback

The vehicular off-axis pitch rate dynamics do not correlate as well as roll rate dynamics, however for the same maneuver the rotor state dynamics illustrates the lead of the Bell 412 ASRA rotor disc tilt over either helicopter's attitude-rate as shown in Figures 4.26 and 4.27.

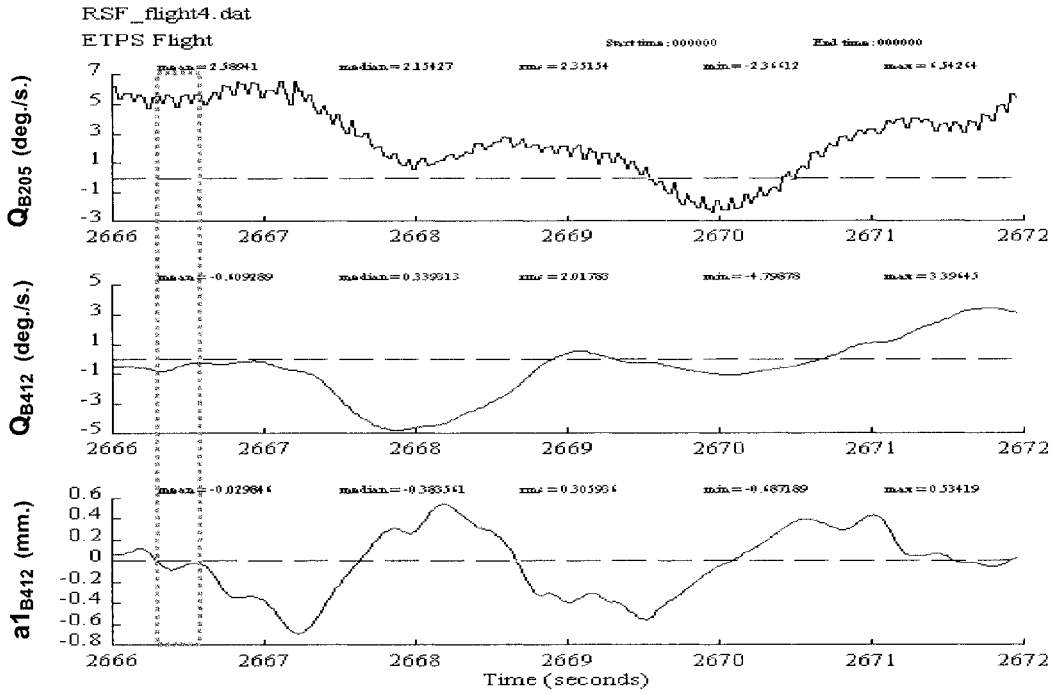

Figure 4.26 Flight Dynamics Response – Slalom Event, Rotor-Body Physics in Pitch - With Turbulence and Rotor State Feedback

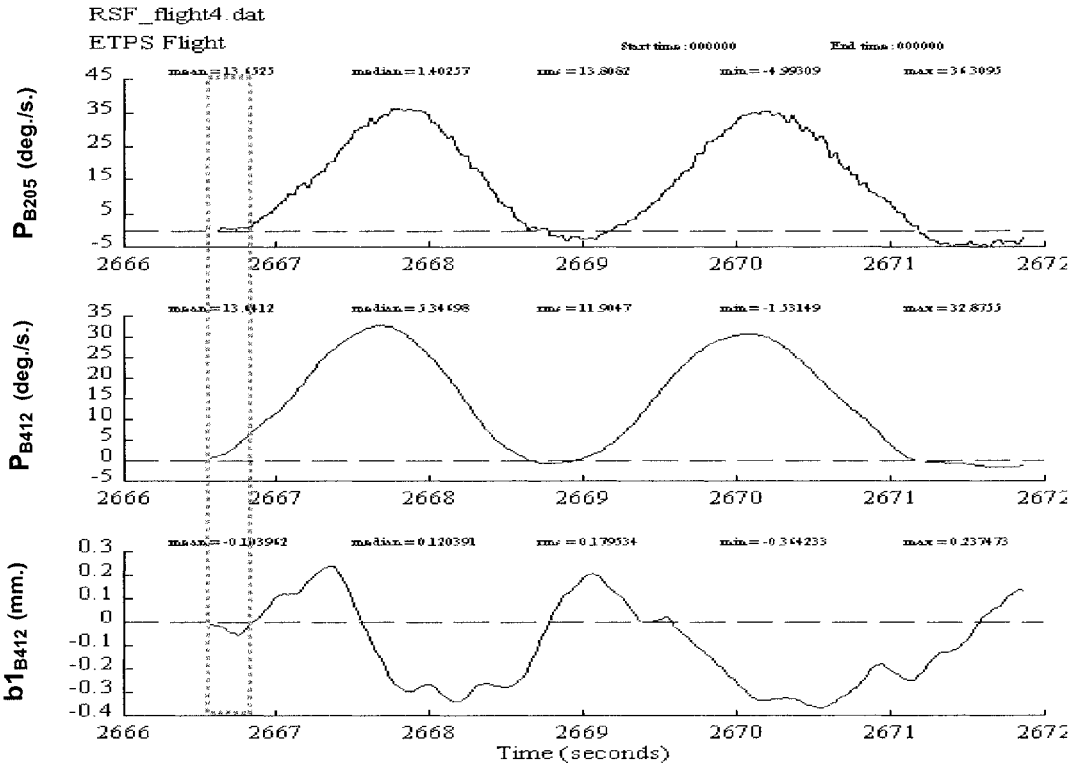

Figure 4.27 Flight Dynamics Response – Slalom Event, Rotor-Body Physics in Roll - With Turbulence and Rotor State Feedback

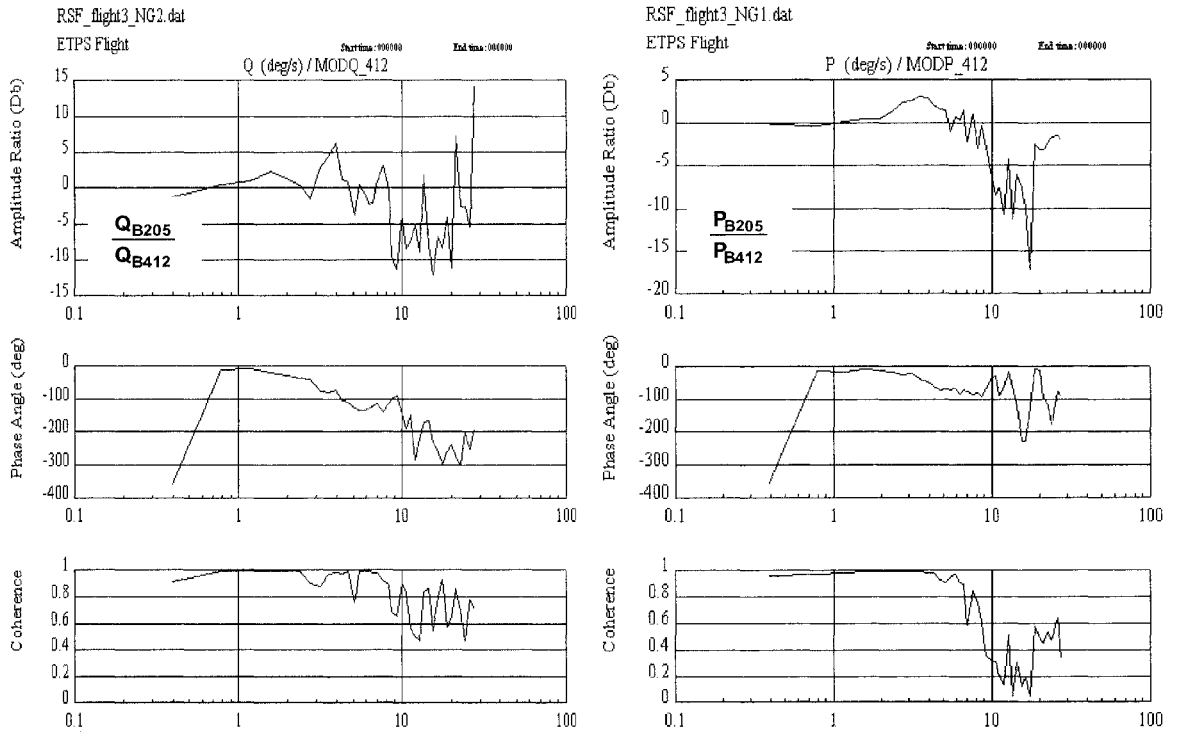

Figure 4.28 Bell 205A AS Model Following Limits - Pitch (Left), Roll (Right) - Without Rotor State Feedback

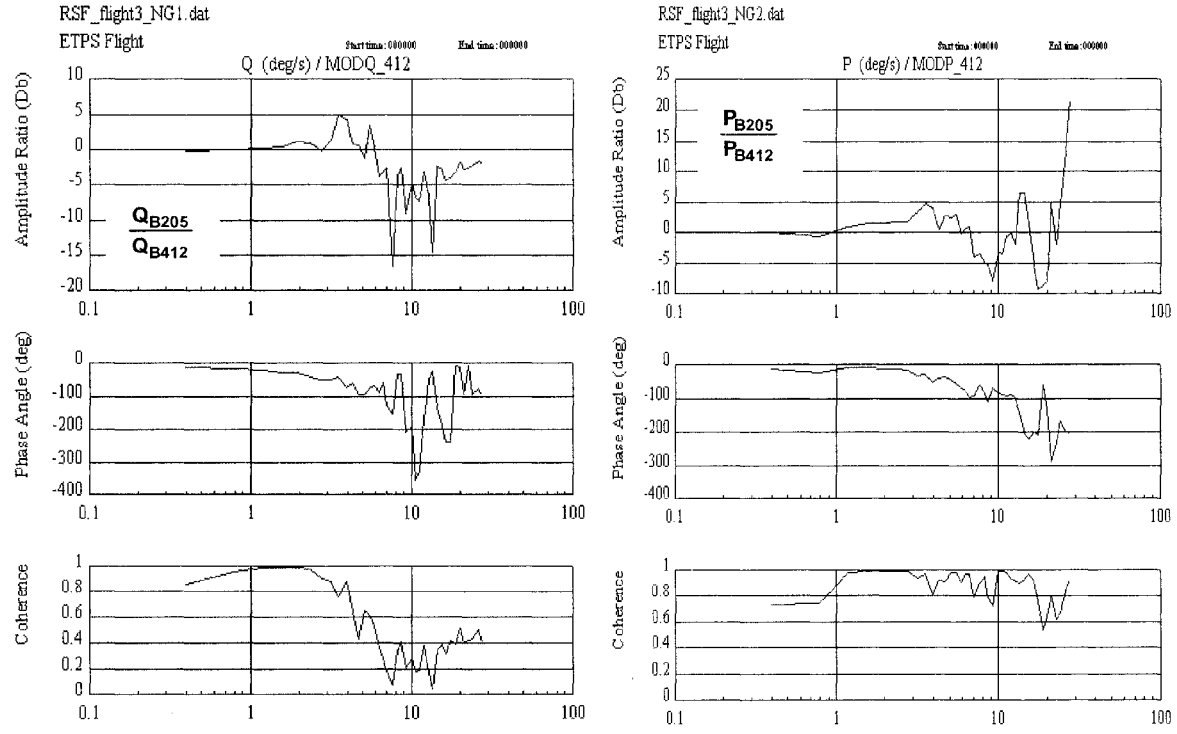

Figure 4.29 Bell 205A AS Model Following Limits - Pitch (Left), Roll (Right) - With Rotor State Feedback

The model following capabilities of the host Bell 205A AS aircraft are depicted the Figures 4.28 and 4.29. The model following bandwidth limits without rotor state feedback is illustrated by resonant peaks in the frequency magnitudes and phase roll-off under frequency responses with good signal coherence. Typically, coherences of greater than 0.8 are used in system identification and controls research to establish the quality of the signal. Here, without rotor state feedback the limits identified in flight were 4.0 rad./sec. and 3.5 rad./sec. in pitch and roll, respectively. In the presence of rotor state feedback, the limits were curtailed in pitch to 3.6 rad./sec.

From these results it was judged that the quality of the model following was suitable for handling qualities assessment of the rotor state feedback controllers.

4.5.3 Bandwidth Attainment With and Without Rotor State Feedback

The frequency sweep and maneuver dynamics all had spectral contents necessary for extracting bandwidth values. The MFCA as implemented in flight-testing required filtering (to alleviate model state divergences) and time delay adjustments (to realistically correlate the Bell 205A AS and Bell 412ASRA responses) in the presence of the nominal Bell 205A AS FBW rotor/control architecture.

As such, in addition to FBW digital implementation time and phase latency, the assessment/tabulation of latency contributions for handling qualities assessment requires that 72msec. of latency be added to the Bell 412ASRA simulation data for correlation with Bell 205A AS flight test results. This latency would adjust the TA+T assessments as shown in Table 4.6 as well as Figures 4.30, 4.31, and 4.32 by increased phase delay and reduced bandwidth towards improved correlation between the MFCA model and flight test results.

AXIS	ACHIEVED BANDWIDTH (BW) PERFORMANCE FLIGHT TEST POINT: FREQUENCY SWEEPS							
	BELL205 BW_{NRSF} (rad./sec.)	RATING	BELL412 BW_{NRSF} (rad./sec.)	RATING	BELL205 BW_{RSF} (rad./sec.)	RATING	BELL412 BW_{RSF} (rad./sec.)	RATING
PITCH	3.0	L1	4.8	L1	2.5	L1	3.5	L1
ROLL	2.9	L2	4.2	L1	2.6	L3	3.4	L1

Notation:
NRSF = **Without** Rotor State Feedback
RSF = **With** Rotor State Feedback
L1, L2, L3 = Level 1, Level 2, Level 3, with respect to ADS-33EPRF Compliance

Table 4.6 Summary of Eigenstructure Assignment Control (EAC) Flight Test Bandwidth Performance -Frequency Sweep Test Points

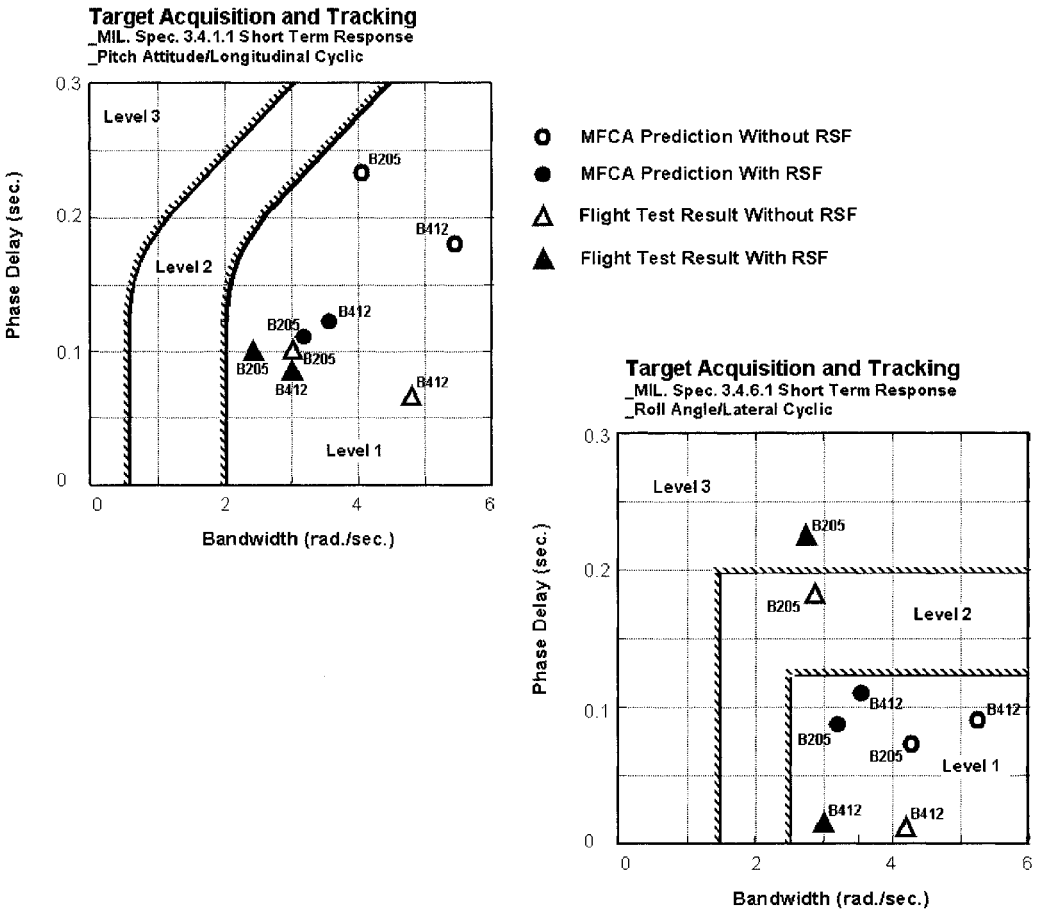

Figure 4.30 EAC Flight Test Compliances due to Effective Rotor State Feedback – ADS-33E-PRF

For flight-testing with turbulence inactive, the predicted and achieved bandwidths for the Bell 412 ASRA in-flight simulation are tabulated in Table 4.6 and Figure 4.30. The results suggest that both the MFCA predictions were good overall for the rotor state feedback cases. The correlation in predicted to flight test results show that RSF_ON pitch-axis dynamics cases lie in the bandwidth and phase delay ranges of 2-4 rad./sec. and 0.08-0.13 sec.; in roll-axis dynamics, 2.5-6 rad./sec and 0-0.13 sec. are evaluated.

Comparing MFCA prediction to flight test results, the bandwidths of Bell 412ASRA RSF_OFF cases were higher than RSF_ON cases for either the pitch or roll axes; the same trend held for the Bell 205A AS. In terms of phase delays, in the pitch axis the Bell 412 ASRA phase delay was higher in prediction for RSF_OFF. This compared to the phase delay being higher for RSF_ON cases in flight test. The Bell 205A AS phase delays remained the same for both RSF_ON and RSF_OFF cases.

In the roll axis, the phase delays for RSF_OFF cases were lower than those achieved in flight testing for the Bell 412 ASRA; the same trend held for the Bell 205A AS.

During flight-testing the Bell 412 ASRA achieved bandwidth was always higher than the host aircraft in either pitch or roll axes. The phase delays were always lower for the Bell 412 ASRA than those of the Bell 205A AS. Some large deviations in prediction to flight test result were found without this feedback. In the roll axis the Bell 205 flight test points in Level 2 and Level 3 bounds suggest non-optimal control law design or analytical error. The former case is more likely since pilots reported minor deficiencies in handling qualities with or without rotor state feedback engaged.

Overall the above tabulation was favorable indicating desirable control and model following optimality. (Note: The bandwidths determined in the presence of turbulence are presented for comparative purposes. Their interpretation is clouded by low control-response coherence brought about by the presence the simulated atmospheric disturbances.)

ACHIEVED BANDWIDTH (BW) PERFORMANCE
FLIGHT TEST POINT: SLALOM HANDLING QUALITIES ASSESSMENT

CASE: WITHOUT TURBULENCE ENGAGED

AXIS	BELL205 BW_{NRSF} (rad./sec.)	RATING	BELL412 BW_{NRSF} (rad./sec.)	RATING	BELL205 BW_{RSF} (rad./sec.)	RATING	BELL412 BW_{RSF} (rad./sec.)	RATING
PITCH	1.8	L3	4.6	L1	2.9	L1	2.8	L1
ROLL	4.1	L1	4.9	L1	3.2	L1	4.0	L1

CASE: WITH TURBULENCE ENGAGED

AXIS	BELL205 BW_{NRSF} (rad./sec.)	RATING	BELL412 BW_{NRSF} (rad./sec.)	RATING	BELL205 BW_{RSF} (rad./sec.)	RATING	BELL412 BW_{RSF} (rad./sec.)	RATING
PITCH	0.98	L2	2.8	L1	1.7	L2	2.9	L1
ROLL	3.9	L1	4.9	L1	3.5	L1	4.0	L1

Notation:
NRSF = **Without** Rotor State Feedback
RSF = **With** Rotor State Feedback
L1, L2, L3 = Level 1, Level 2, Level 3, with respect to ADS-33EPRF Compliance

Table 4.7 Summary of Eigenstructure Assignment Control (EAC) Flight Test Bandwidth Performance -Slalom Handling Qualities Assessment

The overall handling qualities flight test evaluation of rotor state feedback due to turbulence by the slalom mission task element is tabulated in Table 4.7 and plotted in Figures 4.31 and 4.32. Assessments of Slalom and Target Acquisition and Tracking (TA+T) maneuvers do not correlate in terms of piloted flight dynamics mainly due to level of accuracy and aggression applied. However, the following analysis is performed in consideration of the following conditions for qualitative pilot Handling Qualities Ratings (HQR) of the task due to rotor state feedback and simulated turbulence:

- **Condition 1:** HQR's indicate pilots' assessment of aircraft performance
- **Condition 2:** HQR's qualify pilots' assessment of workload required to achieve task performance

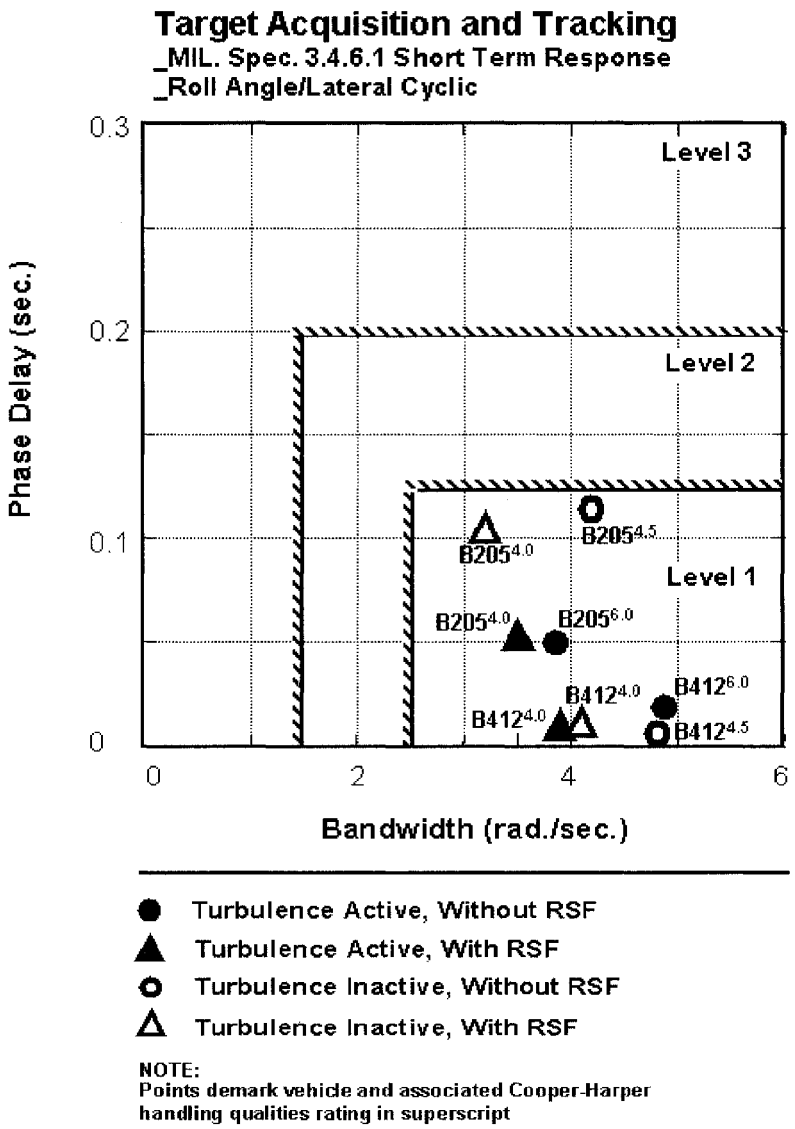

Figure 4.31 EAC Flight Test Roll Axis Compliances due to Combined Rotor State Feedback and Turbulence Injection - ADS-33E-PRF

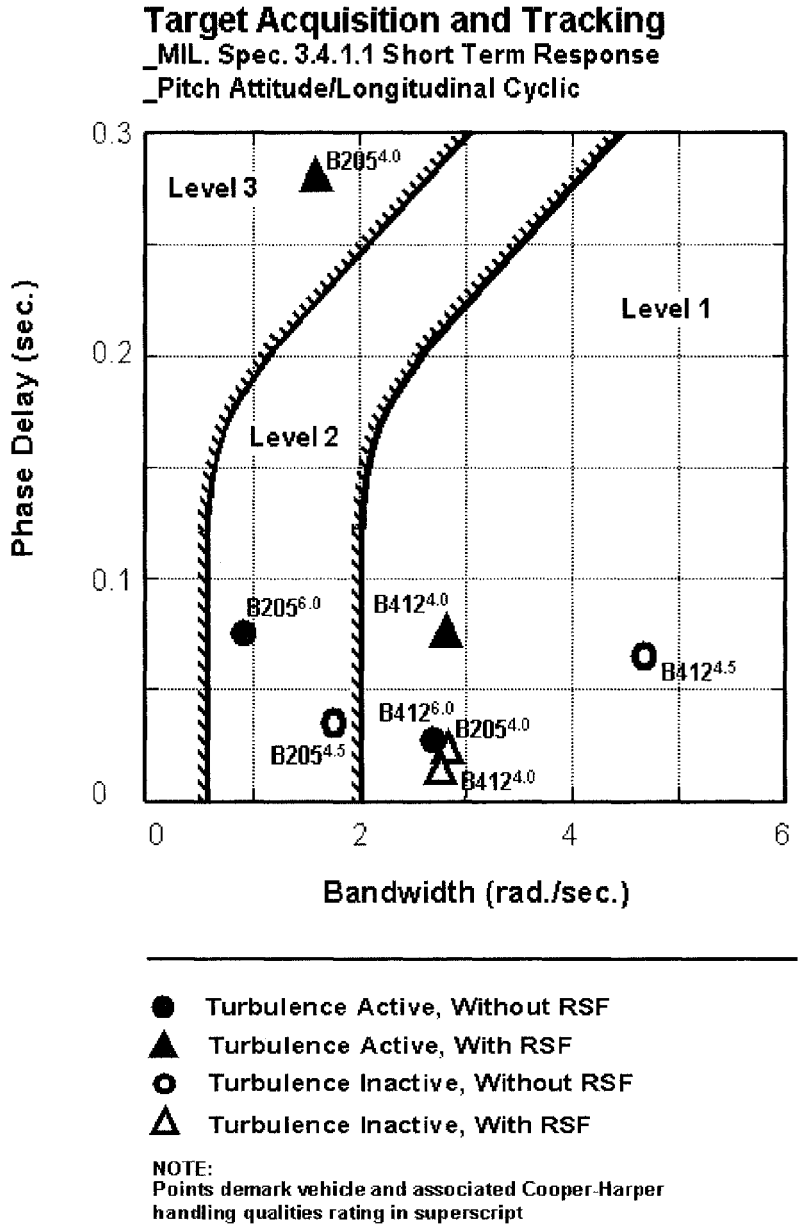

Figure 4.32 EAC Flight Test Pitch Axis Compliances due to Combined Rotor State Feedback and Turbulence Injection - ADS-33E-PRF

The depicted pitch and roll compliances are generally very good with the exception of several out-lying points again associated with the Bell 205A AS.

The results indicate that in roll, the pilot evaluated the Bell 205A AS with better handling qualities for lower bandwidth configurations whether RSF_ON with TURBULENCE_ON or RSF_OFF with TURBULENCE_OFF cases. The best ratings were assessed for the RSF_ON with or without turbulence. The worst rating was assessed for the TURBULENCE_ON case without rotor state feedback.

The pitch axis results show that the Bell 205A AS was assessed to have better handling qualities at higher bandwidths. The best HQR applied to the RSF_ON case without turbulence and the worst to RSF_OFF with turbulence.

Overall the results suggest that the pilots were very sensitive to changes in phase delay associated with EAC rotor state feedback control. In pitch, increases in phase delay were associated with higher HQR's and lower handling qualities Levels; in roll the opposite trend was evaluated for increases in phase delay. This trend in roll is uncorroborated.

In what follows the effects of rotor state feedback are explored more closely to highlight rotor state feedback performance characteristics.

4.5.4 Attitude Capture Accuracy

EVENT	RSF CASE	TURBULENCE CASE	MANUEVER	EVALUATION PILOT COMMENTS
1	ON	OFF	Roll Capture	±5° Roll, with ±1° Pitch excursions; "**Sharp but wobbly**" capture of roll attitude
2	OFF	OFF	Roll Capture	±3° Roll, with ±1° Pitch excursion, with "**Better**" capture of roll attitude

Table 4.8 Case Study of Attitude Capture

For a roll-attitude capture task, the pilot evaluated that the RSF_OFF case provided an improved capture of the desired attitude with ±3° roll- and ±1° pitch-attitude excursions as shown in Table 4.8. This was due to some instability caused by the controller when engaged. It was suggested that biomechanical feedback, sensitivity settings, and gearing could be the cause of this effect. The pilot's expectations were that the RSF_ON case would perform better based on the progression of his evaluation results. The author supports this assumption since in Chapter 3 both attitude capture on- and off-axis performance were substantially improved over baseline control. In Figures 4.33 and 4.34, the trend does show slightly more oscillation on capture with the RSF_ON than with the RSF_OFF case.

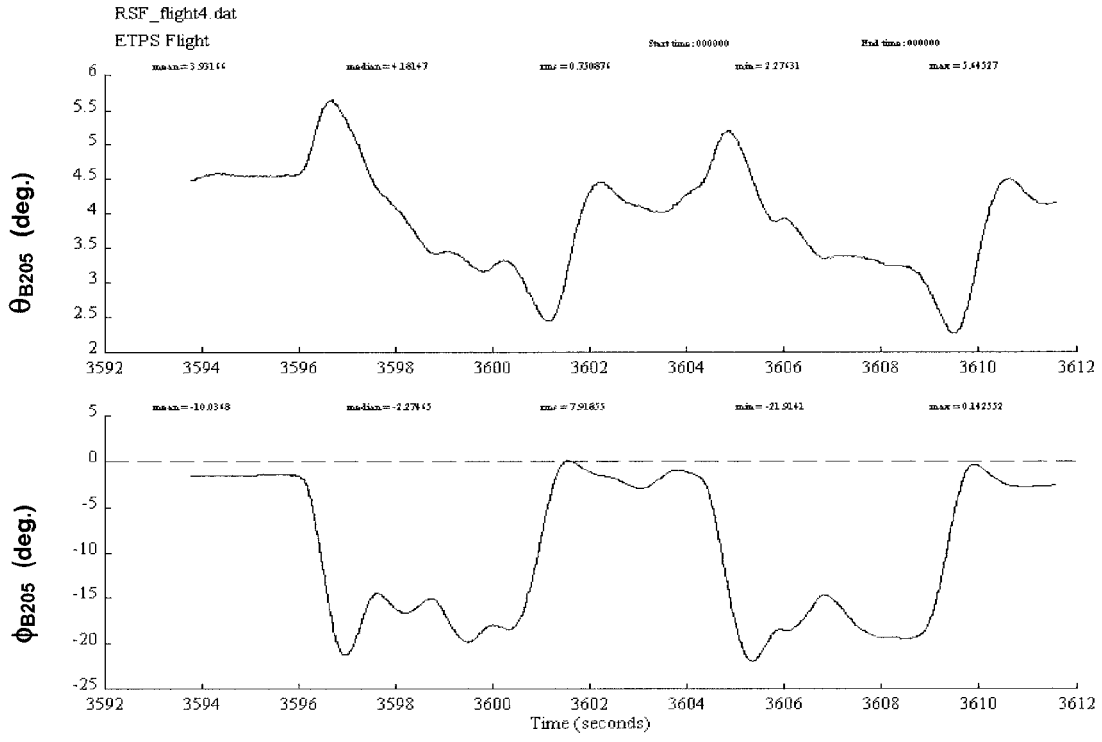

Figure 4.33 Bell 205 Attitude Capture Without Rotor State Feedback in Roll

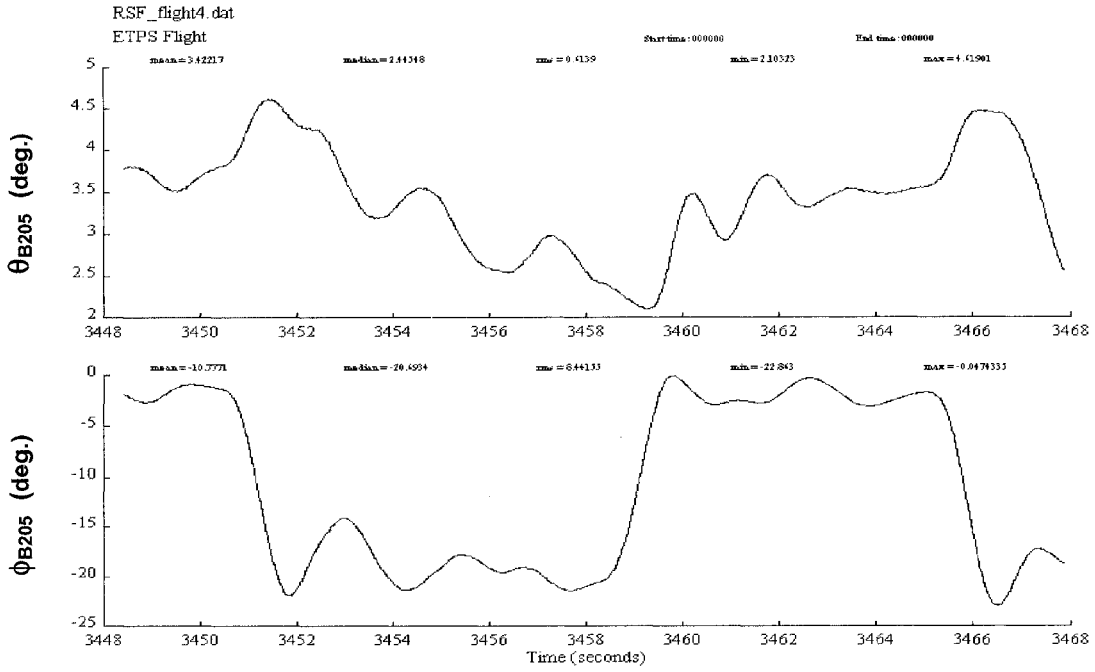

Figure 4.34 Bell 205 Attitude Capture With Rotor State Feedback in Roll

The oscillations are believed to correlate with a mode interaction; the nature of the oscillation as viewed in Figure 4.34 could point to an excessive bandwidth condition, a coupled-rotor-body response, or a biodynamic instability. This latter point is important since the pilots were under high workload (i.e.; low level flight, active traffic pattern, etc.), using position-sensing inceptors, and adjusting the control sensitivities to perform their experimental mission tasks. Though the EAC controllers did not perform well in the attitude capture task, pilots commented that during their aggressive maneuvering there was noticeable airspeed tracking.

4.5.5 Axis Decoupling

EVENT	RSF CASE	TURBULENCE CASE	MANUEVER	EVAULATION PILOT COMMENTS
ALL	ON	ALL	ALL	No pitch-roll cross-couplings evaluated in either RSF_ON or RSF_OFF cases
ALL	OFF	ALL	ALL	

Table 4.9 Case Study of Axis Decoupling

The evaluation pilot commented that during the handling qualities engagement, he assessed no pitch-roll coupling events in either RSF_ON or RSF_OFF cases as shown in Table 4.9. This was significant since;

- The Bell 205A AS was emulating a much more coupled hingeless rotor helicopter.
- The divided attention of the pilots was high thus workload inducing cross coupling could have rendered tasks unattainable.

In Figures 4.35 to 4.37, several important findings with respect to axis decoupling and disturbance rejection are highlighted by depicting axis cross-control relationships. In Figures 4.35 to 4.36 the RSF_ON cases without and with turbulence shows coherence thresholds of 0.8 and 0.4. The turbulence produces lower coherence between pilot input and vehicle response. Notice here how rotor state feedback in roll-to-pitch maintains phase correlation. In Figures 4.37 and 4.38 for the RSF_OFF cases with and without turbulence, the effect is the same, however as depicted by phase response, phase information has low correlation with controlled dynamics in the presence of turbulence.

In Figures 4.35 and 4.37 comparing the RSF_ON and RSF_OFF cases without turbulence it is noted that rotor state feedback can cause heightened cross-axis coherences. (Note: Assessing a narrow bandwidth of 2-5 rad./sec. for example shows similar response dynamics in general.). Lastly, in Figures 4.36 and 4.38 for the RSF_ON and RSF_OFF cases with turbulence, rotor state feedback is shown to substantially develop lower response coherence between control and rigid-body response while maintaining meaningful phase information in the presence of turbulence. This last point illustrates a combined decoupling and disturbance rejection effect being produced by rotor state feedback.

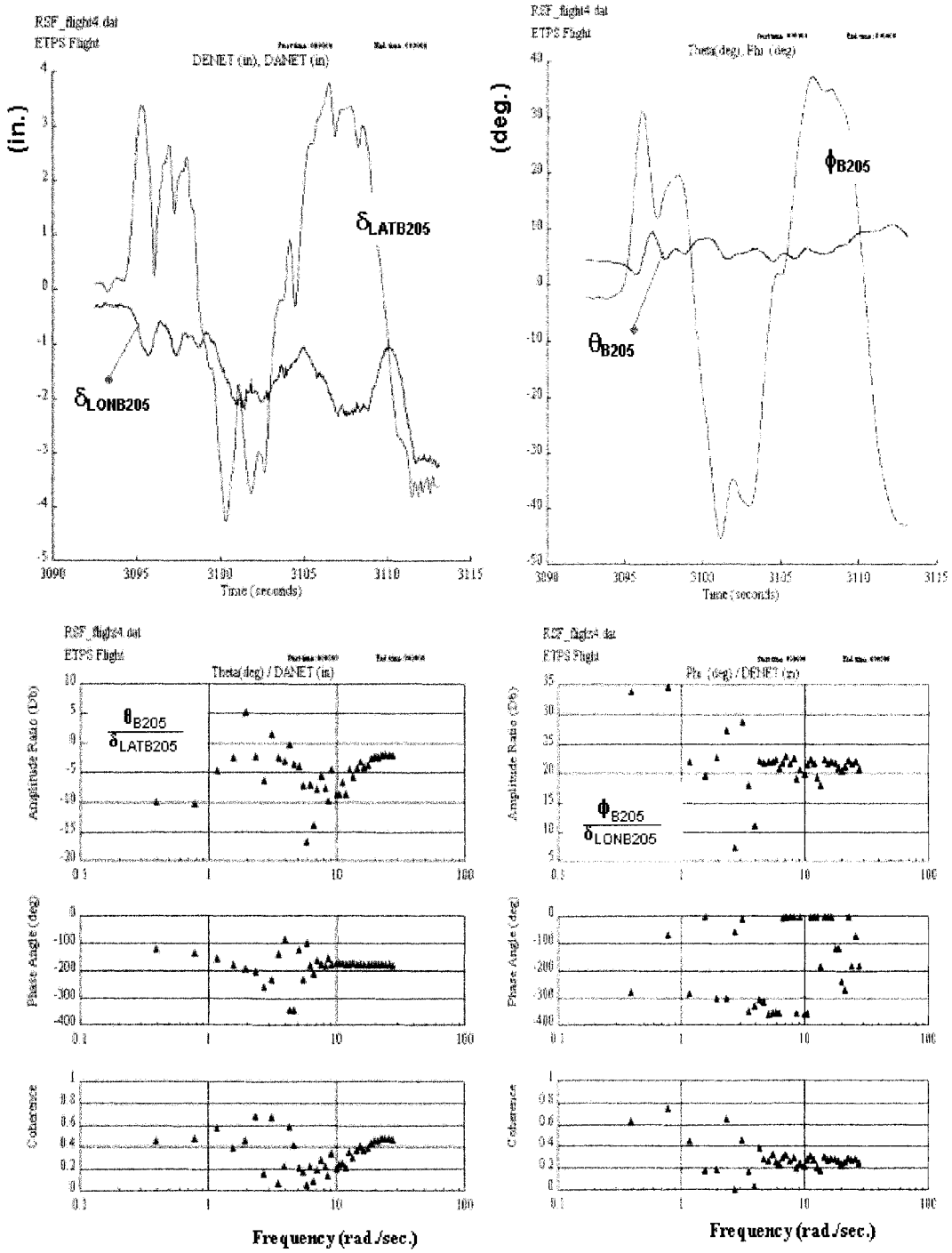

Figure 4.35 Bell 205 Response Couplings, RSF_ON, TURB_OFF - Input and Pitch Attitude to Lateral Cyclic (left), Output and Roll Attitude to Longitudinal Cyclic(right)

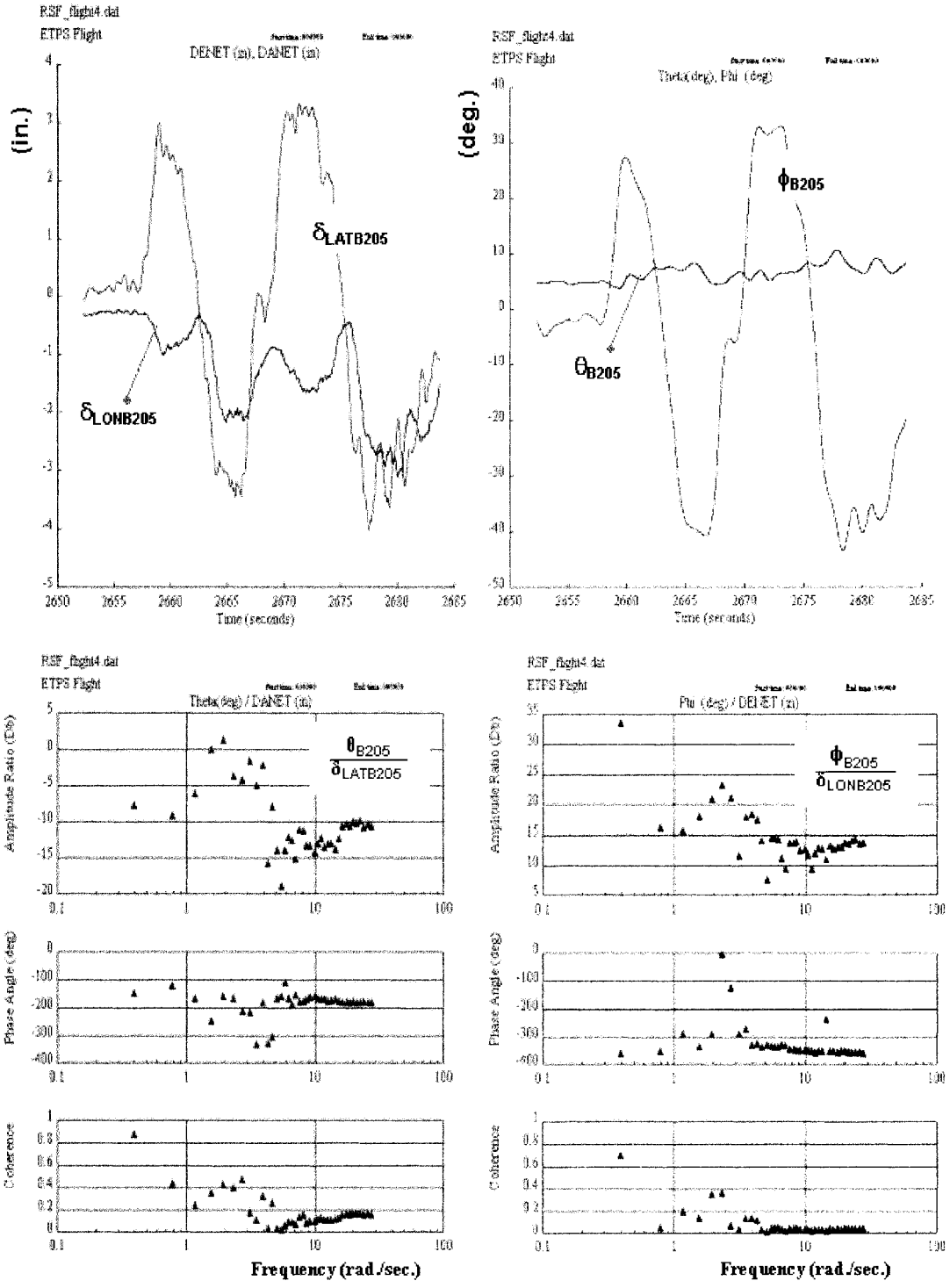

Figure 4.36 Bell 205 Response Couplings, RSF_ON, TURB_ON - Input and Pitch Attitude to Lateral Cyclic (left), Output and Roll Attitude to Longitudinal Cyclic(right)

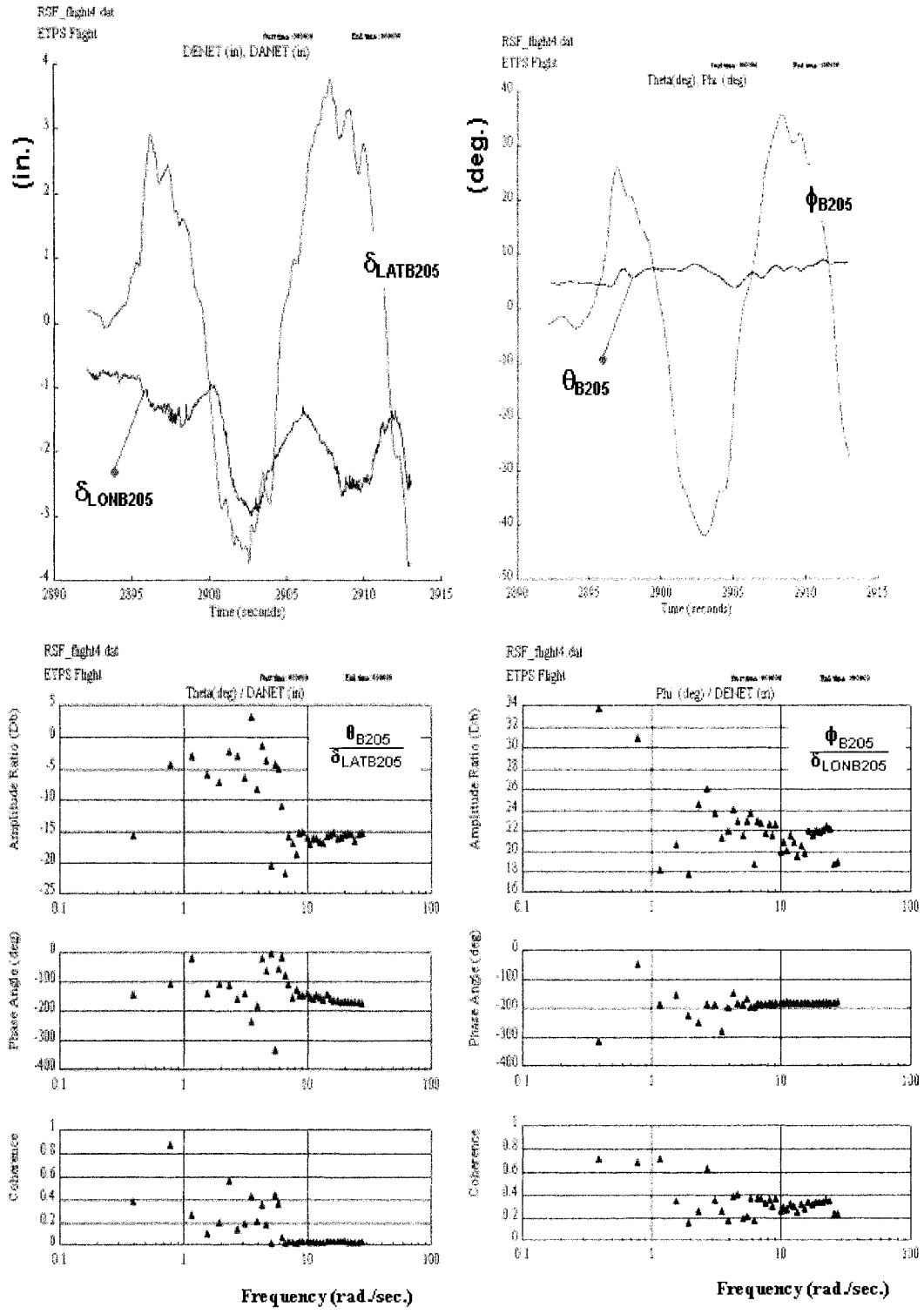

Figure 4.37 Bell 205 Response Couplings, RSF_OFF, TURB_OFF- Input and Pitch Attitude to Lateral Cyclic (left), Output and Roll Attitude to Longitudinal Cyclic(right)

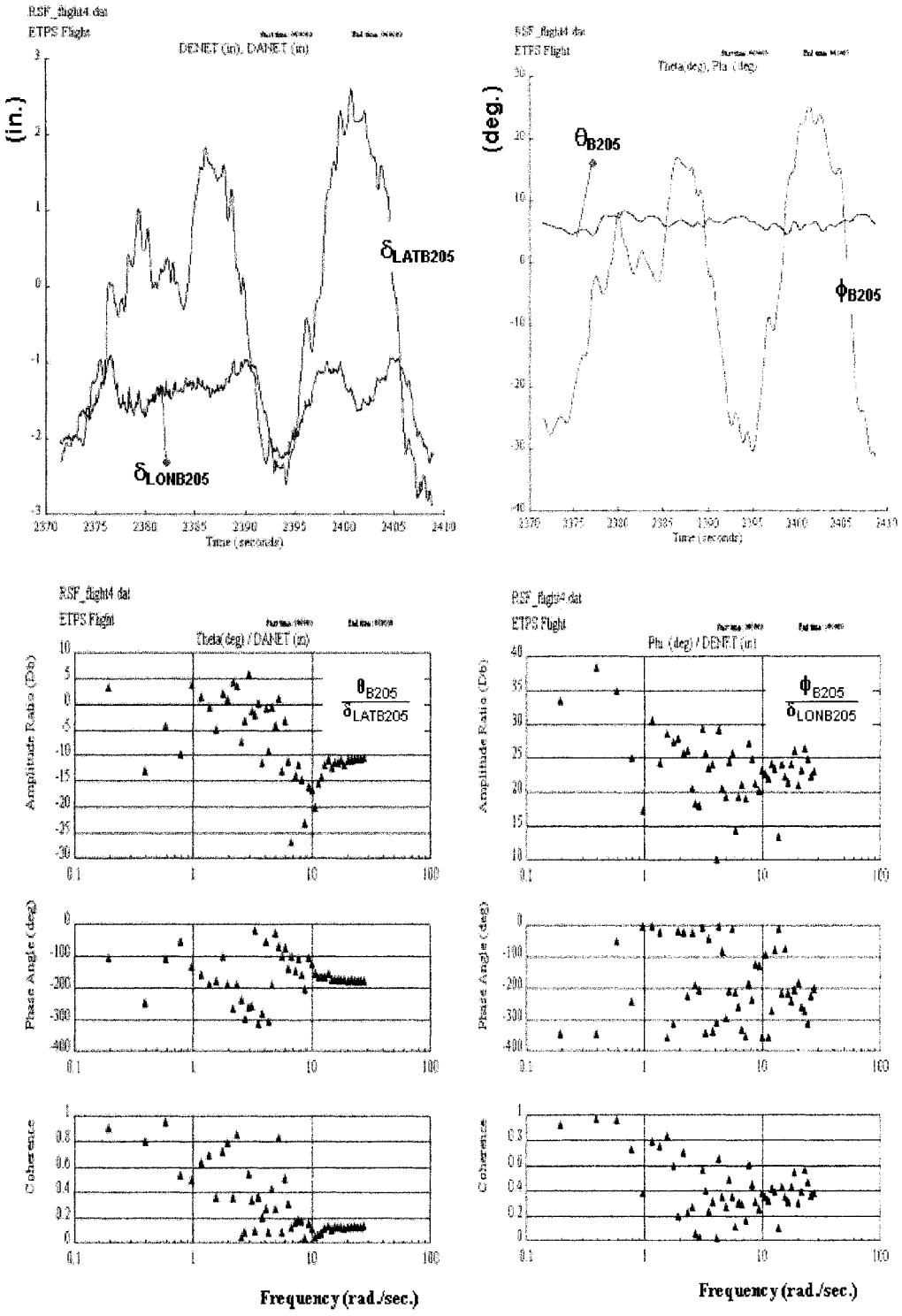

Figure 4.38 Bell 205 Response Couplings, RSF_OFF, TURB_ON - Input and Pitch Attitude to Lateral Cyclic (left), Output and Roll Attitude to Longitudinal Cyclic(right)

4.5.6 Vehicular Disturbance Rejection

The disturbance rejection results were compelling in demonstration of the effects of rotor state feedback in both attenuation of rigid-body excursions in the host Bell 205A AS and rotor response excursions in the simulated Bell 412ASRA which were induced by the MFCA turbulence model. For the flight engagements for slalom maneuvers the pilots commented that there was significant reduction in disturbance activity felt during the execution of the mission task when rotor state feedback was engaged. The evaluation pilot reported this attenuation as a striking 5:1 reduction in vehicular rigid-body response while in aggressive maneuvering which assisted in the achievement of task.

Table 4.10 shows that with RSF_ON and TURBULENCE_OFF the handling qualities rating (HQR) went from 4.5 to.4.0 with a Level 2 placement as represented in the Cooper-Harper ratings scale. (Figure 4.22)

EVENT	RSF CASE	TURBULENCE CASE	MANUEVER	SPEED (KNOTS)	HANDLING QUALITIES RATING	HANDLING QUALITIES LEVEL
1	ON	ON	SLALOM	60	**4.0**	**2.0**
2	OFF	OFF	SLALOM	60	**4.5**	**2.0**
3	ON	OFF	SLALOM	60	**4.0**	**2.0**
4	OFF	ON	SLALOM	45	**6.0**	**2.0**

Table 4.10 Case Study of Disturbance Rejection

The same trend held true with RSF_ON and TURBULENCE_ON indicating that the EAC controller with rotor state feedback attenuated the effects of turbulence or allowed the pilot to perform the MTE more compliantly.

Another trend also shows the beneficial performance of this controller. With TURBULENCE_ON for both RSF_OFF and RSF_ON cases, the pilots rated the MTE performance as 6.0 and 4.0, respectively. This showed that the EAC controller with rotor state feedback improved task performance in the presence of the simulated turbulence.

The disturbance rejection behavior characterized is decisively shown by quantitative analysis of the flight test data. Two events are assessed based on RSF_ON and RSF_OFF cases with TURBULENCE_ON. The effects of the turbulence response on Bell 412 ASRA and Bell 205A AS vehicular dynamics in both the time and frequency domains are depicted in Figure 4.39.

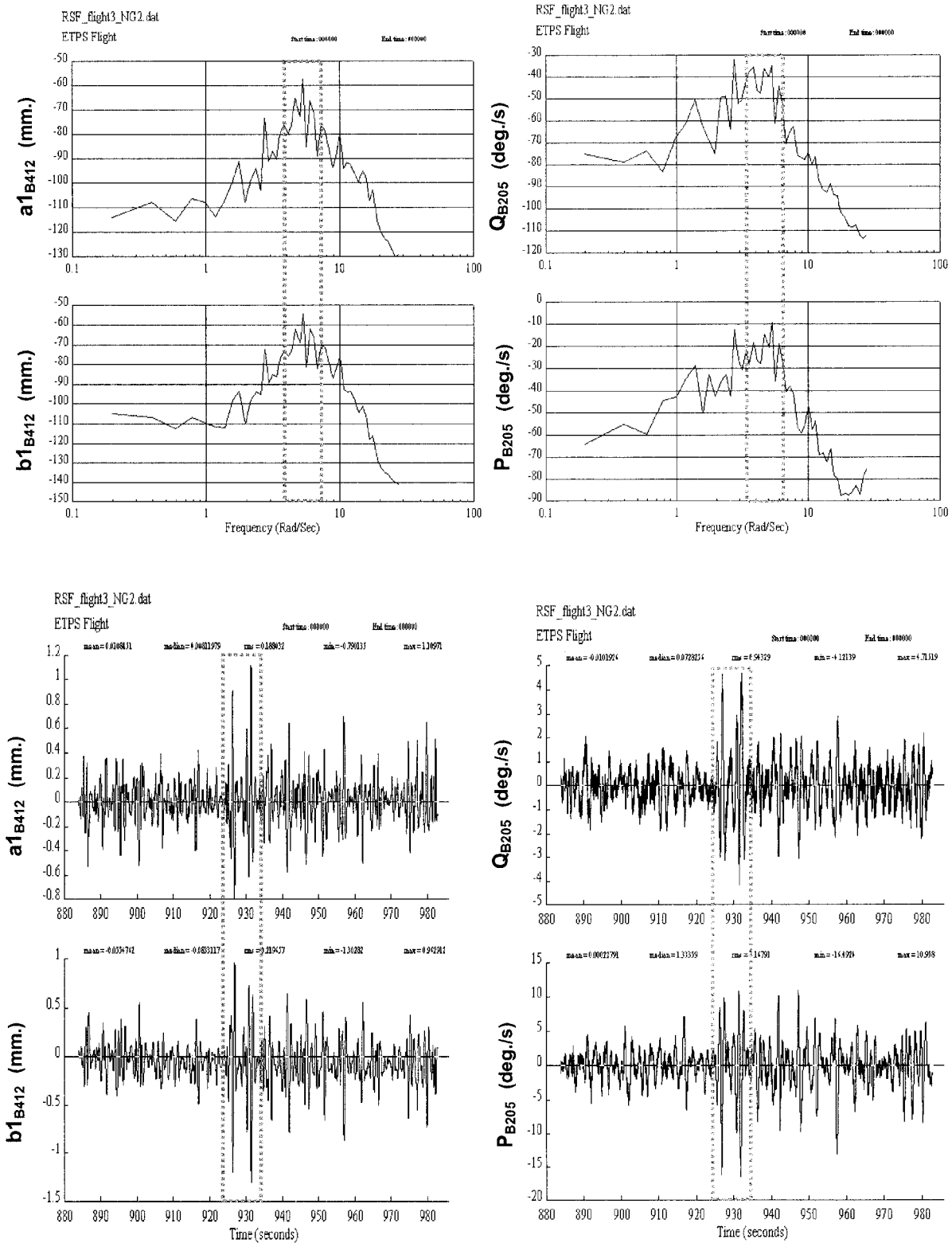

Figure 4.39 Onset of Turbulence – Frequency and Time History Responses, (Left) Bell 412 ASRA, (Right) Bell 205A AS

The Bell 412 ASRA longitudinal and lateral disc tilt responds to introduced turbulence by excitation at 5.5 rad./sec. In transient response this excitation is onset at 9.2 seconds of the event by the pilot. Peak-to-peak excitation of the rotor hub yoke is as much as 1.7 mm. Comparatively the Bell 205 rigid-body pitch and roll attitude-rate excitations appear at 2.8 rad./sec., and 5.3 rad./sec., respectively. In transient response, these excitations produce peak-to-peak attitude-rate excursions of 9 deg./sec. and 22 deg./sec. in pitch and roll, respectively. Notice that the turbulence peaks highlighted correlate between Bell 412 ASRA rotor response and Bell 205 rigid body response.

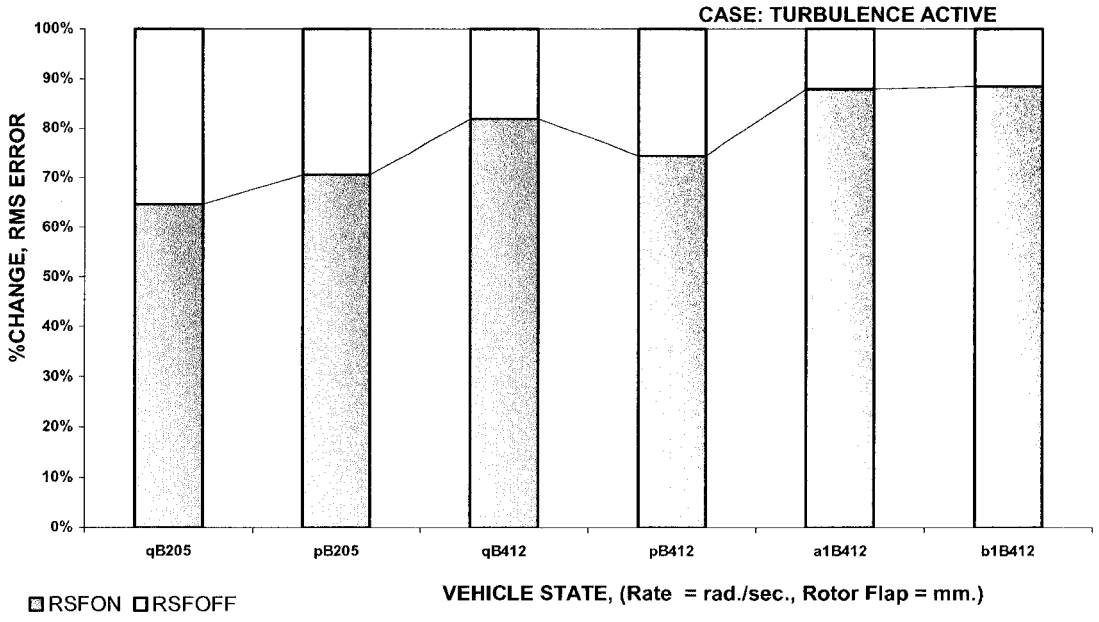

Figure 4.40 Percent Change RMS (Root Mean Square) State Errors due to Rotor State Feedback with Turbulence Active

The disturbance rejection capability of the EAC rotor state feedback controller in-flight is decisive. As shown by Figure 4.40 which depicts the reductions in Root Mean Square (RMS) state error for the host, rigid-body and rotor state responses due to simulated turbulence are attenuated in the Bell 205A AS and the Bell 412ASRA in in-flight simulation. This effect, proven in simulation in Chapter 3, occurs due to the EAC modern multivariable controller's application of rotor state feedback in the reduction of sensitivity to the imposed disturbances. For the Bell 205A AS, the RMS state error reductions are 54.7% and 41.5% in pitch- and roll-rate, while for the Bell 412ASRA the reductions are 22.1%, 34.2%, 13.8%, and 13.1% in pitch- and roll-rate, and longitudinal- and lateral-rotor disc tilt RMS state activity errors.

4.6 Summary of the Flight Test Engagement

The flight test investigation successfully engaged the variable stability capability of the Bell 205A AS in the model following of Bell 412 ASRA rotor state feedback induced rigid-body attitude and attitude-rate dynamics. The results indicate the developmental simulations including nonlinear flight control development environment (FCDE) in Chapter 3, and the present MFCA have predicted fundamental helicopter physics associated with both teetering and hingeless rotor dynamics. Several of these important identified trends include:

- Rotor-body coupling stability and response time frame modeling.
- Prediction of the benefits of rotor state feedback in flight test that include bandwidth modification, attitude and trim velocity tracking, axis decoupling, and rigid-body disturbance rejection.

The flight-testing of the Eigenstructure Assignment Control (EAC) based rotor state feedback control algorithm resulted in the following successful conclusions in application to rigid-rotor helicopters:

- The first investigation of rotor state feedback in flight test at the NRC-FRL facility.
- The validation of a model following control architecture (MFCA) incorporating a system identified turbulence model. Results depicted excellent correlations between the vehicle attitudes and attitude-rates.
- Quantitatively highly desirable Level-1 ADS-33E-PRF handling qualities compliances and qualitatively minor deficient Level-4 Cooper Harper handling qualities compliances.
- Excessive bandwidth and biodynamic instability events that provided a compelling conclusion regarding the application of rotor state feedback in bandwidth optimization as opposed to solely bandwidth augmentation.
- Highly robust control effects to off-design conditions including elevated pilot workload/divided-attention environments, parameter offsets (including altitude, weight/balance, and airspeed), and inclement weather test points.
- Moderate attitude capturing tracking performance with excellent commanded task velocity tracking.
- A combined benefit effect of axis decoupling and rigid-body disturbance rejection. Pilots report low discernable axis cross-coupling while data shows a decisive attenuation of rigid-body pitch and roll rate excursions due to simulated turbulence.
- The EAC algorithm provided an efficient and effective control law that provided insightful understanding of rigid-rotor helicopter modal dynamics for real-time high bandwidth flight control applications in the area of rotor state feedback control.

Chapter 5.0

Summary, Contributions, and Conclusions

5.1 Research Summary, Contributions, and Conclusions

This research involved supporting a major NRC-FRL initiative in higher-order helicopter rotor dynamics and high bandwidth flight control. The project encompassed the parameter estimation of an 8 Degree-Of-Freedom Hybrid Mathematical Model Structure (HMMS) of the Bell 412 ASRA incorporating explicit rigid-body and soft inplane hingeless rotor state measurement data from the vehicle fuselage and rotor state measurement systems (FSMS/RSMS), respectively. Through simulation using a variety of non-linear simulation tools (including the flight control law development environment (FCDE), and model following control architecture (MFCA)), the dynamics of higher order rotor hub yoke dynamics were investigated based on high bandwidth flight control requirements of variable stability helicopters. Root Locus Method (RLM), Classical Multivariable Control (CMC), and Eigenstructure Assignment Control (EAC) control algorithms were applied to investigate rigid-body and rotor state dynamics and feedbacks. Finally, a comprehensive model following in-flight investigation applying the host Bell 205A AS and simulated Bell 412 ASRA flight dynamics successfully evaluated in a realistic flight environment the effects of rotor state feedback on helicopter handling and ride qualities.

The following discussion will highlight major contributions and findings of this investigation.

❖ **Commissioning of the Rotor State Measurement System**

A digital, radio frequency Rotor State Measurement System was integrated into the Bell 412 ASRA by NRC-FRL for supporting this and other research in higher order rotor dynamics.

This project has significantly contributed to the commissioning of the RSMS integration, functionality, and data validity. Important contributions to the integration include the tabulation and analysis of RSMS hub yoke referenced sensing validity for rotor blade dynamics correlation. Important contributions to the functionality and data validation include comparative analysis of RSMS data with previous research in RSMS programs and validation of RSMS data through physics analyses employing a variety of helicopter flight dynamics simulation tools. A co-authored paper was presented at the 59th Annual American Helicopter Society Forum (Phoenix, Arizona) entitled, "Development of a Rotor State Measurement System for the NRC Bell 412 Advanced Systems Research Aircraft".

Major findings are as follows:

- The RSMS capability to capture soft-inplane rotor hub yoke dynamics by Hall Effect Sensor and Radio Frequency technologies for system identification and flight control law research has been verified. Current operational capabilities for the support of 15Hz flight control law research in handling and ride qualities include 300Hz rotor flap and lead-lag data rate bandwidth capability, first-mode rotor yoke flexure capturing, capability to measure blade azimuth angle and rotor speed to within 2 degrees and 0.5 RPM, a signal-to-noise ratio of 30dB, and a data transmission latency of less than 5 msec.

- The author suggests that in its current form the RSMS integration has the potential to support significant future contributions to research in the handling and ride qualities bandwidths. However, the RSMS has limited fidelity in aeromechanical and aeroservoelastic contexts due to single-point, off-blade sensing.

❖ **Development of an 8DOF Hybrid Mathematical Model Structure (HMMS)**

An 8DOF rigid-body mathematical model with rotor longitudinal and lateral rotor disc tilt dynamics of the Bell 412 ASRA was developed by the NRC-FRL by using rotor state measurements from the recently developed rotor state measurement system (RSMS).
This research made significant contributions in the application of a Maximum Likelihood Estimation (MLE) procedure for time domain parameter estimation based on coupled rotor-body equations developed by Chen[93] and Talbot[92] et al., development of fundamental structural dynamics and kinematics compatibility relationships of the rotor hub yoke and RSMS installations, and the execution and data analysis of a data gathering flight test for the 60-knot design point.

Major findings are as follows:

- The HMMS has captured by explicit rotor equations (including coupled rotor –body approximation and rigid-blade offset hinge modeling) time and frequency response effects of helicopter physics that go beyond quasi-steady 6DOF modeling. These effects include the second-order behavior of rotor flap dynamics, response correlation of attitude-rate and rotor flap dynamics, and response lead of rotor flap dynamics over rigid body dynamics. The HMMS parameterization was also shown to provide a good approximation of theoretical rotor lead-lag dynamics.
- The HMMS is highly robust to both desk-top and real-time in-flight simulation requirements for high bandwidth flight control applications. This finding is important since few of the HMMS reviewed in this research have been applied in real-time flight test conditions.
- The author further highlights that the HMMS did show deficiencies in off-axis response correlation and prediction, and demonstrated parameter convergence anomalies such as 12 derivatives with Cramer-Rao Bounds of greater than 20%. These deficiencies are typical of the current state of the art in helicopter system identification research and in light of the uncertainties accrued in this research. (i.e.; RSMS integration limitations, rotor dynamics assumptions, and neglected dynamics).

❖ **Development of a Root Locus Analysis Technique for Time and Frequency Domain Response**

A comprehensive 3-part analysis of coupled rotor-body dynamics was developed based on Root Locus Methodology. The analysis extended typical pole-zero mapping of helicopter flight dynamics to include frequency domain (Bode plot) and time domain (Step response) trajectories based on full-order and reduced-order transfer function modeling of axis flight dynamics. The frequency domain extension yielded bandwidth effects due to feedback on coupled rotor-body mode interaction out to the rotor flap regressive mode frequency. The time domain extension yielded transient response trajectories illustrating vehicle coupling, response type, and aeromechanical behaviors directly.

Major findings are as follows:

- The RLM analysis showed that rotor states placed limits on attainable bandwidth
- It was further shown that pitch and roll rate feedbacks had significant effects on mode trajectories that could be important causes of coupled rotor-body interactions. This points to the cautious selection of gains to be applied in rigid-body and rotor state feedback in view of aeromechanical and aeroservoelastic stability concerns.

❖ **Development of Classical and Modern Multivariable Control Laws Applying Explicit Rotor State Feedback Compliant to ADS-33E-PRF Specifications**

A synthesis of a rotor state feedback based Eigenstructure Assignment Controller (EAC) demonstrated optimal and insightful modal control (based on pole placement/interaction and resultant helicopter physics) as well as a sound methodology for adherence to Level-1 ADS-33-E-PRF handling qualities in both desk-top simulation and flight testing. A synthesis of a rotor state feedback based Classical Multivariable Controller (CMC) produced non-optimal control over helicopter physics. It is purported that lack of translation velocity components in the gain structure led to poor modal control and overall low Level-3 handling qualities in desk-top simulation.

Major findings include:

- The EAC algorithm was validated in desk-top simulation and variable-stability flight testing illustrating a robust method for high bandwidth, model following flight control applying full-state, high-order rotor state feedback.
- Rotor state feedback by EAC has demonstrated in simulation for the Bell 412 ASRA, significant improvements in inter-axis decoupling, rigid-body and rotor-response disturbance rejection, optimal actuator/control and rotor dynamics, command tracking accuracy, and rigid-body bandwidth performance.

❖ **NRC-FRL FBW Assessment of Rotor State feedback by Model Following Control**

A model following control architecture (MFCA) developed by Ellis and Gubbels was applied in the flight test evaluations of this research. Employing the host Bell 205A AS and simulated Bell 412ASRA rigid-rotor dynamics, the benefits of rotor state feedback by EAC have been validated in compliance with military handling qualities (ADS-33E-PRF) and Cooper-Harper pilot ratings.

Major findings for this flight test include:

- Rotor state feedback by EAC has demonstrated significant improvements in inter-axis decoupling and rigid-body disturbance rejection.
- Level-1 compliances with ADS-33E-PRF handling qualities requirements have been illustrated by quantitative data analyses, while Cooper-Harper ratings of HQR-4 were evaluated by pilots.
- Highly robust control effects to off-design conditions including elevated pilot workload/divided-attention environments, parameter offsets (including altitude, weight/balance, and airspeed), and inclement weather test points were demonstrated.
- The important finding that in rotorcraft high bandwidth control, rotor state feedback is an important tool in the optimization helicopter performance by axis bandwidth modification as opposed to solely bandwidth augmentation for next generation helicopters.
- Moderate attitude capturing performance with excellent commanded task velocity tracking was demonstrated.
- The combined benefit of axis-decoupling and rigid-body disturbance rejection is compelling. Pilots report low discernable axis cross-coupling while both pilot comments and data show a decisive attenuation of rigid-body pitch and roll rate excursions due to simulated turbulence.

5.2 Recommended Future Research

The successful completion of this investigation highlights many areas providing significant potential for research innovations and contributions to the National Research Council – Flight Research Laboratory variable stability rotorcraft investigations specific to measured higher-order rotor dynamics.

- **Bell 412 ASRA Rotor State Feedback (RSF) Flight Testing**: It is recommended that the NRC-FRL proceed with the flight test engagement of the Bell 412 ASRA to allow investigation of Rotor State Feedback on hingeless rotor helicopters. The objective of the flight test engagement would be to further confirm the wide-ranging benefits of RSF based on the validated control strategies that were originally developed for this rigid-rotor type. The exploration of the effects of RSF by allowing pilots to explore safe gain/stability thresholds through an incremental-gains approach is recommended. The author suggests that further optimization of the control laws be undertaken to explore effective flight control law design procedures based on coupled rotor-body modal control.

- **Rotor State Measurement System (RSMS) Technology Development:** The concept of Rotor State Measurement was validated here by a novel sensor technology. The author recommends that the RSMS be further developed as a comprehensive higher-order dynamics measurement system to greater levels of fidelity. Several areas for development include on blade sensing (flap and lead-lag displacements, pressures, temperatures) and blade root sensing (torsion dynamics) capabilities. This comprehensive systems integration would allow for research in domains such as airloads and flow characterization (inflow, wake), rotor based health and usage monitoring (vibration spectra), active rotor control concepts (innovative blade control concepts), and rotor noise attenuation (blade vortex interaction).

- **Development of Higher-Order Dynamics Capabilities:** Fidelity improvements in high bandwidth rotor state flight dynamics research requires consistent/compatible problem analyses and parameterization. For a given rotorcraft problem (e.g.; system identification, flight control law design, handling qualities assessment, aeromechanical stability assessment, etc.) technologies must provide adequate quality data, analyses must apply the required levels of physics fidelity, and results must be bound by limitations imposed by uncertainty. In this research then not only does the RSMS require development but so too are the analytical tools applied to support it. The author points out that some limitations in this project were imposed by the system identification technique (time domain based parameter estimation) and by the analytical-simulation environment (selected coupled rotor-body equations and use of linearly based simulation tools such as Matlab/Simulink).
  The recommendation presented here then is to maintain problem compatibility by development of the analytical tools to support rotor state research. Areas include the development of frequency domain

based system identification techniques and the application of industry/research tools specifically directed at supporting the highly non-linear dynamics present in rotorcraft. The selection or development of other rotor physics representations is highly dependent of the capability (data fidelity and quality) of the RSMS.

- **Suggested Future Research in Higher-Order Rotor Dynamics:** There are many areas for innovative application and research in the area higher-order rotor dynamics. The author suggests two areas. The first is directed at the development of modern high bandwidth helicopter handling qualities. With rotor state descriptions improving the understanding of helicopter physics, performance optimization of specific helicopter types could benefit from incorporating rotor state dynamics directly in modern handling qualities specifications. Areas might include rotor mode placement/trajectory/interaction metrics (for specifications aimed at agile military and inflight variable stability rotorcraft) and rotor design metrics (for specifications aimed at optimal bandwidth conditions). The second area proposed involves rotor state measurement and feedback in active rotor control research. Early experiments could focus on using helicopter variable-stability capabilities in higher harmonic flight control (HHFC) by sending control signals to FBW control actuators and/or swashplate for performance evaluation.

Appendices

APPENDIX A

A Guide to the Analytical Assessment of Military Handling Qualities Specifications

The objective of flight-test validation of rotor state measurement and feedback research on a variable stability helicopter dictates that the response of the vehicle will be modified over a wide frequency spectrum. As reviewed by the introductory chapter, the benefits and hazards must be constantly evaluated throughout the simulated and flight test stages of the control law development. The flying qualities of the helicopter reflect 2 subdivisions in flight dynamics. Handling qualities reflect the aircraft's behavior in response to pilot controls. These standards and much of the mission capability of the vehicle are committed in the early definition stages of a new development program. Ride qualities reflect the response of the vehicle to external disturbances. With the advent of active augmentation for attainment of operational flight envelope (OFE) requirements of next generation's military helicopters, the US Army developed ADS-33 handling qualities requirements. The latest requirement is ADS-33E-PRF and for this study a subset of forward flight specifications for the Target Acquisition and Tracking (TA+T) task are assessed for the Bell 412 ASRA bare-airframe and controlled dynamics.

Definitions

The specifications **3.4.1.**, **3.4.6.**, and **3.4.8** below, place limits on the allowable **bandwidth** and **phase delay** of the system in question. Once the limits are set in the particular specification, the satisfaction of the requirements are quantified by "**Levels**" such that;

- **Level 1** – Satisfactory. No improvement needed. The Mission Task Element (MTE) may be completed with moderate pilot workload.
- **Level 2** – Marginal. Warrants improvement, but not required. The MTE may be completed with increased pilot workload.
- **Level 3** – Deficient. Requires improvement. Maintaining control requires high pilot workload; completion of the MTE is not possible.

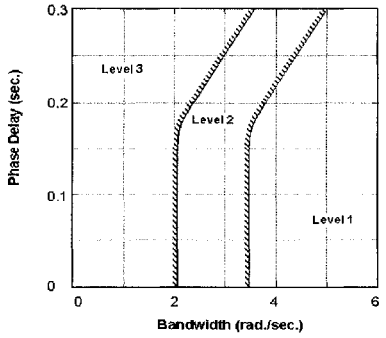

Figure A.1 Typical Bandwidth and Phase Delay Specification

Phase Delay

The phase delay is a measure of the sensitivity of the system beyond the neutral stability frequency. It is found by measuring the change in phase between the neutral stability frequency, which is always -180°, and twice the neutral stability frequency. Phase delay measures the lag in the response of the system to an input of a given frequency.

Bandwidth

The bandwidth is the frequency at which the output response sinusoid first suffers significant reduction in amplitude.

Stability in the Frequency Domain

- A system is stable if the gain is less than 0 dB at the neutral stability frequency (i.e.; the frequency at which the phase = -180°.
- Pilots have demonstrated that if the phase changes rapidly beyond the neutral stability frequency, the vehicle is susceptible to Pilot-Induced-Oscillations (PIO).

Method of Compliance for Bandwidth and Phase Limited Specifications

To determine the compliance with the bandwidth and phase limited requirements such as Figure A.1, a Bode frequency response plot is developed for each axis of concern. There are 2 bandwidths to be assessed: gain and phase bandwidth. The first step is to find the **neutral stability frequency** (where; phase = -180°), ω_{-180}. The **phase bandwidth**, $\omega_{BW_{PHASE}}$, is the frequency at which the controlled system has 45° of phase margin, (i.e.; has a -135° crossover). The **gain bandwidth**, $\omega_{BW_{GAIN}}$, is the frequency at which the controlled system has 6dB of gain margin, this corresponds to the doubling of the response amplitude. (Pilots could thus double the magnitude of their control inputs without risking stability.)

S3.4.1.1, S3.4.6.1, and S3.4.8.1: Short Term Response Compliance

These are bandwidth and phase limited specifications for on-axis longitudinal, lateral, and directional dynamics (Figure A.2). Compliance to these specifications is met by the methods outlined above.

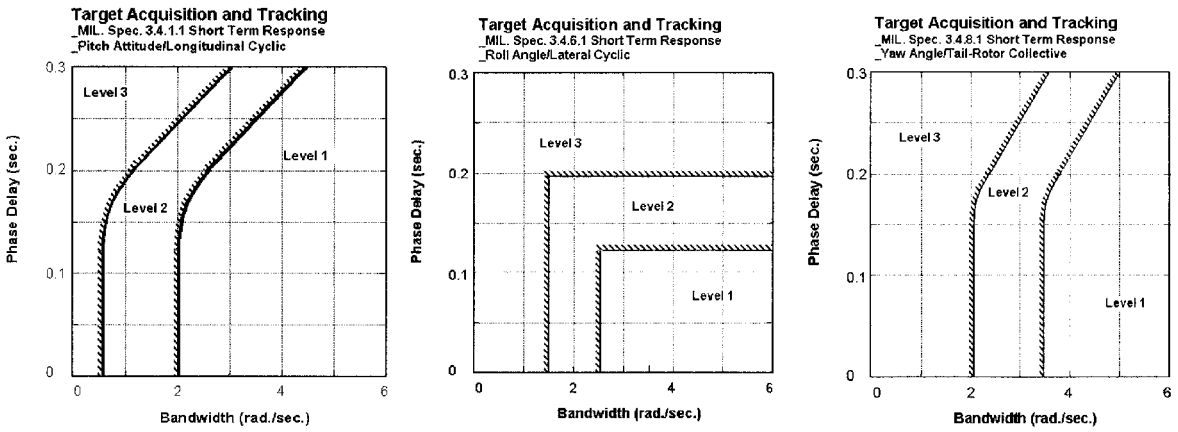

Figure A.2 Short Term Response – (Forward Flight)

S3.3.2(ADS-33C): Small Amplitude, Mid-Term Response Compliance

- **S3.3.2 (Allowable Pole Placement of Rigid Body Response)**

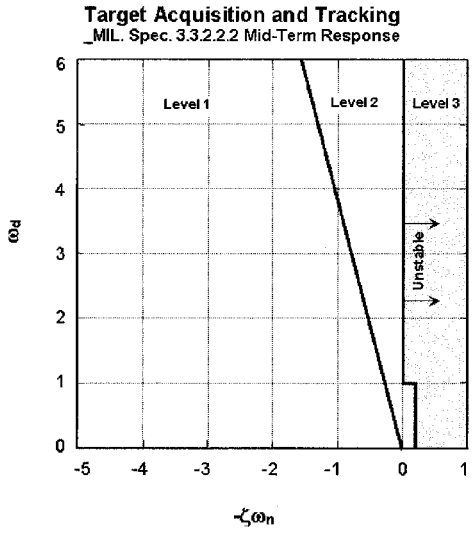

Figure A.3 Spec.3.3.2 Midterm Response – Rigid Body Pole Placement (ADS-33C Low-speed)

This requirement defines the allowable placement of rigid body poles defining the behavior of the helicopter beyond the initial seconds following an input from pilot controls or gusts. This specification is designed to assess the relationship between the pilot action through diverted attention workload and the vehicle flight profile without undue excursions for short periods of time. Thus the vehicle must allow for

this diverted attention flight control in light of the TA+T MTE where pilots are concentrating on multiple subtasks including acquisition, tracking, controlling, and cockpit management.

Compliance with this specification requires the assessment of rigid body mode damping and frequency for placement in the region of compliance shown in Figure A.3. Poles for Level 1 will have at least 0.35 damping ratio, while in the Level 2 region as long as the natural frequency is small, slight instabilities are tolerated.

S3.3.9(Low Speed))/S3.4.5.(ADS-33E-PRF): Inter-axis Coupling Compliance

- **S3.3.9.1 Yaw due to Collective for Aggressive Agility**

To demonstrate compliance the time histories of yaw rate and vertical velocity following a step input of collective pitch are plotted. Three parameters are read from these time histories. The first is the magnitude of the value of the first yaw rate peak within 3 seconds, in deg./sec. If no peak exists in that time parameter, r_1 is the magnitude of the yaw rate after one second. The second parameter, also from the yaw rate plot is labeled, r_3, and is the difference between the magnitude of the yaw rate at 3 seconds and the r_1 value. The third and final parameter is the magnitude of the vertical velocity, $\dot{h}(3)$, after 3 seconds in ft./sec. The quantities are plotted on their respective axes as shown in Figure A.4.

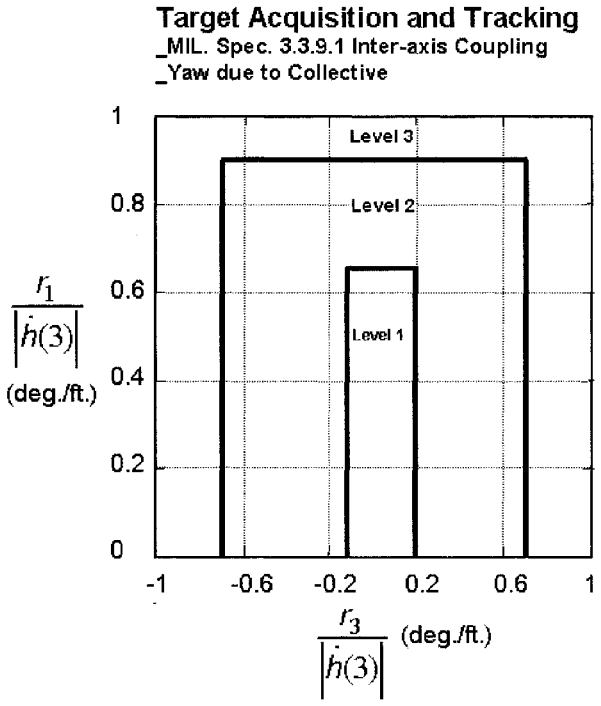

Figure A.4 Spec.3.3.9.1 Inter-axis Coupling – Yaw due to Collective (Low Speed)

- **S3.4.5.4: Pitch due to Roll and Roll due to Pitch for Aggressive Agility**

To demonstrate compliance the two-frequency response pairs are plotted to form the coupled rate ratios. First the frequency responses of pitch rate to lateral cyclic, roll rate to lateral cyclic, and pitch attitude to longitudinal cyclic are plotted. The average frequency, F1avg., between the bandwidth and neutral stability (phase = -180°) frequencies is evaluated from the pitch attitude to longitudinal cyclic response. Using the dB conversion, $y\,dB = 20\log_{10}(x)$, the magnitudes of the pitch rate and roll rate frequencies are calculated at the average frequency, F1avg., based on their respective frequency response plots. The coupling ratio of roll rate to pitch rate, p/q, is then calculated and converted back to its dB equivalent. Secondly the frequency responses of roll rate to longitudinal cyclic, pitch rate to longitudinal cyclic, and pitch attitude to longitudinal cyclic are plotted. The average frequency, F2avg., between the bandwidth and neutral stability (phase = -180°) is evaluated from the roll attitude to lateral cyclic response. Using the dB conversion, $y\,dB = 20\log_{10}(x)$, the magnitudes of the roll rate and pitch rate frequencies are calculated at the average frequency, F2avg., based on their respective frequency response plots. The coupling ratio of pitch rate to roll rate, q/p, is then calculated and converted back to its dB equivalent.

These coupling ratios are then plotted on their respective axes as shown in Figure A.5.

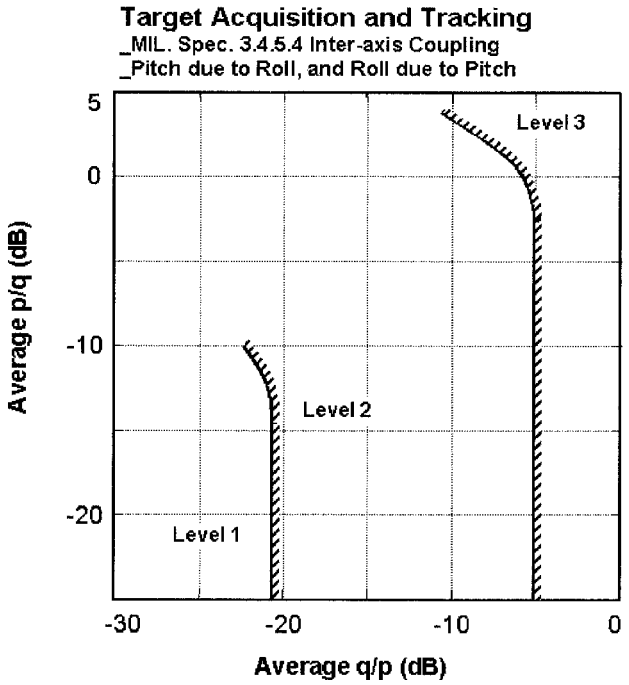

Figure A.5 Spec.3.4.5.4 Inter-axis Coupling – Pitch due to Roll and Roll due to Pitch (Forward Flight)

APPENDIX B

Bell 412 ASRA – Hybrid Mathematical Model Structure (HMMS)

- Controls (in.), Velocities (m/sec.), Attitude-Rates: (rads./sec.), Attitudes: (rads.)
- Yoke Flap Displacement: (mm.)

	u	v	w	p	q	r	a1	b1	lon	coll	lat	ped
X	-0.001129	0.009713	0.08167	0.02195	-0.01884	1.061	-1.034	0.000	0.4997	0.1252	-0.1501	0.2944
Y	0.02173	-0.05061	-0.01498	1.789	-0.08964	0.9608	0.000	-0.4235	0.1683	-0.1087	-0.4643	0.1640
Z	-0.009245	-0.03057	-0.8362	0.9814	-0.1027	0.7715	0.000	0.000	1.052	-2.610	0.3410	-0.08873
L	-0.01467	-0.05309	0.03192	-0.0682	0.000	0.6463	0.2392	-0.8468	-0.1806	-0.01694	0.1562	0.2722
M	0.006139	0.01090	-0.006283	0.000	0.000	-0.07925	-0.6859	-0.4389	0.1263	0.06222	-0.1397	0.01922
N	-0.02921	0.009517	-0.05194	-1.791	0.3000	-1.341	1.485	1.372	-0.7683	0.02580	0.6788	-0.4557
a1	0.000	0.000	0.000	0.000	13.000	0.000	-10.500	-3.633	5.230	0.000	-1.465	0.000
b1	0.000	0.000	0.000	14.000	0.000	0.000	3.633	-10.500	0.1163	0.000	-4.184	0.000

Non-Zero Stability Derivatives	Parameter Values	Cramer-Rao Bounds (%)
Xu	-0.001129	128.88
Xv	0.009713	11.03
Xw	0.08167	3.03
Xp	0.02195	187.97
Xq	-0.01884	413.96
Xr	1.061	3.53
Xa1	-1.034	6.64
Yu	0.02173	6.26
Yv	-0.05061	1.961
Yw	-0.01498	14.04
Yp	0.9814	5.46
Yq	-0.08964	70.62
Yr	0.9608	3.42
Yb1	-0.4235	11.24
Zu	-0.009245	61.86
Zv	-0.03057	13.21
Zw	-0.8362	1.04
Zp	0.9814	11.24
Zq	-0.1027	233.7
Zr	0.7715	16.75
Lu	-0.01467	9.24
Lv	-0.05309	1.75
Lw	0.03192	7.29
Lp	-0.0682	---
Lr	0.6463	6.62
La1	0.2392	35.69
Lb1	-0.8468	4.27
Mu	0.006139	5.25
Mv	0.01090	2.36
Mw	-0.006283	8.87
Mr	-0.07925	12.82
Ma1	-0.6859	2.01
Mb1	-0.4389	1.79
Nu	-0.02921	5.37
Nv	0.009517	11.33
Nw	-0.05194	5.05
Np	-1.791	---
Nq	0.3000	---
Nr	-1.341	3.40
Na1	1.485	6.23
Nb1	1.372	2.80
a1q	13.000	---
a1a1	-10.500	---
a1b1	-3.633	---
b1p	14.000	---
b1a1	3.633	---
b1b1	-10.500	---

Non-Zero Control Derivatives	Parameter Values	Cramer-Rao Bounds (%)
Xδlon	0.4997	5.34
Xδcol	0.1252	7.78
Xδlat	-0.1501	6.08
Xδped	0.2944	4.28
Yδlon	0.1683	5.37
Yδcol	-0.1087	7.72
Yδlat	-0.4643	3.72
Yδped	0.1640	6.33
Zδlon	1.052	2.74
Zδcol	-2.610	1.43
Zδlat	0.3410	8.84
Zδped	-0.08873	52.67
Lδlon	-0.1806	19.68
Lδcol	-0.01694	58.41
Lδlat	0.1562	9.39
Lδped	0.2722	5.22
Mδlon	0.1263	---
Mδcol	0.06222	4.53
Mδlat	-0.1397	---
Mδped	0.01922	22.25
Nδlon	-0.7683	5.47
Nδcol	0.02580	38.79
Nδlat	0.6788	2.63
Nδped	-0.4557	3.23
a1δlon	5.230	1.29
a1δlat	-1.465	2.69
b1δlon	0.1163	98.89
b1δlat	-4.184	2.48

References

List of References

1. Padfield, G.D., Helicopter Flight Dynamics: The Theory and Application of Flying Qualities and Simulation Modeling, AIAA Education Series, Reston, VA, 1999.
2. Padfield, G.D., Helicopter Handling Qualities: An American Helicopter Society Workshop, Washington, May 2001.
3. Johnson, W.; Helicopter Theory; Dover Publications, New York; 1980.
4. A.R.S. Bramwell, Done, G., Balmford, D.; Bramwell's Helicopter Dynamics -2nd Edition; Co-published - American Institute of Aeronautics and Astronautics and Butterworth-Heinemann; 2001.
5. Bielawa, R.L.; Rotary Wing Structural Dynamics and Aeroelasticity; AIAA Education Series; Washington, D.C.; 1992.
6. Chopra, I; Helicopter Dynamics ENAE 633; University of Maryland – Center for Rotorcraft Education and Research
7. Prouty; Helicopter Performance, Stability and Control; Prindle, Weber & Schmidt; ISBN 0-534-06360-8; 1986.
8. Schafer; Helicopter Maintenance; Jepperson, Sanderson Training Products; ISBN 0-89100-281-2; 1980.
9. Stepniewski; Keys; Rotary-Wing Aerodynamics; Dover Publications; ISBN 0-486-64647-5; 1984.
10. Vuillet; "Rotor and Blade Aerodynamic Design"; Aerospatiale Helicopter Division – France; AGARD – FDP, Special Course on Aerodynamics of Rotorcraft; AGARD-R-781; April-May 1990.
11. Langrebe, A.J.; "Overview of Helicopter Wake and Airloads Technology"; 12[1] European Rotorcraft Forum; Garmisch-Partenkirchen; Paper 18; September 1986.
12. Chen, R.T.N.; Hindson, W.S.; "Influence of Dynamic Inflow on the Helicopter Vertical Response"; Vertica ; Volume 11, Number ½ pp 77-91; 1987.
13. United States Army Aviation and Missile Command; "Handling Qualities Requirements for Military Rotorcraft: ADS-33E-PRF"; Aeronautical Design Standard Performance Specification, March 2000.
14. United States Army Aviation and Troop Command; "Handling Qualities Requirements for Military Rotorcraft: ADS-33D"; Aeronautical Design Standard, July 1994.
15. Military Specification; "Flight Control Systems - Design, Installation and Test of Piloted Aircraft General Specification For: MIL-F-9490D"; June 1975.
16. Hohenemser; "Hingeless Rotorcraft Flight Dynamics"; Washington University; AGARD Report: AGARD-AG-197; September 1974.
17. Loewy; "Review of Rotary-Wing V/STOL Dynamic and Aeroelastic Problems"; AIAA/AHS VTOL Research, Design, and Operations Meeting; 1969.
18. Miao; "Rotor Aeroelastic Stability", Sikorsky Aircraft Division, Stratford Connecticut; Publication Source Unknown
19. Chopra, I.; "Perspectives in Aeromechanical Stability of Helicopter Rotors"; American Helicopter Society National Specialist's Meeting on Rotorcraft Dynamics; November 1989.
20. Taylor; Caldwell; "An overview of the Effects of Aeroservoelasticity on the Design of Flight Control Systems"; UK; IEE Colloquium on Multivariable Methods for Flight Control Applications; Accession Number: 4869806; 1994.
21. Noll, T.E., Perry III, B., Kehoe, M.W., "A Quarter Century of NASA Wind-Tunnel and Flight Experiments Involving Aeroservoelasticity", Structures and Materials Panel Specialists' Meeting on Advanced Aeroservoelastic Testing and Data Analysis, Rotterdam, The Netherlands, May 1995.
22. Huber; "Will Rotor Hubs Lose Their Bearings? – A Survey of Bearingless Main Rotor Development"; 18th European Rotorcraft Forum, France; Paper No. 506/SP-06; September 1992.
23. Mayo; Occhiato; Hong; "Helicopter Modeling Requirements for Full Mission Simulation and Handling Qualities Assessment"; Sikorsky Aircraft Corporation

24. Ingle, Weber, Miller; "Concurrent Handling Qualities and Aeroservoelastic Specification Compliance for the RAH-66 Comanche"; American Helicopter Society Aeromechanical Specialist Conference; January 1994.
25. Dryfoos, J.B., Mayo, J.; "An Approach to Reducing Rotor-Body Coupled Roll Oscillations on the RAH-66 Comanche Using Modified Roll Rate Feedback"; 55th Annual American Helicopter Society Forum; Phoenix, Arizona; May 1999.
26. Reichert, G., Ewald, J.; "Helicopter Ground and Air Resonance Dynamics"; 14th European Rotorcraft Forum; Milan, Italy; September 1988.
27. Reichert; Huber; "Dynamic Aspects in the Design of Advanced Rotor Systems"; AHS/NAI International Seminar on "The Theoretical Basis of Helicopter Technology"; November 1985.
28. Kufeld; Johnson; "The Effects of Control System Stiffness Models on the Dynamic Stall Behavior of a Helicopter"; 54th American Helicopter Society Forum, Washington; May 1998.
29. Alexander, M.; Behdinan, K.; "Integrating Active Rotor Control into Helicopters"; Ryerson University Undergraduate Thesis, Aerospace Engineering; April 2000.
30. Yu; Gmelin; Splettstoesser; Philippe; Prieur; Brooks; "Reduction of Helicopter Blade-Vortex Interaction Noise by Active Control Technology"; Aerospace Science – Volume 33, pp. 647-687, 1997.
31. Splettstoesser; Kube; Wagner; Selhorst; Boutier; Micheli; Mercker; Pengel; "Key Results From a Higher Harmonic Control Aeroacoustic Rotor Test (HART)"; European Rotorcraft Forum; 1995.
32. Tettenborn; Kessler; Reichert; "Comparison of IBC with Active Controllers Using a Conventional Swashplate to Suppress Ground and Air Resonance"; Institute of Flight Mechanics and Space Flight Technology, Germany
33. Weller, W.; "Fuselage State Feedback for Aeromechanical Stability Augmentation of a Bearingless Main Rotor"; United Technologies Research Center; Journal of the American Helicopter Society; 1996.
34. Weller, W.; "Active Aeromechanical Stability Augmentation using Fuselage State Feedback"; 53rd Annual Forum of the American Helicopter Society, Virginia Beach, Virginia, April – May 1997.
35. Hathaway, E.; Gandhi, F.; "Individual Blade Control For Alleviation of Helicopter Ground Resonance"; American Institute for Aeronautics and Astronautics; AIAA-98-2006
36. Straub, F.K., Warmbrodt, W., "The Use of Active Controls to Augment Rotor/Fuselage Stability," Journal of the American Helicopter Society, Vol. 30, No. (3), July 1985.
37. Ellis, C.; "Effects of Articulated Rotor Dynamics on Helicopter Automatic Control System Requirements"; Kaman Aircraft Corporation; Aeronautical Engineering Review; July 1953.
38. Kelley B., "Helicopter Stability with Young's Lifting Rotor", Bell Aircraft Corporation, SAE Journal Transactions, Vol. 53, (12), December 1945.
39. Miller, R.H., "A Method of Improving the Inherent Stability and Control Characteristics of Helicopters", Rotary Wing Aircraft Session - 17th Annual Meeting, New York, January 1949.
40. Hall Jr., W.E., Bryson Jr., A.E., "Inclusion of Rotor Dynamics in Controller Design for Helicopters", Journal of Aircraft, Vol. 10, (4), April 1973.
41. Potthast, A.J., Kerr, A.W.; "Rotor Moment Control with Flap-Moment Feedback"; Lockheed Aircraft Corporation; American Helicopter Society 30th Annual Forum, Washington, D.C., May1974.
42. Curtiss, H.C.; Stability and Control Modeling"; Vertica; Volume 12, Number 4; pp. 381-394; 1988.
43. Curtiss, H.C.; "Physical Aspects of Rotor Body Coupling in Stability and Control"; American Helicopter Society 46th Annual Forum, Washington, D.C., May 1990.
44. Curtiss, H.C. Jr.; "The Use of Complex Coordinates in the Study of Rotor Dynamics"; American Institute for Aeronautics and Astronautics 2nd Atmospheric Flight Mechanics Conference; Palo Alto, California; AIAA Paper No. 72-954; September 1972.
45. Hohenemser, K.H., Yin, S.K.; "On the Use of First Order Rotor Dynamics in Multiblade Coordinates" 30th AHS Forum Proceedings, Washington, D.C.; 1974.
46. Hohenemser, K.H., Yin, S.K.; "Some Applications of the Method of Multiblade Coordinates"; Journal of the American Helicopter Society; July 1972.

47. DuVal, Ronald; "Use of Multiblade Sensors for On-Line Rotor Tip-Path-Plane Estimation"; Journal of the American Helicopter Society; October 1980.
48. Fuller, J.W., "Rotor State Estimation for Rotorcraft", American Helicopter Society Northeast Region National Specialists' Meeting on Helicopter Vibration – Technology for the Jet Smooth Ride, Hartford, Connecticut, November 1981.
49. McKillip R.M.; "Kinematic Observers for Active Control of Helicopter Rotor Vibration"; 12th European Rotorcraft Forum; Garmisch-Partenkirchen; September 1986.
50. Takahashi, M.D., "Rotor-State Feedback in the Design of Flight Control Laws for a Hovering Helicopter", Journal of the American Helicopter Society, Vol. 39, (1), January 1994.
51. Takahashi, M.D., "H-Infinity Flight Control Law Design With and Without Rotor State Feedback"; Journal of Guidance, Control, and Dynamics, Vol. 17, (6), November-December 1994.
52. Chen, R.T.N., "An Exploratory Investigation of the Flight Dynamic Effects of Rotor RPM Variations and Rotor State Feedback in Hover", 18th European Rotorcraft Forum, Avignon, France, September 1992.
53. Howitt, J., Howell, S.E., McCallum, A.T., Brinson, P.R., "Experimental Evaluation of Flight Control System Designs Exploiting Rotor State Feedback", American Helicopter Society 57th Annual Forum, Washington, D.C., May 2001.
54. Briczinski, S.J., Cooper, D.E., "Flight Investigation of Rotor/Vehicle State Feedback", NASA CR – 132546, SER – 50905.
55. Diftler, M.A.; "UH-60A Helicopter Stability Augmentation Study"; 14th European Rotorcraft Forum; Milano, Italy; Paper No. 74; September 1988.
56. Cunningham, T.B., Nunn. E.C.; "Helicopter High Gain Control"; NASA CR-159052
57. Hohenemser, K.H., Yin, S.K.; "The Effects of Some Rotor Feedback Systems on Rotor-Body Dynamics"; NASA CR-114709; 1973.
58. Alexander, M., Gubbels, A.W., Dillon, J.; "Development of a Rotor State Measurement System for the Bell 412 Advanced Systems Research Aircraft", 59th Annual American Helicopter Society Forum; Phoenix, Arizona; May 2003.
59. Knight Jr., V.H., Haywood Jr., W.S., Williams, M.L., "A Rotor Mounted Digital Instrumentation System for Helicopter Blade Flight Research Measurements", NASA Technical Paper 1146, April 1978.
60. Kufeld, R., Loschke, P., "UH-60 Airloads Program: Status and Plans", AIAA Aircraft Design Systems and Operations Meeting, Baltimore, MD, September 1991.
61. Ellerbrock, P.J., Halmos, Z., Shanthakumaran, P., "Development of New Health and Usage Monitoring System Tools Using a NASA/Army Rotorcraft", American Helicopter Society 55th Annual Forum, Montreal, Canada, May 1999.
62. Fletcher, J.W., Tischler, M.B., "Improving Helicopter Flight Mechanics Models with Laser Measurements of Blade Flapping", American Helicopter Society 53rd Annual Forum, Virginia Beach, VA, April-May 1997.
63. Arnold, U.T.P., Strecker, G., "Certification, Ground, and Flight Testing of an Experimental IBC System for the CH-53G Helicopter", American Helicopter Society International 58th Annual Forum, Montreal, Canada, June 2002.
64. Splettstoesser, W.R., Schultz, K.-J., van der Wall, B., Buchhloz, H., "Helicopter Noise Reduction by Individual Blade Control (IBC) – Selected Flight Test and Simulation Results", RTO AVT Symposium on Active Control Technologies for Enhanced Performance Operational Capabilities of Military Aircraft, Land Vehicles, and Sea Vehicles, Braunschweig, Germany, May 2000.
65. Okuno, Y., Matayoshi, N., "Development of a New Research Helicopter MuPAL-ε", American Helicopter Society 57th Annual Forum, Washington, D.C., May 2001.
66. McKillip Jr., R., "A Novel Instrumentation System for Measurement of Helicopter Rotor Motions and Loads Data", American Helicopter Society 58th Annual Forum, Montreal, Canada, June 2002.
67. Brinson, P., Mullen, G., Howitt, J., Woodrow, I., "Experimental Investigation of Control System Design Methods for Helicopters", 21st European Rotorcraft Forum, Saint Petersburg, Russia, August-September 1995.

68. Hermans, C., Hakkart, J., Panosetti, G., Preatoni, G., Mikulla, V., Chery, F., Serr, C., "Overview of the NH90 Wind Tunnel Test Activities and Benefits to the Helicopter Development", American Helicopter Society 53rd Annual Forum, Virginia Beach, VA, April-May 1997.
69. Lorber, P., Park, C., Polak, D., O'Neil, J., Welsh, W., "Active Rotor Experiments at Mach Scale Using Root Pitch IBC", American Helicopter Society 57th Annual Forum, Washington, D.C., May 2001.
70. Norman, T.R., Shinoda, P.M., Kitaplioglu, C., Jacklin, S.A., Sheikman, A., "Low-Speed Wind Tunnel Investigation of a Full-Scale UH-60 Rotor System", American Helicopter Society 58th Annual Forum, Montreal, Canada, June 2002.
71. Ham, N.D., McKillip Jr., R.M., "Research on Measurement and Control of Helicopter Rotor Response Using Blade-Mounted Accelerometers", 18th European Rotorcraft Forum, Avignon, France, September 1992.
72. Chen, R.T.N.; Hindson, W.S.; "Influence of Higher-Order Dynamics on Helicopter Flight-Control System Bandwidth", Journal of Guidance, Vol. 9, No. (2), March-April 1986.
73. Manness, M.A., Gribble, J.J., Murray-Smith, D.J., "Multivariable Methods for Helicopter Flight Control Law Design: A Review", 17th European Rotorcraft Forum, Glasgow, Scotland, September 1990.
74. Tischler, M.B., Advances in Aircraft Flight Control, Taylor and Francis Publishers, 1996
75. Ingle, S.J., Celi, R., "Effects of Higher Order Dynamics on Helicopter Flight Control Law Design", American Helicopter Society 48th Annual Forum, Washington, D.C., June 1992.
76. Miller, D.G., White, F., "A Treatment of the Impact of Rotor-Fuselage Coupling on Helicopter Handling Qualities", 43rd Annual National Forum of the American Helicopter Society, May 1987.
77. Mullen, G.J., Brinson, P.R.; "Experimental Evaluation of Multivariable Rotor Control Schemes"; The Aeronautical Journal; December 1999.
78. Tischler, M.B., "Digital Control of Highly Augmented Combat Rotorcraft", NASA-Technical Memorandum 88346, May 1987.
79. Liu, G.P., Patton, R.J.; Eigenstructure Assignment for Control System Design, John Wiley and Sons, England, 1998.
80. Brinson, P.R., Mullen, G.J., Howitt, J., Woodrow, I.; "Experimental Investigation of Control System Design Methods For Helicopters", 21st European Rotorcraft Forum, Saint-Petersburg, Russia, August-September 1995.
81. Zhao, X., Curtiss, H.C.; "A Study of Helicopter Stability and Control Including Blade Dynamics"; NASA-CR-183245; October 1988.
82. Rozak, J.N.; "Impact of Robust Control on Handling Qualities and Fatigue of Rotorcraft", The Pennsylvania State University, May 1995.
83. Rozak, J.N., Ray, A., "Technical Note - Robust Multivariable Control of Rotorcraft in Forward Flight: Impact of Bandwidth on Fatigue Life", Journal of the American Helicopter Society, Vol. 43 (3), July 1998.
84. Tischler, M.B., Lee, J.A., Colburne, J.D., "Comparison of Flight Control System Design Methods Using the Conduit Design Tool", Journal of Guidance, Control, and Dynamics, Vol. 25, (3), May-June 2002.
85. Walker, D.J., Turner, M.C., Gubbels, A.W., "Practical Aspects of Implementing H-Infinity Controllers on a FBW Research Helicopter", RTO AVT Symposium – Active Control Technology for Enhanced Performance Operational Capabilities of Military Aircraft, Land Vehicles and Sea Vehicles, Braunschweig, Germany, May 2000.
86. Walker, D.J., "Multivariable Control of the Longitudinal and Lateral Dynamics of a Fly-By-Wire Helicopter", Control Engineering Practice 11, 2003.
87. Takahashi; Fletcher; Tischler; "Development of a Model Following Control Law for Inflight Simulation Using Analytical and Identifies Models"; 51st Annual American Helicopter Society Forum; Fort Worth; May 1995.
88. Lewis; "An Aeroelastic Model Structure Investigation for a Manned Real-Time Rotorcraft Simulation"; US Army - Virginia; 49th American Helicopter Society Forum, St. Louis, Missouri; May 19-21 – 1993.
89. Maine R.E., Iliff, K.W.; "User's Manual for MMLE3, a General FORTRAN Program fro Maximum Likelihood Parameter Estimation"; NASA Technical Paper 1563, November 1980.

90. AGARD Lecture Series: "Rotorcraft System Identification"; AGARD-LS-178; October 1991.
91. Tischler, M.B., "Frequency-Response Identification of XV-15 Tilt-Rotor Aircraft Dynamics", NASA-Technical Memorandum 89428, May 1987.
92. Talbot, P.D., Bruce, T.E., Decker, W.A., Chen, R.T.N.; "A Mathematical Model of a Single Main Rotor Helicopter for Piloted Simulation"; NASA Technical Memorandum 84281; 1982.
93. Chen, R.T.N.; "Effects of Primary Rotor Parameters on Flapping Dynamics", NASA Technical Paper 1431, January 1980.
94. Padfield, G.D., DuVal, R.W.; "Application Areas for Rotorcraft System Identification Simulation Validation"; AGARD Lecture Series: Rotorcraft System Identification; AGARD-LS-178; October 1991.
95. Kaletka, J.; Von Grunhagen, W.; "Identification of Mathematical Derivative Models for the Design of a Model Following Control System"; 45th Annual American Helicopter Society Forum and Technology Display; Boston, M.A.; May 1989.
96. Kaletka, J., Von Grunhagen, W., Tischler, M.B., Fletcher, J.W.; "Time and Frequency Domain Identification and Verification of Bo105 Dynamic Models"; 15th European Rotorcraft Forum; Amsterdam; September 1989.
97. Fu, K.-H.; Kaletka, J.; "Frequency-Domain Identification of Bo105 Derivative Models with Rotor Degrees of Freedom"; Journal of the American Helicopter Society; January 1993
98. Hansen, R.; "Towards a Better Understanding of Helicopter Stability Derivatives"; 8th European Rotorcraft Forum", Aix-En-Provence, France; September 1982.
99. Hui, K.; "Improving Prediction: The Incorporation of Simplified Rotor Dynamics in a Mathematical Model of the Bell 412HP", Canadian Aeronautics and Space Journal, Vol. 40 (4), December 1994.
100. Hui, K., "The Inclusion of Higher-Order Rotor Dynamics to Improve the Dynamic Model of a Single Rotor Helicopter in Hover", System Identification for Integrated Aircraft Development and Flight Testing, RTO Systems Concepts and Integration Panel (SCI) Symposium, Madrid, Spain, May 1998.
101. Blackwell, J., Feik, R.A., Perrin, R.H.; "Identification of Rotor Dynamic Effects in Flight Data", 15th European Rotorcraft Forum, Amsterdam, Paper 68, September 1999.
102. Tischler, M.B., "System Identification Requirements for High-Bandwidth Rotorcraft Flight Control System Design", Journal of Guidance, Vol. 13, (5), September-October 1990.
103. Tischler, M.B., Cauffman, M.G., "Frequency-Response Method for Rotorcraft System Identification with Applications to the BO-105 Helicopter", American Helicopter Society 46th Annual Forum, Washington, D.C., May 1990.
104. Tomashofski, C.A., Tischler, M.B.; "Flight Test Identification of SH-2G Dynamics in Support of Digital Flight Control System Development"; American Helicopter Society 55th Annual Forum, Montreal, Canada; May 1999.
105. Tischler, M.B., Colbourne, J.D., Jenkins, J.L., Cicolanti, L.S., Cheung, K.K., Wright, S.C., Acunzo, A.C., Yakzan, N.S., Sahasrabudhe, V.; "Integrated System Identification and Flight Control Optimization in S-92 Handling-Qualities Development"; American Helicopter Society 57th Annual Forum, Washington, D.C., May 2001.
106. Kim, F., Celi, R., Tischler, M.B.; "Higher-Order State Space Simulation Models of Helicopter Flight Mechanics"; American Helicopter Society 46th Annual Forum, Washington, D.C.; May 1990.
107. Aponso, B., Johnston, D.E., Johnson, W.A., Magdaleno, R.,E., "Identification of Higher-Order Helicopter Dynamics Using Linear Modeling Methods"; American Helicopter Society 47th Annual Forum, Washington, D.C.; May 1991.
108. Cresap, W.L., Myers, A.W., "Design and Development of the Model 412 Helicopter", American Helicopter Society 36th Annual Forum, Washington, D.C., May 1980.
109. Myers, A.W., Phillips, N.B., Snyder, D.E., "The Model 412 Multi-Bladed Rotor System", American Helicopter Society Mid-East Region National Specialists' Meeting - Rotor System Design, Philadelphia, Pennsylvania, October 1980.
110. Erdos, R.T., Gubbels A.W., Ellis, D.K, "Variable Stability Airborne Simulation: Application in Flight Testing", American Helicopter Society 58th Annual Forum, Montreal, PQ, June 2002.

111. Gubbels, A.W., Carignan, S.J.R.P.; "The NRC Bell 412 Advanced Systems Research Aircraft – A New Facility for Airborne Simulation"; Canadian Aeronautics and Space Journal; Volume 46, Number 2; June 2000.
112. Baillie, S., Morgan, M.;"The Effects of Control Bandwidth, Control Sensitivity, and Disturbance Rejection Ability on Rotorcraft Handling Qualities", National Research Council Canada, LTR-FR-111, March 1990.
113. Lusardi, J.A., Blanken, C.L., Tischler, M.B.; "Piloted Evaluation of a UH-60 Mixer Equivalent Turbulence Simulation Model", American Helicopter Society 59th Annual Forum, Phoenix, Arizona, May 2003.
114. Cooke, A., Fitzpatrick, E., Helicopter Test and Evaluation, Blackwell Publishing – QinetiQ Limited, 2002.
115. Tischler, M.B., Williams, J.N., Ham, J.A., "Flight Test Manual – Rotorcraft Frequency Domain Flight Testing", U.S. Army Aviation Technical Test Center, AQTD Project No. 93-14, September 1995.
116. Turnour, S.R., Celi, R., "Modeling of Flexible Rotor Blades for Helicopter Flight Dynamics Applications"; 19th European Rotorcraft Forum, Cernobbio, Italy; September 1995.